

**ASYMMETRIC SYNTHESIS MEDIATED BY NOVEL
ORGANOCATALYSTS AND REACTIONS OF
2-ALKENYL-*p*-BENZOQUINONES**

A THESIS

*Submitted in partial fulfilment of the
requirements for the award of the degree*

of

DOCTOR OF PHILOSOPHY

in

CHEMISTRY

by

RASHMI RANI



**DEPARTMENT OF CHEMISTRY
INDIAN INSTITUTE OF TECHNOLOGY ROORKEE
ROORKEE-247 667 (INDIA)**

JANUARY, 2011

**©INDIAN INSTITUTE OF TECHNOLOGY ROORKEE, ROORKEE-2011
ALL RIGHTS RESERVED**



INDIAN INSTITUTE OF TECHNOLOGY ROORKEE
ROORKEE

CANDIDATE'S DECLARATION

I hereby certify that the work which is being presented in the thesis entitled '**Asymmetric Synthesis Mediated by Novel Organocatalysts and Reactions of 2-Alkenyl-*p*-benzoquinones**' in partial fulfilment of the requirements for the award of the degree of Doctor of Philosophy and submitted in the Department of Chemistry of the Indian Institute of Technology Roorkee, Roorkee is an authentic record of my own work carried out during a period from July 2006 to Jan 2011 under the supervision of Dr. Rama Krishna Peddinti, Assistant Professor, Department of Chemistry, Indian Institute of Technology Roorkee, Roorkee.

The matter presented in the thesis has not been submitted by me for the award of any other degree of this or any other Institute.

Rashmi
(Rashmi Rani)

This is to certify that the above statement made by the candidate is correct to the best of my knowledge.

R. K. Peddinti
(R. K. Peddinti)
Supervisor

Date: 3.2.2011

The Ph.D. Viva-Voice Examination of **Ms. RASHMI RANI**, Research Scholar, has been held on 22.6.2011

R. K. Peddinti
Signature of Supervisor

Ajay
Signature of External Examiner

ACKNOWLEDGEMENTS

First and foremost, I must thank my supervisor, **Dr. Rama Krishna Peddinti**, who exemplified to me the meaning of research with his distinct vision and meticulous guidance. At this day of my career, when I pause to look back to my research period I find that at every stage his perpetual encouragement, constructive criticism and above all morale boosting inspiration served a vital source to bring the present work to conclusion. Further his bold initiative and compromising gesture made a highly challenging path feasible.

I am highly grateful to Prof. Ravi Bhushan, Prof. Kamaluddin and Prof. V. K. Gupta the former and present Heads of the Department of Chemistry, Indian Institute of Technology-Roorkee for providing me with the necessary facilities and support to carry out these investigations.

With great pleasure I would like to thank my labmates Jyoti, Garima, Seshi, Naganjaneyulu, Ram Tilak, Deepika, Sankha, Anju, Santosh, Arun and Naresh for their invaluable suggestions, motivation and encouragement in the progress of this research work. Their help and co-operation are unforgettable.

I will always cherish my friendship with Jyoti, Shivani, Varu, Priti who contributed directly or indirectly towards successful completion of this project in their own special way.

I would like to thank all my friends and specially my senior Sandeep Kumar, who boosted my morale with their ever buoyant expression.

My grandparents and parents deserve a special line of respect and sincere gratitude for whatever they did for me. These pages wouldn't be sufficient to mention the enormous efforts my parents have made to educate me and to take care of my entire requirements.

I am in dearth of proper words to express my abounding feeling to *bhaiya Ravi, bhabhi Anshu* for their, encouragement and the love they showed on me at every stage.

A few words for Aaruhi and Aarush, my little niece and nephew, when "they" grow up they can see their sweet names in my thesis.

Special thanks to my fiancée Anurag who has provided me unflinching support and encouragement when I really needed it.

I am also grateful to faculty members and staff of Chemistry Department for their

cooperation and timely help which provided a good environment to develop my skills as a researcher.

My sincere thanks to Prof. Ritu Barthwal, Coordinator, NMR facility at IIC of the Institute for her support. I also thank Dr. Raghavaiah, School of Chemistry, University of Hyderabad for useful discussions on single crystal X-ray analysis.

The financial assistance provided by Department of Science and Technology (DST) and Council for Scientific and Industrial Research (CSIR), New Delhi that made my research work very smooth and prompt is gratefully acknowledged.

At the end, I would like to thank Almighty who instilled in me courage, confidence and patience to fulfill my task.

RASHMI RANI

CONTENTS

	Page No.
Candidate's Declaration	
Acknowledgements	
Abbreviations	i
Abstract	iii
Appendix-1 (List of Schemes)	ix
Appendix-2 (List of Figures)	xiii
Appendix-3 (List of Tables)	xv
Appendix-4 (List of Spectra)	xvii
CHAPTER-1 Introduction	
1.1. Chirality, chiral compounds and enantiomers	1
1.2. Asymmetric synthesis	3
1.3. Organocatalysis	5
1.3.1. Lewis bases as organocatalysts	7
1.3.1.1. Enamine catalysis	7
1.3.1.2. Iminium catalysis	14
1.3.2. Lewis acids as organocatalysts	19
1.3.3. Brønsted bases as organocatalysts	21
1.3.4. Brønsted acids as organocatalysts	22
1.4. <i>p</i> -Benzoquinones in organic synthesis	24
1.5. References	29
CHAPTER-2 Synthesis and Characterization of Novel Camphorsulfonamide-Based Prolinamide Organocatalysts	
2.1. Introduction	39
2.2. Objective	40
2.3. Results and discussion	41
2.3.1. Synthesis of 2-aminocamphor-10-sulfonamides II-14a,b , II-15a,b and II-16a,b	41
2.3.2. Synthesis of camphorsulfonamide-based prolinamides Cat-1a , Cat-2a , Cat-3a and 3b	53

2.4.	Conclusion	55
2.5.	Experimental	56
2.5.1.	General	56
2.6.	References	70

CHAPTER-3 Asymmetric Aldol Reaction Catalyzed by Camphorsulfonamide-Based Prolinamides

3.1.	Introduction	73
3.2.	Objective	74
3.3.	Results and discussion	75
3.3.1.	Aldol reaction catalyzed by camphorsulfonamide-based prolinamides	75
3.3.2.	Determination of absolute configuration of III-3d by single crystal X-Ray analysis	85
3.3.3.	Desymmetrization	87
3.3.4.	Structure determination of aldol product III-18a by NOESY experiment	89
3.3.5.	Proposed mechanism	90
3.3.6.	Proposed transition state	91
3.4.	Conclusion	91
3.5.	Experimental	92
3.5.1.	General	92
3.5.2.	Instrumentation	92
3.5.3.	General Procedure	92
	HPLC Charts	109
3.6.	References	118

CHAPTER-4 Asymmetric Michael Reaction Catalyzed by Camphorsulfonamide-Based Prolinamides

4.1.	Introduction	125
4.2.	Objective	126
4.3.	Results and discussion	126
4.3.1.	Michael reaction catalyzed by camphorsulfonamide-based prolinamides	126
4.3.2.	Proposed mechanism	134
4.3.3.	Proposed transition state	135
4.4.	Conclusion	136
4.5.	Experimental	137

4.5.1. General	137
4.5.2. Instrumentation	137
4.5.3. General Procedure	137
HPLC Charts	147
4.6. References	152

CHAPTER-5 Domino Reactions of Alkenyl-1,4-benzoquinones

5.1. Introduction	155
5.2. Objective	157
5.3. Results and discussion	157
5.4. Conclusion	180
5.5. Experimental	181
5.6. References	191

NMR Spectra of Selected Compounds	193
--	-----

List of Publications

LIST OF ABBREVIATIONS

Ac	acetyl
Boc	<i>tert</i> -butoxycarbonyl
Bn	benzyl
<i>n</i> -Bu	<i>n</i> -butyl
<i>t</i> -Bu	<i>tert</i> -butyl
Bu	butyl
Bz	benzoyl
CAN	ceric ammonium nitrate
COSY	correlation spectroscopy
CSA	camphor-10-sulfonic acid
DCC	<i>N,N</i> -dicyclohexylcarbodiimide
DCM	dichloromethane
DDQ	2,3-dichloro-5,6-dicyano-1,4-benzoquinone
DEPT	distortionless enhancement by polarization transfer
DHF	2,3-dihydrofuran
DHP	2,3-dihdropyran
DMAP	4-dimethylaminopyridine
DMF	<i>N,N</i> -dimethylformamide
DMSO	dimethylsulfoxide
dr	diastereomeric ratio(s)
ee	enantiomeric excess(es)
EVE	ethyl vinyl ether
EWG	electron-withdrawing group
FT-IR	fourier transform infrared spectroscopy
GC	gas chromatography
HPLC	high pressure liquid chromatography
HRMS	high resolution mass spectroscopy

HSQC	heteronuclear single quantum coherence
IPA	isopropanol
ⁱ Pr	isopropyl
LUMO	lowest unoccupied molecular orbital
<i>m</i> -CPBA	<i>meta</i> -chloroperbenzoic acid
MS	mass spectroscopy
<i>N</i> -Boc	<i>tert</i> -butyl carbamate
NBS	<i>N</i> -bromosuccinamide
NMR	nuclear magnetic resonance
NOESY	nuclear Overhauser effect spectroscopy
ORTEP	oak ridge thermal ellipsoid plot program
PG	protecting group
PMP	<i>p</i> -methoxyphenyl
ROESY	rational frame nuclear Overhauser effect spectroscopy
rt	room temperature
TBDPS	<i>tert</i> -butyldiphenylsilyl
TBSO	<i>tert</i> -butyldimethylsilyl
TCA	trichloroacetic acid
Tf ₂ NH	trifluoromethanesulfonimide
TFA	trifluoroacetic acid
THF	tetrahydrofuran
THP	tetrahydropyran
TLC	thin layer chromatography
TMS	tetramethylsilane
TMSCN	trimethylsilyl cyanide
TMSN ₃	trimethylsilyl azide
TPFPB	tris(pentafluorophenyl)borane
TsOH	<i>p</i> -toluenesulfonic acid
UV	ultraviolet

Abstract

The thesis entitled “**Asymmetric Synthesis Mediated by Novel Organocatalysts and Reactions of 2-Alkenyl-*p*-benzoquinones**” is divided into five chapters.

Novel Camphor-based prolinamides have been synthesized and employed as efficient chiral organocatalysts for the C-C bond forming reactions such as aldol and Michael addition reactions. Furthermore, stereoselective domino reactions of alkenyl-1,4-benzoquinones with enol ethers have been carried out to furnish novel angular fused heterocyclic quinoid ring systems.

CHAPTER-1: Introduction

Enantioselective synthesis has become most important area in synthetic organic chemistry, medicinal chemistry, agricultural chemistry, natural products chemistry and pharmaceutical industries. New catalytic asymmetric reactions give us the opportunities to develop more efficient methods for the synthesis of various highly potent chiral compounds, with successful applications for the synthesis of various complex natural products as well as industrial production. However, in catalytic approach, catalytic amount of small organic molecules or chiral metal complexes is employed in the reaction and its regeneration and participation in parallel catalytic cycle complete the reaction. Though, metal catalysts have significant advantages in asymmetric synthesis over the organic molecules as wide substrate scope with catalytic activity, they offer some troubles also such as potential heavy metals high price, toxicity, pollution, waste treatment, etc. On the other hand, metal free organocatalytic reactions unlike metal-ligand complexes, generally tolerate aerobic conditions and do not require rigorous exclusion of water. They enjoy a broad spectrum of substrates than enzymes and can be used in various organic solvents. Thus the development of enantioselective organocatalysts is one of the most challenging and formidable endeavors in modern science and technology.

This chapter also details a brief review on reactions of *p*-benzoquinones and domino reactions. Benzoquinones are versatile intermediates in organic synthesis. Owing to functionalities such as enone, *p*-benzoquinones undergo Diels-Alder reactions and [3+2] cycloaddition reactions. These cross conjugated dienones can be utilized for the synthesis of carbocyclic and heterocyclic ring systems.

CHAPTER-2: Synthesis and Characterization of Novel Camphorsulfonamide-based Prolinamide organocatalysts

This chapter deals with synthesis and characterization of novel camphor-based prolinamide organocatalysts. Chiral monoterpene such as camphor, known to be used in several medicines antiseptics and insecticides having rigid bicyclic structure are widely used synthons in asymmetric synthesis. Camphor and its derivatives can afford a simple, inexpensive scaffold around which to build a chiral catalyst. Such molecules arouse our attention to use these molecules as chiral scaffold to develop proline-based chiral organocatalysts for asymmetric synthesis. For this purpose we synthesized camphor and proline based organocatalysts as shown in figure 1.

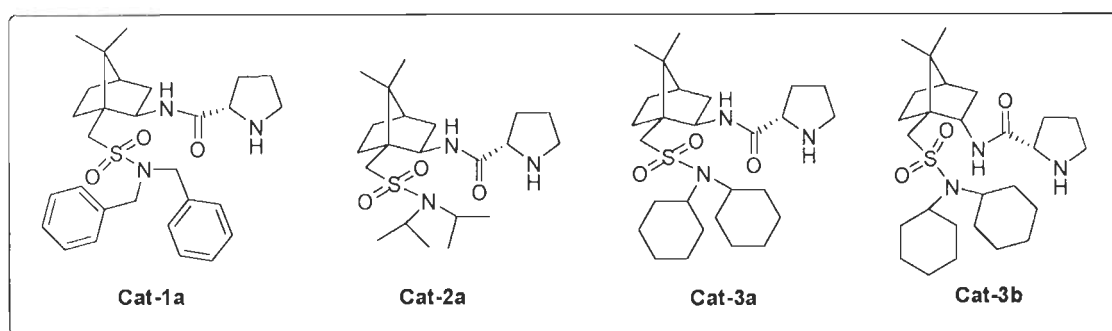
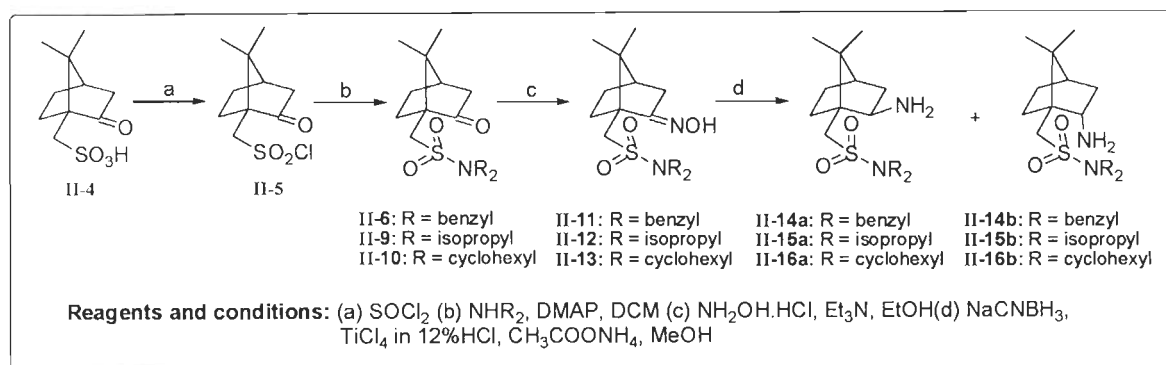


Figure 1: structures of camphor-based organocatalysts

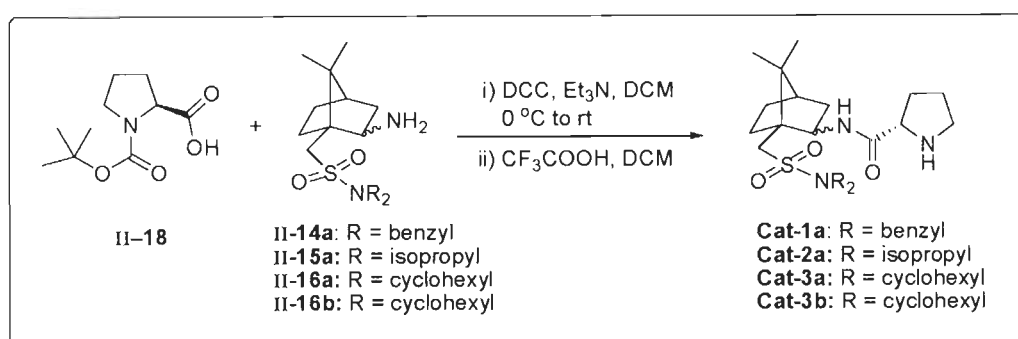
In our synthetic approach proline unit was anchored to the host camphor based system by following five steps. Initially, we synthesized compounds **II-14a-b**, **II-15a-b**, **II-16a-b** starting from (1*S*)-(+)-10-camphorsulfonic acid as shown in scheme 1. All intermediates otherwise mentioned were isolated and fully characterized by ¹H and ¹³C NMR & DEPT.



Scheme 1: synthesis of camphorsulfonamide-based primary amines

The *exo* and *endo* amines were characterized by ^1H and ^{13}C NMR, ^1H - ^1H COSY & HSQC and ^1H - ^1H NOSEY experiments.

After synthesizing the camphor-based primary amines, we converted these amines in to corresponding prolinamides by coupling with N-Boc proline. All prolinamides were isolated and purified by silica gel chromatography method and characterized by standard spectroscopic methods. The IR, ^1H & ^{13}C NMR, and HRMs were found to be in agreement with the assigned structure for **Cat-1a**, **Cat-2a**, **Cat-3a** and **Cat-3b**.

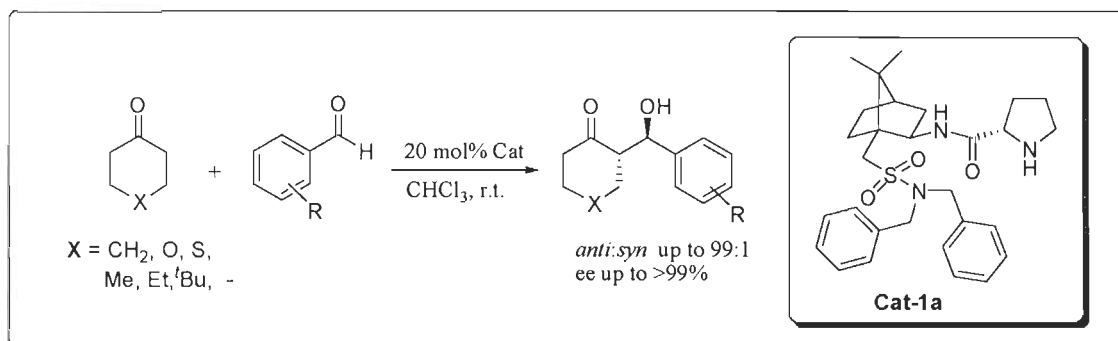


Scheme 2: Synthesis of camphorsulfonamide-based prolinamides

CHAPTER-3: Asymmetric Aldol Reaction Catalyzed by Camphorsulfonamide -based Prolinamide

In this chapter we have discussed the applications of these potential organocatalysts for asymmetric aldol reactions between cyclic and acyclic ketones as aldol donor with various aromatic aldehydes containing diversified substituents as aldol acceptors. Probing for an effective catalyst, We performed reaction between cyclohexanone and 2-nitrobenzaldehyde as a model reaction in presence of prolinamides **Cat-1a**, **Cat-2a**, **Cat-3a**, **Cat-3b** in various conditions. By proper screening of solvents and other conditions, prolinamide **Cat-1a** (20 mol%) in chloroform at room temperature was found to be most appropriate catalyst for aldol reaction and the corresponding aldol products were obtained in excellent chemical yields with high levels of *anti*-diastereoselectivity (up to 99:1) and enantioselectivity (up to >99%) (Scheme 3).

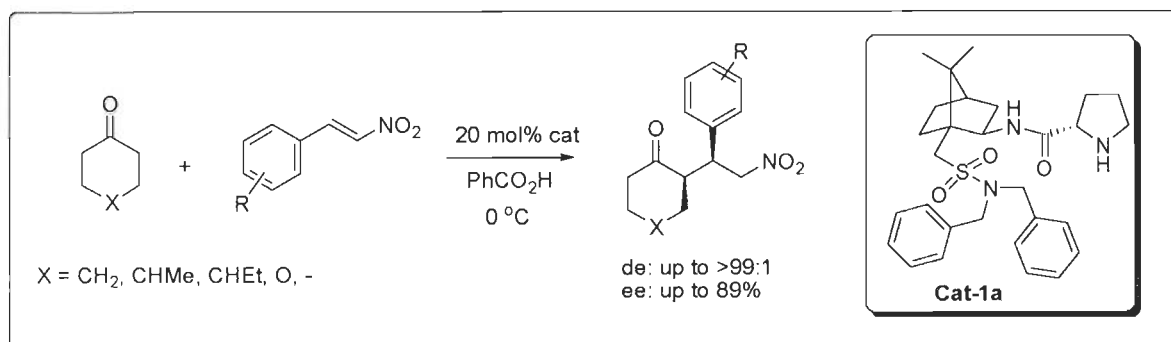
All aldol adducts were purified by column chromatography and fully characterized by IR, ^1H and ^{13}C NMR. finally, enantioselectivity of pure product was determined by HPLC analysis using chiral stationary phase column and hexane-isopropanol as eluting solvent.



Scheme 3: Asymmetric aldol reactions catalyzed by camphorsulfonamide-based prolinamides

CHAPTER-4: Asymmetric Michael Reaction Catalyzed by Camphorsulfonamide - based Prolinamide

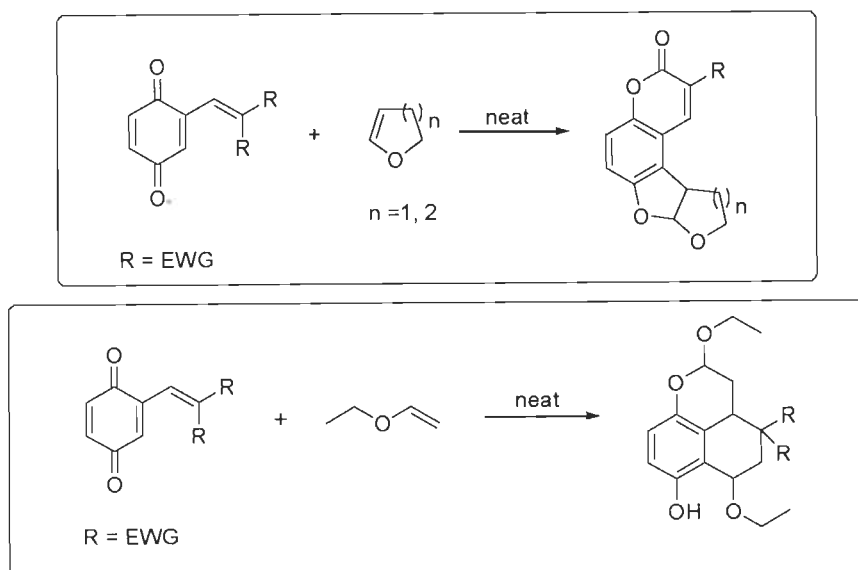
In continuation of our work on asymmetric synthesis we envisaged that these bifunctional organocatalysts can play a significant role in determining stereochemical outcome of amine catalyzed Michael addition of ketones to nitroolefins also. In this chapter these Novel camphor sulfonamide based organocatalysts were evaluate for their catalytic activity in Michael reaction of ketones with nitroolefins, leading to (1*R*,2*S*)-*syn* adducts as major antipodes. For studying asymmetric Michael addition we have chosen the addition of cyclohexanone to β -nitrostyrene (**IV-2a**) as model reaction by using these organocatalysts in numerous polar and non polar solvents. To our surprise we got best results in neat condition (without using any additional solvent) in presence of prolinamide **Cat-1a** (20 mol%). The asymmetric induction was further improved by conducting the reaction at different temperature, under solvent free conditions using catalyst and a co-catalyst. The addition of 15 mol% carboxylic acid as co-catalyst significantly accelerated the reaction rate relative to that carried out in the absence of co-catalyst. Among the employed carboxylic acids benzoic acid afforded the best result to afford Michael adducts in high yields (up to 97%) and excellent distereoselectivities (up to >99:1) with good enantioselectivity (up to 89%) (Scheme 4). All michael adducts were purified by column chromatography and fully characterized by IR, ^1H and ^{13}C NMR. finally, enantioselectivity of pure product was determined by HPLC analysis using chiral stationary phase column and hexane-isopropanol as eluting solvent.



Scheme 4: Asymmetric Michael addition catalyzed by camphorsulfonamide-based prolinamides

CHAPTER-5: Domino Reactions of Alkenyl-*p*-benzoquinones

In this chapter we have discussed the results on the synthesis of alkenyl-*p*-benzoquinones and their reactions with enol ethers to provide tri- and tetra-cyclic systems such as furo-furocoumarins via domino reaction pathway. Quinones are highly reactive substrates in Diels-Alder reactions with various dienes and provide the wide scope for the reaction. These reactions are highly useful for the synthesis of natural products and other complex molecules. *p*-Quinones are starting compounds for the synthesis of furobezofuran ring systems such as natural products such as aflatoxin B₂. Studies on synthesis of alkenyl-*p*-benzoquinones and their reactions with enol ethers are described in this chapter (Scheme 5).



Scheme 5: Reactions of alkenyl-*p*-benzoquinones

APPENDIX-1

LIST OF SCHEMES

	Page No.
CHAPTER-1	
Scheme 1: Hajos-Parrish-Eder-Sauer-Wiechert Robinson annulation.	5
Scheme 2: Formation of enamine.	7
Scheme 3: Enamine catalysis.	8
Scheme 4: Proline-catalyzed intermolecular aldol reaction.	8
Scheme 5: Hydrogen bonding control vs. steric control in enamine catalysis.	9
Scheme 6: Proline catalyzed aldol reactions.	11
Scheme 7: Direct three-component Mannich reaction.	11
Scheme 8: Transition states in aldol and Mannich reaction.	12
Scheme 9: Asymmetric enamine-catalyzed Michael additions with aldehyde donors.	13
Scheme 10: Domino <i>O</i> -nitroso aldol-conjugate addition.	14
Scheme 11: Iminium catalysis.	15
Scheme 12: [4+2] Cycloaddition of α,β -unsaturated aldehydes.	15
Scheme 13: Friedel-Craft acylation reaction between α,β -unsaturated aldehydes and substituted benzene.	16
Scheme 14: [4+2] Cycloaddition of 3-hydroxypyrones and α,β -unsaturated ketones.	17
Scheme 15: [3+2] Cycloaddition using MacMillan imidazolidinone catalyst.	18
Scheme 16: Organocatalytic hydrogenation.	19
Scheme 17: Diels-Alder reaction catalyzed by a chiral silyl salt.	20
Scheme 18: Cycloalkylsilyl triflimides.	20
Scheme 19: Enantioselective Friedel-Crafts alkylation.	21
Scheme 20: Cinchona alkaloids as organocatalysts.	22
Scheme 21: Different conjugate addition of cinchona alkaloids.	22
Scheme 22: Biginelli reaction: scope and proposed reaction pathway.	23
Scheme 23: Diels-Alder reaction of ethyl vinyl ketone with silyloxydienes.	23
Scheme 24: The Diels-Alder reaction between cyclopentadiene and <i>p</i> -benzoquinone.	24

Scheme 25: The Diels-Alder reaction as a key-step in the total synthesis of steroid hormones cortisone and cholesterol.	25
Scheme 26: The [4+2] cycloaddition between alkenylindoles and <i>p</i> -benzoquinone.	25
Scheme 27: The [4+2] cycloaddition between alkenyl-1,4-benzoquinone and 2,3-dihydrofuran.	26
Scheme 28: Reaction between substituted <i>p</i> -benzoquinone and 2,3-dihydrofuran.	26
Scheme 29: Reaction between alkenyl-1,4-benzoquinone and cyclic enol ethers.	26
Scheme 30: Chiral oxazaborolidinium ion mediated enantioselective [3+2] cycloaddition between 2-methoxy-1,4-benzoquinone and 2,3-dihydrofuran.	27
Scheme 31: The Diels-Alder reaction as a key-step in the total synthesis of dimeric metabolite acremine G.	27

CHAPTER-2

Scheme 1: Camphor scaffold embedded chiral thiourea catalyst for aldol reaction.	39
Scheme 2: Chiral pyrrolidine camphor derivative catalyzed Michael addition.	40
Scheme 3: Synthesis of camphorsulfonamide II-6 .	42
Scheme 4: Synthesis of camphorsulfonamides II-9 and II-10 .	43
Scheme 5: Synthesis of camphor oxime derivatives II-11 , II-12 & II-13 .	43
Scheme 6: Reduction of oxime II-11 .	44
Scheme 7: Synthesis of 2-aminocamphorsulfonamides II-14-16 .	46
Scheme 8: Synthesis of <i>N-tert</i> -butoxycarbonyl-(<i>S</i>)-proline II-18 .	53
Scheme 9: Synthesis of prolinamide Cat-1a .	53
Scheme 10: Synthesis of prolinamides Cat-2a and Cat-3a .	54
Scheme 11: Synthesis of prolinamide Cat-3b .	54

CHAPTER-3

Scheme 1: Prolinamide catalyzed asymmetric aldol reaction.	74
Scheme 2: Proposed mechanism for asymmetric aldol reaction.	90

CHAPTER-4

Scheme 1: Prolinamide catalyzed asymmetric Michael reaction.	126
---	-----

Scheme 2: Possible four diastereoisomers from the reaction of cyclohexanone with nitrostyrene.	127
Scheme 3: Michael reaction of acetone with substituted β -nitrostyrenes in presence of Cat-1a .	134
Scheme 4: Proposed mechanism for asymmetric Michael reaction.	135
Scheme 5: Possible transition state for Michael reaction.	136

CHAPTER-5:

Scheme 1: Biomimetic domino synthesis of tropinone.	155
Scheme 2: Biosynthesis of steroids from squalene epoxides.	156
Scheme 3: Diels-Alder and [3+2] cycloaddition in the total synthesis of (-)-vindorosine.	156
Scheme 4: Formylation of <i>p</i> -methoxyphenol.	158
Scheme 5: Reaction between <i>p</i> -methoxysalicylaldehyde and dimethyl malonates.	158
Scheme 6: Methylation of <i>p</i> -methoxysalicylaldehyde.	158
Scheme 7: Synthesis of alkenylarene V-4 .	159
Scheme 8: Synthesis of alkenylarene V-5 .	159
Scheme 9: Synthesis of alkenyl <i>p</i> -benzoquinones.	159
Scheme 10: Formation of furo-furocoumarin V-8 by conjugate addition/double cyclization domino process.	161
Scheme 11: Conjugate addition/double cyclization domino process of alkenyl <i>p</i> -benzoquinone V-7 with DHF.	162
Scheme 12: Conjugate addition/double cyclization domino process of alkenyl <i>p</i> -benzoquinones V-6 and V-7 with DHP.	168
Scheme 13: Domino reaction of alkenyl- <i>p</i> -benzoquinones V-6 and V-7 and ethyl vinyl ether.	172
Scheme 14: Plausible mechanism for the formation of tetrahydro-benzochromene derivative V-14 by a domino process.	173
Scheme 15: The triple Diels-Alder cycloaddition domino process in the formation of nonacyclic adduct V-19 .	178
Scheme 16: The Diels-Alder cycloaddition between alkenyl- <i>p</i> -benzoquinone V-7 and 2-methylfuran.	179
Scheme 17: The Diels-Alder cycloaddition between alkenyl- <i>p</i> -benzoquinone V-6 and 2-methylfuran.	179

APPENDIX-2

LIST OF FIGURES

	Page No.
CHAPTER-1	
Figure 1: Chiral molecule containing a tetrahedral stereocenter.	1
Figure 2: Examples of enantiomers with different biological effects.	2
Figure 3: Enantioselective synthesis.	3
Figure 4: Classification of asymmetric synthesis.	4
Figure 5: Examples of organocatalysts.	6
Figure 6: Selected examples of enamine catalysts.	10
Figure 7: Stereocontrol elements in the iminium ion.	16
CHAPTER-2	
Figure 1: Design of camphorsulfonamide-based organocatalysts.	40
Figure 2: Camphorsulfonamide-based organocatalysts.	41
Figure 3: Aliphatic region of the 500 MHz ¹ H NMR spectra of 2-amino camphorsulfonamides II-14a,b , II-15a,b and II-16a,b .	45
Figure 4: ¹ H- ¹ H and ¹ H- ¹³ C (HSQC) COSY spectra of II-15a .	49
Figure 5: ¹ H- ¹ H and ¹ H- ¹³ C (HSQC) COSY spectra of II-15b .	50
Figure 6: 500 MHz NOESY Spectrum of II-16a in CDCl ₃ .	52
Figure 7: 500 MHz NOESY Spectrum of II-16b in CDCl ₃ .	52
CHAPTER-3	
Figure 1: ORTEP Diagram of crystal structure of 2-[hydroxy-(2-bromophenyl) methyl]cyclohexanone (III-3d).	85
Figure 2: 500 MHz NOESY Spectrum of III-18a in CDCl ₃ .	89
Figure 3: Plausible transition state.	91
Figure 4: HPLC Chromatograms of aldol adducts III-3a , III-3b , III-3c and III-3d .	109
Figure 5: HPLC Chromatograms of aldol adducts III-3e , III-3f , III-3g and III-3h .	110
Figure 6: HPLC Chromatograms of aldol adducts III-3i , III-3j , III-3k and III-3l .	111

Figure 7: HPLC Chromatograms of aldol adducts III-6a, III-6b, III-7a and III-7b.	112
Figure 8: HPLC Chromatograms of aldol adducts III-9a, III-9b, III-9c and III-9d.	113
Figure 9: HPLC Chromatograms of aldol adducts III-9e, III-9f, III-11a and III-11b.	114
Figure 10: HPLC Chromatograms of aldol adducts III-11c, III-11d, III-11e and III-11f.	115
Figure 11: HPLC Chromatograms of aldol adducts III-16a, III-16b, III-17a and III-17b.	116
Figure 12: HPLC Chromatograms of aldol adducts III-18a, III-18b.	117

CHAPTER-4

Figure 1: HPLC Chromatograms of Michael adducts IV-3a, IV-3b, IV-3c and IV-3d.	147
Figure 2: HPLC Chromatograms of Michael adducts IV-3e, IV-3f, IV-3g and IV-3h.	148
Figure 3: HPLC Chromatograms of Michael adducts IV-3i, IV-3j, III-3k and III-8a.	149
Figure 4: HPLC Chromatograms of Michael adducts IV-8b, IV-9a, IV-10a and IV-11a.	150
Figure 5: HPLC Chromatograms of Michael adduct IV-13a.	151

CHAPTER-5

Figure 1: Structures of alkenyl- <i>p</i> -benzoquinones and enol ethers.	157
Figure 2: ¹ H- ¹ H and ¹ H- ¹³ C (HSQC) COSY spectra of V-8.	164
Figure 3: ¹ H- ¹ H and ¹ H- ¹³ C (HSQC) COSY spectra of V-11.	165
Figure 4: 500 MHz NOESY Spectrum of V-11 in CDCl ₃ .	166
Figure 5: ORTEP Diagram of crystal structure of tetracyclic compound V-11.	166
Figure 6: ¹ H- ¹ H and ¹ H- ¹³ C (HSQC) COSY spectra of V-12.	170
Figure 7: ¹ H- ¹ H and ¹ H- ¹³ C (HSQC) COSY spectra of V-13.	171
Figure 8: 500 MHz ROESY Spectrum of V-13 in CDCl ₃ .	172
Figure 9: ¹ H- ¹ H and ¹ H- ¹³ C (HSQC) COSY spectra of V-14.	175
Figure 10: ¹ H- ¹ H and ¹ H- ¹³ C (HSQC) COSY spectra of V-15.	176
Figure 11: Structures of isomeric nonacyclic systems V-19a and V-19b.	177

APPENDIX-3

LIST OF TABLES

	Page No.
CHAPTER-2	
Table 1: Proton and carbon chemical shifts and proton-proton coupling constants for <i>exo</i> and <i>endo</i> isomers II-14a and II-14b .	46
Table 2: Proton and carbon chemical shifts and proton-proton coupling constants for <i>exo</i> and <i>endo</i> isomers II-15a and II-15b .	48
Table 3: Proton and carbon chemical shifts and proton-proton coupling constants for <i>exo</i> and <i>endo</i> isomers II-16a and II-16b .	51
CHAPTER-3	
Table 1: Effect of solvent on direct aldol reaction of cyclohexanone with 2-nitrobenzaldehyde in presence of Cat-1a .	76
Table 2: Screening of organocatalysts.	78
Table 3: Aldol reaction of cyclohexanone with substituted benzaldehydes in the presence of Cat-1a .	79
Table 4: Aldol reaction of 4-oxa, 4-thia-cyclohexanones with substituted benzaldehydes in the presence of Cat-1a .	81
Table 5: Aldol reaction of cyclopentanone with substituted benzaldehydes in the presence of Cat-1a .	82
Table 6: Aldol reaction of acetone with substituted benzaldehydes in the presence of Cat-1a .	83
Table 7: Comparison of enantioselectivity of aldol reactions catalyzed by Cat-1a and proline (III-12).	84
Table 8: Crystallographic data for (2 <i>S</i> ,1' <i>R</i>)-2-[hydroxy(2-bromophenyl)methyl]cyclohexanone (III-3d).	86
Table 9: Aldol reaction between 4-substituted cyclohexanones and substituted benzaldehydes in the presence of Cat-1a .	88
Table 10: HPLC data table for aldol products obtained from the reaction between cyclohexanone and substituted benzaldehydes in presence of Cat-1a .	104

Table 11: HPLC data table for aldol products obtained from the reactions between cyclopentanone and substituted benzaldehydes in presence of Cat-1a .	106
Table 12: HPLC data table for aldol products obtained from the reaction between acetone and substituted benzaldehydes in presence of Cat-1a .	107
Table 13: HPLC data table for aldol products derived from the reaction between 4-substituted cyclohexanones and substituted aromatic aldehydes in presence of Cat-1a .	108

CHAPTER-4

Table 1: Screening of reaction conditions and organocatalysts.	128
Table 2: Effect of additives on Michael reaction of cyclohexanone with β -nitrostyrene (IV-2a) in presence of Cat-1a .	130
Table 3: Michael reaction of cyclohexanone with substituted β -nitrostyrenes IV-2a-k in presence of Cat-1a .	131
Table 4: Michael reaction of ketones with substituted β -nitrostyrenes in presence of Cat-1a .	133
Table 5: HPLC data for Michael adducts obtained from camphorsulfonamide-based prolinamide Cat-1a catalyzed Michael reactions.	144

CHAPTER-5

Table 1: Optimization conditions for the synthesis of tetracyclic compound V-8 .	160
Table 2: Spectral data for tetracyclic compounds V-8 and V-11 .	163
Table 3: Crystallographic data for furo-furocoumarin derivative V-11 .	167
Table 4: Spectral data for tetracyclic compounds V-12 and V-13 .	169
Table 5: Spectral data for tricyclic compounds V-14 and V-15 .	174

APPENDIX-4

LIST OF SPECTRA

	Page No.
Figure S-1: ^1H NMR (500 MHz, CDCl_3) Spectrum of Cat-1a .	194
Figure S-2: ^{13}C DEPT (125 MHz, CDCl_3) Spectra of Cat-1a .	195
Figure S-3: ^1H NMR (500 MHz, CDCl_3) Spectrum of Cat-2a .	196
Figure S-4: ^{13}C DEPT (125 MHz, CDCl_3) Spectra of Cat-2a .	197
Figure S-5: ^1H NMR (500 MHz, CDCl_3) Spectrum of Cat-3a .	198
Figure S-6: ^{13}C DEPT (125 MHz, CDCl_3) Spectra of Cat-3a .	199
Figure S-7: ^1H NMR (500 MHz, CDCl_3) Spectrum of Cat-3b .	200
Figure S-8: ^{13}C NMR (125 MHz, CDCl_3) Spectrum of Cat-3b .	201
Figure S-9: ^1H NMR (500 MHz, CDCl_3) Spectrum of II-6 .	202
Figure S-10: ^{13}C DEPT (125 MHz, CDCl_3) Spectra of II-6 .	203
Figure S-11: ^1H NMR (500 MHz, CDCl_3) Spectrum of II-10 .	204
Figure S-12: ^{13}C DEPT (125 MHz, CDCl_3) Spectra of II-10 .	205
Figure S-13: ^1H NMR (500 MHz, CDCl_3) Spectrum of II-11 .	206
Figure S-14: ^{13}C DEPT (125 MHz, CDCl_3) Spectra of II-11 .	207
Figure S-15: ^1H NMR (500 MHz, CDCl_3) Spectrum of II-12 .	208
Figure S-16: ^{13}C DEPT (125 MHz, CDCl_3) Spectra of II-12 .	209
Figure S-17: ^1H NMR (500 MHz, CDCl_3) Spectrum of II-13 .	210
Figure S-18: ^{13}C DEPT (125 MHz, CDCl_3) Spectra of II-13 .	211
Figure S-19: ^1H NMR (500 MHz, CDCl_3) Spectrum of II-14a .	212
Figure S-20: ^{13}C DEPT (125 MHz, CDCl_3) Spectra of II-14a .	213
Figure S-21: ^1H - ^1H COSY (500 MHz, CDCl_3) Spectrum of II-14a .	214
Figure S-22: HSQC (^1H - ^{13}C) (125 MHz, CDCl_3) Spectrum of II-14a .	215
Figure S-23: ^1H NMR (500 MHz, CDCl_3) Spectrum of II-14b .	216
Figure S-24: ^{13}C NMR (125 MHz, CDCl_3) Spectrum of II-14b .	217
Figure S-25: ^1H - ^1H COSY (500 MHz, CDCl_3) Spectrum of II-14b .	218
Figure S-26: HSQC (^1H - ^{13}C) (125 MHz, CDCl_3) Spectrum of II-14b .	219
Figure S-27: ^1H NMR (500 MHz, CDCl_3) Spectrum of II-15a .	220
Figure S-28: ^{13}C DEPT (125 MHz, CDCl_3) Spectra of II-15a .	221
Figure S-29: ^1H - ^1H COSY (500 MHz, CDCl_3) Spectrum of II-15a .	222

Figure S-30: HSQC (^1H - ^{13}C) (125 MHz, CDCl_3) Spectrum of II-15a .	223
Figure S-31: ^1H NMR (500 MHz, CDCl_3) Spectrum of II-15b .	224
Figure S-32: ^{13}C DEPT (125 MHz, CDCl_3) Spectra of II-15b .	225
Figure S-33: ^1H - ^1H COSY (500 MHz, CDCl_3) Spectrum of II-15b .	226
Figure S-34: HSQC (^1H - ^{13}C) (125 MHz, CDCl_3) Spectrum of II-15b .	227
Figure S-35: ^1H NMR (500 MHz, CDCl_3) Spectrum of II-16a .	228
Figure S-36: ^{13}C DEPT (125 MHz, CDCl_3) Spectra of II-16a .	229
Figure S-37: ^1H - ^1H COSY (500 MHz, CDCl_3) Spectrum of II-16a .	230
Figure S-38: HSQC (^1H - ^{13}C) (125 MHz, CDCl_3) Spectrum of II-16a .	231
Figure S-39: ^1H NMR (500 MHz, CDCl_3) Spectrum of II-16b .	232
Figure S-40: ^{13}C DEPT (125 MHz, CDCl_3) Spectra of II-16b .	233
Figure S-41: ^1H - ^1H COSY (500 MHz, CDCl_3) Spectrum of II-16b .	234
Figure S-42: HSQC (^1H - ^{13}C) (125 MHz, CDCl_3) Spectrum of II-16b .	235
Figure S-43: ^1H NMR (500 MHz, CDCl_3) Spectrum of III-3a .	236
Figure S-44: ^{13}C NMR (125 MHz, CDCl_3) Spectrum of III-3b .	237
Figure S-45: ^1H NMR (500 MHz, CDCl_3) Spectrum of III-6b .	238
Figure S-46: ^{13}C NMR (125 MHz, CDCl_3) Spectrum of III-6b .	239
Figure S-47: ^1H NMR (500 MHz, CDCl_3) Spectrum of IV-3d .	240
Figure S-48: ^{13}C NMR (125 MHz, CDCl_3) Spectrum of IV-3d .	241
Figure S-49: ^1H NMR (500 MHz, CDCl_3) Spectrum of IV-3h .	242
Figure S-50: ^{13}C NMR (125 MHz, CDCl_3) Spectrum of IV-3h .	243
Figure S-51: ^1H NMR (500 MHz, CDCl_3) Spectrum of V-4 .	244
Figure S-52: ^{13}C DEPT (125 MHz, CDCl_3) Spectra of V-4 .	245
Figure S-53: ^1H NMR (500 MHz, CDCl_3) Spectrum of V-5 .	246
Figure S-54: ^{13}C DEPT (125 MHz, CDCl_3) Spectra of V-5 .	247
Figure S-55: ^1H NMR (500 MHz, CDCl_3) Spectrum of V-7 .	248
Figure S-56: ^{13}C DEPT (125 MHz, CDCl_3) Spectra of V-7 .	249
Figure S-57: ^1H NMR (500 MHz, CDCl_3) Spectrum of V-8 .	250
Figure S-58: ^{13}C DEPT (125 MHz, CDCl_3) Spectra of V-8 .	251
Figure S-59: ^1H NMR (500 MHz, CDCl_3) Spectrum of V-11 .	252
Figure S-60: ^{13}C DEPT (125 MHz, CDCl_3) Spectra of V-11 .	253
Figure S-61: ^1H NMR (500 MHz, CDCl_3) Spectrum of V-12 .	254
Figure S-62: ^{13}C DEPT (125 MHz, CDCl_3) Spectra of V-12 .	255
Figure S-63: ^1H NMR (500 MHz, CDCl_3) Spectrum of V-13 .	256

Figure S-64: ^{13}C DEPT (125 MHz, CDCl_3) Spectra of V-13 .	257
Figure S-65: ^1H NMR (500 MHz, CDCl_3) Spectrum of V-14 .	258
Figure S-66: ^{13}C DEPT (125 MHz, CDCl_3) Spectra of V-14 .	259
Figure S-67: ^1H NMR (500 MHz, CDCl_3) Spectrum of V-15 .	260
Figure S-68: ^{13}C DEPT (125 MHz, CDCl_3) Spectra of V-15 .	261
Figure S-69: ^1H NMR (500 MHz, CDCl_3) Spectrum of V-19 .	262
Figure S-70: ^{13}C DEPT (125 MHz, CDCl_3) Spectra of V-19 .	263
Figure S-71: ^1H NMR (500 MHz, CDCl_3) Spectrum of V-20 .	264
Figure S-72: ^{13}C DEPT (125 MHz, CDCl_3) Spectra of V-20 .	265
Figure S-73: ^1H NMR (500 MHz, CDCl_3) Spectrum of V-22 .	266
Figure S-74: ^{13}C DEPT (125 MHz, CDCl_3) Spectra of V-22 .	267

Introduction

1.1. CHIRALITY, CHIRAL COMPOUNDS AND ENANTIOMERS

The importance of chirality is now well recognized in connection with physiological and pharmaceutical properties of natural and artificial organic compounds. Chirality [1] is the property of a molecule which is generated due to the asymmetry in its chemical structure arising from different spatial arrangements of atoms or groups around the asymmetric center. On molecular level, chirality is an intrinsic property of the “building blocks of life,” such as amino acids and sugars, and therefore, of peptides, proteins and polysaccharides. A molecule that is not identical to its mirror image, although the two have identical composition and same connectivity of atoms, is asymmetric and named chiral. Such non-identical pairs of molecular mirror images are called enantiomers and are related to each other in the same way as our left and right hands. Enantiomers have identical physical and chemical properties, but differ when they are placed in a chiral environment, e.g., when interacting with other chiral compounds or when subjected to plane-polarized light. A 50/50 mixture of enantiomers is called a racemic mixture or a racemate. The molecule and its mirror image are not superimposable with each other and thus are enantiomers (Figure 1).

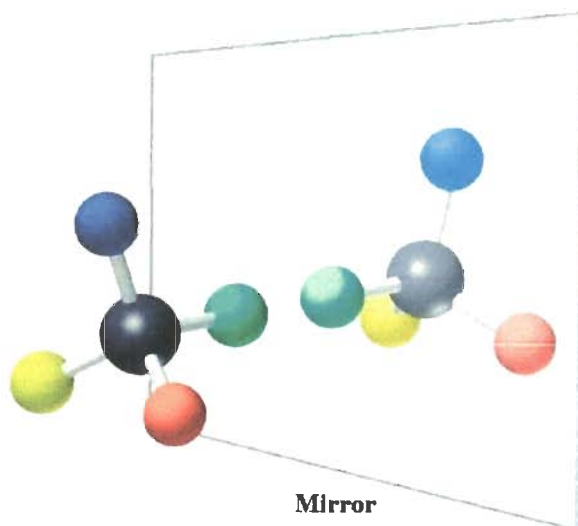


Figure 1: Chiral molecule containing a tetrahedral stereocenter.

Most of the commercial drugs exist in stereoisomeric forms. Many drugs developed from organic synthesis are still administered as a racemic mixture which may even disturb biological processes and may cause several other side effects. Therefore, enantioselective analysis of compounds containing one or more stereogenic centers is extremely important in medicinal [2], pharmaceutical, agricultural, environmental and food chemistry. Some examples of the variation of biological activities of various enantiomeric pairs are shown in Figure 2. The most infamous example of an enantiomeric drug having unwanted side effects is thalidomide. Thalidomide was prescribed in the 1960's to relieve pregnant women of symptoms associated with morning sickness. The (*R*)-enantiomer was effective in combating morning sickness. However, the (*S*)-enantiomer caused serious birth defects in children. This is an example of how important it is to identify and separate harmful stereoisomers for biological applications.

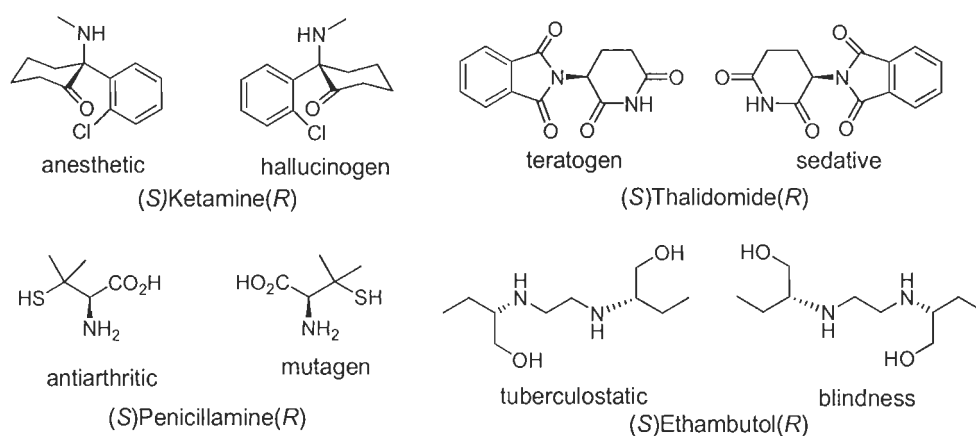


Figure 2: Examples of enantiomers with different biological effects.

The development of methods for obtaining enantiomerically enriched molecules has become one of the most important goals in the fields of organic and bioorganic chemistry. The importance of enantiomerically pure molecules stems from the central role of enantiomer recognition in biological activity. The dependence of biological activity of several chemical products on the enantiomeric purity of several pharmaceutical molecules has led chemists to investigate a variety of approaches to such a sort of molecules. Consequently, a number of chiral reagents, chiral catalysts and synthetic strategies have been developed for the synthesis of optically active molecules. One field of particular prominence in asymmetric synthesis is asymmetric catalysis, including both enzyme and transition metal catalysis.

1.2. ASYMMETRIC SYNTHESIS

Asymmetric synthesis, in which a chiral organic molecule catalyzes an enantioselective transformation, is an exciting and rapidly developing field. Over the past decades, asymmetric synthesis has been developed rapidly and extensively to provide enantiomerically enriched products. Since the importance of spatial arrangement within molecule to the fundamental properties of the substance was recognized, enantioselective synthesis has become most important in various domains such as synthetic organic chemistry, medicinal chemistry [3], agricultural chemistry, biological and natural products chemistry [4-8] and pharmaceutical industries [9-11]. There are several routes for asymmetric synthesis. Of particular importance is the enantioselective catalysis, which is one of the most efficient processes in terms of chirality, economy and environmental benignity [11-13].

Historically, enantiomerically enriched compounds were generated either by chemical transformation of an enantiomerically enriched precursor, often derived directly or indirectly from nature's chiral pool, or by resolving an equimolar (racemic) mixture of the two enantiomers. Both of these approaches suffer from potentially severe drawbacks, the former in requiring stoichiometric amounts of a suitable precursor and the latter in typically yielding only up to 50% of the desired enantiomer. Asymmetric synthesis, in which each molecule of chiral catalyst, by virtue of being continually regenerated, can yield many molecules of chiral product, has significant potential advantages over these older procedures [Figure 3].

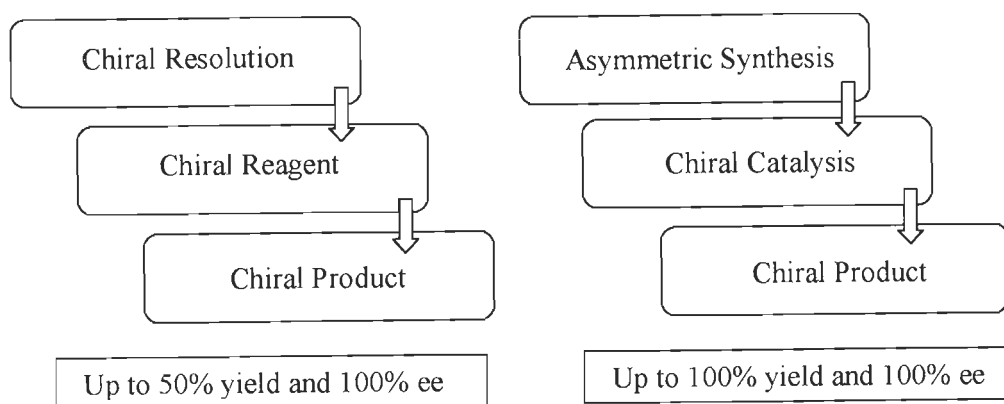


Figure 3: Enantioselective synthesis.

New catalytic asymmetric reactions give us the opportunities to develop more efficient methods for the synthesis of various highly potent chiral compounds, with successful applications for the synthesis of various complex natural products as well as industrial production. As mentioned above, asymmetric synthesis involves the synthesis of enantiomerically enriched compounds starting from prochiral substrates by using efficient chiral catalysts or chiral auxiliaries. The catalytic reactions have been rapidly emerging since a smaller amount of chiral material is sufficient unlike mole-for-mole use of chiral material required for chiral auxiliary-based reactions. Therefore, a large quantity of naturally and unnaturally occurring chiral materials are directly obtained through asymmetric catalysis with no need for further manipulation for removal and recovery of the chiral auxiliary. However, in catalytic approach, catalytic amount of small organic molecules or chiral metal complexes is employed in reaction followed by the regeneration in parallel catalytic cycle for further use. Though, metal catalysts have significant advantages in asymmetric synthesis over the organic molecules as wide substrate scope with catalytic activity, they offer some troubles also such as potential heavy metals high price, toxicity, pollution, waste treatment, *etc.* On the other hand, metal free organocatalytic reactions unlike metal-ligand complexes, generally tolerate aerobic conditions and do not require rigorous exclusion of water. They enjoy a broad spectrum of substrates than enzymes and can be used in various organic solvents (Figure 4).

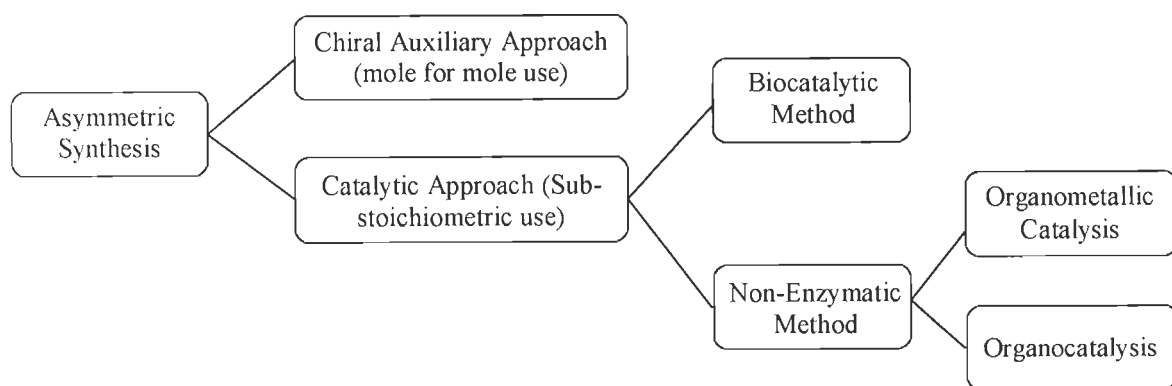


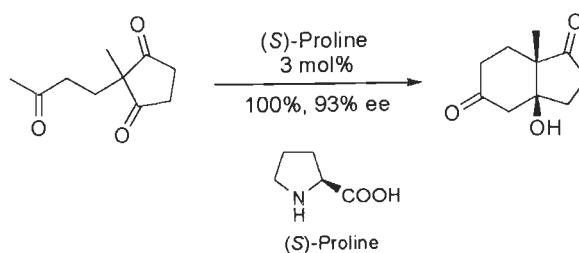
Figure 4: Classification of asymmetric synthesis.

There are certain limitations for asymmetric transformations especially for catalytic asymmetric carbon-carbon bond forming reactions such as substrate generality, catalyst efficiency, enantioselectivity, chemical yield, and reliability when applied to a large scale.

1.3. ORGANOCATALYSIS

The development of enantioselective organocatalysts is one of the most challenging and formidable endeavors in modern science and technology. Until a few years ago, it was generally accepted that transition metal complexes [14] and enzymes were the two main classes of very efficient asymmetric catalysts. A change in perception occurred during the last few years when several reports confirmed that relatively simple organic molecules could be highly effective and remarkable enantioselective catalysts for a variety of fundamentally important organic transformations [11-23]. Thus organocatalysis is an approach catalyzed by small chiral organic molecules to synthesize the enantiomerically pure compounds. These small chiral molecules are known as organocatalysts. These are low-molecular weight organic compounds composed of carbon, hydrogen, nitrogen, sulfur and phosphorous without having any metal atom. Generally these are nontoxic, inexpensive and readily available catalysts. These novel asymmetric catalysts are widely employed in phase transfer catalysis, kinetic resolutions as well as in a variety of asymmetric synthesis. In recent years it has been established that small organic molecules, in addition to metal complexes and biocatalysts, can be highly selective and efficient catalysts.

In 1971, a landmark publication on asymmetric organocatalysis emerged from literature from Hajos-Parrish-Eder-Sauer-Wiechert demonstrating for the first time that asymmetry could be induced in a Robinson-type annulation using a meso-triketone and simply adding a catalytic amount of D- or L-proline (Scheme 1) [15,16]. Later on the discoveries from the laboratories of MacMillan [17], List [18], and Jørgensen [19] have established asymmetric organocatalysis using naturally available amino acid L-proline and its derivatives and related amines.



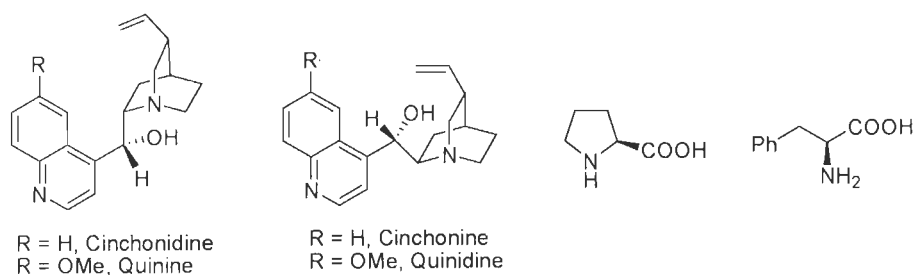
Scheme 1: Hajos-Parrish-Eder-Sauer-Wiechert Robinson annulation.

Proline is one of the most important and naturally occurring small amino acid molecules which was found to be efficient, and enantioselective organocatalyst. After obtaining successful

results from proline catalyzed asymmetric aldol reaction, the catalytic activity of proline was further extended to several other enantioselective transformations. An increased number of research groups have been attracted by the advantages of asymmetric organocatalysis. The recent past has seen tremendous development in this area as well [20-22]. Within a few years, powerful organocatalysts for a wide range of reactions have been designed and developed. Organocatalysis is gaining importance in asymmetric synthesis and has been proved highly selective and efficient chiral catalysts. Some examples of important organocatalysts based on natural compounds such as alkaloids, proline and related compounds are shown in Figure 5.

Most but not all organocatalysts can be classified as Lewis bases, Lewis acids, Brønsted bases and Brønsted acids. Lewis base activates the electrophilic substrates by nucleophilic addition to provide the intermediate which undergo a reaction to release the product and catalyst.

Natural organocatalysts



Synthetic organocatalysts

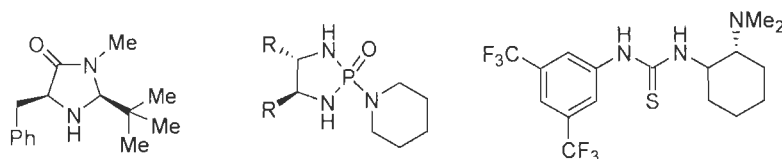


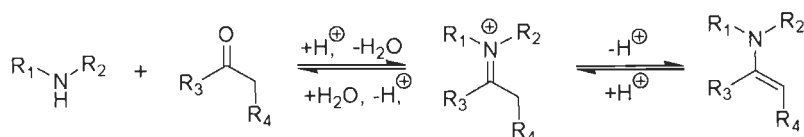
Figure 5: Examples of organocatalysts.

For further turnover and operates the reactions through enamine and iminium [23,24] mechanism and convert the substrates to activated nucleophiles or electrophiles. Lewis acids activate the nucleophilic substrates by electrophilic addition in the same manner. Brønsted bases and acids initiate the catalytic cycle *via* deprotonation and protonation, respectively.

1.3.1. Lewis bases as organocatalysts

1.3.1.1. Enamine catalysis

An enamine is an unsaturated compound derived by the reaction of an aldehyde or ketone with an amine followed by loss of H₂O. Enamines are among the most reactive neutral carbon nucleophiles, exhibiting rates that are even comparable to some charged nucleophiles, such as enolates [25,26]. Most enamines, unfortunately, are sensitive to hydrolysis. The parent



Scheme 2: Formation of enamine.

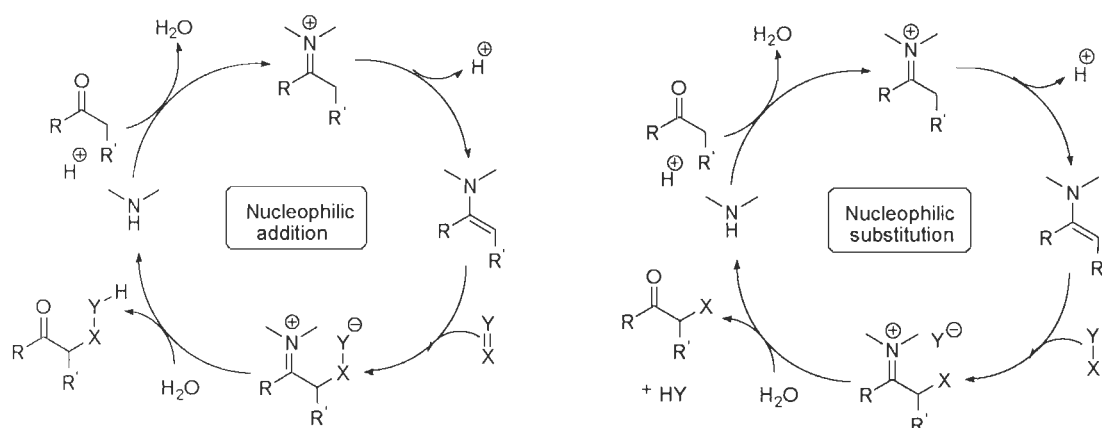
enamine, *N,N*-dimethylvinylamine was prepared but appeared to be unstable, but enamine of cyclic ketones and many aldehydes can readily be isolated. The utility of enamine as nucleophiles was believed to be diminished due to its instability but actually this property can be viewed as an added benefit. Enamines can be readily and rapidly generated catalytically by using a suitable amine and a carbonyl compound (Scheme 2).

Catalytic formation of enamine

The catalysis of primary and secondary amines of electrophilic substitution reactions in α -position of carbonyl compounds and related reactions *via* enamine intermediate is called enamine catalysis [27,28]. Stork did pioneer work in classical preformed enamine chemistry [29,30] proceed *via* addition or substitution route depending on the nature of the reaction partner (electrophile). Thus a vast array of transformations has been achieved *via* preformed enamine chemistry [25]. Therefore a catalytic version of this chemistry was highly desirable.

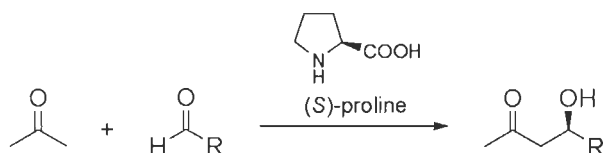
Recent years have witnessed an explosive growth, particularly, in the field of asymmetric enamine catalysis, and it became apparent that, in addition to being almost ideally atom and step economic, the scope of the catalytic version (Scheme 3) and its potential for enantioselective synthesis by far exceeds those of the stoichiometric approach. The basic for enamine catalysis is the reversibly generated enamine from a catalytic amount of an amine and a carbonyl compound. There are two modes of enamine catalysis nucleophilic addition reactions of double

bond containing electrophiles such as imine, aldehyde and Michael acceptor and nucleophilic substitution reactions of single bond containing electrophiles such as alkyl halides and lead to stoichiometric byproducts.



Scheme 3: Enamine catalysis.

The concept of enamine catalysis has three fundamental routes: (1) the stoichiometric chemistry of enamines as developed by Stork and others [29,30] used enamines as nucleophiles in organic synthesis. (2) Biological approach towards C-C bond formation *via* enamine catalysis. (3) The Hajos-Parrish-Eder-Sauer-Wiechert reaction, a proline-catalyzed aldol reaction that proceed *via* enamine intermediate although this reaction was discovered in early 1970's but the revival of this chemistry was initiated at the beginning of this century, with the discovery of the proline-catalyzed direct asymmetric intermolecular aldol reaction by List *et al.* (Scheme 4) [18].



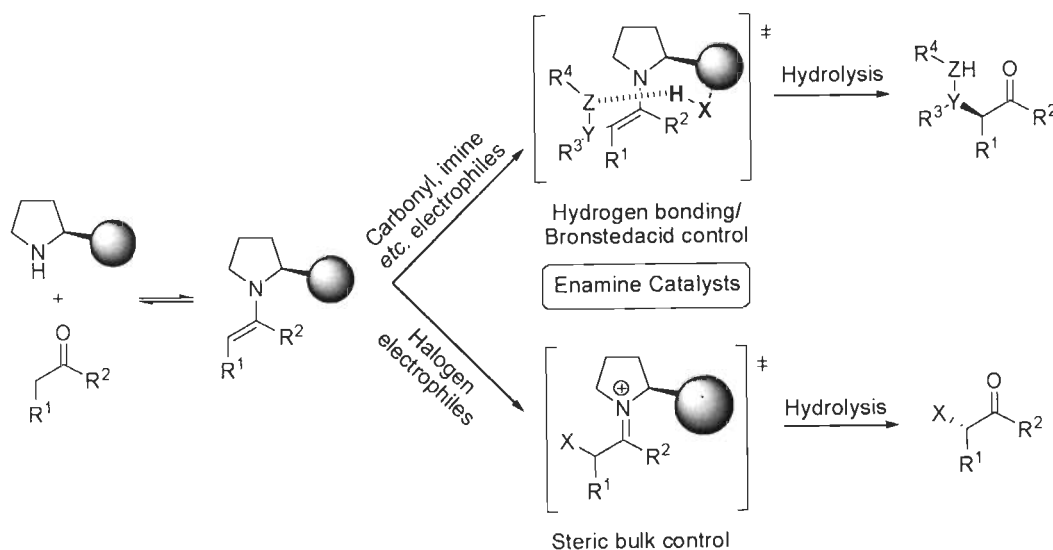
Scheme 4: Proline-catalyzed intermolecular aldol reaction.

Since then, the field of asymmetric organocatalysis and particularly, amine catalysis has unfurled at a breathtaking pace new catalysts are being designed, new reactions are being discovered and applied in asymmetric synthesis, and the mechanistic picture is becoming increasingly clear.

Generic modes of activation for enamine catalysis

In general, the most nucleophilic enamines are those where the nitrogen lone pair is most effectively delocalized. Most of the successful enamine catalysts are based on the pyrrolidine skeleton. This can be explained by the increased propensity of five-membered rings to accept sp^2 -hybridized atoms into the ring compared to the six-membered rings. In recent years, primary amines have also emerged as interesting alternatives to the cyclic amine catalysts.

In enantioselective enamine catalysis, the enamine can control the approach of the electrophile either by the steric bulk of the enamine or by directing the electrophile with an activating group. As for unreactive electrophiles, such as aldehydes, ketones or imines, additional assistance for catalysis can be provided by suitably positioned hydrogen bond donors and/or other acids. Mechanistically, enamine catalysis might be better described as bifunctional catalysis because the amine containing catalyst such as proline typically interacts with a ketone substrate to form an enamine intermediate but simultaneously engages with an electrophilic



Scheme 5: Hydrogen bonding control vs. steric control in enamine catalysis.

reaction partner either through hydrogen bonding or through electrostatic attraction. On the basis of these modes of activation enamine catalysts can be divided into two types (Scheme 5) [31].

(1) It includes an internal acid as cocatalyst/hydrogen bond donor to orient the approach of the electrophile. These are simple amino acids, such as proline and most of their derivatives such as tetrazole and various sulfonamides. These catalysts are typically used for aldol, Mannich, α -amination and α -oxygenation reactions where the electrophile can readily be activated by hydrogen bonding. (Figure 6) [20,21,27,28].

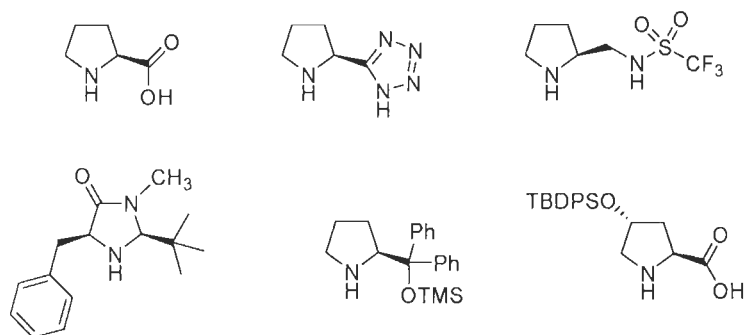
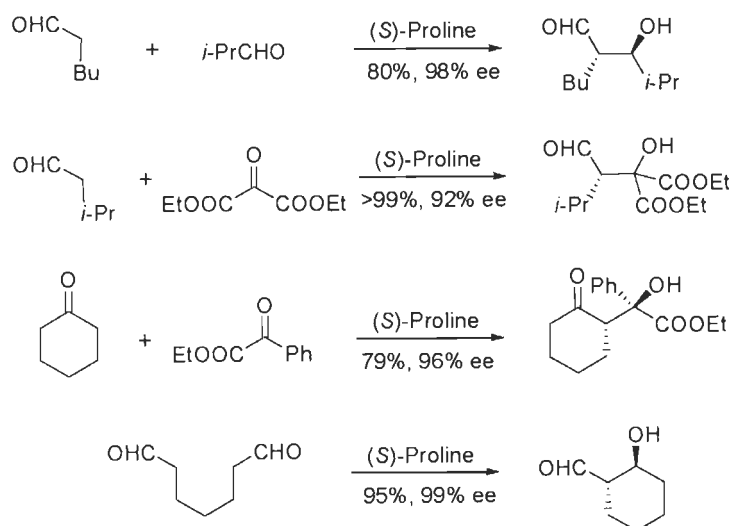


Figure 6: Selected examples of enamine catalysts.

(2) In these a bulky, nonacidic group is used to orient enamine and to block the approach of the electrophile from one side. These are recently developed and include the diarylprolinol ethers (developed by the Hayashi and Jørgensen groups) and its derivatives [32-36] as well as the MacMillan imidazolidinone catalysts (Figure 6) [37,38]. These modes of activation have now been used in a wide range of enantioselective carbonyl α -functionalization processes.

Aldol and related reactions

This is the addition of an enamine to a carbonyl compound and subsequent hydrolysis to generate aldol product. In this process one or two stereocenters are generated and one carbon-carbon bond formation occurs. The component that forms enamine is called aldol donor and the electrophilic component is known as aldol acceptor. Since 2000, significant development in the utility of the enamine-catalyzed aldol reaction has been made. This reaction has been extended to other substrate combinations (aldehyde to aldehyde, aldehyde to ketone, ketone to ketone) and to enolendo-enolexo aldolization [39-43] as depicted in Scheme 6.



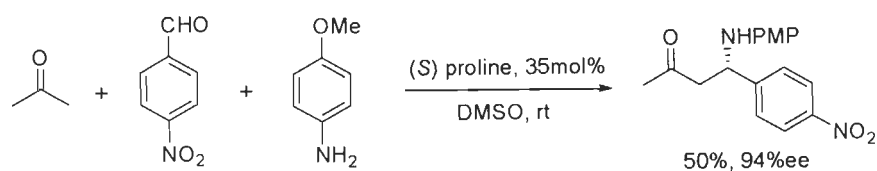
Scheme 6: Proline catalyzed aldol reactions.

Remarkable efforts have been made to develop more efficient variants of proline [18,44-49], and other amino acids and peptides bearing primary amino groups [50,51], chiral imidazolidinones cinchona alkaloid-derived amines [52] for the asymmetric aldol reactions as depicted in Figure 6.

Mannich type reactions

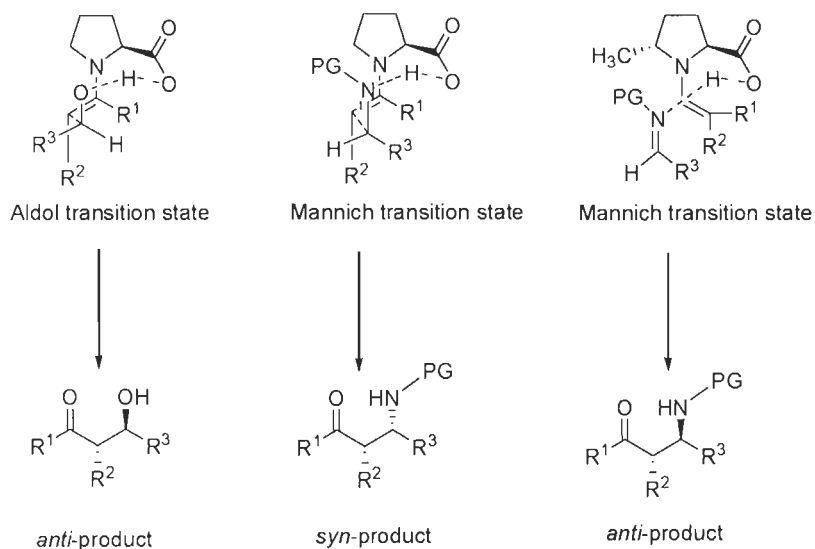
In enamine catalyzed aldol reaction, acceptor aldehyde adds to enamine resulting from the condensation of carbonyl group with amine catalyst followed by its reaction with to afford aldol product. However, in Mannich reaction, instead of aldehyde, imine is used as acceptor to provide β -amino carbonyl compound as Mannich product.

The first three-component asymmetric proline-catalyzed Mannich reactions between numerous cyclic and acyclic aliphatic ketones as donor and aromatic imines as acceptors *via*



Scheme 7: Direct three-component Mannich reaction.

enamine catalysis were reported by List in 2000 (Scheme 7) [53]. After that substrate scope has been expanded to donors such as heteroatom substituted ketones, cyclic ketones [54], and aldehydes [55,56] and *N*-Boc protected imine acceptors for Mannich reaction to afford Mannich product. In recent years, many other catalysts were also employed successfully for this transformation to afford Mannich products in high yields with excellent enantioselectivity.

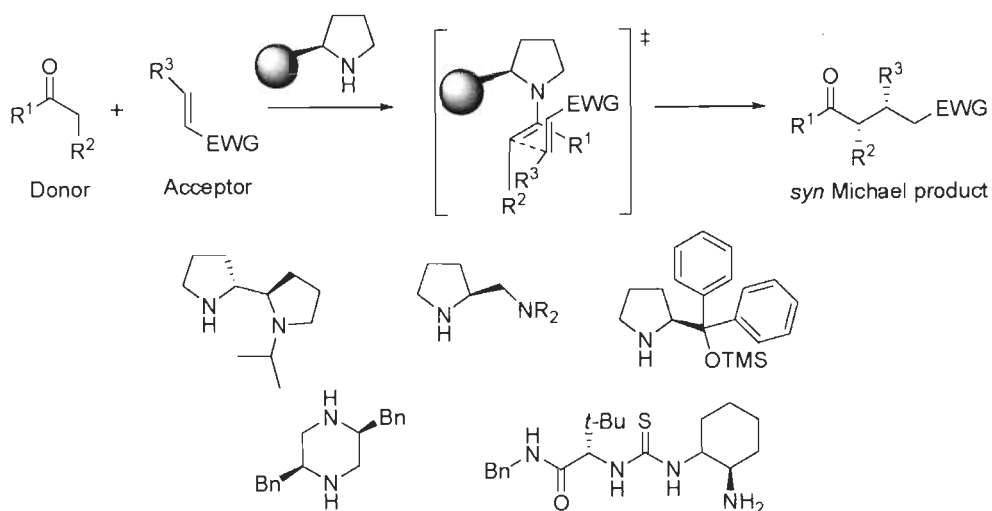


Scheme 8: Transition states in aldol and Mannich reaction.

In contrast to aldol adducts, Mannich products are usually *syn* selective. This may be attributed to the fact that larger size of imine acceptor forces the approach of imine and enamine in a manner different to that of aldehyde acceptor of enamine. These differences explain the reversal of selectivity in proline catalyzed aldol and Mannich reactions. By modification of the proline catalyst to it is also possible to obtain *anti* Mannich adducts [57]. An additional methyl group attached at 5th position of proline forces a specific enamine approach and the transition state which is now a 10-membered ring with addition in *anti* mode as shown in Scheme 8.

Conjugate addition reactions

Michael addition is the nucleophilic addition of enamine with α,β -unsaturated ketones, nitro and sulfonyl compounds [58-60]. Both aldehydes and ketones can be used as donors [61]. It belongs to the larger class of conjugate addition. This is an important atom-economical method for diastereoselective and enantioselective C-C bond formation. Initially, proline and its



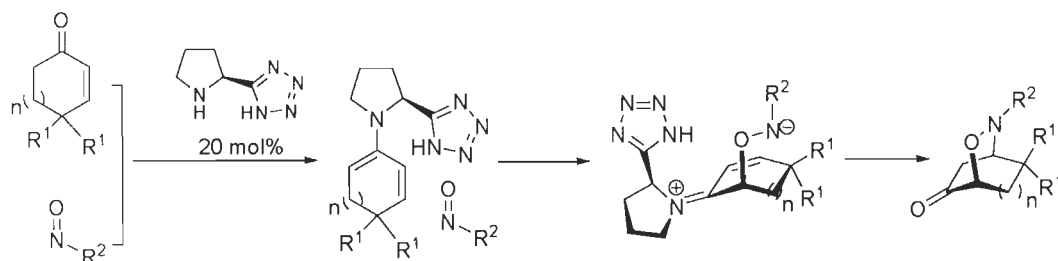
Scheme 9: Asymmetric enamine-catalyzed Michael additions with aldehyde donors.

analogues were used as chiral catalyst for conjugate reaction with modest results. However, in recent years many efficient catalysts consisting an additional hydrogen bond donor, such as thiourea moiety [62] or an acidic triflimide group [63], *etc.*, were developed for conjugate addition reactions. Conjugate addition of C-nucleophiles to a variety of α,β -unsaturated carbonyl compounds and to nitro olefins can currently be performed with readily available organocatalysts operating by intermediate formation of enamine or iminium ions as shown in Scheme 9.

Domino processes

Organic reactions are traditionally viewed as linear and stepwise processes in which isolation and purification of key intermediates often lead to reduced yields. Domino reactions, on the other hand, allow access to a myriad of complex molecules with high stereocontrol in an efficient, atom-economical manner. According to Tietze, a domino reaction is defined as a process in which two or more bond-forming transformations occur based on functionalities formed in the previous step. Furthermore, neither additional reagents, catalysts, and additives can be added to the reaction vessel, under unaltered reaction conditions [64]. Although several metal and enzyme catalyzed domino reactions are known, a few domino reactions have been catalyzed by chiral organic molecules [65,66].

Many recent synthetic efforts took advantage of the orthogonal modes of carbonyl activation in the context of a domino reaction. Amine catalysts activate carbonyls by the formation of an iminium ion or an enamine. Reaction of unsaturated iminium ions with nucleophiles provides enamine. On the contrary, enamine reacts with electrophiles to afford electrophilic iminium ions which readily react with nucleophiles. This dual nature of enamine-iminium catalysis leads to unique possibilities in domino processes. Many reports are available for the domino reactions using enamine catalysis [67-69].



Scheme 10: Domino *O*-nitroso aldol-conjugate addition.

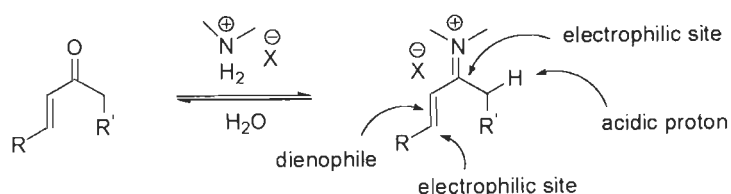
Yamamoto and coworkers published a highly enantioselective asymmetric domino process including *O*-nitroso aldol-conjugate addition sequence by using cyclic enones and aromatic nitroso compounds as shown in Scheme 10 [70].

The scope of enantioselective enamine catalysis has been expanded in scope more rapidly than perhaps any other field of asymmetric catalysis. Other important and remarkably useful enamine catalytic nucleophilic substitution reactions have been developed subsequently and include enantioselective α -chlorinations [71], α -fluorinations [72], α -brominations [73], α -iodinations and α -sulfonylations [74].

1.3.1.2. Iminium catalysis

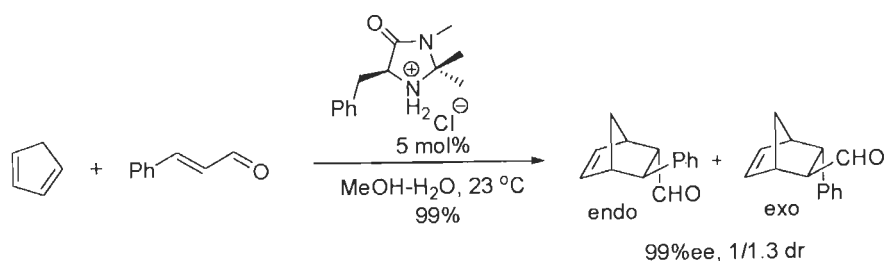
The condensation of aldehydes or ketones with amine catalysts forms a highly deficient iminium ion through reversible reaction. It should be emphasized that the activation provided by iminium ion formation is a common phenomenon, and many different types of nucleophile-electrophile interactions can be envisaged. This includes cycloadditions, nucleophilic additions, attacks by bases (resulting in deprotonation and enamine formation), and retroaldol type

processes such as decarboxylation. Iminium ion catalysis provides an organocatalytic alternative to conventional Brønsted and Lewis acid catalysis of α,β -unsaturated compounds (Figure 7). The operational simplicity of iminium catalysis makes them attractive alternatives to Lewis acid catalysis.



Scheme 11: Iminium catalysis.

Iminium-catalyzed cycloadditions were not discovered until the turn of the century. In 1976, Baum and Viehe reported that iminium salts provide significant acceleration in the Diels-Alder reaction [75]. However, it was not until 2000 that MacMillan and co-workers disclosed a more general catalysis strategy for the Diels-Alder reaction, using enantioselective iminium catalysis. They successfully employed chiral imidazolidinone catalyst for enantioselective Diels-Alder reaction of unsaturated aldehydes and ketones with diene (Scheme 12). Condensation of chiral imidazolidinone catalyst with an enal forms iminium ion. The LUMO of the iminium species is lowered in energy such that it can now interact with suitable coupling partner diene



Scheme 12: [4+2] Cycloaddition of α,β -unsaturated aldehyde.

leading to a Diels-Alder cycloaddition. The catalyst is designed in such a way that in the active species single iminium ion geometry is formed. The dimethyl substitution forces the bulk of the iminium ion away from this large group and a potential stabilization by a π -interaction with the benzyl group unit enforces this conformation and leads to high facial selectivity during attack on

the alkene. The reactions on the alkenyl portion of the iminium ion can be split into two types, cycloaddition processes and conjugate additions as shown in Figure 7.

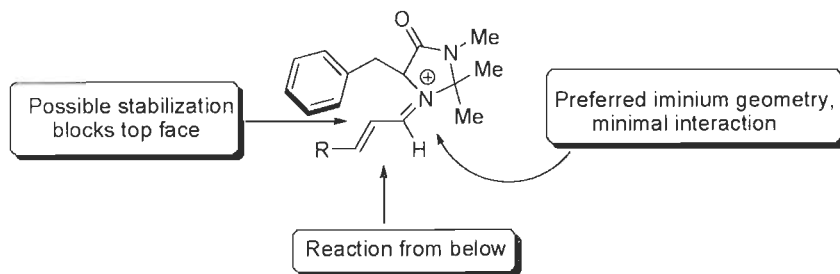
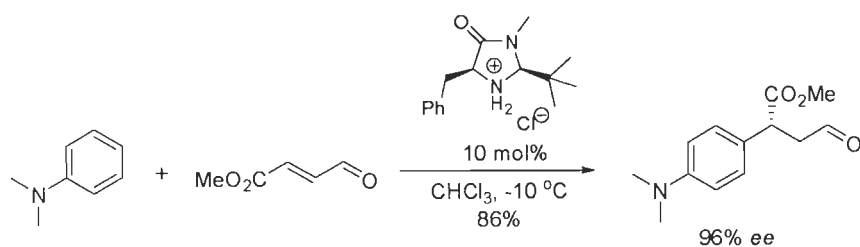


Figure 7: Stereocontrol elements in the iminium ion.

The concept of iminium catalysis has further been extended to other reactions of α,β -unsaturated aldehydes, such as [3+2] cycloaddition with nitrones (up to 98% yields, dr = 98 : 2, and 99% ee) [76,77], Friedel–Crafts alkylation with pyrroles [78], indoles [37] and benzenes (up to 97% yield and 99% ee) (Scheme 13) [79] and Mukaiyama–Michael reactions (up to 93% yield and 98% ee) [80] and Michael addition of malonates [81] and nitroalkanes [82] to enones using (*S*)-proline or a similar catalyst system. In all cases, high yields and enantioselectivities were achieved.

Other reactions that can be attained through iminium catalysis are the conventional [4+2], nitron [3+2], and [4+3] cycloadditions and 1,3-dipolar cycloadditions [76,83,84]. In addition, highly enantioselective epoxidations [85] and cyclopropanations [86] have been recently developed.

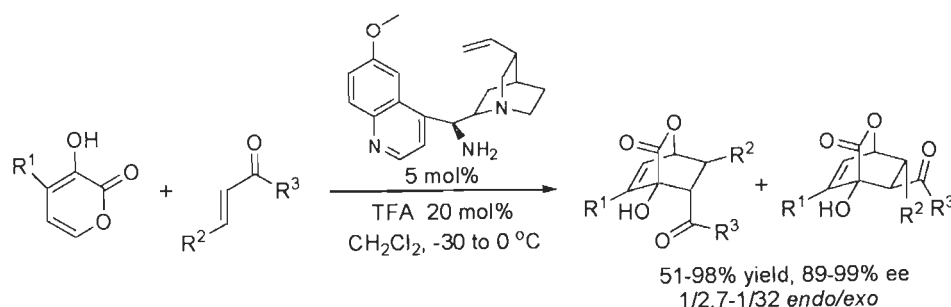


Scheme 13: Friedel–Crafts acylation reaction between α,β -unsaturated aldehyde and substituted benzene.

Cycloaddition reactions

(i) [4+2] Cycloaddition reactions

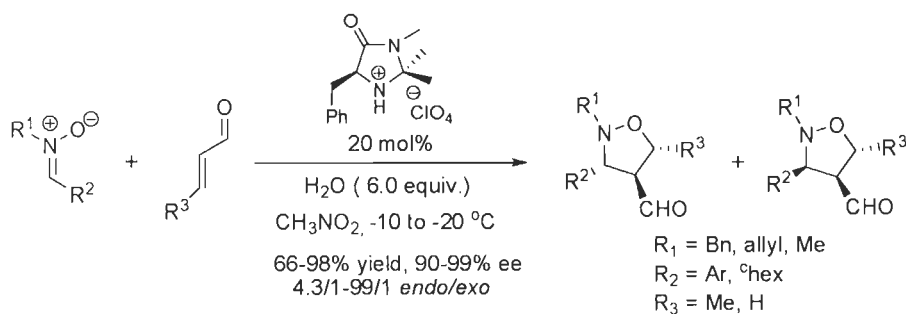
MacMillan *et al.* reported the first examples of [4+2] cycloaddition of α,β -unsaturated aldehydes and ketones with dienes using the chiral imidazolidinone catalyst [83]. Following this, numerous secondary amine organocatalysts as biaryl catalysts [87], diarylprolinol silyl ethers [88], hydrazide catalysts [89], and variants of imidazolidinone catalysts [90] have been used to catalyze this cycloaddition process. These catalysts yielded the Diels-Alder product with high chemical yields with high level of asymmetric induction. However, many primary amine containing organocatalysts as primary cinchona alkaloids [91] and binaphthyl catalysts [92] were also successfully employed for enantioselective [4+2] cycloaddition reactions as depicted in Scheme 14.



Scheme 14: [4+2] Cycloaddition of 3-hydroxypyrones and α,β -unsaturated ketones.

(ii) [3+2] Cycloaddition reactions

The [3+2] addition between enals and nitrones is another major class of organocatalytic cycloaddition. These cycloadditions produce valuable intermediates for the construction of biologically important amino acids, alkaloids, amino carbohydrates and β -lactams. MacMillan and co-workers reported the first examples of imidazolidinone catalyzed [3+2] cycloaddition (Scheme 15) between nitrones and α,β -unsaturated aldehydes in 2000 [76].



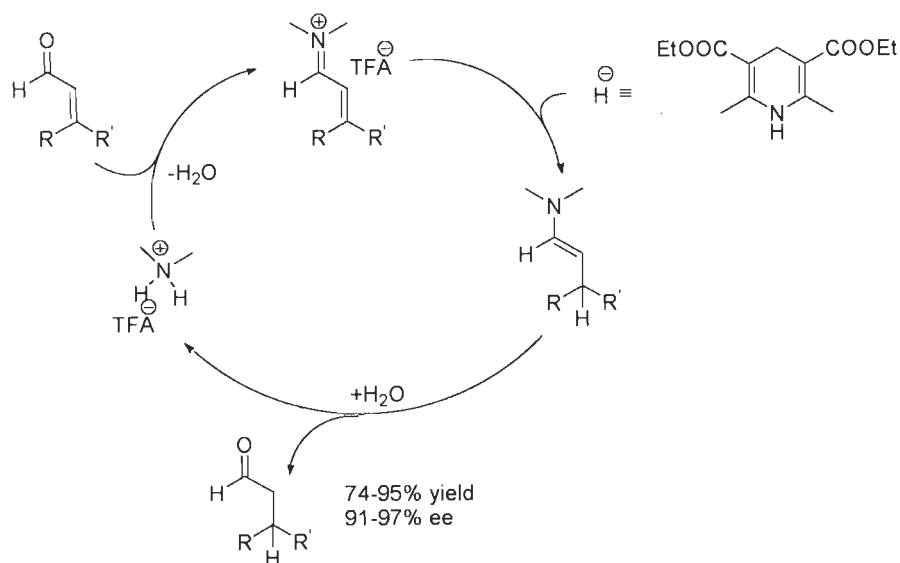
Scheme 15: [3+2] Cycloaddition using MacMillan imidazolidinone catalyst.

Later other catalysts such as hydrazides, prolinol derived catalysts [93], primary amine containing cinchona alkaloids [94] were also used for enantioselective [3+2] cycloaddition reactions.

Organocatalytic conjugate addition

These organocatalytic additions involve the attack of nucleophiles on electron deficient double and triple bonds generating one or more stereogenic centers, under the influence of an external chiral ligand or chiral catalyst. Enormous number of methods and catalysts has been developed for the addition of carbon-, nitrogen-, oxygen-, sulfur-, and hydride-based nucleophiles to α,β -unsaturated aldehydes and ketones *via* iminium ion activation. A range of aromatic, heteroaromatic and nonaromatic nucleophiles can be added to enals to form many functionalities that are common in pharmaceutical compounds. In particular, the indole and aniline motifs are readily incorporated into an asymmetric framework and modified to synthetically useful compounds [37,80]. For C-C bond formation reactions, nucleophiles can be divided into two classes: aryl, heteroaromatic and vinyl nucleophiles, which undergo Friedel-Crafts type alkylation and C-H acids such as 1,3-dicarbonyl compounds and nitroalkanes.

Yang *et al.*, in 2004 [95] reported the first metal free organocatalytic transfer hydrogenation of α,β -unsaturated aldehydes (Scheme 16). Dibenzylammonium trifluoroacetate was used as an efficient catalyst for this reaction. A variety of functional groups that are sensitive to standard hydrogenation conditions (nitro, nitrile, benzyloxy, and alkene functional groups) were tolerated in the process. On the basis of this protocol an example of asymmetric catalytic version was also presented. This protocol was subsequently optimized and a highly enantioselective



Scheme 16: Organocatalytic hydrogenation.

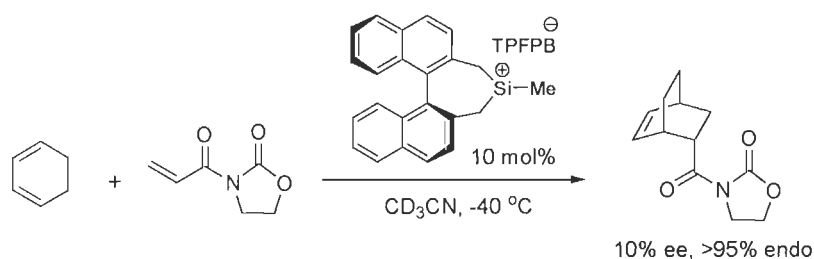
variant using the trichloroacetate salt of MacMillan's second generation imidazolidinone as the catalyst. Another concept introduced into the field of iminium ion activation is asymmetric counteranion-directed catalysis. For the introduction of asymmetry in transition metal, phase transfer and organocatalyzed processes, the use of non-reactive chiral anions as effective tools is receiving significant attention [96,97].

Iminium catalysis has now been an exciting and vibrant area of research in recent years. The catalysts are usually bench stable, robust, reliable and easily available and carried out the reactions at room temperature in the presence of moisture and air with high yield and optical purity. Additionally, iminium catalysis can be applied to tandem, cascade and multi-component coupling reactions for the formation of desired products from simple achiral precursors in a single step.

1.3.2. Lewis acids as organocatalysts

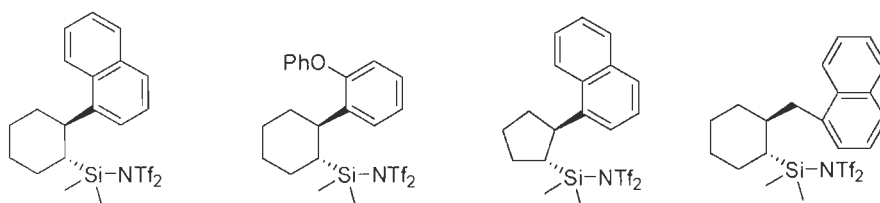
Generally metal salts like AlCl_3 , TiCl_3 , *etc.*, are referred to as Lewis acid catalysts. However, not only metal centers can function as Lewis acids. Carbenium, silyl or phosphonium cations and phosphorus- and hypervalent silicon-based compounds also display Lewis acid catalytic activity. A broad variety of reactions can be catalyzed with these Lewis acids. In 1998 Jørgenson and Helmchen reported the first binaphthyl derived chiral silyl cationic salt as

catalyst for enantioselective Diels-Alder reaction with 95% yield and *endo* selective was higher than 95%, though the enantioselectivity of the reaction was very low (10%) (Scheme 17) [98]. Since silyl cations are highly reactive and moisture sensitive so they were prepared *in situ* from air and moisture stable precursor *via* hydride transfer [99,100].



Scheme 17: Diels-Alder reaction catalyzed by chiral silyl salt.

Later Jonas, Ghosez and coworkers have reported several enantiopure cycloalkylsilyl triflimides as silicon containing chiral molecules as depicted in Scheme 18 and tested in the Diels-Alder reaction of methyl acrylate and cyclopentadiene [101, 102].



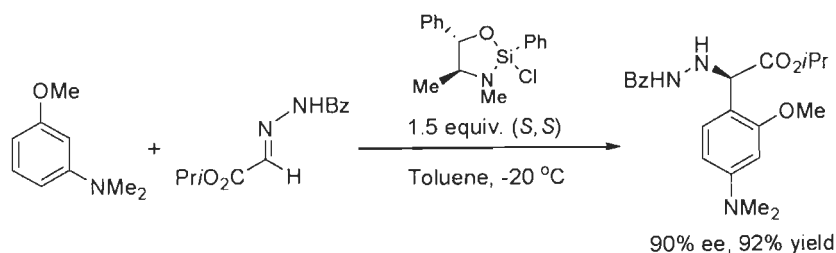
Scheme 18: Cycloalkylsilyl triflimides.

Another example of Lewis acid catalysts is hypervalent silicon-based catalysts. Hypervalent silanes are crucial intermediates in silicon-based carbon-carbon bond-forming reactions. Chemistry of penta and/or hexavalent silicon compounds has recently attracted much attention because of the possibility to develop organocatalyzed enantioselective reactions in the presence of cheap, low toxic and environmental friendly species such as hypervalent silicates. Recently Leighton *et al.* have discovered simple hypervalent chiral silane Lewis acid, synthesized in a single step from enantiopure pseudoephedrine and phenyltrichlorosilane [103]. They employed successfully this catalyst in Friedel-Crafts alkylation with benzoylhydrazones and obtained 90% yield and up to 90% enantioselectivity (Scheme 19). By inspiring these

results, they reported enantioselective [3+2] cycloaddition reactions catalyzed by the same catalyst with improved diastereo- and enantio-selectivity of the corresponding products [104].

The other class of Lewis acid-based organocatalysts is phosphonium and carbocation based catalysts. A series of different phosphonium salts, prepared from hydroxyl phosphine oxides or phosphinates are known and investigated for Diels-Alder reaction between cyclopentadiene and α,β -unsaturated ketones [105]. Carbocations are highly active catalysts. A group at Merck developed the first efficient chiral phase-transfer catalyst, *N*-benzylcinchoninium salt for the asymmetric α -methylation of indanone in 95% yield and 92% ee [106].

The other types of Lewis acid chiral catalysts include the ionic liquids and organic salts. Nevertheless, due to the broad variety of possible reactions, which are catalyzed by Lewis acids, this research field possesses a large potential, still improvement and further investigation for asymmetric induction of the reactions is needed.

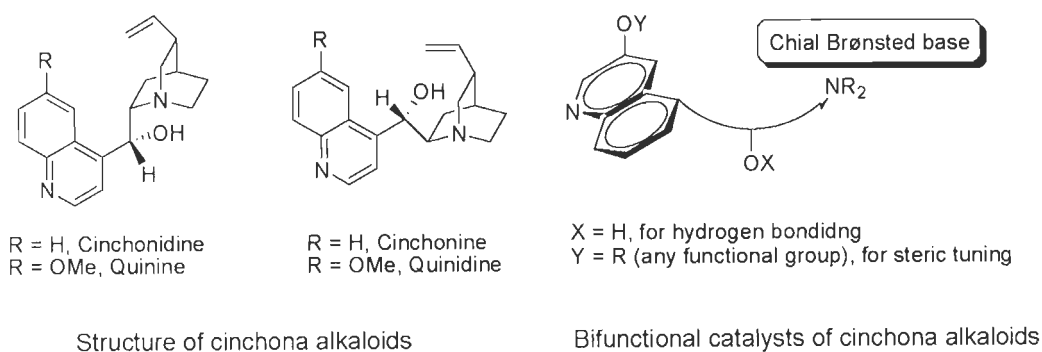


Scheme 19: Enantioselective Friedel-Crafts alkylation.

1.3.3. Brønsted bases as organocatalysts

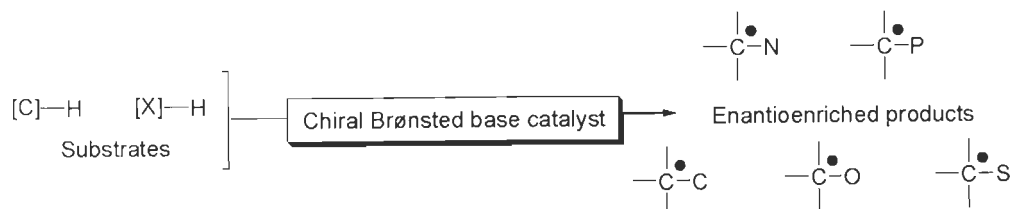
Chiral, metal-free Brønsted bases have been demonstrated capable of catalyzing several types of C–C and C–X bond-forming reactions with high chemical and stereochemical efficiency, thereby complementing other major organocatalytic asymmetric approaches such as enamine catalysis. Bifunctional catalysts, containing both Brønsted base and H-activating functionalities, have proven to be very applicable to an array of reactions type. The chiral Brønsted base catalysis has been upright with the recognition of cinchona alkaloids as excellent chiral catalysts [107]. Later, the study on the importance of a rigid backbone with basic functionality and the absence or presence of a hydrogen-bond donor within same molecule led to the synthesis of novel cinchona alkaloid-based catalysts broadened the scope of their utility.

Cinchona alkaloids, acting as a bifunctional organocatalyst (Scheme 20) or ligand, are key contributors in asymmetric reactions and enantioselective transformations of conjugate additions subdivided into substrate categories of enones, imines, azodicarboxylates, nitroalkenes, sulfones and α -ketoesters (Strecker, Michael, Mannich, Aldol, Baylis–Hillman and Henry reactions) and



Scheme 20: Cinchona alkaloids as organocatalysts.

cycloaddition reactions, phase-transfer reactions, β -lactone synthesis, aziridination, desymmetrization studies, decarboxylations, epoxidation and hydrogenations [108]. Other examples of the catalysts include cinchona alkaloid-derived thiourea catalysts, chiral guanidine catalysts, chiral cyclohexane-diamine catalysts, chiral binaphthyl-derived amines, *etc.*

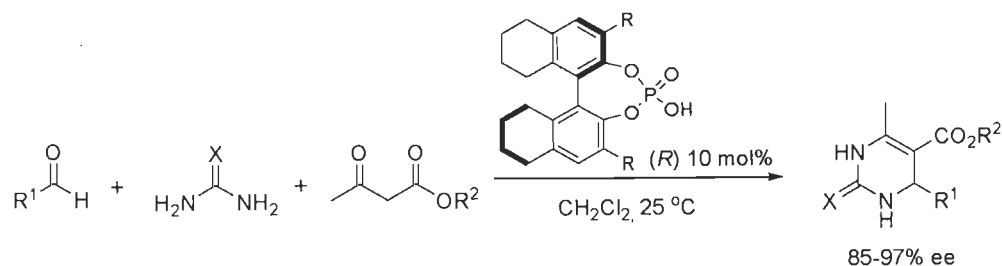


Scheme 21: Different conjugate addition of cinchona alkaloids.

1.3.4. Brønsted acids as organocatalysts

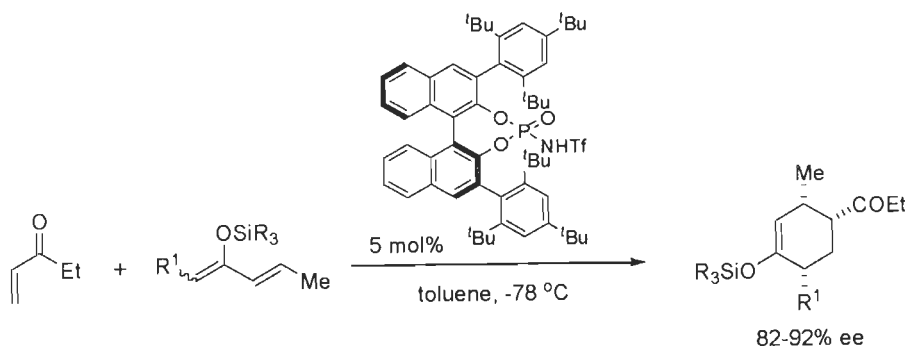
Chiral Brønsted acids have emerged as a new class of organocatalysts over the last few years. The field of asymmetric Brønsted acid catalysis can be divided into general acid catalysis and specific acid catalysis. In general in acid catalysis substrate is activated *via* hydrogen bonding whereas in specific acid catalysis substrate is activated *via* protonation. Since 2004 after the pioneering studies of the groups of Akiyama and Terada [109,110] on chiral BINOL

phosphates as powerful Brønsted acid catalysts in asymmetric Mannich-type reactions, numerous imine activated catalytic asymmetric transformations have been studied by means of this catalyst class, including among others Pictet–Spengler, Friedel–Crafts, Strecker, cycloaddition reactions, transfer hydrogenations, and reductive aminations. More recently, in 2006, Gong



Scheme 22: Biginelli reaction: scope and proposed reaction pathway.

and coworkers [111] described the first highly enantioselective organocatalytic Biginelli reaction (Scheme 22) by using chiral BINOL phosphates. Recently several research groups reported on the use of chiral BINOL phosphates as Brønsted acids in numerous multicomponent and cascade reactions.



Scheme 23: Diels-Alder reaction of ethyl vinyl ketone with silyloxydienes.

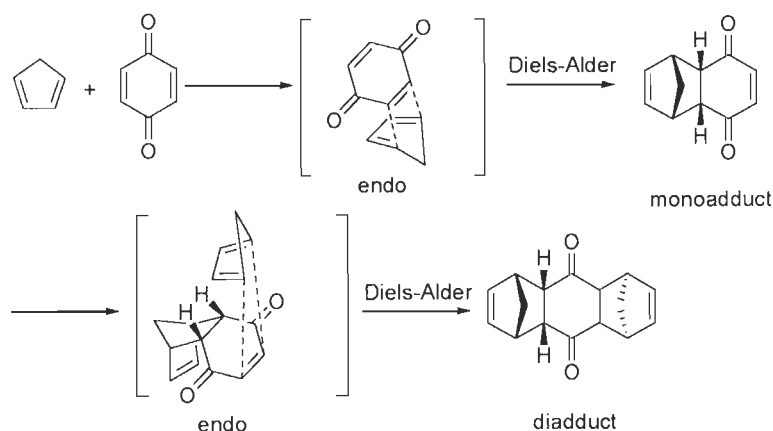
Imines are the reactive substrates for Brønsted acid catalysis. In 2006 with the introduction of chiral BINOL-derived *N*-triflylphosphoramidates for Diels-Alder reaction of α,β -unsaturated ketones with silyloxydienes as depicted in Scheme 23 [112], asymmetric Brønsted acid catalysis is not restricted to reactive substrates. Electron-rich alkenes (enecarbamates, enamides), aziridines and certain carbonyl compounds can be activated through these stronger Brønsted acid catalysts. In dealing with sensitive substrate classes, chiral dicarboxylic acids proved of particular value. Thus, chiral Brønsted acid catalysis is a rising field within the

domain of asymmetric organocatalysis and the introduction of stronger chiral Brønsted acid provides more opportunities to develop a variety of asymmetric transformations.

In summary, enantioselective organocatalysis has a major role in organic synthesis since a decade and helped in the development of numerous enantioselective catalytic reactions. At the same time, use of newly synthesized organocatalysts will bring new magnitude of developments in the field of asymmetric synthesis.

1.4. *p*-BENZOQUINONES IN ORGANIC SYNTHESIS

The Diels-Alder reaction is one of the most versatile and synthetically useful reactions due to its inherent potential to generate up to four new stereogenic centers besides forming two new carbon-carbon/carbon-heteroatom/heteroatom-heteroatom bonds in a single laboratory operation [113-115]. The utility of this cycloaddition arises from its versatility and remarkable selectivity for constructing simple and complex molecules. The landmark 1928 paper by Diels

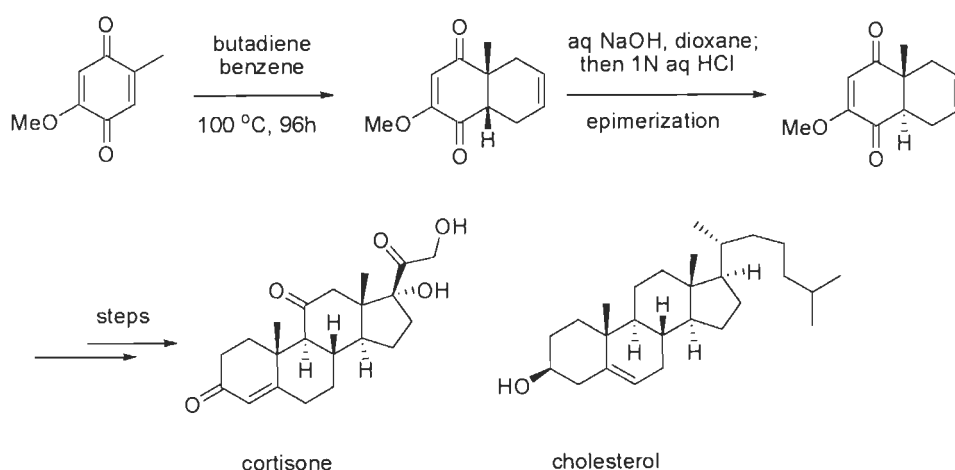


Scheme 24: The Diels-Alder reaction between cyclopentadiene and *p*-benzoquinone.

and Alder on the discovery of [4+2] cycloaddition describes proper identification of products formed during the reaction between cyclopentadiene and *p*-benzoquinone which is considered to be a historical event in the field of chemistry [116].

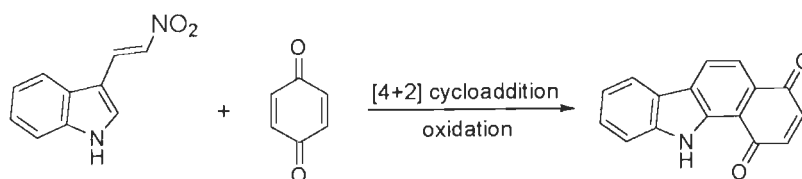
p-Benzoquinones are powerful intermediates in organic synthesis. Due to their high electron-deficiency, these cross-conjugated dienones undergo reactions with wide variety of reaction partners including electron-rich species. For more than seven decades, the Diels-Alder reaction of dienophilic quinones has provided a powerful construction for functionalized *cis*-

fused decalin sub-structures. Several syntheses of complex natural products have been uncovered in which the quinone Diels-Alder reaction has been used to incorporate an initial arrangement of rings and stereocenters giving the way for expansion of the final target structure by a series of selective reactions thereafter. Some of the most prominent achievements in complicated synthetic chemistry are the total syntheses of steroids, reserpine, ibogamine, dendrobine, gibberellic acid, trichodermol, and euonyminol [117].



Scheme 25: The Diels-Alder reaction as a key-step in the total synthesis of steroid hormones cortisone and cholesterol.

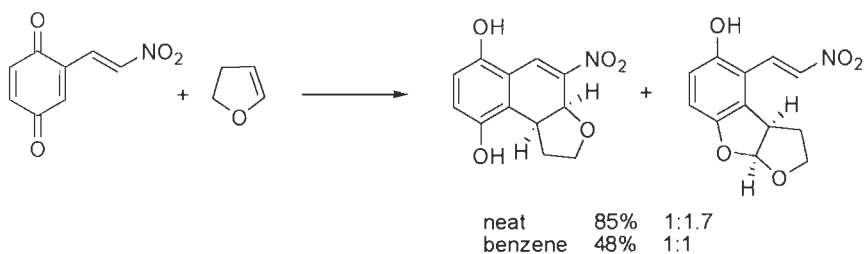
The normal electron demand [4+2] cycloadditions of 3-(2-nitrovinyl)indoles with parent *p*-benzoquinone producing benzo[*a*]carbazole-1,4-diones was reported (Scheme 26). The 3-alkenyl indole derivative participated as diene in this Diels-Alder reaction [118].



Scheme 26: The [4+2] cycloaddition between alkenylindoles and *p*-benzoquinone.

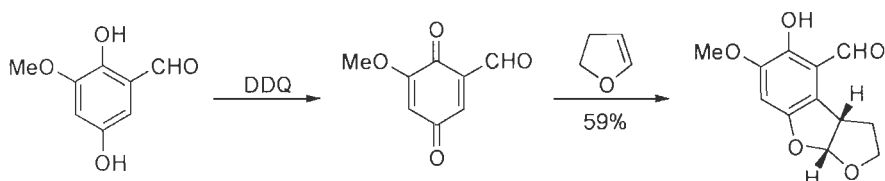
The reaction of 2,3-dihydrofuran with β -nitroalkenyl-1,4-benzoquinone afforded a mixture of two products resulted from [4+2] cycloaddition and subsequent conjugate addition of

enol ether followed by tautomerization to a phenolic nucleophile and ring closure [119]. The product distribution depends on the reaction conditions (Scheme 27).



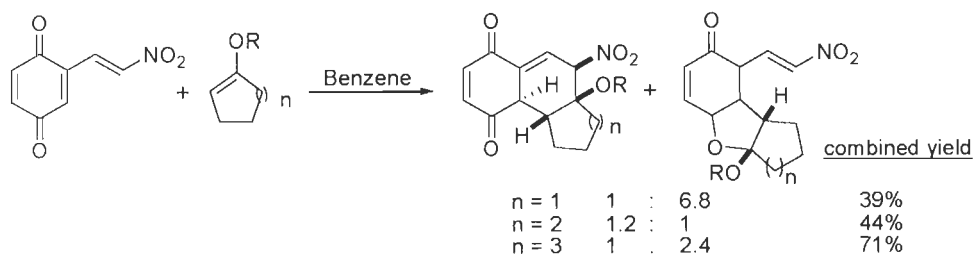
Scheme 27: The [4+2] cycloaddition between alkenyl-1,4-benzoquinone and 2,3-dihydrofuran.

Noland and Kedrowski studied the reaction between substituted *p*-benzoquinones and 2,3-dihydrofuran for the synthesis of furobenzofuran ring systems [120]. The *in situ* generated 2-formyl-6-methoxy-1,4-benzoquinone on treatment with dihydrofuran furnished the substituted furobenzofuran derivative *via* [3+2] cycloaddition to O-4 and C-3 of the quinone in good yield (Scheme 28).



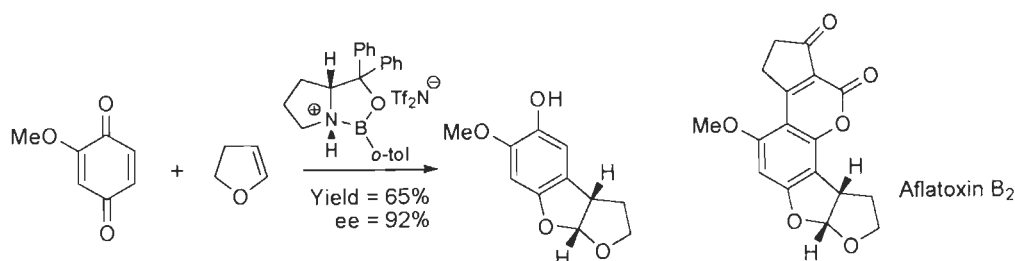
Scheme 28: Reaction between substituted *p*-benzoquinone and 2,3-dihydrofuran.

The reactions of β -nitroalkenyl-1,4-benzoquinone was also studied with cyclic enol ethers [121]. The reaction proceeded to furnish a mixture of carbocyclic and benzofuran derivatives in varied ratio in moderate to good combined yields (Scheme 29).



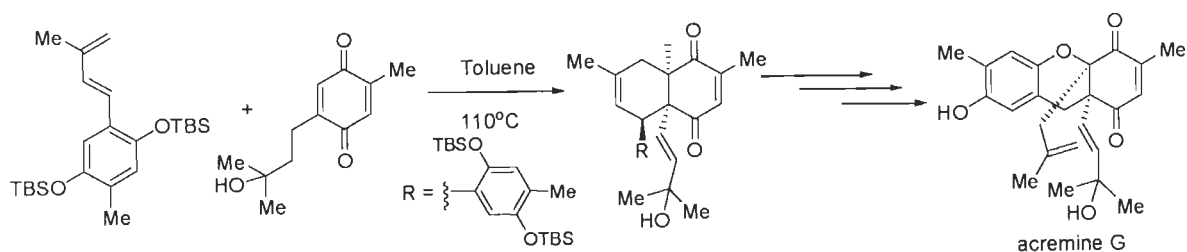
Scheme 29: Reaction between alkenyl-1,4-benzoquinone and cyclic enol ethers.

Several *p*-benzoquinone derivatives were used as dienophiles in enantioselective Diels-Alder reaction catalyzed by chiral oxazaborolidinium ions in early key steps for the total syntheses of complex natural products [122]. Recently Zhou and Corey reported the usefulness of asymmetric [3+2] cycloaddition step between 2-methoxy-1,4-benzoquinone and 2,3-dihydrofuran as a key step in the enantioselective total synthesis of the potent naturally occurring mutagen aflatoxin B₂ [123]. A chiral oxazaborolidinium ion derived from α,α -diphenylprolinol catalyzed the [3+2] cycloaddition of *p*-benzoquinone derivative and dihydrofuran to furnish furobenzofuran derivative by conjugate addition of enol ether followed by tautomerization to a phenolic nucleophile and subsequent ring closure (Scheme 30).



Scheme 30: Chiral oxazaborolidinium ion mediated enantioselective [3+2] cycloaddition between 2-methoxy-1,4-benzoquinone and 2,3-dihydrofuran.

An alkenyl *p*-benzoquinone derivative was used as a dienophile in the highly selective Diels-Alder reaction step for a biomimetic synthesis of dimeric *Acremonium byssoides* metabolite acremine G [124]. The cycloaddition was carried out at reflux temperature in toluene to provide *endo* product as major adduct (Scheme 31).



Scheme 31: The Diels-Alder reaction as a key-step in the total synthesis of dimeric metabolite acremine G.

In conclusion, *p*-benzoquinones are versatile intermediates in organic synthesis. These cross-conjugated diene-diones and their alkenyl derivatives undergo useful cycloaddition reactions to generate complex molecular architectures. The domino processes of these alkenyl-1,4-benzoquinones with suitable reacting partners would unravel the rapid synthesis of compounds of molecular complexity with profound selectivity.

Chapter-1

INTRODUCTION

1.5. REFERENCES

- 1 G.H. Wagnière, *On Chirality and the Universal Asymmetry: Reflection Image and Mirror Image*, Wiley-VCH: Weinheim, 2007.
- 2 E. Francotte, W. Lindner, *Chirality in Drug Research*, Wiley-VCH: Weinheim, 2006.
- 3 J.K. Khalaf, A. Datta, A Concise, *Asymmetric Synthesis of (2R,3R)-3-Hydroxyaspartic Acid*, *Amino Acids* 35 (2008) 507.
- 4 A.M. Gómez, A. Barrio, A. Pedregosa, S. Valverde, J.C. López, *Three-Component Assembly of Amines, Boronic Acids, and a Polyfunctionalized Furanose: A Concise Entry to Furanose-Based Carbohydrate Template*, *J. Org. Chem.* 74 (2009) 6323.
- 5 V. Kumar, N.G. Ramesh, *A Versatile Strategy for the Synthesis of N-linked Glycoamino- Acids from Glycols*, *Org. Biomol. Chem* 5 (2007) 3847.
- 6 J.P. Reddy, V.R. Pedireddi, *Synthesis and Analysis of Some Adducts of 3,5-Dinitrobenzamide*, *Tetrahedron* 60 (2004) 8817.
- 7 J.V.B. Kanth, M. Periasamy, *Convenient Method for the Synthesis of Chiral α,α -Diphenyl-2-pyrrolidinemethanol*, *Tetrahedron* 49 (1993) 5127.
- 8 S. Hajra, A.K. Giri, S. Hazra, *Asymmetric Syntheses of (-)-Enterolactone and (7'R)-7'-Hydroxyenterolactone via Organocatalyzed Aldol Reaction*, *J. Org. Chem.* 74 (2009) 7978.
- 9 G.S. Rao, N. Sudhakar, B.V. Rao, S.J. Basha, *The Formal Synthesis of 3-epi Jaspine B Using Stereoselective Intramolecular Oxa-Michael Addition*, *Tetrahedron: Asymm.* 21 (2010) 1963.
- 10 L. Yaouancq, L. René, M.-E.T.H. Dau, B. Badet, *Toward Synthesis of α -Alkyl Amino Glycines (A3G), New Amino Acid Surrogates*, *J. Org. Chem.* 67 (2002) 5408.
- 11 E.N. Jacobsen, A. Pfaltz, H. Yamamoto (Eds.), *Comprehensive Asymmetric Catalysis, Vol. I-III* Springer, 1999.
- 12 A. Berkessel, H. Gröger (Eds.), *Asymmetric Organocatalysis*, Wiley, Weinheim, 2005.
- 13 P.I. Dalko (Ed.), *Enantioselective Organocatalysis*, Wiley, Weinheim, 2007.
- 14 D.J. Ramon, M. Yus, *In the Area of Enantioselective Synthesis, Titanium Complexes Wear the Laurel Wreath*, *Chem. Rev.* 106 (2006) 2126.

- 15 U. Eder, G. Sauer, R. Wiechert, *Total Synthesis of Optically Active Steroids 6. New Type of Asymmetric Cyclization to Optically Active Steroid CD Partial Structures*, *Angew. Chem. Int. Ed. Engl.* 10 (1971) 496.
- 16 Z.G. Hajos, D.R. Parrish, *Asymmetric Synthesis of Bicyclic Intermediates of Natural Product Chemistry*, *J. Org. Chem.* 39 (1974) 1615.
- 17 K.A. Ahrendt, J.B. Christopher, D.W.C. MacMillan, *New Strategies for Organic Catalysis: The First Highly Enantioselective Organocatalytic Diels-Alder Reaction*, *J. Am. Chem. Soc.* 122 (2000) 4243.
- 18 B. List, R.A. Lerner, C.F. Barbas III, *Proline-Catalyzed Direct Asymmetric Aldol Reactions*, *J. Am. Chem. Soc.* 122 (2000) 2395.
- 19 N. Kumaragurubaran, K. Juhl, W. Zhuang, A. Bogevig, K.A. Jørgensen, *Direct L-Proline-Catalyzed Asymmetric α -Amination of Ketones*, *J. Am. Chem. Soc.* 124 (2002) 6254.
- 20 M.S. Taylor, E.N. Jacobsen, *Asymmetric Catalysis by Chiral Hydrogen-Bond Donors*, *Angew. Chem. Int. Ed.* 45 (2006) 1520.
- 21 A.G. Doyle, E.N. Jacobsen, *Small-Molecule H-Bond Donors in Asymmetric Catalysis*, *Chem. Rev.* 107 (2007) 5713.
- 22 T. Akiyama, *Stronger Brønsted Acids*, *Chem. Rev.* 107 (2007) 5744.
- 23 S. Mukherjee, J.W. Yang, S. Hoffmann, B. List, *Asymmetric Enamine Catalysis*, *Chem. Rev.* 107 (2007) 5471.
- 24 A. Erkkilä, I. Majander, P.M. Pihko, *Iminium Catalysis*, *Chem. Rev.* 107 (2007) 5416.
- 25 Z. Rappoport (Ed.), *The Chemistry of Enamines*, Wiley, New York, 1994.
- 26 P.W. Hickmott, *Enamines: Recent Advances in Synthetic, Spectroscopic, Mechanistic, and Stereochemical Aspects*, *Tetrahedron* 38 (1982) 1975.
- 27 B. List, *Asymmetric Aminocatalysis*, *Synlett.* (2001) 1675.
- 28 B. List, *Enamine Catalysis is a Powerful Strategy for the Catalytic Generation and Use of Carbanion Equivalents*, *Acc. Chem. Res.* 37 (2004) 548.
- 29 G. Stork, A. Brizzolara, H. Landesman, J. Szmuszkovicz, R. Terrell, *The Enamine Alkylation and Acylation of Carbonyl Compounds*, *J. Am. Chem. Soc.* 85 (1963) 207.
- 30 G. Stork, N.A. Saccomano, *Enantioselective Synthesis of an Intermediate for the Intramolecular Diels-Alder Construction of 11-Keto Steroids*, *Tetrahedron Lett.* 28 (1987) 2087.

- 31 C. Palomo, A. Mielgo, *Diarylprolinol ethers: Expanding the Potential of Enamine/Iminium-ion Catalysis*, *Angew. Chem. Int. Ed.* 45 (2006) 7876.
- 32 J. Franzen, M. Marigo, D. Fielenbach, T.C. Wabnitz, A. Kjrsgaard, K.A. Jørgensen, *A General Organocatalyst for Direct α -Functionalization of Aldehydes: Stereoselective C-C, C-N, C-F, C-Br, and C-S Bond-Forming Reactions. Scope and Mechanistic Insights*, *J. Am. Chem. Soc.* 127 (2005) 18296.
- 33 Y. Hayashi, H. Gotoh, T. Hayashi, M. Shoji, *Diphenylprolinol Silyl Ethers as Efficient Organocatalysts for the Asymmetric Michael Reaction of Aldehydes and Nitroalkenes*, *Angew. Chem. Int. Ed.* 44 (2005) 4212.
- 34 M. Marigo, D. Fielenbach, A. Braunton, A. Kjoersgaard, K.A. Jørgensen, *Enantioselective Formation of Stereogenic Carbon-Fluorine Centers by a Simple Catalytic Method*, *Angew. Chem. Int. Ed.* 44 (2005) 3703.
- 35 N. Halland, A. Braunton, S. Bachmann, M. Marigo, K.A. Jørgensen, *Direct Organocatalytic Asymmetric α -Chlorination of Aldehydes*, *J. Am. Chem. Soc.* 126 (2004) 4790.
- 36 P. Diner, A. Kjaersgaard, M.A. Lie, K.A. Jørgensen, *On the Origin of the Stereoselectivity in Organocatalysed Reactions with Trimethylsilyl-Protected Diarylprolinol*, *Chem. Eur. J.* 14 (2008) 122.
- 37 J.F. Austin, D.W.C. MacMillan, *Enantioselective Organocatalytic Indole Alkylations. Design of a New and Highly Effective Chiral Amine for Iminium Catalysis*, *J. Am. Chem. Soc.* 124 (2002) 1172.
- 38 D.W.C. MacMillan, G. Lelais, *History and Perspective of Chiral Organic Catalysis*, K. Mikami, M. Koichi (Eds.), *New Frontiers in Asymmetric Catalysis*, (2007) 313.
- 39 D. Cuperly, C. Crévisy, R. Grée, *Application of a New Tandem Isomerization-Aldolization Reaction of Allylic Alcohols to the Synthesis of Three Diastereoisomers of (2R)-1,2-O-Isopropylidene-4-methylpentane-1,2,3,5-tetraol*, *J. Org. Chem.* 68 (2003) 6392.
- 40 A.B. Northrup, D.W.C. MacMillan, *The First Direct and Enantioselective Cross-Aldol Reaction of Aldehydes*, *J. Am. Chem. Soc.* 124 (2002) 6798.
- 41 A. Bøgevig, N. Kumaragurubaran, K.A. Jørgensen, *Direct Catalytic Asymmetric Aldol Reactions of Aldehydes*, *Chem. Commun.* (2002) 620.

- 42 O. Tokuda, T. Kano, W-G. Gao, T. Ikemoto, K. Maruoka, *A Practical Synthesis of (S)-2-Cyclohexyl-2-phenylglycolic Acid via Organocatalytic Asymmetric Construction of a Tetrasubstituted Carbon Center*, *Org. Lett.* 7 (2005) 5103.
- 43 C. Pidathala, L. Hoang, N. Vignola, B. List, *Direct Catalytic Asymmetric Enolexo Aldolizations*, *Angew. Chem. Int. Ed.* 42 (2003) 2785.
- 44 D. Gryko, R. Lipinski, *L-Prolinethioamides - Efficient Organocatalysts for the Direct Asymmetric Aldol Reaction*, *Adv. Synth. Catal.* 347 (2005) 1948.
- 45 Y. Zhou, Z. Shan, *Chiral Diols: A New Class of Additives for Direct Aldol Reaction Catalyzed by L-Proline*, *J. Org. Chem.* 71 (2006) 9510.
- 46 B. List, P. Pojarliev, C. Castello, *Proline-Catalyzed Asymmetric Aldol Reactions Between Ketones and α -Unsubstituted Aldehydes*, *Org. Lett.* 3 (2001) 573.
- 47 D. Enders, C. Grondal, *Direct Organocatalytic De Novo Synthesis of Carbohydrates*, *Angew. Chem. Int. Ed.* 44 (2005) 1210
- 48 A.B. Northrup, I.K. Mangion, F. Hettche, D.W.C. MacMillan, *Enantioselective Organocatalytic Direct Aldol Reactions of α -Oxy-aldehydes: Step One in a Two-Step Synthesis of Carbohydrates*, *Angew. Chem. Int. Ed.* 43 (2004) 2152.
- 49 S. Chandrasekhar, K. Vijeender, C. Sridhar, *L-Proline-Catalyzed One-Pot Synthesis of 2-Aryl-2,3-Dihydroquinolin-4(1H)-ones*, *Tetrahedron Lett.* 48 (2007) 4935.
- 50 A. Córdova, W. Zou, I. Ibrahim, E. Reyes, M. Engqvist, W.W. Liao, *Acyclic Amino Acid Catalyzed Direct Asymmetric Aldol Reactions: Alanine, The Simplest Stereoselective Organocatalyst*, *Chem. Commun.* (2005) 3586.
- 51 X.Y. Xu, Y.Z. Wang, L.Z. Gong, *Design of Organocatalysts for Asymmetric Direct syn-Aldol Reactions*, *Org. Lett.* 9 (2007) 4247.
- 52 B.L. Zheng, Q.Z. Liu, C.S. Guo, X.L. Wang, L. He, *Highly Enantioselective Direct Aldol Reaction Catalyzed by Cinchona Derived Primary Amines*, *Org. Biomol. Chem.* 5 (2007) 2913.
- 53 B. List, *The Direct Catalytic Asymmetric Three-Component Mannich Reaction*, *J. Am. Chem. Soc.* 122 (2000) 9336.
- 54 Y. Hayashi, T. Urushima, S. Aratake, T. Okano, K. Obi, *Organic Solvent-Free Enantio- and Diastereoselective Direct Mannich Reaction in the Presence of Water*, *Org. Lett.* 10 (2008) 21.

- 55 I. Ibrahim, A. Córdova, *Amino Acid-Catalyzed Direct Enantioselective Synthesis of β -Amino- α -oxyaldehydes*, *Tetrahedron Lett.* 46 (2005) 2839.
- 56 P. Dzedzic, I. Ibrahim, A. Córdova, *Direct Catalytic Asymmetric Three-Component Mannich Reactions with Dihydroxyacetone: Enantioselective Synthesis of Amino Sugar Derivatives*, *Tetrahedron Lett.* 49 (2008) 803.
- 57 S. Mitsumori, H. Zhang, P.H. Cheong, K.N. Houk, F. Tanaka, C.F. Barbas III, *Direct Asymmetric anti-Mannich-Type Reactions Catalyzed by a Designed Amino Acid*, *J. Am. Chem. Soc.* 128 (2006) 1040.
- 58 D. Almaşi, D.A. Alonso, C. Nájera, *Organocatalytic Asymmetric Conjugate Additions*, *Tetrahedron: Asymm.* 18 (2007) 299.
- 59 S.B. Tsogoeva, *Recent Advances in Asymmetric Organocatalytic 1,4-Conjugate Additions*, *Eur. J. Org. Chem.* (2007) 1701.
- 60 S. Sulzer-Mossé, A. Alexakis, *Chiral Amines as Organocatalysts for Asymmetric Conjugate Addition to Nitro Olefins and Vinyl Sulfones via Enamine Activation*, *Chem. Commun.* (2007) 3123.
- 61 H.G. Lindwall, J.S. MacLennan, *Condensation of Acetophenone with Isatin by the Knoevenagel Method*, *J. Am. Chem. Soc.* 54 (1932) 4739.
- 62 H. Huang, E.N. Jacobsen, *Highly Enantioselective Direct Conjugate Addition of Ketones to Nitroalkenes Promoted by a Chiral Primary Amine-Thiourea Catalyst*, *J. Am. Chem. Soc.* 128 (2006) 7170.
- 63 J. Wang, H. Li, L. Zu, W. Wang, *Highly Enantioselective Organocatalytic Michael Addition Reactions of Ketones with Chalcone Derivatives*, *Adv. Synth. Catal.* 348 (2006) 425.
- 64 L.F. Tietze, *Domino Reactions in Organic Synthesis*, *Chem. Rev.* 96 (1996) 115.
- 65 H-G. Guo, J-A. Ma, *Catalytic Asymmetric Tandem Transformations Triggered by Conjugate Additions*, *Angew. Chem.* 45 (2006) 354.
- 66 D. Enders, C. Grondal, M.R.M. Hüttl, *Asymmetric Organocatalytic Domino Reactions*, *Angew. Chem. Int. Ed.* 46 (2007) 1570.
- 67 S. Mukherjee, J.W. Yang, S. Hoffmann, B. List, *Asymmetric Enamine Catalysis*, *Chem. Rev.* 107 (2007) 5471.

- 68 H. Sundén, I. Ibrahim, L. Eriksson, A. Córdova, *Direct Catalytic Enantioselective Aza-Diels-Alder Reactions*, *Angew. Chem. Int. Ed.* 44 (2005) 4877.
- 69 A. Erkkilä, I. Majander, P.M. Pihko, *Iminium Catalysis*, *Chem. Rev.* 107 (2007) 5416.
- 70 Y. Yamamoto, N. Momiyama, H. Yamamoto, *Enantioselective Tandem O-Nitroso Aldol/Michael Reaction*, *J. Am. Chem. Soc.* 63 (2004) 5962.
- 71 M.P. Brochu, S.P. Brown, D.W.C. MacMillan, *Direct and Enantioselective Organo-catalytic α -Chlorination of Aldehydes*, *J. Am. Chem. Soc.* 126 (2004) 4108.
- 72 D. D. Steiner, N. Mase, C. F. Barbas III, *Direct Asymmetric α -Fluorination of Aldehydes*, *Angew. Chem. Int. Ed.* 44 (2005) 3706.
- 73 S. Bertelsen, N. Halland, S. Bachmann, M. Marigo, A. Braunton, K.A. Jørgensen, *Organocatalytic Asymmetric α -Bromination of Aldehydes and Ketones*, *Chem. Commun.* (2005) 4821.
- 74 M. Marigo, T.C. Wabnitz, D. Fielenbach, K.A. Jørgensen, *Enantioselective Organo-Catalyzed α -Sulfonylation of Aldehydes*, *Angew. Chem. Int. Ed.* 44 (2005) 794.
- 75 J.S. Baum, H.G. Viehe, *Synthesis and Cycloaddition Reactions of Acetylenic Iminium Compounds*, *J. Org. Chem.* 41 (1976) 183.
- 76 W.S. Jen, J.J.M. Wiener, D.W.C. MacMillan, *New Strategies for Organic Catalysis: The First Enantioselective Organocatalytic 1,3-Dipolar Cycloaddition*, *J. Am. Chem. Soc.* 122 (2000) 9874.
- 77 S. Karlsson, H.E.H. Ogberg, *Catalytic Enantioselective 1,3-Dipolar Cycloaddition of Nitrones to Cyclopent-1-enecarbaldehyde*, *Tetrahedron: Asymm.* 13 (2002) 923.
- 78 N.A. Paras, D.W.C. MacMillan, *New Strategies in Organic Catalysis: The First Enantioselective Organocatalytic Friedel-Crafts Alkylation*, *J. Am. Chem. Soc.* 123 (2001) 4370.
- 79 N.A. Paras, D.W.C. MacMillan, *The Enantioselective Organocatalytic 1,4-Addition of Electron-Rich Benzenes to α,β -Unsaturated Aldehydes*, *J. Am. Chem. Soc.* 124 (2002) 7894.
- 80 S.P. Brown, N.C. Goodwin, D.W.C. MacMillan, *The First Enantioselective Organocatalytic Mukaiyama-Michael Reaction: A Direct Method for the Synthesis of Enantioenriched γ -Butenolide Architecture*, *J. Am. Chem. Soc.* 125 (2003) 1192.

- 81 M. Yamaguchi, T. Shiraishi, M. Hirama, *Asymmetric Michael Addition of Malonate Anions to Prochiral Acceptors Catalyzed by L-Proline Rubidium Salt*, J. Org. Chem. 61 (1996) 3520.
- 82 S. Hanessian, V. Pham, *Catalytic Asymmetric Conjugate Addition of Nitroalkanes to Cycloalkenones*, Org. Lett. 2 (2000) 2975.
- 83 A.B. Northrup, D.W.C. MacMillan, *The First General Enantioselective Catalytic Diels-Alder Reaction with Simple α,β -Unsaturated Ketones*, J. Am. Chem. Soc. 124 (2002) 2458.
- 84 M. Harmata, K.S. Ghosh, H. Xuechuan, W. Sumrit, K. Patrick, *Asymmetric Organocatalysis of [4+3] Cycloaddition Reactions*, J. Am. Chem. Soc. 125 (2003) 2058.
- 85 M. Marigo, J. Franzen, B.T. Poulsen, W. Zhuang, K.A. Jørgensen, *Asymmetric Organocatalytic Epoxidation of α,β -Unsaturated Aldehydes with Hydrogen Peroxide*, J. Am. Chem. Soc. 127 (2005) 6964.
- 86 K.R. Kunz, D.W.C. MacMillan, *Enantioselective Organocatalytic Cyclopropanations. The Identification of a New Class of Iminium Catalyst Based upon Directed Electrostatic Activation*, J. Am. Chem. Soc. 127 (2005) 3240.
- 87 T. Kano, Y. Tanaka, K. Maruoka, *Exo-Selective Asymmetric Diels-Alder Reaction Catalyzed by Diamine Salts as Organocatalysts*, Asian Journal 2 (2007) 1161.
- 88 H. Gotoh, Y. Hayashi, *Diarylprolinol Silyl Ether as Catalyst of an exo-Selective, Enantioselective Diels-Alder Reaction*, Org. Lett. 9 (2007) 2859.
- 89 M. Lemay, L. Aumand, W.W. Ogilvie, *Design of a Conformationally Rigid Hydrazide Organic Catalyst*, Adv. Synth. Catal. 349 (2007) 441.
- 90 S.A. Selkala, J. Tois, M.P. Pihko, M.P.A. Koskinen, *Asymmetric Organocatalytic Diels-Alder Reactions on Solid Support*, Adv. Synth. Catal. 344 (2002) 941.
- 91 R.P. Singh, K. Bartelson, Y. Wang, H. Su, X. Lu, L. Deng, *Enantioselective Diels-Alder Reaction of Simple α,β -Unsaturated Ketones with a Cinchona Alkaloid Catalyst*, J. Am. Chem. Soc. 130 (2008) 2422.
- 92 A. Sakakura, K. Suzuki, K. Nakano, K. Ishihara, *Chiral 1,1'-Binaphthyl-2,2'-diammonium Salt Catalysts for the Enantioselective Diels-Alder Reaction with α -Acloxyacroleins*, Org. Lett. 8 (2006) 2229.

- 93 S.S. Chow, M. Nevalainen, C.A. Evans, C.W. Johannes, *A New Organocatalyst for 1,3-Dipolar Cycloaddition of Nitrones to α,β -Unsaturated Aldehydes*, *Tetrahedron Lett.* 48 (2007) 277.
- 94 W. Chen, W. Du, Y.Z. Duan, Y. Wu, S.Y. Yang, Y.C. Chen, *Enantioselective 1,3-Dipolar Cycloaddition of Cyclic Enones Catalyzed by Multifunctional Primary Amines: Beneficial Effects of Hydrogen Bonding*, *Angew. Chem. Int. Ed.* 46 (2007) 7667.
- 95 J.W. Yang, M.T.H. Fonseca, B. List, *A Metal-Free Transfer Hydrogenation: Organocatalytic Conjugate Reduction of α,β -Unsaturated Aldehydes*, *Angew. Chem. Int. Ed.* 43 (2004) 6660.
- 96 J. Lacour, H.V. Virginie, *Recent Developments in Chiral Anion Mediated Asymmetric Chemistry*, *Chem. Soc. Rev.* 32 (2003) 373.
- 97 G.L. Hamilton, E.J. Kang, M. Mba, F.D. Toste, *A Powerful Chiral Counterion Strategy for Asymmetric Transition Metal Catalysis*, *Science* 317 (2007) 496.
- 98 M. Johannsen, K.A. Jørgensen, G. Helmchen, *Synthesis and Application of the First Chiral and Highly Lewis Acidic Silyl Cationic Catalyst*, *J. Am. Chem. Soc.* 120 (1998) 7637.
- 99 J.Y. Corey, *Generation of a Silicenium Ion in Solution*, *J. Am. Chem. Soc.* 97 (1975) 3237.
- 100 J.Y. Corey, R. West, *Hydrogen-Halogen Exchange between Silanes and Triphenylmethyl Halides*, *J. Am. Chem. Soc.* 85 (1963) 2430.
- 101 G. Simchen, S. Jonas, *Highly Reactive Trialkylsilylation Reagents Derived from bis(trifluoromethanesulfonyl)imide. Silylation of Functional Groups, Alkynes, and Reactive Aromatics*, *J. Prakt. Chem.* 340 (1998) 506.
- 102 B. Mathieu, L. de Fays, L. Ghosez, *The Search for Tolerant Lewis Acid Catalysts. Part 1. Chiral Silicon Lewis Acids Derived from (-)-Myrtenal*, *Tetrahedron Lett.* 41 (2000) 9561.
- 103 S. Shirakawa, R. Berger, J.L. Leighton, *Enantioselective Friedel-Crafts Alkylations with Benzoylhydrazones Promoted by a Simple Strained Silacycle Reagent*, *J. Am. Chem. Soc.* 127 (2005) 2858.

- 104 S. Shirakawa, P.J. Lombardi, J.L. Leighton, *A Simple and General Chiral Silicon Lewis Acid for Asymmetric Synthesis: Highly Enantioselective [3+2] Acylhydrazone-Enol Ether Cycloadditions*, *J. Am. Chem. Soc.* 127 (2005) 9974.
- 105 M. Terada, M. Kouchi, *Novel Metal Free Lewis Acid Catalysis by Phosphonium Salts through Hypervalent Interaction*, *Tetrahedron* 62 (2006) 401.
- 106 U.-H. Dolling, P. Davis, E.J.J. Grabowski, *Efficient Catalytic Asymmetric Alkylations Enantioselective Synthesis of (+)-Indacrinone via Chiral Phase-Transfer Catalysis*, *J. Am. Chem. Soc.* 106 (1984) 446.
- 107 J. Seayad, B. List, *Asymmetric Organocatalysis*, *Org. Biomol. Chem.* 3 (2005) 719.
- 108 K. Kacprzak, J. Gawronski, *Cinchona Alkaloids and their Derivatives: Versatile Catalysts and Ligands in Asymmetric Synthesis*, *Synthesis* 7 (2001) 961.
- 109 T. Akiyama, J. Itoh, K. Yokota, K. Fuchibe, *Enantioselective Mannich-Type Reaction Catalyzed by a Chiral Brønsted Acid*, *Angew. Chem. Int. Ed.* 43 (2004) 1566.
- 110 D. Uraguchi, M. Terada, *Chiral Brønsted Acid-Catalyzed Direct Mannich Reactions via Electrophilic Activation*, *J. Am. Chem. Soc.* 126 (2004) 5356.
- 111 X.-H. Chen, X.-Y. Xu, H. Liu, L.-F. Cun, L.-Z. Gong, *Highly Enantioselective Organocatalytic Biginelli Reaction*, *J. Am. Chem. Soc.* 128 (2006) 14802.
- 112 D. Nakashima, H. Yamamoto, *Design of Chiral N-Triflyl Phosphoramidate as a Strong Chiral Brønsted Acid and Its Application to Asymmetric Diels-Alder Reaction*, *J. Am. Chem. Soc.* 128 (2006) 9626.
- 113 E.J. Corey, *Catalytic Enantioselective Diels-Alder Reactions: Methods, Mechanistic Fundamentals, Pathways, and Applications*, *Angew. Chem. Int. Ed.* 41 (2002) 165.
- 114 K.C. Nicolaou, S.A. Snyder, T. Montagnon, G. Vassilikogiannakis, *The Diels-Alder Reaction in Total Synthesis*, *Angew. Chem. Int. Ed.* 41 (2002) 1668.
- 115 E.M. Stocking, R.M. Williams, *Chemistry and Biology of Biosynthetic Diels-Alder Reactions*, *Angew. Chem. Int. Ed.* 42 (2003) 3078.
- 116 O. Diels, K. Alder, *Synthesen in Der Hydroaromatischen Reihe*, *Justus Liebigs Ann. Chem.* 460 (1928) 98.
- 117 E.J. Corey, R.L. Danheiser, S. Chandrasekaran, P. Siret, G.E. Keck, J.-L. Gras, *Stereospecific Total Synthesis of Gibberellic Acid*, *J. Am. Chem. Soc.* 100 (1978) 8031.

- 118 W.E. Noland, M.S. Tempesta, R.D. Cink, D.M. Powers, *Diels-Alder Reactions of 3-(2-Nitrovinyl)indoles: Formation of Carbazoles and Bridged Carbazoles*, *J. Heterocycl. Chem.* 30 (1993) 183.
- 119 W.E. Noland, B.L. Kedrowski, *Synthesis of Angular Quinoid Heterocycles from 2-(2-Nitrovinyl)-1,4-benzoquinone*, *J. Org. Chem.* 64 (1999) 596.
- 120 W.E. Noland, B. L. Kedrowski, *Quinone Approaches toward the Synthesis of Aflatoxin B2*, *Org. Lett.* 2 (2000) 2109.
- 121 W.E. Noland, B.L. Kedrowski, *Reactivity of Nitrovinylquinones with Cyclic and Acyclic Enol Ethers*, *J. Org. Chem.* 67 (2002) 8366.
- 122 Q.Y. Hu, G. Zhou, E.J. Corey, *Application of Chiral Cationic Catalysts to Several Classical Syntheses of Racemic Natural Products Transforms Them into Highly Enantioselective Pathways*, *J. Am. Chem. Soc.* 126 (2004) 13708.
- 123 G. Zhou, E.J. Corey, *Short, Enantioselective Total Synthesis of Aflatoxin B2 Using an Asymmetric [3+2]-Cycloaddition Step*, *J. Am. Chem. Soc.* 127 (2005) 11958.
- 124 E. Arkoudis, I.N. Lykakis, C. Gryparis, M. Stratakis, *Biomimetic Synthesis of Dimeric Metabolite Acremine G via a Highly Regioselective and Stereoselective Diels-Alder Reaction*, *Org. Lett.* 11 (2009) 2988.

Chapter-2

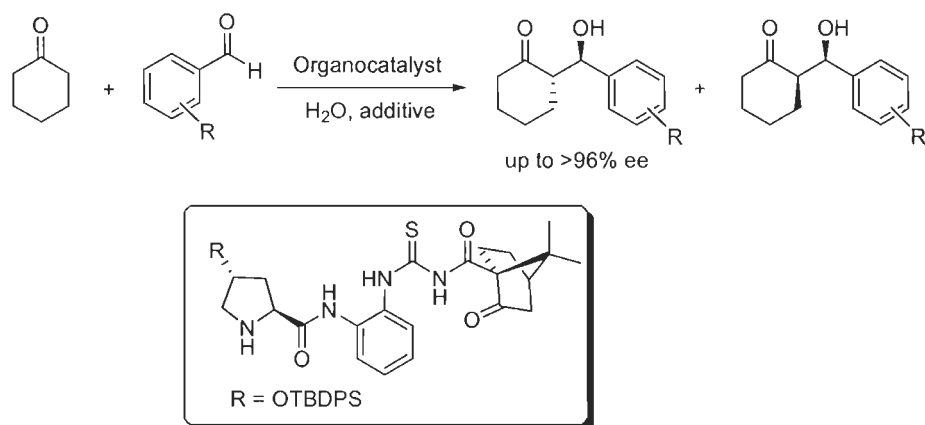
SYNTHESIS AND CHARACTERIZATION OF NOVEL CAMPHORSULFONAMIDE-BASED PROLINAMIDE ORGANOCATALYSTS

Synthesis and Characterization of Novel Camphorsulfonamide-based Prolinamide Organocatalysts

2.1. INTRODUCTION

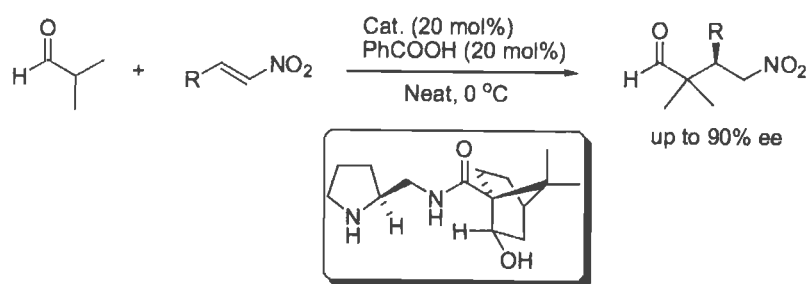
Organocatalysis has emerged as a rapidly growing and important field in organic chemistry [1,2]. Organocatalysts consist of small, low-molecular-weight organic compounds, containing carbon, hydrogen, nitrogen, sulfur and phosphorus [3-5]. The advantages of organocatalysts include their tolerance towards moisture and oxygen, their ready availability, low cost and low toxicity, which confers a huge direct benefit in the production of pharmaceutical intermediates when compared with transition-metal catalysts [6-11]. In recent years, several organocatalysts have been developed for numerous asymmetric transformations. Among them, prolinamides have been established as another class of organocatalysts. Presence of secondary amine and introduction of amide linkage provide opportunities for the catalytic activity of these prolinamides to synthesize various chiral compounds.

Certain organic compounds of natural origin are the primary source of chirality in organic synthesis and are used to prepare other chiral compounds of interest. Among the various types of natural chiral products, monoterpenes such as camphor and their derivatives have been successfully employed as primary chirality sources [12-20]. Camphor exists extensively in nature and it is a flexible chiral substance, easily derivatized at any of its ten carbons to give



Scheme 1: Camphor scaffold embedded chiral thiourea catalyst for aldol reaction.

camphor derived compounds. Furthermore, the different position of the gem-dimethyl group in camphor derivative confers dissimilar topology, often reflected in the capacity of chirality transfer. In past few years, camphor-derivatives have been proved as highly versatile and powerful ligands or auxiliaries in organic synthesis [21-28]. During our work progress, in 2008 Chen *et al.* reported new class of organocatalyst bearing camphor scaffold with thiourea motif for aldol reaction (Scheme 1) [29]. After this, they reported pyrrolidine-camphor derivative as an organocatalyst for another asymmetric transformation (Scheme 2) [30]. To our surprise, the camphor moiety had never been used as part of prolinamide catalyst for asymmetric synthesis.



Scheme 2: Chiral pyrrolidine camphor derivative catalyzed Michael addition.

2.2 OBJECTIVE

Chiral monoterpenes such as camphor, known to be used in the manufacture of cellulose nitrate, polyvinylchloride and several medicines antiseptics and insecticides, *etc.*, having rigid bicyclic structures, are widely used as synthons in asymmetric synthesis. Camphor and its derivatives such as camphor-10-sulfonic acid are readily available in optically pure forms and

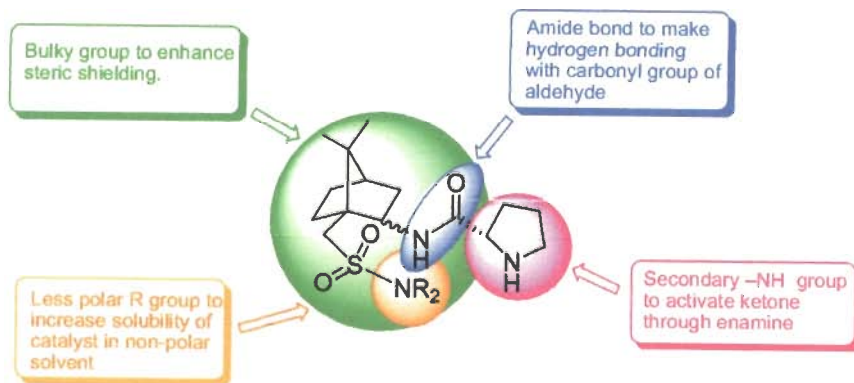


Figure 1: Design of camphorsulfonamide-based organocatalysts.

can afford a simple, inexpensive scaffold from which a chiral catalyst can be built. Such molecules arouse our attention to employ these molecules as chiral scaffolds to develop prolinamide-based chiral organocatalysts for asymmetric synthesis. For this purpose, our objective was to synthesize novel organocatalysts having camphor scaffold and proline moiety to activate carbonyl donor through enamine catalysis and utilize them for various asymmetric transformations. On the other hand, the presence of tunable *N,N*-dialkyl group on camphor sulfonamide moiety will facilitate to increase the solubility of these catalysts in non-polar solvents and thereby achieving rapid reaction in the medium taken. Given these considerations, we were interested to synthesize camphorsulfonamide-based prolinamides **Cat-1a**, **Cat-2a**, **Cat-3a** and **Cat-3b** having camphor scaffold and proline moiety through appended prolinamide linkage to examine their catalytic activity for the asymmetric aldol and Michael reactions. We rationalized the anticipated catalytic activity of these catalysts in the projected reactions on the basis of stabilization of the transition state *via* hydrogen bonding between aldehyde or nitrostyrenes and amide moiety of the enamine formed from catalyst and ketone and effective shielding of one of the faces of enamine by camphor unit of the catalyst.

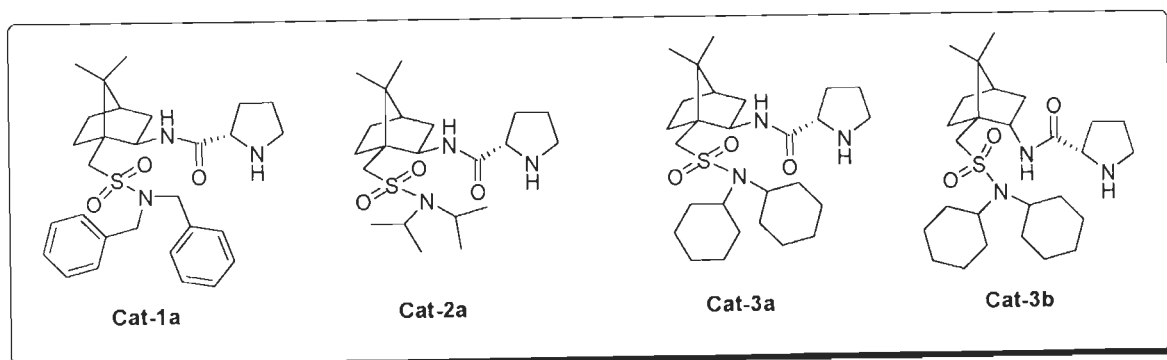


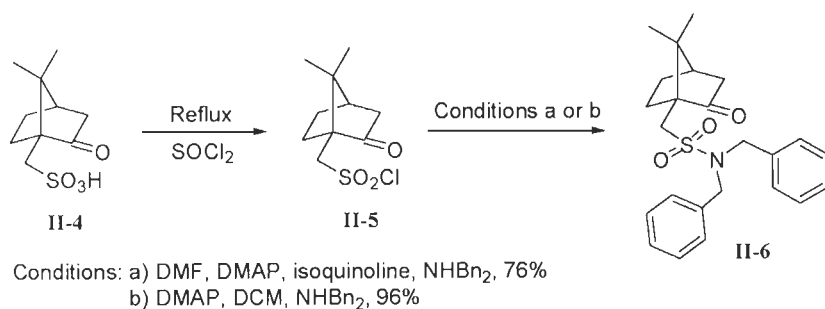
Figure 2: Camphorsulfonamide-based organocatalysts.

2.3. RESULTS AND DISCUSSION

2.3.1. Synthesis of 2-aminocamphor-10-sulfonamides II-14a,b, II-15a,b and II-16a,b

In our synthetic approach, proline unit was anchored to the host camphor-based system in five synthetic steps. Initially, we synthesized compounds **II-14a,b**, **II-15a,b** and **II-16a,b**

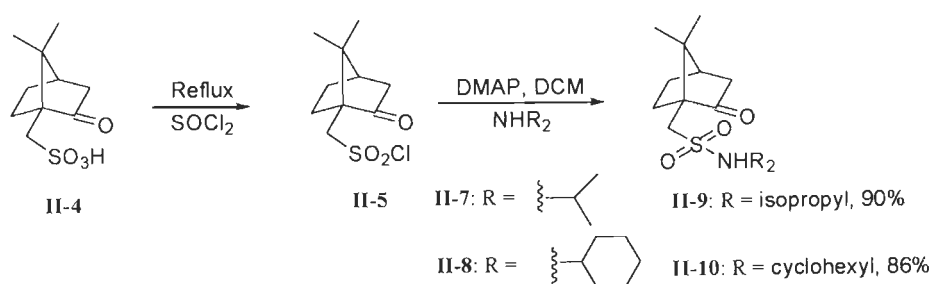
starting from (1*S*)-(+)-camphor-10-sulfonic acid. The first step involves the conversion of camphorsulfonic acid **II-4** into camphorsulfonyl chloride **II-5** by treating with thionyl chloride at reflux temperature [31]. The treatment of camphorsulfonyl chloride **II-5** with dibenzylamine in presence of DMAP and isoquinoline in DMF at room temperature produced (1*S*)-(+)-camphors-10-sulfonamide (**II-6**) in 76% yield. Alternatively, this reaction was performed with dibenzylamine in presence of DMAP in dry DCM by following literature procedure [32] to furnish the desired product **II-6** in excellent yield.



Scheme 3: Synthesis of camphorsulfonamide **II-6**.

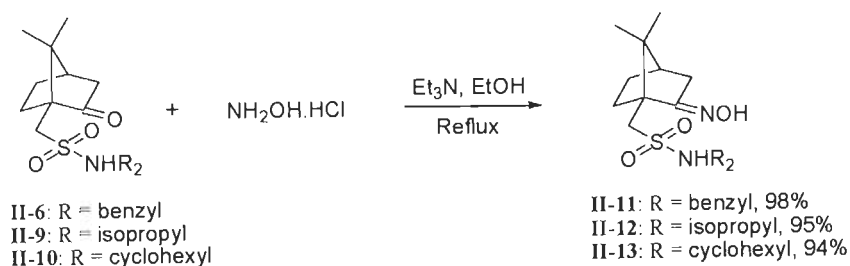
This method was extended to synthesize products **II-9** and **II-10** from **II-4**. However, yields of the products vary with the substituent. While sulfonamide **II-6** having dibenzylamine group was obtained in 95% yield, the sulfonamide **II-9** bearing diisopropylamine was achieved in 90% yield along with 8% of the acid **II-4** and the compound **II-10** having dicyclohexylamine was acquired in 86% yield with 10% recovery of reactant **II-4**. Our efforts to improve the chemical yield of the latter two sulfonamides by using more equivalents of DMAP were not successful. The structure of **II-6** was established on the basis of its IR, ^1H and ^{13}C NMR spectral data and CHNS analysis. In IR spectrum, an intense peak at 1740 cm^{-1} shows the presence of $-\text{CO}$ group and peaks at 1335 and 1146 cm^{-1} show the presence of $-\text{SO}_2$ group. ^1H NMR spectrum signal at δ 4.36 (AB quartet, $J = 15.0, 35.5\text{ Hz}$, 4H) and aromatic [δ 7.39-7.30 (m, 10H)] protons show the presence of two benzyl groups and signals at δ 1.15 (s, 3H), δ 0.80 (s, 3H) show the presence of bridgehead methyl groups of camphor moiety of the compound. Proton decoupled ^{13}C NMR spectrum in CDCl_3 (125 MHz) was fully consistent with the assigned structure of **II-6**. The structures of **II-9** and **II-10** were also established on the basis of their spectral analysis.

The conversion of carbonyl function of the above camphorsulfonamides into oxime group was carried out following a literature procedure [33]. Thus the reaction of camphorsulfonamide **II-6** with hydroxylamine hydrochloride in the presence of triethylamine in absolute ethanol at reflux temperature reached 100% conversion of the reactant in 8 h and 98% of the product **II-11** was isolated. This is the typical example of nucleophilic addition reaction in which water is eliminated from the initially formed tetrahedral intermediate with subsequent formation of a new C=N bond. In a similar fashion, the oximes **II-12** and **II-13** were also synthesized in excellent yields (Scheme 5).



Scheme 4: Synthesis of camphorsulfonamides **II-9** and **II-10**.

The structure of **II-11** was established on the basis of its IR, ^1H and ^{13}C NMR spectral data and CHNS analysis. The intense peaks at 3448 (OH), 1643 (C=N), 932 (N–O) cm^{-1} in IR spectrum show the presence of oxime functionality. ^1H NMR spectrum signal at δ 4.37 (AB quartet, $J = 15.0, 91.5$ Hz, 4H) and aromatic [δ 7.35–7.27 (m, 10H)] protons show the presence of two benzyl groups. Signal at δ 7.93 (s, 1H) which got disappeared in D_2O exchange experiment shows the presence of –OH group and signals at δ 0.98 (s, 3H) and δ 0.67 (s, 3H) show the

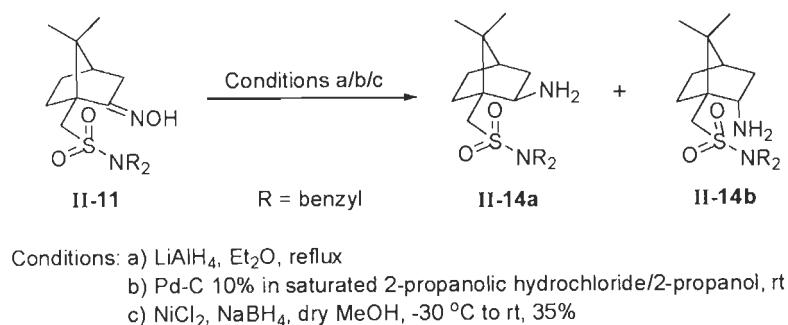


Scheme 5: Synthesis of camphor oxime derivatives **II-11**, **II-12** and **II-13**.

presence of two bridgehead methyl groups of camphor entity of the compound. The proton decoupled ^{13}C NMR spectrum in CDCl_3 (125 MHz) is fully consistent with the assigned

structure of **II-11**. The signals in the upfield region at δ 52.3 and 49.8 refer to quaternary carbons and signal at δ 50.1 is due to $-\text{CH}_2\text{Ph}$ and the signals at δ 51.5, 32.7, 28.1 and 27.2 are due to methylene carbons of camphor moiety. The signal at δ 43.3 is assigned to the methine carbon and the signals at δ 19.3 and 19.1 are due to the geminal methyl groups of camphor moiety and the remaining signals are of carbons of arene systems. The structures of **II-12** and **II-13** were also established on the basis of their IR, ^1H and ^{13}C NMR spectral data and CHNS analysis.

Having oximes **II-11–13** in hand, our next step was to convert the oxime group into amino group on C-2. We attempted the reduction of oxime **II-11** function with usual methods such as i) refluxing with LiAlH_4 in Et_2O for 4 h, ii) reaction with 10% Pd-C in saturated 2-propanolic hydrogen chloride/2-propanol at room temperature and iii) reaction with NiCl_2 and NaBH_4 in dry MeOH under inert atmosphere. No conversion was observed in the first method and 100% starting compound **II-11** was recovered. In the second method no desired product was obtained. However, when camphor oxime was treated with 2 equiv. of NiCl_2 and 10 equiv. of NaBH_4 in dry MeOH at $-30\text{ }^\circ\text{C}$ to room temperature for 4 h, 42% conversion (^1H NMR) of the reactant was observed and *exo* and *endo* amines **II-14a,b** were isolated in a combined yield of 35% (Scheme 6).



Scheme 6: Reduction of oxime **II-11**.

At this juncture, the reduction of oxime **II-11** was carried out with NaCNBH_3 , in the presence of TiCl_3 (12% in HCl) and $\text{CH}_3\text{COONH}_4$ in dry MeOH to afford *exo* and *endo* amines **II-14a,b** (Scheme 7). The TLC analysis showed two isomers at different R_f values (0.60 and 0.35 in 4:96 methanol: dichloromethane solvent system; later confirmed to be *exo* and *endo* isomers, respectively on the basis of 2D NMR experiments, (*vide infra*). Further, the ^1H NMR analysis of crude sample revealed the presence of two isomers *exo* **II-14a** and *endo* **II-14b**. We

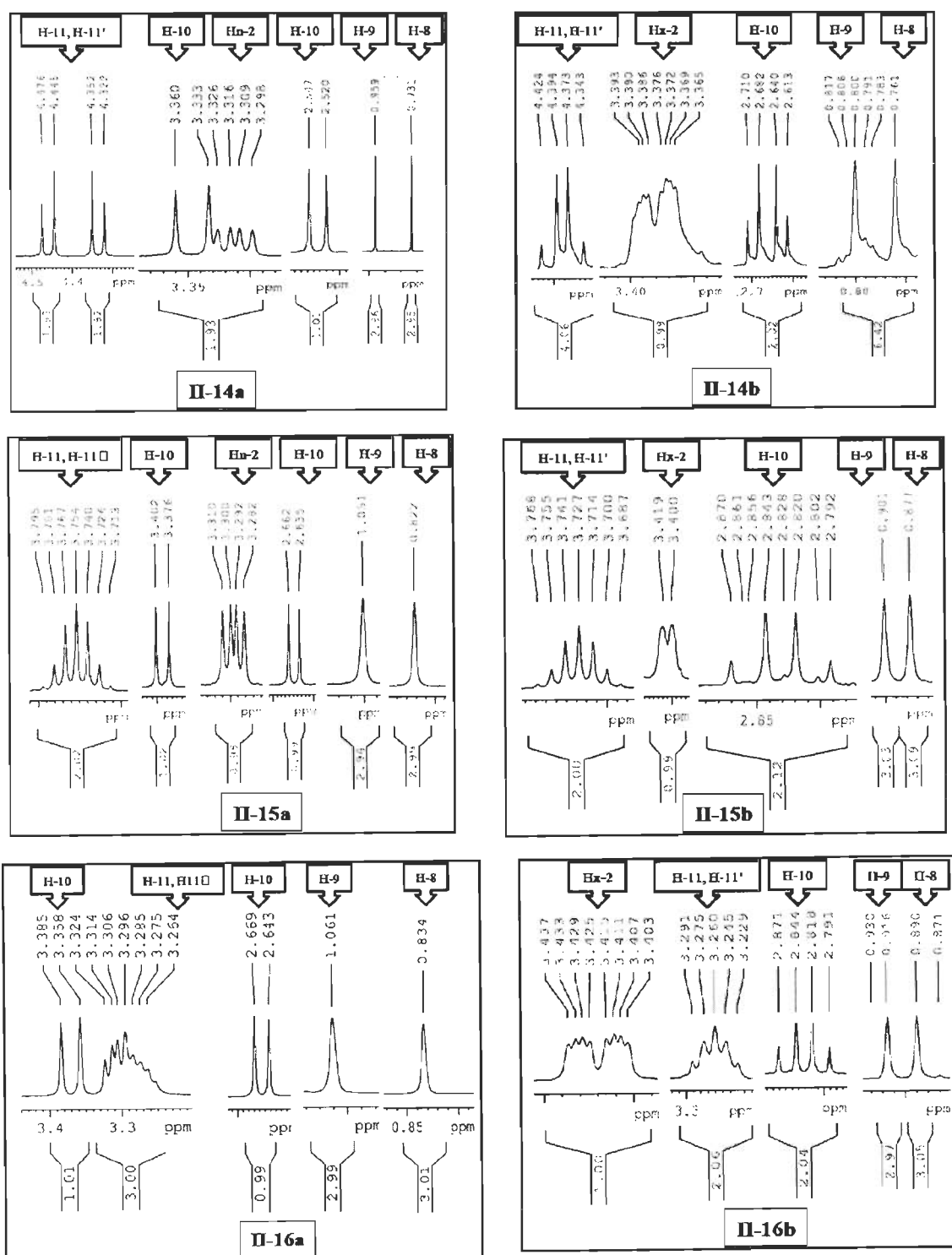
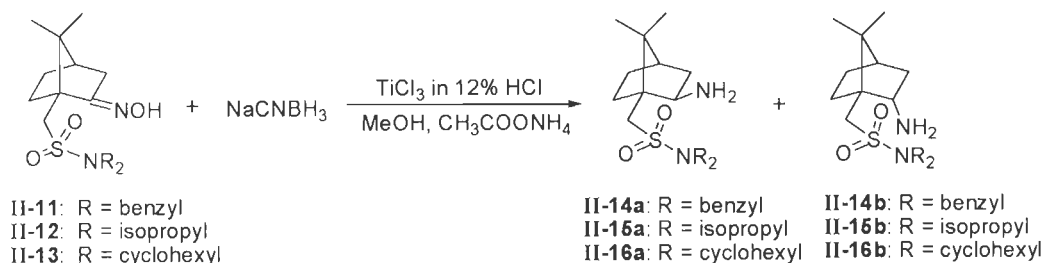


Figure 3: Aliphatic region of the 500 MHz ^1H NMR spectra of 2-aminocamphorsulfonamides **II-14a,b**, **II-15a,b** and **II-16a,b**.

separated the diastereomers **II-14a,b** by silica gel column chromatography in a combined yield of 68%. Similarly, 2-aminocamphorsulfonamides **II-15a,b** and **II-16a,b** were synthesized and the isomers were separated by column chromatography.



Scheme 7: Synthesis of 2-aminocamphorsulfonamides **II-14-16**.

Table 1: Proton and carbon chemical shifts and proton-proton coupling constants for *exo* and *endo* isomers **II-14a** and **II-14b**.

Position	 II-14a		 II-14b	
	δ_{H} (ppm)	δ_{C} (ppm)	δ_{H} (ppm)	δ_{C} (ppm)
C-2	3.31 (dd, $J = 5.5, 9.0$ Hz)	57.1	3.38 (qd, $J = 2.0, 10.5$ Hz)	55.6
C-3	-	-	2.40-2.31 (m), 0.86 (dd $J = 3.0, 11.0$ Hz)	39.9
C-8	0.73 (s)	21.1	0.76 (s)	20.5
C-9	0.96 (s)	19.9	0.80 (s)	18.6
C-10	3.35 (d, $J = 13.5$ Hz), 2.53 (d, $J = 13.5$ Hz)	52.0	2.66 (AB quartet, $J = 13.5, 34.5$ Hz)	56.3
C-11, C-11'	4.40 (AB quartet, $J = 15.0, 61.5$ Hz)	50.2	4.38 (AB quartet, $J = 15.0, 25.5$ Hz)	50.1

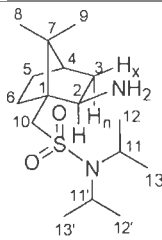
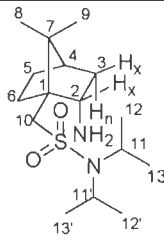
The structure elucidation of isomers **II-14a** and **14b** is on the basis of collective information that obtained from ^1H and ^{13}C NMR and 2D (^1H - ^1H and ^1H - ^{13}C COSY) experiments of pure and isolated isomers. The two dimensional ^1H and ^{13}C correlation spectroscopy identifies the connectivity between protons and carbons. The ^1H - ^1H COSY identifies protons that are coupled with each other. For instance, the spectrum of **II-14b** shows zero-coupling between H-3 n and H-4 protons, where the dihedral angle between the planes containing these protons is close to 90° . This is in accordance with Karplus correlation *i.e.*, relationship between the dihedral angle and vicinal coupling constants. The proton H-3 n shows couplings with H-2 ($^3J_{2,3n} = 3.0$ Hz) and H-3 x ($^2J_{3x,3n} = 11.0$ Hz). The small coupling constant between H-3 n and H-2 clearly indicates that the dihedral angle between the planes containing these protons is 50 - 60° and confirms H-2 x proton. This is further validated by the coupling ($^3J_{2x,3x} = 10.5$ Hz) between H-2 x and H-3 x . ^1H NMR of *exo* isomer **II-14a** signal for proton at C-2 appears as dd at δ 3.31 ppm while in *endo* isomer **II-14b** signal for proton at C-2 shifts little towards downfield and resonate at δ 3.38 ppm. In *exo* **II-14a**, signal for C-10 protons appears as doublet at δ 3.35 and 2.53 ppm while in *endo* **II-14b** it appears as AB quartet at δ 2.66 ppm (Table 1). The gem dimethyl groups of *exo* **II-14a** resonate at 0.96 and 0.73 ppm and those of *endo* **II-14b** resonate at 0.80 and 0.76 ppm. This further confirms that the $-\text{NH}_2$ substituent at C-2 is *exo* and a deshielding proximity effect is in operation in *exo* **II-14a** due to which C-8 methyl group resonates upfield of 0.96 ppm. The NMR data of selected protons and carbons of these isomers is depicted in Table 1.

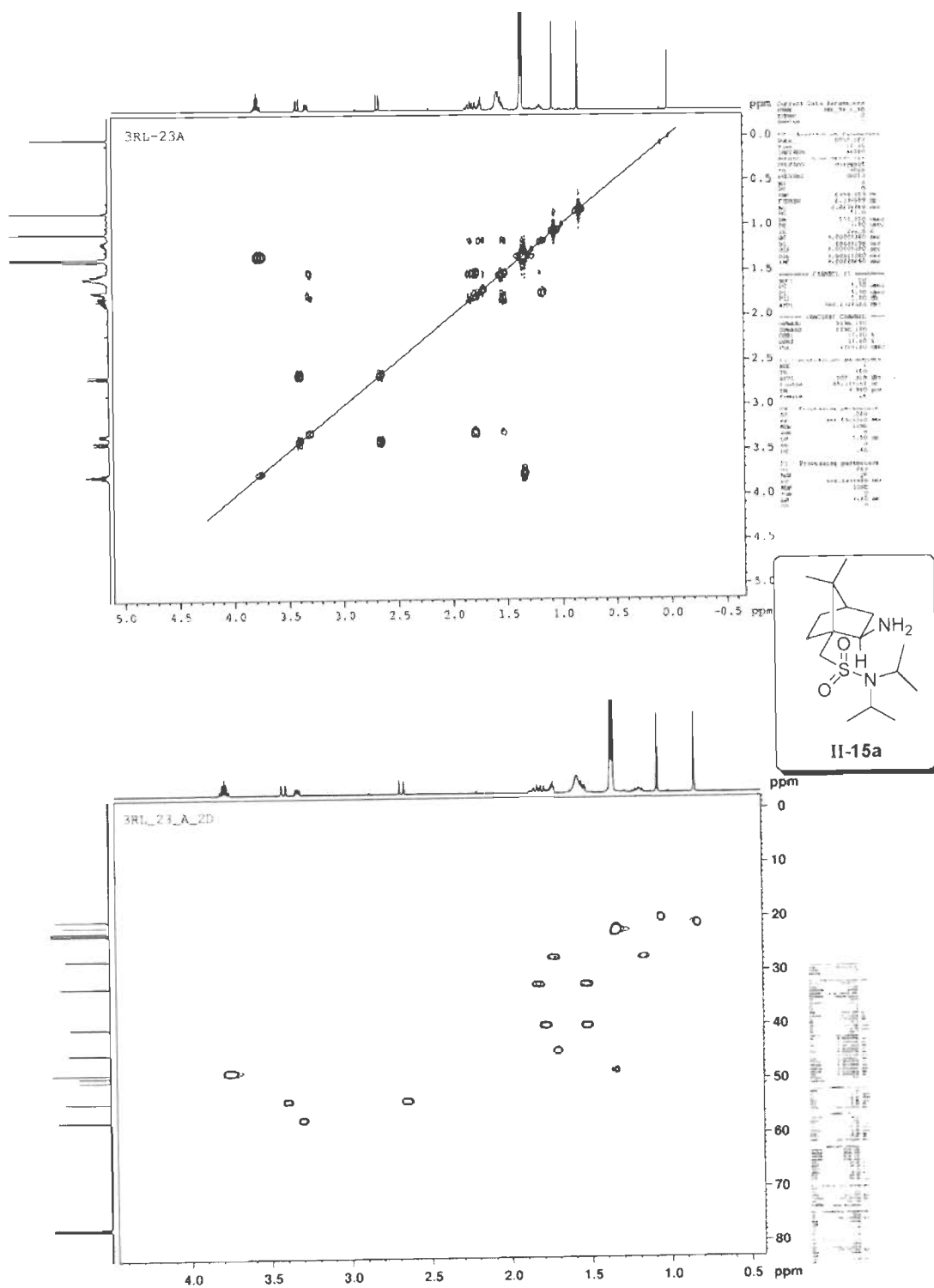
The structures of *exo* **II-15a** and *endo* **II-15b** were also confirmed by studies of ^1H and ^{13}C NMR and 2D (^1H - ^1H and ^1H - ^{13}C COSY) experiments carried out at 500 MHz. These experiments facilitated to identify the chemical shifts and connectivity of ^1H and ^{13}C signals. The resonance and coupling pattern of these signals parallels to that of previous pair *exo* **II-14a** and *endo* **II-14b**. The NMR data of isomers **II-15a,b** is tabulated in the following page.

The δ values for different protons as well as carbons of both *exo* and *endo* isomers **II-15a** and **II-15b** were assigned based on ^1H - ^1H COSY and HSQC experiments (Figures 4 and 5). A more resolved spectrum was observed for *endo* **II-15b**. The deshielding effect of $-\text{NH}_2$ function is clearly visible in *exo* **II-15a**. The two protons at C-10 of *exo* **II-15a** appear as two doublets at δ 3.39 and 2.65 and those of *endo* **II-15b** appear as AB quartet at δ 2.83 ppm. The H-2 n and H-

2x protons of *exo* **II-15a** and *endo* **II-15b** resonate δ 3.30 (dd) and 3.41 (d), respectively. It is observed that the carbon chemical shifts of *endo* **II-15b**, in general, moved slightly upfield in comparison to those of *exo* **II-15a**.

Table 2: Proton and carbon chemical shifts and proton-proton coupling constants for *exo* and *endo* isomers **II-15a** and **II-15b**.

Position	 II-15a				 II-15b			
	δ_H (ppm) (multiplicity)	δ_C (ppm)	Correlation	J_{H-H} (Hz)	δ_H (ppm) (multiplicity)	δ_C (ppm)	Correlation	J_{H-H} (Hz)
C-1	-	49.7	-	-	-	51.3	-	-
C-2	3.30 (dd)	57.1	H2-H3 H2-H3	5.0 9.0	3.41 (d)	55.5	H2-H3	9.5
C-3	1.60-1.49 (m) 1.86-1.69 (m)	40.2	-	-	2.37-2.29 (m) 0.79 (dd)	39.6	H2-H3 H3-H3	- 13.0
C-4	1.86-1.69 (m)	44.7	-	-	1.58 (t)	43.9	H3-H4-H5	4.5
C-5	1.86-1.69 (m) 1.22-1.13 (m)	27.4	-	-	2.25-2.18 (m) 1.65-1.60 (m)	24.4	-	-
C-6	1.86-1.69 (m) 1.60-1.49 (m)	32.4	-	-	1.27-1.21 (m) 1.83-1.70 (m)	28.3	-	-
C-7	-	48.9	-	-	-	48.3	-	-
C-8	0.82 (s)	21.2	-	-	0.88 (s)	20.6	-	-
C-9	1.05 (s)	20.1	-	-	0.90 (s)	18.7	-	-
C-10	3.39 (d) 2.65 (d)	53.7	H10a-H10b H10a-H10b	13.0 13.5	2.83 (AB quartet)	58.1	H10a-H10b	14.0 25.5
C-11, 11'	3.75 (septet)	48.3	H11-H12- H13	6.5	3.73 (septet)	48.3	H11-H12- H13	6.5
C-12, 12'	1.33 (dd)	22.2	-	3.0, 6.5	1.30 (d)	22.3	-	7.0
C-13, 13'	-	22.7	-	-	-	22.2	-	-

Figure 4: ^1H - ^1H and ^1H - ^{13}C (HSQC) COSY spectra of II-15a.

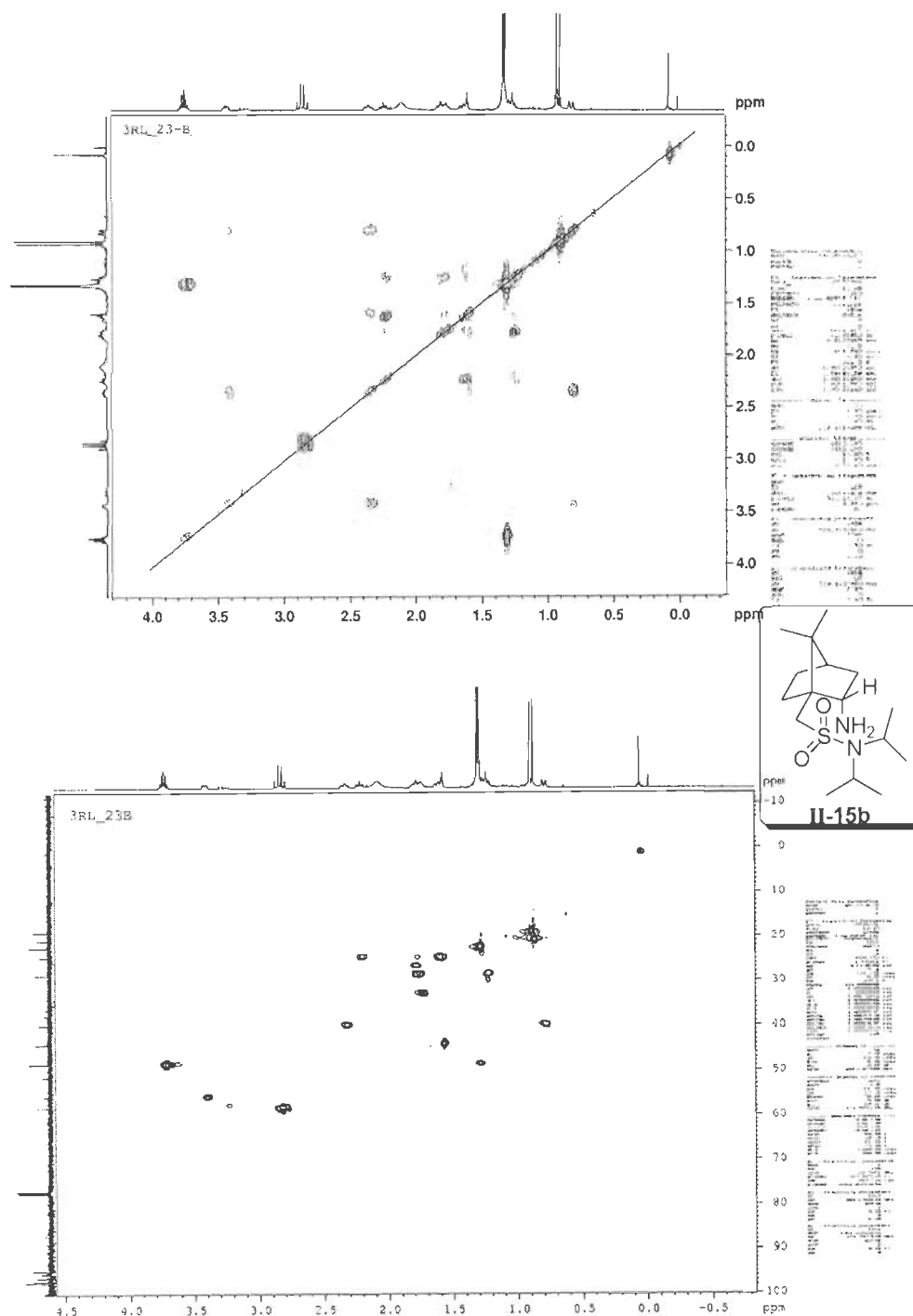
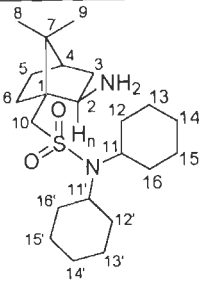
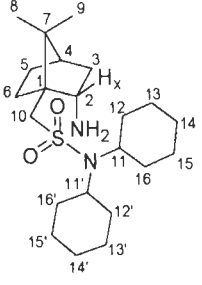


Figure 5: ^1H - ^1H and ^1H - ^{13}C (HSQC) COSY spectra of II-15b.

The dicyclohexyl 2-aminocamphorsulfonamides **II-16a,b** were characterized in a similar fashion using 1D and 2D NMR experiments. In case of *exo* **II-16a** signal for H-2_n proton appears as multiplet at δ 3.33-3.25 (mixed with 2-CH protons of cyclohexyl rings), while H-2_x of *endo* **II-16b** resonates at δ 3.43 as quartet of doublet. While the H-10 protons of *exo* **II-16a** appear as doublets at δ 3.37 and 2.66, those of *endo* **II-16b** appear as quartet at δ 2.83 (Table 3). The stereochemistry of *exo* **II-16a** and *endo* **II-16b** was unequivocally confirmed by NOESY ¹H NMR experiments. The NOESY study on *exo* isomer **II-16a** showed a cross-peak between H-2_n and the H-10 protons; while similar study on *endo* **II-16b** showed a cross-peak between H-2_x and CH₃-8 protons as shown in Figures 6 and 7.

Table 3: Proton and carbon chemical shifts and proton-proton coupling constants for *exo* and *endo* isomers **II-16a** and **II-16b**.

Position	 II-16a		 II-16b	
	δ_{H} (ppm) (multiplicity)	δ_{C} (ppm)	δ_{H} (ppm) (multiplicity)	δ_{C} (ppm)
C-2	3.33-3.25 (m)	57.1	3.43 (qd, $J = 2.0, 11.0$ Hz)	55.5
C-3	-	-	2.39-2.29 (m), 0.78 (dd, $J = 4.0, 8.5$ Hz)	39.8
C-8	0.83 (s)	21.2	0.89 (s)	20.6
C-9	1.06 (s)	20.1	0.92 (s)	18.7
C-10	3.37 (d, $J = 13.5$ Hz), 2.66 (d, $J = 13.0$ Hz)	54.6	2.83 (q, $J = 13.5$ Hz)	59.0
C-11, C-11'	3.33-3.25 (m)	57.1	3.26 (quintet, $J = 8.0$ Hz)	57.5

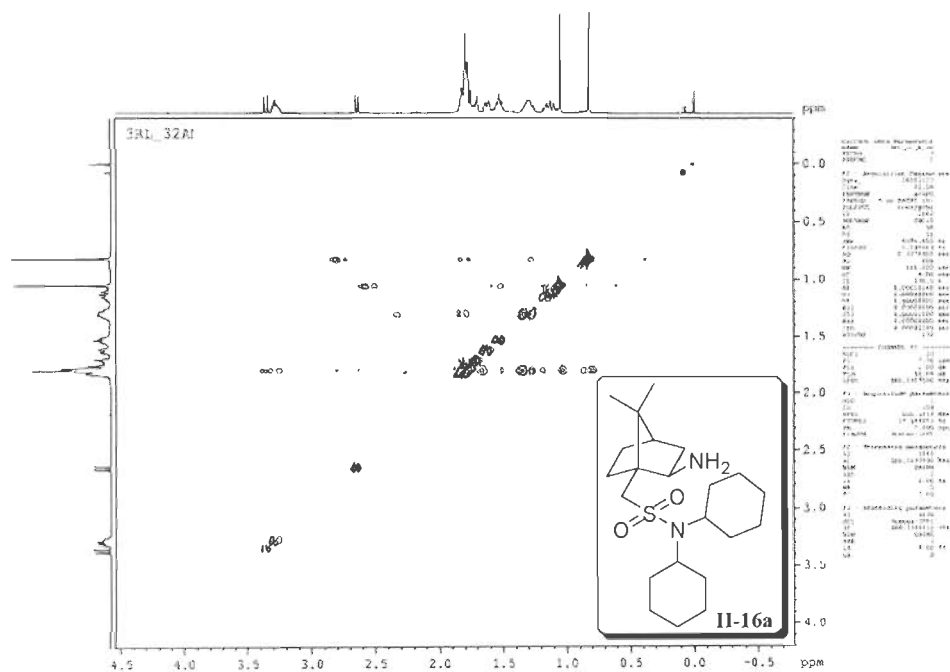


Figure 6: 500 MHz NOESY Spectrum of II-16a in CDCl₃.

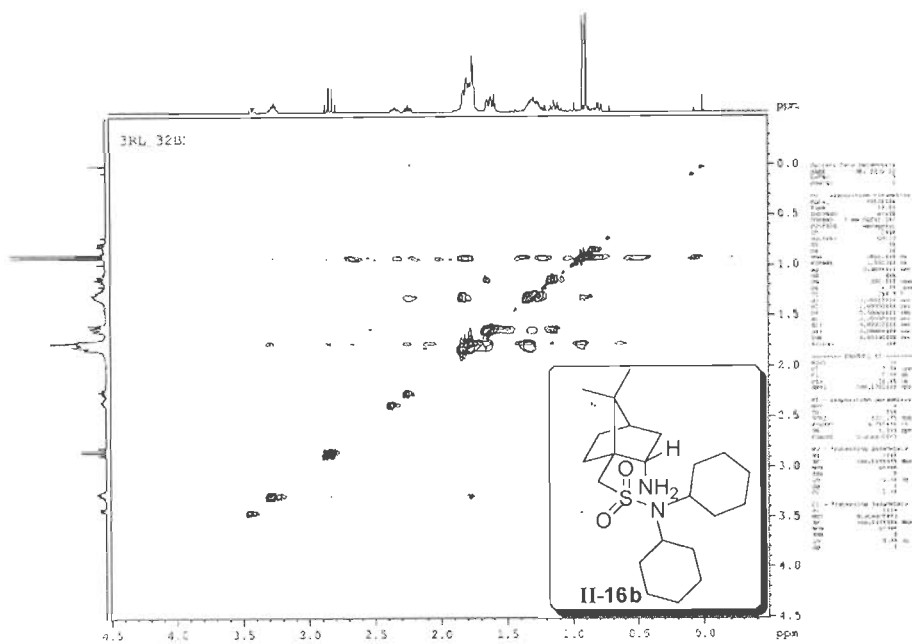
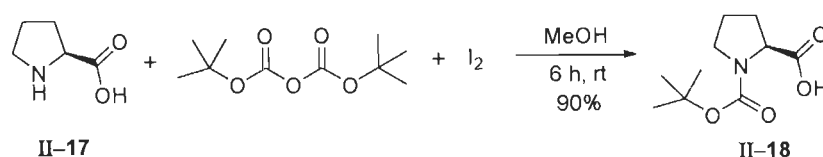


Figure 7: 500 MHz NOESY Spectrum of II-16b in CDCl₃.

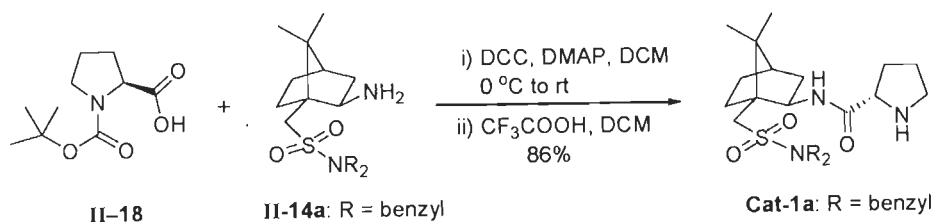
2.3.2. Synthesis of camphorsulfonamide-based prolinamides **Cat-1a**, **Cat-2a** and **Cat-3a,b**

Having dialkyl 2-amino-camphorsulfonamides in hand, we then proceeded to convert these amines into the corresponding prolinamides by coupling them with (*S*)-proline. Initially, we protected –NH group of proline as –NBoc with *tert*-butoxycarbonyl anhydride. This reaction was performed by stirring a solution of (*S*)-proline, with *tert*-butoxycarbonyl anhydride in methanol at room temperature in presence of catalytic amount of iodine. The desired *N*-*tert*-butoxycarbonyl-(*S*)-proline was obtained in excellent yield (Scheme 8).



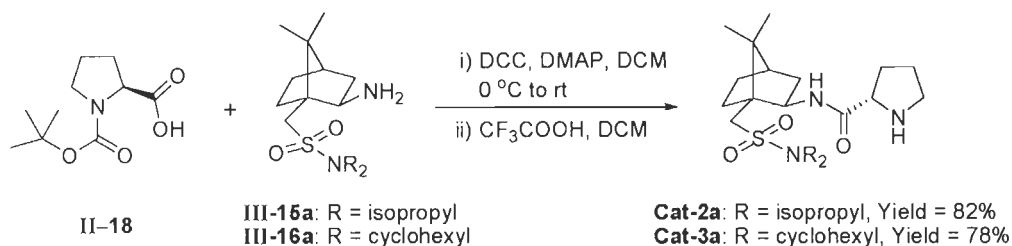
Scheme 8: Synthesis of *N*-*tert*-butoxycarbonyl-(*S*)-proline.

The coupling of primary amine **II-14a** with **II-18** was affected with dehydrating reagent dicyclohexylcarbodiimide. Thus to a solution of *N*-Boc proline under stirring, was added sequentially a solution of chiral amine and a solution of DCC and DMAP at 0 °C. The resulting reaction mixture was allowed to warm up to room temperature and stirred further for 16 h. After the usual workup, the crude reaction mixture was obtained which was further treated with trifluoroacetic acid to afford the prolinamide **Cat-1a** as a crude solid. Purification of this residue by silica gel chromatography furnished **Cat-1a** as yellowish solid in 86% yield from two steps (Scheme 9).



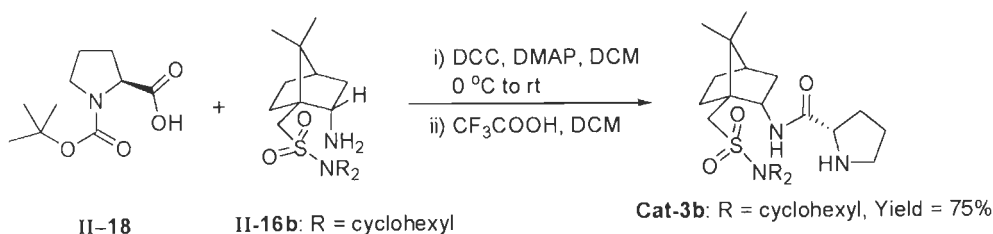
Scheme 9: Synthesis of prolinamide **Cat-1a**.

The other prolinamide derivatives were also synthesized by following same procedure as described above. The *exo* amines **II-15a** and **II-16a** were treated with *N*-protected proline **II-18** to provide the corresponding prolinamides **Cat-2a** and **Cat-3a**, respectively, in high yields (Scheme 10).



Scheme 10: Synthesis of prolinamides **Cat-2a** and **Cat-3a**.

After synthesizing prolinamides from *exo* isomers, *endo* isomer **II-16b** was subjected to coupling with *N*-protected proline **II-18**. Thus the reaction between *endo* **II-16b** and **II-18** was performed following the procedure described for the synthesis of **Cat-3a** to furnish **Cat-3b** in very high yield (Scheme 11).



Scheme 11: Synthesis of prolinamide **Cat-3b**.

All prolinamides were isolated by silica gel column chromatography and characterized by standard spectroscopic methods. The IR, ^1H and ^{13}C NMR, and HRMS were found to be in agreement with the assigned structure for **Cat-1a**, **Cat-2a**, **Cat-3a** and **Cat-3b**.

For **Cat-1a**, in IR the single stretching band at 3330 cm^{-1} indicates amide linkage of secondary amide and the amide I band (C=O stretching) and the amide II band (NH bending) appear at 1664 cm^{-1} . In ^1H NMR the signal at $\delta 8.11$ (d, $J = 7.5\text{ Hz}$, 1H) was assigned for $-\text{NH}$ proton of amide group on the basis of D_2O exchange experiment. The NH proton of pyrrolidine ring resonates at around $\delta 1.7$. The signal at $\delta 4.36$ as AB quartet with coupling constant $J = 15.0, 96.5\text{ Hz}$ is due to the benzylic protons. The signals at $\delta 0.98$ (s, 3H), $\delta 0.79$ (s, 3H) show the presence of two methyl groups C8 and C9 of camphor core in the compound and signals at $\delta 3.36$ and $\delta 2.59$ are due to the protons attached to C-10 carbon. Proton decoupled ^{13}C NMR and DEPT experiments in CDCl_3 (125 MHz) were also fully consistent with assigned structure

for **Cat-1a**. The HRMS (ES) spectrum was also in support of assigned structure for **Cat-1a**. HRMS (ES) spectrum shows (M+H) value 510.2791 (calculated 510.2746) was in agreement with molecular formula $C_{29}H_{39}N_3O_3S$ (M^+). The spectral data of organocatalysts **Cat-2a**, **Cat-3a** and **Cat-3b** is analogous to that of **Cat-1a**.

2.4. CONCLUSION

The novel prolinamide organocatalysts presented herein were synthesized from *N,N*-dialkyl camphorsulfonamides. The *endo* and *exo* 2-amino-camphorsulfonamides derived from reduction of the corresponding oximes were separated by silica gel column chromatography in good yields. Thus we have synthesized *N,N*-dialkyl 2-amino-camphorsulfonamides *exo* **II-14a-16a** and *endo* **II-14b-16b** for the first time. These amines were coupled with (2*S*)-proline to provide hitherto unknown prolinamides **Cat-1a**, **Cat-2a**, **Cat-3a** and **Cat-3b**. The *N,N*-dialkyl 2-amino-camphorsulfonamides and prolinamide organocatalysts were well characterized by modern analytical tools including 2D NMR.

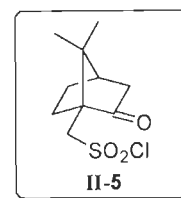
2.5. EXPERIMENTAL

2.5.1 General

All solvents were dried by using standard methods. Reagents were purchased at the highest commercial quality and used without further purification, unless otherwise mentioned. Yields refer to chromatographically homogeneous materials, unless otherwise stated. Reactions were monitored by thin-layer chromatography (TLC) carried out on 0.25 mm E. Merck silica gel plates (60F-254) using UV light as visualizing agent and/or iodine as developing agent. Silica gel (particle size 100- 200 mesh; SD Fine Chem Ltd.) was used for column chromatography. Melting points are uncorrected. IR spectra of the compounds were recorded on a Thermo Nicolet FT-IR NexusTM and are expressed as wavenumbers (cm⁻¹). ¹H NMR (500.13 MHz) and ¹³C NMR (125.76 MHz) spectra were recorded on Brüker AMX-500 instrument. The following abbreviations were used to explain the multiplicities: s = singlet, d = doublet, t = triplet, q = quartet, m = multiplet, b = broad. Elemental analyses were performed on VarioEL III CHNS instrument.

Synthesis of (7,7-dimethyl-2-oxobicyclo[2.2.1]heptan-1-yl)methanesulfonyl chloride (**II-5**)

(1S)-(+)-Camphor-10-sulfonic acid (**II-4**, 5.10 g, 22 mM) was added portion-wise to thionyl chloride (5.57 mL, 77 mM) and heated at reflux for 4 h. After completion of the reaction, excess of thionyl chloride was distilled off and the last traces of thionyl chloride were removed by azeotropic distillation with dry toluene (5 mL) to get the product **II-5** and used as such for next step without further purification.



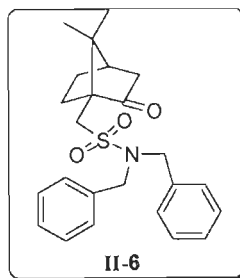
Time: 4 h.

Yield: 5.39 g (98%) as brown viscous liquid.

Synthesis of *N,N*-dibenzyl (7,7-dimethyl-2-oxobicyclo[2.2.1]heptan-1-yl)methanesulfonamide (**II-6**):

To a stirred solution of dibenzylamine (3.84 mL, 20 mM) and 4-*N,N*-dimethylaminopyridine (2.68 g, 22 mM) in dry DCM (20 mL) at 0 °C, a solution of sulfonyl chloride **II-5** (5.0 g, 20 mM) in dry DCM (20 mL) was added dropwise. After 1 h stirring at 0 °C, the resulting reaction

mixture was stirred at room temperature further for 5 h. After completion of the reaction, the reaction solution was diluted with ethyl acetate (160 mL). This solution was washed with water, then 1 N HCl followed by water. The combined organic layers were dried with anhyd. sodium sulfate and concentrated to dryness. The crude mixture was subjected to silica gel column chromatography using ethyl acetate/hexanes (10:90-30:70) to obtain pure product **II-6** as white solid.



Time: 6 h.

Yield: 7.80 g (95%) as white solid.

IR (KBr) ν_{\max} : 2961, 2925, 1740, 1450, 1335, 1146, 1044, 896, 789, 758, 700 cm^{-1} .

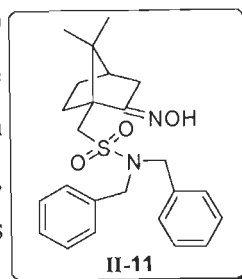
$^1\text{H NMR}$ (CDCl_3 , 500 MHz): δ 7.39-7.30 (m, 10H), 4.36 (AB quartet, $J = 15.0, 35.5$ Hz, 4H, CH_2Ph), 3.32 (d, $J = 14.5$ Hz, 1H), 2.64 (d, $J = 14.5$ Hz, 1H), 2.62-2.55 (m, 1H), 2.38 (td, $J = 3.5, 18.5$ Hz, 1H), 2.13-2.04 (m, 2H), 1.95 (d, $J = 18.5$ Hz, 1H), 1.75-1.67 (m, 1H), 1.48-1.41 (m, 1H), 1.15 (s, 3H), 0.80 (s, 3H) ppm.

$^{13}\text{C NMR}$ (CDCl_3 , 125 MHz): δ 215.2 (CO), 135.8 (C), 128.9, 128.7, 128.0 (C, Ph), 58.6 (C), 50.2 (CH_2), 49.4 (CH_2), 47.8 (C), 42.8 (CH), 42.6 (CH_2), 27.0 (CH_2), 25.4 (CH_2), 20.1 (CH_3), 19.7 (CH_3) ppm.

Elemental analysis: $\text{C}_{24}\text{H}_{29}\text{NO}_3\text{S}$; calcd. C 70.04, H 7.10, N 3.40, O 11.66, S 7.79; found C 70.00, H 7.04, N 3.25, O 11.58, S 7.70

Synthesis of *N,N*-dibenzyl 2-(hydroxyimino)-7,7-dimethylbicyclo[2.2.1]heptan-1-ylmethanesulfonamide (**II-11**):

To a solution of compound **II-6** (6.98 g, 17 mM) in absolute ethanol (80 mL), hydroxylamine hydrochloride (5.86 g, 85 mM) and triethylamine (10.64 mL, 76.5 mM, 4.5 equiv.) were added and resulting reaction mixture was refluxed at 80 °C for 16 h. After completion of the reaction, the resulting mixture was concentrated and diluted with ethyl acetate. This solution was washed twice with water and the combined organic layers



were dried over anhyd. Na_2SO_4 and concentrated under reduced pressure to give crude product. Crude reaction mixture was purified by silica gel column chromatography using ethyl acetate/hexanes (10:90) to furnish pure **II-11** as white solid.

Time: 16 h.

Yield: 7.10 g (98%) as white solid.

IR (KBr) ν_{max} : 3448, 2956, 2917, 1643, 1549, 1456, 1384, 1335, 1141, 1066, 932, 783, 742, 690 cm^{-1} .

^1H NMR (CDCl_3 , 500 MHz): δ 7.93 (s, 1H), 7.35-7.27 (m, 10H), 4.37 (AB quartet, $J = 15.0$, 91.5 Hz, 4H, CH_2Ph), 3.33 (d, $J = 14.0$ Hz, 1H), 2.72 (d, $J = 14.5$ Hz, 1H), 2.50-2.41 (m, 2H), 2.02 (d, $J = 18.0$ Hz, 1H), 1.94-1.85 (m, 2H), 1.84-1.77 (m, 1H), 1.33-1.25 (m, 1H), 0.98 (s, 3H), 0.67 (s, 3H) ppm.

^{13}C NMR (CDCl_3 125 MHz): δ 136.0 (C), 128.9, 128.6, 127.9 (C, Ph), 52.3 (C), 51.5 (CH_2), 50.1 (CH_2), 49.8 (C), 43.3 (CH), 32.7 (CH_2), 28.1 (CH_2), 27.2 (CH_2), 19.3 (CH_3), 19.1 (CH_3) ppm.

Elemental analysis: $\text{C}_{24}\text{H}_{30}\text{N}_2\text{O}_3\text{S}$; calcd. C 67.58, H 7.09, N 6.57, O 11.25, S 7.52; found C 67.50, H 7.00, N 6.48, O 11.20, S 7.45.

Synthesis of (2-amino-7,7-dimethylbicyclo[2.2.1]heptan-1-yl)-*N,N*-dibenzylmethanesulfonamide (II-14a and II-14b):

To a stirred solution of compound **II-11** (6.96 g, 14 mM) in dry methanol (50 mL) at 0 °C, ammonium acetate (12.93 g, 168 mM) and sodium cyanoborohydride (3.47 g, 56 mM) was added at 0 °C. To this, a solution of TiCl_3 (12% in HCl, 45.25 mL, 42 mM) was added slowly at the same temperature. The resultant reaction mixture was brought to room temperature by removing the cooling bath and stirring was continued at room temperature for further 7 h. Then the reaction was quenched by the addition of saturated NaHCO_3 solution and filtered through celite and the product was extracted twice with ethyl acetate from the filtrate. Combined organic layers were dried with anhyd. sodium sulfate and concentrated under reduced pressure to yield the crude product as a mixture of two (*exo* and *endo*) isomers in 80:20 ratio. This crude mixture

was subjected to silica gel chromatography using MeOH:DCM:hexanes (5:45:50) to obtain 3.12 g of *exo*-isomer **II-14a** and 0.782 g of *endo*-isomer **II-14b** in 68% combined yield.

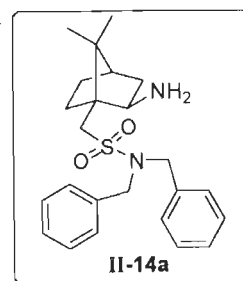
Time: 7 h.

(2-Amino-7,7-dimethylbicyclo[2.2.1]heptan-1-yl)-*N,N*-dibenzylmethanesulfonamide (*exo* amine II-14a):

Yield: 3.12g (54%) as light yellow solid.

IR (KBr) ν_{\max} : 3401, 3330, 3039, 2945, 2877, 1742, 1601, 1454, 1331, 1143, 1055, 934, 905, 794, 746, 703 cm^{-1} .

$^1\text{H NMR}$ (CDCl_3 , 500 MHz): δ 7.41-7.31 (m, 10H), 4.40 (AB quartet, $J = 15.0, 61.5$ Hz, 4H, CH_2Ph), 3.35 (d, $J = 13.5$ Hz, 1H), 3.31 (dd, $J = 5.5, 9.0$ Hz, 1H), 2.53 (d, $J = 13.5$ Hz, 1H), 1.87-1.69 (m, 4H), 1.60-1.49 (m, 4H), 1.23-1.16 (m, 1H), 0.96 (s, 3H), 0.73 (s, 3H) ppm.



$^{13}\text{C NMR}$ (CDCl_3 , 125 MHz): δ 135.9 (C), 128.8, 128.7, 128.0, (C, Ph), 57.1 (CH), 52.0 (CH_2), 50.2 (CH_2), 49.5 (C), 49.1 (C), 44.6 (CH), 40.1 (CH_2), 32.2 (CH_2), 27.4 (CH_2), 21.1 (CH_3), 19.9 (CH_3) ppm.

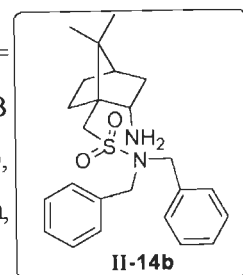
HRMS (ES⁺): (M^+H) $\text{C}_{24}\text{H}_{32}\text{N}_2\text{O}_2\text{S}$, calcd. 413.2218; found 413.2261.

(2-Amino-7,7-dimethylbicyclo[2.2.1]heptan-1-yl)-*N,N*-dibenzylmethanesulfonamide (*endo* amine II-14b):

Yield: 0.782 g (14%) as light brown viscous liquid.

IR (KBr) ν_{\max} : 3400, 3331, 3035, 2940, 2800, 1740, 1640, 1455, 1320, 1145, 1030, 746, 706 cm^{-1} .

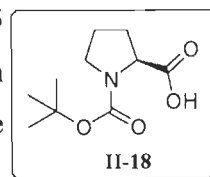
$^1\text{H NMR}$ (CDCl_3 , 500 MHz): δ 7.43-7.28 (m, 10H), 4.38 (AB quartet, $J = 15.0, 25.5$ Hz, 4H, CH_2Ph), 3.38 (qd, $J = 2.0, 10.5$ Hz, 1H), 2.66 (AB quartet, $J = 13.5, 34.5$ Hz, 2H), 2.40-2.31 (m, 1H), 2.30-2.20 (m, 1H), 1.84-1.69 (m, 2H), 1.62-1.55 (m, 2H), 1.31-1.22 (m, 1H), 1.01-0.88 (m, 1H), 0.86 (dd, $J = 3.0, 11.0$ Hz, 1H), 0.80 (s, 3H), 0.76 (s, 3H) ppm.



^{13}C NMR (CDCl_3 , 125 MHz): δ 135.6 (C), 128.8, 128.7, 128.0, (C, Ph), 56.3 (CH), 55.6 (CH_2), 51.5 (CH_2), 50.9 (C), 50.1 (C), 44.0 (CH), 39.9 (CH_2), 28.4 (CH_2), 24.2 (CH_2), 20.5 (CH_3), 18.6 (CH_3) ppm.

Synthesis of *N*-Boc proline (II-18):

To a solution of (*S*)-proline (5.75 g, 50 mM) in MeOH, $(\text{Boc})_2\text{O}$ (1.19 g, 5.5 mM) and iodine (1.26 g, 5 mM) were added and the resulting reaction mixture was stirred for 5 h at room temperature. After completion of the reaction, the solvent was evaporated to dryness. The residue was redissolved in ethyl acetate and washed successively with water, sodium thiosulphate and brine solution. The organic layer was dried over anhyd. Na_2SO_4 and evaporated under reduced pressure to get the crude product. The crude solid was recrystallized in ethyl acetate-hexanes to furnish the product **II-18** as white crystalline solid.



Time: 5 h.

Yield: 9.6 g (90%) as white crystalline solid.

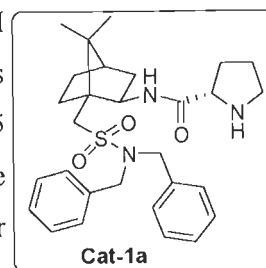
IR (KBr) ν_{max} : 3668, 2918, 2853, 2712, 1721, 1613, 1495, 1463, 1365, 1093, 1052 cm^{-1} .

^1H NMR (CDCl_3 , 500 MHz): δ 4.36-4.20 (m, 1 H), 3.60-3.31 (m, 2 H), 2.39-2.22 (m, 1 H), 2.02-2.01 (m, 1 H), 1.99-1.83 (M, 2 H), 1.48 and 1.42 (s, 9 H).

^{13}C NMR (CDCl_3 , 125 MHz): δ 178.3, 176.2, 155.6, 153.9, 80.7, 80.3, 58.9, 46.7, 46.2, 30.7, 29.1, 28.3, 28.1, 24.2, 23.5.

[2-(*L*-Prolyl)amido-7,7-dimethylbicyclo[2.2.1]heptan-1-yl]-*N,N*-dibenzylmethanesulfonamide (*exo* isomer **Cat-1a**):

To a stirred solution of *N*-Boc-proline (**II-18**, 1.07 g, 5 mM) in DCM (10 mL), *exo* amine **II-14a** (2.0 g, 5 mM) in dry DCM (10 mL) was added at room temperature. To this, a solution of DMAP (61 mg, 0.5 mM) and DCC (2.06 g, 10 mM) in dry DCM (15 mL) was added. The resulting reaction mixture was stirred for further 16 h. After completion of the reaction, the contents were filtered and washed



successively with 1 N HCl, water, saturated NaHCO₃ and brine solution. The organic layer was dried over anhyd. Na₂SO₄, concentrated under reduced pressure and the residue was purified by flash column chromatography to afford the corresponding *N*-Boc-prolinamide (2.79 g) as off white solid. This solid was dissolved in DCM (10 mL) and TFA (5.2 g, 46 mM) was added to it. The resulting reaction mixture was stirred for 1 h. After completion of the reaction, the mixture was evaporated to dryness and re-dissolved in DCM and washed with saturated Na₂CO₃ solution and brine. The organic layer was dried over anhyd. Na₂SO₄ and concentrated under reduced pressure. The residue was purified by silica gel chromatography using ethyl acetate:hexanes (20:80) to afford prolinamide **Cat-1a**.

Time: 16 h (1st step) and 1 h (2nd step).

Yield: 2.19 g (86%, two steps) as light yellow solid.

IR (KBr) ν_{\max} : 3330, 2931, 2846, 1664, 1567, 1508, 1453, 1336, 1198, 1145, 1052, 933, 900, 795, 701 cm⁻¹.

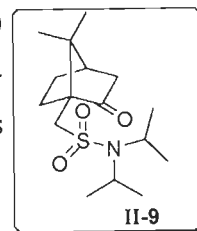
¹H NMR (CDCl₃, 500 MHz): δ 8.11 (d, J = 7.5 Hz, 1H), 7.39-7.30 (m, 10H), 4.36 (AB quartet, J = 15.0, 96.5 Hz, 4H, CH₂Ph), 4.13 (sextet, J = 4.5 Hz, 1H), 3.94 (t, J = 7.5 Hz, 1H), 3.36 (d, J = 14.5 Hz, 1H), 2.97-2.91 (m, 1H), 2.86-2.77 (m, 1H), 2.59 (d, J = 14.0 Hz, 1H), 2.12-1.90 (m, 5H), 1.82-1.66 (m, 6H), 1.32-1.24 (m, 1H), 0.98 (s, 3H), 0.79 (s, 3H) ppm.

¹³C NMR (CDCl₃, 125 MHz): δ 135.8 (C), 128.7, 128.7, 127.9 (C, Ph), 60.3 (CH), 55.0 (CH), 52.1 (CH₂), 50.3 (CH₂), 49.6 (C), 49.4 (C), 46.7 (CH₂), 44.6 (CH), 39.9 (CH₂), 33.1 (CH₂), 29.1 (CH₂), 27.2 (CH₂), 25.8 (CH₂), 20.4 (CH₃), 20.1 (CH₃) ppm.

HRMS (ES⁺): (M⁺+H) C₂₉H₃₉N₃O₃S, calcd. 510.2746; found 510.2791.

Synthesis of *N,N*-diisopropyl (7,7-dimethyl-2-oxobicyclo[2.2.1]heptan-1-yl)methanesulfonamide (**II-9**):

Compound **II-9** was synthesized from diisopropylamine (2.79 mL, 20 mM) and compound **II-5** (5.0 g, 20 mM) in presence of 4-*N,N*-dimethylamino-pyridine (2.68 g, 22 mM) following the procedure described for the synthesis of sulfonamide **II-6**.



Time: 5 h.

Yield: 5.67 g (90%) as white solid.

IR (KBr) ν_{\max} : 3458, 2963, 2923, 1705, 1628, 1457, 1415, 1297, 1145, 938, 878, 723, 597 cm^{-1} .

^1H NMR (CDCl_3 , 500 MHz): δ 3.80 (septet, $J = 7.0$ Hz, 2H), 3.34 (d, $J = 14.5$ Hz, 1H), 2.80 (d, $J = 14.5$ Hz, 1H), 2.65-2.58 (m, 1H), 2.38 (td, $J = 3.5, 18.5$ Hz, 1H), 2.11-2.01 (m, 2H), 1.94 (d, $J = 18.0$ Hz, 1H), 1.67-1.59 (m, 1H), 1.44-1.38 (m, 1H), 1.35 (t, $J = 7.0$ Hz, 12H), 1.18 (s, 3H), 0.90 (s, 3H) ppm.

^{13}C NMR (CDCl_3 , 125 MHz): δ 210.5 (CO), 138.2 (C), 56.2 (CH_2), 52.0 (C), 49.4 (C), 45.3 (CH), 43.4 (CH), 31.6 (CH_2), 30.6 (CH_2), 28.1 (CH_2), 23.7 (CH_3), 22.8 (CH_3), 20.1 (CH_3), 19.3 (CH_3).

Elemental analysis: $\text{C}_{16}\text{H}_{29}\text{NO}_3\text{S}$; calcd. C 60.92, H 9.27, N 4.44, O 15.21, S 10.16; found C 60.88, H 9.20, N 4.40, O 15.16, S 10.10.

Synthesis of *N,N*-diisopropyl (2-(hydroxyimino)-7,7-dimethylbicyclo[2.2.1]heptan-1-yl)methanesulfonamide (II-12):

Compound **II-12** was synthesized from compound **II-9** (4.72 g, 15 mM) and hydroxylamine hydrochloride (5.17 g, 75 mM) in presence of triethylamine (9.39 mL) following the procedure described for the synthesis of oxime **II-11**.

Time: 16 h.

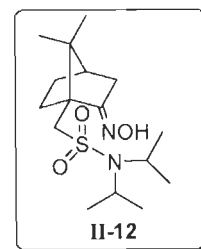
Yield: 4.70 g (95%) as white solid.

IR (KBr) ν_{\max} : 3414, 2967, 2941, 2877, 1634, 1459, 1382, 1324, 1191, 1130, 981, 774, 697 cm^{-1} .

^1H NMR (CDCl_3 , 500 MHz): δ 7.43 (s, OH, 1H), 3.79 (septet, $J = 7.0$ Hz, 2H), 3.41 (d, $J = 14.0$ Hz, 1H), 2.91 (d, $J = 14.5$ Hz, 1H), 2.63-2.52 (m, 2H), 2.08 (d, $J = 18.0$ Hz, 1H), 1.98-1.90 (m, 2H), 1.78-1.71 (m, 1H), 1.34 (t, $J = 7.0$ Hz, 13H), 1.12 (s, 3H), 0.87 (s, 3H) ppm

^{13}C NMR (CDCl_3 , 125 MHz): δ 168.2 (C), 53.1 (CH_2), 52.8 (C), 49.4 (C), 48.3 (CH), 43.7 (CH), 32.7 (CH_2), 28.2 (CH_2), 27.1 (CH_2), 22.7 (CH_3), 22.1 (CH_3), 19.5 (CH_3), 19.4 (CH_3) ppm.

Elemental analysis: $\text{C}_{16}\text{H}_{30}\text{N}_2\text{O}_3\text{S}$; calcd. C 58.15, H 9.15, N 8.48, O 14.52, S 9.70; found C 58.10, H 9.08, N 8.38, O 14.45, S 9.65.



Synthesis of (2-amino-7,7-dimethylbicyclo[2.2.1]heptan-1-yl)-*N,N*-diisopropylmethanesulfonamide (II-15a and II-15b):

The *exo* amine **II-15a** and *endo* amine **15b** were synthesized by the reduction of compound **II-12** (3.96 g, 12 mM) with sodium cyanoborohydride (4 equiv.) and solution of TiCl_3 (12% in HCl, 38.79 mL, 36 mM) in presence of ammonium acetate (12 equiv.) following the procedure described for the synthesis of isomeric amines **II-14a** and **II-14b**. The crude product was obtained as a mixture of two isomers (*exo* and *endo*) in 70:30 ratio. This crude mixture was subjected to silica gel chromatography using MeOH:DCM:hexanes (5:45:50) to afford 1.55 g of *exo* isomer **II-15a** and 0.657 g of *endo* isomer **II-15b** in 58% combined yield.

Time: 8.5 h.

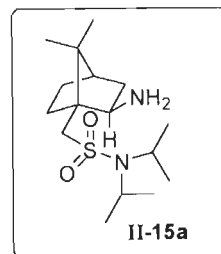
(2-Amino-7,7-dimethylbicyclo[2.2.1]heptan-1-yl)-*N,N*-diisopropylmethanesulfonamide (*exo* isomer **II-15a**):

Yield: 1.55 g (41%) as yellow solid.

IR (KBr) ν_{max} : 3742, 3451, 3399, 2947, 2872, 1640, 1463, 1381, 1324, 1127, 979, 886, 769, 651 cm^{-1} .

^1H NMR (CDCl_3 , 500 MHz): δ 3.75 (septet, $J = 6.5$ Hz, 2H), 3.39 (d, $J = 13.0$ Hz, 1H), 3.30 (dd, $J = 5.0, 9.0$ Hz, 1H), 2.65 (d, $J = 13.5$ Hz, 1H), 1.86-1.69 (m, 4H), 1.60-1.49 (m, 4H, 2H D_2O exchangeable), 1.33 (dd, $J = 3.0, 6.5$ Hz, 12H), 1.22-1.13 (m, 1H), 1.05 (s, 3H), 0.82 (s, 3H) ppm

^{13}C NMR (CDCl_3 , 125 MHz): δ 57.1 (CH), 53.7 (CH_2), 49.7 (C), 48.9 (C), 48.3 (CH), 44.7 (CH), 40.2 (CH_2), 32.4 (CH_2), 27.4 (CH_2), 22.7 (CH_3), 22.2 (CH_3), 21.2 (CH_3), 20.1 (CH_3) ppm.



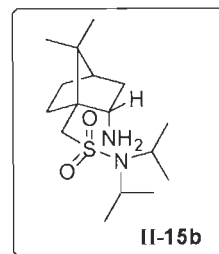
HRMS (ES⁺): ($\text{M}^+ + \text{H}$) $\text{C}_{16}\text{H}_{32}\text{N}_2\text{O}_2\text{S}$, calcd. 317.2218; found 317.2263.

(2-Amino-7,7-dimethylbicyclo[2.2.1]heptan-1-yl)-*N,N*-diisopropylmethanesulfonamide (*endo* isomer **II-15b**):

Yield: 0.657 g (17%) as light brown viscous liquid.

IR (KBr) ν_{max} : 3740, 3445, 3390, 2945, 2868, 1647, 1457, 1380, 1314, 1130, 979, 884, 779, 661 cm^{-1} .

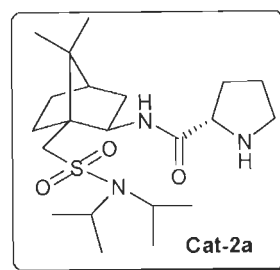
$^1\text{H NMR}$ (CDCl_3 , 500 MHz): δ 3.73 (septet, $J = 6.5$ Hz, 2H), 3.41 (d, $J = 9.5$ Hz, 1H), 2.83 (AB quartet, $J = 14.0, 25.5$ Hz, 2H), 2.37-2.29 (m, 1H), 2.25-2.18 (m, 1H), 1.83-1.70 (m, 3H), 1.65-1.60 (m, 1H), 1.58 (t, $J = 4.5$ Hz, 1H), 1.30 (d, $J = 7.0$ Hz, 12H), 1.27-1.21 (m, 1H), 0.90 (s, 3H), 0.88 (s, 3H), 0.79 (dd, $J = 4.0, 13.0$ Hz, 1H) ppm.



$^{13}\text{CNMR}$ (CDCl_3 , 125 MHz): δ 58.1 (CH_2), 55.5 (CH), 51.3 (C), 48.3 (CH), 43.9 (CH), 39.6 (CH_2), 28.3 (CH_2), 24.4 (CH_2), 22.3 (CH_3), 22.2 (CH_3), 20.6 (CH_3), 18.7 (CH_3) ppm.

[2-(L-prolyl)amido-7,7-dimethylbicyclo[2.2.1]heptan-1-yl]-N,N-diisopropylmethanesulfonamide (*exo* isomer **Cat-2a):**

To a stirred solution of *N*-Boc-proline (**II-18**, 1.71 g, 8 mM) in DCM (12 mL), compound **II-15a** (2.52 g, 8 mM) in dry DCM (12 mL) was added at room temperature. To this, a solution of DMAP (97 mg, 0.8 mM) and DCC (3.29 g, 16 mM) in dry DCM (18 mL) were added. The resulting reaction mixture was stirred for further 16 h. After completion of the reaction, the reaction mixture was filtered and the



filtrate was washed with 1N HCl, water, saturated NaHCO_3 and brine solution. The organic layer was dried over anhyd. Na_2SO_4 and evaporated under reduced pressure and the residue was purified by flash column chromatography to afford the corresponding *N*-Boc-prolinamide (3.66 g) as off white solid. This solid was dissolved in DCM (10 mL) and TFA (8.0 g, 71 mM) was added to it. The resulting reaction mixture was stirred for 1 h. After completion of the reaction, the reaction mixture was evaporated to dryness, re-dissolved in DCM and washed with saturated Na_2CO_3 solution and brine. The organic layer was dried over anhyd. Na_2SO_4 and evaporated under reduced pressure and the residue was purified by silica gel chromatography using ethyl acetate:hexanes (20:80) to afford pure prolinamide **Cat-2a**.

Time: 15 h (1st step) and 1 h (2nd step).

Yield: 2.70 g (82%, two steps) as off white solid.

IR (KBr) ν_{max} : (KBr) 3376, 3300 (OH, NH_2), 3068, 3036, 2993, 2966, 2872, 2835, 1576, 1455 cm^{-1} .

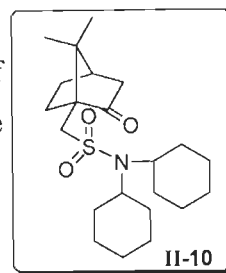
^1H NMR (CDCl₃, 500 MHz): δ 8.07 (d, J = 7.0 Hz, 1H), 4.07 (dt, J = 5.0, 8.5 Hz, 1H), 3.97 (t, J = 7.0 Hz, 1H), 3.72 (septet, J = 6.5 Hz, 2H), 3.38 (d, J = 14.5 Hz, 1H), 3.18-3.11 (m, 1H), 3.05-2.97 (m, 1H), 2.77 (d, J = 14.0 Hz, 1H), 2.18-2.08 (m, 3H), 1.99-1.68 (m, 7H), 1.32 (d, J = 6.5 Hz, 6H), 1.31 (d, J = 6.0 Hz, 6H), 1.26-1.21 (m, 2H), 1.07 (s, 3H), 0.98 (s, 3H) ppm.

^{13}C NMR (CDCl₃, 125 MHz): δ 171.4 (CO), 60.3 (CH), 55.8 (CH), 54.2 (CH₂), 50.0 (C), 48.9 (C), 48.3 (CH), 46.8 (CH₂), 45.0 (CH), 39.6 (CH₂), 33.1 (CH₂), 29.3 (CH₂), 27.1 (CH₂), 26.0 (CH₂), 22.8 (CH₃), 21.7 (CH₃), 20.8 (CH₃), 20.1 (CH₃) ppm.

HRMS (ES⁺): (M⁺+H) C₂₁H₃₉N₃O₃S, calcd. 414.2746; found 414.2791.

Synthesis of *N,N*-dicyclohexyl (7,7-dimethyl-2-oxobicyclo[2.2.1]heptan-1-yl)methanesulfonamide (II-10):

The sulfonamide **II-10** was synthesized from dicyclohexylamine (3.97 mL, 20 mM) and camphorsulfonyl chloride **II-5** (5.0 g, 20 mM) in presence of 4-*N,N*-dimethylaminopyridine (2.68 g, 22 mM) following the procedure described for the synthesis of sulfonamide **II-6**.



Time: 6 h.

Yield: 6.79 g (86%) as white solid.

IR (KBr) ν_{max} : 2931, 2854, 1746, 1635, 1453, 1331, 1152, 1047, 979, 773, 738 cm⁻¹.

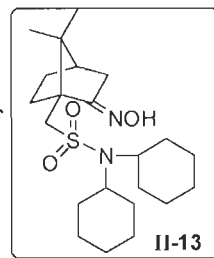
^1H NMR (CDCl₃, 500 MHz): δ 3.38-3.27 (m, 3H), 2.81 (d, J = 14.0 Hz, 1H), 2.68-2.59 (m, 1H), 2.39 (td J = 3.5, 18.5 Hz, 1H), 2.13-2.02 (m, 2H), 1.94 (d, J = 18.5 Hz, 1H), 1.89-1.78 (m, 13H), 1.69-1.60 (m, 2H), 1.46-1.28 (m, 4H), 1.20 (s, 3H), 1.14 (tq, J = 3.5, 13.5 Hz, 2H), 0.92 (s, 3H) ppm.

^{13}C NMR (CDCl₃, 125 MHz): δ 215.7 (CO), 59.0 (C), 57.7 (CH), 52.2 (CH₂), 47.5 (C), 43.0 (CH), 42.6 (CH₂), 33.0 (CH₂), 32.6 (CH₂), 26.9 (CH₂), 26.5 (CH₂), 26.5 (CH₂), 25.3 (CH₂), 25.2 (CH₂), 20.3 (CH₃), 19.9 (CH₃) ppm.

Elemental analysis: C₂₂H₃₇NO₃S; calcd. C 66.79, H 9.43, N 3.54, O 12.13, S 8.11; found C 66.70, H 9.38, N 3.47, O 12.10, S 8.08.

Synthesis of *N,N*-dicyclohexyl (2-(hydroxyimino)-7,7-dimethylbicyclo[2.2.1]heptan-1-yl)-methanesulfonamide (**II-13**):

The oxime **II-13** was synthesized from sulfonamide **II-10** (5.92 g, 15 mM) and hydroxylamine hydrochloride (5.17 g, 75 mM) in presence of triethylamine (9.39 mL) following the procedure described for the synthesis of oxime **II-11**.



Time: 18 h.

Yield: 5.78 g (94%) as white solid.

IR (KBr) ν_{\max} : 3380, 2933, 2859, 1635, 1450, 1329, 1151, 1107, 1047, 981, 780, 741 cm^{-1} .

^1H NMR (CDCl_3 500 MHz): δ 7.88 (s, 1H), 3.39 (d, $J = 9.0$ Hz, 1H), 3.37-3.27 (m, 2H), 2.91 (d, $J = 14.5$ Hz, 1H), 2.64-2.53 (m, 2H), 2.10 (d, $J = 17.5$ Hz, 1H), 1.98-1.90 (m, 2H), 1.86-1.75 (m, 12H), 1.69-1.63 (m, 3H), 1.41-1.26 (m, 5H), 1.21-1.00 (m, 5H), 0.87 (s, 3H) ppm.

^{13}C NMR (CDCl_3 125 MHz): δ 168.0 (CO), 57.5 (CH), 54.0 (CH_2), 52.8 (C), 49.5 (C), 43.6 (CH), 33.1 (CH_2), 33.0 (CH_2), 32.4 (CH_2), 28.2 (CH_2), 27.1 (CH_2), 26.5 (CH_2), 26.5 (CH_2), 25.2 (CH_2), 19.5 (CH_3), 19.4 (CH_3) ppm.

Elemental analysis: $\text{C}_{22}\text{H}_{38}\text{N}_2\text{O}_3\text{S}$; calcd. C 64.35, H 9.33, N 6.82, O 11.69, S 7.81; found C 64.30, H 9.30, N 6.58, O 11.60, S 7.75.

Synthesis of (2-amino-7,7-dimethylbicyclo[2.2.1]heptan-1-yl)-*N,N*-dicyclohexylmethanesulfonamide (**II-16a** and **II-16b**):

The amines **II-16a** and **16b** were synthesized from the reduction of oxime **II-13** (4.92 g, 12 mM), with sodium cyanoborohydride (4 equivalent) and solution of TiCl_3 (12% in HCl, 38.79 mL, 36 mM) in presence of ammonium acetate (12 equiv.) following the procedure described for the synthesis of amines **II-14a** and **II-14b**. The crude product was obtained as a mixture of two isomers (*exo* and *endo*) in 60:40 ratio. This crude mixture was subjected to silica gel chromatography using MeOH:DCM:hexanes (5:45:50) to furnish 1.84 g of *exo* isomer **II-16a** and 1.23 g of *endo* isomer **II-16b** in 65% combined yield.

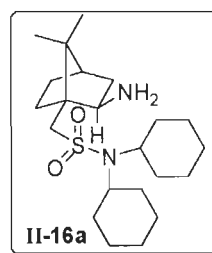
Time: 8.0 h.

(2-Amino-7,7-dimethylbicyclo[2.2.1]heptan-1-yl)-*N,N*-dicyclohexylmethanesulfonamide
(*exo*-isomer II-16a):

Yield: 1.84 g (39%) as yellow solid.

IR (KBr) ν_{\max} : 3463, 3401, 2932, 2860, 1633, 1457, 1319, 1141, 1045, 984, 817, 774, 639 cm^{-1}

^1H NMR (CDCl_3 , 500 MHz): δ 3.37 (d, $J = 13.5$ Hz, 1H), 3.33-3.25 (m, 3H), 2.66 (d, $J = 13.0$ Hz, 1H), 1.86-1.60 (m, 19H, 1H D_2O exchangeable), 1.58-1.50 (m, 3H, 1H D_2O exchangeable), 1.37-1.26 (m, 4H), 1.21-1.10 (m, 3H), 1.06 (s, 3H), 0.83 (s, 3H) ppm.



^{13}C NMR (CDCl_3 , 125 MHz): δ 57.6 (CH), 57.1 (CH), 54.6 (CH_2), 49.8 (C), 48.9 (C), 44.7 (CH), 40.0 (CH_2), 33.0 (CH_2), 32.7 (CH_2), 32.5 (CH_2), 27.4 (CH_2), 26.5 (CH_2), 25.2 (CH_2), 21.2 (CH_3), 20.1 (CH_3) ppm.

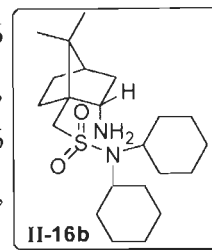
HRMS (ES $^+$): (M^+H) $\text{C}_{22}\text{H}_{40}\text{N}_2\text{O}_2\text{S}$, calcd. 397.2844; found 397.2887.

(2-Amino-7,7-dimethylbicyclo[2.2.1]heptan-1-yl)-*N,N*-dicyclohexylmethanesulfonamide
(*endo* isomer II-16b):

Yield: 1.23 g (26%) as light brown viscous liquid.

IR (KBr) ν_{\max} : 3460, 3395, 2925, 2850, 1630, 1456, 1311, 1137, 1042, 970, 810, 770, 628 cm^{-1} .

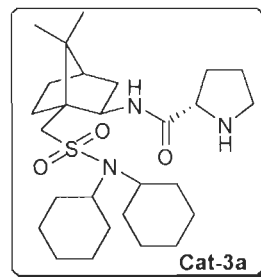
^1H NMR (CDCl_3 , 500 MHz): δ 3.43 (qd, $J = 2.0, 11.0$ Hz, 1H), 3.26 (quintet, $J = 8.0$ Hz, 2H), 2.83 (q, $J = 13.5$ Hz, 2H), 2.39-2.29 (m, 1H), 2.28-2.20 (m, 1H), 1.86-1.71 (m, 15H, 1H D_2O exchangeable), 1.66-1.56 (m, 4H), 1.36-1.20 (m, 5H), 1.11 (tq, $J = 3.5, 13.5$ Hz, 2H), 0.92 (s, 3H), 0.89 (s, 3H), 0.78 (dd, $J = 4.0, 8.5$ Hz, 1H) ppm.



^{13}C NMR (CDCl_3 , 125 MHz): δ 59.0 (CH_2), 57.5 (CH), 55.5 (C), 54.6 (CH_2), 51.3 (C), 43.9 (CH), 39.8 (CH_2), 32.7 (CH_2), 32.6 (CH_2), 28.4 (CH_2), 26.3 (CH_2), 25.1 (CH_2), 24.4 (CH_2), 20.6 (CH_3), 18.7 (CH_3) ppm.

[2-(*L*-propyl)amido-7,7-dimethylbicyclo[2.2.1]heptan-1-yl)-*N,N*-dicyclohexylmethanesulfonamide (*exo* isomer **Cat-3a):**

To a stirred solution of *N*-Boc-proline (**II-18**, 1.71 g, 8 mM) in DCM (12 mL), compound **II-16a** (3.16 g, 8 mM) in dry DCM (12 mL) was added at room temperature. To this a solution of DMAP (97 mg, 0.8 mM) and DCC (3.29 g, 16 mM) in dry DCM (18 mL) was added. The resulting reaction mixture was stirred for further 16 h. After completion of the reaction, the reaction mixture was filtered and the filtrate was



washed with 1N HCl, water, saturated NaHCO₃ and brine solution. The organic layer was dried over anhyd. Na₂SO₄ and evaporated under reduced pressure. The residue was purified by flash column chromatography to afford the corresponding *N*-Boc-prolinamide (3.66 g) as off white solid. The solid was dissolved in DCM (10 mL) and TFA (8.0 g, 71 mM) was added to it. The resulting reaction mixture was stirred for 1 h. After completion of the reaction, the reaction mixture was evaporated to dryness and re-dissolved in DCM and washed with saturated Na₂CO₃ solution and brine. The organic layer was dried over anhyd. Na₂SO₄ and evaporated under reduced pressure. The resultant residue was purified by silica gel chromatography using ethyl acetate:hexanes (20:80) to afford pure prolinamide **Cat-3a**.

Time: 16 h (1st step) and 1 h (2nd step).

Yield: 3.08 g (78%, two steps) as light yellow solid.

IR (KBr) ν_{\max} : 3443, 3305, 2931, 2859, 1671, 1516, 1457, 1326, 1144, 1048, 984, 893, 723, 645 cm⁻¹.

¹H NMR (CDCl₃, 500 MHz): δ 8.03 (d, J = 7.5 Hz, 1H), 4.04 (dt, J = 4.5, 8.5 Hz 1H), 3.91 (t, J = 7.0 Hz, 1H), 3.33 (d, J = 14.0 Hz, 1H), 3.25 (quintet, J = 7.5 Hz, 2H), 3.18-3.10 (m, 1H), 3.04-2.97 (m, 1H), 2.80 (d, J = 14.5 Hz, 1H), 2.13 (q, J = 6.5 Hz, 3H), 1.97-1.68 (m, 20H), 1.68-1.60 (m, 2H), 1.37-1.20 (m, 5H), 1.15-1.06 (m, 2H), 1.07 (s, 3H), 1.00 (s, 3H) ppm.

¹³C NMR (CDCl₃ 125 MHz): δ 60.4 (CH), 57.6 (CH), 56.0 (CH), 55.4 (CH₂), 50.4 (C), 48.7 (C), 46.8 (CH₂), 45.2 (CH), 39.5 (CH₂), 33.2 (CH₂), 33.1 (CH₂), 32.5 (CH₂), 27.1 (CH₂), 26.5 (CH₂), 26.4 (CH₂), 26.2 (CH₂), 25.2 (CH₂), 20.9 (CH₃), 20.1 (CH₃) ppm.

HRMS (ES⁺): (M⁺+H) C₂₇H₄₇N₃O₃S, calcd. 494.3372; found 494.3317.

[2-(L-prolyl)amido-7,7-dimethylbicyclo[2.2.1]heptan-1-yl)-N,N-dicyclohexylmethanesulfonamide (*endo* isomer **Cat-3b):**

The **Cat-3b** was synthesized from *N*-Boc-proline (**II-18**, 0.43 g, 2 mM) and compound **II-16b** (0.986 g, 2 mM) in presence of DMAP (24 mg, 0.2 mM) and DCC (0.820 g, 4 mM) following the procedure described for the synthesis of **Cat-3a**.

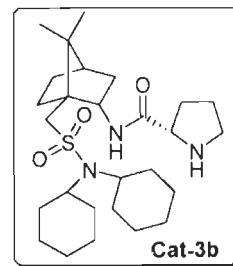
Time: 16 h (1st step) and 1 h (2nd step).

Yield: 0.915 g (75%, two steps) as light yellow solid.

IR (KBr) ν_{max} : 3440, 3308, 2930, 2857, 1670, 1513, 1455, 1324, 1140, 1045, 982, 891, 725, 640 cm^{-1} .

^1H NMR (CDCl_3 , 500 MHz): δ 7.91 (d, $J = 8.0$ Hz, 1H), 4.34-4.26 (m, 1H), 3.80-3.75 (m, 1H), 3.29-3.18 (m, 2H), 3.09-2.98 (m, 3H), 2.84 (d, $J = 14.0$ Hz, 1H), 2.45-2.35 (m, 1H), 2.20-2.10 (m, 1H), 1.94-1.88 (m, 2H), 1.82-1.68 (m, 16H), 1.65-1.58 (m, 3H), 1.28-1.24 (m, 4H), 1.09 (tq, $J = 4.0, 13.5$ Hz, 3H), 0.97 (s, 3H), 0.95 (s, 3H) ppm.

^{13}C NMR (CDCl_3 , 125 MHz): δ 60.7 (CH), 57.8 (CH), 57.3 (CH), 53.9 (CH_2), 50.6 (C), 50.2 (C), 46.7 (CH_2), 44.2 (CH), 37.8 (CH_2), 33.1 (CH_2), 32.4 (CH_2), 31.9 (CH_2), 30.2 (CH_2), 28.2 (CH_2), 26.4 (CH_2), 25.7 (CH_2), 25.2 (CH_2), 20.1 (CH_3), 18.9 (CH_3) ppm.



2.6. REFERENCES

1. P.I. Dalko, *Enantioselective Organocatalysis: Reactions and Experimental Procedures*, Wiley VCH: Weinheim 2007.
2. P.I. Dalko, L. Moisan, *In the Golden Age of Organocatalysis*, *Angew. Chem. Int. Ed.* 43 (2004) 5138.
3. M.J. Gaunt, C.C.C. Johansson, A. McNally, N.T. Vo, *Enantioselective Organocatalysis*, *Drug discov. Today* 12 (2007) 8.
4. D. Enders, C. Grondal, M.R.M. Hüttl, *Asymmetric Organocatalytic Domino Reactions*, *Angew. Chem. Int. Ed.* 46 (2007) 1570.
5. P.I. Dalko, L. Moisan, *Enantioselective Organocatalysis*, *Angew. Chem. Int. Ed.* 40 (2001) 3726.
6. P. Kočovský, A.V. Malkov, *Organocatalysis in Organic Synthesis*, *Tetrahedron* 62 (2006) 243.
7. B. List, *Introduction: Organocatalysis*, *Chem. Rev.* 107 (2007) 5413.
8. D. Enders, C. Grondal, M.R.M. Hüttl, *Asymmetric Organocatalytic Domino Reactions*, *Angew. Chem. Int. Ed.* 46 (2007) 1570.
9. H. Pellissier, *Asymmetric Organocatalysis*, *Tetrahedron* 63 (2007) 9267.
10. A. Dondoni, A. Massi, *Asymmetric Organocatalysis: From Infancy to Adolescence*, *Angew. Chem. Int. Ed.* 47 (2008) 4638.
11. D.W.C. MacMillan, *The Advent and Development of Organocatalysis*, *Nature* 455 (2008) 304.
12. T. Money, *Camphor: A Chiral Starting Material in Natural Product Synthesis*, *Nat. Prod. Rep.* 2 (1985) 253.
13. W. Oppolzer, *Camphor Derivatives as Chiral Auxiliaries in Asymmetric Synthesis*, *Tetrahedron* 43 (1987) 1969.
14. B.H. Kim, D.P. Curran, *Asymmetric Thermal Reactions with Oppolzer's Camphor Sultam*, *Tetrahedron* 49 (1993) 293.
15. R. Noyori, M. Kitamura, *Enantioselective Addition of Organometallic Reagents to Carbonyl Compounds: Chirality Transfer, Multiplication, and Amplification*, *Angew. Chem. Int. Ed. Engl.* 30 (1991) 49.

16. T.H. Yan, C.W. Tan, H.C. Lee, H.C. Lo, T.Y. Huang, *Asymmetric Aldol Reactions: A Novel Model for Switching Between Chelation- and Non-Chelation-Controlled Aldol Reactions*, *J. Am. Chem. Soc.* 115 (1993) 2613.
17. K. Tanaka, H. Uno, H. Osuga, H. Suzuki, *Stereocontrolled Cyclopropanation of α,β -Unsaturated Carboxamides Derived from Bicyclic Amino Alcohols*, *Tetrahedron: Asymm.* 5 (1994) 1175.
18. G. Helmchen, U. Leikauf, I. Taufer-Knoepfel, *Enantio- and anti-Diastereoselective Aldol Additions of Acetates and Propionates via O-Silylketene Acetals*, *Angew. Chem. Int. Ed. Engl.* 97 (1985) 874.
19. K. Soai, S. Niwa, *Enantioselective Addition of Organozinc Reagents to Aldehydes*, *Chem. Rev.* 92 (1992) 833.
20. I.V. Komarov, M.V. Gorichko, M.Yu. Kornilov, *Synthesis of Chiral Functionalized Phosphine Ligands Based on Camphor Skeleton*, *Tetrahedron: Asymm.* 8 (1997) 435.
21. M.V. Goricho, O.O. Grygorenko, I.V. Komarov, *A Chiral Tricyclic Proline Analogue Obtained from Camphor*, *Tetrahedron Lett.* 43 (2002) 9411.
22. T. Saito, D. Akiba, M. Sakairi, S. Kanazawa, *Preparation of a Novel, Camphor-Derived Sulfide and its Evaluation as a Chiral Auxiliary Mediator in Asymmetric Epoxidation via the Corey–Chaykovsky Reaction*, *Tetrahedron Lett.* 42 (2001) 57.
23. T. Saito, M. Sakairi, D. Akiba, *Enantioselective Synthesis of Aziridines from Imines and Alkyl Halides Using a Camphor-Derived Chiral Sulfide Mediator via the Imino Corey–Chaykovsky Reaction*, *Tetrahedron Lett.* 42 (2001) 5451.
24. Y. Li, X.-Q. Wang, C. Zheng, S.-L. You, *Highly Enantioselective Intramolecular Michael Reactions by D-Camphor-Derived Triazolium Salts*, *Chem. Commun.* (2009) 5823.
25. P. Bañuelos, J.M. García, E.G.-Bengoa, A. Herrero, J.M. Odriozola, M. Oiarbide, C. Palomo, J. Razkin, *(1R)-(+)-Camphor and Acetone Derived α -Hydroxy Enones in Asymmetric Diels-Alder Reaction: Catalytic Activation by Lewis and Brønsted Acids, Substrate Scope, Applications in Syntheses, and Mechanistic Studies*, *J. Org. Chem.* 75 (2010) 1458.

26. A.G.M. Barrett, D.C. Braddock, P.W.N. Christan, D. Pilipauskas, A.J.P. White, D.J. Williams, *Diastereoselective Conjugate Addition to (+)-Camphorsulfonic Acid Derived Nitroalkenes: Synthesis of α -Hydroxy and α -Amino Acids*, J. Org. Chem. 63 (1998) 5818.
27. J.-W. Chang, D.-P Jang, B.-J. Uang, F.-L. Liao, S.-L. Wang, *Enantioselective Synthesis of α -Hydroxy Acids Employing (1S)-(+)-N,N-Diisopropyl-10-Camphorsulphonamide as Chiral Auxiliary*, Org. Lett. 1 (1999) 2061.
28. V. Vaillancourt, M.R. Agharahimi, U.N. Sundram, O. Richou, D.J. Faulkner, K.F. Albizati, *Synthesis and Absolute Configuration of the Antiparasitic Furanoseliterpenes (-)-Furodysin and (-)-Furodysin. Camphor as a Six-Membered Ring Chiral Pool Template*, J. Org. Chem. 56 (1991) 378
29. Z.H. Tzeng, H.Y. Chen, C.T. Huang, K. Chen, *Camphor Containing Organocatalysts in Asymmetric Aldol Reaction In Water*, Tetrahedron Lett. 49 (2008) 4134.
30. C. Chang, S.H. Li, J.R. Reddy, K. Chen, *Pyrrolidine-Camphor Derivative as an Catalyst for Asymmetric Michael Additions of α,α -Disubstituted Aldehydes to β -Nitroalkenes: Construction of Quaternary Carbon-Bearing Aldehydes Under Solvent-Free Conditions*, Adv. Synth. Catal. 351 (2009) 1273.
31. A. Gayet, C. Bolea, P.G. Andersson, *Development of New Camphor Based N,S Chiral Ligands and Their Application in Transfer Hydrogenation*, Org. Biomol. Chem. 2 (2004) 1887.
32. M. Marzi, P. Minetti, G. Moretti, M.O. Tinti, F.D. Angelis, *Efficient Enantioselective Synthesis of (R)-(-)-Carnitine from Glycerol*, J. Org. Chem. 65 (2000) 6766.
33. O. Prieto, D.J. Ramoan, M. Yus, *Camphordisulfonamides: Good Chiral Ligands for the Addition of Dialkylzinc to Aliphatic Aldehydes*, Tetrahedron: Asymm. 11 (2000) 1629.

Chapter-3

ASYMMETRIC ALDOL REACTION CATALYZED BY CAMPHORSULFONAMIDE- BASED PROLINAMIDES

Asymmetric Aldol Reaction Catalyzed by Camphorsulfonamide-based Prolinamides

3.1. INTRODUCTION

The aldol reaction, discovered in 1838 [1], is arguably one of the most significant carbon-carbon bond forming reactions available to synthetic organic chemists [2-13]. This is a reliable transformation which can be applied to a broad range of substrates for the construction of new carbon-carbon bonds in a regio-, diastereo-, and enantioselective manner. In last few years, most attention has been focused on the use of small organic compounds as organocatalysts for asymmetric aldol reaction. In particular, the proline and its derivatives catalyzed aldol reaction attracted great attention, because of their synthetic value as well as mechanistic aspects [14-28]. This powerful organocatalytic protocol allows the direct cross-coupling between ketones and aldehydes. Most of the reactions catalyzed by proline or proline embedded molecules are performed in polar solvents such as DMF and DMSO [29-33].

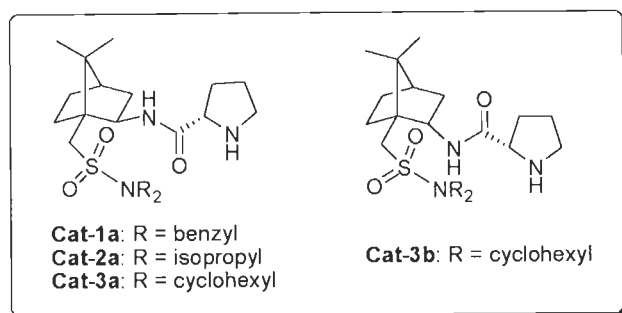
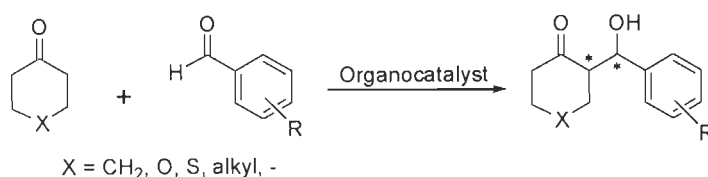
In the aldol reaction, condensation of enamine to a carbonyl compound followed by hydrolysis affords aldol adduct. The component that forms enamine is called aldol donor and the electrophilic component is known as aldol acceptor and the selective formation of any stereoisomer in this reaction constitutes an asymmetric process.

The Hajos-Parrish-Eder-Sauer-Wiechert reaction is an important example of an intramolecular enamine catalyzed aldol reaction. However, it was not until 2000 when List and Barbas demonstrated the same reaction in intermolecular fashion, using proline as a simple enamine catalyst [34,35]. After the pioneering work reported by List, Barbas and Lerner which proves proline as an active and versatile organocatalyst in the asymmetric aldol reaction, numerous organocatalysts have been designed for this reaction. Since 2000 significant developments in the utility of the enamine-catalyzed aldol reaction have been made. Simultaneously, remarkable efforts have been done to develop more efficient variants of proline [38,39], amino acids and peptides bearing primary amino groups [40,41], chiral imidazolidinones [42], cinchona alkaloid-derived amines for the asymmetric aldol reaction to furnish aldol adducts in excellent chemical as well as optical yields. In recent years, prolinamides have been established as another

class of organocatalysts for the direct asymmetric aldol reaction [43-56]. During our work was in progress reports on prolinamide-based organocatalysts [56-63] and camphor scaffold with thiourea motif [54] were appeared. Although the derivatization of amino functionality to groups such as amide provides more opportunity to perform reactions in various organic solvents, some drawbacks such as longer reaction times and low selectivities are associated with prolinamide catalysis.

3.2. OBJECTIVE

As mentioned in the previous chapter, we synthesized novel camphorsulfonamide-based organocatalysts **Cat-1a**, **2a**, **3a** and **3b**. These catalysts have been designed by rational combination of proline with amino group of amino-camphorsulfonamide entity through prolinamide functionality. We envisaged that these chiral catalysts can play a significant role for stereochemical control in aldol reaction of ketone with aromatic aldehydes which proceed *via* enamine



Scheme 1: Prolinamide catalyzed asymmetric aldol reaction.

intermediate formed between secondary amine of proline with carbonyl group of ketones. These catalyst architectures bearing amide linkage between proline and amino group of amino-camphorsulfonamide moiety would catalyze the aldol reaction *via* hydrogen bonding between the amide moiety of the catalyst with the carbonyl group of aldehyde and the alkyl groups on nitrogen of sulfonamide moiety would effectively block one of the faces of the substrate leading to diastereo- and enantioselective formation of the products. In addition, the solubility of these

catalysts is expected to increase in polar as well as non-polar organic solvents due to the presence of *N,N*-dialkyl camphorsulfonamide moiety (Scheme 1). Thus we planned to utilize the aforementioned camphorsulfonamide-based prolinamides as organocatalysts for direct intermolecular aldol reaction between cyclic/acyclic ketones as aldol donor and various aromatic aldehydes containing diversified substituents as aldol acceptors.

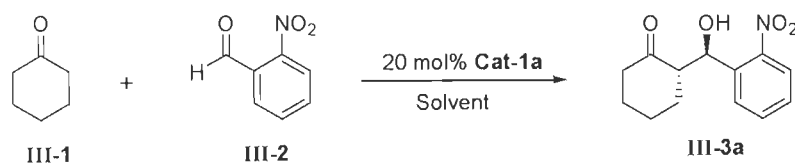
3.3. RESULTS AND DISCUSSION

3.3.1. Aldol reaction catalyzed by camphorsulfonamide-based prolinamides

The prolinamides **Cat-1a**, **Cat-2a**, **Cat-3a**, and **Cat-3b** were used as organocatalysts for asymmetric aldol reaction between ketones and aryl aldehydes. As a prelude to this objective, carried out the aldol reaction between cyclohexanone (**III-1**) and 2-nitrobenzaldehyde as a model reaction in presence of prolinamide **Cat-1a** derived from *N,N*-dibenzyl camphor-10-sulfonamide bearing *exo*-NH group at C-2 position of camphorsulfonamide moiety. Reactions were performed with cyclohexanone (0.4 mM) and 2-nitrobenzaldehyde (0.2 mM) in the presence of organocatalyst **Cat-1a** (0.04 mM, 20 mol%) in 0.5 mL of solvent. After completion of the reaction, crude product was submitted to ¹H NMR to find out diastereoselectivity and the residue was purified by silica gel column chromatography. The enantioselectivity of pure product **III-3a** was determined by HPLC analysis on a chiral stationary phase column (Chiralcel OD-H) using hexanes-isopropanol as eluting solvent. When the reaction was performed under neat conditions by using 15 equivalents of cyclohexanone without solvent at room temperature, it reached completion within 7 h to provide **III-3a** with excellent yield (90%) and diastereoselectivity (97:3) and good enantioselectivity (51%). Subsequently, we focused our attention on the effect of temperature on the outcome of the reaction anticipating better selectivity by lowering the reaction temperature. It was observed that enantioselectivity of adduct was slightly increased when the reaction was performed at low temperature. For example, in neat condition, the ee value for the aldol product **III-3a** was 51 and 58% (Table 1, entries 1 and 2) at room temperature and 0 °C, respectively. Encouraged by these results, we further lowered the reaction temperature and thus at -20 °C *anti* product was obtained in excellent yield with enhancement in enantioselectivity (Table 1, entry 3). When the reaction was performed in water as solvent, the product was obtained in poor enantioselectivity (17%). Then several polar and relatively non-polar solvents such as DMF, DMSO, CHCl₃ and CH₃CN were screened and the results are

summarized in Table 1. These studies identified chloroform as the optimal solvent for the reaction. Thus the reaction in chloroform at room temperature produced the aldol product **III-3a** in 66 h in excellent chemical yield (96%) and diastereoselectivity (99:1) with 97% ee for the major *anti* isomer (Table 1, entry 7). As the optimum results were obtained with 20 mol% catalyst **Cat-1a** loading, the reaction conditions were further tested by using 10 and 30 mol%

Table 1: Effect of solvent on direct aldol reaction of cyclohexanone with 2-nitrobenzaldehyde in presence of **Cat-1a**.^{a)}



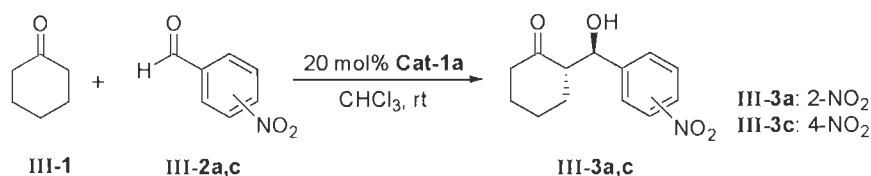
Entry	Solvent	Temp	Time	Yield (%)	dr (<i>anti:syn</i>) ^{b)}	ee (%) ^{c)}
1	neat	rt	7 h	90	97:3	51
2	neat	0 °C	10 h	89	92:8	58
3	neat	-20 °C	22 h	98	92:8	72
4	H ₂ O	rt	20 h	92	93:7	17
5	DMF	rt	62 h	92	95:5	80
6	CH ₂ Cl ₂	rt	70 h	90	90:10	50
7	CHCl₃	rt	66 h	96	99:1	97
8	DMSO	rt	80 h	88	85:15	80
9	DMSO-H ₂ O ^{d)}	rt	88 h	90	99:1	88
10	CH ₃ CN	rt	80 h	89	94:6	80
11	MeOH	rt	92 h	91	67:33	64

^{a)} Reactions were performed with cyclohexanone (0.4 mM) and 2-nitrobenzaldehyde (0.2 mM) in presence of **Cat-1a** (20 mol%) in 0.5 mL of solvent. ^{b)} Determined by ¹H NMR analysis of the crude sample. ^{c)} Of *anti* isomer and determined by HPLC analysis (Chiralcel OD-H). ^{d)} 0.5 mL of DMSO and 36 μL of H₂O were used.

catalyst **Cat-1a** loading (Table 2, entries 1 and 3). Though, we observed decrease in enantioselectivity (80%) and diastereoselectivity (92:8) of *anti* aldol product with 10 mol% catalyst loading, the reaction with 30 mol% catalyst loading provided **III-3a** of 97:3 diastereomeric ratio and 94% enantioselectivity. Thus the screening of the catalyst in various conditions identified the optimal solvent CHCl_3 at room temperature to carry out further asymmetric aldol reactions.

Encouraged by the preliminary data, we carried on to modify the hydrophobic groups on the nitrogen of the camphorsulfonamide moiety of the catalyst to examine the effect in rate, yield and diastereo- and enantio-selectivities of the reaction. The catalyst **Cat-2a**, derived from *N,N*-diisopropyl camphor-10-sulfonamide, having *exo*-NH group at C-2 position of camphorsulfonamide and the catalysts **Cat-3a** and **Cat-3b**, derived from *N,N*-dicyclohexyl camphor-10-sulfonamide, having both *exo*- and *endo*-NH groups at C-2 position of camphorsulfonamide moiety, respectively, were used as catalysts in 20 mol% for the aldol reaction of cyclohexanone with nitrobenzaldehydes. The results are summarized in Table 2. When catalytic activity of **Cat-2a** was examined in CHCl_3 at room temperature, the reaction was completed in favour of *anti* product **III-3a** in 72 h with 80% ee (Table 2, entry 4). In case of **Cat-3a** and **Cat-3b**, the reaction reached completion in 96 and 85 h to provide **III-3a** with 88 and 55% ee, respectively. Thus the asymmetric induction of the reaction catalyzed by **Cat-3b** bearing *endo*-NH group at C-2 position of camphorsulfonamide diastereoselectivity was diminished in comparison to that of the reaction catalyzed by **Cat-3a** catalyst bearing *exo*-NH group at C-2 position of camphorsulfonamide (Table 2, entries 5 and 6).

With optimal catalyst and reaction parameters established, a variety of aromatic aldehydes with diversified substituents were then evaluated as substrates and the results are summarized in Table 3. Several electron-rich and electron-deficient aldehydes with different substitution patterns gave rise to aldol products in high yields and with high levels of diastereo- and enantio-selectivity (Table 3). All the reactions proceeded smoothly at room temperature in CHCl_3 as solvent with 20 mol% of organocatalyst **Cat-1a** and reached completion in 3–4 days providing the products in high to excellent yields and dr in almost all cases studied. The *anti* aldol products were obtained as major adducts in high to excellent enantioselectivities (89–100%).

Table 2: Screening of organocatalysts.^{a)}

Entry	Catalyst (mol%)	Time (h)	Product	Yield (%)	dr(<i>anti:syn</i>) ^{b)}	ee (%) ^{c)}
1	Cat-1a (10)	120	III -3a	89	92:8	80
2	Cat-1a (20)	66	III -3a	96	99:1	97
3	Cat-1a (30)	68	III -3a	95	97:3	94
4	Cat-2a (20)	72	III -3a	91	90:10	80
5	Cat-3a (20)	96	III -3a	93	91:9	88
6	Cat-3b (20)	85	III -3a	90	70:30	55
7	Cat-1a (20)	72	III -3c	96	90:10	91
8	Cat-2a (20)	96	III -3c	89	89:11	58
9	Cat-3a (20)	72	III -3c	91	92:8	77

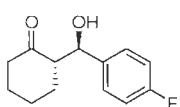
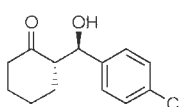
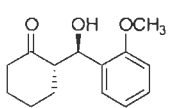
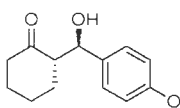
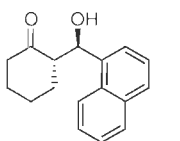
^{a)} Reactions were performed with cycloalkanone (0.4 mM) and aldehyde (0.2 mM) in the presence of organocatalyst **Cat-1a** (20 mol%) in 0.5 mL of CHCl₃. ^{b)} Determined by ¹H NMR analysis of the crude sample. ^{c)} Of *anti* isomer and determined by HPLC analysis (Chiralcel OD-H).

The reactions of cyclohexanone with *o*-, *m*- and *p*-nitrobenzaldehydes provided the corresponding aldol adducts **III-3a**, **III-3b** and **III-3c** with good to excellent diastereo- and enantioselectivity (Table 3, entries 1-3). The reactions of cyclohexanone with *o*-bromo- and *o*-chloro-benzaldehydes provided the corresponding aldol adducts **III-3d** and **III-3f** in good diastereoselectivity (96:4) and enantioselectivity (92% and 96% ee). The products **III-3e** and **III-3g** with *p*-bromo- and *p*-chloro-substitutions were obtained in comparable diastereoselectivity (92:8) and enantioselectivities (91 and 92% ee). In case of *p*-fluorobenzaldehyde, the diastereoselectivity was less in comparison to other halo-substituted aldol products. However, the fluoro adduct **III-3h** was obtained in excellent enantioselectivity (92% ee). The reaction of cyclohexanone with 1-naphthaldehyde furnished *anti* adduct **III-3i** as major product along with

15% of *syn* isomer. The *anti* aldol adduct **III-3l** was obtained in >99.9% enantiomeric purity, (Table 3, entry 12). While the aldol products **III-3j** and **III-3k** from *ortho* and *para*-substituted methoxy-benzaldehydes were obtained in 89 and 98% enantioselectivities, respectively, diastereoselectivity for *para*-substituted aldol product was less than *ortho*-substituted aldol product (Table 3, entries 10 and 11). The reactions of benzaldehydes bearing electron-withdrawing group are relatively faster than those with halo-substituent. No product was observed under the reaction conditions when benzaldehyde was used as a substrate.

Table 3: Aldol reaction of cyclohexanone with substituted benzaldehydes in the presence of **Cat-1a**.^{a)}

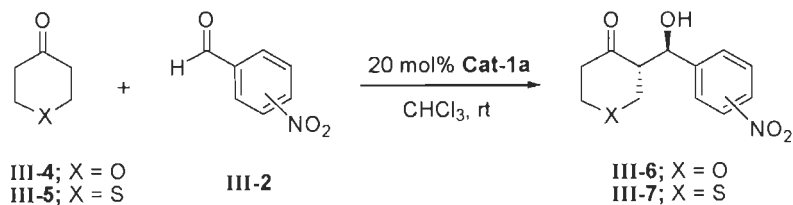
Entry	Product	Time	Yield (%)	dr (<i>anti</i> : <i>syn</i>) ^{b)}	ee (%) ^{c)}
1	III-3a	66 h	96	99:1	97
2	III-3b	72 h	94	95:5	90
3	III-3c	72 h	96	90:10	91
4	III-3d	88 h	89	96:4	92 ^{d)}
5	III-3e	90 h	91	92:8	91
6	III-3f	88 h	90	96:4	96
7	III-3g	90 h	92	92:8	92

8		III-3h	88 h	93	79:21	92
9		III-3i	72 h	95	94:6	92 ^{d)}
10		III-3j	72 h	90	95:5	89
11		III-3k	70 h	89	79:21	98 ^{d)}
12		III-3l	72 h	92	85:15	>99 ^{e)}

^{a)} Reactions were performed with cyclohexanone (0.4 mM) and aldehyde (0.2 mM) in the presence of an organocatalyst **Cat-1a** (20 mol%) in 0.5 mL of CHCl₃. ^{b)} Determined by ¹H NMR analysis of the crude sample. ^{c)} Of *anti* isomer and determined by HPLC analysis (Chiralcel OD-H). ^{d)} Of *anti* isomer and determined by HPLC analysis (Chiralpak AD-H). ^{e)} Of *anti* isomer and determined by HPLC analysis (on columns Chiralcel OD-H and Chiralpak AD-H) (see page 104 for Table 10 and page 109 for HPLC charts).

Encouraged by these results, we next probed the aldol reaction between aryl aldehydes and other six-membered cyclic ketones such as tetrahydropyran-4-one and tetrahydrothiopyran-4-one using catalyst **Cat-1a**. Again in these reactions, the aldol adducts exhibited in excellent diastereoselectivities and enantioselectivities. These reactions were carried out with 0.2 mM of aromatic aldehyde and 0.4 mM of tetrahydrothiopyran-4-one in 0.5 mL of CHCl₃ to afford corresponding aldol products. The reactions of tetrahydropyran-4-one and tetrahydrothiopyran-4-one with *o*-nitrobenzaldehyde provided the corresponding adducts **III-6a** and **III-7a** in very good yields with 95:5 and 97:3 diastereomeric ratios and 98% ee as shown in Table 4 (entries 1 and 3). The *p*-nitro products **III-6b** and **III-7b** derived from tetrahydropyran-4-one and tetrahydrothiopyran-4-one, respectively, were obtained in good diastereoselectivities but the enantioselectivity of **III-7b** was better than that of **III-6b**. The results are summarized in Table 4.

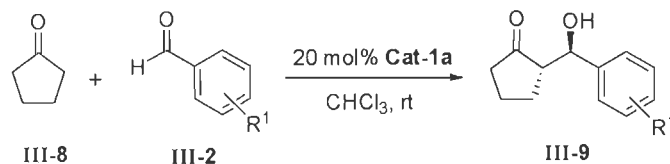
Encouraged by the results obtained from the six membered cyclic ketones, we then investigated the reactions of cyclopentanone and the results are summarized in Table 5. In the

Table 4: Aldol reaction of 4-oxa, 4-thia-cyclohexanones with substituted benzaldehydes in the presence of **Cat-1a**.^{a)}

Entry	Product	Time	Yield (%)	dr (<i>anti:syn</i>) ^{b)}	ee (%) ^{c)}
1	 III-6a	60 h	96	95:5	98
2	 III-6b	62 h	94	98:2	87
3	 III-7a	60 h	97	97:3	98 ^{d)}
4	 III-7b	62 h	95	96:4	95

^{a)} Reactions were performed with cycloalkanone (0.4 mM) and aldehyde (0.2 mM) in the presence of 20 mol% **Cat-1a** in 0.5 mL of CHCl_3 at rt. ^{b)} Determined by ^1H NMR (500 MHz) analysis of the crude sample. ^{c)} Of *anti* isomer and determined by HPLC analysis (Chiralpak AD-H) unless otherwise mentioned. ^{d)} Of *anti* isomer and determined by HPLC analysis (Chiralcel OD-H) (see page 104 for Table 10 and page 112 for HPLC charts).

reaction of cyclopentanone with substituted benzaldehydes, though the diastereoselective outcome of these reactions is not impressive, both the *syn* and *anti* products were obtained in high enantioselectivities. In all cases aldol adducts from nitrobenzaldehydes and halo-benzaldehydes were obtained in high enantiomeric excess with diminished diastereoselectivity. In case of 2-substituted bromobenzaldehyde and 4-substituted nitro- and fluoro-benzaldehydes, the diastereomers were obtained in near 1:1 ratio (Table 5, entries 3, 4 and 6). All reactions were furnished the corresponding aldol adducts **III-9a-f** with high to excellent chemical yields in 40-60 h.

Table 5: Aldol reaction of cyclopentanone with substituted benzaldehydes in the presence of **Cat-1a**.^{a)}

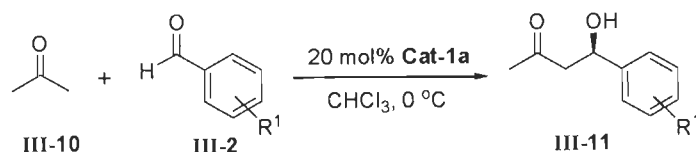
Entry	Product	Time	Yield (%)	dr (<i>anti:syn</i>) ^{b)}	ee(%) ^{c),d)}
1	III-9a	40 h	90	60:40	90 (74)
2	III-9b	48 h	89	45:55	90 (78) ^{e)}
3	III-9c	52 h	91	53:47	86 (84)
4	III-9d	58 h	87	51:49	87 (94)
5	III-9e	60 h	85	40:60	92 (84)
6	III-9f	58 h	86	48:52	79 (75)

^{a)} Reactions were performed with cyclopentanone (0.4 mM) and aldehyde (0.2 mM) in the presence of 20 mol% **Cat-1a** in 0.5 mL of CHCl_3 at room temperature. ^{b)} Determined by ^1H NMR (500 MHz) analysis of the crude sample. ^{c)} Of *anti* isomer, and the value in parenthesis of *syn* isomer. ^{d)} Determined by HPLC analysis (Chiralpak AD-H) unless otherwise mentioned. ^{e)} Determined by HPLC analysis (Chiralcel OD-H) (see page 106 for Table 11 and page 113 for HPLC charts).

To examine the generality of this organocatalytic approach, the reactions of acetone were investigated with nitro- and halo-benzaldehydes. The reaction of acetone with *o*-nitrobenzaldehyde in the presence of 20 mol% **Cat-1a** at room temperature afforded the aldol adduct **III-11a** in 88% yield and 77% ee in 24 h. When the same reaction was performed at 0 °C, the adduct **III-**

11a was obtained in excellent chemical and optical yields. In case of *m*- and *p*-nitrobenzaldehydes yield was excellent but enantioselectivity was diminished (Table 6, entries 2 and 3). The reactions of acetone with halo-benzaldehydes were carried out under similar conditions and results are summarized in Table 6. The asymmetric induction in organocatalyst **Cat-1a** mediated aldol reaction of acetone was high. The chemical yields of these adducts were very high as no dehydration products were observed. When the above results obtained from **Cat-1a** catalysis were compared to the results obtained from the proline (**III-12**) catalysis reported in literature,

Table 6: Aldol reaction of acetone with substituted benzaldehydes in the presence of **Cat-1a**.^{a)}

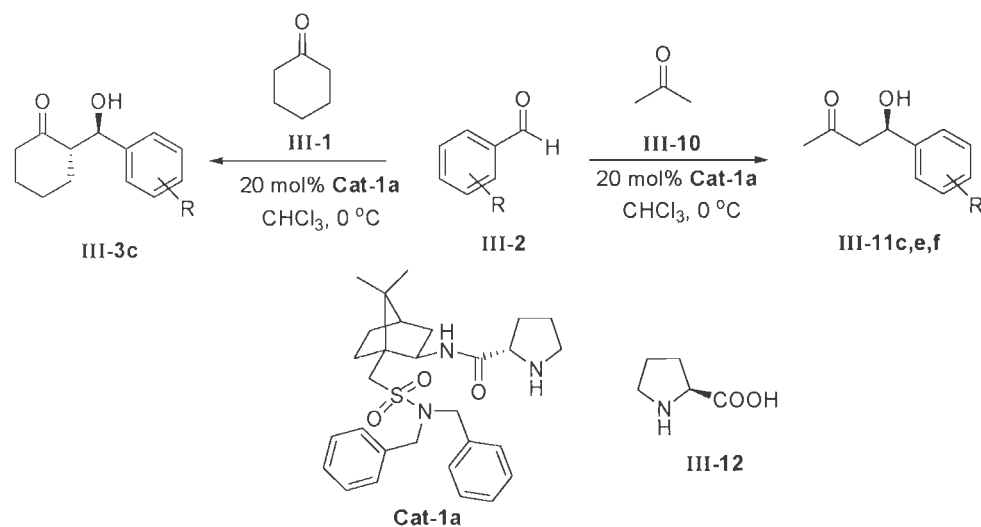


Entry	Product	Time	Yield (%)	ee (%) ^{b)}
1	III-11a	36h	98	91
2	III-11b	35h	94	73
3	III-11c	40h	92	77
4	III-11d	48h	82	78
5	III-11e	48h	88	90
6	III-11f	48h	90	92

^{a)} Reactions were performed with acetone (0.6 mM) and aldehyde (0.2 mM) in the presence of organocatalyst **Cat-1a** (20 mol%) in 0.5 mL of CHCl₃ at 0 °C. ^{b)} Determined by HPLC analysis (Chiralpak AD-H) (see page 107 for Table 12 and page 114 for HPLC charts).

the asymmetric induction in aldol reaction was found to be better in the former case in comparison with those catalyzed by proline. The results obtained from **Cat-1a** catalyzed aldol reaction with those obtained from proline-catalyzed aldol reaction are compared in Table 7.

Table 7: Comparison of enantioselectivity of aldol reactions catalyzed by **Cat-1a** and proline (**III-12**).



Entry	Catalyst	Solvent	Product	Yield (%)	dr (<i>anti:syn</i>)	ee (%)	
1	Cat-1a (20 mol%)	CHCl ₃		III-3c	96	90:10	91
2	III-12 (30 mol%)	DMSO			65	63:37	89
3	Cat-1a (20 mol%)	CHCl ₃		III-11c	92	-	77
4	III-12 (30 mol%)	DMSO			68	-	76
5	Cat-1a (20 mol%)	CHCl ₃		III-11e	88	-	91
6	III-12 (30 mol%)	DMSO			74	-	65
7	Cat-1a (20 mol%)	CHCl ₃		III-11f	90	-	92
8	III-12 (30 mol%)	DMSO			94	-	69

3.3.2. Determination of absolute configuration of III-3d by single crystal X-ray analysis

The absolute configuration of the major antipodes from the current study was determined by comparing the retention times on HPLC of the products with the literature data [32,45,48,49,52,53,64,65]. We were pleased to obtain single crystals for heavy 'bromine' atom containing aldol product **III-3d** with 92% ee from ethyl acetate-hexanes solvent system. This paved us way to determine its absolute configuration by X-ray crystallographic method. The Sheldrick least-squares refinement gave a Flack x parameter = 0.021(15). The expected values are 0 for correct and +1 for incorrect absolute configuration. Analysis of Flack parameter confirmed $2S,1'R$ configuration in our crystal. A view of the molecular structure of $(2S,1'R)$ -**III-3d** is shown in Figure 1.

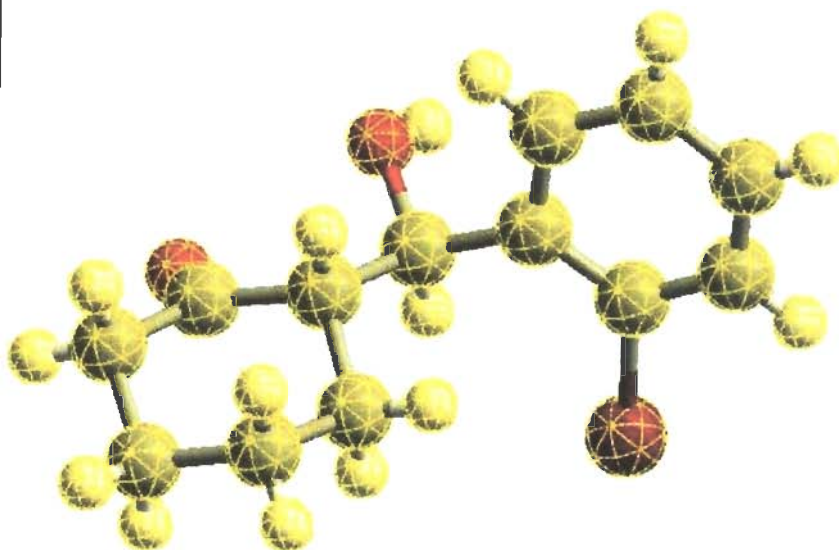
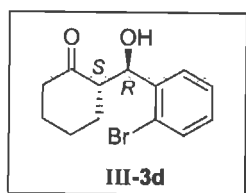


Figure 1: ORTEP Diagram of crystal structure of 2-[hydroxy-(2-bromophenyl)methyl]cyclohexanone (**III-3d**).

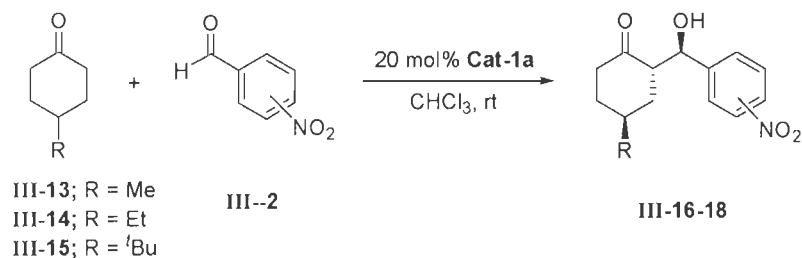
Table 8: Crystallographic data for (2*S*,1'*R*)-2-[hydroxy(2-bromophenyl)methyl]cyclohexanone (III-3d).

Empirical Formula	C ₁₃ H ₁₅ Br O ₂
Formula Weight	283.16
Crystal System	orthorhombic
Space group	P 2 ₁ 2 ₁ 2 ₁
Unit cell dimensions	
a(Å)	9.4921(5)
b(Å)	10.6559(8)
c(Å)	12.3890(9)
α	90.00
β	90.00
γ	90.00
V(Å ³)	1253.11(15)
Z	4
D _{cal} (g/cm ³)	1.501
Data collection	
Temperature (°K)	293
μ(Mo Kα) (cm ⁻¹)	3.263
θ _{max} (°)	26.37
No. of measured Reflections	2564
No. of observed Reflections	1170
Data/ restraints/ parameters	2564/0/149
R	0.0402
R _w	0.0894

3.3.3. Desymmetrization

The catalyst **Cat-1a** has proven to be an efficient and highly enantioselective organocatalyst for direct aldol reaction between aromatic aldehydes and cyclic/acyclic ketones. Encouraged by these results, we next evaluated its catalytic behaviour for asymmetric desymmetrization of 4-substituted cyclic ketones. The desymmetrization of such substances represents a powerful approach to access chiral nonracemic products. The desymmetrization of substituted cyclic ketones through their aldolization with aldehydes is a great challenge as the prochiral center is remote to the carbon of cyclic ketones where the aldolization takes place. The chiral catalyst must have strong ability to control the diastereo- and enantio-selectivities, and more importantly, to distinguish the stereogenicity of the carbon remote to the reactive site. As part of our continuous efforts to explore the camphorsulfonamide-based prolinamides for new organocatalytic processes, we considered the possibility to remove the symmetry of substituted cyclic ketones using the asymmetric direct aldol reaction under the catalytic influence of prolinamides synthesized in our studies. The results from desymmetrization studies are presented in Table 8. The enantioselective desymmetrization of 4-substituted cyclic ketones *via* organocatalytic direct aldol reaction simultaneously generated three stereogenic centers in high ee (up to 97%).

Prolinamide **Cat-1a** has proven to be efficient and highly enantioselective organocatalysts for direct aldol reactions of aromatic aldehydes with acetone. So under same conditions (20 mol% **Cat-1a**, CHCl₃ as solvent) we performed the aldol reaction of 4-methylcyclohexanone (**III-13a**) with 2-nitrobenzaldehyde at room temperature, indeed leading to an enantioselective desymmetrization and yielding **III-16a** as a major product with excellent enantioselectivity (96% ee). The minor products that were identified to be isomers of **III-16a** were obtained in less than 5% total yield (Table 9, Entry 1). This methodology was applied to other symmetric cyclic ketones and we were pleased to observe that the catalytic activity of **Cat-1a** is very good for desymmetrization. The reaction of 4-nitrobenzaldehyde with 4-methylcyclohexanone also provided the expected isomer **III-16b** in excellent chemical yield and enantioselectivity. Further, the reactions of 4-ethylcyclohexanone with 2-nitro and 4-nitro-benzaldehydes provided the corresponding adduct **III-17a** and **III-17b** in excellent chemical yield and enantioselectivity (Table 9, entries 3 and 4). Similar results were obtained in the reactions between 4-*tert*-butylcyclohexanone and *o*- and *p*-nitro benzaldehydes producing aldol adducts **III-18a** and **III-18b** (Table 9, entries 5 and 6).

Table 9: Aldol reaction between 4-substituted cyclohexanones and substituted benzaldehydes in the presence of **Cat-1a**.^{a)}

Entry	Product	Time	Yield (%) ^{b)}	ee (%) ^{c)}
1		68 h	96	96
2		72 h	95	92 ^{d)}
3		70 h	91	97
4		76 h	94	90 ^{d)}
5		78 h	95	95
6		80 h	93	87 ^{d)}

^{a)} Reactions were performed with 4-substituted cyclohexanone (0.4 mM) and aldehyde (0.2 mM) in the presence of 20 mol% **Cat-1a** in 0.5 mL of CHCl₃. ^{b)} Of the major isomer. ^{c)} Of the major isomer and determined by HPLC analysis (Chiralcel AD-H) unless otherwise mentioned. ^{d)} Of the major isomer and determined by HPLC analysis (Chiralpak OD-H) (see page 108 for Table 12 and page 116 for HPLC charts).

3.3.4. Structure determination of aldol product **III-18a** by NOESY experiment

Stereochemistry at C-2 and C-4 of **III-18a** was confirmed by NOESY experiment. The NOESY experiment conducted upon **III-18a** reveals a correlation between H-2 and protons of *tert*-butyl group together with the absence of interactions between H-2 and H-4 which is pinpointing the *anti* stereochemistry between C-2 and C-4. Thus NOESY experiment confirms the stereochemistry at C-2 and C-4 for compound **III-18a**.

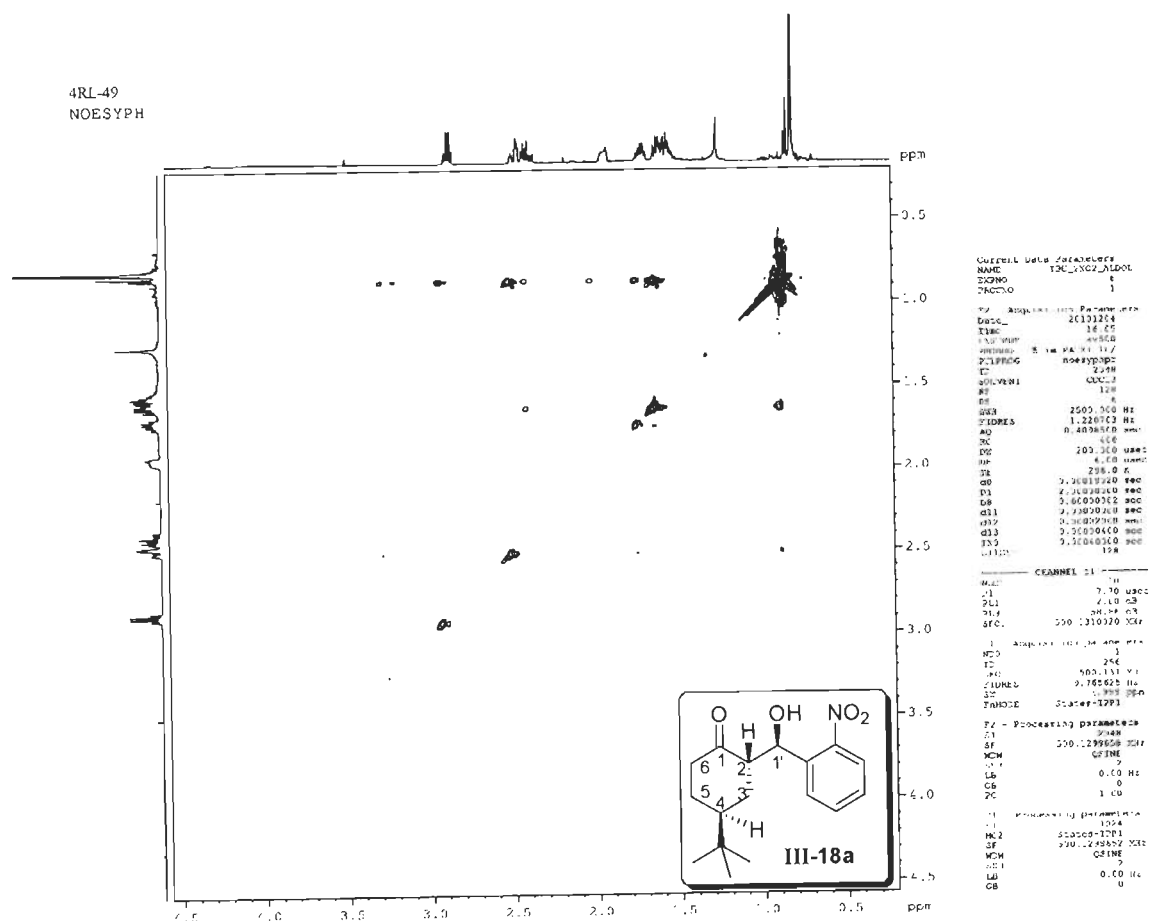
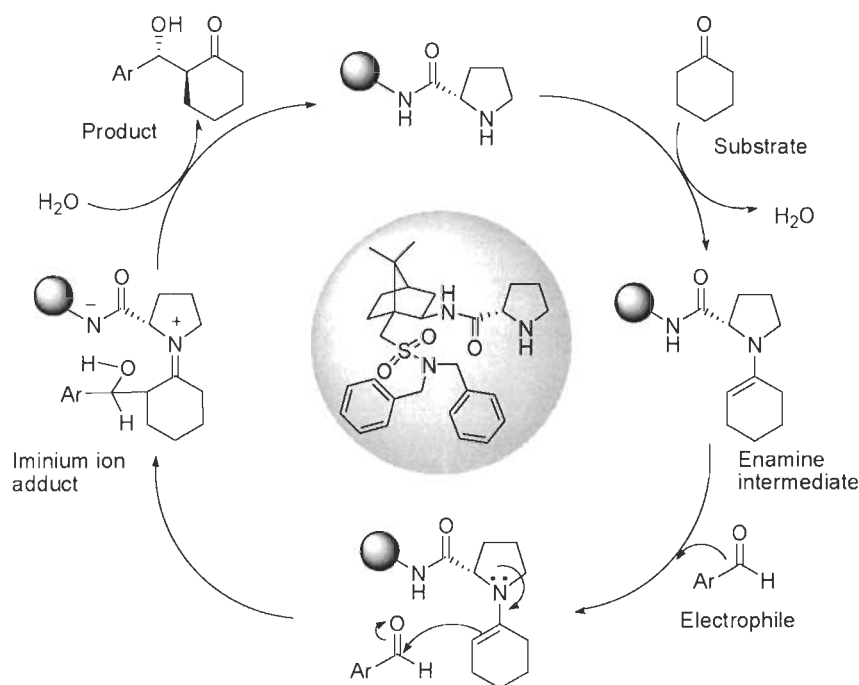


Figure 2: 500 MHz NOESY Spectrum of **III-18a** in CDCl_3 .

3.3.5. Proposed mechanism

The aldol reaction is a powerful means of forming carbon-carbon bonds in organic chemistry. The reaction combines two carbonyl compounds *via* nucleophilic addition of ketone to an aldehyde to form β -hydroxy carbonyl compound as aldol adduct. In **Cat-1a** catalyzed aldol addition reactions, the condensation of the secondary amino group of prolinamide with a carbonyl group of ketone substrate leads to the formation of a nucleophilic enamine intermediate. The adjacent amide group of the enamine intermediate then directs the approach of the electrophile (aldehyde) by formation of a specific hydrogen bonding between $-NH$ of amide group of the catalyst and carbonyl group of the ketone in the transition state. This provides both pre-organization of the substrates and stabilization of the transition state. The bulky benzyl group on the catalyst framework could effectively shield one of the faces of enamine, leaving another face exposed for enantioselective bond formation with the electrophile. Upon electrophilic capture of the enamine derivative, the resulting iminium ion is hydrolyzed to release the product and the catalyst to participate in the catalytic cycle.



Scheme 2: Proposed mechanism for asymmetric aldol reaction.

3.3.6. Proposed transition state

According to the stereochemical outcome in the current reactions catalyzed by **Cat-1a**, we propose that *N,N*-dibenzyl camphorsulfonamide-based prolinamide catalyst could catalyze the direct aldol reaction *via* the transition state shown in Figure 3. The aldehyde could be activated by the hydrogen bonding with $-NH$ of the catalyst. The bulky benzyl group on the catalyst framework could effectively shield the *Re*-face of the enamine, leaving its *Si*-face exposed for enantioselective bond formation on the *Re*-face of the aldehyde that leads to (*2S,1'R*)-isomer.

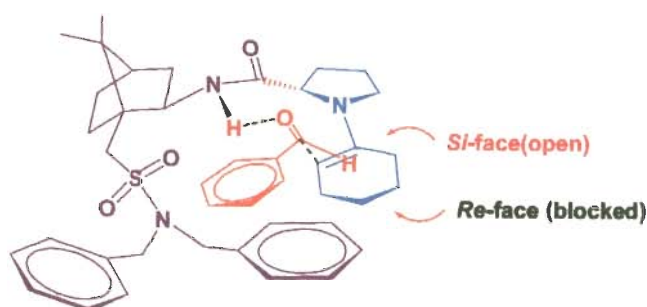


Figure 3: Plausible transition state.

3.4. CONCLUSION

In conclusion, we have synthesized camphorsulfonamide-based prolinamides and investigated their catalytic behaviour in direct aldol reaction. The organocatalyst **Cat-1a** showed remarkable selectivities in the reactions between cyclic/acyclic ketones and aromatic aldehydes. The excellent results displayed by **Cat-1a** may be attributed to the stabilization of transition state *via* hydrogen bonding between aldehyde and amide moiety of the enamine formed from catalyst and ketone and effective shielding of one of the faces of enamine by benzyl moiety of the catalyst.

3.5. EXPERIMENTAL

3.5.1. General

All reagents were purchased at the highest commercially quality and used without further purification. The solvents were purified by standard methods. Yields refer to chromatographically homogeneous materials, unless otherwise stated. Reactions were monitored by thin-layer chromatography (TLC) carried out on 0.25 mm E. Merck silica gel plates (60F-254) using UV light as visualizing or in an iodine chamber. Silica gel (particle size 100-200 mesh; SD Fine Chem Ltd) was used for column chromatography with ethyl acetate-hexanes as eluent system. Melting points are uncorrected.

3.5.2. Instrumentation

IR spectra of the compounds were recorded on a Thermo Nicolet FT-IR NexusTM and are expressed as wavenumbers. NMR spectra were recorded in CDCl₃ using TMS as internal standard on Brüker AMX-500 instrument. Chemical shifts of ¹H NMR spectra were given in parts per million with respect to TMS and the coupling constants *J* were measured in Hz. The signals from solvent CDCl₃, 7.26 and 77.0 ppm, are set as the reference peaks in ¹H NMR and ¹³C NMR spectra, respectively. Mass spectra were recorded by GC-MS (Perkin-Elmer Clarus 500, EI, 70 eV). The following abbreviations were used to explain the multiplicities: s = singlet, d = doublet, t = triplet, q = quartet, m = multiplet, br = broad. Analytical HPLC measurements were carried out on a Shimadzu SPD-20A with UV detector by using Chiralpak AS-H, AD-H and Chiralcel OD-H columns.

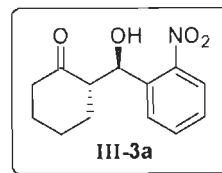
3.5.3. General Procedure

A solution of aldehyde (0.2 mmol), organocatalyst **Cat-1a** (0.04 mmol, 20 mol%) and cycloalkanone (0.4 mmol) in CHCl₃ (0.5 mL) was stirred at room temperature for a period of time mentioned in Table 3. The reaction was monitored by TLC at regular intervals. Upon completion of the reaction, the crude product was submitted for ¹H NMR (500 MHz) to determine the diastereomeric excess. The residue was subjected to column chromatography on silica gel to afford a pure product. The HPLC analysis of the aldol product was performed on a chiral stationary phase using hexanes–isopropanol as eluting solvent.

(2*S*,1'*R*)-2-[Hydroxy(2-nitrophenyl)methyl]cyclohexanone (III-3a):

IR (KBr) ν_{\max} : 3517, 3478, 2924, 2845, 1720, 1613, 1519, 1325, 1129, 1101, 695 cm^{-1}

$^1\text{H NMR}$ (CDCl_3 , 500 MHz): δ 7.86 (dd, $J = 1.5, 8.5$ Hz, 1H), 7.76 (dd, $J = 1.5, 7.5$ Hz, 1H), 7.64 (dt, $J = 1.0, 8.5$ Hz, 1H), 7.44 (dt, $J = 1.5, 8.5$ Hz, 1H), 5.44 (d, $J = 7.0$, 1H), 4.19 (s, 1H, $-\text{OH}$), 2.80-2.72 (m, 1H), 2.49-2.42 (m, 1H), 2.33 (dt, $J = 6.5, 13.5$ Hz, 1H), 2.14-2.07 (m, 1H), 1.89-1.80 (m, 1H), 1.80-1.53 (m, 4H) ppm.

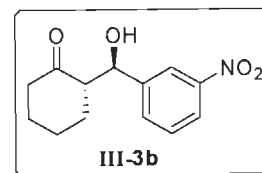


$^{13}\text{C NMR}$ (CDCl_3 , 125 MHz): δ 214.9, 148.7, 136.6, 133.1, 129.0, 128.4, 124.1, 69.7, 57.3, 42.8, 31.1, 27.8, 25.0 ppm.

(2*S*,1'*R*)-2-[Hydroxy(3-nitrophenyl)methyl]cyclohexanone (III-3b):

IR (KBr) ν_{\max} : 3348, 2495, 2879, 1719, 1535, 1349, 1250, 1159, 1033, 809, 727, 686 cm^{-1} .

$^1\text{H NMR}$ (CDCl_3 , 500 MHz): δ 8.22-8.17 (m, 2H), 7.70 (d, $J = 8.0$ Hz, 1H), 7.56 (t, $J = 8.0$ Hz, 1H), 4.92 (dd, $J = 3.0, 8.5$ Hz, 1H), 4.14 (d, $J = 3.0$, 1H, $-\text{OH}$), 2.68-2.62 (m, 1H), 2.57-2.49 (m, 1H), 2.45-2.36 (m, 1H), 2.19-2.12 (m, 1H), 1.90-1.83 (m, 1H), 1.73-1.55 (m, 3H), 1.48-1.38 (m, 1H) ppm.

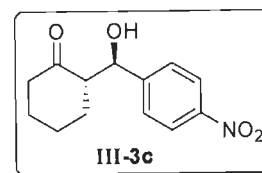


$^{13}\text{C NMR}$ (CDCl_3 , 125 MHz): δ 214.8, 148.3, 143.3, 133.2, 129.3, 122.8, 122.0, 74.0, 57.1, 42.6, 30.7, 27.6, 24.6 ppm.

(2*S*,1'*R*)-2-[Hydroxy(4-nitrophenyl)methyl]cyclohexanone (III-3c):

IR (KBr) ν_{\max} : 3517, 3481, 2934, 2855, 1696, 1603, 1517, 1345, 1130, 1109, 856 cm^{-1} .

$^1\text{H NMR}$ (CDCl_3 , 500 MHz): δ 8.22-8.19 (m, 2H), 7.53-7.48 (m, 2H), 4.90 (dd, $J = 3.5, 8.5$ Hz, 1H), 3.99 (d, $J = 3.5$, 1H, $-\text{OH}$), 2.69-2.56 (m, 1H), 2.52-2.47 (m, 1H), 2.40-4.32 (m, 1H), 2.15-2.07 (m, 1H), 1.89-1.80 (m, 1H), 1.72-1.53 (m, 3H), 1.45-1.35 (m, 1H) ppm.

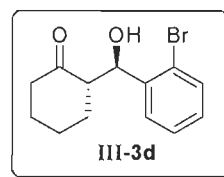


$^{13}\text{C NMR}$ (CDCl_3 , 125 MHz): δ 214.6, 148.5, 147.7, 127.8, 123.5, 74.0, 57.2, 42.6, 30.7, 27.6, 24.7 ppm.

(2*S*,1'*R*)-2-[Hydroxy(2-bromophenyl)methyl]cyclohexanone (III-3d):

IR (KBr) ν_{\max} : 3513, 2933, 2860, 1696, 1438, 1387, 1301, 1126, 751 cm^{-1} .

$^1\text{H NMR}$ (CDCl_3 , 500 MHz): δ 7.56 (dd, $J = 1.5, 4.0$ Hz, 1H), 7.55 (dd, $J = 1.5, 4.0$ Hz, 1H), 7.39 (dt, $J = 1.0, 8.0$ Hz, 1H), 7.19-7.15 (m, 1H), 5.33 (dd, $J = 4.0, 8.5$ Hz, 1H), 4.12 (d, $J = 3.5$ Hz, 1H, $-\text{OH}$), 2.75-2.67 (m, 1H), 2.52-2.46 (m, 1H), 2.42-2.34 (m, 1H), 2.16-2.09 (m, 1H), 1.92-1.82 (m, 1H), 1.77-1.55 (m, 4H) ppm.

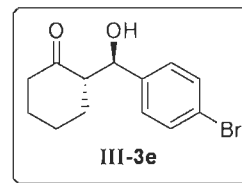


$^{13}\text{C NMR}$ (CDCl_3 , 125 MHz): δ 215.1, 140.8, 132.4, 129.1, 128.5, 127.9, 123.4, 72.8, 57.7, 42.7, 30.6, 27.8, 24.9 ppm.

(2*S*,1'*R*)-2-[Hydroxy(4-bromophenyl)methyl]cyclohexanone (III-3e):

IR (KBr) ν_{\max} : 3512, 2953, 2865, 1689, 1508, 1445, 1387, 1220, 1042, 835 cm^{-1} .

$^1\text{H NMR}$ (CDCl_3 , 500 MHz): δ 7.52-7.48 (m, 2H), 7.25-7.21 (m, 2H), 4.78 (dd, $J = 3.0, 9.0$ Hz, 1H), 4.00 (d, $J = 3.0$ Hz, 1H, $-\text{OH}$), 2.62-2.2.55 (m, 1H), 2.54-2.48 (m, 1H), 2.42-2.34 (m, 1H), 2.15-2.09 (m, 1H), 1.87-1.80 (m, 1H), 1.73-1.52 (m, 3H), 1.38-1.27 (m, 1H) ppm.

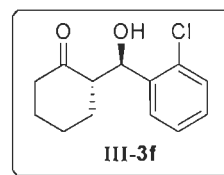


$^{13}\text{C NMR}$ (CDCl_3 , 125 MHz): δ 215.2, 140.1, 131.5, 128.8, 121.7, 74.2, 57.3, 42.7, 30.7, 27.7, 24.7 ppm.

(2*S*,1'*R*)-2-[Hydroxy(2-chlorophenyl)methyl]cyclohexanone (III-3f):

IR (KBr) ν_{\max} : 3437, 2929, 2858, 1696, 1480, 1445, 1104, 699 cm^{-1} .

$^1\text{H NMR}$ (CDCl_3 , 500 MHz): δ 7.54 (dd, $J = 1.5, 7.5$ Hz, 1H), 7.34-7.29 (m, 2H), 7.22 (dt, $J = 2.0, 8.0$ Hz, 1H), 5.35 (dd, $J = 3.0, 8.0$ Hz, 1H), 4.07 (d, $J = 4.0$ Hz, 1H, $-\text{OH}$), 2.71-2.63 (m, 1H), 2.50-2.44 (m, 1H), 2.34 (ddt, $J = 1.0, 6.0, 13.5$ Hz, 1H), 2.13-2.05 (m, 1H), 1.85-1.80 (m, 1H), 1.72-1.50 (m, 4H) ppm.



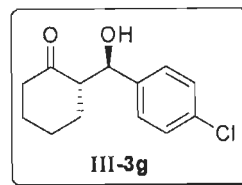
$^{13}\text{C NMR}$ (CDCl_3 , 125 MHz): δ 215.2, 139.1, 133.0, 129.2, 128.7, 128.3, 127.2, 70.4, 57.6, 42.7, 30.4, 27.8, 24.9 ppm.

(2*S*,1'*R*)-2-[Hydroxy(4-chlorophenyl)methyl]cyclohexanone (III-3g) :

IR (KBr) ν_{\max} : 3427, 2928, 2858, 2695, 1485, 1443, 1120, 828 cm^{-1} .

$^1\text{H NMR}$ (CDCl_3 , 500 MHz): δ 7.37-7.32 (m, 2H), 7.31-7.26 (m, 2H), 4.79 (d, $J = 8.5$ Hz, 1H), 4.01 (d, $J = 2.0$ Hz, 1H, $-\text{OH}$), 2.61-2.56 (m, 1H), 2.54-2.48 (m, 1H), 2.43-2.34 (m, 1H), 2.16-2.09 (m, 1H), 1.86-1.79 (m, 1H), 1.75-1.52 (m, 3H), 1.38-1.26 (m, 1H) ppm.

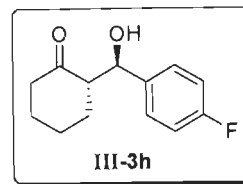
$^{13}\text{C NMR}$ (CDCl_3 , 125 MHz): δ 215.3, 139.5, 133.6, 128.5, 128.4, 74.1, 57.4, 42.7, 30.8, 27.7, 24.7 ppm.

**(2*S*,1'*R*)-2-[Hydroxy(4-fluorophenyl)methyl]cyclohexanone (III-3h):**

IR (KBr) ν_{\max} : 3517, 2943, 2860, 1698, 1510, 1449, 1393, 1223, 1040, 837 cm^{-1} .

$^1\text{H NMR}$ (CDCl_3 , 500 MHz): δ 7.35-7.27 (m, 2H), 7.08-7.04 (m, 2H), 4.80 (dd, $J = 1.0, 8.5$ Hz, 1H), 4.01 (d, $J = 2.0$ Hz, 1H, $-\text{OH}$), 2.63-2.56 (m, 1H), 2.55-2.45 (m, 1H), 2.43-2.34 (m, 1H), 2.16-2.08 (m, 1H), 1.92-1.80 (m, 2H), 1.78-1.64 (m, 1H), 1.62-1.54 (m, 1H), 1.36-1.25 (m, 1H) ppm.

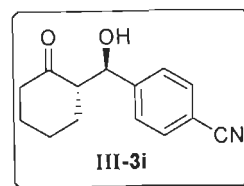
$^{13}\text{C NMR}$ (CDCl_3 , 125 MHz): δ 215.4, 163.3 (d, $J = 245.0$ Hz), 136.8, 128.7 (d, $J = 8.75$ Hz), 115.2 (d, $J = 21.25$ Hz), 74.1, 57.5, 42.6, 30.7, 27.7, 24.6 ppm.

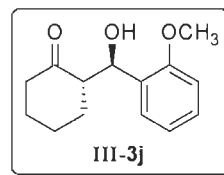
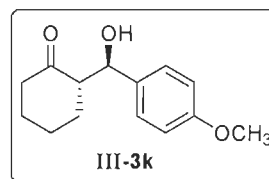
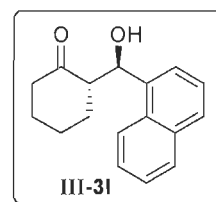
**(2*S*,1'*R*)-2-[Hydroxy(4-cyanophenyl)methyl]cyclohexanone (III-3i):**

IR (KBr) ν_{\max} : 3510, 3315, 2964, 2845, 1705, 1600, 1510, 1340, 1130, 1100, 858 cm^{-1} .

$^1\text{H NMR}$ (CDCl_3 , 500 MHz): δ 7.68-7.62 (m, 2H), 7.44 (d, $J = 8.5$ Hz, 2H), 4.84 (dd, $J = 3.0, 8.5$ Hz, 1H), 4.03 (d, $J = 3.0$ Hz, 1H, $-\text{OH}$), 2.60-2.53 (m, 1H), 2.52-2.45 (m, 1H), 2.35 (ddt, $J = 1.0, 6.0, 13.5$ Hz, 1H), 2.15-2.07 (m, 1H), 1.86-1.80 (m, 1H), 1.72-1.61 (m, 1H), 1.59-1.50 (m, 2H), 1.41-1.30 (m, 1H) ppm.

$^{13}\text{C NMR}$ (CDCl_3 , 125 MHz): δ 214.2, 146.4, 132.1, 127.7, 118.7, 111.6, 74.2, 57.2, 42.5, 30.7, 27.6, 24.6 ppm.

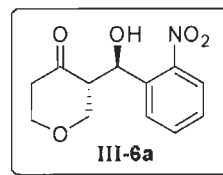


(2*S*,1'*R*)-2-[Hydroxy(2-methoxyphenyl)methyl]cyclohexanone (III-3j):**IR (KBr) ν_{\max} :** 3511, 2930, 2858, 1690, 1585, 1440, 1389, 1300, 1127, 752 cm^{-1} . **$^1\text{H NMR}$ (CDCl_3 , 500 MHz):** δ 7.39 (dd, $J = 1.5, 7.5$ Hz, 1H), 7.28-7.23 (m, 1 H), 7.01-6.96 (m, 1H), 6.86 (d, $J = 8.0$ Hz, 1H), 5.25 (d, $J = 9.0$ Hz, 1H), 3.81 (s, 3 H), 2.78-2.70 (m, 1H), 2.50-2.43 (m, 1H), 2.39-2.31 (m, 1 H), 2.09-2.01 (m, 1H), 1.82-1.75 (m, 1H), 1.74-1.50 (m, 3H), 1.48-1.38 (m, 1H) ppm. **$^{13}\text{C NMR}$ (CDCl_3 , 125 MHz):** δ 215.6, 156.7, 129.6, 128.6, 127.8, 120.9, 110.5, 68.6, 57.3, 55.4, 42.6, 30.5, 28.0, 24.7 ppm.**(2*S*,1'*R*)-2-[Hydroxy(4-methoxyphenyl)methyl]cyclohexanone (III-3k):****IR (KBr) ν_{\max} :** 3504, 2937, 2862, 1700, 1612, 1513, 1451, 1248, 1176, 1034, 835 cm^{-1} . **$^1\text{H NMR}$ (CDCl_3 , 500 MHz):** δ 7.25-7.21 (m, 2H), 6.88 (d, $J = 8.5$ Hz, 2 H), 4.74 (dd, $J = 2.5, 9.0$ Hz, 1H), 3.91 (d, $J = 3.0$ Hz, 1H, $-\text{OH}$), 3.80 (s, 3H), 2.63-2.49 (m, 1H), 2.51-2.41 (m, 1H), 2.40-2.31 (m, 1H), 2.12-2.05 (m, 1H), 1.82-1.75 (m, 1H), 1.72-1.63 (m, 1H), 1.61-1.50 (m, 2H), 1.24-1.19 (m, 1H) ppm. **$^{13}\text{C NMR}$ (CDCl_3 , 125 MHz):** δ 215.7, 159.3, 133.2, 128.2, 113.8, 74.3, 57.5, 55.3, 42.7, 30.8, 27.8, 24.7 ppm.**(2*S*,1'*R*)-2-[Hydroxy(1-naphthyl)methyl]cyclohexanone (III-3l):****IR (KBr) ν_{\max} :** 3475, 2931, 2860, 1695, 1510, 1347, 1253, 1128, 1048, 802, 755, 697 cm^{-1} . **$^1\text{H NMR}$ (CDCl_3 , 500 MHz):** δ 8.28 (d, $J = 8.0$ Hz, 1H), 7.92-7.87 (m, 1 H), 7.83 (d, $J = 8.5$ Hz, 1H), 7.59 (d, $J = 8.0$ Hz, 1H), 7.56-7.48 (m, 3 H), 5.61 (dd, $J = 3.0, 8.5$ Hz, 1H), 4.15 (d, $J = 3.0$ Hz, 1H, $-\text{OH}$), 3.10- 2.99 (m, 1H), 2.58-2.52 (m, 1H), 2.43 (dt, $J = 6.0, 13.5$ Hz, 1H), 2.15-2.08 (m, 1H), 1.79-1.65 (m, 2H), 1.55- 1.35 (m, 3H) ppm. **$^{13}\text{C NMR}$ (CDCl_3 , 125 MHz):** δ 215.7, 136.9, 134.0, 131.4, 128.9, 128.4, 126.0, 125.5, 125.4, 125.3, 124.0, 72.1, 57.4, 42.8, 31.4, 27.9, 24.9 ppm.

(2*S*,1'*R*)-2-[Hydroxy(2-nitrophenyl)methyl]tetrahydropyran-4-one (III-6a):

IR (KBr) ν_{\max} : 3525, 3478, 2925, 2830, 1720, 1612, 1515, 1337, 1125, 1100, 1045, 799 cm^{-1} .

$^1\text{H NMR}$ (CDCl_3 , 500 MHz): δ 7.92 (dd, $J = 1.5, 8.5$ Hz, 1H), 7.81 (dd, $J = 1.5, 8.0$ Hz, 1H), 7.67 (dt, $J = 1.0, 8.0$ Hz, 1H), 7.48-7.44 (m, 1H), 5.47 (d, $J = 6.5$, 1H), 4.15 (s, 1H, $-\text{OH}$), 4.24-4.19 (m, 1H), 3.92 (ddd, $J = 1.5, 6.5, 11.5$ Hz, 1H), 3.84-3.74 (m, 2H), 3.06 (dtd, $J = 1.0, 6.0, 10.0$ Hz 1H), 2.71-2.64 (m, 1 H), 2.51 (td, $J = 3.5, 14.5$ Hz, 1H) ppm.

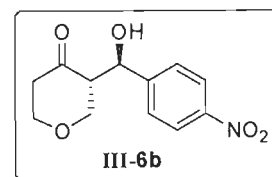


$^{13}\text{C NMR}$ (CDCl_3 , 125 MHz): δ 209.6, 148.1, 136.1, 133.6, 128.9, 128.8, 124.4, 70.5, 68.4, 67.4, 57.9, 43.3 ppm.

(2*S*,1'*R*)-2-[Hydroxy(4-nitrophenyl)methyl]tetrahydropyran-4-one (III-6b):

IR (KBr) ν_{\max} : 3524, 3475, 2932, 2865, 1705, 1615, 1517, 1345, 1130, 1105, 1050, 998, 855 cm^{-1} .

$^1\text{H NMR}$ (CDCl_3 , 500 MHz): δ 8.27-8.24 (m, 2H), 7.56-7.52 (m, 2H), 5.01 (d, $J = 8.0$ Hz, 1H), 4.15-4.20 (m, 1H), 3.79 (dd, $J = 3.5, 11.0$ Hz, 1 H), 3.76- 3.72 (m, 1H), 3.47 (dd, $J = 10.0, 11.5$ Hz, 1H), 2.95-2.88 (m, 1H), 2.74-2.66 (m, 2H), 2.55 (td, $J = 3.0, 14.5$ Hz, 1H) ppm.

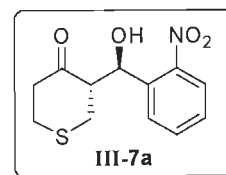


$^{13}\text{C NMR}$ (CDCl_3 , 125 MHz): δ 209.3, 147.8, 147.4, 127.5, 123.9, 71.3, 69.8, 68.9, 57.6, 42.9, ppm.

(2*S*,1'*R*)-2-[Hydroxy(2-nitrophenyl)methyl]tetrahydrothiopyran-4-one (III-7a):

IR (KBr) ν_{\max} : 3512, 3489, 2924, 2835, 1719, 1612, 1585, 1505, 1335, 1129, 1055, 797 cm^{-1} .

$^1\text{H NMR}$ (CDCl_3 , 500 MHz): δ 8.20-8.16 (m, 2H), 7.71-7.64 (m, 1H), 7.56 (t, $J = 8.0$ Hz, 1H), 4.97 (d, $J = 8.0$, 1H), 4.25-4.18 (m, 1H), 3.78-3.68 (m, 2H), 3.45 (t, $J = 11.5$ Hz, 1H), 2.96-2.89 (m, 1H), 2.56-2.49 (m, 1H) ppm.

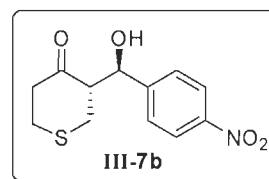


$^{13}\text{C NMR}$ (CDCl_3 , 125 MHz): δ 209.8, 148.4, 142.4, 132.8, 128.9, 123.4, 121.7, 71.4, 69.8, 67.9, 57.6, 42.8 ppm.

(2*S*,1'*R*)-2-[Hydroxy(4-nitrophenyl)methyl]tetrahydrothiopyran-4-one (III-7b):

IR (KBr) ν_{\max} : 3534, 3472, 2928, 2860, 1710, 1615, 1530, 1448, 1356, 1152, 1100, 1050, 856 cm^{-1} .

^1H NMR (CDCl_3 , 500 MHz): δ 8.22 (d, $J = 8.5$ Hz, 2H), 7.53 (d, $J = 8.5$ Hz, 2H), 5.05 (dd, $J = 8.0, 3.5$ Hz, 1H), 3.66 (s, 1H, $-\text{OH}$), 3.02-2.96 (m, 3H), 2.85-2.76 (m, 2H), 2.70-2.63 (m, 1H), 2.54-2.49 (m, 1H) ppm.

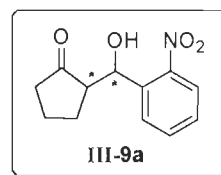


^{13}C NMR (CDCl_3 , 125 MHz): δ 211.2, 147.7, 147.5, 127.6, 123.9, 73.2, 59.4, 44.5, 32.4, 30.7 ppm.

2-[Hydroxy(2-nitrophenyl)methyl]cyclopentanone (III-9a):

IR (KBr) ν_{\max} : 3527, 3488, 2925, 2846, 1725, 1600, 1550, 1529, 1485, 1340, 1119, 1110, 798 cm^{-1} .

^1H NMR (CDCl_3 , 500 MHz): δ 7.81-7.78 (m, 2H), 7.72-7.59 (m, 1H), 7.57-7.38 (m, 1H), 5.90 (d, $J = 3$ Hz, CHOH (*syn*)), 4.42 (d, $J = 8.4$ Hz, CHOH (*anti*)), 4.50 (s, 1H), 2.85-2.65 (m, 1H), 2.60-2.26 (m, 2H), 2.26-1.95 (m, 2H), 1.81-1.69 (m, 2H) ppm.

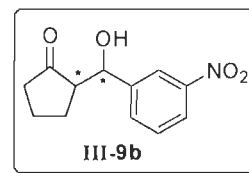


^{13}C NMR (CDCl_3 , 125 MHz): δ 219.1, 146.9, 138.6, 133.3, 133.1, 128.9, 128.6, 128.5, 127.9, 124.4, 123.9, 69.0, 66.4, 55.3, 54.7, 38.6, 26.5, 22.8, 20.4, 20.1 ppm.

2-[Hydroxy(3-nitrophenyl)methyl]cyclopentanone (III-9b):

IR (KBr) ν_{\max} : 3350, 2490, 2875, 1728, 1535, 1350, 1201, 1159, 1045, 809, 727 cm^{-1}

^1H NMR (CDCl_3 , 500 MHz): δ 8.26-8.22 (m, 1H), 8.17 (qd, $J = 1.0, 8.5$ Hz, 0.5 H), 8.15-8.12 (m, 0.5H), 7.72-7.66 (m, 1H), 7.56-7.50 (m, 1H), 5.43 (t, $J = 4.0$ Hz, 0.5H (*syn*)), 4.83 (d, $J = 4.5$ Hz, 0.5H (*anti*)), 4.79 (d, $J = 1.0$ Hz, $-\text{OH}$ (*anti*)), 2.55-2.25 (m, 2H), 2.21-2.10 (m, 1 H), 2.09-1.96 (m, 2 H), 1.81-1.68 (m, 2 H) ppm.

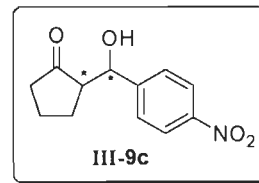


^{13}C NMR (CDCl_3 , 125 MHz): δ 214.9, 216.1, 148.4, 145.2, 143.7, 132.7, 131.7, 129.5, 129.3, 123.0, 122.2, 121.6, 120.6, 74.4, 70.2, 56.1, 55.1, 39.0, 38.6, 26.8, 22.4, 20.4 ppm.

2-[Hydroxy(4-nitrophenyl)methyl]cyclopentanone (III-9c):

IR (KBr) ν_{\max} : 3442, 2953, 2875, 1725, 1601, 1516, 1346, 1159, 1103, 861 cm^{-1} .

^1H NMR (CDCl_3 , 500 MHz): δ 8.23-8.19 (m, 2 H), 7.56-7.50 (m, 2H), 5.42 (t, $J = 3.5$ Hz, 0.5H (*syn*)), 4.53 (d, $J = 8.5$ Hz, 0.5H (*anti*)), 4.52 (s, -OH (*anti*)), 2.45 (d, $J = 5.0$ Hz, 1H), 2.51-2.45 (m, 1H), 2.43-2.35 (m, 1H), 2.07-2.05 (m, 2H), 1.76-1.67 (m, 2H) ppm.

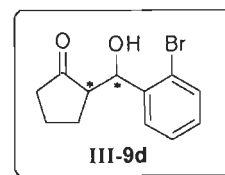


^{13}C NMR (CDCl_3 , 125 MHz): δ 214.7, 213.6, 150.3, 147.2, 127.4, 126.4, 123.7, 123.6, 74.4, 70.4, 56.1, 55.1, 38.9, 38.6, 26.8, 22.4, 20.3 ppm.

2-[Hydroxy(2-bromophenyl)methyl]cyclopentanone (III-9d):

IR (KBr) ν_{\max} : 3455, 2950, 2882, 1725, 1600, 1515, 1420, 1100, 756 cm^{-1} .

^1H NMR (CDCl_3 , 500 MHz): δ 7.60-7.55 (m, 1 H), 7.54-7.49 (m, 1 H), 7.39-7.31 (m, 1 H), 7.17-7.12 (m, 1 H), 5.63 (d, $J = 2.0$ Hz, 0.5 H (*syn*)), 5.27 (d, $J = 9.0$ Hz, 0.5 H (*anti*)), 4.51 (brs, -OH (*anti*)), 2.74-2.67 (m, 0.5 H), 2.51-2.38 (m, 1 H), 2.38-2.28 (m, 1 H), 2.22-2.12 (m, 0.5 H), 2.06-1.96 (m, 1.5 H), 1.80-1.70 (m, 1.5 H), 1.69-1.64 (m, 1 H) ppm.

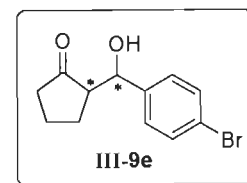


^{13}C NMR (CDCl_3 , 125 MHz): δ 215.2, 214.0, 141.8, 140.7, 132.6, 132.5, 129.3, 128.7, 128.0, 127.9, 127.4, 122.7, 121.0, 72.7, 69.9, 55.5, 53.5, 39.1, 38.7, 26.6, 22.3, 20.6, 20.4 ppm.

2-[Hydroxy(4-bromophenyl)methyl]cyclopentanone (III-9e):

IR (KBr) ν_{\max} : 3435, 2970, 2879, 1728, 1605, 1510, 1420, 1215, 1165, 845 cm^{-1} .

^1H NMR (CDCl_3 , 500 MHz): δ 7.49-7.45 (m, 2H), 7.24-7.19 (m, 2H), 5.26 (t, $J = 4.0$ Hz, 0.6H (*syn*)), 4.68 (d, $J = 9.0$ Hz, 0.4H (*anti*)), 4.57 (s, -OH (*anti*)), 2.46-2.40 (m, 1.7H), 2.40-2.31 (m, 1H), 2.30-2.20 (m, 0.4 H), 2.17-2.09 (m, 0.6H), 2.04-1.90 (m, 1.7H), 1.85-1.65 (m, 2.2H), 1.54-1.43 (m, 0.4H) ppm.

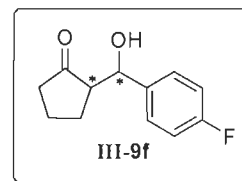


^{13}C NMR (CDCl_3 , 125 MHz): δ 215.6, 214.2, 141.8, 140.5, 131.6, 131.4, 128.3, 127.3, 121.8, 121.0, 74.6, 70.9, 56.0, 55.2, 39.1, 38.7, 26.9, 22.7, 20.4, 20.4 ppm.

2-[Hydroxy(4-fluorophenyl)methyl]cyclopentanone (III-9f):

IR (KBr) ν_{\max} : 3431, 2964, 2880, 1727, 1604, 1509, 1405, 1223, 1157, 1032, 845 cm^{-1} .

^1H NMR (CDCl_3 , 500 MHz): δ 7.35-7.27 (m, 2H), 7.05-7.00 (m, 2H), 5.27 (d, $J = 3.0$ Hz, 0.5H (*syn*)), 4.69 (d, $J = 9.5$ Hz, 0.5H (*anti*)), 4.58 (brs, -OH (*anti*), 0.5H), 2.50 (brs, -OH (*syn*), 0.5H), 2.45-2.31 (m, 2H), 2.30-2.20 (m, 0.5H), 2.18-2.08 (m, 0.5H), 2.03-1.92 (m, 1.6H), 1.85-1.63 (m, 2H), 1.56-1.42 (m, 0.5H) ppm.

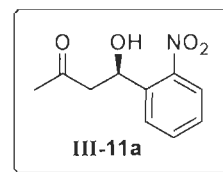


^{13}C NMR (CDCl_3 , 125 MHz): δ 218.2, 217.3, 150.3, 147.2, 127.4, 126.4, 123.7, 123.6, 74.4, 70.4, 56.1, 55.1, 38.9, 38.6, 26.8, 22.4, 20.3 ppm.

(4R)-4-[Hydroxy-4-(2-nitrophenyl)butan-2-one (III-11a):

IR (KBr) ν_{\max} : 3445, 2922, 2858, 1705, 1515, 1490, 1395, 1055, 750 cm^{-1} .

^1H NMR (CDCl_3 , 500 MHz): δ 7.96 (dd, $J = 1.0, 8.0$ Hz, 1H), 7.90 (dd, $J = 1.0, 7.5$ Hz, 1H), 7.67 (dt, $J = 1.0, 8.0$ Hz, 1H), 7.46-7.42 (m, 1H), 5.68 (dd, $J = 2.0, 9.5$ Hz, 1H), 3.14 (dd, $J = 2.5, 18.0$ Hz, 1H), 3.73 (s, 1H, -OH), 2.72 (dd, $J = 9.5, 17.5$ Hz, 1H), 2.24 (s, 3 H) ppm.

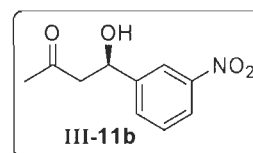


^{13}C NMR (CDCl_3 , 125 MHz): δ 208.8, 147.1, 138.4, 133.8, 128.3, 128.2, 124.4, 65.6, 51.0, 30.4 ppm.

(4R)-4-[Hydroxy-4-(3-nitrophenyl)butan-2-one (III-11b):

IR (KBr) ν_{\max} : 3441, 2925, 1701, 1515, 1490, 1395, 1100, 802, 745 cm^{-1} .

^1H NMR (CDCl_3 , 500 MHz): δ 8.25-8.21 (m, 1H), 8.12 (qd, $J = 1.5, 8.5$ Hz, 1H), 7.72-7.68 (m, 1H), 7.52 (t, $J = 8.0$ Hz, 1H), 5.25 (t, $J = 5.5$ Hz, 1H), 3.66 (s, 1H, -OH), 2.89-2.85 (m, 2H), 2.22 (s, 3 H) ppm.

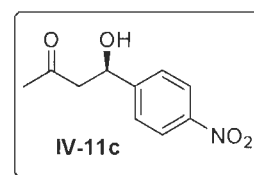


^{13}C NMR (CDCl_3 , 125 MHz): δ 208.6, 148.3, 145.1, 131.9, 129.5, 122.5, 120.7, 68.8, 51.6, 30.7 ppm.

(4R)-4-[Hydroxy-4-(4-nitrophenyl)butan-2-one (III-11c):

IR (KBr) ν_{\max} : 3440, 2923, 2859, 1708, 1518, 1398, 850 cm^{-1} .

^1H NMR (CDCl_3 , 500 MHz): δ 8.23-8.19 (m, 2H), 7.56-7.52 (m, 2H),



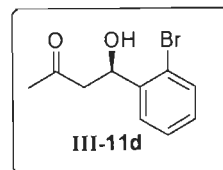
5.29-5.24 (m, 1H), 3.57 (d, $J = 3.5$ Hz, 1H, $-OH$), 2.87-2.83 (m, 2H), 2.22 (s, 3H) ppm

^{13}C NMR ($CDCl_3$, 125 MHz): δ 208.5, 150.0, 147.3, 126.4, 123.8, 68.9, 51.5, 30.9 ppm

(4*R*)-4-[Hydroxy-4-(2-bromophenyl)butan-2-one (III-11d):

IR (KBr) ν_{max} : 3395, 2925, 2827, 1697, 1517, 1397, 1112, 755 cm^{-1} .

1H NMR ($CDCl_3$, 500 MHz): δ 7.62 (dd, $J = 1.5, 8.0$ Hz, 1H), 7.50 (dd, $J = 1.0, 8.0$ Hz, 1H), 7.35 (dd, $J = 1.0, 7.5$ Hz, 1H), 7.14 (dt, $J = 2.0, 8.0$ Hz, 1H), 5.50-5.44 (m, 1H), 3.52 (d, $J = 3.5$, 1H, $-OH$), 3.01 (dd, $J = 2.0, 18.0$ Hz, 1H), 2.65 (dd, $J = 10.0, 18.0$ Hz, 1H), 2.20 (s, 3H) ppm.

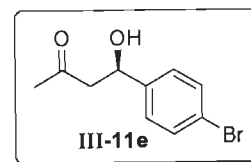


^{13}C NMR ($CDCl_3$, 125 MHz): δ 209.1, 140.7, 132.6, 129.0, 127.9, 127.3, 121.2, 68.8, 50.2, 30.6 ppm.

(4*R*)-4-[Hydroxy-4-(4-bromophenyl)butan-2-one (III-11e):

IR (KBr) ν_{max} : 3441, 2925, 2850, 1697, 1515, 1396, 1054, 814 cm^{-1} .

1H NMR ($CDCl_3$, 500 MHz): δ 7.53-7.48 (m, 2H), 7.29-7.23 (m, 2H), 5.13 (dd, $J = 4.0, 8.5$ Hz, 1H), 2.84 (d, $J = 8.5$ Hz, 1H), 2.82 (d, $J = 4.0$ Hz, 1H), 2.20 (s, 3H) ppm.

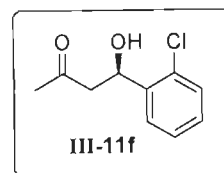


^{13}C NMR ($CDCl_3$, 125 MHz): δ 208.5, 150.0, 147.3, 126.4, 123.8, 68.9, 51.5, 30.9 ppm.

(4*R*)-4-[Hydroxy-4-(2-chlorophenyl)butan-2-one (III-11f):

IR (KBr) ν_{max} : 3420, 2910, 2875, 1695, 1500, 1483, 1387, 1102, 748 cm^{-1} .

1H NMR ($CDCl_3$, 500 MHz): δ 7.61 (dd, $J = 1.5, 8.0$ Hz, 1H), 7.34-7.28 (m, 2H), 7.21 (dt, $J = 2.0, 7.5$ Hz, 1H), 5.51 (dd, $J = 2.0, 9.5$ Hz, 1H), 3.56 (br, s, 1H, $-OH$), 2.98 (dd, $J = 2.0, 17.5$ Hz, 1H), 2.67 (dd, $J = 10.0, 18.0$ Hz, 1H), 2.21 (s, 3H) ppm.

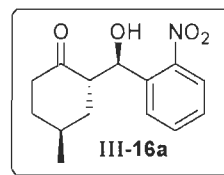


^{13}C NMR ($CDCl_3$, 125 MHz): δ 209.1, 140.2, 131.1, 129.3, 128.6, 127.2, 127.1, 66.6, 50.1, 30.6 ppm.

(2*S*,4*S*,1'*R*)-2-[Hydroxy(2-nitrophenyl)methyl]-4-methylcyclohexanone (III-16a):

IR (KBr) ν_{max} : 3330, 3100, 2955, 2920, 2855, 1702, 1605, 1575, 1530, 1369, 850, 770 cm^{-1} .

^1H NMR (CDCl₃, 500 MHz): δ 7.85 (dd, $J = 1.5, 8.5$ Hz, 1H), 7.75 (dd, $J = 1.5, 8.0$ Hz, 1H), 7.67 (dt, $J = 1.5, 8.5$ Hz, 1H), 7.46-7.41 (m, 1H), 5.43 (d, $J = 7.5$, 1H), 4.0 (br, s, -OH), 2.97-2.89 (m, 1H), 2.55-2.42 (m, 1H), 2.36 (td, $J = 5.0, 14.0$ Hz, 1H), 2.16-2.08 (m, 1H), 1.99-1.83 (m, 2H), 1.80-1.72 (m, 1H), 1.56-1.48 (m, 1H), 1.09 (d, $J = 7.0$ Hz, 3H) ppm.

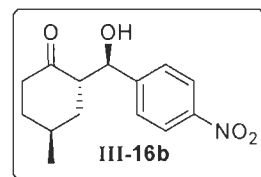


^{13}C NMR (CDCl₃, 125 MHz): δ 215.1, 148.8, 136.8, 133.2, 128.9, 128.5, 124.1, 69.9, 52.9, 38.5, 36.7, 33.2, 26.9, 18.2 ppm.

(2S,4S,1'R)-2-[Hydroxy(4-nitrophenyl)methyl]-4-methylcyclohexanone (III-16b):

IR (KBr) ν_{max} : 3489, 3100, 2965, 1700, 1599, 1498, 1342, 700 cm⁻¹.

^1H NMR (CDCl₃, 500 MHz): δ 8.26-8.21 (m, 2H), 7.55-7.50 (m, 2H), 4.94 (d, $J = 9.0$, 1H), 2.80-2.72 (m, 1H), 2.61-2.52 (m, 1H), 2.41 (td, $J = 5.0, 14.5$ Hz, 1H), 2.14-2.06 (m, 1H), 1.99-1.91 (m, 1H), 1.86-1.78 (m, 1H), 1.65-1.57 (m, 2H), 1.08 (d, $J = 7.0$ Hz, 3H) ppm.

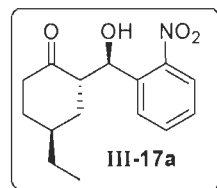


^{13}C NMR (CDCl₃, 125 MHz): δ 214.9, 148.4, 147.6, 127.8, 123.6, 74.1, 52.8, 38.1, 36.0, 32.9, 26.6, 18.4 ppm.

(2S,4S,1'R)-2-[Hydroxy(2-nitrophenyl)methyl]-4-ethylcyclohexanone (III-17a):

IR (KBr) ν_{max} : 3331, 3105, 2949, 2919, 2853, 1703, 1607, 1578, 1528, 1370, 851, 772 cm⁻¹.

^1H NMR (CDCl₃, 500 MHz): δ 7.88 (dd, $J = 1.0, 8.0$ Hz, 1H), 7.79 (dd, $J = 1.0, 8.0$ Hz, 1H), 7.67 (m, 1H), 7.44 (m, 1H), 5.45 (d, $J = 7.0$, 1H), 4.15 (br, s, 1H, -OH), 2.92-2.85 (m, 1H), 2.52-2.43 (m, 1H), 2.38 (td, $J = 5.0, 9.5$ Hz, 1H), 1.99-1.91 (m, 1H), 1.90-1.83 (m, 2H), 1.81-1.71 (m, 1H), 1.69-1.51 (m, 1H), 1.54-1.44 (m, 2H), 0.89 (t, $J = 7.5$ Hz, 3H) ppm.

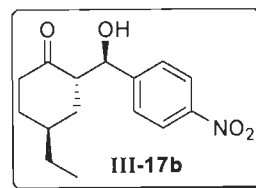


^{13}C NMR (CDCl₃, 125 MHz): δ 215.3, 148.8, 136.8, 133.2, 128.9, 128.5, 124.1, 69.9, 53.0, 38.7, 34.1, 33.9, 30.9, 24.8, 12.0 ppm.

(2S,4S,1'R)-2-[Hydroxy(4-nitrophenyl)methyl]-4-ethylcyclohexanone (III-17b):

IR (KBr) ν_{max} : 3490, 3101, 3060, 2965, 2910, 2842, 1705, 1600, 1585, 1500, 1340, 860 cm⁻¹.

$^1\text{H NMR}$ (CDCl_3 , 500 MHz): δ 8.26-8.21 (m, 2H), 7.55-7.51 (m, 2H), 4.94 (d, $J = 8.5$ Hz, 1H), 2.73-2.66 (m, 1H), 2.55-2.46 (m, 1H), 2.41 (td, $J = 5.0, 14.5$ Hz, 1H), 1.96-1.88 (m, 2H), 1.78-1.71 (m, 1H), 1.61-1.44 (m, 2H), 1.44-1.35 (m, 2H), 0.83 (t, $J = 7.5$ Hz, 3H) ppm.

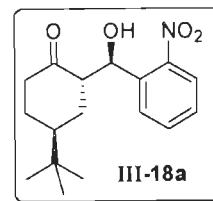


$^{13}\text{C NMR}$ (CDCl_3 , 125 MHz): δ 215.1, 148.4, 147.6, 127.8, 123.8, 74.2, 53.0, 38.4, 33.7, 33.5, 30.5, 24.8, 12.0 ppm

(2*S*,4*S*,1'*R*)-2-[Hydroxy(2-nitrophenyl)methyl]-4-*tert*-butylcyclohexanone (III-18a):

IR (KBr) ν_{max} : 3455, 2949, 2921, 2851, 1703, 1605, 1575, 1393, 1320, 1249, 720, 685 cm^{-1} .

$^1\text{H NMR}$ (CDCl_3 , 500 MHz): δ 7.89 (dd, $J = 1.0, 8.0$ Hz, 1H), 7.78-7.75 (m, 1H), 7.68-7.63 (m, 1H), 7.48-7.43 (m, 1H), 5.48 (d, $J = 7.0$, 1H), 2.87 (q, $J = 7.5$ Hz, 1H), 2.51-2.43 (m, 1H), 2.43-2.34 (m, 1H), 1.96-1.90 (m, 1H), 1.74-1.66 (m, 1H), 1.64-1.52 (m, 3H), 0.8 (s, 9H).

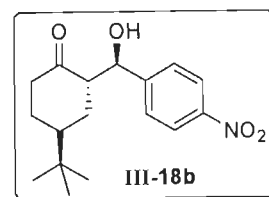


$^{13}\text{C NMR}$ (CDCl_3 , 125 MHz): δ 216.2, 148.7, 136.9, 133.3, 129.1, 128.7, 124.3, 69.7, 53.6, 42.4, 39.5, 32.8, 27.6, 27.0, 24.3.

(2*S*,4*S*,1'*R*)-2-[Hydroxy(4-nitrophenyl)methyl]-4-*tert*-butylcyclohexanone (III-18b):

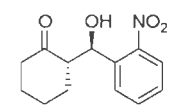
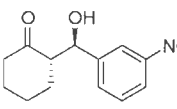
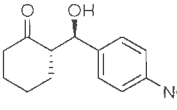
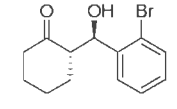
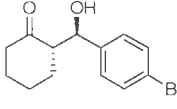
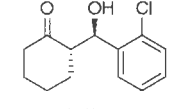
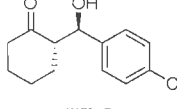
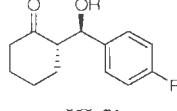
IR (KBr) ν_{max} : 3455, 2950, 2920, 2855, 1700, 1603, 1515, 1385, 1333, 1255, 1220, 856 cm^{-1} .

$^1\text{H NMR}$ (CDCl_3 , 500 MHz): δ 8.28-8.25 (m, 2H), 7.59-7.55 (m, 2H), 4.99 (d, $J = 9.0$ Hz, 1H), 2.68 (q, $J = 9.0$ Hz, 1H), 2.59-2.52 (m, 1H), 2.49-2.40 (m, 1H), 1.67-1.57 (m, 3H), 1.48-1.39 (m, 2H), 0.81 (s, 9H) ppm.



$^{13}\text{C NMR}$ (CDCl_3 , 125 MHz): δ 215.7, 148.1, 147.8, 127.5, 123.7, 74.0, 54.3, 42.2, 39.3, 32.7, 26.9, 26.8, 24.2 ppm.

Table 10: HPLC data table for aldol products obtained from the reaction between cyclohexanone and substituted benzaldehydes in presence of **Cat-1a**.

S.No.	¹ H NMR (CDCl ₃ -CHOH, δ)		HPLC data						
	<i>syn</i>	<i>anti</i>	Column	λ (nm)	Flow rate	Solvent IPA:Hex	<i>anti</i> product		
							<i>t_R</i> (min)	<i>t_R</i> (min)	
1		5.94	5.44	Chiralcel OD-H	254	1ml/min	5:95	18.3	22.2
2		5.51	4.92	Chiralcel OD-H	254	1ml/min	5:95	24.4	34.7
3		5.46	4.90	Chiralcel OD-H	254	1ml/min	5:95	29.9	43.9
4		5.67	5.33	Chiralpak AD-H	225	0.3ml/min	10:90	32.0	36.8
5		5.38	4.78	Chiralpak AD-H	254	0.3ml/min	10:90	39.4	44.4
6		5.70	5.35	Chiralcel OD-H	254	1ml/min	5:95	9.6	12.0
7		5.39	4.79	Chiralcel OD-H	254	1ml/min	5:95	11.5	16.4
8		5.39	4.80	Chiralcel OD-H	210	1ml/min	5:95	12.1	22.1

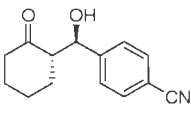
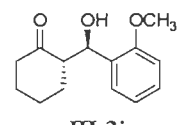
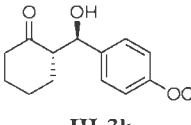
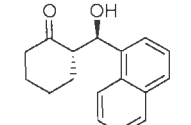
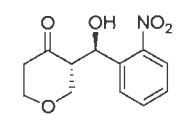
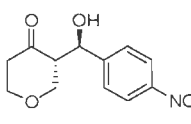
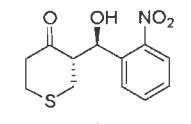
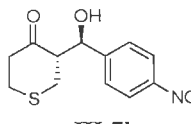
9	 III-3i	5.43	4.84	Chiralpak AD-H	234	0.3ml/min	10:90	61.7	78.2
10	 III-3j	5.61	5.25	Chiralcel OD-H	210	0.5ml/min	3:97	28.2	39.2
11	 III-3k	5.33	4.74	Chiralpak AD-H	254	1ml/min	5:95	35.5	36.8
12	 III-3l	6.37	5.61	Chiralcel OD-H	280	0.5ml/min	10:90	35.7	42.4
13	 III-6a	6.03	5.47	Chiralcel OD-H	254	1ml/min	10:90	53.4	59.1
14	 III-6b	5.53	5.01	Chiralpak AD-H	254	1ml/min	10:90	38.5	48.0
15	 III-7a	5.46	4.97	Chiralcel OD-H	254	1ml/min	10:90	33.8	42.5
16	 III-7b	5.94	5.05	Chiralpak AD-H	254	1ml/min	10:90	45.7	56.0

Table 11: HPLC data table for aldol products obtained from the reactions between cyclopentanone and substituted benzaldehydes in presence of **Cat-1a**.

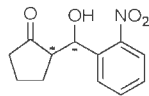
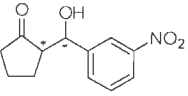
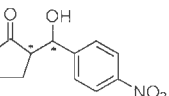
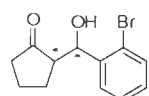
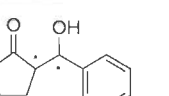
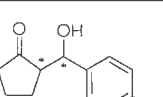
S.No.	Product	¹ H NMR (CDCl ₃ - CH ₂ OH, δ)		HPLC data							
		<i>syn</i>	<i>anti</i>	Column	λ (nm)	Flow rate (ml/min)	Solvent IPA:Hex	<i>syn</i> product		<i>anti</i> product	
								<i>t_R</i> (min)	<i>t_R</i> (min)	<i>t_R</i> (min)	<i>t_R</i> (min)
1	 III-9a	5.90	4.42	Chiralpak AD-H	254	1	5:95	15.3	19.1	23.5	26.9
2	 III-9b	5.43	4.83	Chiralcel OD-H	254	0.5	3:97	35.0	41.2	44.5	54.1
3	 III-9c	5.42	4.53	Chiralpak AD-H	254	1	5:95	24.4	27.6	35.2	36.3
4	 III-9d	5.63	5.27	Chiralpak AD-H	220	0.9	2:98	6.4	8.0	13.1	15.0
5	 III-9e	5.26	4.68	Chiralpak AD-H	220	1	5:95	12.1	15.7	18.4	20.3
6	 III-9f	5.27	4.69	Chiralpak AD-H	220	0.9	2:98	24.6	30.4	31.7	35.5

Table 12: HPLC data table for aldol products obtained from the reaction between acetone and substituted benzaldehydes in presence of **Cat-1a**.

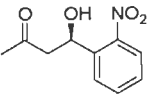
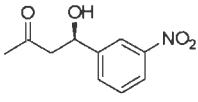
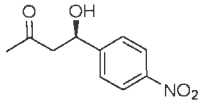
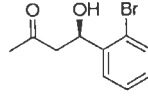
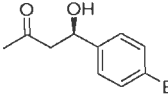
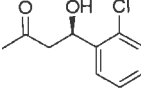
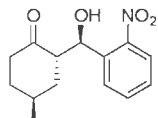
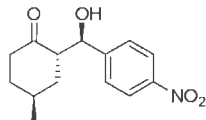
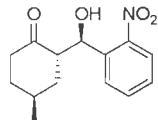
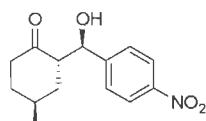
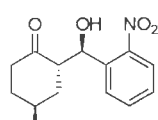
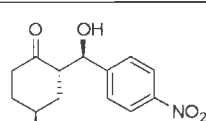
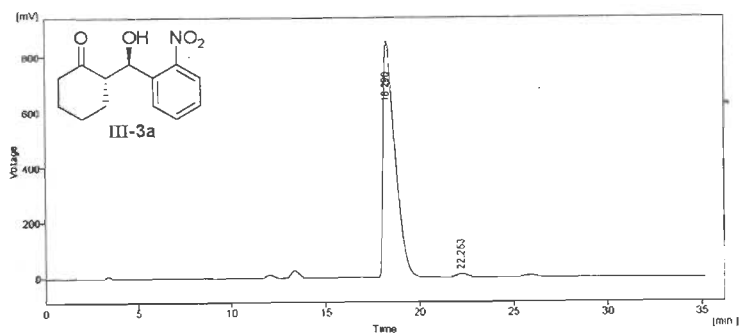
S.No.	Product	HPLC data					
		Column	λ (nm)	Flow rate	Solvent IPA:Hex	t_R (min)	t_R (min)
1	 III-11a	Chiralpak AD-H	254	0.5ml/min	3:97	48.7	51.6
2	 III-11b	Chiralpak AD-H	254	1ml/min	5:95	69.6	76.0
3	 III-11c	Chiralpak AD-H	254	1ml/min	5:95	10.7	13.6
4	 III-11d	Chiralpak AD-H	254	0.5ml/min	5:95	13.4	16.1
5	 III-11e	Chiralpak AD-H	254	0.5ml/min	7:93	23.8	25.7
6	 III-11f	Chiralpak AD-H	254	0.3ml/min	8:92	36.1	40.3

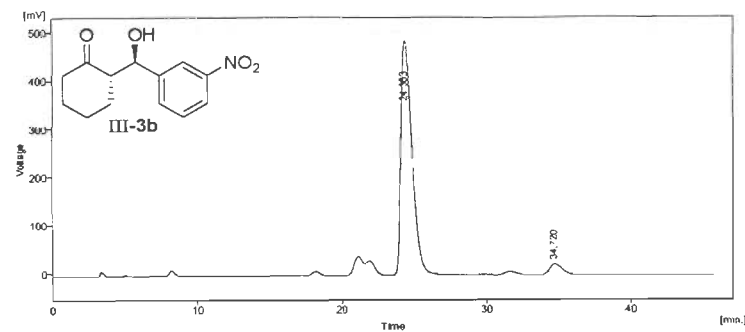
Table 13: HPLC data table for aldol products derived from the reaction between 4-substituted cyclohexanones and substituted aromatic aldehydes in presence of **Cat-1a**.

S.No.	Product	HPLC data					
		Column	λ (nm)	Flow rate	Solvent IPA:Hex	t_R (min)	t_R (min)
1	 III-16a	Chiralpak AD-H	254	0.5 ml/min	5:95	53.7	63.1
2	 III-16b	Chiralcel OD-H	254	1 ml/min	90:10	44.5	52.6
3	 III-17a	Chiralpak AD-H	254	0.5 ml/min	5:95	47.6	58.2
4	 III-17b	Chiralcel OD-H	254	0.5 ml/min	5:95	57.0	64.4
5	 III-18a	Chiralpak AD-H	254	0.5 ml/min	95:5	43.1	55.4
6	 III-18b	Chiralcel OD-H	280	0.5ml/min	8:92	53.4	63.1



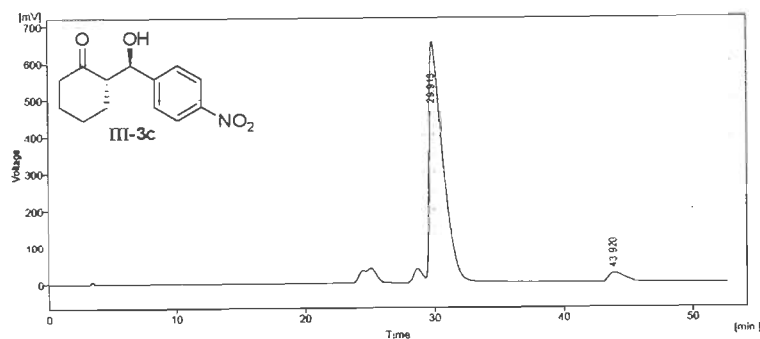
Result Table (Uncal - F:\RASHMI\FINAL DATA\RL_21_ONO2)

Reten Time (min)	Area (mv.s)	Height (mv)	Area (%)	Height (%)	WDS (min)	
1	16.290	38223.936	896.960	98.3	58.5	0.99
2	22.263	648.247	11.325	1.7	1.5	0.73
Total		38869.183	908.686	100.0	100.0	



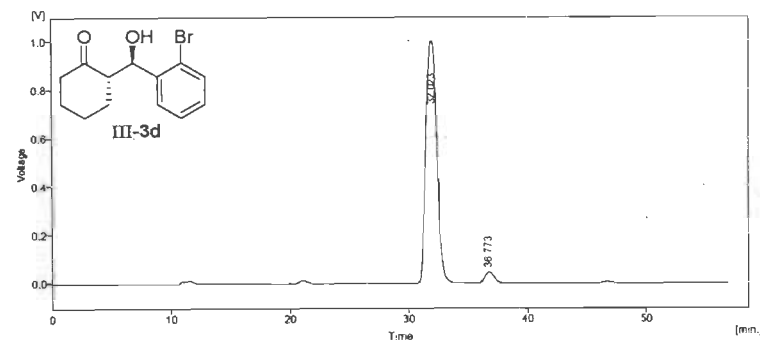
Result Table (Uncal - F:\RASHMI\FINAL DATA\RL_44-02_1)

Reten Time (min)	Area (mv.s)	Height (mv)	Area (%)	Height (%)	WDS (min)	
1	24.283	29620.811	486.611	99.2	99.7	0.81
2	34.720	1906.296	21.756	4.8	1.3	0.96
Total		26526.748	508.347	100.0	100.0	



Result Table (Uncal - F:\RASHMI\FINAL DATA\4_NO2_HO)

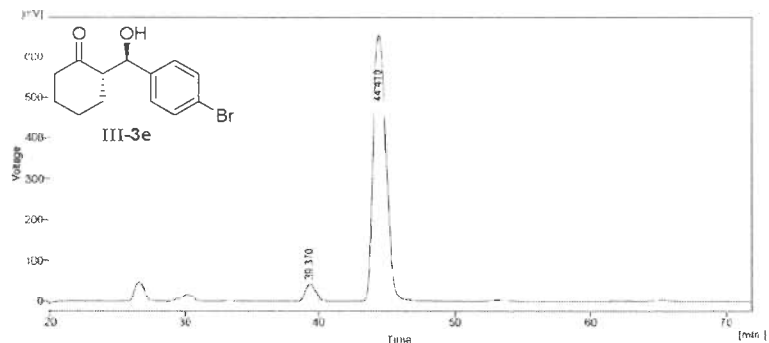
Reten Time (min)	Area (mv.s)	Height (mv)	Area (%)	Height (%)	WDS (min)	
1	29.913	48236.183	643.374	95.4	98.2	1.11
2	43.920	2242.563	25.310	4.6	3.8	1.36
Total		48551.726	668.684	100.0	100.0	



Result Table (Uncal - F:\RASHMI\FINAL DATA\RL_33_OBR)

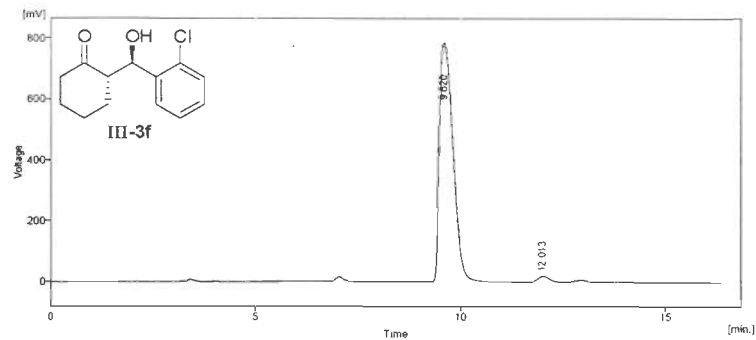
Reten Time (min)	Area (mv.s)	Height (mv)	Area (%)	Height (%)	WDS (min)	
1	32.023	63196.447	959.145	96.2	95.6	1.02
2	36.773	2524.022	45.936	3.8	4.4	0.97
Total		65720.469	1045.080	100.0	100.0	

Figure 4: HPLC Chromatograms of aldol adducts III-3a, III-3b, III-3c and III-3d.



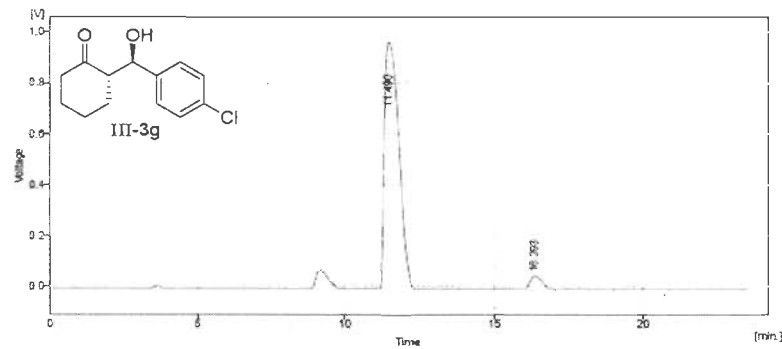
Result Table (Uncal - F:\asymmetric\data\IRL_47_p61)

Reten. Time [min]	Area [mV s]	Height [mV]	Area [%]	Height [%]	W05 [min]
1	39.370	167.296	37.931	4.5	5.6
2	44.810	41453.964	652.397	95.4	54.3
Total	43441.343	590.266	100.0	100.0	



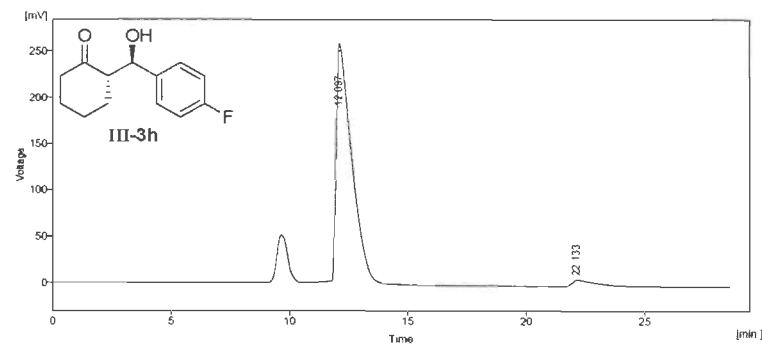
Result Table (Uncal - F:\asymmetric\data\IRL_48_OCL_r1)

Reten. Time [min]	Area [mV s]	Height [mV]	Area [%]	Height [%]	W05 [min]
1	9.620	17377.975	787.101	97.9	97.6
2	12.013	377.053	19.367	2.1	2.4
Total	17755.028	806.468	100.0	100.0	



Result Table (Uncal - F:\asymmetric\data\O-Cl_r0)

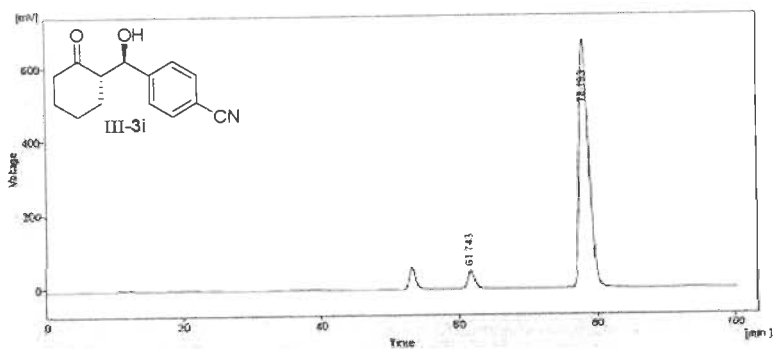
Reten. Time [min]	Area [mV s]	Height [mV]	Area [%]	Height [%]	W05 [min]
1	11.490	31880.171	968.046	95.1	95.2
2	16.393	1299.410	49.337	3.9	4.2
Total	33179.581	1017.384	100.0	100.0	



Result Table (Uncal - F:\asymmetric\data\IRL_48_F-10p61)

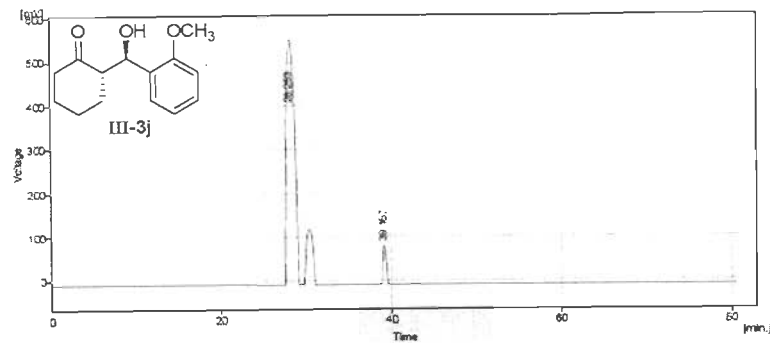
Reten. Time [min]	Area [mV s]	Height [mV]	Area [%]	Height [%]	W05 [min]
1	12.097	11590.257	256.988	96.2	97.4
2	22.130	452.286	6.769	3.9	2.6
Total	12042.543	265.457	100.0	100.0	

Figure 5: HPLC Chromatograms of aldol adducts III-3e, III-3f, III-3g and III-3h.



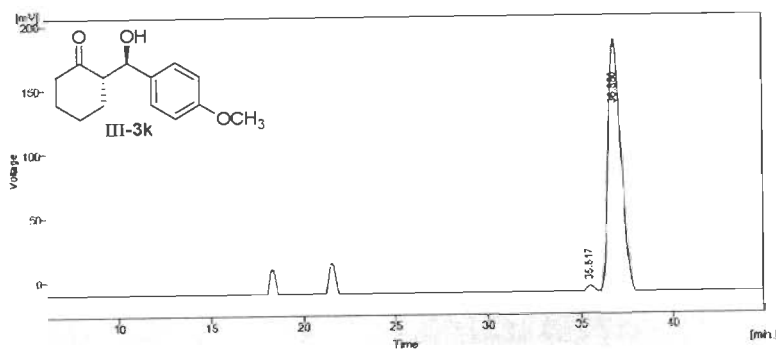
Result Table (User: F:\msd\msd\data\201_43_CN_1)

Reten. Time [min]	Area [mV.s]	Height [mV]	Area [%]	Height [%]	W05 [min]	
1	61743	2501474	42.721	4.0	5.8	0.07
2	76193	8150881	672102	96.6	94.0	1.41
Total	54132155	714827	100.0	100.0		



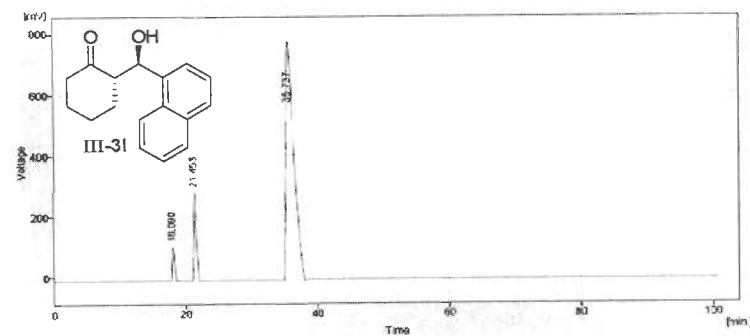
Result Table (User: F:\msd\msd\data\201_084_01)

Reten. Time [min]	Area [mV.s]	Height [mV]	Area [%]	Height [%]	W05 [min]
1	28.252	27499206	94.3	94.4	1.15
2	30.167	2265006	6.7	13.6	0.45
Total	35765.512	648.529	100.0	100.0	



Result Table (User: F:\2014\ALDOL\FinalView\Folder14JA_22b)

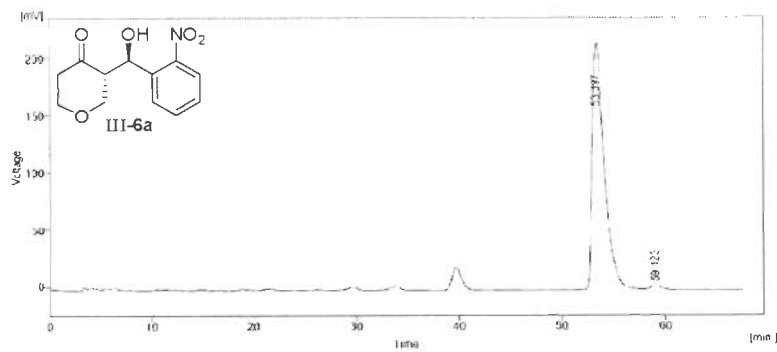
Reten. Time [min]	Area [mV.s]	Height [mV]	Area [%]	Height [%]	W05 [min]	
1	35.517	114005	47.6	1.2	2.3	0.43
2	36.680	9234574	196238	98.8	97.7	0.75
Total	5349442	203955	100.0	100.0		



Result Table (User: F:\msd\msd\data\201_084_02)

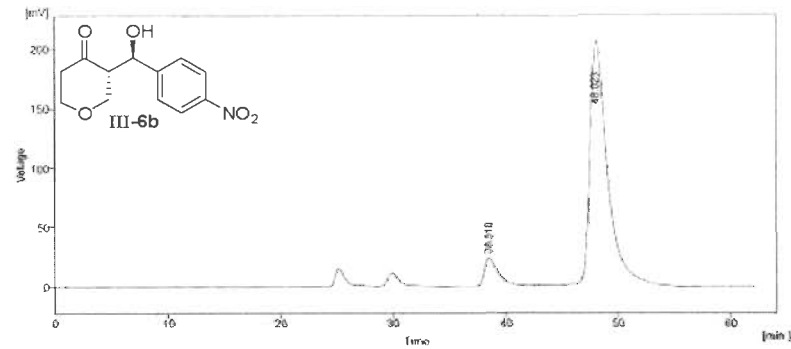
Reten. Time [min]	Area [mV.s]	Height [mV]	Area [%]	Height [%]	W05 [min]	
1	18.080	2767171	111585	3.6	9.4	0.43
2	21.453	9002685	290456	12.2	24.5	0.51
3	35.737	61953164	793086	84.0	66.1	1.24
Total	73640221	1165090	100.0	100.0		

Figure 6: HPLC Chromatograms of aldol adducts III-3i, III-3j, III-3k and III-3l.



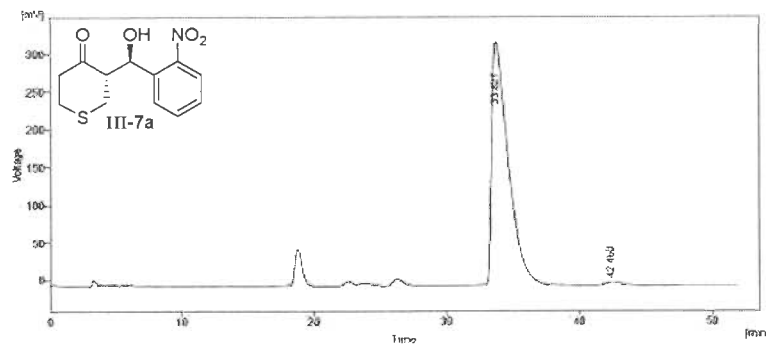
Result Table (Linear - F:\data\final\data\New Folder\New Folder\Furans_2\NO2)

Reten. Time [min]	Area [int. s]	Height [int.]	Area [%]	Height [%]	WCS [min]
1	53.287	16925.154	214.457	98.8	88.6
2	59.122	202.325	2.656	1.2	1.21
Total	17.127.478	217.123	100.0	100.0	



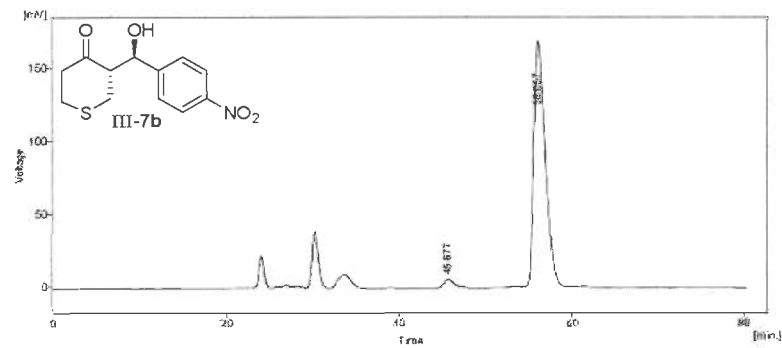
Result Table (Linear - F:\data\final\data\New Folder\New Folder\Furans_2\NO2)

Reten. Time [min]	Area [int. s]	Height [int.]	Area [%]	Height [%]	WCS [min]
1	36.910	1725.342	21.055	9.1	3.6
2	48.510	22141.755	266.660	90.9	50.4
Total	24478.137	228.624	100.0	100.0	



Result Table (Linear - F:\data\final\data\New Folder\New Folder\Furans_2\NO2)

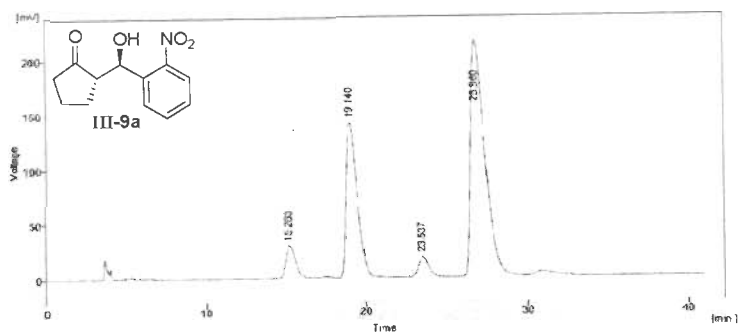
Reten. Time [min]	Area [int. s]	Height [int.]	Area [%]	Height [%]	WCS [min]
1	35.232	27502.935	324.857	98.8	88.7
2	42.460	384.365	4.629	1.2	1.3
Total	28267.301	329.486	100.0	100.0	



Result Table (Linear - F:\data\final\data\New Folder\New Folder\Furans_2\NO2)

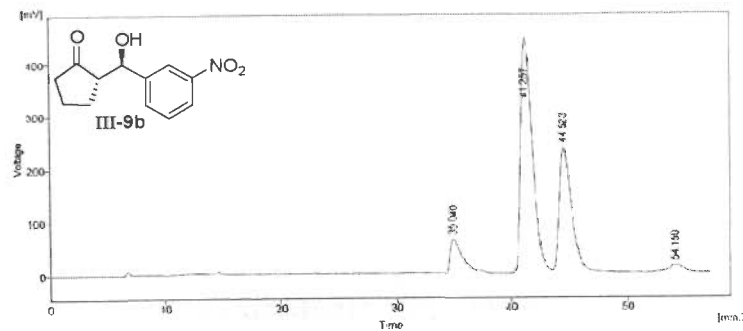
Reten. Time [min]	Area [int. s]	Height [int.]	Area [%]	Height [%]	WCS [min]
1	45.817	427.671	5.654	2.7	3.3
2	57.820	15515.485	188.004	97.3	96.7
Total	15943.156	173.658	100.0	100.0	

Figure 7: HPLC Chromatograms of aldol adducts III-6a, III-6b, III-7a and III-7b.



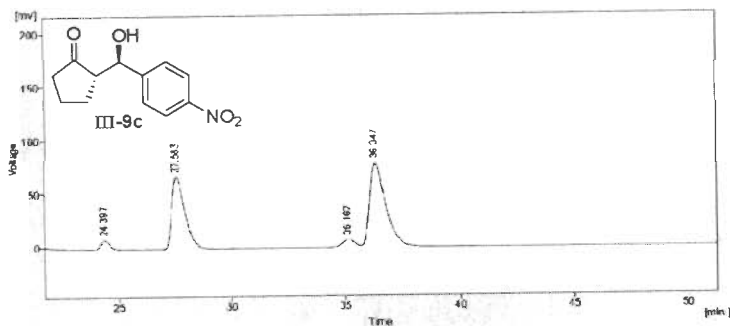
Result Table (Local - F:\asymmetric\data\New Folder\MO2_P1_)

Reten. Time [min]	Area [mV.s]	Height [mV]	Area [%]	Height [%]	WOS [min]
1	15.263	306.516	26.804	4.8	4.6
2	19.140	6670.817	142.063	51.1	55.3
3	23.577	683.360	17.029	5.2	4.3
4	25.900	13110.323	216.429	61.1	53.6
Total		21484.815	432.186	100.0	100.0



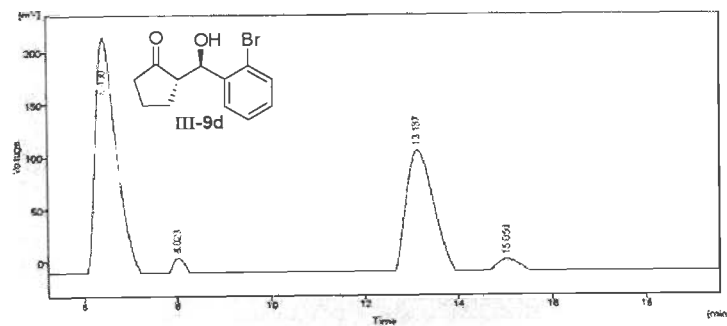
Result Table (Local - F:\asymmetric\data\New Folder\Folder_369_563)

Reten. Time [min]	Area [mV.s]	Height [mV]	Area [%]	Height [%]	WOS [min]
1	35.043	2687.792	60.167	7.2	1.02
2	41.287	30697.013	445.016	56.1	1.07
3	44.823	17403.046	245.810	30.0	1.12
4	54.150	947.165	1.112	1.5	1.36
Total		52855.504	751.015	100.0	100.0



Result Table (Local - F:\asymmetric\data\New Folder\Folder_369_563)

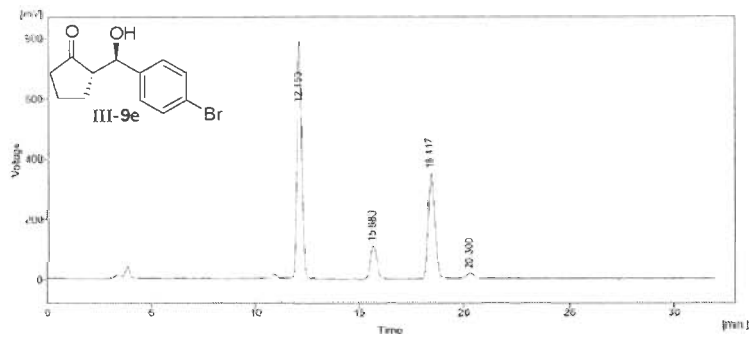
Reten. Time [min]	Area [mV.s]	Height [mV]	Area [%]	Height [%]	WOS [min]
1	24.997	221.756	6.660	5.2	3.42
2	27.843	2721.494	81.964	58.2	3.42
3	35.187	382.973	7.582	4.0	3.56
4	36.241	3476.272	78.897	54.3	4.56
Total		7142.501	142.429	100.0	100.0



Result Table (Local - F:\asymmetric\data\New Folder\Folder_369_563)

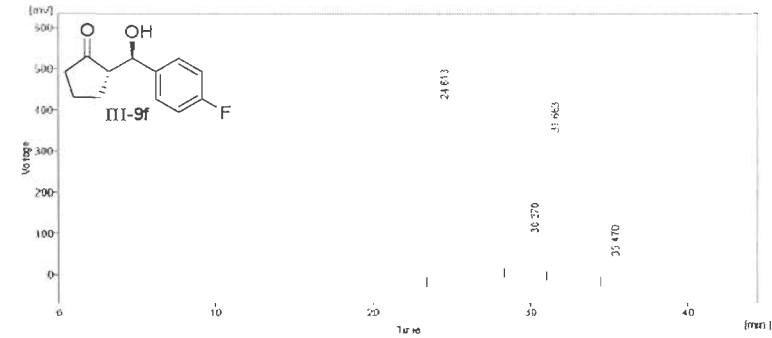
Reten. Time [min]	Area [mV.s]	Height [mV]	Area [%]	Height [%]	WOS [min]
1	6.410	6828.676	226.406	56.0	61.7
2	8.023	218.838	15.904	1.9	3.8
3	13.157	4698.777	174.361	38.0	37.0
4	15.050	117.822	10.531	2.8	2.8
Total		11969.214	383.105	100.0	100.0

Figure 8: HPLC Chromatograms of aldol adducts III-9a, III-9b, III-9c and III-9d.



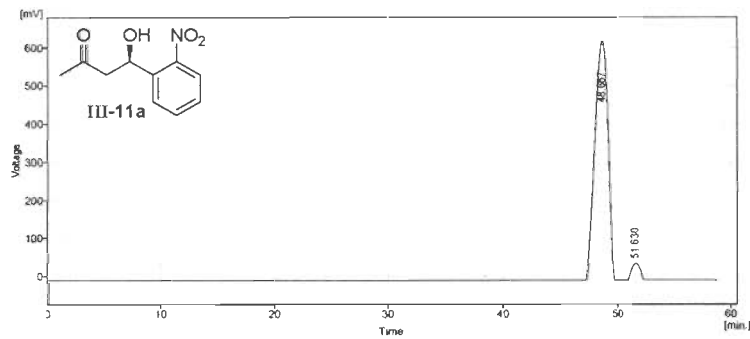
Result Table (Uncal - F:\RASHM\FINAL DATA\3RL_24_10_17)

Reten. Time [min]	Area [mV s]	Height [mV]	Area [%]	Height [%]	W05 [min]
1	12.153	12905.312	75.215	64.3	0.25
2	15.690	1128.575	7.215	5.1	0.26
3	18.417	7994.537	548.498	36.4	0.36
4	20.300	313.710	14.872	1.4	0.35
Total		17442.237	1227.873	100.0	100.0



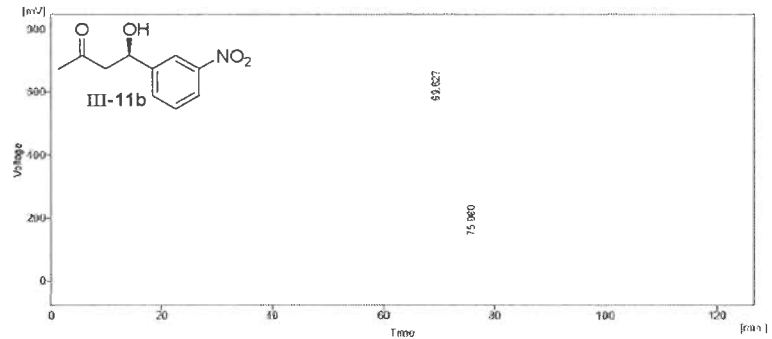
Result Table (Uncal - F:\RASHM\FINAL DATA\New Folder (2)\Cyclopentop_F_1)

Reten. Time [min]	Area [mV s]	Height [mV]	Area [%]	Height [%]	W05 [min]
1	24.613	25760.051	562.614	57.7	0.73
2	30.270	3694.212	35.085	3.4	0.65
3	31.665	14070.862	335.771	33.3	0.65
4	35.476	1673.636	35.058	3.5	0.58
Total		46427.911	1036.539	100.0	100.0



Result Table (Uncal - F:\RASHM\FINAL DATA\3RL_62_ONO2_A)

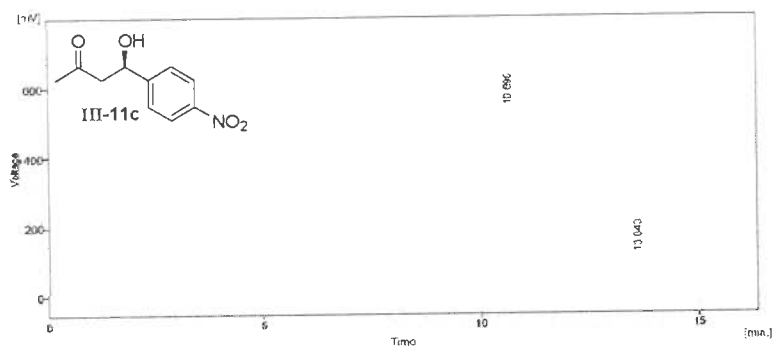
Reten. Time [min]	Area [mV s]	Height [mV]	Area [%]	Height [%]	W05 [min]
1	48.827	49079.488	625.579	95.6	1.30
2	51.630	2249.701	43.100	4.4	0.91
Total		51326.186	669.679	100.0	100.0



Result Table (Uncal - F:\RASHM\FINAL DATA\NO2_A)

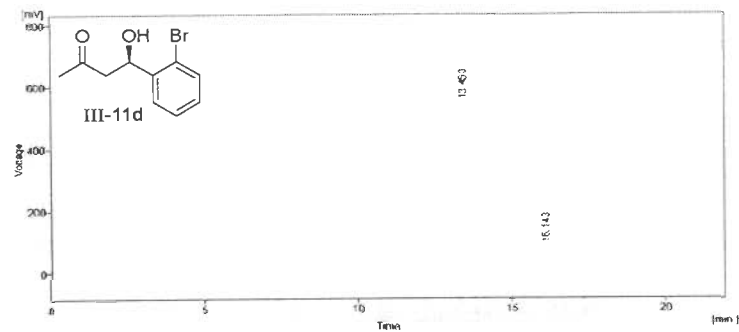
Reten. Time [min]	Area [mV s]	Height [mV]	Area [%]	Height [%]	W05 [min]
1	69.627	116596.291	767.075	80.6	2.47
2	75.960	18182.661	124.751	7.5	2.33
Total		134778.952	891.826	100.0	100.0

Figure 9: HPLC Chromatograms of aldol adducts III-9e, III-9f, III-11a and III-11b.



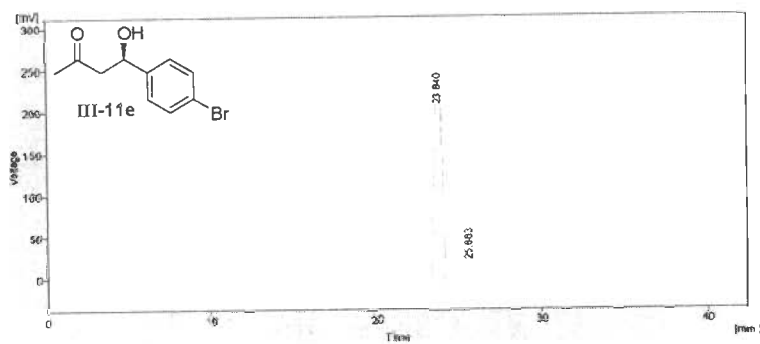
Result Table (LUNA[®]-P₁₈ACQUINOVIAL DATA_02_03A)

Peak	Time [min]	Area [mV*s]	Height [mV]	Area [%]	Height [%]	WDS [mm]
1	10.860	15462.881	729.748	88.7	89.3	0.40
2	13.640	2341.060	87.456	11.3	11.3	0.42
Total	20604.150	797.204	100.0	100.0		



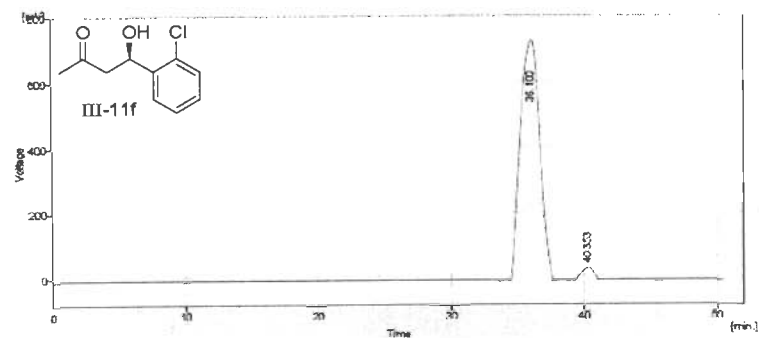
Result Table (LUNA[®]-P₁₈ACQUINOVIAL DATA_02_03A)

Peak	Time [min]	Area [mV*s]	Height [mV]	Area [%]	Height [%]	WDS [mm]
1	13.803	25480.341	784.150	86.8	86.7	0.50
2	16.143	3211.148	87.331	11.2	10.5	0.39
Total	28694.409	851.525	100.0	100.0		



Result Table (LUNA[®]-P₁₈ACQUINOVIAL DATA_02_03A)

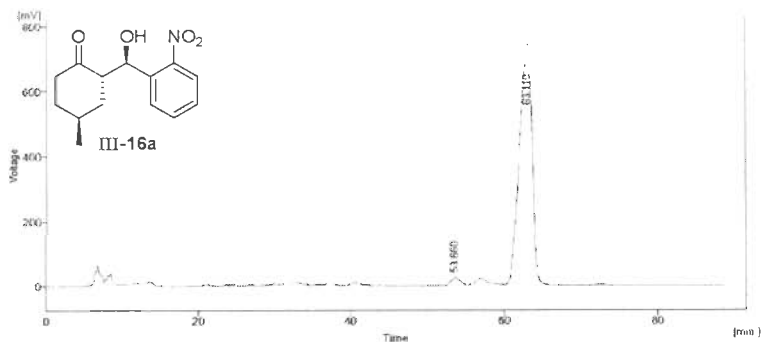
Peak	Time [min]	Area [mV*s]	Height [mV]	Area [%]	Height [%]	WDS [mm]
1	23.840	3310.609	280.616	86.3	92.1	0.48
2	25.663	477.324	21.340	4.7	7.4	0.38
Total	3792.931	317.961	100.0	100.0		



Result Table (LUNA[®]-P₁₈ACQUINOVIAL DATA_02_03A)

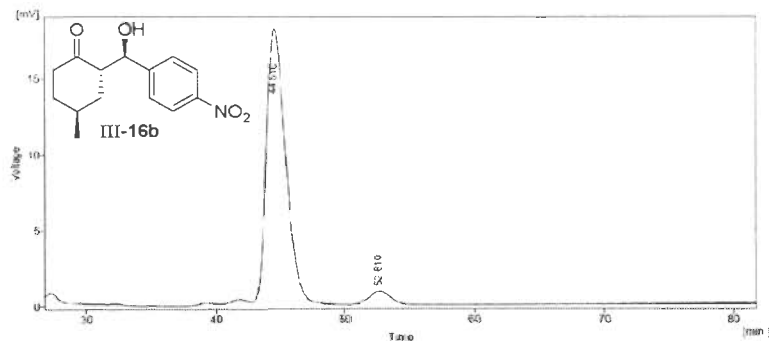
Peak	Time [min]	Area [mV*s]	Height [mV]	Area [%]	Height [%]	WDS [mm]
1	35.100	66031.273	630.306	96.8	93.9	1.53
2	40.363	2887.223	40.676	4.2	6.1	1.11
Total	60096.296	670.982	100.0	100.0		

Figure 10: HPLC Chromatograms of aldol adducts III-11c, III-11d, III-11e and III-11f.



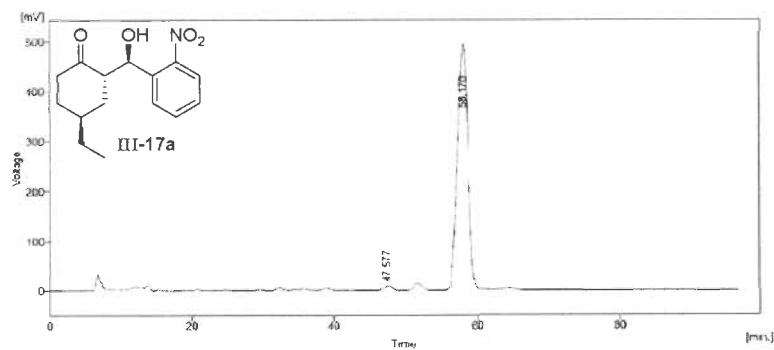
Result Table (Local - F:\msd\msd\data\New Folder\New Folder\nc_Div2)

Reten. Time [min]	Area [mV s]	Height [mV]	Area [%]	Height [%]	WGS [min]
1	53 660	1042 765	25 150	2 2	3 3
2	52 110	80117 100	741 736	97 8	96 7
Total	57053 1623	712 346	100 0	100 0	



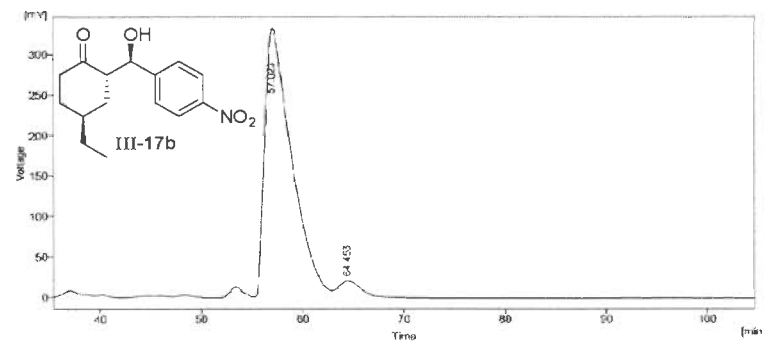
Result Table (Local - F:\msd\msd\data\New Folder\New Folder\nc_Div2)

Reten. Time [min]	Area [mV s]	Height [mV]	Area [%]	Height [%]	WGS [min]
1	44 510	1700 285	16 015	95 9	1 05
2	52 610	76 016	0 799	4 1	4 2
Total	1469 501	16 814	100 0	100 0	



Result Table (Local - F:\msd\msd\data\New Folder\New Folder\ET_1_Civ2)

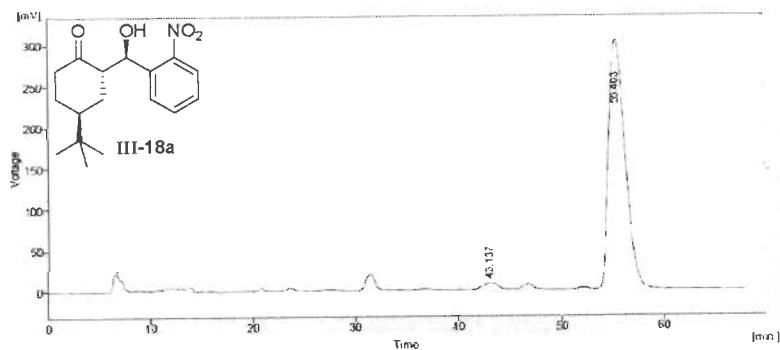
Reten. Time [min]	Area [mV s]	Height [mV]	Area [%]	Height [%]	WGS [min]
1	47 827	475 764	2 506	1 4	1 4
2	58 170	48196 896	490 420	99 6	98 4
Total	49269 593	501 346	100 0	100 0	



Result Table (Local - F:\msd\msd\data\New Folder\New Folder\ET_1\NC2_03)

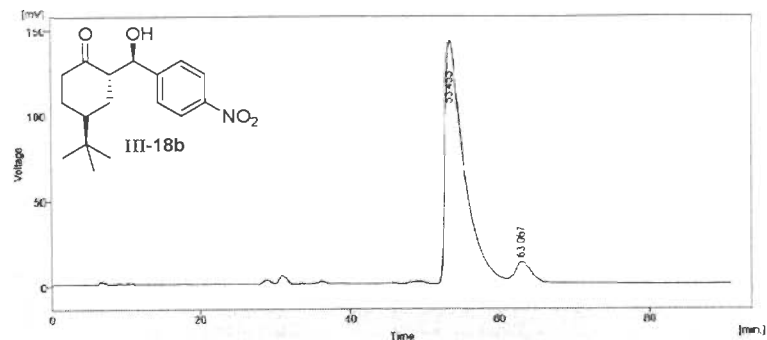
Reten. Time [min]	Area [mV s]	Height [mV]	Area [%]	Height [%]	WGS [min]
1	57 220	61277 547	204 051	94 5	94 5
2	64 463	3297 666	20 545	5 5	5 5
Total	64665 147	154 596	100 0	100 0	

Figure 11: HPLC Chromatograms of aldol adducts III-16a, III-16b, III-17a and III-17b.



Result Table (Unreal - F:\asymmetric\data\new folder\new folder\11-bor_C102)

	Reten. Time [min]	Area [mV s]	Height [mV]	Area [%]	Height [%]	W05 [min]
1	43.137	775.810	6.055	2.2	2.6	1.55
2	55.805	33943.513	305.411	97.8	97.4	1.28
	Total	34719.323	311.476	100.0	100.0	



Result Table (Unreal - F:\asymmetric\data\new folder\new folder\11-bor)

	Reten. Time [min]	Area [mV s]	Height [mV]	Area [%]	Height [%]	W05 [min]
1	52.453	24841.957	142.528	93.3	92.2	2.46
2	63.067	1766.428	17.087	6.7	7.8	2.71
	Total	26608.385	159.615	100.0	100.0	

Figure 12: HPLC Chromatograms of aldol adducts **III-18a** and **III-18b**.

3.6. REFERENCES

- 1 R. Kane, *Aldol Reaction (Condensation)*, *Ann. Phys. Chem.* 44 (1838) 475.
- 2 A. Berkessel, H. Gröger (Eds.), *Asymmetric Organocatalysis: From Biomimetic Concepts to Applications in Asymmetric Synthesis*, Wiley-VCH: Weinheim, 2005.
- 3 P.I. Dalko (Ed.), *Enantioselective Organocatalysis: Reactions and Experimental Procedures*, Wiley-VCH: Weinheim, 2007.
- 4 B. List, *Introduction: Organocatalysis*, *Chem. Rev.* 107 (2007) 5413.
- 5 D. Enders, C. Grondal, M.R.M. Huettl, *Asymmetric Organocatalytic Domino Reactions*, *Angew. Chem. Int. Ed.* 46 (2007) 1570.
- 6 P. Hélène, *Asymmetric Organocatalysis*, *Tetrahedron* 63 (2007) 9267.
- 7 D. Alessandro, M. Alessandro, *Asymmetric Organocatalysis: From Infancy to Adolescence*, *Angew. Chem. Int. Ed.* 47 (2008) 4638.
- 8 D.W.C. MacMillan, *The Advent and Development of Organocatalysis*, *Nature* 455 (2008) 304.
- 9 H. Gröger, J. Wilken, *The Application of L-Proline as an Enzyme Mimic and Further New Asymmetric Syntheses Using Small Organic Molecules as Chiral Catalysts*, *Angew. Chem. Int. Ed.* 40 (2001) 529.
- 10 B. List, *Asymmetric Aminocatalysis*, *Synlett* (2001) 1675.
- 11 M. Movassaghi, E.N. Jacobsen, *Perspectives: Chemistry: The Simplest "Enzyme"*, *Science* 298 (2002) 1904.
- 12 B. List, *Enamine Catalysis is a Powerful Strategy for the Catalytic Generation and Use of Carbanion Equivalents*, *Acc. Chem. Res.* 37 (2004) 548.
- 13 S. Saito, H. Yamamoto, *Design of Acid-Base Catalysis for the Asymmetric Direct Aldol Reaction*, *Acc. Chem. Res.* 37 (2004) 570.
- 14 W. Notz, F. Tanaka, C.F. Barbas III, *Enamine-Based Organocatalysis with Proline and Diamines: The Development of Direct Catalytic Asymmetric Aldol, Mannich, Michael, and Diels-Alder Reactions*, *Acc. Chem. Res.* 37 (2004) 580.
- 15 U. Kazmaier, *Amino Acids-Valuable Organocatalysts in Carbohydrate Synthesis*, *Angew. Chem. Int. Ed.* 44 (2005) 2186.
- 16 B.S. Chetter, R. Mahrwald, *Modern Aldol Methods for the Total Synthesis of Polyketides*, *Angew. Chem. Int. Ed.* 45 (2006) 7506.

- 17 B. List, *The Ying and Yang of Asymmetric Aminocatalysis*, Chem. Commun. (2006) 819.
- 18 S. Mukherjee, J.W. Yang, S. Hoffmann, B. List, *Asymmetric Enamine Catalysis*, Chem. Rev. 107 (2007) 5471.
- 19 G. Guillena, C. Nájera, D.J. Ramon, *Enantioselective Direct Aldol Reaction: The Blossoming of Modern Organocatalysis*, Tetrahedron: Asymm. 18 (2007) 2249.
- 20 L.M. Geary, P.G. Hultin, *The State of the Art in Asymmetric Induction: The Aldol Reaction as a Case Study*, Tetrahedron: Asymm. 20 (2009) 131.
- 21 K. Sakthivel, W. Notz, T. Bui, C.F. Barbas III, *Amino Acid Catalyzed Direct Asymmetric Aldol Reactions: A Bioorganic Approach to Catalytic Asymmetric Carbon-Carbon Bond-Forming Reactions*, J. Am. Chem. Soc. 123 (2001) 5260.
- 22 A.B. Northrup, I.K. Mangion, F. Hettche, D.W.C. MacMillan, *Enantioselective Organocatalytic Direct Aldol Reactions of α -Oxy-Aldehydes: Step One in a Two-Step Synthesis of Carbohydrates*, Angew. Chem. Int. Ed. 43 (2004) 2152.
- 23 Q. Pan, B. Zou, Y. Wang, D. Ma, *Diastereoselective Aldol Reaction of N,N -Dibenzyl- α -amino Aldehydes with Ketones Catalyzed by Proline*, Org. Lett. 6 (2004) 1009.
- 24 S. Chandrasekhar, Ch. Narsihmulu, N.R. Reddy, S.S. Sultana, *L-Proline Catalyzed Asymmetric Transfer Aldol Reaction between Diacetone Alcohol and Aldehydes*, Chem. Commun. (2004) 2450.
- 25 R. Thayumanavan, F. Tanaka, C.F. Barbas III, *Direct Organocatalytic Asymmetric Aldol Reactions of α -Amino Aldehydes: Expedient Syntheses of Highly Enantiomerically Enriched anti- β -Hydroxy- α -amino Acids*, Org. Lett. 6 (2004) 3541.
- 26 D. Enders, C. Grondal, *Direct Organocatalytic de Novo Synthesis of Carbohydrates*, Angew. Chem. Int. Ed. 44 (2005) 1210.
- 27 J. Casas, M. Engqvist, I. Ibrahim, B. Kaynak, A. Córdova, *Direct Amino Acid Catalyzed Asymmetric Synthesis of Polyketide Sugars*, Angew. Chem. Int. Ed. 44 (2005) 1343.
- 28 J.T. Suri, D.B. Ramachary, C.F. Barbas III, *Mimicking Dihydroxy Acetone Phosphate-Utilizing Aldolases through Organocatalysis: A Facile Route to Carbohydrates and Aminosugars*, Org. Lett. 7 (2005) 1383.
- 29 H. Sunden, R. Rios, I. Ibrahim, G.-L. Zhao, L. Eriksson, A. Córdova, *A Highly Enantioselective Catalytic Domino Aza-Michael/Aldol Reaction: One-Pot Organocatalytic Asymmetric Synthesis of 1,2-Dihydroquinolines*, Adv. Synth. Catal. 349 (2007) 827.

- 30 A. Russo, G. Botta, A. Lattanzi, *Highly Stereoselective Direct Aldol Reactions Catalyzed by (S)-NOBIN-L-Prolinamide*, *Tetrahedron* 63 (2007) 11886.
- 31 Y. Hayashi, T. Itoh, S. Aratake, H. Ishikawa, *A Diarylprolinol in an Asymmetric Catalytic and Direct Crossed-Aldol Reaction of Acetaldehyde*, *Angew. Chem. Int. Ed.* 47 (2008) 2082.
- 32 X.-W. Liu, T.N. Le, Y. Lu, Y. Xiao, J. Ma, X. Li, *An Efficient Synthesis of Chiral Phosphinyl Oxide Pyrrolidines and their Application to Asymmetric Direct Aldol Reactions*, *Org. Biomol. Chem.* 6 (2008) 3997.
- 33 F.-Z. Peng, Z.-H. Shao, X.-W. Pu, H.-B. Zhang, *Highly Diastereo- and Enantioselective Direct Aldol Reactions Promoted by Water-Compatible Organocatalysts Bearing Central and Axial Chiral Elements*, *Adv. Synth. Catal.* 350 (2008) 2199.
- 34 B. List, R.A. Lerner, C.F. Barbas III, *Proline-Catalyzed Direct Asymmetric Aldol Reactions*, *J. Am. Chem. Soc.* 122 (2000) 2395.
- 35 W. Notz, B. List, *Catalytic Asymmetric Synthesis of anti-1,2-Diols*, *J. Am. Chem. Soc.* 122 (2000) 7386.
- 36 Z. Tang, Z.-H. Yang, X.-H. Chen, L.-F. Cun, A.-Q. Mi, Y.-Z. Jiang, L.-Z. Gong, *A Highly Efficient Organocatalyst for Direct Aldol Reactions of Ketones with Aldehydes*, *J. Am. Chem. Soc.* 127 (2005) 9285.
- 37 G. Guillena, M.C. Hita, C. Nájera, S.F. Viozquez, *Solvent-Free Asymmetric Direct Aldol Reactions Organocatalyzed by Recoverable (S)-Binam-L-Prolinamide*, *Tetrahedron: Asymm.* 18 (2007) 2300.
- 38 Y. Zhou, Z. Shan, *Chiral Diols: A New Class of Additives for Direct Aldol Reaction Catalyzed by L-Proline*, *J. Org. Chem.* 71 (2006) 9510.
- 39 B. List, P. Pojarliev, C. Castello, *Proline-Catalyzed Asymmetric Aldol Reactions Between Ketones and α -Unsubstituted Aldehydes*, *Org. Lett.* 3 (2001) 573.
- 40 A. Córdova, W. Zou, I. Ibrahim, E. Reyes, M. Engqvist, W.W. Liao, *Acyclic Amino Acid Catalyzed Direct Asymmetric Aldol Reactions: Alanine, The Simplest Stereoselective Organocatalyst*, *Chem. Commun.* (2005) 3586.
- 41 X.Y. Xu, Y.Z. Wang, L.Z. Gong, *Design of Organocatalysts for Asymmetric Direct syn-Aldol Reactions*, *Org. Lett.* 9 (2007) 4247.

- 42 B.L. Zheng, Q.Z. Liu, C.S. Guo, X.L. Wang, L. He, *Highly Enantioselective Direct Aldol Reaction Catalyzed by Cinchona Derived Primary Amines*, *Org. Biomol. Chem.* 5 (2007) 2913.
- 43 L. He, J. Jiang, Z. Tang, X. Cui, A.-Q. Mi, Y.-Z. Jiang, L.-Z. Gong, *Highly Diastereo- and Enantioselective Direct Aldol Reactions of Cycloketones with Aldehydes Catalyzed by a trans-4-tert-Butyldimethylsiloxy-L-Proline Amide*, *Tetrahedron: Asymm.* 18 (2007) 265.
- 44 S. Sathapornvajana, T. Vilaivan, *Prolinamides Derived from Aminophenols as Organocatalysts for Asymmetric Direct Aldol Reactions*, *Tetrahedron* 63 (2007) 10253.
- 45 G.L. Puleo, A. Iuliano, *Methyl 12-[D-prolinoylamino]cholate as a Versatile Organocatalyst for the Asymmetric Aldol Reaction of Cyclic Ketones*, *Tetrahedron: Asymm.* 18 (2007) 2894.
- 46 X.-Y. Xu, Y.-Z. Wang, L.-F. Cun, L.-Z. Gong, *L-Proline Amides Catalyze Direct Asymmetric Aldol Reactions of Aldehydes with Methylthioacetone and Fluoroacetone*, *Tetrahedron: Asymm.* 18 (2007) 237.
- 47 G. Guillena, M.C. Hita, C. Nájera, S.F. Viozquez, *A Highly Efficient Solvent-Free Asymmetric Direct Aldol Reaction Organocatalyzed by Recoverable (S)-Binam-L-Prolinamides. ESI-MS Evidence of the Enamine-Iminium Formation*, *J. Org. Chem.* 73 (2008) 5933.
- 48 J.-R. Chen, X.-L. An, X.-Y. Zhu, X.-F. Wang, W.-J. Xiao, *Rational Combination of Two Privileged Chiral Backbones: Highly Efficient Organocatalysts for Asymmetric Direct Aldol Reactions between Aromatic Aldehydes and Acyclic Ketones*, *J. Org. Chem.* 73 (2008) 6006.
- 49 S. Gandhi, V.K. Singh, *Synthesis of Chiral Organocatalysts Derived from Aziridines: Application in Asymmetric Aldol Reaction*, *J. Org. Chem.* 73 (2008) 9411.
- 50 M. Gruttadauria, F. Giacalone, A.M. Marculescu, R. Noto, *Novel Prolinamide-Supported Polystyrene as Highly Stereoselective and Recyclable Organocatalyst for the Aldol Reaction*, *Adv. Synth. Catal.* 350 (2008) 1397.
- 51 Y.-C. Teo, G.-L. Chua, *A Recyclable Non-Immobilized Siloxy Serine Organocatalyst for the Asymmetric Direct Aldol Reaction*, *Tetrahedron Lett.* 49 (2008) 4235.

- 52 F. Chen, S. Huang, H. Zhang, F. Liu, Y. Peng, *Proline-Based Dipeptides with Two Amide Units as Organocatalyst for the Asymmetric Aldol Reaction of Cyclohexanone with Aldehydes*, *Tetrahedron* 64 (2008) 9585.
- 53 S.S. Chimni, S. Singh, D. Mahajan, *Protonated (S)-Prolinamide Derivatives-Water Compatible Organocatalysts for Direct Asymmetric Aldol Reaction*, *Tetrahedron: Asymm.* 19 (2008) 2276.
- 54 Z.-H. Tzeng, H.-Y. Chen, C.-T. Huang, K. Chen, *Camphor Containing Organocatalysts in Asymmetric Aldol Reaction on Water*, *Tetrahedron Lett.* 49 (2008) 4134.
- 55 R.S. Schwab, F.Z. Galetto, J.B. Azeredo, A.L. Braga, D.S. Luedtke, M.W. Paixao, *Organocatalytic Asymmetric Aldol Reactions Mediated by a Cysteine-Derived Prolinamide*, *Tetrahedron Lett.* 49 (2008) 5094.
- 56 M.R. Vishnumaya, V.K. Singh, *Highly Efficient Small Organic Molecules for Enantioselective Direct Aldol Reaction in Organic and Aqueous Media*, *J. Org. Chem.* 74 (2009) 4289.
- 57 A.M. Bernard, A. Frongia, P.P. Piras, F. Secci, M. Spiga, *Synthesis of Enantiomerically Enriched Secondary and Tertiary Phenylthio- and Phenoxy-Aldols*, *Tetrahedron Lett.* 49 (2008) 3037.
- 58 J.-F. Zhao, L. He, J. Jiang, Z. Tang, L.-F. Cun, L.-Z. Gong, *Organo-Catalyzed Highly Diastereo- and Enantio-Selective Direct Aldol Reactions in Water*, *Tetrahedron Lett.* 49 (2008) 3372.
- 59 S.-P. Zhang, X.-K. Fu, S.-D. Fu, *Rationally Designed 4-Phenoxy Substituted Prolinamide Phenols Organocatalyst for the Direct Aldol Reaction in Water*, *Tetrahedron Lett.* 50 (2009) 1173.
- 60 M. Gruttadauria, F. Giacalone, R. Noto, *Water in Stereoselective Organocatalytic Reactions*, *Adv. Synth. Catal.* 351 (2009) 33.
- 61 H. Yang, R.G. Carter, *N-(p-Dodecylphenylsulfonyl)-2-pyrrolidinecarboxamide: A Practical Proline Mimetic for Facilitating Enantioselective Aldol Reactions*, *Org. Lett.* 10 (2008) 4649.
- 62 Z.-H. Tzeng, H.-Y. Chen, R.J. Reddy, C.-T. Huang, K. Chen, *Highly Diastereo- and Enantioselective Direct Aldol Reactions Promoted by Water-Compatible Organocatalysts Bearing A Pyrrolidinyl-Camphor Structural Scaffold*, *Tetrahedron* 65 (2009) 2879.

- 63 S.-P. Zhang, X.-K. Fu, S.-D. Fu, J.-F. Pan, *Highly Efficient 4-Phenoxy Substituted Organocatalysts Derived from N-Prolylsulfonamide for the Asymmetric Direct Aldol Reaction in Water*, *Catal. Commun.* 10 (2009) 401.
- 64 S.-T. Tong, P.W.R. Harris, D. Baker, M.A. Brimble, *Use of (S)-5-(2-Methylpyrrolidin-2-yl)-1H-tetrazole as a Novel and Enantioselective Organocatalyst for the Aldol Reaction*, *Eur. J. Org. Chem.* (2008) 164.
- 65 B. Rodríguez, T. Rantanen, C. Bolm, *Solvent-Free Asymmetric Organocatalysis in a Ball Mill*, *Angew. Chem. Int. Ed.* 45 (2005) 6924.

Chapter-4

*ASYMMETRIC MICHAEL REACTION
CATALYZED BY CAMPHORSULFONAMIDE-
BASED PROLINAMIDES*

Asymmetric Michael Reaction Catalyzed by Camphorsulfonamide-based Prolinamides

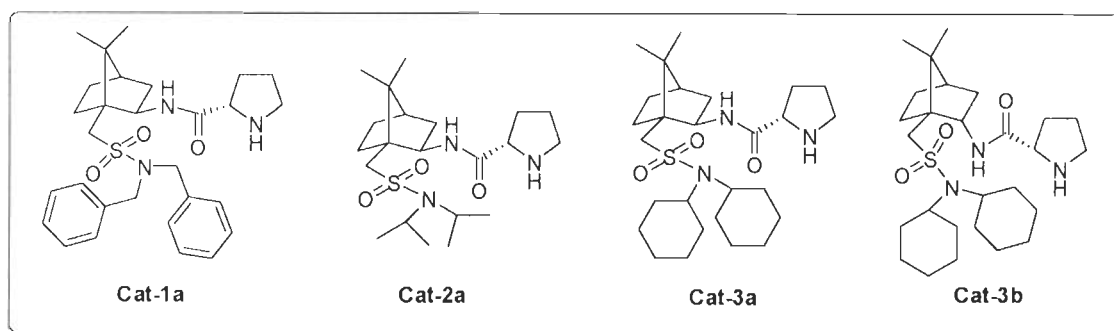
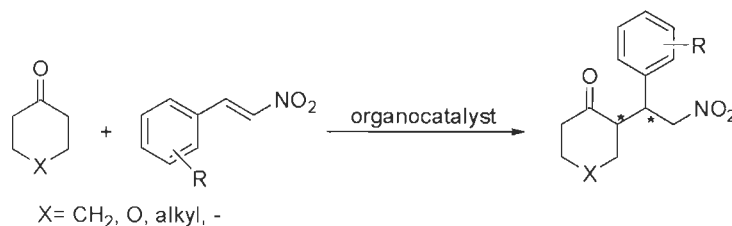
4.1. INTRODUCTION

The development of organocatalytic asymmetric reactions has drawn much attention in recent years since environmentally friendly and metal-free transformations are desired within catalytic asymmetric processes [1,2]. Michael addition plays an important role among the numerous asymmetric carbon-carbon bond-forming reactions, since it represents one of the most elegant and attractive ways to introduce chirality into a Michael acceptor. The conjugate addition of carbon nucleophile to the electron deficient nitroalkene is particularly interesting and challenging as it involves the generation of two chiral centers in a single synthetic operation [3-6]. Furthermore, thus obtained nitro compounds can be converted into a wide range of synthetically useful compounds such as amines, ketones, carboxylic acids, nitrile oxides, *etc.*, which are valuable building blocks for the preparation of several agricultural and pharmaceutical compounds [7].

Due to the simplicity of the asymmetric organocatalytic approach, the Michael addition of various donors and acceptors has been studied in the presence of organocatalysts. The proline-catalyzed Michael addition between ketones and *trans*- β -nitrostyrene was first demonstrated by Barbas [8], List [9] and Enders [10] where the adducts were obtained with good yields albeit in very low enantioselectivities. Since then, extraordinary progress has been made with respect to both stereoselectivity and substrate scope using various primary and secondary amine organocatalysts. In this context, numerous pyrrolidine-based [11-16] and thiourea-based bifunctional [17-20] organocatalysts have been used in asymmetric Michael additions. Michael additions of carbonyl compounds onto nitroalkenes using chiral amines as organocatalysts [21-23], which promote the reaction *via* an enamine pathway, have been studied in several laboratories. Among these, good levels of asymmetric induction could be obtained by proline derivatives where the amide moiety is a part of a chiral cavity in which the reaction takes place. However, only sporadic reports are available in which (2*R*,1'*S*)-*syn* products as the major enantiomers [24, 25].

4.2. OBJECTIVE

We synthesized camphorsulfonamide-based novel organocatalysts **Cat-1a**, **Cat-2a**, **Cat-3a,b** (Chapter 2) with the appended prolinamide group and found that these catalysts did exert good stereochemical control in the aldol reaction (Chapter 3). In continuation of our work on asymmetric synthesis we envisaged that these bifunctional organocatalysts can play a significant role in determining stereochemical outcome of Michael addition of ketones to nitroolefins which proceed *via* an enamine intermediate, similar to the proline-promoted aldol reaction. Our objective was to evaluate the catalytic behaviour of these camphorsulfonamide-based organocatalysts for Michael reaction between ketones such as cyclohexanone, 4-methylcyclohexanone, 4-ethylcyclohexanone and related ketones with various nitroolefins (Scheme 1).



Scheme 1: Prolinamide catalyzed asymmetric Michael reaction.

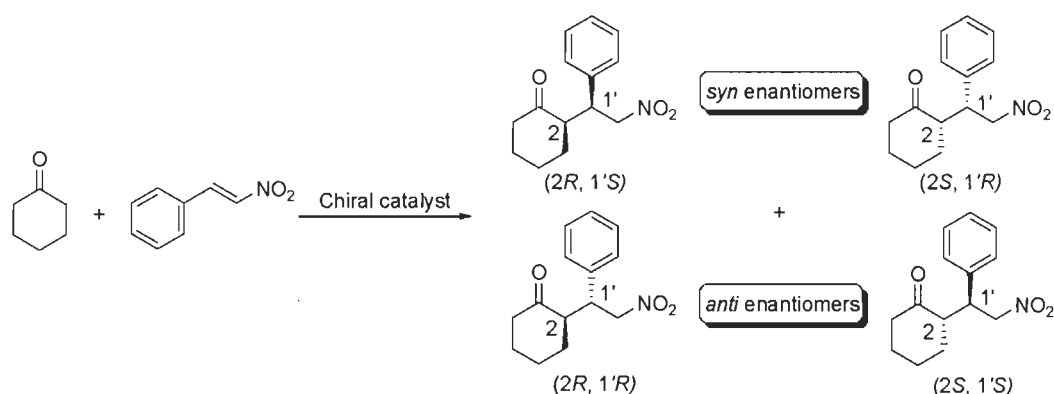
4.3. RESULTS AND DISCUSSION

4.3.1. Michael reaction catalyzed by camphorsulfonamide-based prolinamide

Michael addition of cyclohexanone with *trans*- β -nitrostyrene in presence of chiral catalyst produces Michael adduct with two chiral centers. The two chiral centers in product indicate the possibility of as many as four stereoisomers. These would exist as a pair of two diastereomers (*syn* and *anti*) where each diastereomer is of a pair of enantiomers leading to a

total of four chiral products as shown in Scheme 2. In case of 4-substituted cyclohexanones, three chiral centers would be generated in the product resulting in possible 2^3 stereoisomers.

We have chosen the addition of cyclohexanone to β -nitrostyrene (**IV-2a**) using 20 mol% organocatalyst **1a** as model study for asymmetric Michael addition. The reaction was performed by adding β -nitrostyrene (**IV-2a**, 29 mg, 0.2 mM) to a solution of cyclohexanone (41 μ L, 0.4 mM) and **Cat-1a** (20 mol%) in dichloromethane (0.5 mL) at room temperature. The progress of

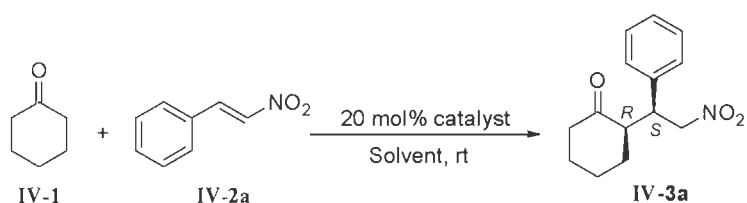


Scheme 2: Possible four diastereoisomers from the reaction of cyclohexanone with nitrostyrene.

the reaction was monitored by TLC analysis at regular intervals and found that the reaction was completed in 16 h. After completion of the reaction, diastereomeric excess was found to be 80:20 as determined ^1H NMR analysis of the crude mixture. The residue was purified by column chromatography to afford pure product **IV-3a**. The optical purity of this product was determined by HPLC using chiralpak AS-H column and hexanes-isopropanol as eluting solvent (Table 1, entry 1). A survey of polar and nonpolar solvents (CH_2Cl_2 , MeOH, CH_3CN , *etc.*) revealed that all the reactions proceeded smoothly and completed within 16-30 h at room temperature without using any co-catalyst. However high chemical yields with poor *syn* and *anti* selectivity were observed for Michael adducts in all cases (Table 1, entries 1-6). To our surprise, when the reaction was performed with 15 equiv. of cyclohexanone without using any solvent, the reaction was completed within 10 h to afford the adduct **IV-3a** with excellent chemical yield and acceptable enantioselectivity (Table 1, entry 8). Optimum results were obtained with 20 mol% catalyst. The use of 15 mol% and 30 mol% organocatalyst led to a minor loss of stereocontrol (Table 1, entries 7 and 9). The prolinamides **Cat-2a** and **Cat-3a,3b** derived from *N,N*-diisopropyl camphor-10-sulfonamide and *N,N*-dicyclohexyl camphor-10-sulfonamide, respectively, showed

less catalytic efficiency for this transformation in comparison to the prolinamide **Cat-1a** derived from *N,N*-dibenzyl camphor-10-sulfonamide (Table 1, entries 8,10-12).

Table 1: Screening of reaction conditions and organocatalysts.



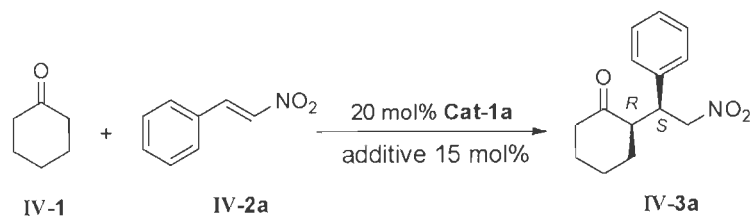
Entry	Catalyst (mol%)	Solvent	Time (h)	Yield (%) ^{a)}	dr (<i>anti</i> : <i>syn</i>) ^{b)}	ee ^{c)}
1	Cat-1a (20)	CH ₂ Cl ₂	16	77	80:20	36
2	Cat-1a (20)	CHCl ₃	20	80	85:15	53
3	Cat-1a (20)	MeOH	20	85	80:20	30
4	Cat-1a (20)	H ₂ O	28	60	65:35	32
5	Cat-1a (20)	H ₂ O:MeOH	30	80	70:30	45
6	Cat-1a (20)	CH ₃ CN	26	65	64:36	30
7	Cat-1a (15)	neat	14	88	88:12	53
8	Cat-1a (20)	neat	10	92	90:10	61
9	Cat-1a (30)	neat	10	90	90:10	59
10	Cat-2a (20)	neat	14	80	92:8	44
11	Cat-3a (20)	neat	8	93	85:15	53
12	Cat-3b (20)	neat	15	85	80:20	40

^{a)} of pure and isolated products ^{b)} determined by ¹H NMR (500 MHz) analysis of the crude sample. ^{c)} determined by HPLC analysis using Chiralpak AS-H column.

The asymmetric induction was further improved by conducting the reaction at low temperature, under solvent free conditions without using co-catalyst (Table 2). Since the optimum results at room temperature were obtained under solvent free conditions by using 20 mol% of **Cat-1a** (Table 1, entry 8), it was decided to perform the reaction at 0 °C anticipating better asymmetric induction by diminishing the rate of the reaction. Thus the reaction between

IV-1 and **IV-2a** at 0 °C was completed in 18 h and the product **IV-3a** was obtained in very high yield with improved diastereo- and enantio-selectivity (Table 2, entry 1). Encouraged by these results, the reaction temperature was further lowered to –30 °C and found significant increase in reaction time while the ee was maintained at the same level.

At this juncture, we used various organic acids as additives to study the stereochemical outcome of the reaction. By increasing the polarization of carbonyl group of ketone during the formation of enamine, these acids are believed to accelerate the rate of reaction and improve the stereochemical outcome of the reaction with concurrent activation of the Michael acceptors through hydrogen bonding. It has been observed that the presence of additive has significant influence on the reaction in terms of asymmetric induction. Initially, we used mild and bulky aromatic carboxylic acids such as benzoic acid, 4-nitro-, 2,4-dinitro-benzoic acids and isobutyric acid to promote the reaction. In the place of acids we also used bases such as Et₃N as additive. The addition of 15 mol% carboxylic acids as co-catalyst significantly accelerated the reaction rate relative to that carried out in the absence of co-catalyst. The use of 10 mol% and 20 mol% co-catalyst led to a minor loss of stereocontrol. Among the employed additives benzoic acid (15 mol%) afforded optimum results in terms of reaction time and selectivity (95:5 dr, 65% ee). Thus acidic co-catalyst has an important role on reaction. Moreover, the reaction temperature was found to be a crucial factor to the enantioselectivity of reaction. The stereoselectivity was gradually increased by decreasing the reaction temperature from rt to 0 °C (Table 2, entries 4 and 9). However, further lowering of the temperature to –30 °C resulted in a slight decrease of the optical purity of the adduct **IV-3a** as well as the reaction rate (Table 2, entry 10). It has been observed that as the temperature of the reaction was decreased, the stereochemical outcome of the reaction was improved. Thus under the optimal reaction conditions (20 mol% catalyst, 15 mol% PhCOOH as the co-catalyst at 0 °C, Table 2, entry 9) organocatalyst **Cat-1a** demonstrated the best catalytic activity. All reactions proceeded with diastereoselectivity in favour of *syn*-diastereoisomer of the corresponding Michael adducts.

Table 2: Effect of additives on Michael reaction of cyclohexanone with β -nitrostyrene (**IV-2a**) in presence of **Cat-1a**.

Entry	Solvent	Additive	Temp	Time (h)	Yield (%) ^{a)}	dr (<i>anti:syn</i>) ^{b)}	ee ^{c)}
1	neat	-	0 °C	18	90	92:8	71
2	neat	-	-30 °C	30	89	90:10	70
3	CHCl ₃	-	0 °C	28	85	85:15	65
4	neat	PhCOOH	rt	7	94	95:5	65
5	CHCl ₃	PhCOOH	rt	18	88	80:20	57
6	neat	4-NO ₂ C ₆ H ₄ COOH	rt	18	85	80:20	53
7	neat	Isobutyric acid	rt	20	72	70:30	51
8	neat	2,4-(NO ₂) ₂ C ₆ H ₃ COOH	rt	28	67	65:35	45
9	neat	PhCOOH	0 °C	12	95	95:5	79
10	neat	PhCOOH	-30 °C	24	92	92:8	75
11	neat	4-NO ₂ C ₆ H ₄ COOH	0 °C	30	80	85:15	59
12	neat	Et ₃ N	0 °C	36	75	93:7	62
13	neat	Isobutyric acid	0 °C	30	70	77:23	60
14	neat	3-CF ₃ C ₆ H ₄ COOH	0 °C	32	89	90:10	61
15	neat	Et ₃ N	-30 °C	42	73	90:10	65

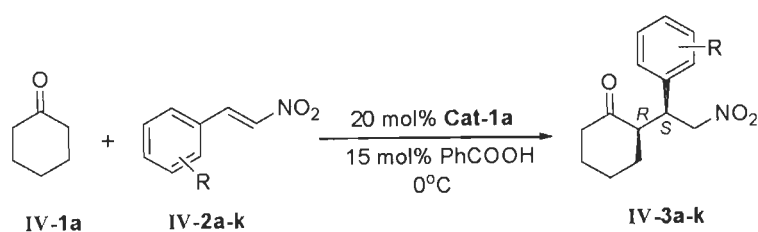
^{a)} of pure and isolated products. ^{b)} determined by ¹H NMR (500 MHz) analysis of the crude sample.

^{c)} determined by HPLC analysis using Chiralpak AS-H column.

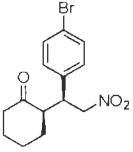
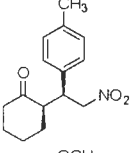
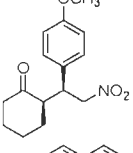
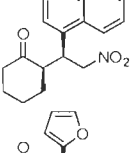
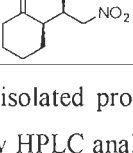
Thus, the screening of the catalysts in various solvents and neat condition and screening of various additives at different temperatures identified the optimal catalyst as well as optimal conditions to carry out further asymmetric Michael reaction. To expand the scope of Michael

addition, we next investigated the reactions of other nitroolefins **IV-2b-k** with cyclohexanone under the optimal reaction conditions in the presence of organocatalyst **Cat-1a**. The results are summarized in Table 3. In all the cases studied, adducts were obtained in very high to excellent chemical yields regardless of the electronic nature of the substitutions on the aromatic nucleus. The diastereomeric discrimination of the products is high to excellent except that of adduct **IV-3i** derived from 4-methoxynitrostyrene (**IV-2i**) (Table 3, entry 9) where the *syn* and *anti* adducts

Table 3: Michael reaction of cyclohexanone with substituted β -nitrostyrenes **IV-2a-k** in presence of **Cat-1a**.



Entry	Product	Time	Yield (%) ^{a)}	dr (<i>syn:anti</i>) ^{b)}	ee (%) ^{c)}
1	IV-3a	12h	95	95:5	79
2	IV-3b	14h	96	97:3	77
3	IV-3c	14h	92	93:7	67
4	IV-3d	18h	94	92:8	69
5	IV-3e	18h	92	97:3	68
6	IV-3f	18h	95	95:5	71

7		IV-3g	18h	92	92:8	70
8		IV-3h	24h	90	95:5	72
9		IV-3i	24h	89	84:16	60
10		IV-3j	16h	94	>99:1	89
11		IV-3k	18h	90	75:5	78

^{a)} of pure and isolated products ^{b)} determined by ¹H NMR (500 MHz) analysis of the crude sample.

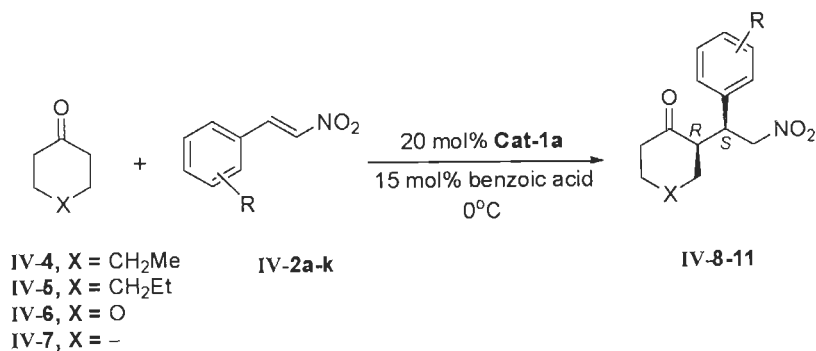
^{c)} determined by HPLC analysis using Chiral columns. (see page 144 for Table 5 and page 147 for HPLC charts).

were obtained in moderate 84:16 ratio. The reaction of nitrostyrene **IV-2b** (R = *o*-NO₂) provided better asymmetric induction in comparison to that of nitrostyrene **IV-2c** (R = *m*-NO₂) (Table 3, entries 2 and 3). However, the halogen-substituted nitrostyrenes **IV-2d-g** afforded the corresponding Michael adducts **IV-3d-g** in comparable optical yields with almost same enantioselectivities (Table 3, entries 4-7). Among Michael acceptors 4-methyl and 4-methoxy-nitroolefins (**IV-2h,i**), the former furnished the Michael adduct in better diastereo- and enantioselectivities (Table 3, entries 8 and 9). The reaction of cyclohexanone with α -naphthyl-nitrostyrene (**IV-2j**) resulted in the formation of adduct **IV-3j** almost exclusively with *syn* stereochemistry and very high optical yield of 89% (Table 3, entry 10). 2-(2-Nitrovinyl)furan (**IV-2k**) yielded the adduct **IV-3k** in very high stereoselectivities.

The use of other symmetrical cycloalkanones such as 4-methyl, 4-ethyl-cyclohexanones and γ -pyrone as Michael donors was evaluated as well, and the products **IV-8a,b**, **IV-9a** and **IV-10a** were obtained in excellent yields with high diastereomeric excess and very good

enantioselectivities. All the reactions were performed with 0.2 mM of *trans*- β -nitrostyrene and 3 mM of 4-substituted cyclohexanone in the presence of 20 mol% organocatalyst and 15 mol% of

Table 4: Michael reaction of ketones with substituted β -nitrostyrenes in presence of **Cat-1a**.



Entry	Product	Time	Yield (%) ^{a)}	dr (<i>anti:syn</i>) ^{b)}	ee (%) ^{c)}	
1		IV-8a	14h	92	-	76
2		IV-8b	14h	96	-	65
3		IV-9a	15h	94	-	71
4		IV-10a	16h	97	93:7	75
5		IV-11a	12h	90	85:15	75

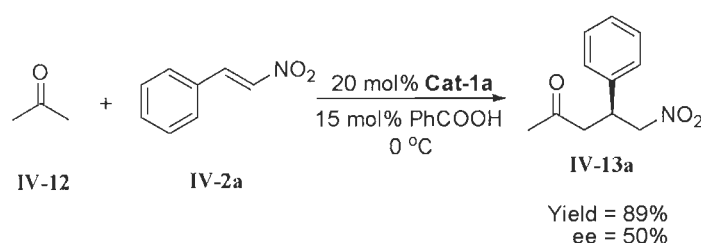
^{a)} of pure and isolated products ^{b)} determined by ¹H NMR (500 MHz) analysis of the crude sample.

^{c)} determined by HPLC analysis using Chiral columns. (see page 144 for Table 5 and page 149 for HPLC charts)

PhCOOH (co-catalyst) at 0 °C. The reaction progress was monitored by thin layer chromatography. After the completion of reaction, obtained crude reaction mixture was submitted to ¹H

NMR to get diastereoselectivity of the corresponding Michael product. Further this crude reaction mixture was purified by silica gel chromatography. The optical purity of these products was determined by HPLC using chiral columns and hexanes-isopropanol as eluting solvent. The results are summarized in Table 4. The reaction of nitrostyrene **IV-2a** with cyclopentanone as a Michael donor was also performed to afford the adduct **IV-11a** with very good optical yield.

The reaction between acetone and nitrostyrene **IV-2a** under the present catalytic system was then examined. The product **IV-13a** was achieved in very high chemical yield albeit in moderate optical purity in 18 h.

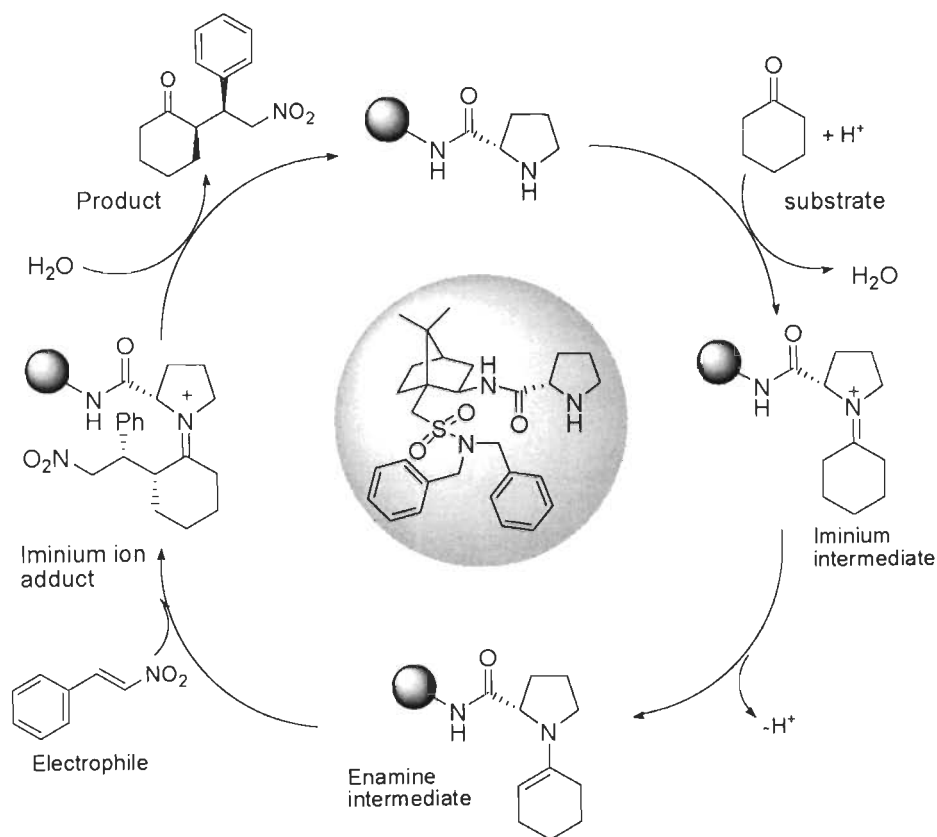


Scheme 3: Michael reaction of acetone with substituted β -nitrostyrenes in presence of **Cat-1a**.

The absolute configuration of Michael adducts were determined by comparing the retention times obtained from HPLC analysis of the products with literature data [21, 26-33].

4.3.2. Proposed mechanism

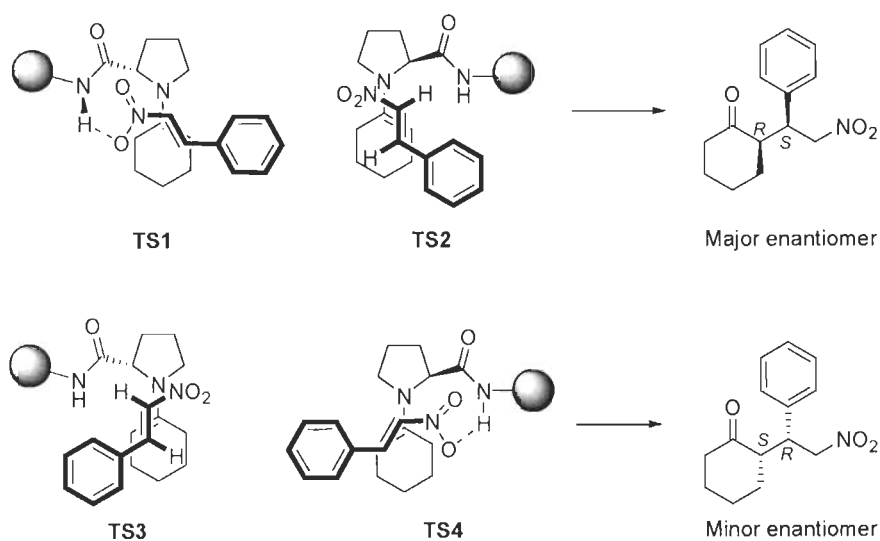
Asymmetric Michael addition is an important carbon-carbon and carbon-hetero atom bond forming reaction. The reaction include the addition of carbonyl compounds to electron deficient nitroolefins to form Michael adduct. The mechanism for the asymmetric Michael addition is outlined in Scheme 4. Initially, an iminium ion is generated by the reversible reaction between chiral organocatalyst **Cat-1a** and cyclohexanone; which can be more easily deprotonated to form the enamine nucleophilic intermediate. This enamine intermediate, react with the electron deficient *trans*- β -nitrostyrene to create the new C-C bond. Upon electrophilic capture of the enamine derivative, the resulting iminium ion is hydrolyzed to release the Michael adduct and the catalyst to participate in the catalytic cycle.



Scheme 4: Proposed mechanism for asymmetric Michael reaction

4.3.3. Proposed transition state

To account for the stereoselectivity of the Michael addition reaction using the designed catalyst system, an enamine activation model is proposed as shown in Scheme 5 using cyclohexanone and *trans*- β -nitrostyrene as an example. Among the four approaches, TS1 and TS4 could form hydrogen bond between $-NH$ of the prolinamide with nitro functionality and the approaches TS2 and TS3 could not be activated through hydrogen bonding. The approach shown in TS1, leading to the major (1*S*,2*R*)-isomer, acquires stability through hydrogen bonding between $-NH$ of the prolinamide with nitro group and is favourable on steric grounds. The approach of nitrostyrene in TS4 experiences repulsive interactions between camphor scaffold and Michael acceptor and hence it is not favourable albeit there is a possibility of hydrogen bond formation.



Scheme 5: Possible transition state for Michael reaction.

4.4. CONCLUSION

In conclusion, new camphorsulfonamide-derived prolinamide organocatalysts containing a structural rigid bicyclic camphor scaffold and amide moiety, were used for the first time in Michael addition. We have demonstrated a practical application of camphor-10-sulfonamide-based prolinamide for Michael addition of ketones with β -nitrostyrenes in which $(2R,1'S)$ -*syn* adducts were obtained as major antipodes. In these transformations, the catalyst exhibited good catalytic activity and the reaction proceeded in excellent diastereoselectivity and good to high enantioselectivity, which may be potentially useful for preparing enantiomerically enriched γ -nitroketones.

4.5. EXPERIMENTAL

4.5.1. General

All solvents and reagents were purchased at the highest commercially quality and used without further purification. Solvents were purified by standard methods yields refer to chromatographically homogeneous materials, unless otherwise stated. Reactions were monitored by thin-layer chromatography (TLC) carried out on 0.25 mm E. Merck silica gel plates (60F-254) using UV light as visualizing or in an iodine chamber. Silica gel (particle size 100-200 mesh; SD Fine Chem Ltd) was used for column chromatography with ethyl acetate-hexanes as an eluent system. Melting points are uncorrected.

4.5.2. Instrumentation

IR spectra of the compounds were recorded on a Thermo Nicolet FT-IR NexusTM and are expressed as wavenumbers (cm^{-1}). NMR spectra were recorded in CDCl_3 using TMS as internal standard on Brüker AMX-500 instrument. Chemical shifts of ^1H NMR spectra were given in parts per million with respect to TMS and the coupling constant J was measured in Hz. The signals from solvent CDCl_3 , 7.26 and 77.0 ppm, are set as the reference peaks in ^1H NMR and ^{13}C NMR spectra, respectively. The following abbreviations were used to explain the multiplicities: s = singlet, d = doublet, t = triplet, q = quartet, m = multiplet, b = broad. Analytical HPLC measurements were carried out on Shimadzu SPD-20A instrument with UV detector by using Chiralpak AS-H, AD-H and Chiralcel OD-H columns.

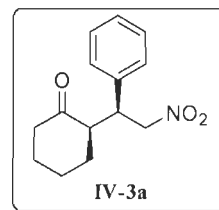
4.5.3. General Procedure

To a mixture of a nitrostyrene (0.2 mM) in cycloalkanone/acetone (15 equiv.), organocatalyst **1a** (0.04 mM) was added and the resulting reaction mixture was stirred at 0 °C. The reaction was monitored by TLC at regular intervals. Upon completion of the reaction, the crude reaction mixture was submitted to ^1H NMR (500 MHz) to determine the diastereomeric ratio of *syn* and *anti* adducts. The residue was subjected to silica gel column chromatography using ethyl acetate and hexanes (10:90 to 20:80) as eluent to afford pure product. The HPLC analysis of the Michael product was performed on a chiral stationary phase using hexanes–isopropanol as eluting solvent.

(2*R*,1'*S*)-2-[1'-Phenyl-2'-nitroethyl]cyclohexanone (IV-3a):

IR (KBr) ν_{\max} : 3024, 2954, 2864, 1695, 1550, 1442, 1380 cm^{-1} .

$^1\text{H NMR}$ (CDCl_3 , 500 MHz): δ 7.34-7.31 (m, 2H), 7.28-7.26 (m, 1H), 7.18-7.14 (m, 2H), 4.94 (dd, $J = 4.5, 12.5$ Hz, 1H), 4.64 (dd, $J = 10.0, 12.5$ Hz, 1H), 3.76 (dt, $J = 4.5, 9.5$ Hz, 1H), 2.73-2.66 (m, 1H), 2.52-2.45 (m, 1H), 2.43-2.35 (m, 1H), 2.12-2.04 (m, 1H), 1.82-1.75 (m, 1H), 1.74-1.60 (m, 3H), 1.28-1.19 (m, 1H) ppm.

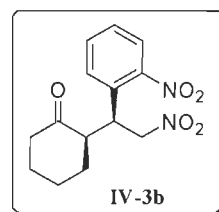


$^{13}\text{C NMR}$ (CDCl_3 , 125 MHz): δ 211.9, 137.7, 128.9, 128.1, 127.7, 78.9, 52.5, 43.9, 42.7, 33.2, 28.5, 25.0 ppm.

(2*R*,1'*S*)-2-[2'-Nitro-1'-(*o*-nitrophenyl)ethyl]cyclohexanone (IV-3b):

IR (KBr) ν_{\max} : 2940, 2865, 1707, 1550, 1522, 1435, 1359, 1128, 1068, 853, 784 cm^{-1} .

$^1\text{H NMR}$ (CDCl_3 , 500 MHz): δ 7.84 (dd, $J = 1.5, 8.0$ Hz, 1H), 7.59 (dt, $J = 1.5, 8.0$ Hz, 1H), 7.47-7.40 (m, 2H), 4.94-4.89 (m, 2H), 4.32 (dt, $J = 5.0, 8.5$ Hz, 1H), 2.98-2.90 (m, 1H), 2.51-2.45 (m, 1H), 2.43-2.32 (m, 1H), 2.14-2.08 (m, 1H), 1.89-1.77 (m, 2H), 1.74-1.58 (m, 2H), 1.53-1.42 (m, 1H) ppm.

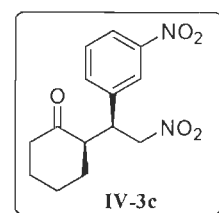


$^{13}\text{C NMR}$ (CDCl_3 , 125 MHz): δ 211.0, 150.8, 133.2, 132.9, 129.4, 128.6, 125.0, 77.6, 52.2, 42.8, 38.8, 33.3, 28.4, 25.4 ppm.

(2*R*,1'*S*)-2-[2'-Nitro-1'-(*m*-nitrophenyl)ethyl]cyclohexanone (IV-3c):

IR (KBr) ν_{\max} : 2940, 2862, 2360, 1705, 1586, 1348, 1107, 898, 804, 735, 689 cm^{-1} .

$^1\text{H NMR}$ (CDCl_3 , 500 MHz): δ 8.17-8.14 (m, 1H), 8.09-8.06 (m, 1H), 7.58-7.50 (m, 2H), 5.00 (dd, $J = 4.5, 13.0$ Hz, 1H), 4.70 (dd, $J = 10.5, 13.0$ Hz, 1H), 3.94 (dt, $J = 4.5, 10.0$ Hz, 1H), 2.78-2.71 (m, 1H), 2.53-2.47 (m, 1H), 2.44-2.36 (m, 1H), 2.16-2.09 (m, 1H), 1.87-1.79 (m, 1H), 1.74-1.56 (m, 3H), 1.33-1.21 (m, 1H) ppm.

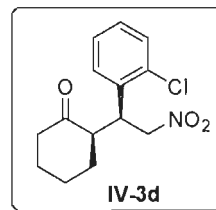


$^{13}\text{C NMR}$ (CDCl_3 , 125 MHz): δ 211.0, 148.5, 140.2, 134.9, 130.0, 123.0, 122.9, 78.1, 52.2, 43.7, 42.8, 33.2, 28.3, 25.1 ppm.

(2*R*,1'*S*)-2-[2'-Nitro-1'-(*o*-chlorophenyl)ethyl]cyclohexanone (IV-3d):

IR (KBr) ν_{max} : 2935, 2860, 1701, 1549, 1440, 1378, 1127, 1059, 747, 694 cm^{-1} .

^1H NMR (CDCl_3 , 500 MHz): δ 7.40-7.36 (m, 1H), 7.26-7.18 (m, 3H), 4.94-4.86 (m, 2H), 4.34-4.24 (m, 1H), 2.98-2.88 (m, 1H), 2.52-2.45 (m, 1H), 2.39 (dt, $J = 6.0, 12.5$ Hz, 1H), 2.14-2.07 (m, 1H), 1.85-1.78 (m, 1H), 1.77-1.62 (m, 3H), 1.33 (dq, $J = 4.0, 12.5$ Hz, 1H) ppm.

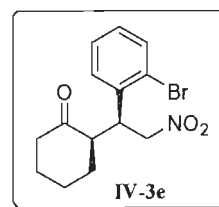


^{13}C NMR (CDCl_3 , 125 MHz): δ 211.6, 135.4, 134.4, 130.2, 129.4, 128.8, 127.3, 77.2, 51.6, 42.7, 40.8, 32.9, 28.4, 25.1 ppm.

(2*R*,1'*S*)-2-[2'-Nitro-1'-(*o*-bromophenyl)ethyl]cyclohexanone (IV-3e):

IR (KBr) ν_{max} : 2937, 2859, 1702, 1549, 1440, 1373, 1128, 1057, 747 cm^{-1} .

^1H NMR (CDCl_3 , 500 MHz): δ 7.47 (dd, $J = 8.0, 1.5$ Hz, 1H), 7.23-7.13 (m, 2H), 7.06-7.00 (m, 1H), 4.87-4.73 (m, 2H), 4.30-4.22 (m, 1H), 2.78 (m, 1H), 2.38-2.28 (m, 2H), 2.03-1.97 (m, 1H), 1.72-1.45 (m, 4H), 1.30-1.26 (m, 1H) ppm.

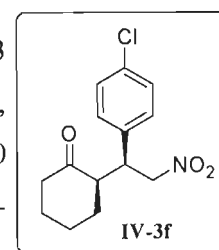


^{13}C NMR (CDCl_3 , 125 MHz): δ 211.6, 137.2, 133.6, 129.0, 127.7, 77.4, 52.0, 43.0, 42.6, 41.8, 32.9, 28.5, 25.0 ppm.

(2*R*,1'*S*)-2-[2'-Nitro-1'-(*p*-chlorophenyl)ethyl]cyclohexanone (IV-3f):

IR (KBr) ν_{max} : 2927, 2859, 1705, 1547, 1379, 1087, 1013, 831 cm^{-1} .

^1H NMR (CDCl_3 , 500 MHz): δ 7.32-7.28 (m, 2H), 7.14-7.10 (m, 2H), 4.93 (dd, $J = 5.0, 13.0$ Hz, 1H), 4.60 (dd, $J = 10.0, 12.5$ Hz, 1H), 3.76 (dt, $J = 4.5, 10.0$ Hz, 1H), 2.68-2.61 (m, 1H), 2.50-2.44 (m, 1H), 2.37 (dt, $J = 6.0, 13.0$ Hz, 1H), 2.14-2.05 (m, 1H), 1.84-1.77 (m, 1H), 1.76-1.52 (m, 3H), 1.30-1.16 (m, 1H) ppm.

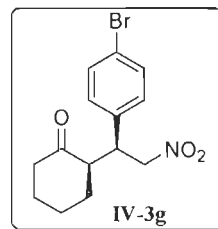


^{13}C NMR (CDCl_3 , 125 MHz): δ 211.5, 136.2, 133.5, 129.5, 129.0, 78.5, 52.3, 43.3, 42.7, 33.1, 28.4, 25.0 ppm.

(2*R*,1'*S*)-2-[2'-Nitro-1'-(*p*-bromophenyl)ethyl]cyclohexanone (IV-3g):

IR (KBr) ν_{\max} : 2937, 2862, 1699, 1552, 1443, 1384, 1302, 1123, 1069, 1010, 821, 714 cm^{-1} .

$^1\text{H NMR}$ (CDCl_3 , 500 MHz): δ 7.47-7.44 (m, 2H), 7.08-7.04 (m, 2H), 4.93 (dd, $J = 4.5, 12.5$ Hz, 1H), 4.60 (dd, $J = 10.0, 12.5$ Hz, 1H), 3.74 (dt, $J = 5.0, 10.0$ Hz, 1H), 2.69-2.61 (m, 1H), 2.51-2.45 (m, 1H), 2.41-2.34 (m, 1H), 2.13-2.05 (m, 1H), 1.83-1.77 (m, 1H), 1.67-1.52 (m, 3H), 1.27-1.20 (m, 1H) ppm.

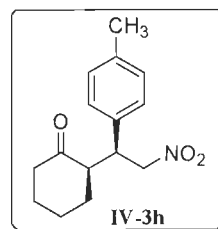


$^{13}\text{C NMR}$ (CDCl_3 , 125 MHz): δ 211.4, 136.8, 132.1, 129.9, 121.7, 78.5, 52.3, 43.4, 42.7, 33.2, 28.4, 25.1 ppm.

(2*R*,1'*S*)-2-[2'-Nitro-1'-(*p*-methylphenyl)ethyl]cyclohexanone (IV-3h):

IR (KBr) ν_{\max} : 2934, 2861, 1699, 1553, 1442, 1383, 1124, 1018, 814 cm^{-1} .

$^1\text{H NMR}$ (CDCl_3 , 500 MHz): δ 7.12 (d, $J = 7.5$ Hz, 2H), 7.04 (d, $J = 8.0$ Hz, 2H), 4.91 (dd, $J = 4.5, 12.0$ Hz, 1H), 4.60 (dd, $J = 10.0, 12.0$ Hz, 1H), 3.72 (dt, $J = 4.5, 10.0$ Hz, 1H), 2.71-2.62 (m, 1H), 2.51-2.44 (m, 1H), 2.44-2.36 (m, 1H), 2.31 (s, 3H), 2.12-2.07 (m, 1H), 1.83-1.62 (m, 3H), 1.63-1.54 (m, 1H), 1.29-1.23 (m, 1H) ppm.

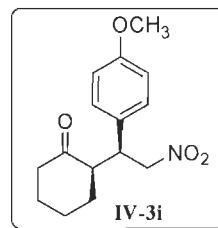


$^{13}\text{C NMR}$ (CDCl_3 , 125 MHz): δ 212.1, 137.5, 134.6, 129.6, 128.0, 79.0, 52.6, 43.5, 42.8, 33.2, 28.6, 25.0, 21.1 ppm.

(2*R*,1'*S*)-2-[2'-Nitro-1'-(*p*-methoxyphenyl)ethyl]cyclohexanone (IV-3i):

IR (KBr) ν_{\max} : 2947, 2845, 1700, 1554, 1513, 1446, 1387, 1299, 1252, 1183, 1024, 821 cm^{-1} .

$^1\text{H NMR}$ (CDCl_3 , 500 MHz): δ 7.13-7.08 (m, 2H), 6.89-6.85 (m, 2H), 4.93 (dd, $J = 4.5, 12.0$ Hz, 1H), 4.61 (dd, $J = 10.0, 12.5$ Hz, 1H), 3.81 (s, 3H), 3.74 (dt, $J = 4.5, 10.0$ Hz, 1H), 2.70-2.63 (m, 1H), 2.53-2.46 (m, 1H), 2.44-2.37 (m, 1H), 2.14-2.05 (m, 1H), 1.85-1.53 (m, 4H), 1.31-1.20 (m, 1H) ppm.

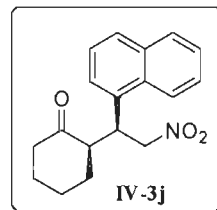


$^{13}\text{C NMR}$ (CDCl_3 , 125 MHz): δ 212.0, 159.0, 129.5, 129.1, 114.3, 79.1, 55.2, 52.6, 43.2, 42.7, 33.1, 28.5, 25.0 ppm.

(2*R*,1'*S*)-2-[2'-Nitro-1'-(1-naphthyl)ethyl]cyclohexanone (IV-3j):

IR (KBr) ν_{\max} : 2928, 2859, 1696, 1552, 1435, 1376, 1252, 1127, 788 cm^{-1} .

$^1\text{H NMR}$ (CDCl_3 , 500 MHz): δ 8.17 (s, 1H), 7.86 (d, $J = 8.0$ Hz, 1H), 7.78 (d, $J = 7.5$ Hz, 1H), 7.59-7.53 (m, 1H), 7.52-7.48 (m, 1H), 7.46 (t, $J = 8.0$ Hz, 1H), 7.38 (dd, $J = 1.0, 7.5$ Hz, 1H), 5.07 (dd, $J = 4.5, 12.5$ Hz, 1H), 4.97-4.88 (m, 1H), 4.83-4.70 (br s, 1H), 2.87 (s, 1H), 2.55-2.48 (m, 1H), 2.46-2.37 (m, 1H), 2.13-2.05 (m, 1H), 1.74-1.62 (m, 4H), 1.31-1.22 (m, 1H) ppm

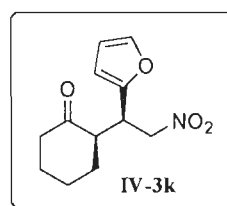


$^{13}\text{C NMR}$ (CDCl_3 , 125 MHz): δ 212.3, 134.0, 129.1, 128.2, 126.8, 125.9, 125.4, 123.6, 122.8, 78.7, 53.9, 42.9, 36.8, 33.3, 29.7, 28.8, 25.3 ppm

(2*R*,1'*S*)-2-[2'-Nitro-1'-(*o*-furanyl)ethyl]cyclohexanone (IV-3k):

IR (KBr) ν_{\max} : 2942, 2865, 1711, 1550, 1435, 1378, 1137, 1018, 745 cm^{-1} .

$^1\text{H NMR}$ (CDCl_3 , 500 MHz): δ 7.38-7.34 (m, 1H), 6.31 (dd, $J = 2.0, 3.0$ Hz, 1H), 6.21 (d, $J = 3.0$ Hz, 1H), 4.81 (dd, $J = 4.5, 12.5$ Hz, 1H), 4.69 (dd, $J = 9.0, 12.5$ Hz, 1H), 3.99 (dt, $J = 5.0, 9.5$ Hz, 1H), 2.81-2.74 (m, 1H), 2.53-2.46 (m, 1H), 2.43-2.34 (m, 1H), 2.17-2.09 (m, 1H), 1.91-1.62 (m, 4H), 1.36-1.25 (m, 1H) ppm

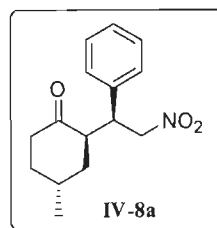


$^{13}\text{C NMR}$ (CDCl_3 , 125 MHz): δ 210.9, 150.9, 142.3, 110.3, 108.9, 76.6, 51.1, 42.5, 37.5, 32.4, 28.2, 25.0 ppm

(2*R*,4*R*,1'*S*)-2-[1'-Phenyl-2'-nitroethyl]-4-methylcyclohexanone (IV-8a):

IR (KBr) ν_{\max} : 3028, 2968, 2860, 1698, 1545, 1442, 1380, 735, 698 cm^{-1} .

$^1\text{H NMR}$ (CDCl_3 , 500 MHz): δ 7.39-7.28 (m, 3H), 7.21-7.17 (m, 2H), 4.72 (dd, $J = 4.5, 13.0$ Hz, 1H), 4.66-4.61 (m, 1H), 3.83 (dt, $J = 5.0, 10.5$ Hz, 1H), 2.78-2.72 (m, 1H), 2.55-2.51 (m, 2H), 2.11-1.98 (m, 2H), 1.70-1.63 (m, 1H), 1.52-1.38 (m, 2H), 1.00 (d, $J = 6.5$ Hz, 3H) ppm

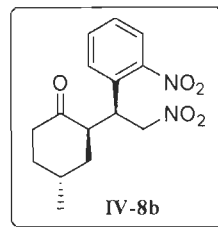


$^{13}\text{C NMR}$ (CDCl_3 , 125 MHz): δ 213.0, 137.3, 129.0, 128.1, 79.0, 50.1, 44.2, 38.7, 37.9, 34.4, 26.4, 19.3 ppm

(2*R*,4*R*,1'*S*)-2-[2'-Nitro-1'-(*o*-nitrophenyl)ethyl]-4-methylcyclohexanone (IV-8b):

IR (KBr) ν_{\max} : 2952, 2868, 1706, 1552, 1520, 1437, 1235, 1126, 1065, 858, 786 cm^{-1} .

^1H NMR (CDCl_3 , 500 MHz): δ 7.84-7.81 (m, 1H), 7.62-7.59 (m, 1H), 7.45-7.39 (m, 2H), 4.85-4.81 (m, 2H), 4.41-4.33 (m, 1H), 3.08-2.98 (m, 1H), 2.57-2.48 (m, 1H), 2.43-2.35 (m, 1H), 2.15-2.04 (m, 1H), 1.99-1.89 (m, 1H), 1.79-1.61 (m, 2H), 1.56-1.47 (m, 1H), 1.05 (d, $J = 6.5$ Hz, 3H) ppm.

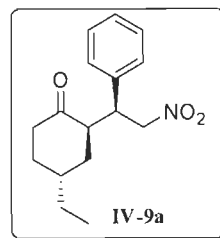


^{13}C NMR (CDCl_3 , 125 MHz): δ 211.9, 150.8, 133.1, 132.6, 128.6, 125.1, 77.7, 48.5, 38.5, 38.4, 33.8, 26.8, 18.5 ppm.

(2*R*,4*R*,1'*S*)-2-[1'-Phenyl-2'-nitroethyl]-4-ethylcyclohexanone (IV-9a):

IR (KBr) ν_{\max} : 3012, 2972, 2865, 1696, 1559, 1440, 1385, 737, 696 cm^{-1} .

^1H NMR (CDCl_3 , 500 MHz): δ 7.37-7.29 (m, 3H), 7.19-7.15 (m, 2H), 4.72 (dd, $J = 4.5, 12.5$ Hz, 1H), 4.61 (dd, $J = 10.5, 13.0$ Hz, 1H), 3.80 (dt, $J = 4.5, 10.5$ Hz, 1H), 2.73-2.66 (m, 1H), 2.52-2.41 (m, 2H), 2.04-1.95 (m, 1H), 1.78-1.57 (m, 3H), 1.47-1.36 (m, 3H), 0.82-0.78 (m, 3H) ppm.

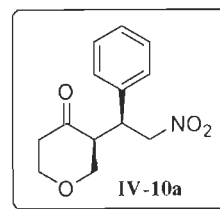


^{13}C NMR (CDCl_3 , 125 MHz): δ 213.0, 137.0, 129.0, 128.1, 79.0, 50.1, 44.0, 38.5, 35.4, 33.2, 32.0, 26.2, 11.5 ppm.

(2*R*,1'*S*)-2-[1'-Phenyl-2'-nitroethyl]pyran-4-one (IV-10a):

IR (KBr) ν_{\max} : 3023, 2957, 2863, 1700, 1550, 1442, 1380, 1065 cm^{-1} .

^1H NMR (CDCl_3 , 500 MHz): δ 7.39-7.30 (m, 3H), 7.23-7.20 (m, 2H), 4.96 (dd, $J = 4.5, 12.5$ Hz, 1H), 4.67 (dd, $J = 10.5, 13.0$ Hz, 1H), 4.20-4.15 (m, 1H), 3.88-3.78 (m, 2H), 3.72 (ddd, $J = 1.0, 5.0, 11.5$ Hz, 1H), 3.30 (dd, $J = 9.0, 11.5$ Hz, 1H), 2.94-2.88 (m, 1H), 2.74-2.66 (m, 1H), 2.59 (td, $J = 4.0, 14.0$ Hz, 1H) ppm.

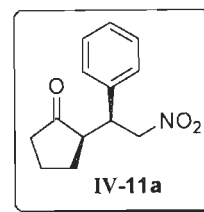


^{13}C NMR (CDCl_3 , 125 MHz): δ 207.4, 136.2, 129.3, 128.3, 127.9, 78.7, 71.6, 69.0, 53.3, 43.0, 41.3 ppm.

(2*R*,1'*S*)-2-[1'-Phenyl-2'-nitroethyl]pentanone (IV-11a):

IR (KBr) ν_{\max} : 2967, 2360, 1731, 1595, 1550, 1377 cm^{-1} .

$^1\text{H NMR}$ (CDCl_3 , 500 MHz): δ 7.33-7.24 (m, 3H), 7.19-7.12 (m, 2H), 5.32 (dd, $J = 5.5, 12.8$ Hz, 1H), 4.63 (dd, $J = 9.5, 12.5$ Hz, 1H), 3.69 (dt, $J = 5.5, 9.5$ Hz, 1H), 2.42-2.33 (m, 2H), 2.19-2.10 (m, 1H), 1.95-1.85 (m, 2H), 1.75-1.60 (m, 2H) ppm.

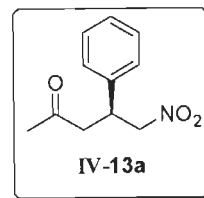


$^{13}\text{C NMR}$ (CDCl_3 , 125 MHz): δ 218.5, 137.6, 137.2, 128.7, 128.5, 78.2, 50.3, 44.0, 38.7, 28.2, 20.1 ppm.

(4*R*)-5-Nitro-4-phenylpentan-2-one (IV-13a):

IR (KBr) ν_{\max} : 3024, 2954, 2864, 1705, 1550, 1442, 1380 cm^{-1} .

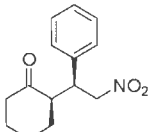
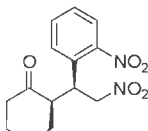
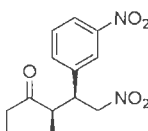
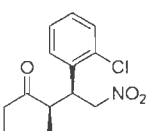
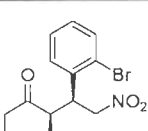
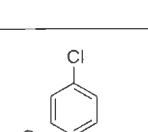
$^1\text{H NMR}$ (CDCl_3 , 500 MHz): δ 7.38-7.29 (m, 3H), 7.26-7.22 (m, 2H), 4.72 (dd, $J = 6.5, 12.0$ Hz, 1H), 4.63 (dd, $J = 8.0, 12.5$ Hz, 1H), 4.04 (quintet, $J = 7.0$ Hz, 1H), 2.95 (d, $J = 7.5$ Hz, 2H), 2.12 (s, 3H) ppm.

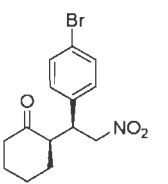
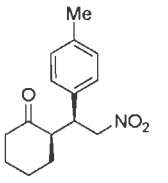
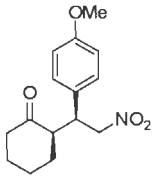
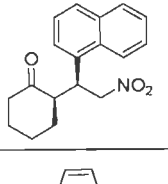
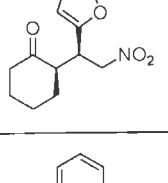
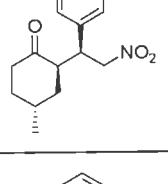
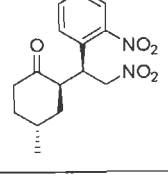
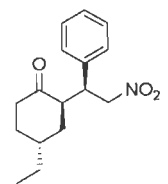


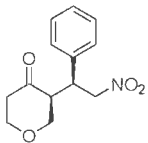
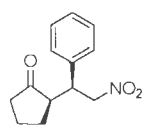
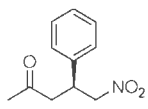
$^{13}\text{C NMR}$ (CDCl_3 , 125 MHz): δ 205.5, 138.8, 129.1, 127.9, 127.4, 79.5, 64.4, 46.1, 39.0, 30.4, 29.7 ppm.

4.5.4. HPLC data table for Michael products

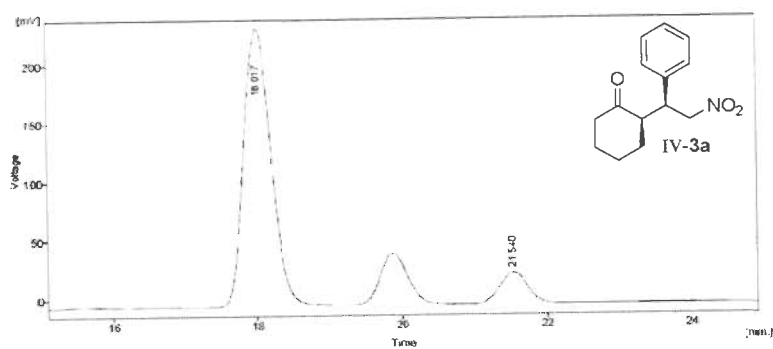
Table 5: HPLC data for Michael adducts obtained from camphorsulfonamide-based prolinamide **Cat-1a** catalyzed Michael reactions.^{a)}

S.No.	Major Product (<i>syn</i>)		HPLC data					
			Column	λ (nm)	Flow rate	Solvent IPA:Hex	t_R (min)	t_R (min)
1		IV-3a	Chiralpak AS-H	220	1ml/min	15:85	18.0	21.5
2		IV-3b	Chiralpak AD-H	254	1ml/min	10:90	9.0	12.9
3		IV-3c	Chiralpak AD-H	230	0.5ml/min	5:95	87.3	106.1
4		IV-3d	Chiralpak AS-H	220	1ml/min	10:90	8.9	13.0
5		IV-3e	Chiralpak AS-H	220	1ml/min	15:85	9.2	14.0
6		IV-3f	Chiralpak AS-H	220	1ml/min	15:85	9.9	15.0

7		IV-3g	Chiralpak AD-H	254	1ml/min	10:90	10.1	16.3
8		IV-3h	Chiralpak AS-H	220	1ml/min	15:85	10.4	14.7
9		IV-3i	Chiralpak AS-H	238	0.7 ml/min	10:90	23.8	35.3
10		IV-3j	Chiralcel AS-H	238	0.7 ml/min	30:70	11.7	16.8
11 ^a		IV-3k	Chiralpak AD-H	254	0.7 ml/min	10:90	13.4	16.1
12		IV-8a	Chiralcel OD-H	254	0.5ml/min	10:90	23.4	27.1
13		IV-8b	Chiralpak AD-H	254	0.8ml/min	2:98	42.1	52.9
14		IV-9a	Chiralpak AS-H	254	0.5ml/min	20:80	23.3	28.5

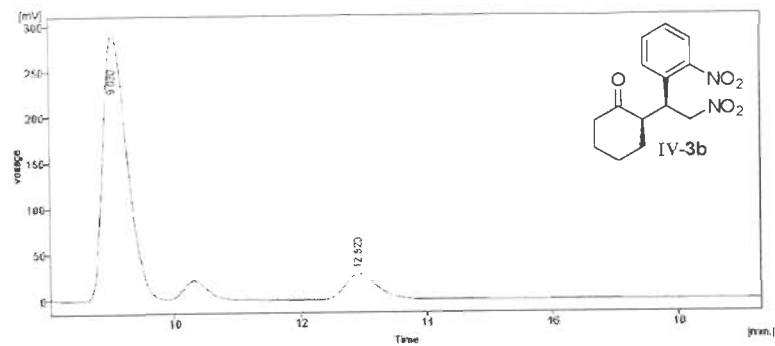
15		IV-10a	Chiralpak AD-H	254	1 ml/min	20:80	18.3	21.9
16		IV-11a	Chiralpak AD-H	254	1ml/min	10:90	7.2	10.7
17		IV-13a	Chiralpak AS-H	254	0.5 ml/min	20:80	31.7	43.1

^{a)} Structure of major enantiomer is shown.



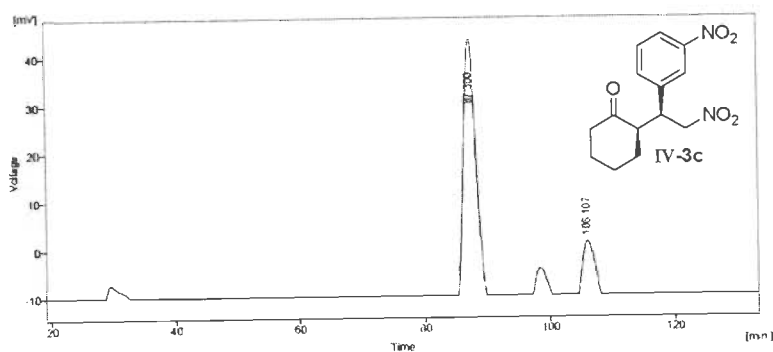
Result Table (Uncat - F:\ashm\data\Fold\147_35)

Reten. Time [min]	Area [mV s]	Height [mV]	Area [%]	Height [%]	W05 [min]	
1	18 017	6190 036	230 472	88 6	89 9	0 41
2	21 540	715 553	28 607	10 4	10 1	0 42
Total		6911 593	263 079	100 0	100 0	



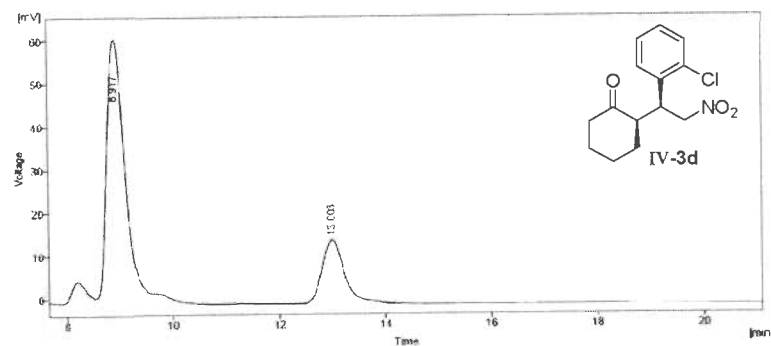
Result Table (Uncat - F:\ashm\data\Fold\147_35)

Reten. Time [min]	Area [mV s]	Height [mV]	Area [%]	Height [%]	W05 [min]	
1	9 030	7750 733	252 092	88 5	91 1	0 42
2	12 910	1009 487	28 478	11 5	8 9	0 54
Total		8760 260	321 600	100 0	100 0	



Result Table (Uncat - F:\ashm\data\Fold\147_35)

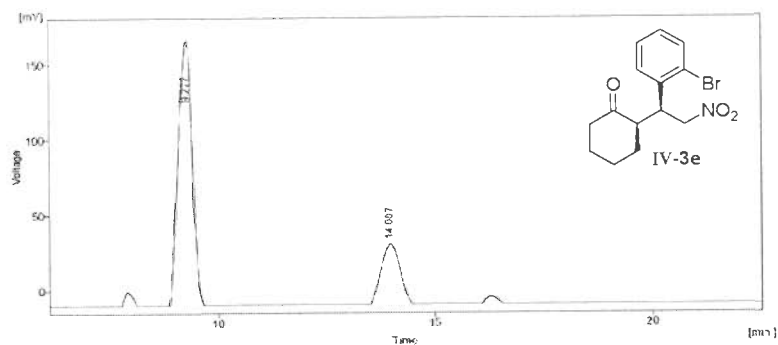
Reten. Time [min]	Area [mV s]	Height [mV]	Area [%]	Height [%]	W05 [min]	
1	87 300	7110 960	53 400	83 6	82 6	2 18
2	106 107	1379 359	11 231	16 2	17 4	2 89
Total		8490 350	64 631	100 0	100 0	



Result Table (Uncat - F:\ashm\data\Fold\147_35)

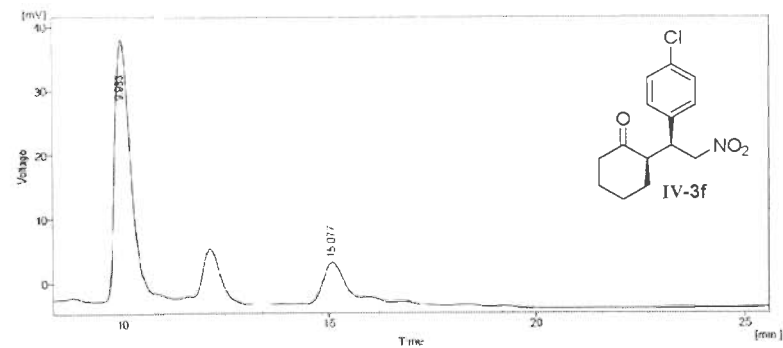
Reten. Time [min]	Area [mV s]	Height [mV]	Area [%]	Height [%]	W05 [min]	
1	8 917	144 014	60 276	84 3	83 6	0 36
2	13 003	264 094	11 835	15 7	16 4	0 39
Total		1709 708	72 111	100 0	100 0	

Figure 1: HPLC Chromatograms of Michael adducts IV-3a, IV-3b, IV-3c and IV-3d.



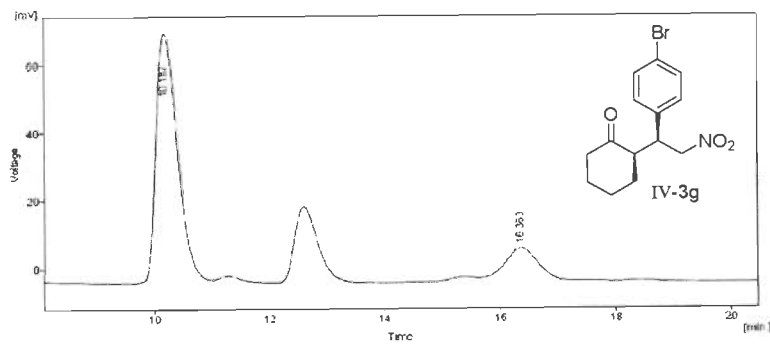
Result Table (Uncal - F:\synth\klausur\FolderNew\FolderNew\Folder148_29_1)

Reten. Time [min]	Area [mV*s]	Height [mV]	Area [%]	Height [%]	WDS [mm]	
1	9.277	3915.786	175.605	84.1	85.6	0.37
2	14.007	142.564	29.633	15.9	14.4	0.41
Total		4058.350	205.237	100.0	100.0	



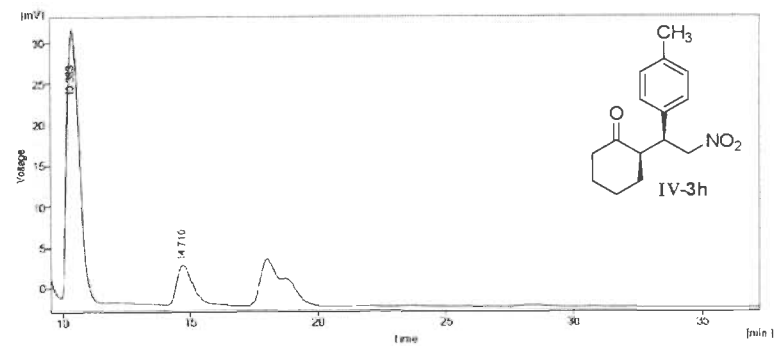
Result Table (Uncal - F:\synth\klausur\FolderNew\FolderNew\Folder148_29_1)

Reten. Time [min]	Area [mV*s]	Height [mV]	Area [%]	Height [%]	WDS [mm]	
1	9.983	1007.890	40.051	85.3	87.2	0.41
2	15.077	196.083	5.962	14.7	12.6	0.51
Total		1272.969	46.013	100.0	100.0	



Result Table (Uncal - F:\synth\klausur\FolderNew\FolderNew\Folder148_29_1)

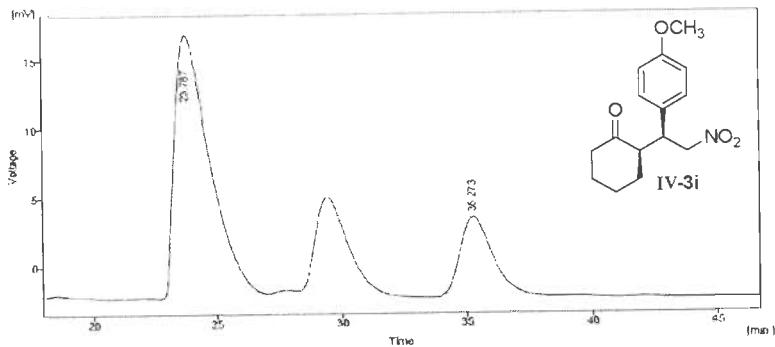
Reten. Time [min]	Area [mV*s]	Height [mV]	Area [%]	Height [%]	WDS [mm]	
1	10.187	1872.348	73.012	85.0	85.1	0.40
2	16.363	329.318	9.030	10.9	10.9	0.58
Total		2201.666	82.042	100.0	100.0	



Result Table (Uncal - HPLC - 120 (06.November.2006))

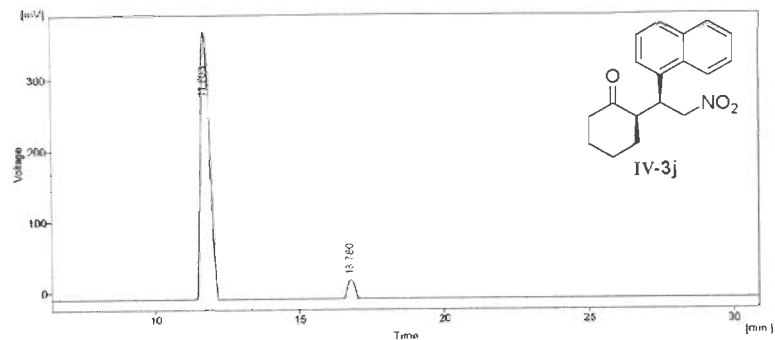
Reten. Time [min]	Area [mV*s]	Height [mV]	Area [%]	Height [%]	WDS [mm]	
1	10.783	1303.110	53.802	86.0	87.8	0.51
2	14.710	177.488	4.597	7.4	12.2	0.65
Total		1270.598	37.749	100.0	100.0	

Figure 2: HPLC Chromatograms of Michael adducts IV-3e, IV-3f, IV-3g and IV-3h.



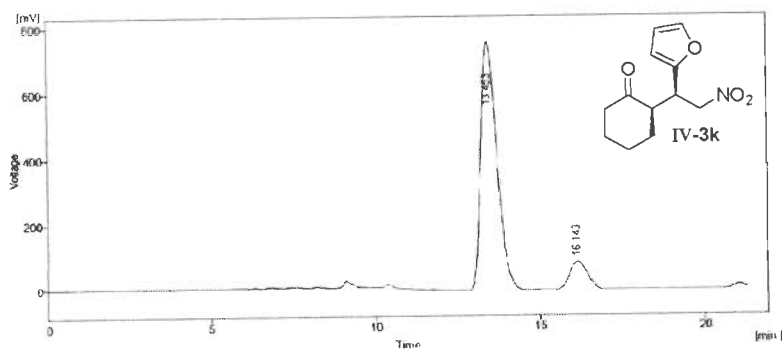
Result Table (Uncal - F:\asym\data\New Folder\New Folder\O-Me)

Reten. Time [min]	Area [mV.s]	Height [mV]	Area [%]	Height [%]	WGS [min]
1	23.787	1250.470	19.081	80.0	1.53
2	36.273	484.182	5.540	20.0	1.24
Total		2322.621	24.620	100.0	100.0



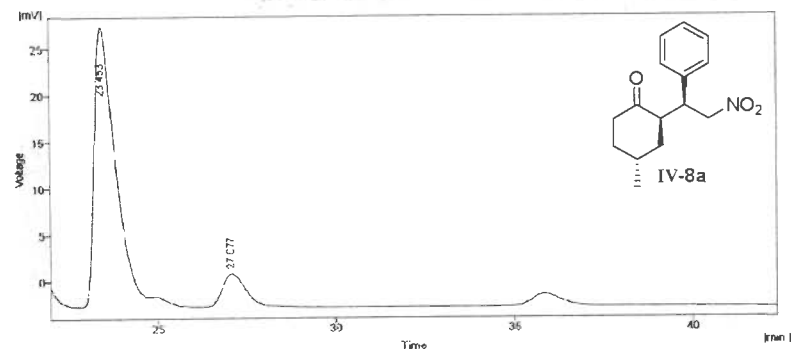
Result Table (Uncal - F:\asym\data\New Folder\New Folder)

Reten. Time [min]	Area [mV.s]	Height [mV]	Area [%]	Height [%]	WGS [min]
1	11.700	8294.644	377.401	94.0	0.98
2	16.760	445.500	26.164	4.9	0.90
Total		8655.643	403.565	100.0	100.0



Result Table (Uncal - F:\asym\data\New Folder (Zulurung))

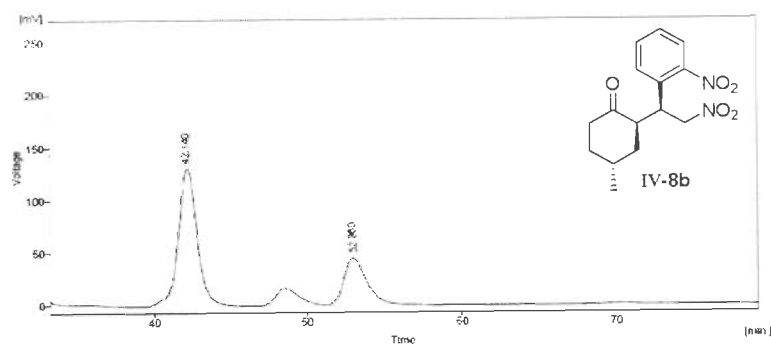
Reten. Time [min]	Area [mV.s]	Height [mV]	Area [%]	Height [%]	WGS [min]
1	13.453	25403.361	764.190	80.8	0.52
2	16.143	3211.148	87.301	11.2	0.55
Total		28614.509	851.492	100.0	100.0



Result Table (Uncal - My GC - 388 (05 April 2018))

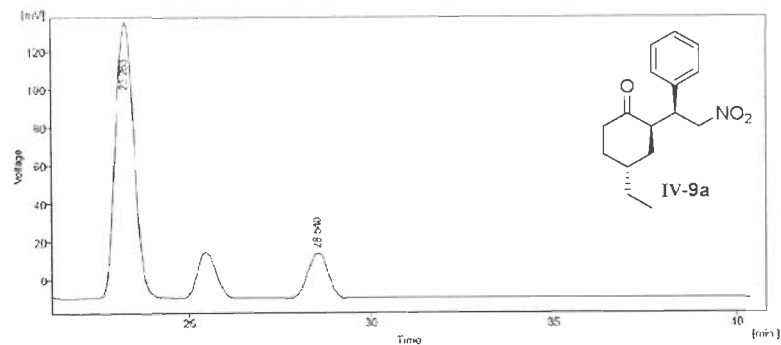
Reten. Time [min]	Area [mV.s]	Height [mV]	Area [%]	Height [%]	WGS [min]
1	23.422	1175.634	29.73	88.2	0.52
2	27.077	127.319	3.265	11.8	0.71
Total		1301.920	33.277	100.0	100.0

Figure 3: HPLC Chromatograms of Michael adducts IV-3i, IV-3j, IV-3k and IV-8a.



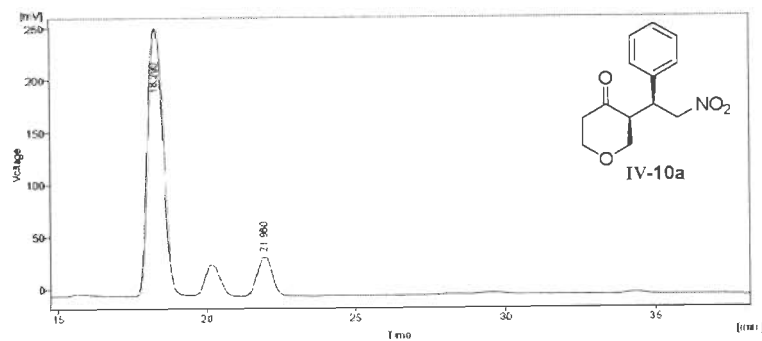
Result Table (Linear - F:\asym\Michael_P\New Folder (2)\p1\4\1\c1\NO2\8b)

Retention Time [min]	Area [mV.s]	Height [mV]	Area [%]	Height [%]	W06 [min]
1	42.140	11262.151	136.531	82.3	80.0
2	52.602	2422.624	32.683	17.7	20.0
Total	13284.775	145.214	100.0	100.0	1.27



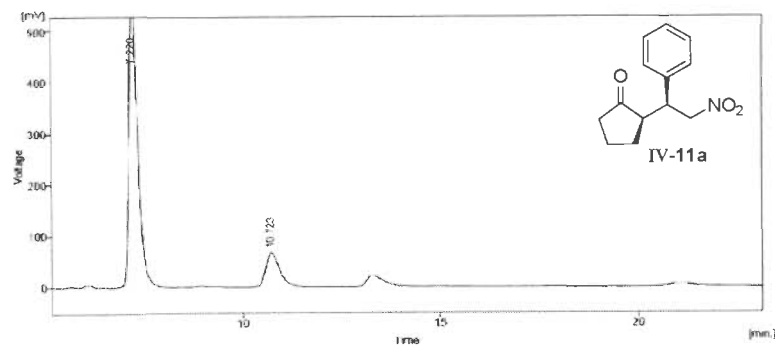
Result Table (Linear - F:\asym\Michael_P\New Folder (2)\p1\4\1\c1\NO2\9a)

Retention Time [min]	Area [mV.s]	Height [mV]	Area [%]	Height [%]	W06 [min]
1	23.263	5199.541	144.976	85.3	80.0
2	28.540	892.046	23.920	14.7	14.0
Total	6078.587	163.254	100.0	100.0	1.17



Result Table (Linear - F:\asym\Michael_P\New Folder (2)\p1\4\1\c1\NO2\10a)

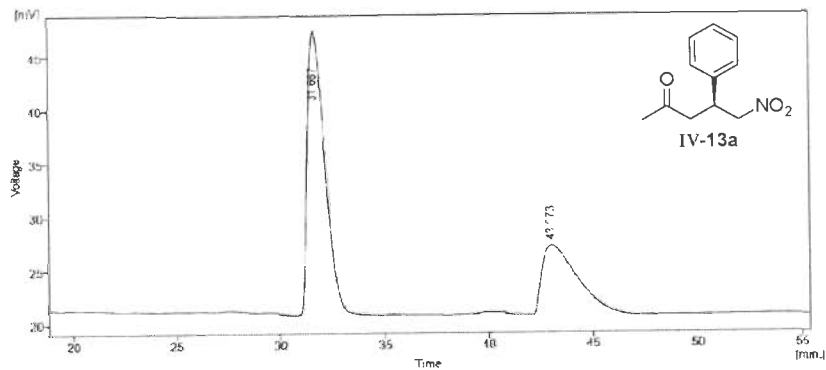
Retention Time [min]	Area [mV.s]	Height [mV]	Area [%]	Height [%]	W06 [min]
1	16.290	8202.148	258.050	97.5	97.3
2	21.940	1120.192	37.792	12.5	12.8
Total	13322.340	254.842	100.0	100.0	3.56



Result Table (Linear - F:\asym\Michael_P\p1\4\1\c1\NO2\11a)

Retention Time [min]	Area [mV.s]	Height [mV]	Area [%]	Height [%]	W06 [min]
1	7.221	8990.780	565.612	92.5	90.5
2	10.723	1269.705	82.922	12.5	9.7
Total	10260.485	626.534	100.0	100.0	0.24

Figure 4: HPLC Chromatograms of Michael adducts IV-8b, IV-9a, IV-10a and IV-11a.



Result Table (Local - F:\sperimentata_nuove_ione_parnet)

Reten. Time [min]	Area [mV·s]	Height [mV]	Area [%]	Height [%]	W05 [min]
1	31.067	1502.940	20.692	75.1	0.90
2	43.073	495.436	6.701	24.9	1.70
Total	3002.363	32.283	100.0	100.0	

Figure 5: HPLC Chromatogram of Michael adduct IV-13a.

4.6. REFERENCES

1. A. Berkessel, H. Gröger (Eds.), *Books on Organocatalysis: Asymmetric Organocatalysis: From Biomimetic Concepts to Applications in Asymmetric Synthesis*, Wiley-VCH: Weinheim, 2005.
2. P.I. Dalko (Ed.), *Enantioselective Organocatalysis: Reactions and Experimental Procedures*, Wiley-VCH: Weinheim, 2007.
3. M. Nielsen, C.B. Jacobsen, N. Holub, W.M. Paixao, K.A. Jørgensen, *Asymmetric Organocatalysis with Sulfones*, *Angew. Chem. Int. Ed.* 49 (2010) 2668.
4. S. Sulzer-Mossè, A. Alexakis, *Chiral Amines as Organocatalysts for Asymmetric Conjugate Addition to Nitroolefins and Vinyl Sulfones via Enamine Activation*, *Chem. Commun.* (2007) 3123.
5. D. Almaşi, D.A. Alonso, C. Nájera, *Organocatalytic Asymmetric Conjugate Additions*, *Tetrahedron: Asymm.* 18 (2007) 299.
6. G.S. Rao, N. Sudhakar, B.V. Rao, S.J. Basha, *The Formal Synthesis of 3-Epi Jaspine B Using Stereoselective Intramolecular Oxa-Michael Addition*, *Tetrahedron: Asymm.* 21 (2010) 1963.
7. O.M. Berner, L. Tedeschi, D. Enders, *Asymmetric Michael Additions to Nitroalkenes*, *Eur. J. Org. Chem.* (2002) 1877.
8. K. Sakthivel, W. Notz, T. Bui, C.F. Barbas III, *Amino Acid Catalyzed Direct Asymmetric Aldol Reactions: A Bioorganic Approach to Catalytic Asymmetric Carbon-Carbon Bond-Forming Reactions*, *J. Am. Chem. Soc.* 123 (2001) 5260.
9. B. List, P. Pojarliev, H.J. Martin, *Efficient Proline-Catalyzed Michael Additions of Unmodified Ketones to Nitro olefins*, *Org. Lett.* 3 (2001) 2423.
10. D. Enders, A. Seki, *Proline-Catalyzed Enantioselective Michael Additions of Ketones to Nitrostyrene*, *Synlett* (2002) 26.
11. Y.-F. Ting, C. Chang, R.J. Reddy, D.R. Magar, K. Chen, *Pyrrolidinyl-Camphor Derivatives as a New Class of Organocatalyst for Direct Asymmetric Michael Addition of Aldehydes and Ketones to β -Nitroalkenes*, *Chem. Eur. J.* 16 (2010) 7030.
12. Quintard, S. Belot, E. Marchal, A. Alexakis, *Animal-Pyrrolidine Organocatalysts - Highly Efficient and Modular Catalysts for α -Functionalization of Carbonyl Compounds*, *Eur. J. Org. Chem.* (2010) 927.

13. A.P. Carley, S. Dixon, J.D. Kilburn, *Pyrrolidine-Based Organocatalysts for Enantioselective Michael Addition of Cyclohexanone to trans- β -Nitrostyrene*, *Synthesis* (2009) 2509.
14. S. Chandrasekhar, B. Tiwari, B.B. Parida, C.R. Reddy, *Chiral Pyrrolidine-Triazole Conjugate Catalyst for Asymmetric Michael and Aldol reactions*, *Tetrahedron: Asymm.* 19 (2008) 495.
15. H. Chen, W. Yu, S. Wei, J. Suna, *L-Proline Derived Triamine as a Highly Stereoselective Organocatalyst for Asymmetric Michael Addition of Cyclohexanone to Nitroolefins*, *Tetrahedron: Asymm.* 18 (2007) 1308.
16. S. Luo, H. Xu, X. Mi, J. Li, X. Zheng, J.-P. Cheng, *Evolution of Pyrrolidine-Type Asymmetric Organocatalysts by "Click" Chemistry*, *J. Org. Chem.* 71 (2006) 9244.
17. D.-Q. Xu, H.-D. Yue, S.-P. Luo, A.-B. Xia, S. Zhang, Z.-Y. Xu, *A Chiral Thiourea Acid as an Effective Additive for Enantioselective Organocatalytic Michael Additions of Nitroolefins*, *Org. Biomol. Chem.* 6 (2008) 2054.
18. Y.-J. Cao, Y.-Y. Lai, X. Wang, Y.-J. Lia W.-J. Xiao, *Michael Additions in Water of Ketones to Nitroolefins Catalyzed by Readily Tunable and Bifunctional Pyrrolidine-Thiourea Organocatalysts*, *Tetrahedron Lett.* 48 (2007) 21.
19. K. Liu, H.-F. Cui, J. Nie, K.-Y. Dong, X.-J. Li, J.-A. Ma, *Highly Enantioselective Michael Addition of Aromatic Ketones to Nitroolefins Promoted by Chiral Bifunctional Primary Amine-thiourea Catalysts Based on Saccharides*, *Org. Lett.* 9 (2007) 923.
20. A. Lu, P. Gao, Y. Wu, Y. Wang, Z. Zhou, C. Tang, *Highly Enantio- and Diastereoselective Michael Addition of Cyclohexanone to Nitroolefins Catalyzed by a Chiral Glucose-Based Bifunctional Secondary Amine-thiourea Catalyst*, *Org. Biomol. Chem.* 7 (2009) 3141.
21. B. Ni, Q. Zhang, A.D. Headley, *Pyrrolidine-Based Chiral Pyridinium Ionic Liquids (ILs) as Recyclable and Highly Efficient Organocatalysts for the Asymmetric Michael Addition Reactions*, *Tetrahedron Lett.* 49 (2008) 1249.
22. M.-K. Zhu, L.-F. Cun, A.-Q. Mi, Y.-Z. Jianga, L.-Z. Gongga, *A Highly Enantioselective Organocatalyst for the Michael Addition of Cyclic Ketones to Nitroolefins*, *Tetrahedron: Asymm.* 17 (2006) 491.

23. B. Ni, Q. Zhang, A.D. Headley, *Highly Enantioselective Michael Addition of Ketones to Nitroolefins Catalyzed by (S)-pyrrolidine Arenesulfonamide*, *Tetrahedron: Asymm.* 18 (2007) 1443.
24. Y. Xu, A. Córdova, *Simple Highly Modular Acyclic Amine-Catalyzed Direct Enantioselective Addition of Ketones to Nitro-olefins*, *Chem. Commun.* (2006) 460.
25. G.L. Puleo, A. Iuliano, *Substrate Control by Means of the Chiral Cavity of Prolinamide Derivatives of Cholic Acid in the Organocatalyzed Michael Addition of Cyclohexanone to Nitroolefins*, *Tetrahedron: Asymm.* 19 (2008) 2045.
26. A.J.A. Cobb, D.M. Shaw, D.A. Longbottom, J.B. Gold, S.V. Ley, *Organocatalysis with Proline Derivatives: Improved Catalysts for the Asymmetric Mannich, Nitro-Michael and Aldol Reactions*, *Org. Biomol. Chem.* 3 (2005) 84.
27. C.-L. Cao, M.-C. Ye, X.-L. Sun, Y. Tang, *Pyrrrolidine-Thiourea as a Bifunctional Organocatalyst: Highly Enantioselective Michael Addition of Cyclohexanone to Nitro-olefins*, *Org. Lett.* 8 (2006) 2901.
28. S. Luo, L. Zhang, X. Mi, Y. Qiao, J.-P. Cheng, *Functionalized Chiral Ionic Liquid Catalyzed Enantioselective Desymmetrizations of Prochiral Ketones via Asymmetric Michael Addition Reaction*, *J. Org. Chem.* 72 (2007) 9350.
29. D.-Q. Xu, B.-T. Wang, S.-P. Luo, H.-D. Yue, L.-P. Wang, Z.-Y. Xu, *Pyrrrolidine-Pyridinium Based Organocatalysts for Highly Enantioselective Michael Addition of Cyclohexanone to Nitroalkenes*, *Tetrahedron: Asymm.* 18 (2007) 1788.
30. B.N.Q. Zhang, A.D. Headley, *Pyrrrolidine-Based Chiral Pyridinium Ionic Liquids (ILs) as Recyclable and Highly Efficient Organocatalysts for the Asymmetric Michael Addition Reactions*, *Tetrahedron Lett.* 49 (2008) 1249.
31. P.L. Wang, Y. Zhang, G. Wang, *Silica Gel Supported Pyrrrolidine-Based Chiral Ionic Liquid as Recyclable Organocatalyst for Asymmetric Michael Addition to Nitrostyrenes*, *Tetrahedron* 64 (2008) 7633.
32. P.J. Chua, B.Tan, X. Zeng, G. Zhong, *L-Prolinol as a Highly Enantioselective Catalyst for Michael Addition of Cyclohexanone to Nitroolefins*, *Bioorg. Med. Chem. Lett.* 19 (2009) 3915.
33. A. Lu, P. Gao, Y. Wu, Y. Wang, Z. Zhou, C. Tang, *Highly Enantio- and Diastereoselective Michael Addition of Cyclohexanone to Nitroolefins Catalyzed by a Chiral Glucose-Based Bifunctional Secondary Amine-Thiourea Catalyst*, *Org. Biomol. Chem.* 7 (2009) 3141.

Chapter-5

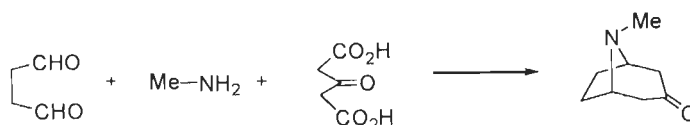
DOMINO REACTIONS OF ALKENYL-1,4-BENZOQUINONES

Domino Reactions of Alkenyl-1,4-benzoquinones

5.1. INTRODUCTION

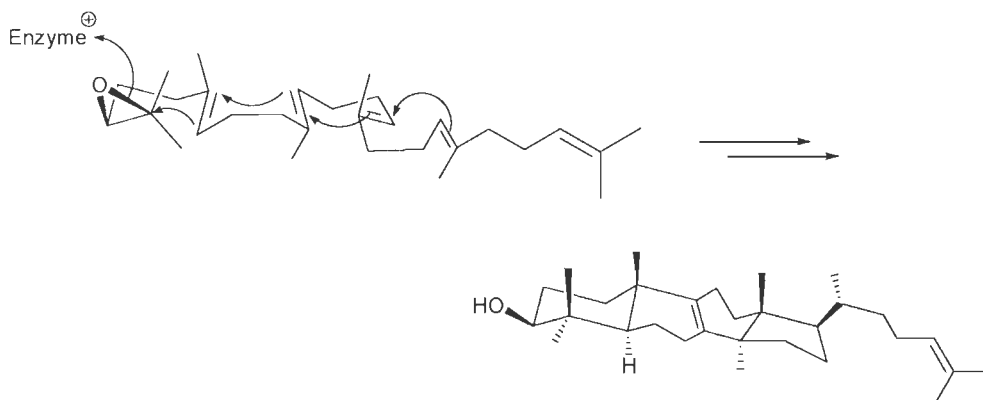
Organic reactions are normally viewed as linear and stepwise processes, in which isolation and purification of key intermediates often lead to diminished yields. The hunt for economical, environmentally benign and more efficient synthetic pathways has led to the development of rapid one-pot multistep processes *viz.*, “tandem”, “domino”, “cascade”, and “sequential”, processes that permit access to an array of molecules of high complexity and stereoselectivity in an efficient and atom-economical manner [1-9]. As duly noted by Nicolaou, terms including “tandem” are frequently used, apparently interchangeably [9]. Tandem reactions, according to Ho, are combinations of two or more reactions whose occurrence is in a specific order, and if they involve sequential addition of reagents the secondary reagents must be integrated into the products [1]. Tietze’s definition of domino reaction is a process involving two or more bond-forming transformations (usually C-C bonds) which take place under the same reaction conditions without adding additional reagents and catalysts, and in which the subsequent reactions result as a consequence of the functionality formed in the previous step [5]. The term “cascade” is another expression for “domino”. In “sequential,” reactions, the functionality for the second reaction has been created but additional reagents must be added in order for the second reaction to occur.

The first domino reaction of a natural product was presented by Robinson in his one-pot synthesis of bicyclic tropinone, a structural component of several alkaloids such as cocaine and atropine, by placing together a mixture of succindialdehyde, methylamine, and acetone-dicarboxylic acid [10]. A double Mannich reaction is the key step in this synthesis (Scheme 1).



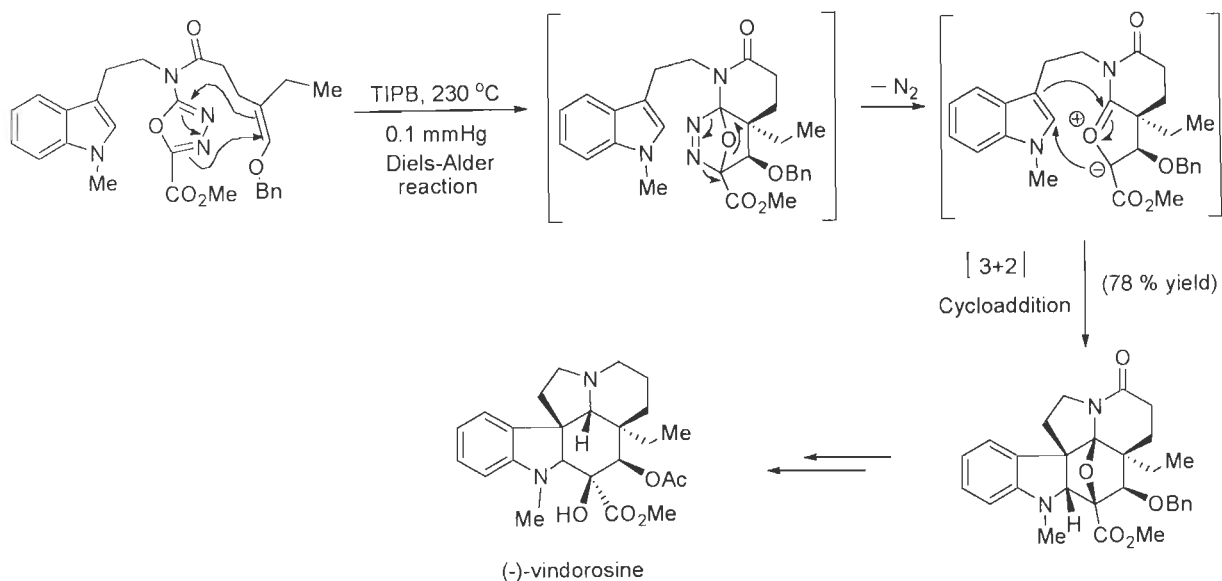
Scheme 1: Biomimetic domino synthesis of tropinone.

An attractive example of domino process is the biosynthesis of steroids from squalene epoxide which is transformed highly selectively into lanosterol with the formation of four C-C bonds and six stereogenic centers [11,12] (Scheme 2).



Scheme 2: Biosynthesis of steroids from squalene epoxides.

Boger *et al.* used domino process involving Diels-Alder and [3+2] cycloadditions in their total synthesis of (-)-vindorosine. Synthesis of a pentacyclic skeleton was achieved by inverse-electron-demand intramolecular Diels-Alder reaction between oxadiazole ring and the tethered enol ether and subsequent 1,3-dipolar cycloaddition [13].



Scheme 3: Diels-Alder and [3+2] cycloaddition in the total synthesis of (-)-vindorosine.

5.2. OBJECTIVE

Pericyclic reactions such as the Diels-Alder, ene, or electrocyclic reactions and non-pericyclic reactions such as conjugate addition reactions are by themselves extremely useful transformations. However, by combining two or more of these reactions the efficiency of the reaction and molecular complexity of the products can be amplified. The domino process would allow an ecologically and economically favorable chemical production with minimization of waste, since the amount of solvents, reagents, and energy would be dramatically decreased, in comparison to stepwise reactions. Often, these domino reactions are accompanied by dramatic increases in molecular complexity and impressive selectivity. This methodology allows for the rapid synthesis of complex compounds from simple substances in a few steps. Addition of nucleophiles and dienic compounds to α,β -unsaturated carbonyl systems such as *p*-benzoquinones, forming carbon-carbon bonds, belong to the central tenet of organic synthesis. Since pericyclic reactions are the most common processes encountered in domino reactions, we were interested to utilize alkenyl-*p*-benzoquinone derivatives as our starting material for domino reactions to synthesize complex molecular architectures.

5.3. RESULTS AND DISCUSSION

We have selected a set of alkenyl-*p*-benzoquinones and enol ethers for the study of domino cycloaddition reactions (Figure 1). The synthesis of alkenyl-*p*-benzoquinones began

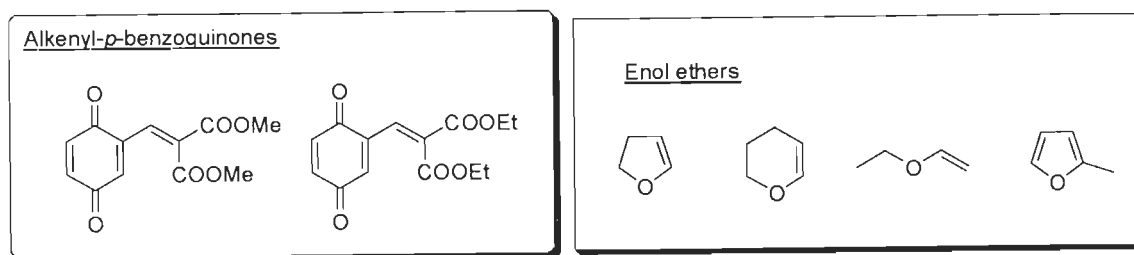
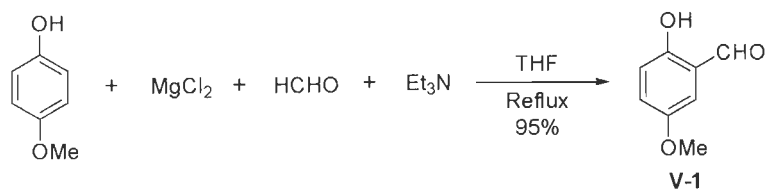


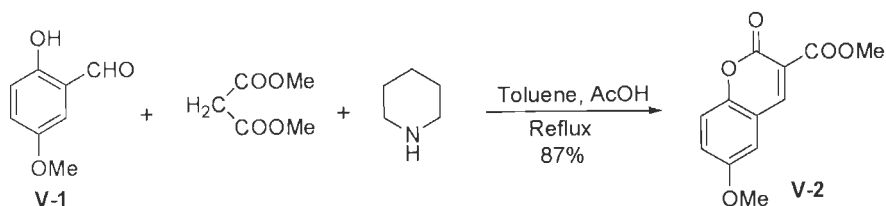
Figure 1: Structures of alkenyl-*p*-benzoquinones and enol ethers.

with the formylation of *p*-methoxyphenol as shown in Scheme 4. The reaction was carried out in dry THF with paraformaldehyde, magnesium chloride and dry triethyl amine according to a known procedure [14] to furnish the desired product in excellent yield.



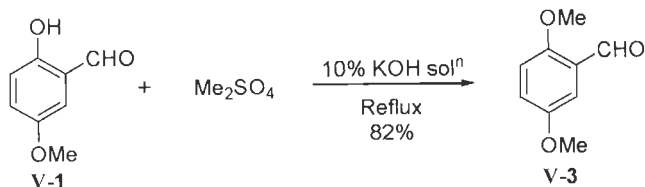
Scheme 4: Formylation of *p*-methoxyphenol.

The Knoevenagel condensation of *p*-methoxysalicylaldehyde with dimethyl malonate was performed in presence of piperidine and acetic acid under reflux conditions using Dean-Stark apparatus. However, under these reaction conditions, instead of desired product alkenyl-*p*-methoxyphenol (**V-4**), the reaction proceeded further with the cyclization to provide coumarin product **V-2** by the attack of phenolic $-\text{OH}$ on the carbonyl carbon of one of the ester moieties (Scheme 5).



Scheme 5: Reaction between *p*-methoxysalicylaldehyde and dimethyl malonates.

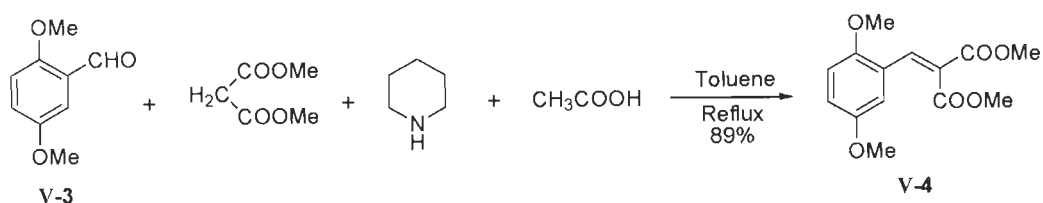
To circumvent the formation of coumarin, the phenolic $-\text{OH}$ function was protected in the form of methyl ether. Thus the methylation of *p*-methoxysalicylaldehyde was performed with Me_2SO_4 in 10% KOH solution. The reaction furnished the dimethyl ether **V-3** in 82% yield (Scheme 6).



Scheme 6: Methylation of *p*-methoxysalicylaldehyde.

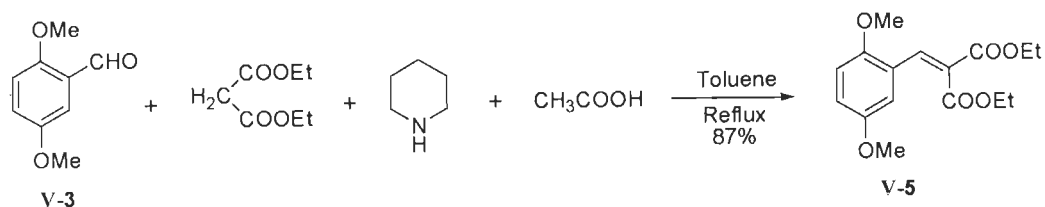
Then Knoevenagel condensation of 2,5-dimethoxybenzaldehyde was carried out with dimethyl malonate in presence of piperidine and acetic acid using Dean-Stark trap as shown in

Scheme 7. The condensation was reached completion in 10 h to afford desired alkenylarene **V-4** in very high yield.



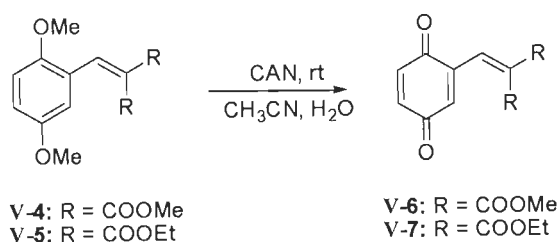
Scheme 7: Synthesis of alkenylarene **V-4**.

Similarly, the condensation of 2,5-dimethoxybenzaldehyde with diethyl malonate was performed under Knoevenagel conditions to furnish styrene **V-5** in 87% yield (Scheme 8).



Scheme 8: Synthesis of alkenylarene **V-5**.

After synthesizing dimethyl ethers of hydroquinone **V-4** and **V-5**, these compounds were subjected to oxidation with ceric ammonium nitrate solution in acetonitrile-water at room temperature to provide corresponding products alkenyl *p*-benzoquinone in excellent yields [15] (Scheme 9).

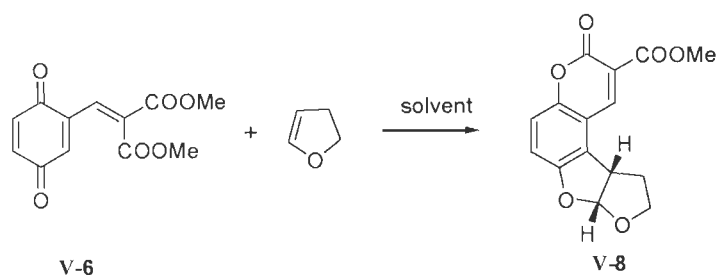


Scheme 9: Synthesis of alkenyl *p*-benzoquinones.

Then the reactions of alkenyl *p*-benzoquinones were carried out with different enol ethers. At the outset, we performed the reaction of alkenyl-*p*-quinone **V-6** with 2,3-dihydrofuran

in various solvent systems at different temperature as shown in Table 1. When the reaction was carried out in DCM, no reaction was observed at room temperature as well as under reflux conditions. When the reaction was performed in other polar solvent THF at room temperature, fura-fused coumarin **V-8** derived from a [3+2] cycloaddition/ring closure domino process was

Table 1: Optimization conditions for the synthesis of tetracyclic compound **V-8**^{a)}.



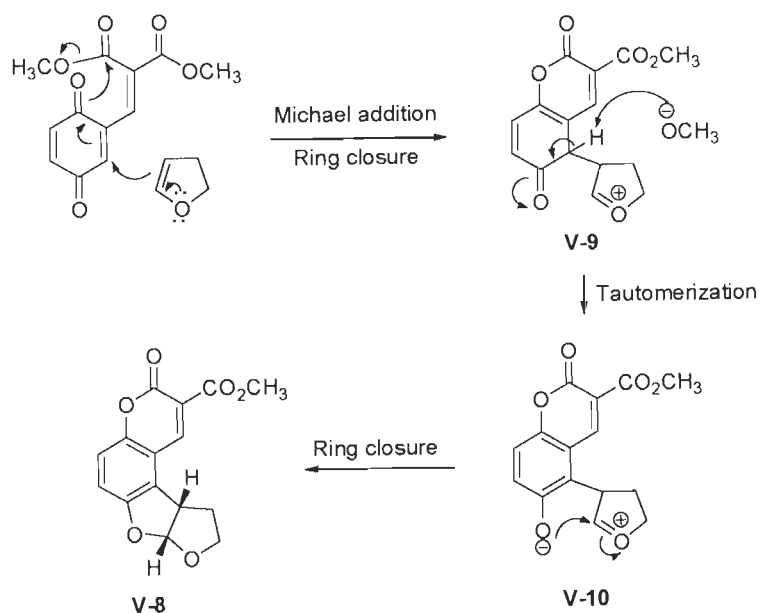
Entry	Solvent	Temp	Time	Yield (%) ^{b)}
1.	DCM	rt	4 d	-
2.	Toluene	rt	36 h	30
3.	THF	rt	2 d	15
4.	DCM	reflux	4 d	-
5.	Toluene	reflux	24 h	40
6.	THF	reflux	2 d	25
7.	Neat	rt	10 h	70
8.	Neat	reflux	8 h	45

^{a)} The reactions in entries 1-3 were carried out with **V-6** (0.3 mM) and DHF (0.5 mM) and that of entries 4-6 were carried out with **V-6** (1.0 mM) and DHF (2.0 mM). The neat reactions (entries 7 and 8) were carried out with **V-6** (1.0 mM) and DHF (2.5 mL). ^{b)} Yield of pure and column chromatographically isolated product.

obtained in 15% yield. However, when both the reactants were treated in less polar solvent toluene, 30% product was achieved in 36 h. To improve the yield of the tetracyclic product **V-8**, the reactions were heated to reflux temperature in THF as well as in toluene. The reactions

furnished the product **V-8** in 25 and 40% yields, in 2 days and 24 h, respectively. When the reactions were heated for longer time, no further conversion of reactant to product was observed. Next we examined the reaction in neat condition. The reaction was performed between diene (1 mM) and dienophile (10 mM) at room temperature for 10 h. Then about 5 mL of hexane was added to the reaction mixture and the flask was kept at 0 °C for 2 h. Gratifyingly, the product **V-8** was obtained as a pure solid in 70% yield after filtration (Table 1, entry 7). However, when the reaction was carried out at reflux temperature in neat condition, only 45% of the product was observed. Thus optimal results were observed as solvent free conditions at room temperature.

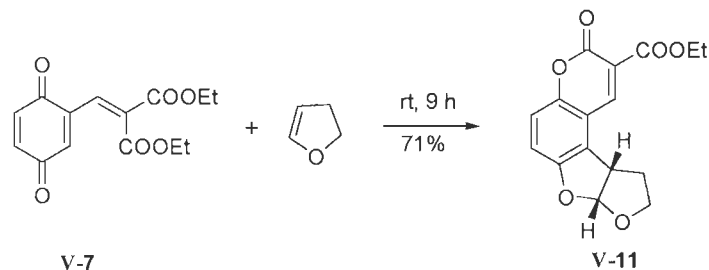
The reaction between alkenyl-*p*-benzoquinone **V-6** and DHF proceeded in a domino conjugate addition of enol ether followed by tautomerization to a phenolic nucleophile and ring closure. The domino process proceeds by (i) conjugate addition of enol ether followed by ring



Scheme 10: Formation of furo-furocoumarin **V-8** by conjugate addition/double cyclization domino process.

closure to generate cationic intermediate **V-9** and (ii) keto-enol tautomerization of **V-9** to a phenolic nucleophile **V-10** and subsequent ring closure to give [3+2] cycloadduct furo-furocoumarin **V-8**. After optimizing the reaction conditions for the synthesis of tetracycle **V-8**, we have performed the reaction between alkenyl-*p*-quinone **V-7** with 2,3-dihydrofuran under

similar conditions. The reaction proceeded at room temperature for 9 h to furnish the tetracyclic product **V-11** in very good yield (Scheme 11).

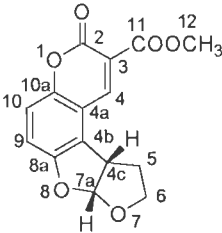
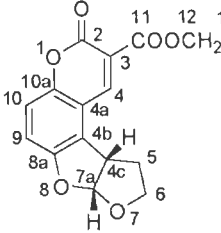


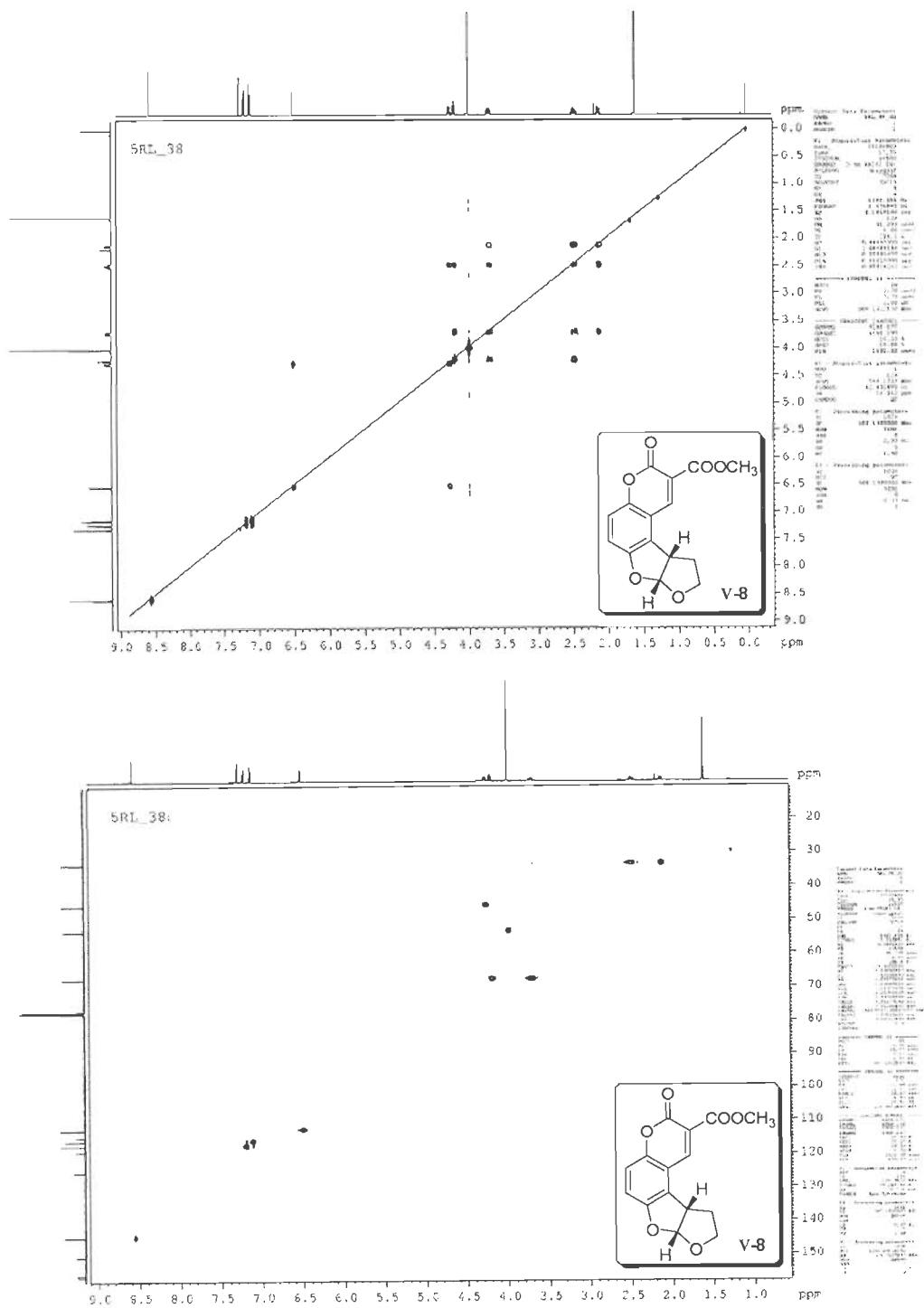
Scheme 11: Conjugate addition/double cyclization domino process of alkenyl *p*-benzoquinone **V-7** with DHF.

The structure elucidation of polycycles **V-8** and **V-11** is on the basis of collective information that obtained from IR, ^1H and ^{13}C NMR and 2D (^1H - ^1H and ^1H - ^{13}C COSY) experiments of pure and isolated products. The identification of protons that are coupled with each other and the connectivity between protons and carbons are realized by ^1H - ^1H COSY and ^1H - ^{13}C COSY, respectively (Table 2, Figures 2 and 3). The carbonyl stretch at 1766 cm^{-1} in IR spectrum of **V-8** is a characteristic band for coumarin systems. The olefinic proton of the lactone ring resonates at δ 8.57 ppm. The two aromatic protons appear as an AB quartet centered at δ 7.17 ppm. The two protons (H-4c and H-7a) present on the fused carbons of five-membered rings resonate at δ 4.27 and 6.52 ppm, respectively. The coupling constant 6.0 Hz between these two protons is indicative of their *cis*-geometry. The ester and lactone carbonyl carbons resonate at δ 164 and 156 ppm, respectively, in ^{13}C NMR. The acetal carbon C-7a resonates at δ 112.3 ppm and the methyl group of carboxylic ester appears at δ 53.1 ppm. The mass value of 288 confirms the molecular weight of this compound.

Similar data was obtained for the tetracycle **V-11** from its IR, ^1H and ^{13}C NMR spectra. The NMR data of protons and selected carbons of the products **V-8** and **V-11** is depicted in Table 2. The small coupling constant obtained for protons at fused rings revealed the *cis*-addition of dihydrofuran to *p*-benzoquinone derivative **V-7**. The NOESY experiment further confirmed the *cis*-geometry of H-4c and H-7a on the fused carbons of five-membered rings of **V-11** (Figure 4).

Table 2: Spectral data for tetracyclic compounds **V-8** and **V-11**.

Position	 V-8		 V-11	
	δ_H (ppm) (multiplicity)	δ_C (ppm)	δ_H (ppm) (multiplicity)	δ_C (ppm)
C-2	-	156.5/155.9	-	156.3/155.7
C-4	8.57 (s)	144.6	8.50 (s)	143.8
C-4c	4.27 (dd, $J = 6.0, 9.0$ Hz)	45.6	4.24 (dd, $J = 5.5, 9.0$ Hz)	45.4
C-5	2.54-2.44 (m), 2.13 (dd, $J = 4.5, 12.0$ Hz)	33.3	2.50-2.40 (m), 2.10 (dd, $J = 5.0, 12.5$ Hz)	33.1
C-6	4.21 (t, $J = 8.0$ Hz), 3.71 (ddd, $J = 5.0, 9.0, 14.0$ Hz)	67.3	4.18 (t, $J = 8.5$ Hz), 3.68 (ddd, $J = 5.0, 9.0, 14.0$ Hz)	67.2
C-7a	6.52 (d, $J = 6.0$ Hz)	112.3	6.49 (d, $J = 5.5$ Hz)	112.2
C-9	7.17 (AB quartet, $J = 8.5, 43.5$ Hz)	115.8	7.13 (AB quartet, $J = 9.0, 46.0$ Hz)	115.4
C-10	7.17 (AB quartet, $J = 8.5, 43.5$ Hz)	117.1	7.13 (AB quartet, $J = 9.0, 46.0$ Hz)	116.8
C-11	-	163.9	-	163.1
C-12	4.00 (s)	53.1	4.44 (q, $J = 7.0$ Hz)	62.0
C-13	-	-	1.42 (t, $J = 7.0$ Hz)	14.1

Figure 2: ^1H - ^1H and ^1H - ^{13}C (HSQC) COSY spectra of V-8.

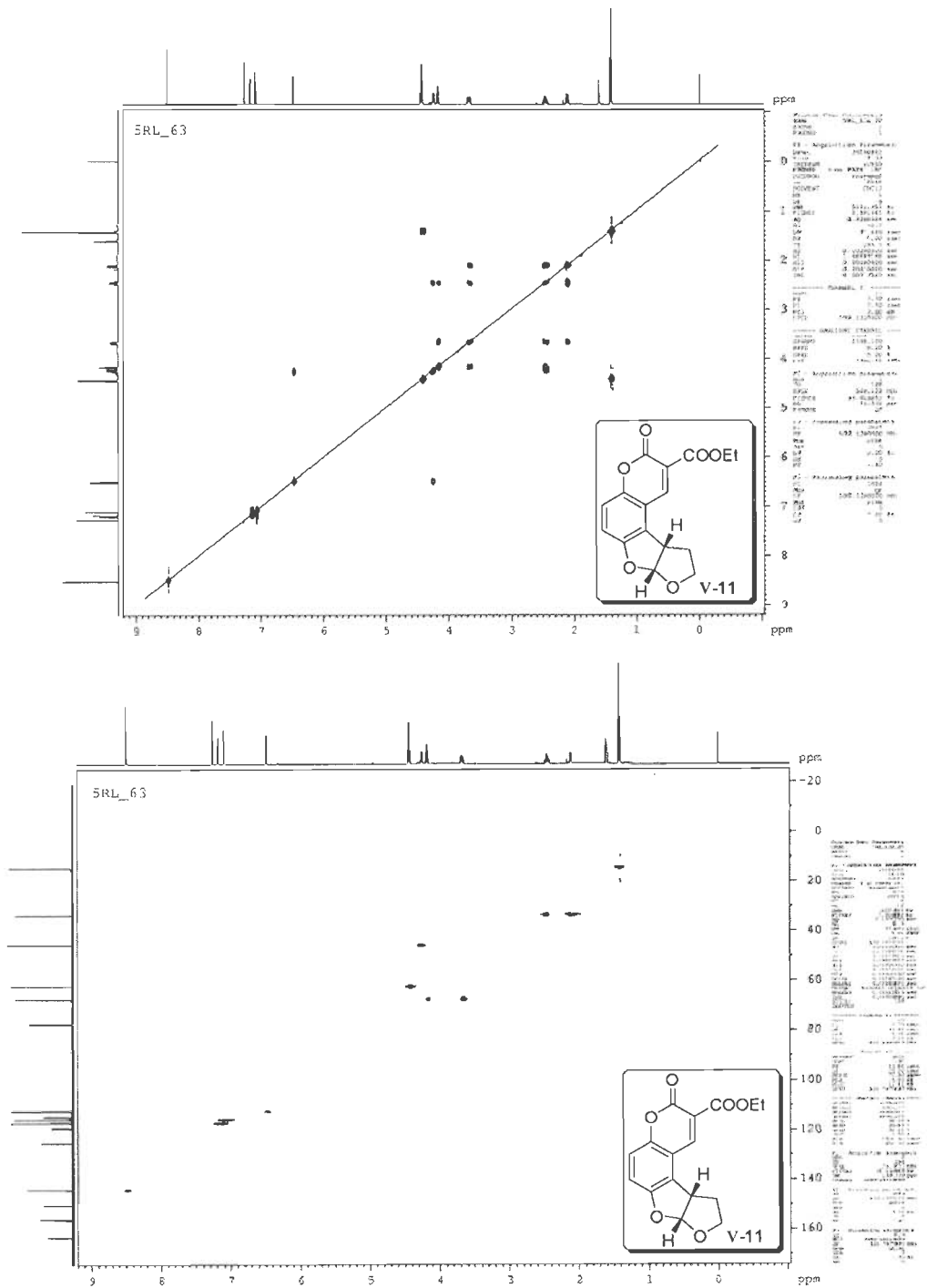


Figure 3: ^1H - ^1H and ^1H - ^{13}C (HSQC) COSY spectra of V-11.

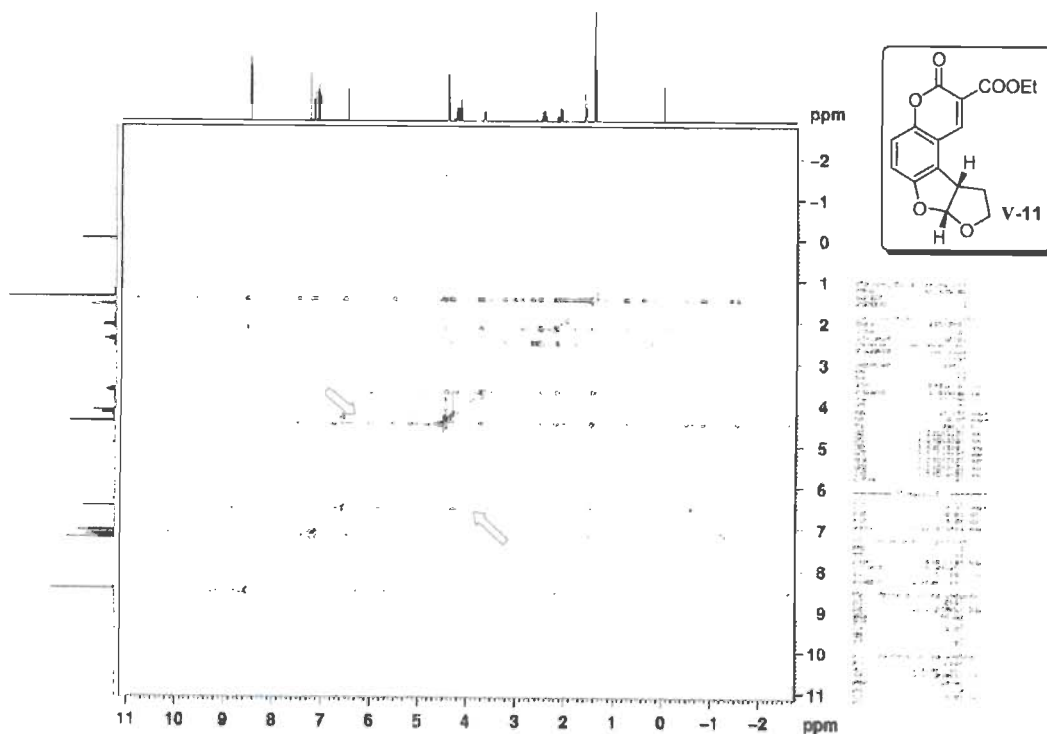


Figure 4: 500 MHz NOESY Spectrum of **V-11** in CDCl_3 .

The structure and stereochemistry of tetracyclic product **V-11** was further confirmed by its single crystal X-ray analysis (Figure 5, Table 3).

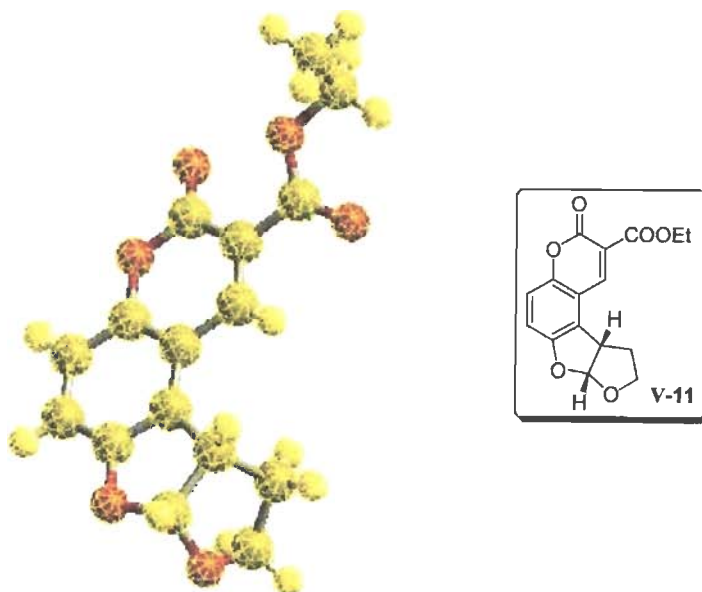


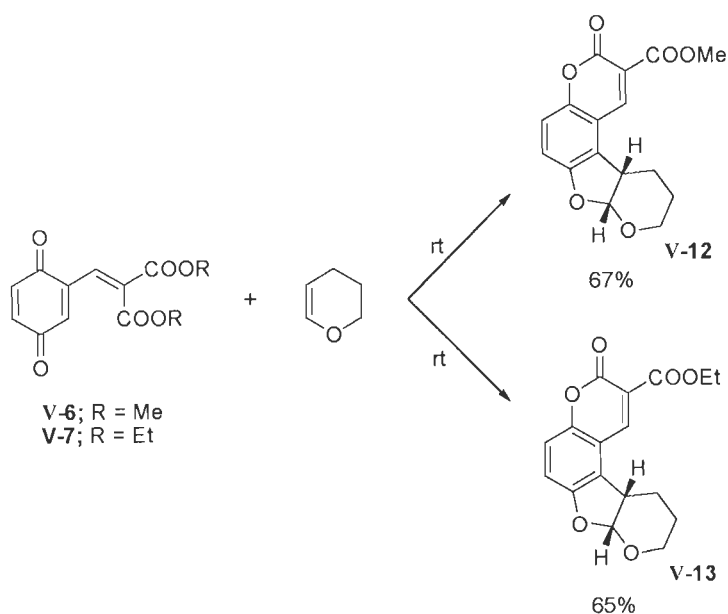
Figure 5: ORTEP diagram of crystal structure of tetracyclic compound **V-11**.

Table 3: Crystallographic data for furo-furocoumarin derivative **V-11**.

Empirical formula	C ₁₆ H ₁₄ O ₆	
Formula weight	302.27	
Temperature	293(2) K	
Wavelength	0.71073 Å	
Crystal system	Triclinic	
Space group	P-1	
Unit cell dimensions	a = 8.756(2) Å	α = 84.180(4)°.
	b = 8.879(2) Å	β = 73.556(4)°.
	c = 9.397(2) Å	γ = 74.346(4)°.
Volume	674.4(3) Å ³	
Z	2	
Density (calculated)	1.489 Mg/m ³	
Absorption coefficient	0.115 mm ⁻¹	
F(000)	316	
Crystal size	0.28 x 0.24 x 0.20 mm ³	
Theta range for data collection	2.26 to 25.84°	
Reflections collected	6397	
Independent reflections	2431 [R(int) = 0.0283]	
Completeness to theta = 25.84°	93.4 %	
Absorption correction	Semi-empirical from equivalents	
Max. and min. transmission	0.9774 and 0.9685	
Refinement method	Full-matrix least-squares on F ²	
Data / restraints / parameters	2431 / 0 / 200	
Goodness-of-fit on F ²	1.037	
Final R indices [I > 2σ(I)]	R1 = 0.0547, wR2 = 0.1347	
R indices (all data)	R1 = 0.0674, wR2 = 0.1440	
Largest diff. peak and hole	0.225 and -0.229 e.Å ⁻³	

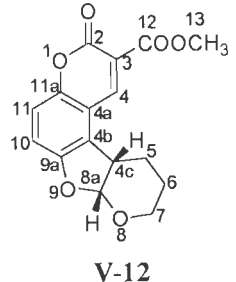
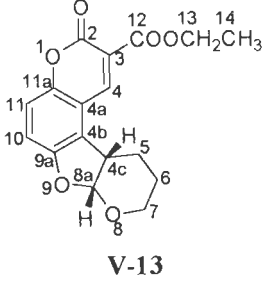
At this juncture we have carried out the domino reaction between alkenyl-*p*-benzoquinones **V-6** and **V-7** with dihydropyran. Thus the reaction of alkenyl-*p*-benzoquinones **V-6** with excess of dihydropyran under neat conditions proceeded smoothly at room temperature to furnish the pyrano-fused furocoumarin derivative **V-12** in very good yield. In a similar fashion the reaction between alkenyl-*p*-benzoquinones **V-7** and excess of dihydropyran provided the tetracyclic compound **V-13** (Scheme 12).

These products were thoroughly characterized by IR, NMR and GC-MS spectral data. The ^1H - ^1H COSY and ^1H - ^{13}C COSY experiments were carried out for these compounds in CDCl_3 to identify the protons that are coupled with each other and the connectivity between protons and carbons, respectively (Table 4, Figures 6 and 7). The coupling constant between H-4c and H-8a of **V-12** and **V-13** is 6.5 Hz; this small value indicates their *cis*-relation. The ROESY experiment performed on these products further confirmed the *cis*-geometry of H-4c and H-8a on the fused carbons of five-membered and six-membered rings of **V-12** and **V-13** (Figure 8).



Scheme 12: Conjugate addition/double cyclization domino process of alkenyl *p*-benzoquinone **V-6** and **V-7** with DHP.

Table 4: Spectral data for tetracyclic compounds V-12 and V-13.

Position	 V-12		 V-13	
	δ_H (ppm) (multiplicity)	δ_C (ppm)	δ_H (ppm) (multiplicity)	δ_C (ppm)
C-2	-	156.5	-	156.6
C-4	8.49 (s)	144.8	8.43 (s)	144.4
C-4c	3.52 (q, $J = 6.5$ Hz)	37.0	3.51 (q, $J = 7$ Hz)	37.1
C-5	1.71-1.60 (m), 1.84-1.74 (m)	20.4	1.70-1.58 (m), 1.83-1.75 (m)	20.5
C-6	1.71-1.60 (m), 2.28-2.21 (m)	25.4	1.70-1.58 (m), 2.28-2.20 (m)	25.5
C-7	3.96-3.91 (m)	61.2	3.95-3.90 (m)	61.3
C-8a	6.06 (d, $J = 6.0$ Hz)	105.5	6.05 (d, $J = 6.5$ Hz)	105.6
C-10	7.18 (AB quartet, $J = 9.0, 18.0$ Hz)	116.4	7.16 (AB quartet, $J = 8.5, 19$ Hz)	116.3
C-11	7.18 (AB quartet, $J = 9.0, 18.0$ Hz)	116.3	7.16 (AB quartet, $J = 8.5, 19$ Hz)	116.3
C-12	-	163.7	-	163.3
C-13	3.99 (s)	52.9	4.48-4.41 (m)	62.1
C-14	-	-	1.43 (t, $J = 7.0$ Hz)	14.2

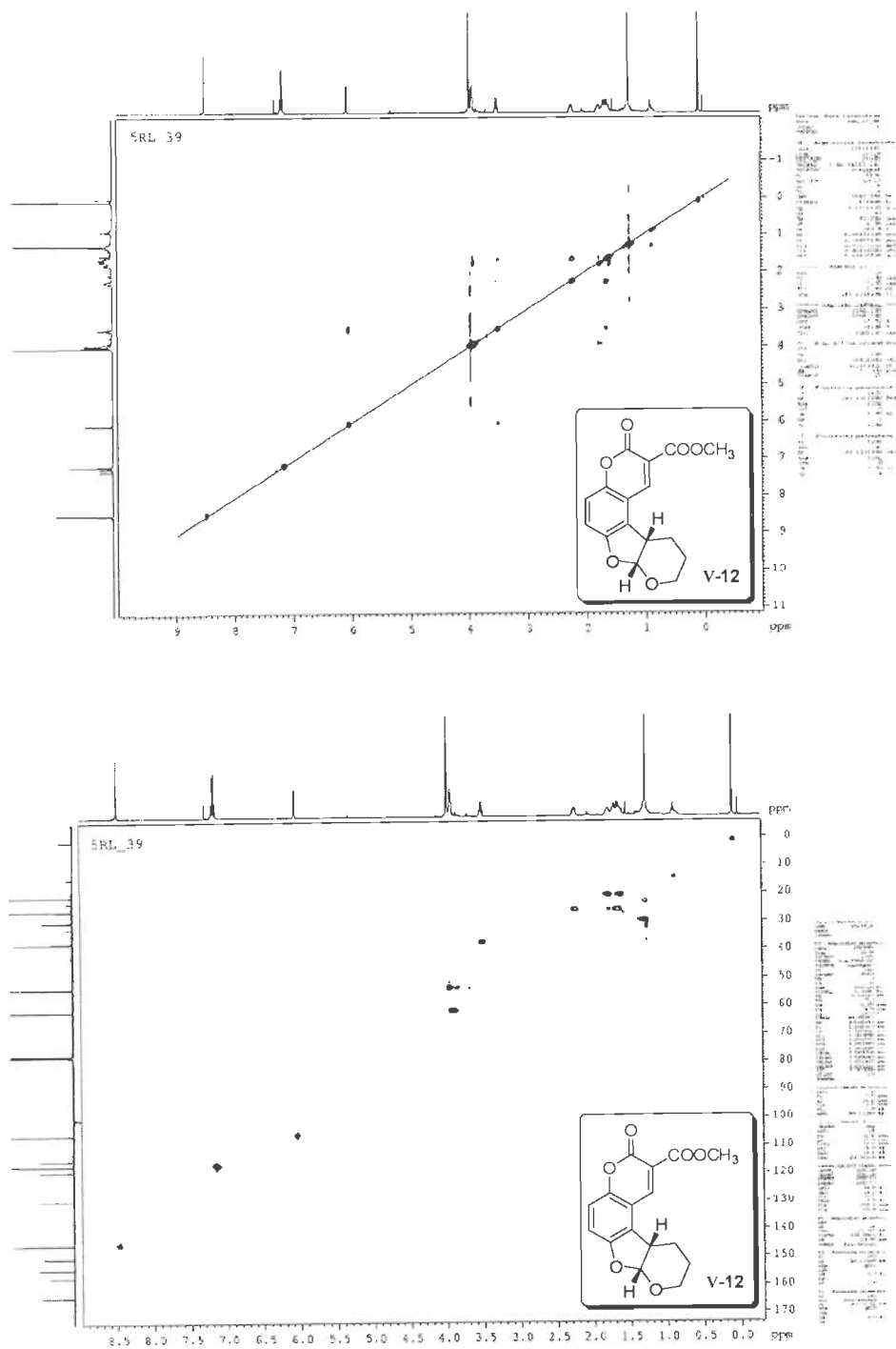


Figure 6: ^1H - ^1H and ^1H - ^{13}C (HSQC) COSY spectra of V-12.

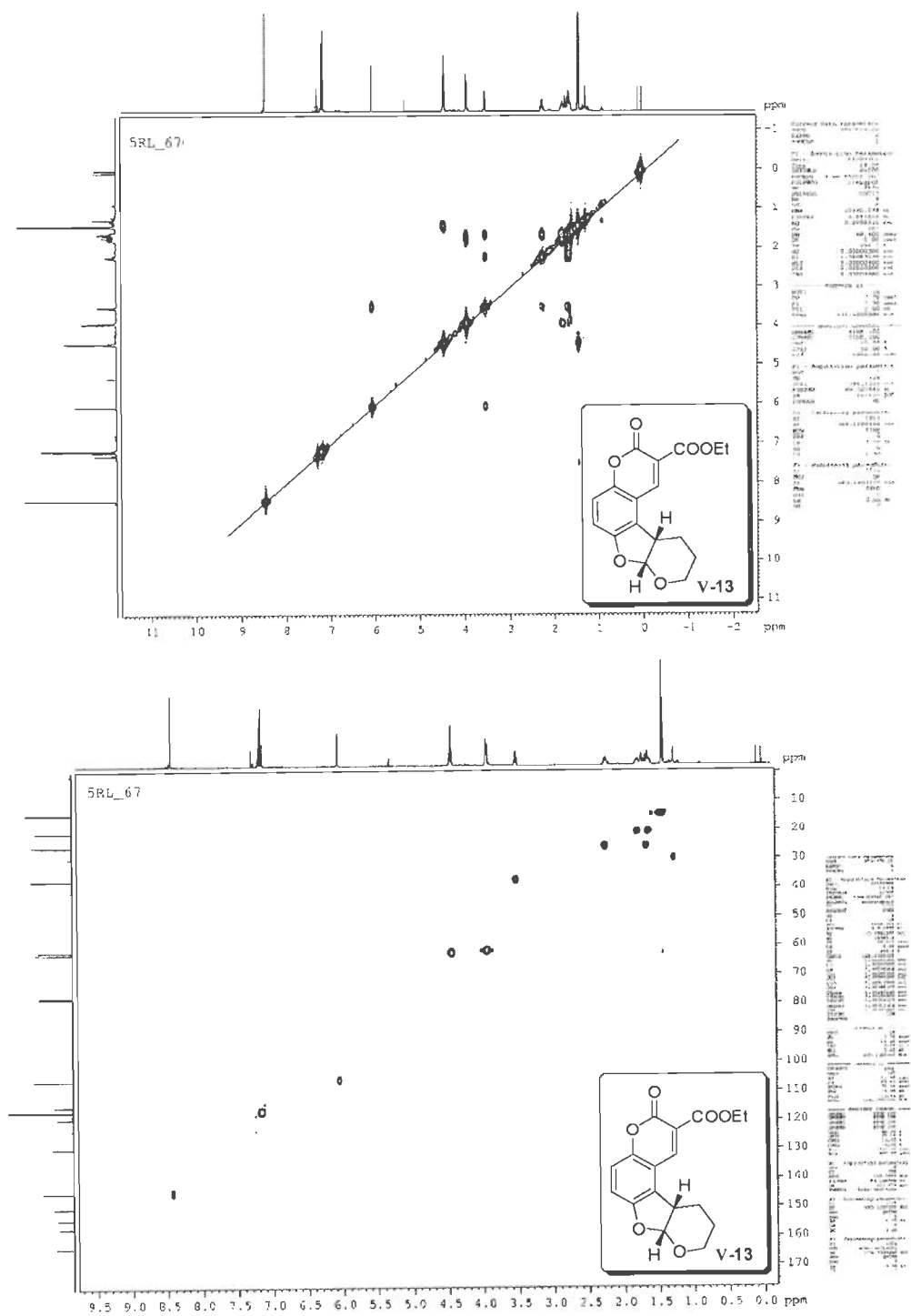


Figure 7: ^1H - ^1H and ^1H - ^{13}C (HSQC) COSY spectra of V-13.

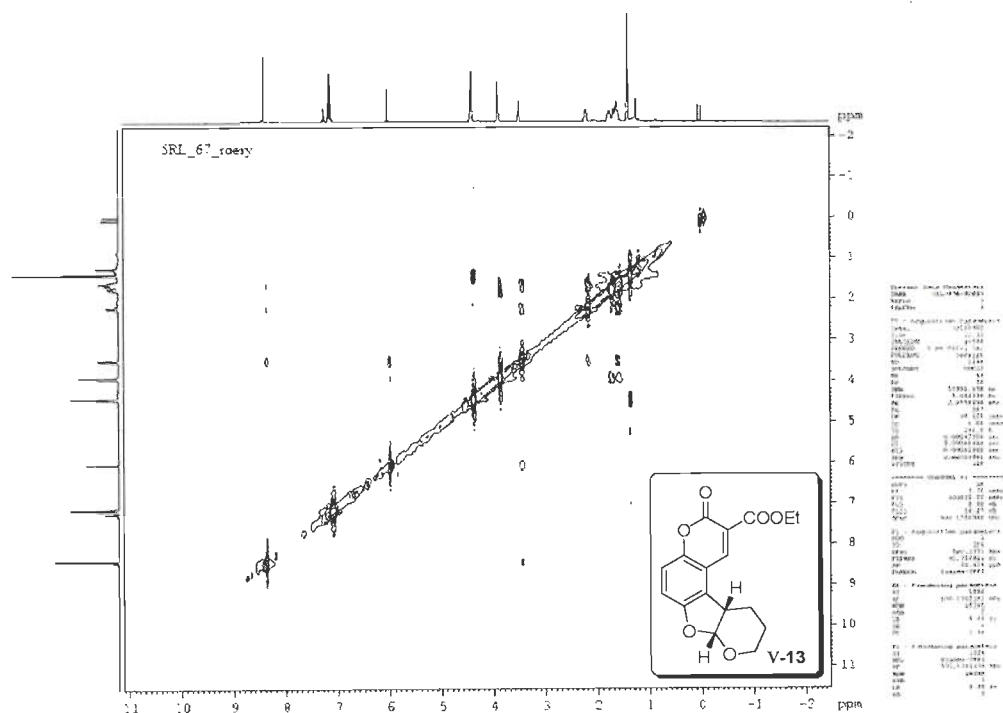
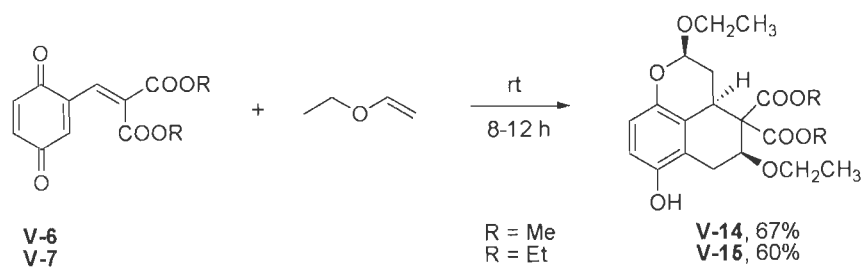


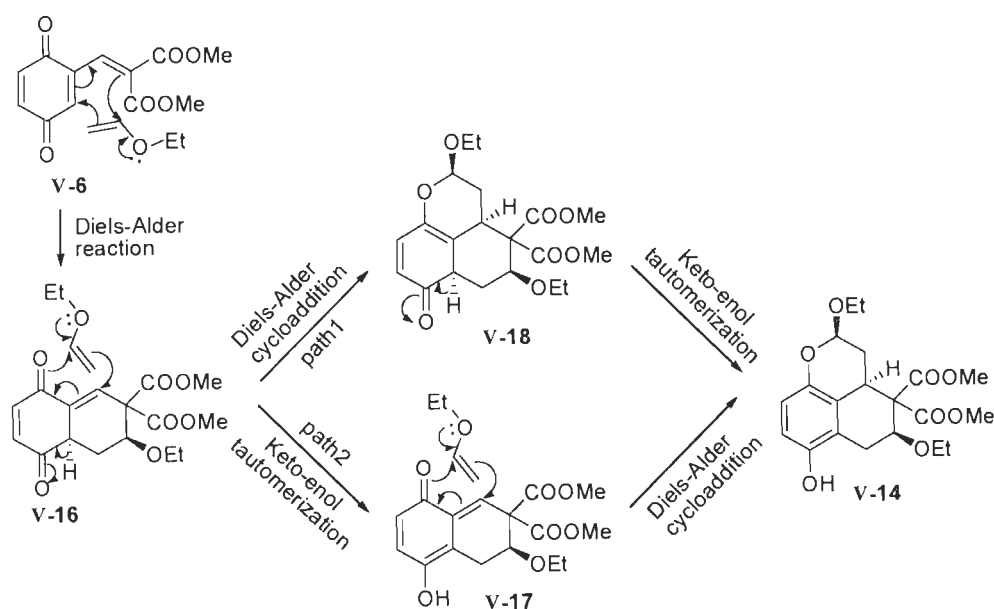
Figure 8: 500 MHz ROESY spectrum of **V-13** in CDCl_3 .

Encouraged by the results from the domino reactions between alkenyl-*p*-benzoquinones **V-6** and **V-7** and cyclic enol ethers DHF and DHP, we next turned our attention on the reactions of **V-6** and **V-7** with acyclic ethyl vinyl ether. Thus, the treatment of alkenyl-*p*-benzoquinone **V-6** with excess ethyl vinyl ether under neat conditions at room temperature provided a tricyclic product **V-14** derived from double Diels-Alder reaction in a domino fashion in 67% isolated yield. The analogous reaction of **V-7** with ethyl vinyl ether was performed under similar conditions. The reaction proceeded smoothly at room temperature and reached completion in 8 h to furnish the tetrahydro-benzochromene derivative **V-15** in good yield.



Scheme 13: Domino reaction of alkenyl-*p*-benzoquinones **V-6** and **V-7** and ethyl vinyl ether.

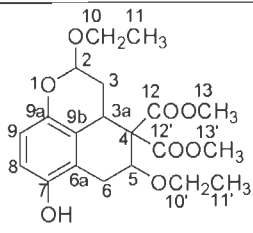
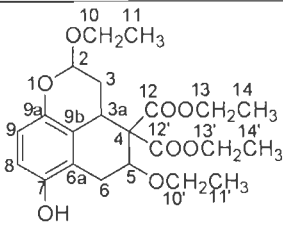
The formation of tetrahydro-benzochromene derivatives **V-14** and **V-15** can be explained based on the probable mechanism for the domino process shown in Scheme 14. The highly electron-deficient diene **V-6/V-7** undergoes inverse electron-demand Diels-Alder cycloaddition with electron-rich dienophilic ethyl vinyl ether to produce Diels-Alder adduct **V-16**. The addition of second molecule of ethyl vinyl ether to **V-16** generates the target tricyclic system **V-14/V-15** via the keto-enol tautomerization of the adduct **V-18**. Another pathway is the addition of second molecule of ethyl vinyl ether to the enol-tautomer **V-17** of **V-16** to deliver the desired product.



Scheme 14: Plausible mechanism for the formation of tetrahydro-benzochromene derivative **V-14** by a domino process.

These products **V-14** and **V-15** were thoroughly characterized by IR, NMR spectral data. The ^1H - ^1H COSY and ^1H - ^{13}C COSY experiments were carried out for these compounds in CDCl_3 to identify the protons that are coupled with each other and the connectivity between protons and carbons, respectively (Table 5, Figures 9 and 10). The 2D COSY experiments indicated the *cis*-geometry of H-2 and H-3a; and H-3a and H-5.

Table 5: Spectral data for tricyclic compounds V-14 and V-15.

Position	 V-14		 V-15	
	δ_{H} (ppm) (multiplicity)	δ_{C} (ppm)	δ_{H} (ppm) (multiplicity)	δ_{C} (ppm)
C-2	5.09 (dd, $J = 2.5, 9.5$ Hz)	100.4	5.08 (dd, $J = 2.5, 9.5$ Hz)	100.4
C-3	2.39 (dt, $J = 9.5, 13.0$ Hz), 2.04 (qd, $J = 2.5, 13.0$ Hz)	30.4	2.40 (dt, $J = 9.5, 12.5$ Hz), 2.06 (qd, $J = 2.5, 12.5$ Hz)	30.4
C-3a	3.59-3.50 (m)	39.9	3.57-3.48 (m)	39.8
C-5	4.15 (dd, $J = 6.5, 10.0$ Hz)	79.6	4.17-4.10 (m)	79.8
C-6	3.20 (dd, $J = 6.5, 17.0$ Hz), 2.89 (dd, $J = 10.5, 17.5$ Hz)	28.5	3.18 (dd, $J = 6.5, 17.0$ Hz), 2.91 (dd, $J = 10.0, 17.0$ Hz)	28.6
C-8	6.57 (dd, $J = 8.5, 17.0$ Hz)	114.6	6.55 (AB quartet, $J = 8.5, 11.5$ Hz)	114.4
C-9	6.57 (dd, $J = 8.5, 17.0$ Hz)	114.4	6.55 (AB quartet, $J = 8.5, 11.5$ Hz)	114.3
C-10	3.68-3.64 (m), 4.10-4.03 (m)	64.5	3.68-3.61 (m), 4.09-4.02 (m)	64.6
C-11	1.28 (t, $J = 7.0$ Hz)	15.2	1.33-1.25 (m)	15.4
C-10'	3.59-3.50 (m), 3.79-3.73 (m)	61.1	3.79-3.71 (m), 3.57-3.48 (m)	66.1
C-11'	1.20 (t, $J = 7.0$ Hz)	15.5	1.18 (t, $J = 7.0$ Hz)	15.2
C-13	3.82 (s)	52.9	4.17-4.10 (m), 4.09-4.02 (m)	60.9
C-13'	3.62 (s)	52.1	4.34-4.22 (m)	62.0
C-14	-	-	1.33-1.25 (m)	15.2
C-14'	-	-	1.08 (t, $J = 7.0$ Hz)	13.8

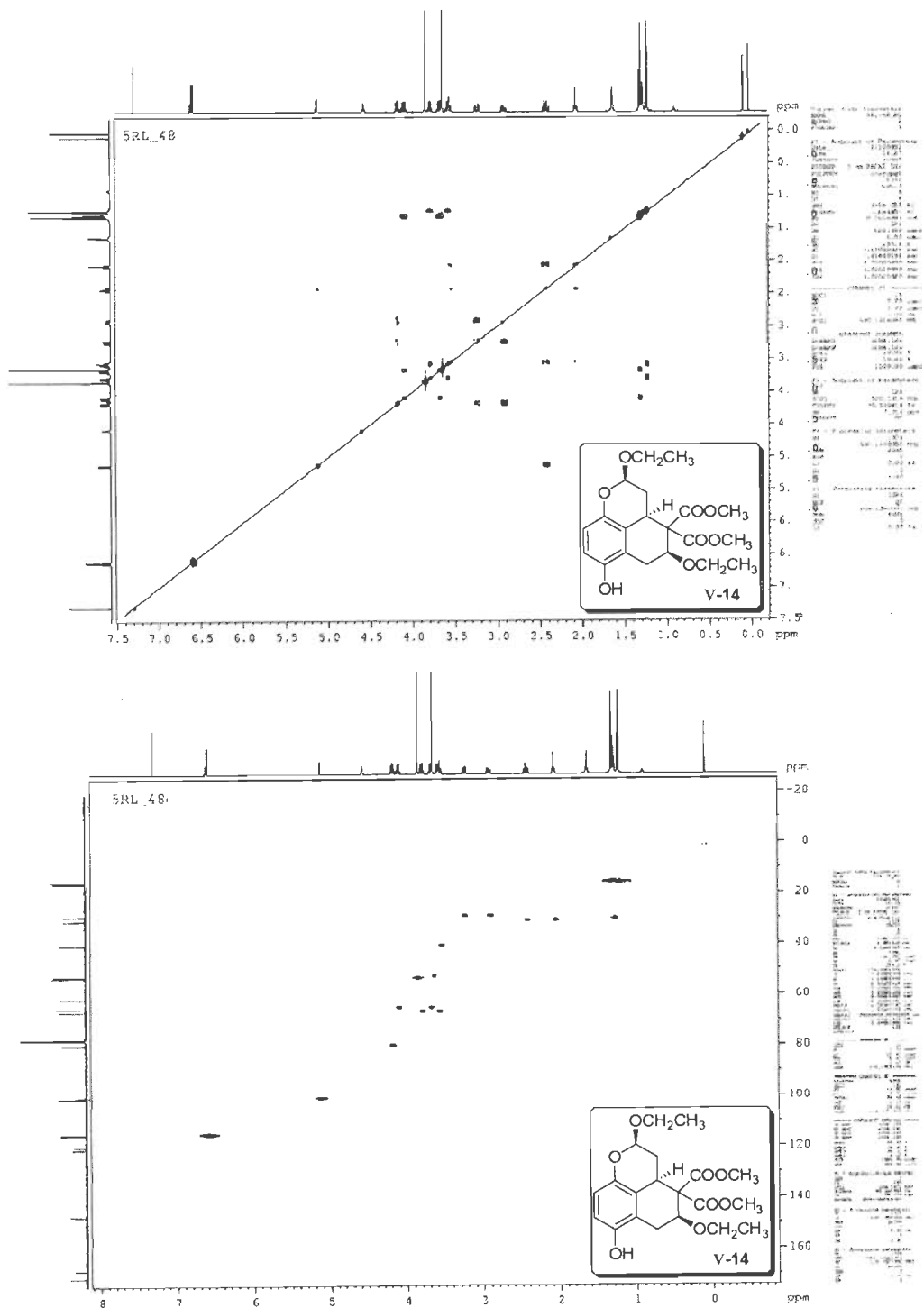
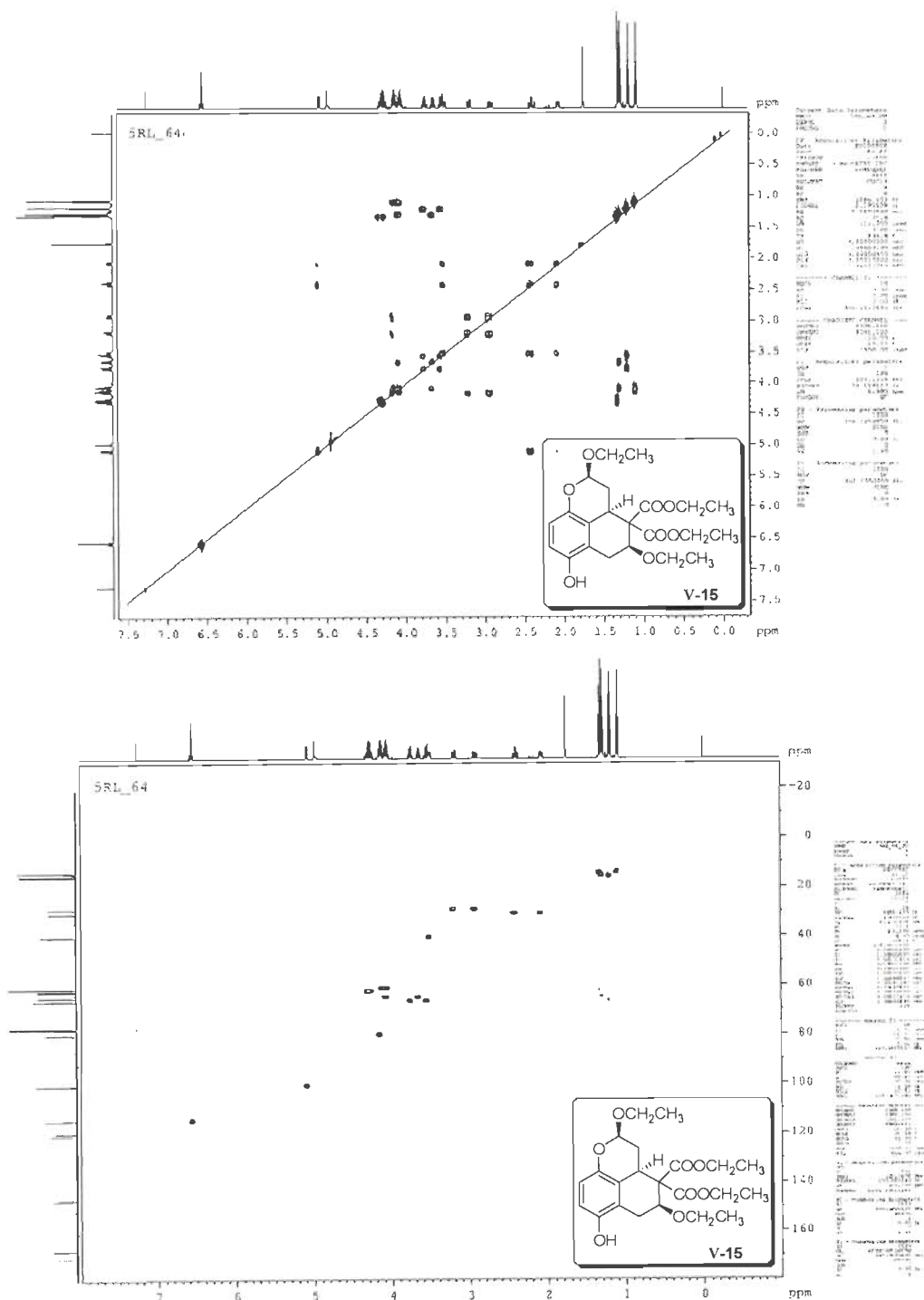


Figure 9: ^1H - ^1H and ^1H - ^{13}C (HSQC) COSY spectra of V-14.

Figure 10: ^1H - ^1H and ^1H - ^{13}C (HSQC) COSY spectra of V-15.

After studying the domino processes of alkenyl-*p*-benzoquinones with cyclic and acyclic enol ethers, we became interested to assess their reactivity with five-membered oxygen heterocycles. Accordingly, the reaction of alkenyl-*p*-benzoquinone **V-7** with 2-methylfuran was tested under neat conditions at room temperature. After usual isolation (*vide supra*) a yellowish solid was obtained in its pure form. The IR spectrum of this compound reveals the presence of hydroxy, ketonic and ester carbonyls, ether functional groups. After careful analysis of its ^1H and ^{13}C NMR and DEPT spectral data it was found to be a nonacyclic compound derived from the addition of two molecules of *p*-benzoquinone derivative **V-7** and three molecules of methylfuran. The ^1H NMR reveals the presence of seven methyl groups in five sets. These signals are centered at δ 1.66 (CH_3), 1.59 (CH_3), 1.56 (CH_3), 1.32 (2 CH_3) and 1.19 (2 CH_3) ppm; the former three are of methyl group bearing allylic proton and the latter two are of ethyl moiety. The signals of four methylenes of ethyl groups appeared as a multiplet at δ 4.40-4.15 ppm. The phenolic hydroxy proton resonates at δ 5.94 ppm. The analysis of ^{13}C NMR and DEPT spectra confirms the presence of seven methyl carbons and four methylene carbons. Further, the appearance of 16 methyne carbons and 16 quaternary carbons in ^{13}C NMR spectrum confirms the presence of 43 carbon atoms in all in the molecule. Based on these spectral data and the reactivity pattern of the dienic alkenyl-*p*-benzoquinone **V-7** and dienophilic 2-methylfuran the isomeric structure **V-19a** or **V-19b** is tentatively assigned for this polycyclic adduct out of which the former is most likely structure (Figure 11). The exact structure and relative stereochemistry await confirmation.

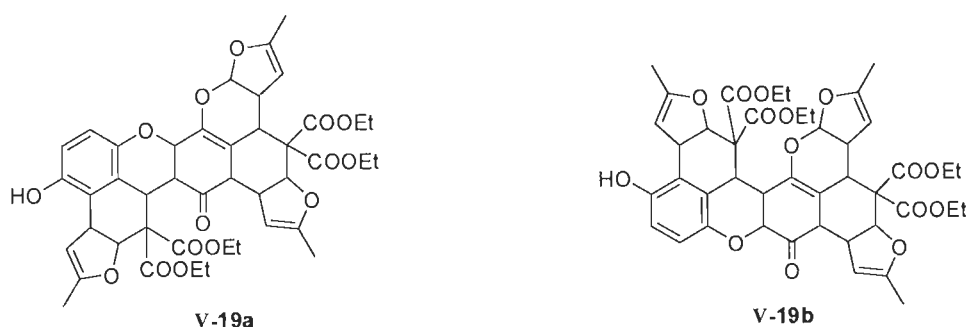
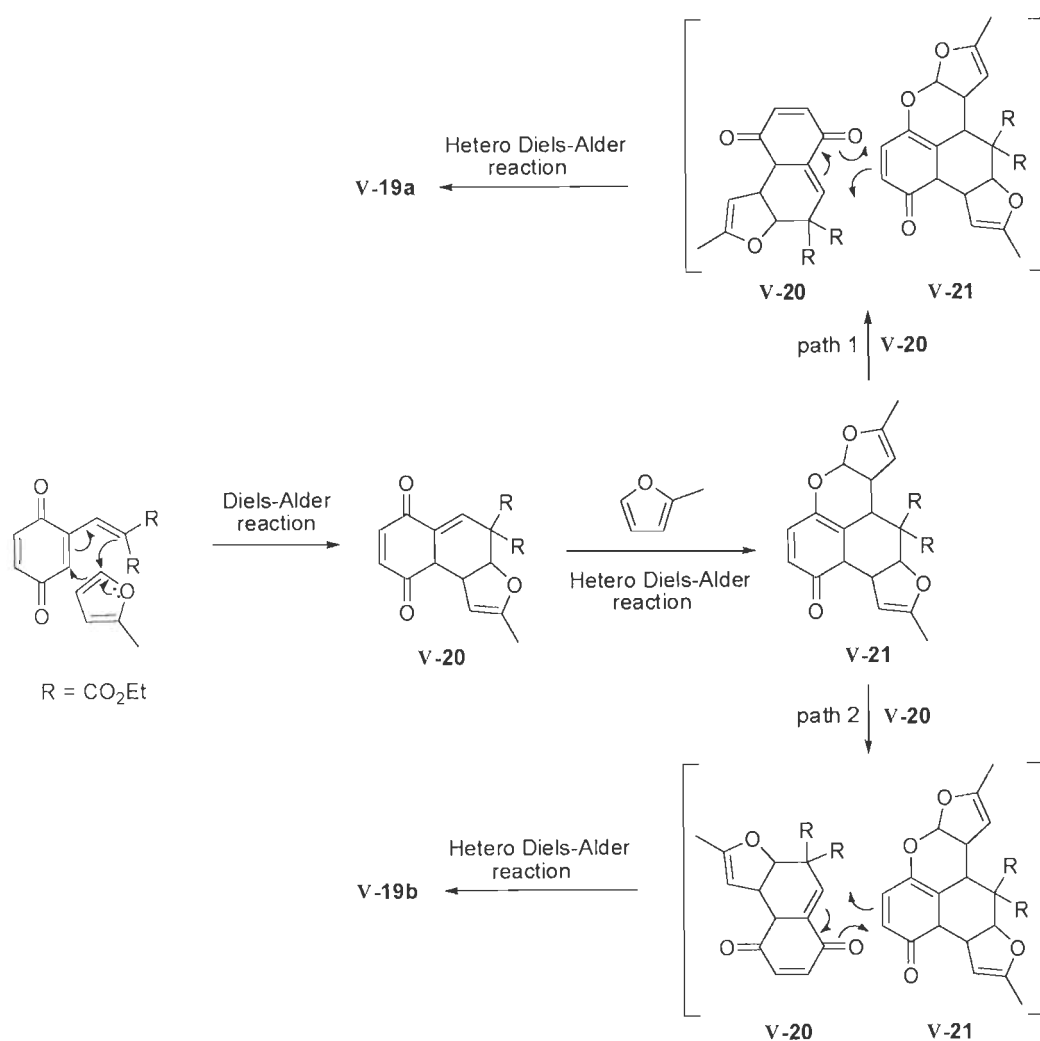


Figure 11: Structures of isomeric nonacyclic systems **V-19a** and **V-19b**.

The plausible sequence of the domino process that resulted in the formation of the adduct **V-19** is depicted in Scheme 15. The initial Diels-Alder reaction between alkenyl-*p*-benzo-

quinone **V-7** and 2-methylfuran produces the cycloadduct **V-20**. The Diels-Alder reaction between heterodiene **V-20** and 2-methylfuran provides the pentacyclic adduct **V-21**. The hetero Diels-Alder reaction between the in situ generated hetero diene **V-20** and pentacyclic enone **V-21**, in a convergent route, enables the formation of final nonacyclic system **V-19**.

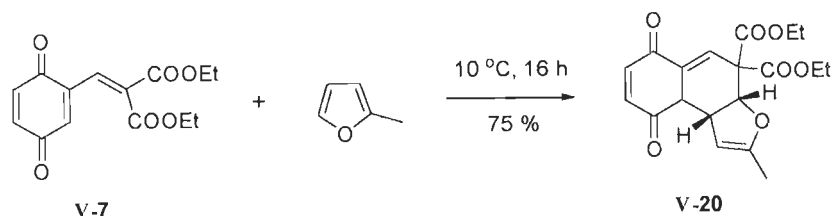
The current one-pot and three-step protocol afforded 62% yield of the polycycle **V-19** with 85% average yield per step. This remarkable, highly efficient and convergent synthesis of the nonacyclic system demonstrates the great power of domino process in the rapid construction



Scheme 15: The triple Diels-Alder cycloaddition domino process in the formation of nonacyclic adduct **V-19**.

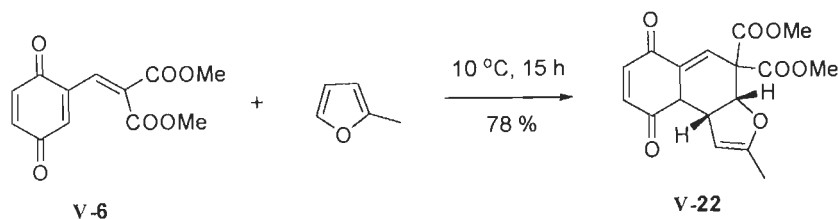
of molecular complexity in a concise fashion; indeed, the domino process described herein enabled the formation of nine rings, six carbon–carbon bonds, two carbon–oxygen bonds and eleven new stereogenic centers in just three steps. *In fact we have isolated a single diastereomer from the possible 1024 diastereomers; or a pair of enantiomers out of possible 2048 stereoisomers!*

We envisioned that by lowering the reaction temperature, the reactivity between alkenyl-*p*-benzoquinone **V-7**, 2-methylfuran and/or the initially formed mono-adduct can be lowered. Thus the reaction between **V-7** and 2-methylfuran was tested at 10 °C under neat conditions. Delightfully, a 1:1 Diels-Alder cycloadduct **V-20** derived from **V-7** and 2-methylfuran was isolated in 75% yield after 16 h (Scheme 16).



Scheme 16: The Diels-Alder cycloaddition between alkenyl-*p*-benzoquinone **V-7** and 2-methylfuran.

The reaction between alkenyl-*p*-benzoquinone **V-6** and 2-methylfuran was also performed at 10 °C under neat conditions. Again, the Diels-Alder cycloadduct **V-22** derived from 1:1 addition of **V-6** and 2-methylfuran was isolated in 78% yield. The *cis*-geometry of the hydrogens present on the five-membered ring junction of [4+2] adducts **V-29** and **V-22** is confirmed on the basis of low coupling constants of these protons in ^1H NMR (Scheme 17).



Scheme 17: The Diels-Alder cycloaddition between alkenyl-*p*-benzoquinone **V-6** and 2-methylfuran.

5.4. CONCLUSION

We have synthesized alkenyl-1,4-benzoquinones and evaluated their reactivity with several electron-rich cyclic and acyclic enol ethers. These reactions provided products from diversified pathways based on the nature of the reacting partners and reaction conditions. However, a single diastereomeric product was isolated in each case although *a priori* many modes of cycloadditions are possible showing that the domino process is highly selective. The chemical yields of these one-pot reactions are noteworthy. The domino processes presented herein furnished the products of molecular complexity with impressive stereocontrol. Thus alkenyl-*p*-benzoquinones have been used as simple starting materials for the domino processes that generated polycyclic products with a plethora of functional groups.

5.5. EXPERIMENTAL

5.5.1. General

All reagents were purchased at the highest commercial quality and used without further purification. Solvents were purified by standard methods. Reactions were monitored by thin-layer chromatography (TLC) carried out on 0.25 mm E. Merck silica gel plates (60F-254) using UV light as visualizing agent and/or iodine as developing agent. Melting points are uncorrected. IR spectra of the compounds were recorded on a Thermo Nicolet FT-IR Nexus™ and are expressed as wavenumbers (cm^{-1}). ^1H NMR (500.13 MHz) and ^{13}C NMR (125.76 MHz) spectra were recorded on Bruker AMX-500 instrument. The following abbreviations were used to explain the multiplicities: s = singlet, d = doublet, t = triplet, q = quartet, m = multiplet, b = broad.

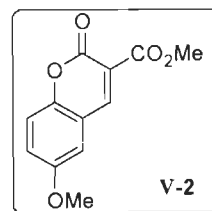
Methyl 6-methoxycoumarin-3-carboxylate (V-2):

To a solution of *p*-methoxysalicylaldehyde (5.0 g, 30 mM) in toluene was added dimethyl malonate (4.13 mL, 36 mM), piperidine (1.7 mL), glacial acetic acid (1.8 mL, 36 mM) successively. The reaction flask was fitted with a Dean-Stark trap and solution was refluxed overnight. After completion of the reaction, the excess toluene was evaporated under reduced pressure then the residue was diluted with ether and washed successively with saturated NaHCO_3 , brine solution and water. The organic layer was dried over anhyd. Na_2SO_4 , concentrated under reduced pressure and the crude mixture was subjected to silica gel column chromatography, EtOAc/hexanes (10:90-20:80) to obtain pure product **V-4** as light yellow solid.

IR (KBr) ν_{max} : 2998, 2985, 1766, 1735, 1728, 1259, 1020, 835, 738, 717 cm^{-1} .

^1H NMR (CDCl_3 , 500 MHz): δ 3.87 (s, 3H), 3.96 (s, 3H), 7.03 (s, 1H), 7.24 (d, $J = 4.5$ Hz, 1H), 7.31 (d, $J = 5.0$ Hz, 1H), 8.53 (s, 1H).

^{13}C NMR (CDCl_3 , 125 MHz): δ 163.8 (C), 156.9 (C), 156.3 (C), 149.8 (C), 149.0 (CH), 122.8 (CH), 118.1 (CH), 117.9 (CH), 110.6 (CH), 55.9 (CH_3), 52.9 (CH_3).



Dimethyl 2-(2,5-dimethoxybenzylidene)malonate (V-4):

Compound **V-4** was synthesized from *p*-methoxysalicylaldehyde (5.0 g, 30 mM) and dimethyl malonate (4.13 mL, 36 mM) following the procedure described for the synthesis of compound **V-2**.

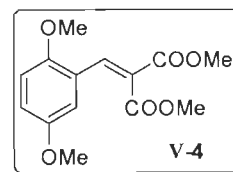
Time: 10 h.

Yield: 7.39 g (88%) as light yellow solid.

MP: 58-60 °C.

IR (KBr) ν_{\max} : 3019, 2949, 1743, 1725, 1625, 1439, 1360, 1248, 1071, 1035, 855, 809, 736 cm^{-1} .

^1H NMR (CDCl_3 , 500 MHz): δ 8.08 (d, $J = 4.0$ Hz, 1H), 6.96-6.89 (m, 2H), 6.84 (dd, $J = 3.5, 8.0$ Hz, 1H), 3.87-3.84 (m, 3H), 3.83-3.78 (m, 6H), 3.76-3.72 (m, 3H) ppm.



^{13}C NMR (CDCl_3 , 125 MHz): δ 167.0 (C), 164.6 (C), 153.1 (C), 152.4 (C), 138.6 (CH), 125.3 (C), 122.4 (C), 117.8 (CH), 113.5 (CH), 111.9 (CH), 55.9 (CH_3), 55.6 (CH_3), 52.4 (CH_3), 52.4 (CH_3).

Diethyl 2-(2,5-dimethoxybenzylidene)malonate (V-5):

Compound **V-5** was synthesized from *p*-methoxysalicylaldehyde (5 g, 30 mM) and diethyl malonate (5.81 mL, 36 mM) following the procedure described for the synthesis of compound **V-2**.

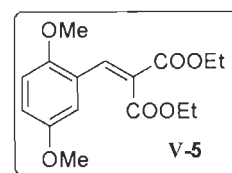
Time: 9 h.

Yield: 8.31 g (90%) as light yellow solid.

MP: 60-62 °C.

IR (KBr) ν_{\max} : 3060, 2991, 1766, 1625, 1459, 1365, 1245, 1085, 947, 917, 821 cm^{-1} .

^1H NMR (CDCl_3 , 500 MHz): δ 8.04 (s, 1H), 6.96 (d, $J = 3.0$ Hz, 1H),



6.91 (dd, $J = 3.0, 8.5$ Hz, 1H), 6.82 (d, $J = 9.0$ Hz, 1H), 4.32-4.25 (m, 4H), 3.81- 3.79 (m, 3H), 3.73-3.71 (m, 3H), 1.32 (t, $J = 7.0$ Hz, 3H), 1.25 (t, $J = 7.0$ Hz, 3H) ppm

^{13}C NMR (CDCl_3 , 125 MHz): δ 166.7 (C), 164.2 (C), 153.1, (C), 152.4 (C), 137.8 (CH), 126.2 (C), 122.5 (C), 117.5 (CH), 113.8 (CH), 111.9 (CH), 61.4 (CH_2), 61.4 (CH_2), 55.9 (CH_3), 55.6 (CH_3), 14.1 (CH_3), 13.8 (CH_3) ppm

Dimethyl 2-[(3,6-dioxocyclohexa-1,4-dienyl)methylene]malonate (V-6):

A solution of ceric ammonium nitrate (14.65 g, 26.7 mM) in CH_3CN (15 mL) and H_2O (15 mL) was poured into a solution of compound V-4 (3 g, 10.7 mM) in CH_3CN (30 mL) with rapid stirring. The colour changed rapidly from orange to red. After 20 min, brine solution was added and the organic layer was separated. The aqueous layer was extracted with chloroform. The combined organic layer was concentrated under reduced pressure and the residue was dissolved in chloroform. The chloroform solution was washed with water to remove inorganic salts. The organic layer was dried over anhyd. Na_2SO_4 , concentrated under reduced pressure. The residue was purified by silica gel chromatography using EtOAc/hexanes (20:80-50:50) to afford pure product V-6.

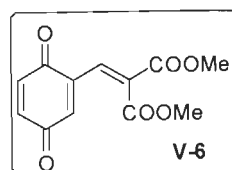
Time: 20 min.

Yield: 2.45 g (92%) as brown dense liquid.

IR (KBr) ν_{max} : 2984, 2943, 1727, 1624, 1496, 1381, 1235, 1062, 877, 810, 709 cm^{-1} .

^1H NMR (CDCl_3 , 500 MHz): δ 7.65 (s, 1H), 6.89-6.81 (m, 3H), 3.89 (s, 3H), 3.86 (s, 3H) ppm

^{13}C NMR (CDCl_3 , 125 MHz): δ 185.4 (C), 184.2 (C), 165.3, (C), 163.6 (C), 136.2 (CH), 136.0 (CH), 133.0 (CH), 132.4 (CH), 13.8 (CH_3), 13.7 (CH_3) ppm



Diethyl 2-[(3,6-dioxocyclohexa-1,4-dienyl)methylene]malonate (V-7):

Compound V-7 was synthesized from V-5 (3 g, 9.7 mM) in CH_3CN (30 mL) was added ceric ammonium nitrate (14.65 g, 26.7 mM) in CH_3CN (15 mL) and H_2O (15 mL) following the procedure described for the synthesis of compound V-6.

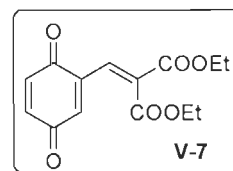
Time: 20 min.

Yield: 2.50 g (93%) as brown dense liquid.

IR (KBr) ν_{max} : 2980, 2945, 1730, 1628, 1489, 1378, 1230, 1065, 875, 796 cm^{-1} .

^1H NMR (CDCl_3 , 500 MHz): δ 7.61 (d, $J = 1.5$ Hz, 1H), 6.90-6.81 (m, 3H), 4.36-4.30 (m, 4H), 1.38-1.30 (m, 6H) ppm.

^{13}C NMR (CDCl_3 , 125 MHz): δ 186.4 (C), 184.6 (C), 164.3, (C), 162.6 (C), 136.7 (CH), 136.4 (CH), 133.6 (CH), 132.6 (CH), 62.1 (CH_2), 61.9 (CH_2), 13.9 (CH_3), 13.8 (CH_3) ppm.



Furo-furocoumarin derivative V-8:

A mixture of DHF (1.5 mL) and alkenyl-*p*-benzoquinone **V-6** (200 mg, 0.8 mM) was stirred at room temperature for 10 h. Then about 5 mL of hexane was added to the reaction mixture and the flask was kept at 0 °C for 2 h. During this period a solid was formed and it was filtered to afford pure product **V-8**.

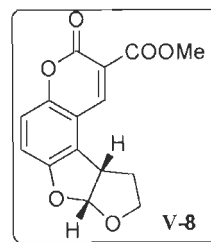
Time: 10 h.

Yield: 161 mg (70%) as yellow solid.

MP: 208-210 °C.

IR (KBr) ν_{max} : 3060, 2991, 1766, 1625, 1571, 1459, 1365, 1245, 1085, 1025, 947, 821 cm^{-1} .

^1H NMR (CDCl_3 , 500 MHz): δ 8.57 (s, 1H), 7.17 (AB quartet, $J = 8.5$, 43.5 Hz, 2H), 6.52 (d, $J = 6.0$ Hz, 1H), 4.27 (dd, $J = 6.0$, 9.0 Hz, 1H), 4.21 (t, $J = 8.0$ Hz, 1H), 4.00 (s, 3H), 3.71 (ddd, $J = 5.0$, 9.0, 14.0 Hz, 1H), 2.54-2.44 (m, 1H), 2.13 (dd, $J = 4.5$, 12.0 Hz, 1H) ppm.



^{13}C NMR (CDCl_3 , 125 MHz): δ 163.9 (C), 156.5 (C), 155.9 (C), 150.3, (C), 144.6 (CH), 125.0 (C), 118.8 (C), 117.1 (CH), 115.8 (CH), 114.5 (C), 112.3 (CH), 67.3 (CH_2), 53.1 (CH_3), 45.6 (CH), 33.3 (CH_2) ppm.

Furo-furocoumarin derivative V-11:

The compound **V-11** was synthesized from DHF (1.5 mL) alkenyl-*p*-benzoquinone **V-7** (200 mg, 0.8 mM) at room temperature following the procedure described for the synthesis of compound **V-8**.

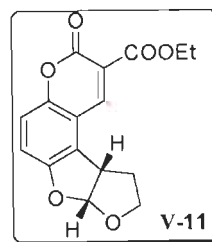
Time: 9 h.

Yield: 154 mg (71%) as yellow solid.

MP: 152-154 °C.

IR (KBr) ν_{\max} : 2991, 2921, 1713, 1669, 1469, 1330, 1243, 1091, 917, 896, 813 cm^{-1} .

^1H NMR (CDCl_3 , 500 MHz): δ 8.50 (s, 1H), 7.13 (AB quartet, $J = 9.0$, 46.0 Hz, 2H), 6.49 (d, $J = 5.5$ Hz, 1H), 4.44 (q, $J = 7.0$ Hz, 2H), 4.24 (dd, $J = 5.5$, 9.0 Hz, 1H), 4.18 (t, $J = 8.5$ Hz, 1H), 3.68 (ddd, $J = 5.0$, 9.0, 14.0 Hz, 1H), 2.50-2.40 (m, 1H), 2.10 (dd, $J = 5.0$, 12.5 Hz, 1H), 1.42 (t, $J = 7.0$ Hz, 3H) ppm



^{13}C NMR (CDCl_3 , 125 MHz): δ 163.1 (C), 156.3 (C), 155.7 (C), 150.1 (C), 143.8 (CH), 124.9 (C), 119.0 (C), 116.8 (CH), 115.4 (CH), 114.4 (C), 112.2 (CH), 67.2 (CH_2), 62.0 (CH_2), 45.4 (CH), 33.1 (CH_2), 14.1 (CH_3) ppm

Pyrano-furocoumarin derivative V-12:

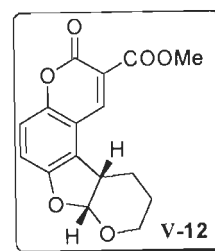
This compound was synthesized from DHP (2 mL) and alkenyl-*p*-benzoquinone **V-6** (250 mg, 1.0 mM) at room temperature following the procedure described for the synthesis of compound **V-8**.

Time: 12 h.

Yield: 202 mg (67%) as yellow solid.

MP: 124-126 °C.

IR (KBr) ν_{\max} : 3012, 2947, 1731, 1684, 1621, 1442, 1261, 1120, 1072, 941, 821, 725 cm^{-1} .



^1H NMR (CDCl_3 , 500 MHz): δ 8.49 (s, 1H), 7.18 (AB quartet, $J = 9.0$, 18.0 Hz, 2H), 6.06 (d, $J = 6.0$ Hz, 1H), 3.99 (s, 3H), 3.96-3.91 (m, 2H), 3.52 (q, $J = 7.0$ Hz, 1H), 2.28-2.21 (m, 1H),

1.84-1.74 (m, 1H), 1.71-1.60 (m, 2H) ppm.

^{13}C NMR (CDCl_3 , 125 MHz): δ 163.7 (C), 156.5 (C), 153.6 (C), 149.7, (C), 144.8 (CH), 129.0 (C), 118.4 (C), 116.4 (CH), 116.3 (CH), 114.5 (C), 105.5 (CH), 61.2 (CH_2), 52.9 (CH_3), 37.0 (CH), 25.4 (CH_2), 20.4 (CH_2) ppm.

Pyrano-furocoumarin derivative V-13:

This compound was prepared from DHP (2 mL) and alkenyl-*p*-benzoquinone V-7 (250 mg, 0.9 mM) at room temperature following the procedure described for the synthesis of compound V-8.

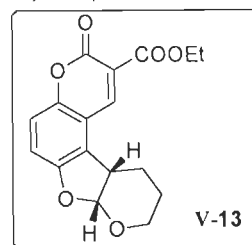
Time: 9 h.

Yield: 183 mg (65%) as yellow solid.

MP: 146-148 °C.

IR (KBr) ν_{max} : 3020, 2952, 1726, 1622, 1460, 1363, 1270, 1186, 1017, 920, 839, 789 cm^{-1} .

^1H NMR (CDCl_3 , 500 MHz): δ 8.43 (s, 1H), 7.16 (AB quartet, $J = 8.5$, 19.0 Hz, 2H), 6.05 (d, $J = 6.5$ Hz, 1H), 4.47-4.41 (m, 2H), 3.95-3.90 (m, 2H), 3.51 (q, $J = 7.0$ Hz, 1H), 2.28-2.20 (m, 1H), 1.83-1.75 (m, 1H), 1.70-1.58 (m, 2H), 1.43 (t, $J = 7.0$ Hz, 3H) ppm.



^{13}C NMR (CDCl_3 , 125 MHz): δ 163.3 (C), 156.6 (C), 153.7 (C), 153.6 (C), 149.7, (C), 144.4 (CH), 129.0 (C), 118.9 (C), 116.3 (CH), 114.7 (C), 105.6 (CH), 62.1 (CH_2), 61.3 (CH_2), 37.1 (CH), 25.5 (CH_2), 20.5 (CH_2), 14.2 (CH_3) ppm.

Dimethyl 2,5-diethoxy-7-hydroxy-3,3a,5,6-tetrahydrobenzo[de]chromene-4,4(2H) dicarboxylate (V-14):

This compound was synthesized from ethyl vinyl ether (2 mL) and alkenyl-*p*-benzoquinone V-6 (250 mg, 1.0 mM) at room temperature following the procedure described for the synthesis of compound V-8.

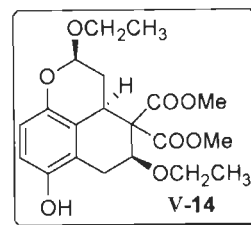
Time: 12 h.

Yield: 274 mg (67%) as cream white solid.

MP: 216-220 °C.

IR (KBr) ν_{\max} : 3464, 2985, 1735, 1610, 1459, 1339, 1250, 1148, 1073, 930, 888, 810 cm^{-1} .

^1H NMR (CDCl_3 , 500 MHz): δ 6.57 (dd, $J = 8.5, 17.0$ Hz, 2H), 5.09 (dd, $J = 2.5, 9.5$ Hz, 1H), 4.50 (s, 1H), 4.15 (dd, $J = 6.5, 10.0$ Hz, 1H), 4.10-4.03 (m, 1H), 3.82 (s, 3H), 3.79-3.73 (m, 1H), 3.68-3.64 (m, 1H), 3.62 (s, 3H), 3.59-3.50 (m, 2H), 3.20 (dd, $J = 6.5, 17.0$ Hz, 1H), 2.89 (dd, $J = 10.5, 17.5$ Hz, 1H), 2.39 (dt, $J = 9.5, 13.0$ Hz, 1H), 2.04 (qd, $J = 2.5, 13.0$ Hz, 1H), 1.28 (t, $J = 7.0$ Hz, 3H), 1.20 (t, $J = 7.0$ Hz, 3H) ppm.



^{13}C NMR (CDCl_3 , 125 MHz): δ 171.0 (C), 168.0 (C), 146.9 (C), 146.7 (C), 120.5 (C), 119.5 (C), 114.6 (CH), 114.4 (CH), 100.4 (CH), 79.6 (CH), 66.2 (CH_2), 64.5 (CH_2), 61.1 (C), 52.9 (CH_3), 52.1 (CH_3), 39.9 (CH), 30.4 (CH_2), 28.5 (CH_2), 15.5 (CH_3), 15.2 (CH_3) ppm.

Diethyl 2,5-diethoxy-7-hydroxy-3,3a,5,6-tetrahydrobenzo[de]chromene-4,4(2H)-dicarboxylate (V-15):

This compound was synthesized from ethyl vinyl ether (2 mL) and alkenyl-*p*-benzoquinone V-7 (300 mg, 1.07 mM) at room temperature following the procedure described for the synthesis of compound V-8.

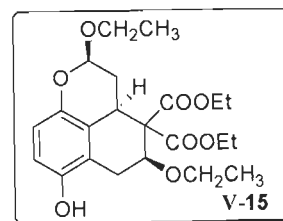
Time: 8 h.

Yield: 263 mg (60%) as cream white solid.

MP: 136-138 $^\circ\text{C}$.

IR (KBr) ν_{\max} : 3446, 2983, 1739, 1613, 1461, 1376, 1253, 1150, 1075, 939, 890, 811 cm^{-1} .

^1H NMR (CDCl_3 , 500 MHz): δ 6.55 (AB quartet, $J = 8.5, 11.5$ Hz, 2H), 5.08 (dd, $J = 2.5, 9.5$ Hz, 1H), 4.98 (s, 1H), 4.34-4.22 (m, 2H), 4.17-4.10 (m, 2H), 4.09-4.02 (m, 2H), 3.79-3.71 (m, 1H), 3.68-3.61 (m, 1H), 3.57-3.48 (m, 2H), 3.18 (dd, $J = 6.5, 17.0$ Hz, 1H), 2.91 (dd, $J = 10.0, 17.0$ Hz, 1H), 2.40 (dt, $J = 9.5, 12.5$ Hz, 1H), 2.06 (qd, $J = 2.5, 12.5$ Hz, 1H), 1.33-1.25 (m, 6H), 1.18 (t, $J = 7.0$ Hz, 3H), 1.08 (t, $J = 7.0$ Hz, 3H) ppm.



^{13}C NMR (CDCl_3 , 125 MHz): δ 170.7 (C), 167.5 (C), 147.3 (C), 146.4 (C), 120.7 (C), 119.6 (C), 114.4 (CH), 114.3 (CH), 100.4 (CH), 79.8 (CH), 66.1 (CH_2), 64.6 (CH_2), 62.0 (CH_2), 60.9 (CH_2), 39.8 (CH), 30.4 (CH_2), 28.6 (CH_2), 15.4 (CH_3), 15.2 (CH_3), 14.1 (CH_3), 13.8 (CH_3) ppm.

Nonacyclic compound V-19a:

This compound was synthesized from 2-methylfuran (2.0 mL) and alkenyl-*p*-benzoquinone **V-7** (200 mg, 0.72 mM) at room temperature following the procedure described for the synthesis of compound **V-8**.

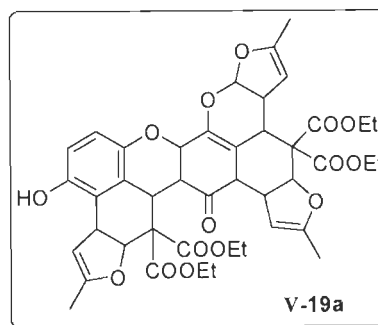
Time: 14 h.

Yield: 178 mg (62%) as yellowish solid.

MP: 152-154 °C.

IR (KBr) ν_{max} : 3446, 2983, 1739, 1613, 1461, 1376, 1345, 1303, 1253, 1150, 1074, 938, 870, 888, 735 cm^{-1} .

^1H NMR (CDCl_3 , 500 MHz): δ 7.60 (dd, $J = 1.0, 3$ Hz, 1H), 6.89 (AB quartet, $J = 10.5, 40.0$ Hz, 2H), 6.69 (dd, $J = 8.5, 10.0$ Hz, 2H), 6.11 (d, $J = 8.0$ Hz, 1H), 5.94 (s, 1H), 5.75 (dd, $J = 3.5, 9.5$ Hz, 1H), 5.37 (qd, $J = 1.0, 7.5$ Hz, 1H), 5.30 (dd, $J = 2.0, 7.5$ Hz, 1H), 4.78 (q, $J = 1.5$ Hz, 1H), 4.40-4.15 (m, 10H), 4.03 (qd, $J = 6.0, 16.5$ Hz, 1H), 3.97 (qd, $J = 3.5, 14.5$ Hz, 1H), 3.85 (d, $J = 1.5$ Hz, 1H), 3.62 (q, $J = 3.0$ Hz, 1H)



1.66 (q, $J = 1.0$ Hz, 3H), 1.59 (t, $J = 1.0$ Hz, 3H), 1.56 (t, $J = 1.0$ Hz, 3H), 1.32 (q, $J = 7.0$ Hz, 6H), 1.19 (dt, $J = 3.5, 7.0$ Hz, 6H) ppm.

^{13}C NMR (CDCl_3 , 125 MHz): δ 193.9 (C), 183.1 (C), 170.6 (C), 170.3 (C), 167.7 (C), 166.7 (C), 160.9 (C), 158.4 (C), 156.3 (C), 150.0 (C), 146.5 (C), 142.4 (CH), 141.4 (CH), 136.6 (CH), 132.5 (C), 122.0 (C), 120.9 (C), 118.7 (CH), 115.2 (CH), 97.4 (CH), 96.3 (CH), 94.4 (CH), 82.7 (CH), 81.1 (CH), 80.7 (CH), 77.7 (CH), 62.6 (CH_2), 62.1 (CH_2), 61.8 (CH_2), 61.8 (CH_2), 58.9 (C), 56.1 (C), 47.7 (CH), 47.6 (CH), 46.3 (CH), 34.9 (CH), 14.1 (CH_3), 14.0 (CH_3), 14.0 (CH_3), 13.8 (CH_3), 13.7 (CH_3), 13.3 (CH_3), 13.3 (CH_3) ppm.

Diethyl 2-methyl-6,9-dioxo-9,9a-dihydronaphtho[1,2-*b*]furan-4,4(3a*H*,6*H*,9*bH*)-dicarboxylate (V-20):

A mixture of 2-methylfuran (2.0 mL) and alkenyl-*p*-benzoquinone **V-7** (300 mg, 1.07 mM) was stirred at 10 °C for 16 h. Then about 5 mL of hexane was added to the reaction mixture and the

flask was kept at 0 °C for 2 h. During this period a solid was formed and it was filtered to afford pure product **V-20**.

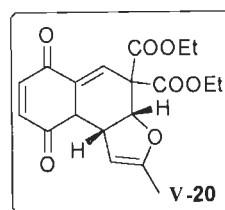
Time: 16 h.

Yield: 288 mg (75%) as yellow solid.

MP: 202-204 °C.

IR (KBr) ν_{max} : 2978, 2930, 1727, 1681, 1614, 1465, 1319, 1251, 1203, 1085, 1013, 852, 730 cm^{-1} .

^1H NMR (CDCl_3 , 500 MHz): δ 7.60 (d, $J = 3.0$ Hz, 1H), 6.90 (AB quartet, $J = 10.5, 40.0$ Hz, 2H), 5.75 (dd, $J = 4.0, 10.0$ Hz, 1H), 4.37-4.26 (m, 2H), 4.25-4.17 (m, 2H), 4.16-4.14 (m, 1H), 4.04 (qd, $J = 7.0, 18.5$ Hz, 1H), 3.63 (t, $J = 3.0$ Hz, 1H), 1.59 (s, 3H), 1.32 (t, $J = 7.0$ Hz, 3H), 1.19 (t, $J = 7.0$ Hz, 3H) ppm.



^{13}C NMR (CDCl_3 , 125 MHz): δ 193.8 (C), 183.1 (C), 167.6 (C), 166.6 (C), 158.3 (C), 142.4 (CH), 141.3 (CH), 136.6 (CH), 132.4 (C), 94.3 (CH), 80.7 (CH), 62.5 (CH_2), 62.0 (CH_2), 58.8 (C), 47.6 (CH), 47.5 (CH), 14.0 (CH_3), 13.8 (CH_3), 13.2 (CH_3).

Dimethyl 2-methyl-6,9-dioxo-9,9a-dihydronaphtho[1,2-*b*]furan-4,4-(3aH,6H,9bH)-dicarboxylate (V-22):

This compound was synthesized from 2-methylfuran (2.0 mL) and alkenyl-*p*-benzoquinone **V-7** (250 mg, 1.0 mM) at 10 °C following the procedure described for the synthesis of **V-20**.

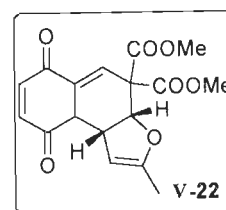
Time: 15 h.

Yield: 258 mg (78%) as yellow solid.

MP: 134-136 °C.

IR (KBr) ν_{max} : 2956, 2852, 1731, 1684, 1622, 1441, 1262, 1219, 1121, 1073, 1018, 941, 824, 725 cm^{-1} .

^1H NMR (CDCl_3 , 500 MHz): δ 7.59 (q, $J = 1.0$ Hz, 1H), 6.92 (AB quartet, $J = 10.5, 40.0$ Hz, 2H), 5.75 (dd, $J = 4.0, 10.0$ Hz, 1H), 4.24 (d, J



= 10.0 Hz, 1H), 4.12 (q, $J = 1.0$ Hz, 1H), 3.84 (s, 3H), 3.68 (s, 3H), 3.61 (t, $J = 3.5$ Hz, 1H), 1.59 (t, $J = 1.5$ Hz, 3H) ppm

^{13}C NMR (CDCl₃, 125 MHz): δ 193.7 (C), 183.0 (C), 168.1 (C), 167.1 (C), 142.3 (CH), 141.4 (CH), 136.2 (CH), 132.6 (C), 94.2 (CH), 80.6 (CH), 58.6 (C), 53.5 (CH₃), 53.1 (CH₃), 47.8 (CH), 47.4 (CH), 13.2 (CH₃).

5.6. REFERENCES

- 1 T. Ho, *Tandem Organic Reactions*, Wiley-Interscience, New York, 1992.
- 2 C. Thebtaranonth, Y. Thebtaranonth, *Cyclization Reactions*, CRC Press: Boca Raton, 1994.
- 3 L.F. Tietze, G. Brasche, K. Gericke, *Domino Reactions in Organic Synthesis*, Wiley-VCH, Weinheim, 2006.
- 4 L.F. Tietze, U. Beifuss, *Sequential Transformations in Organic Chemistry: A Synthetic Strategy with a Future*, *Angew. Chem. Int. Ed. Engl.* 105 (1993) 137.
- 5 L.F. Tietze, *Domino Reactions in Organic Synthesis*, *Chem. Rev.* 96 (1996) 115.
- 6 S.E. Denmark, A. Thorarensen, *Tandem [4+2]/[3+2] Cycloadditions of Nitroalkenes*, *Chem. Rev.* 96 (1996) 137.
- 7 J.D. Winkler, *Tandem Diels-Alder Cycloadditions in Organic Chemistry*. *Chem. Rev.* 96 (1996) 167.
- 8 K.V. Gothelf, K.A. Jørgensen, *Asymmetric 1,3-Dipolar Cycloaddition Reactions*, *Chem. Rev.* 98 (1998) 863.
- 9 K.C. Nicolaou, D.J. Edmonds, P.G. Bulger, *Cascade Reactions in Total Synthesis*, *Angew. Chem. Int. Ed.* 45 (2006) 7134.
- 10 R. Robinson, *Synthesis of Tropinone*, *J. Chem. Soc.* 111 (1917) 762.
- 11 E.J. Corey, W.E. Russey, P.R.O. de Montellano, *2,3-Oxidosqualene, an Intermediate in the Biological Synthesis of Sterols from Squalene*, *J. Am. Chem. Soc.* 88 (1966) 4750.
- 12 E.J. Corey, S.C. Virgil, *An Experimental Demonstration of the Stereochemistry of Enzymic Cyclization of 2,3-Oxidosqualene to the Protosterol System, Forerunner of Lanosterol and Cholesterol*, *J. Am. Chem. Soc.* 113 (1991) 4025.
- 13 G.D. Wilkie, G.I. Elliott, B.S.J. Blagg, S.E. Wolkenberg, D.R. Soenen, M.M. Miller, S. Pollack, D.L. Boger, *Intramolecular Diels-Alder and Tandem Intramolecular Diels-Alder/1,3-Dipolar Cycloaddition Reactions of 1,3,4-Oxadiazoles*, *J. Am. Chem. Soc.* 124 (2002) 11292.
- 14 T.V. Hansena, L. Skattebøl, *A High Yielding One-pot Method for the Preparation of Salen Ligands*, *Tetrahedron Lett.* 46 (2005) 3829.

- 15 P. Jacob III, P.S. Callery, A.T. Shulgin, Jr., N. Castagnoli, *A Convenient Synthesis of Quinones from Hydroquinone Dimethyl Ethers. Oxidative Demethylation with Ceric Ammonium Nitrate*, J. Org. Chem. 41 (1976) 3627.

NMR SPECTRA FOR SELECTED COMPOUNDS

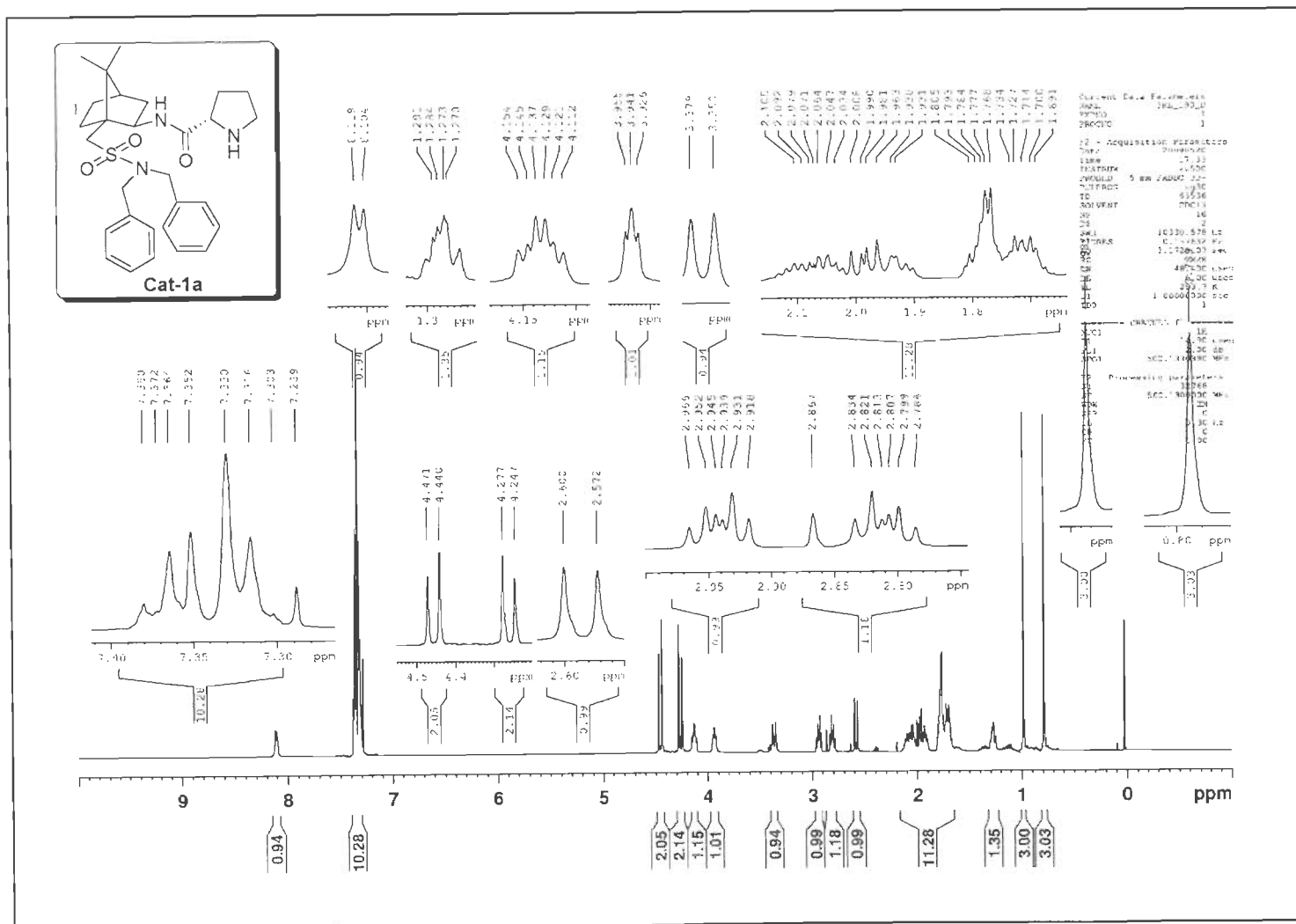


Figure S-1: ¹H NMR (500 MHz, CDCl₃) Spectrum of **Cat-1a**.

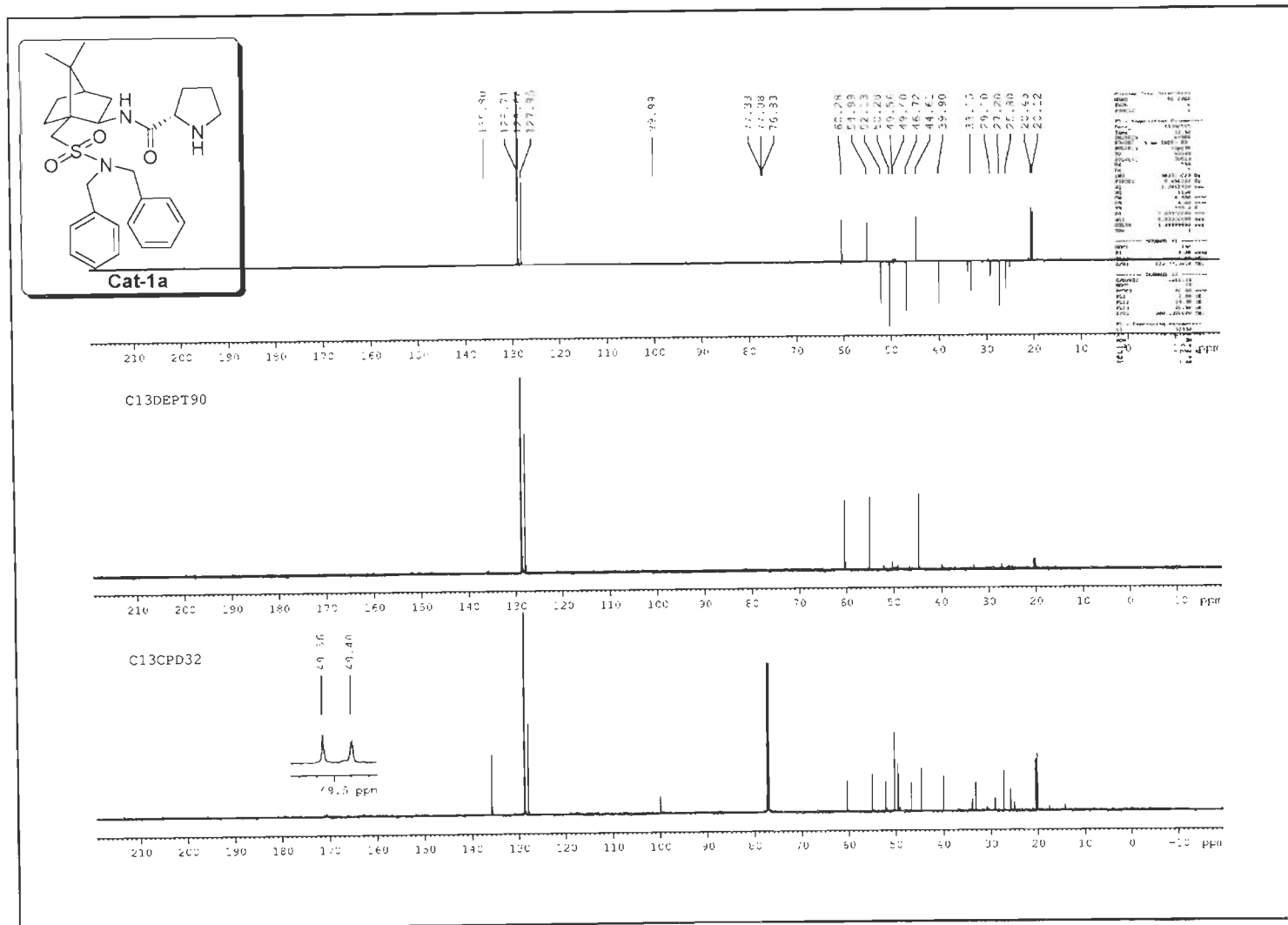


Figure S-2: ¹³C DEPT (125MHz, CDCl₃) Spectra of Cat-1a.

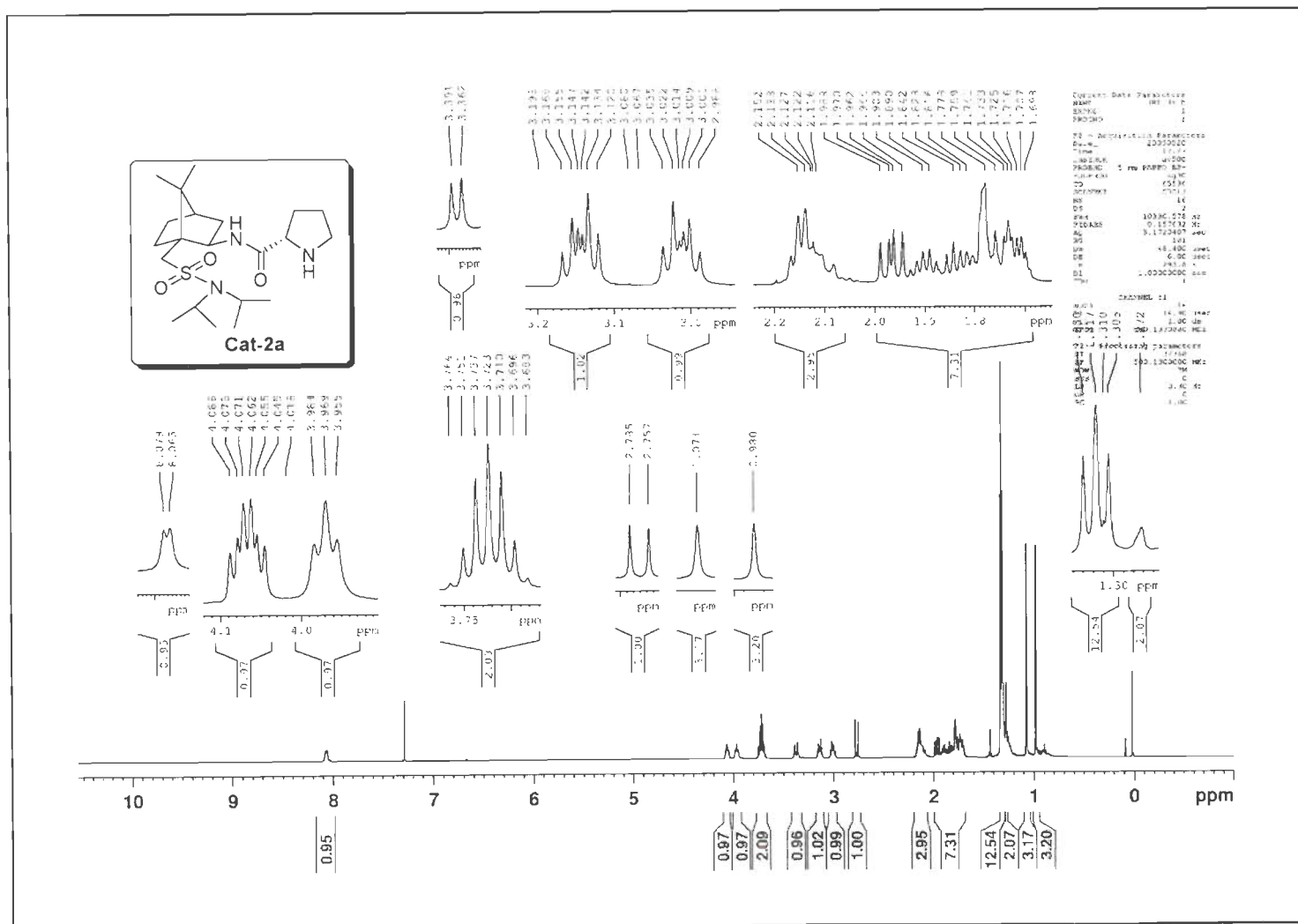


Figure S-3: ^1H NMR (500 MHz, CDCl_3) Spectrum of Cat-2a.

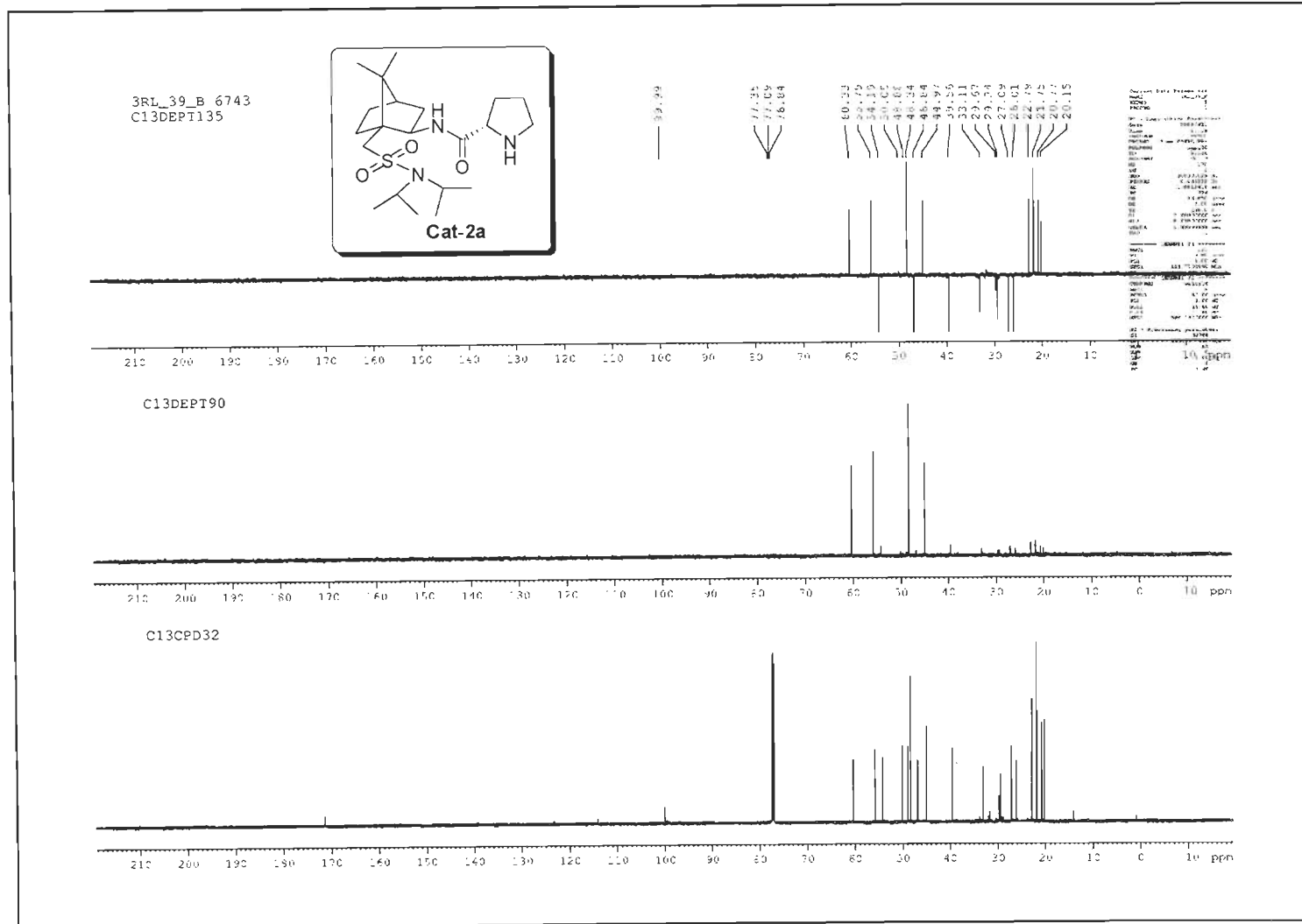


Figure S-4: ¹³C DEPT (125 MHz, CDCl₃) Spectra of Cat-2a.

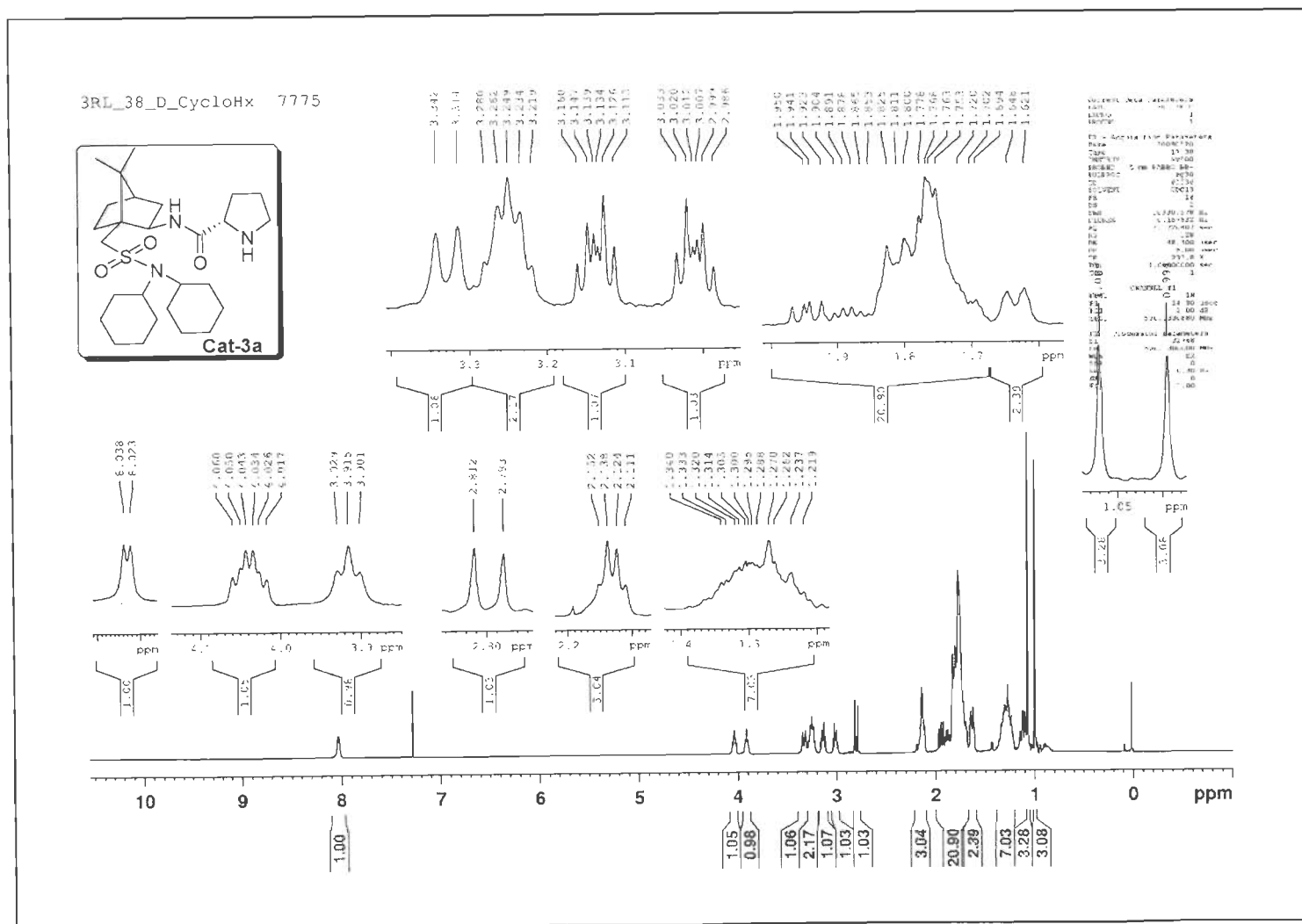


Figure S-5: ^1H NMR (500 MHz, CDCl_3) Spectrum of Cat-3a.

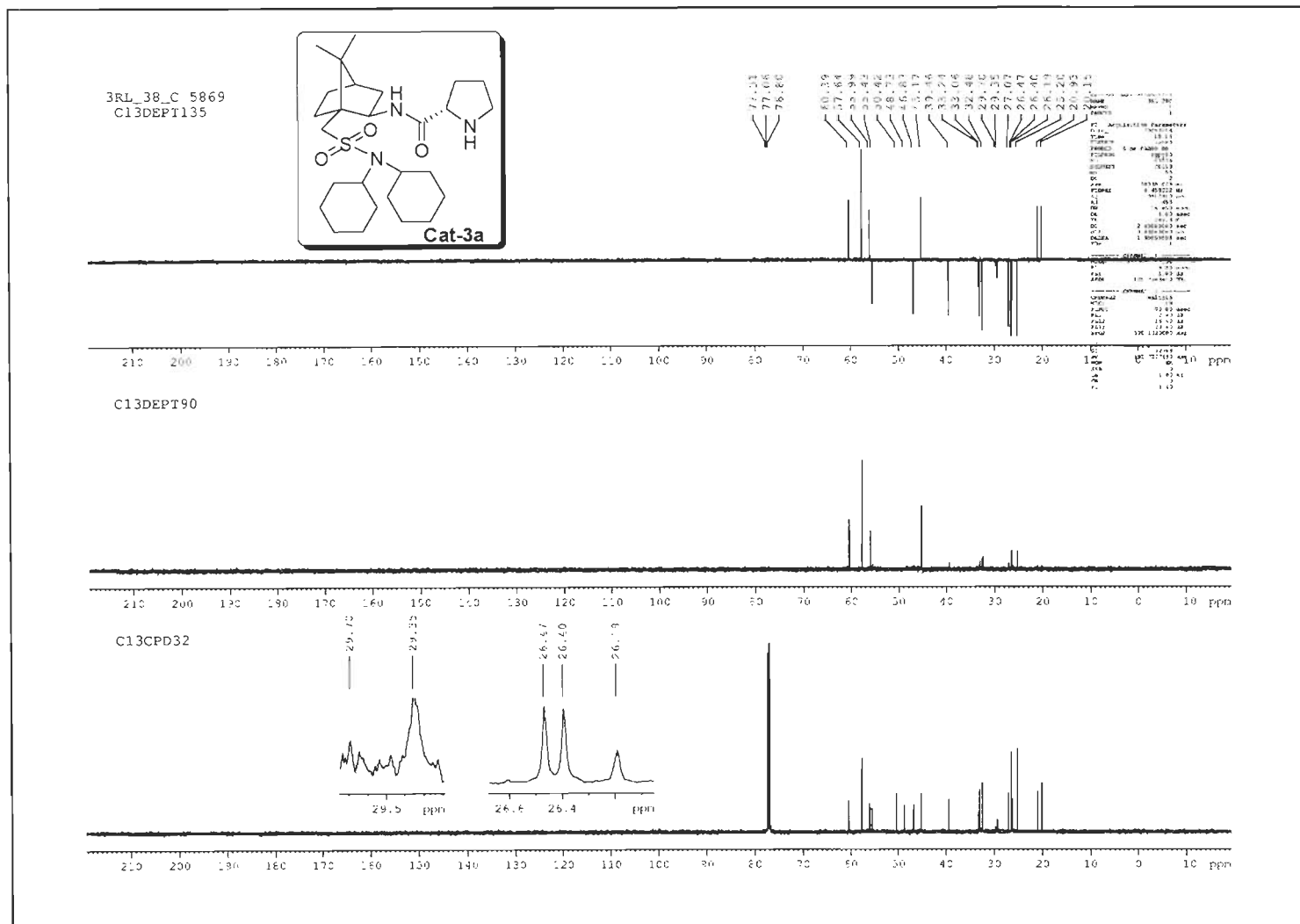
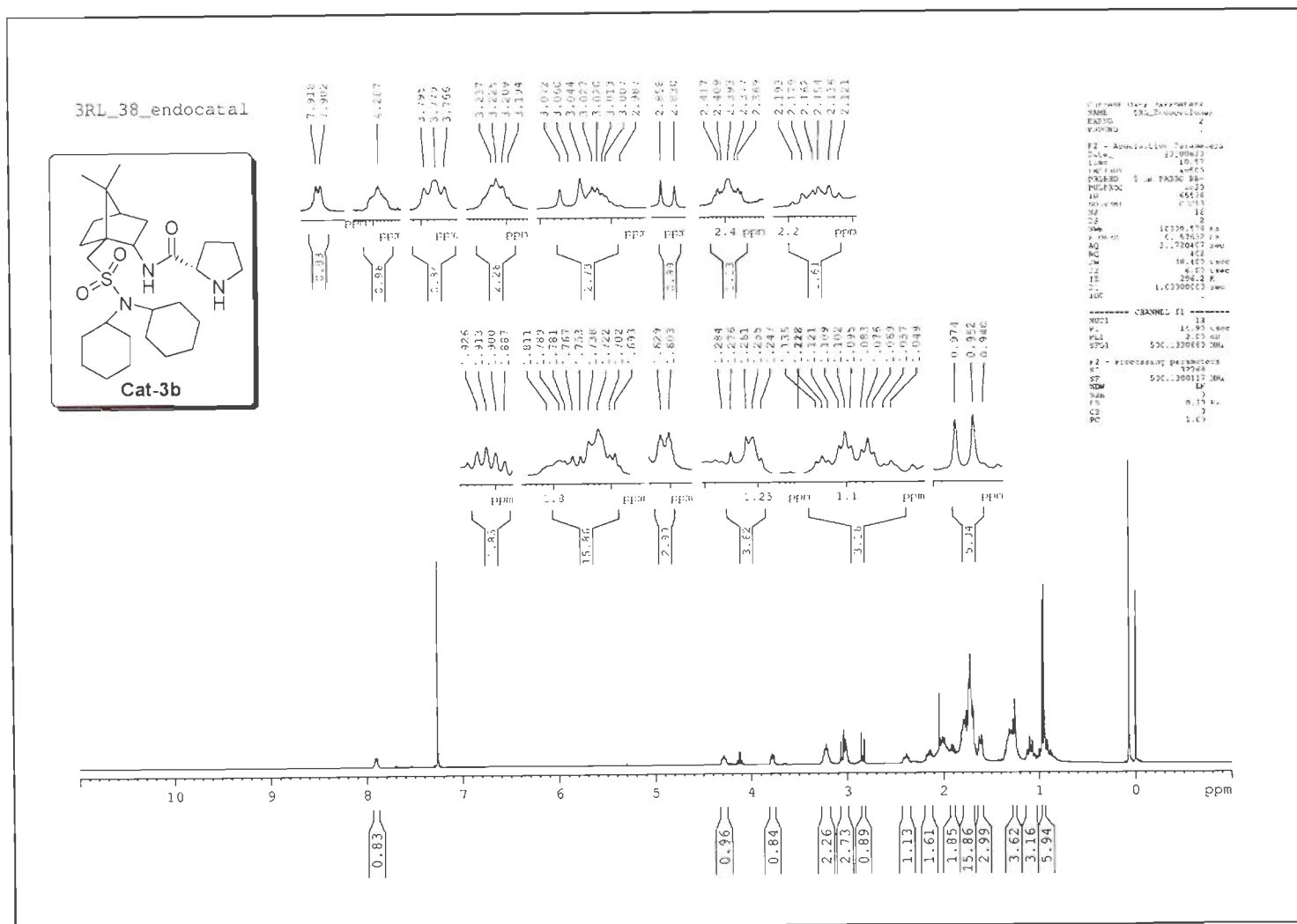


Figure S-6: ¹³C DEPT (125 MHz, CDCl₃) Spectra of Cat-3a.

Figure S-7: ¹H NMR (500 MHz, CDCl₃) Spectrum of Cat-3b.

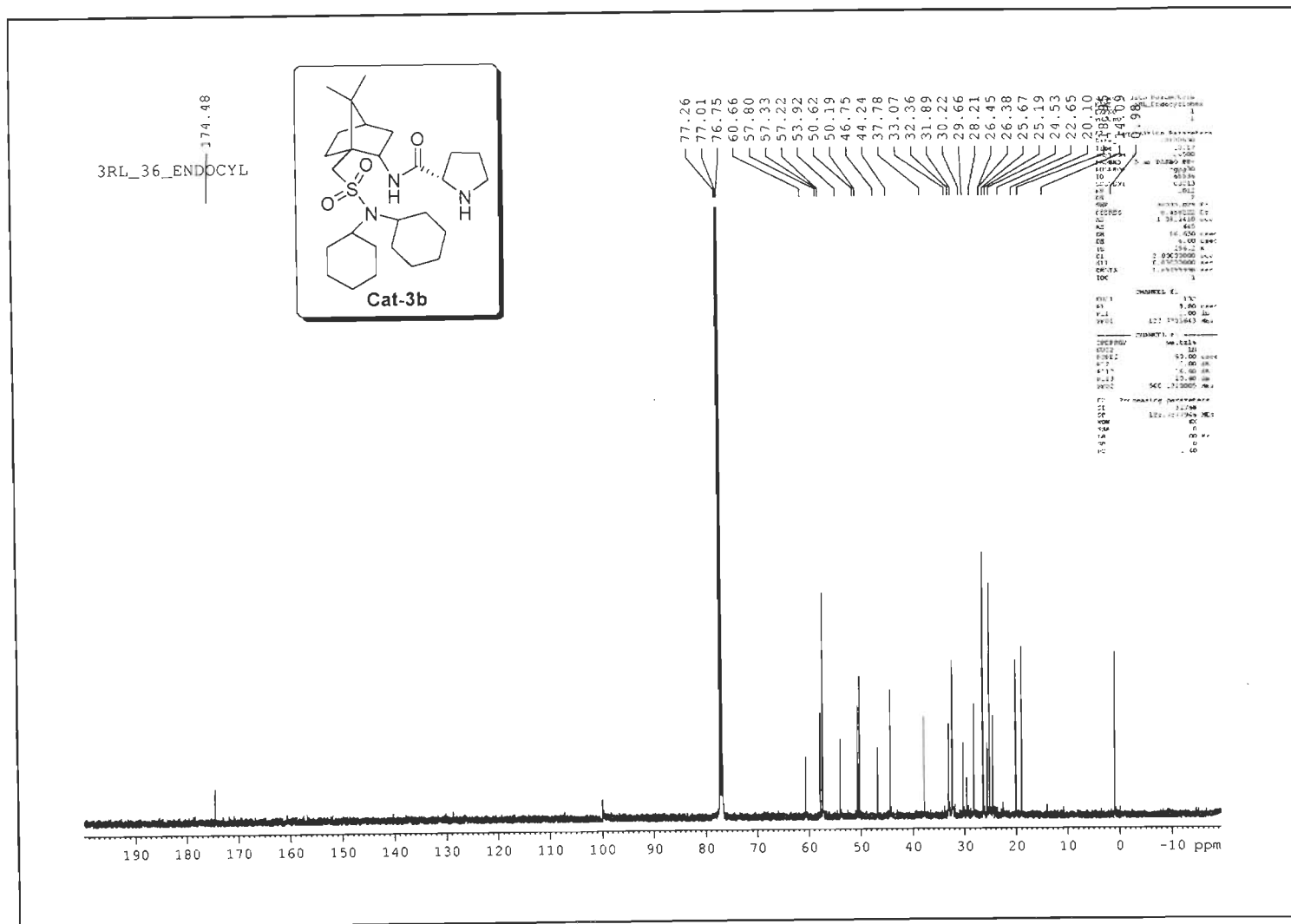


Figure S-8: ^{13}C NMR (125 MHz, CDCl_3) Spectrum of Cat-3b.

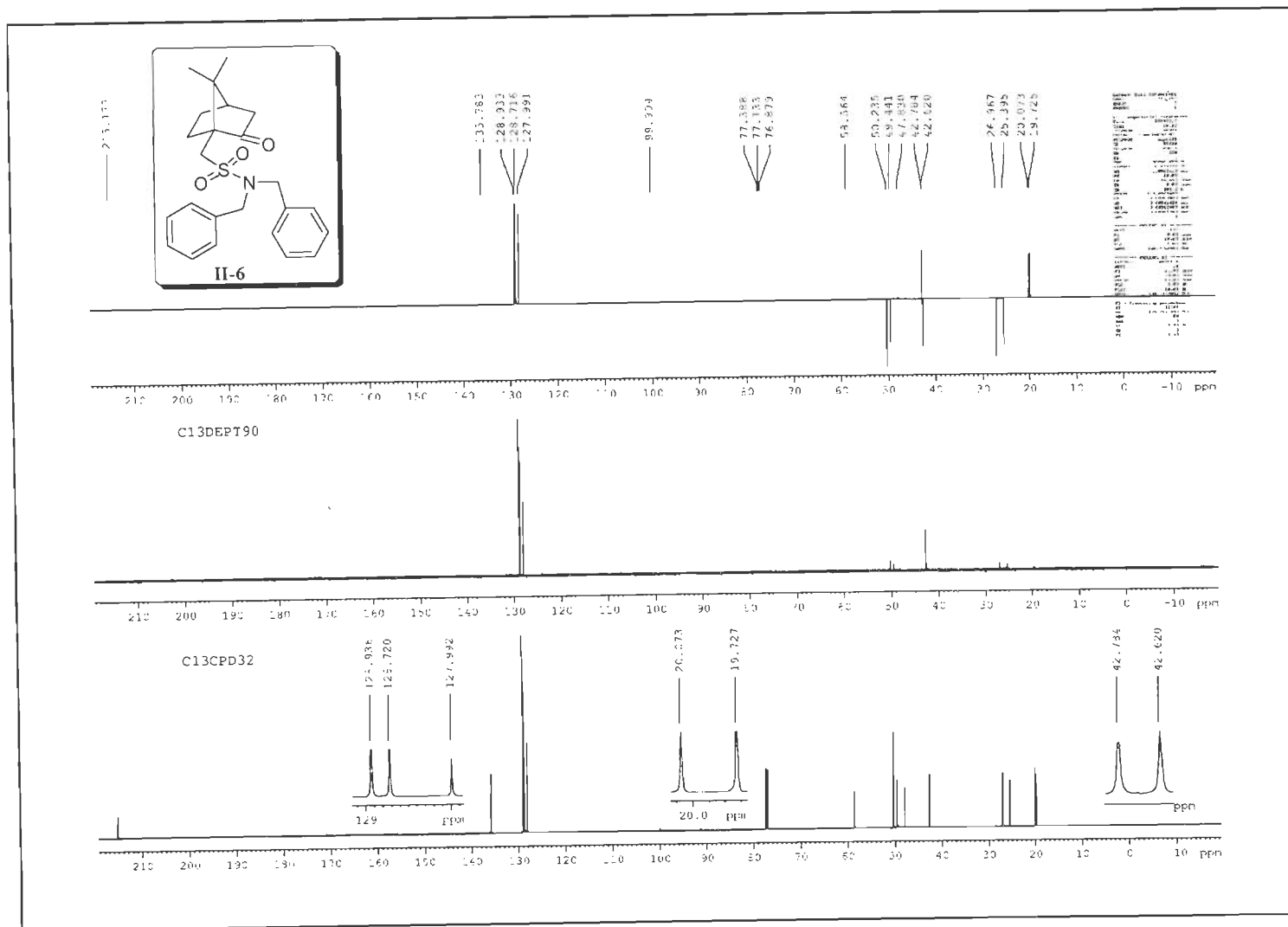


Figure S-10: ^{13}C DEPT (125 MHz, CDCl_3) Spectra of **II-6**.

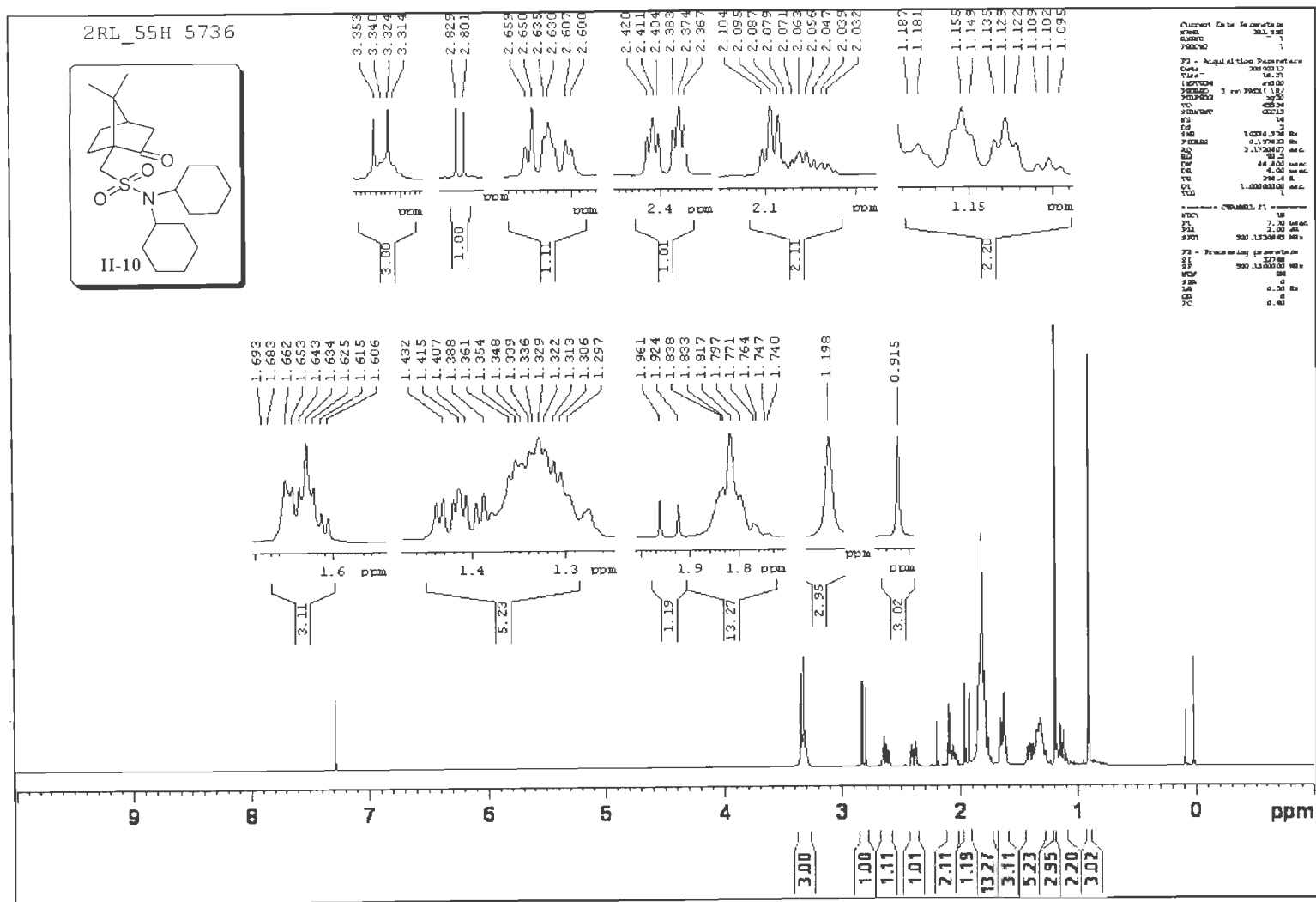


Figure S-11: ^1H NMR (500 MHz, CDCl_3) Spectrum of II-10.

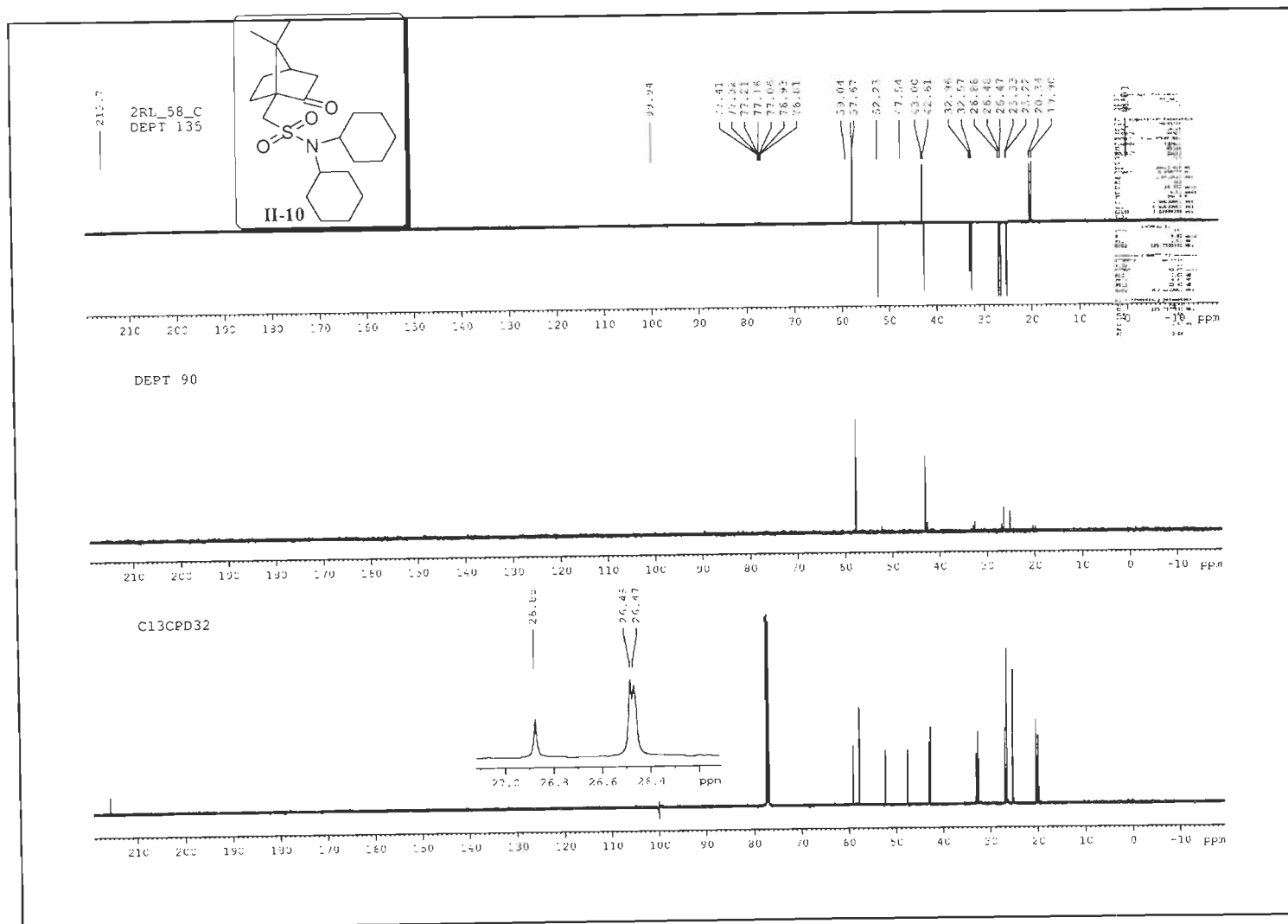


Figure S-12: ^{13}C DEPT (125 MHz, CDCl_3) Spectra of **II-10**.

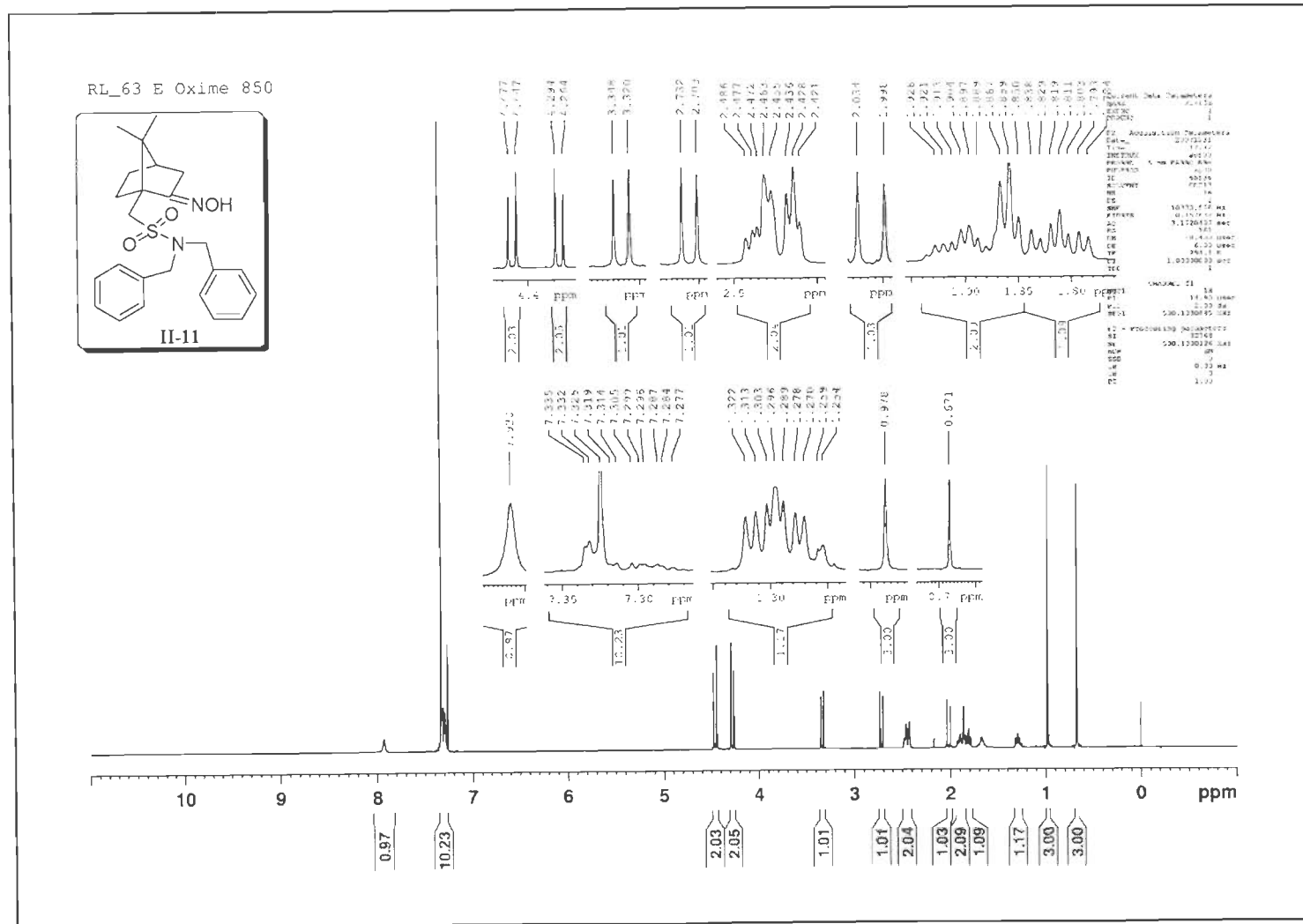


Figure S-13: ${}^1\text{H}$ NMR (500 MHz, CDCl_3) Spectrum of II-11.

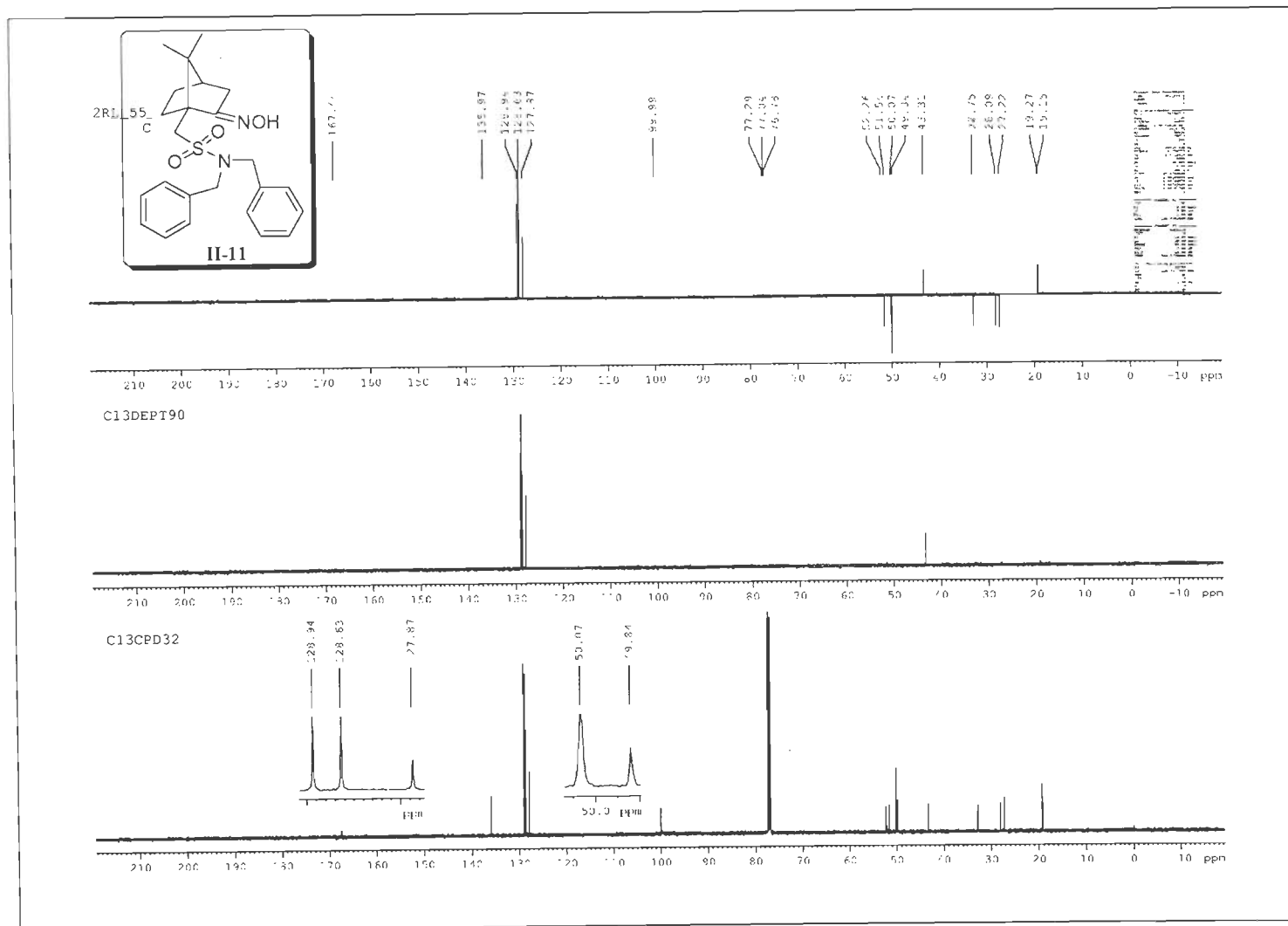
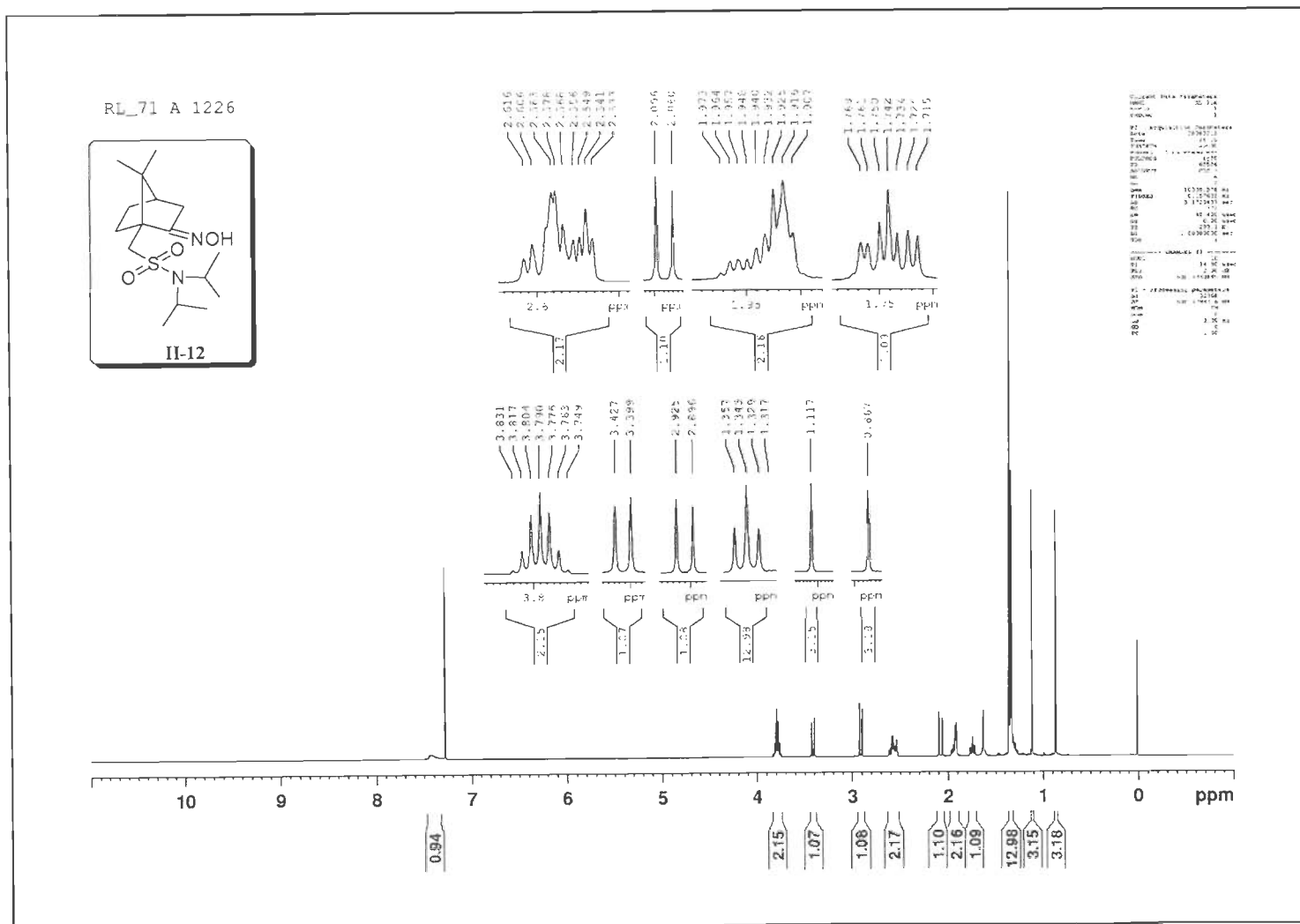


Figure S-14: ^{13}C DEPT (125 MHz, CDCl_3) Spectra of **II-11**.

Figure S-15: ^1H NMR (500 MHz, CDCl_3) Spectrum of II-12.

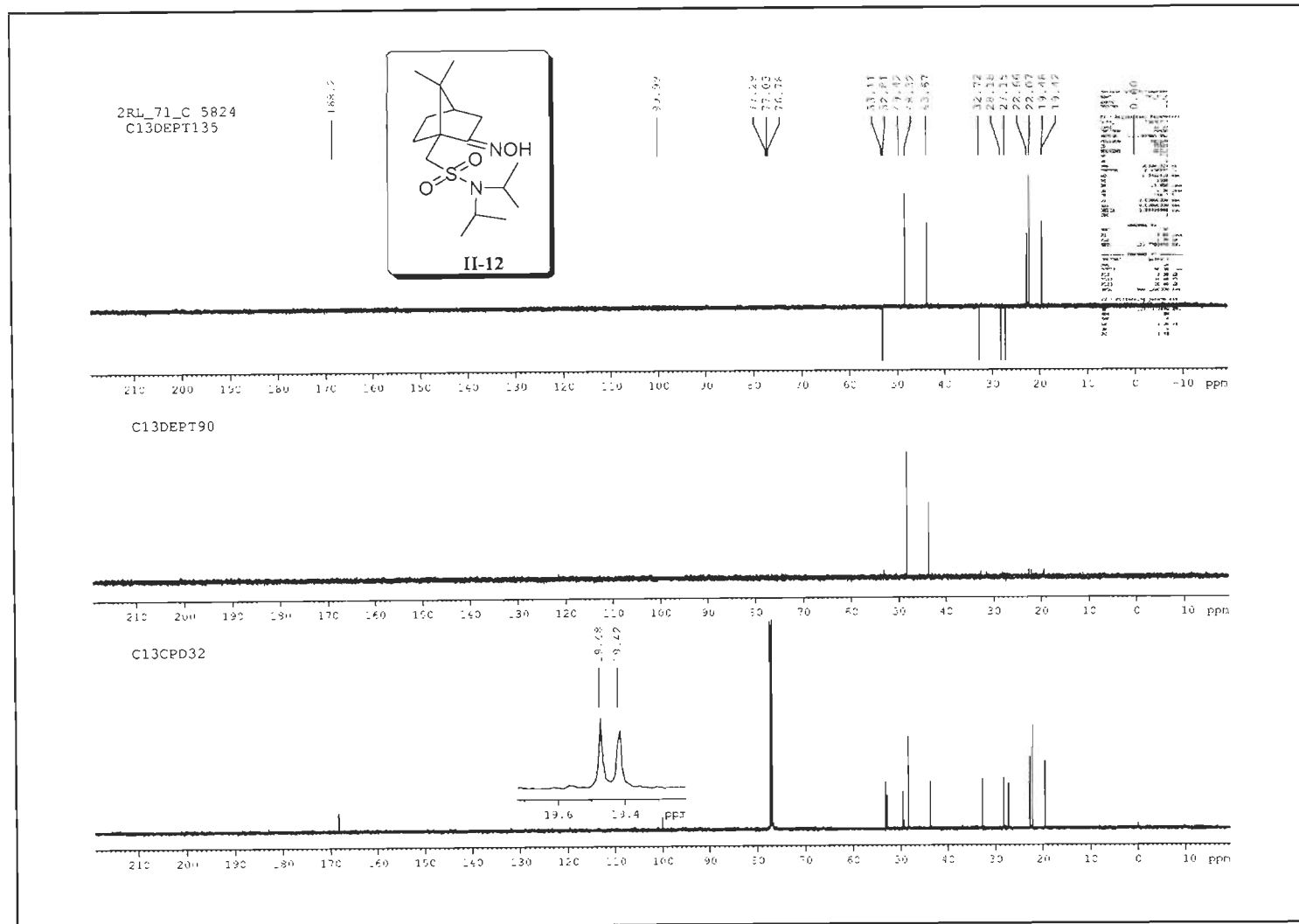


Figure S-16: ^{13}C DEPT (125 MHz, CDCl_3) Spectra of **II-12**.

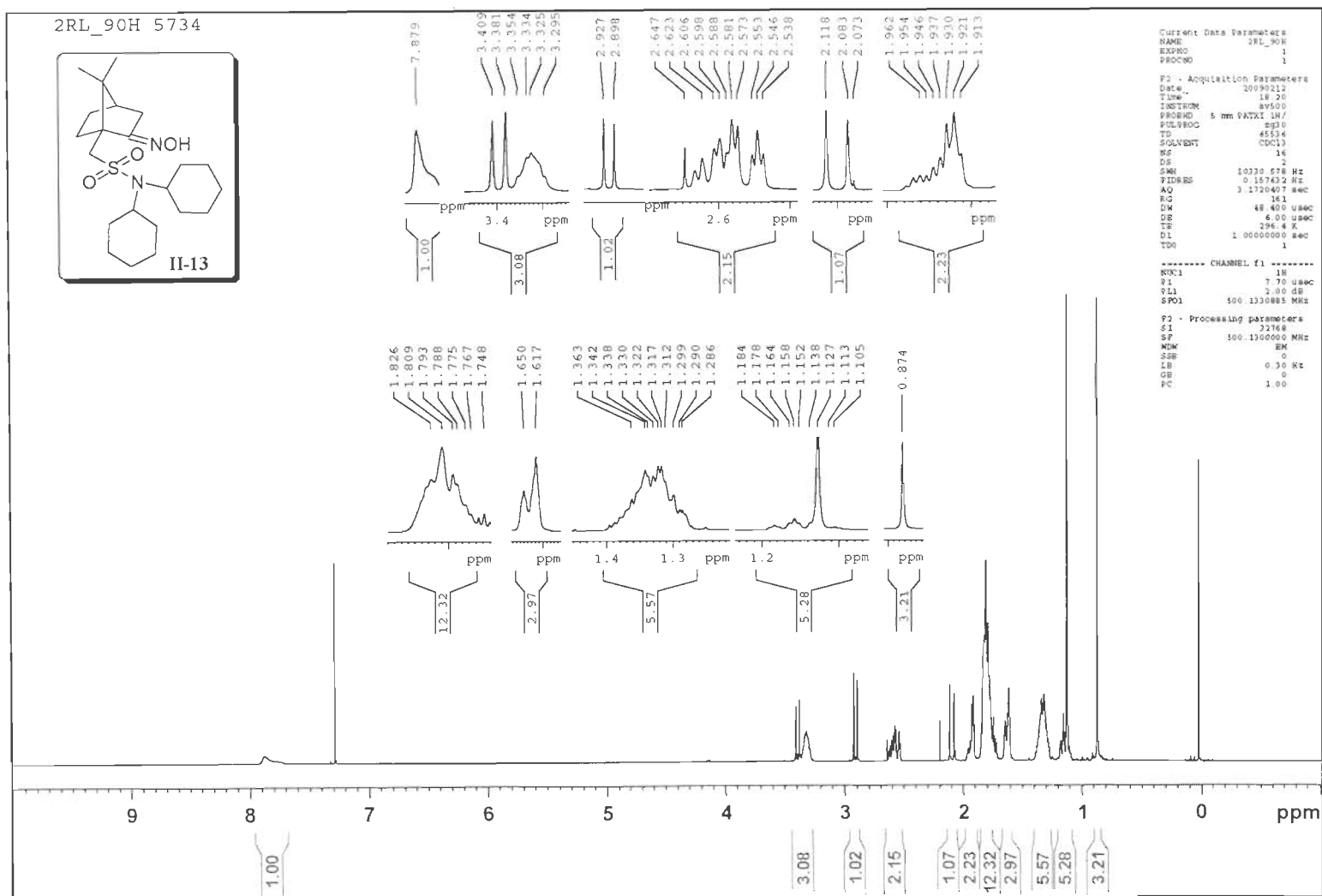


Figure S-17: ^1H NMR (500 MHz, CDCl_3) Spectrum of **II-13**.

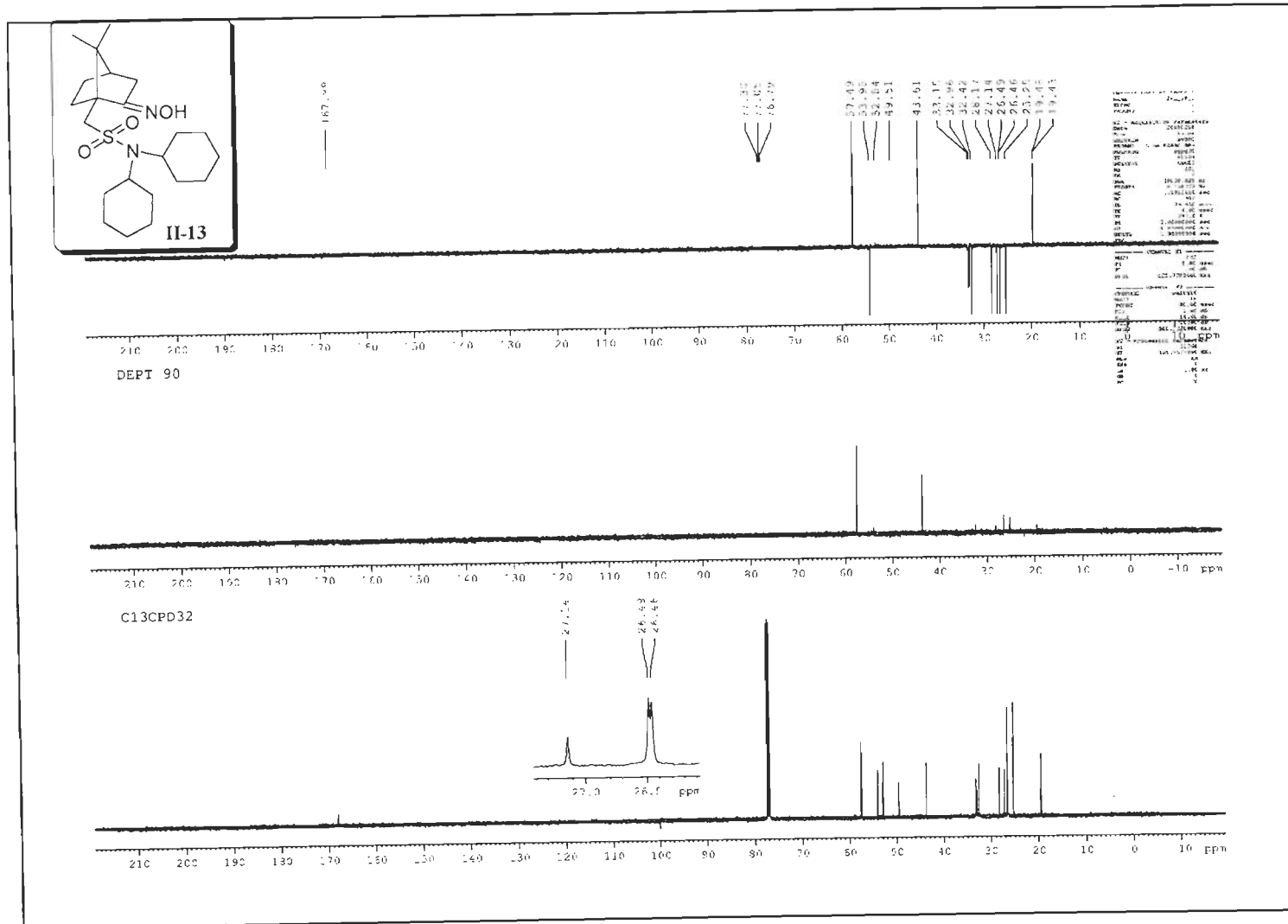


Figure S-18: ^{13}C DEPT (125 MHz, CDCl_3) Spectra of II-13.

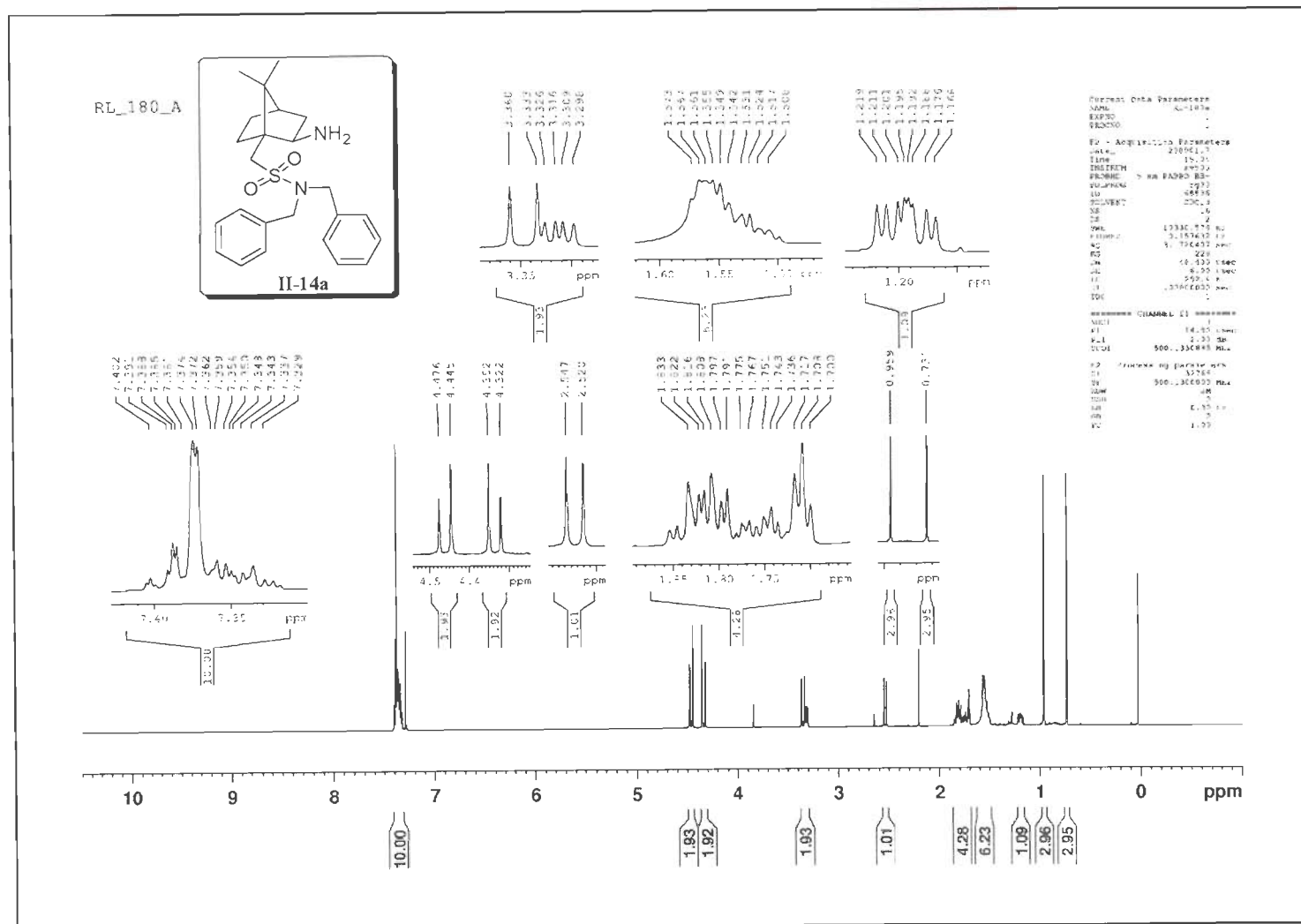


Figure S-19: ^1H NMR (500 MHz, CDCl_3) Spectrum of II-14a.

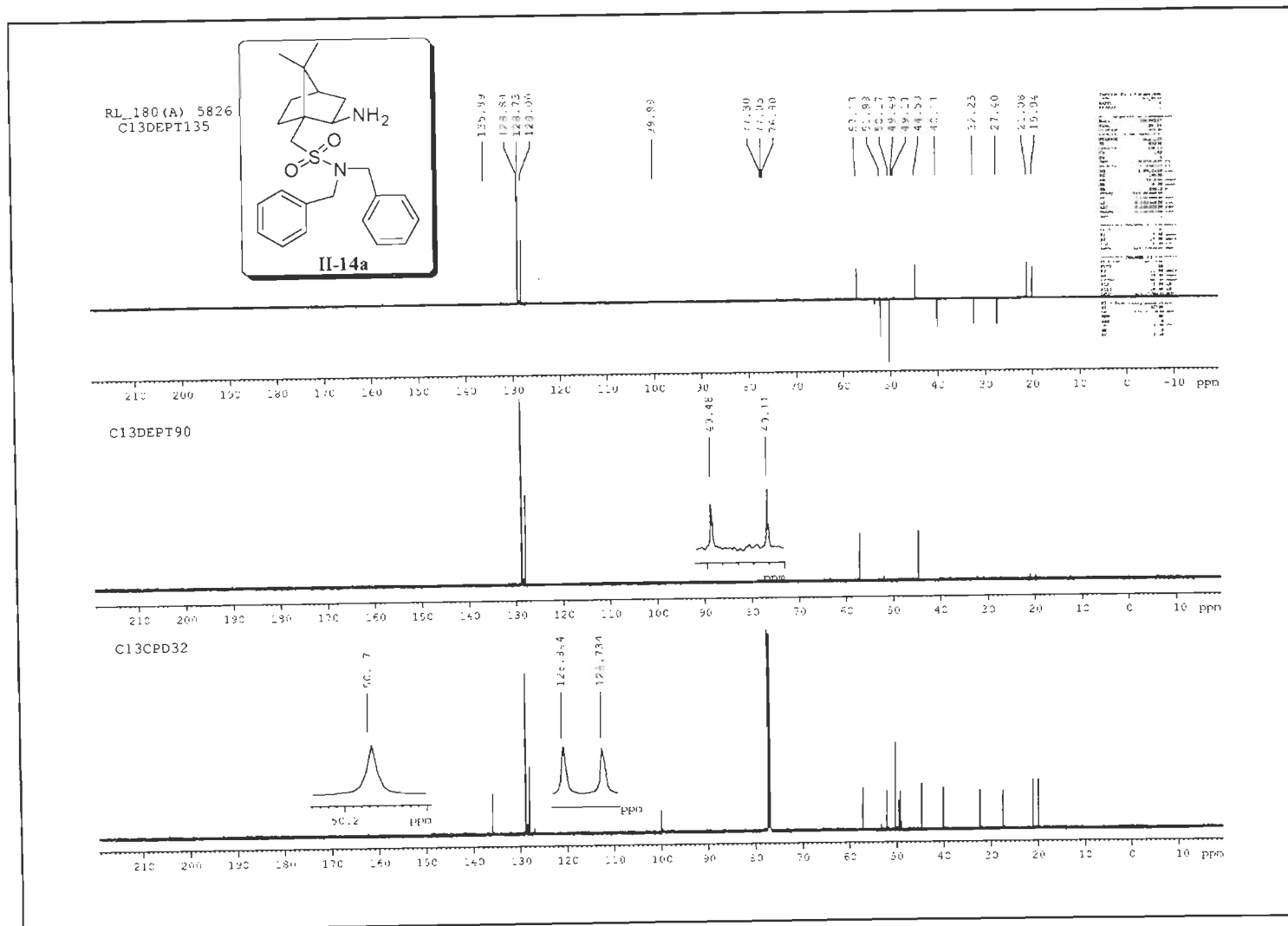
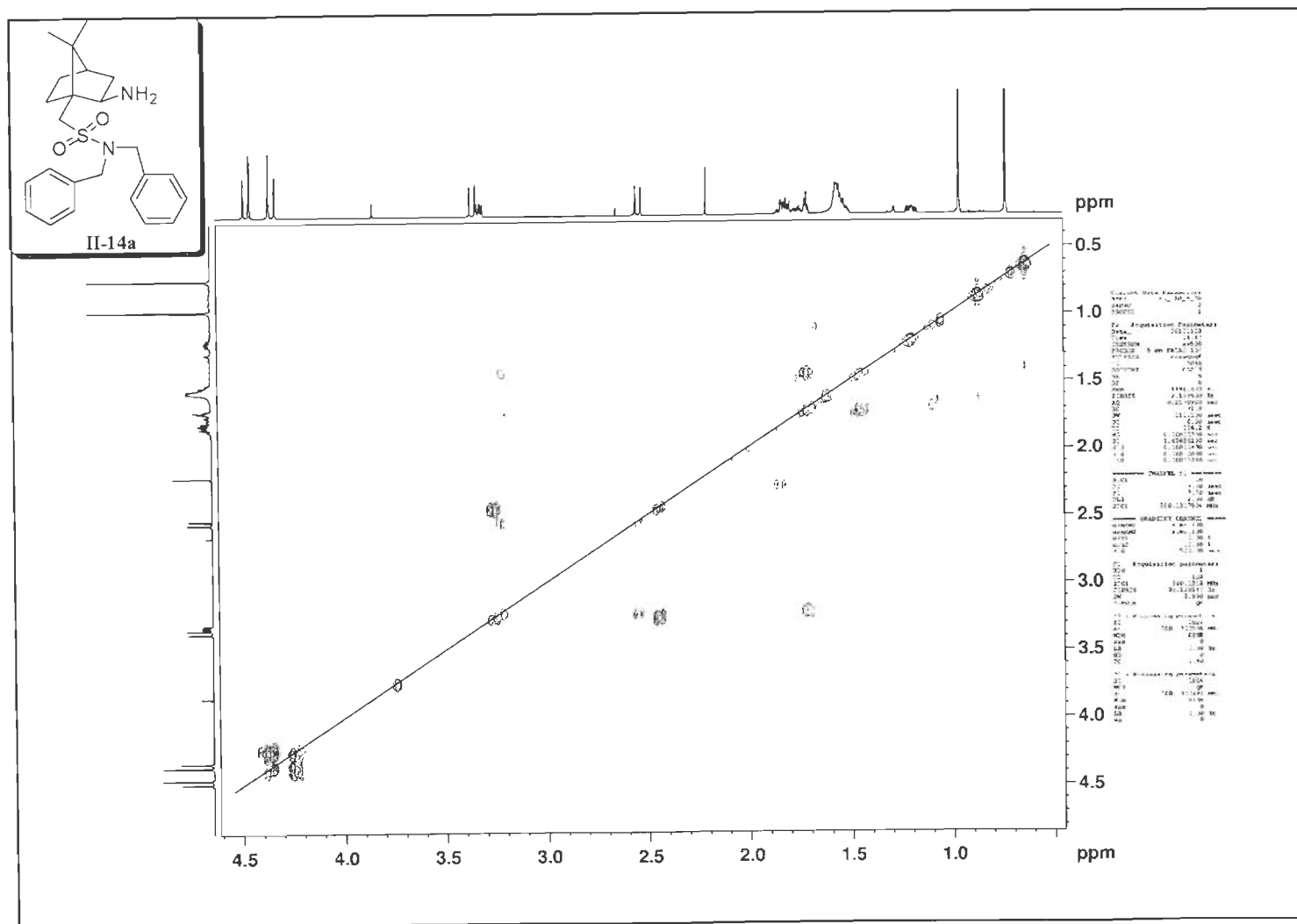


Figure S-20: ^{13}C DEPT (125 MHz, CDCl_3) Spectra of II-14a.

Figure S-21: ^1H - ^1H COSY (500 MHz, CDCl_3) Spectrum of II-14a.

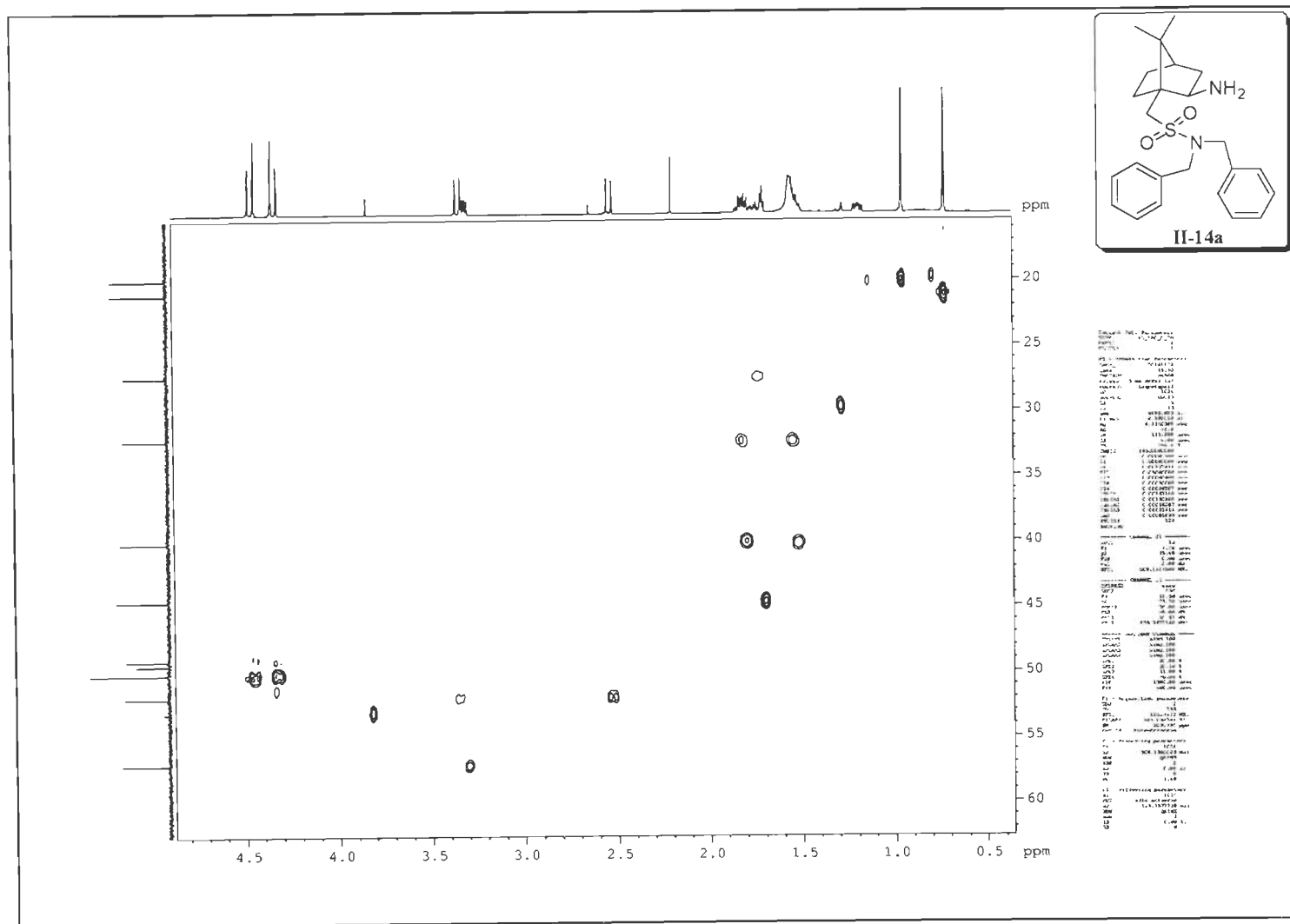


Figure S-22: HSQC (¹H-¹³C) (125 MHz, CDCl₃) Spectrum of II-14a.

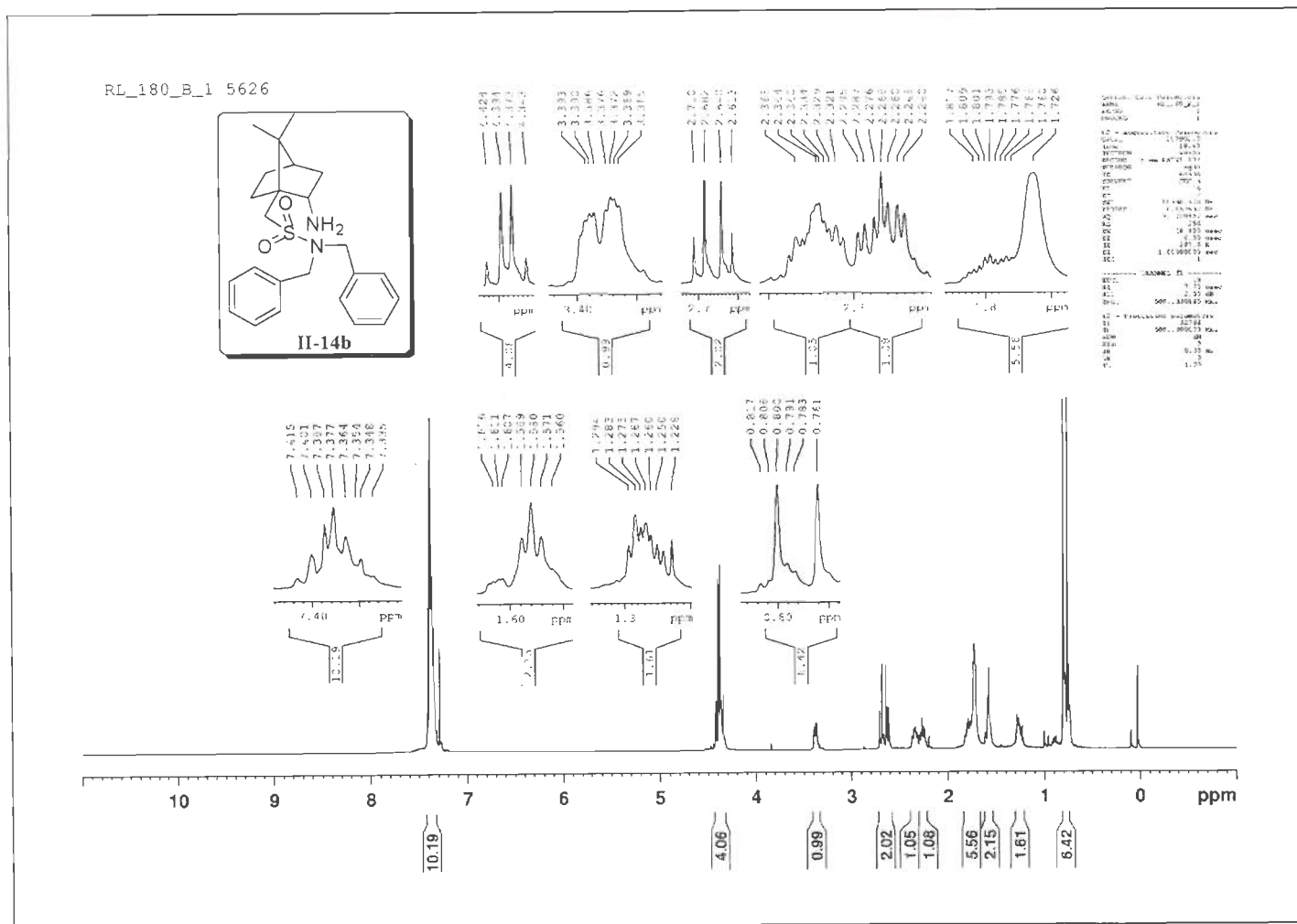


Figure S-23: ^1H NMR (500 MHz, CDCl_3) Spectrum of of **II-14b**.

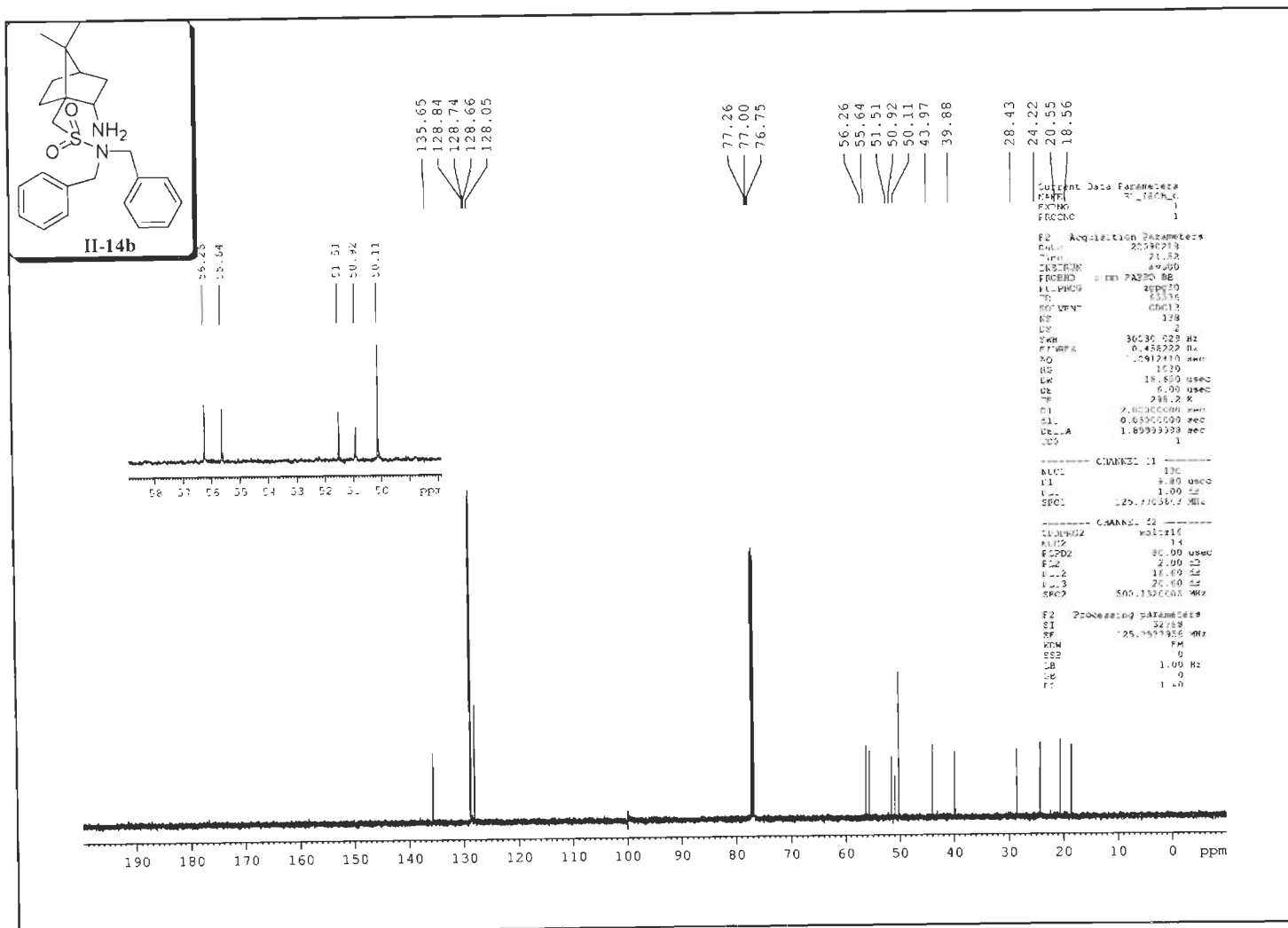


Figure S-24: ^{13}C NMR (125 MHz, CDCl_3) Spectrum of **II-14b**.

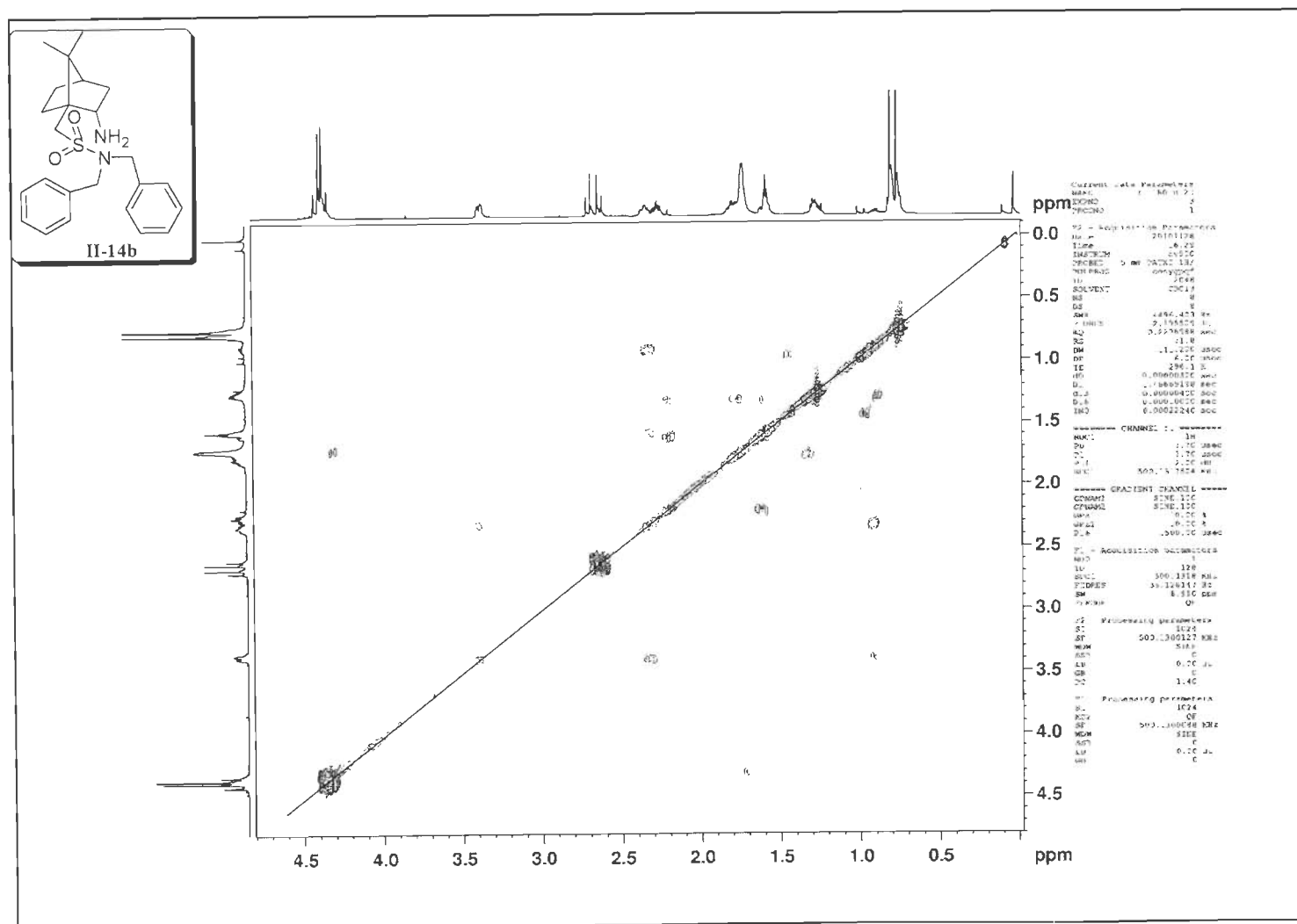


Figure S-25: ^1H - ^1H COSY (500 MHz, CDCl_3) Spectrum of **II-14b**.

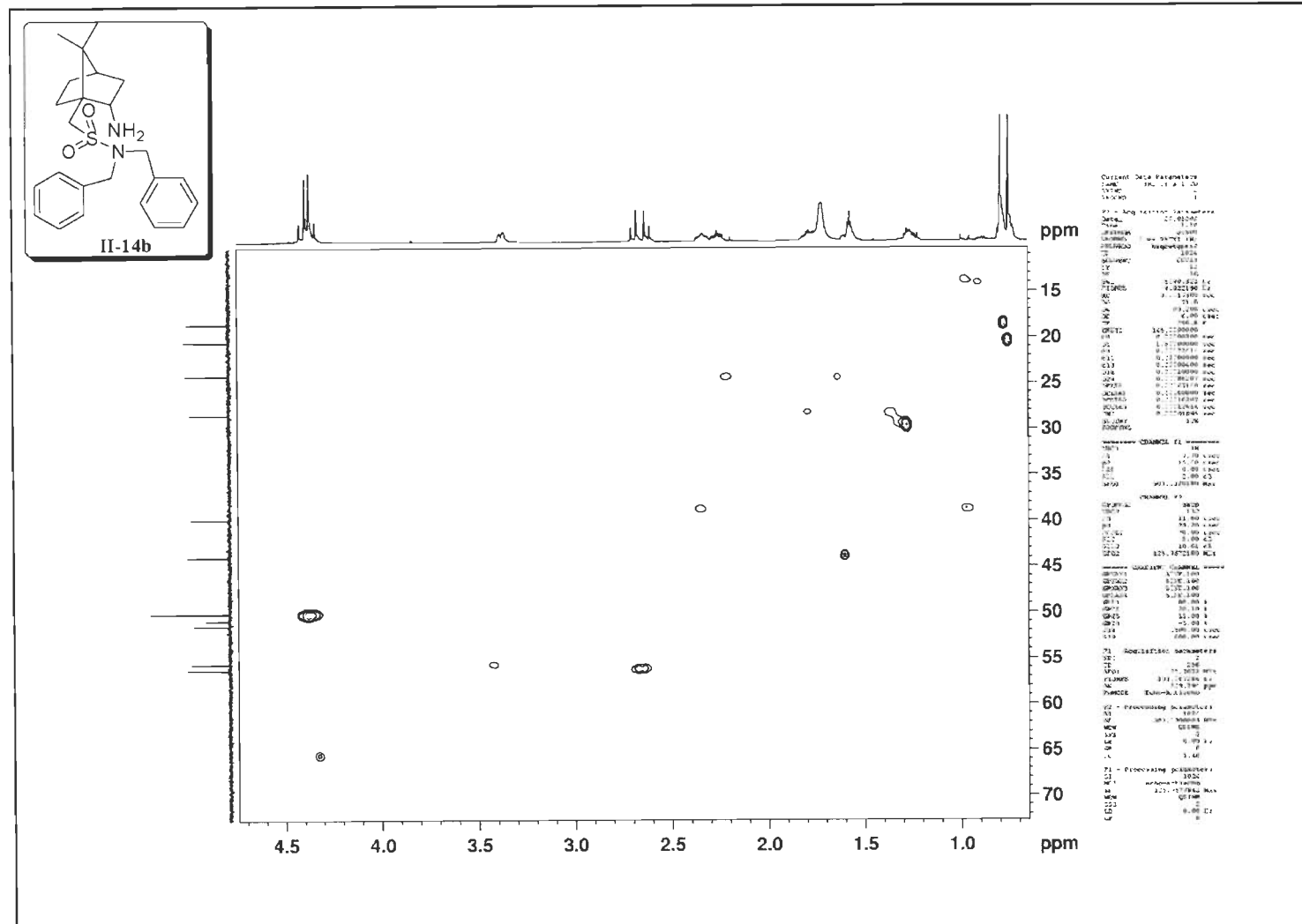


Figure S-26: HSQC (^1H - ^{13}C) (125 MHz, CDCl_3) Spectrum of **II-14b**.

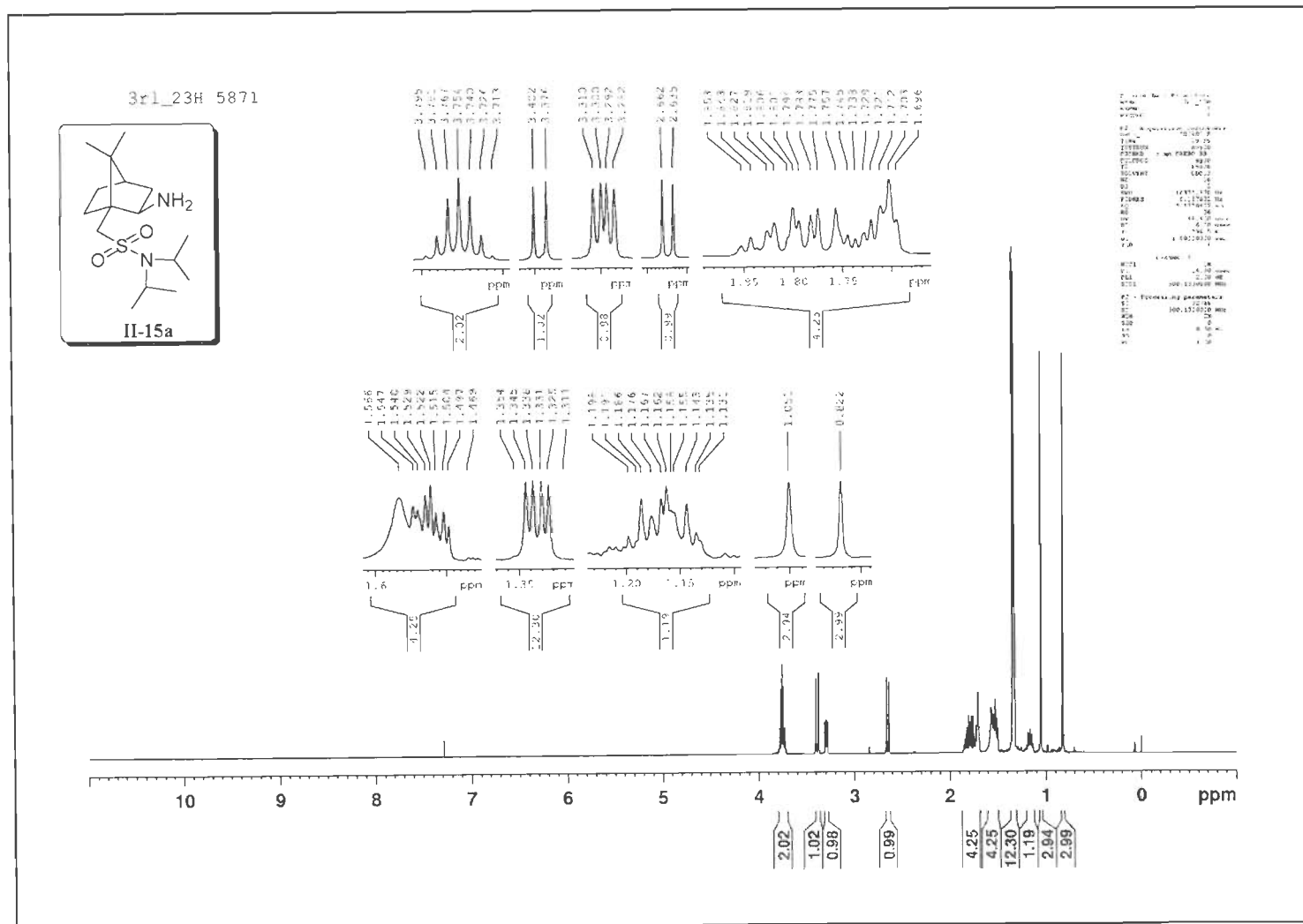


Figure S-27: ^1H NMR (500 MHz, CDCl_3) Spectrum of II-15a.

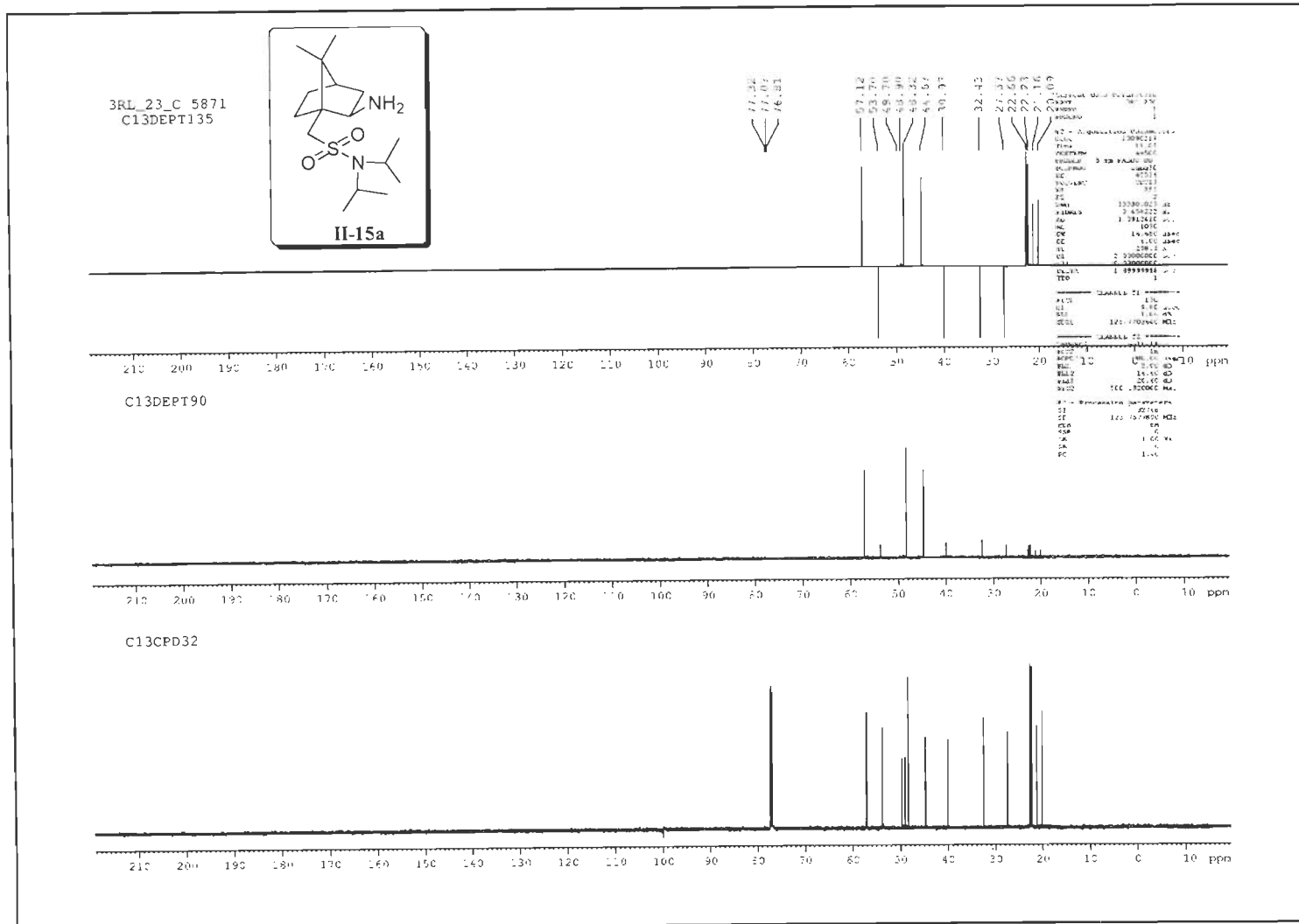


Figure S-28: ^{13}C DEPT (125 MHz, CDCl_3) Spectra of II-15a.

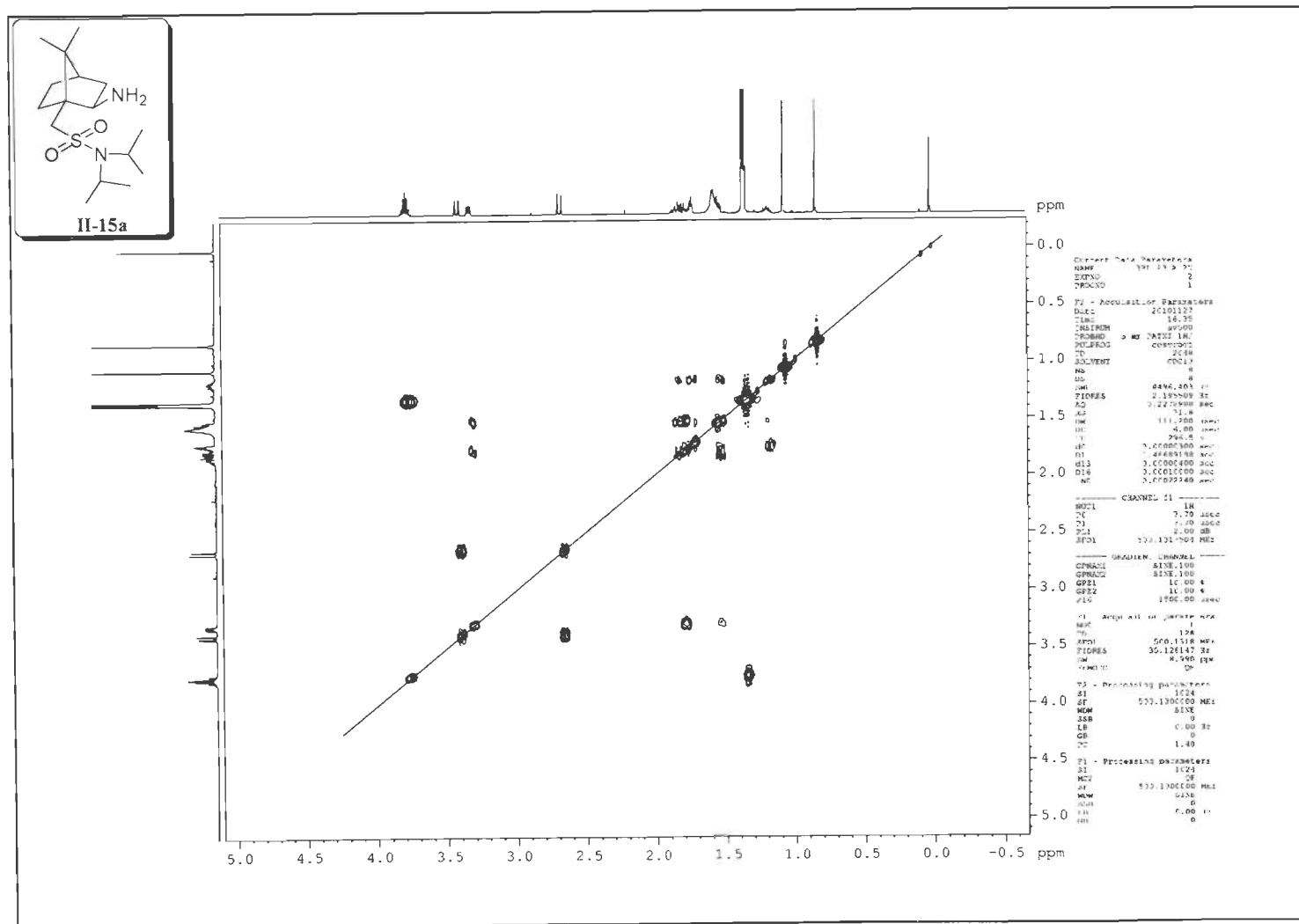
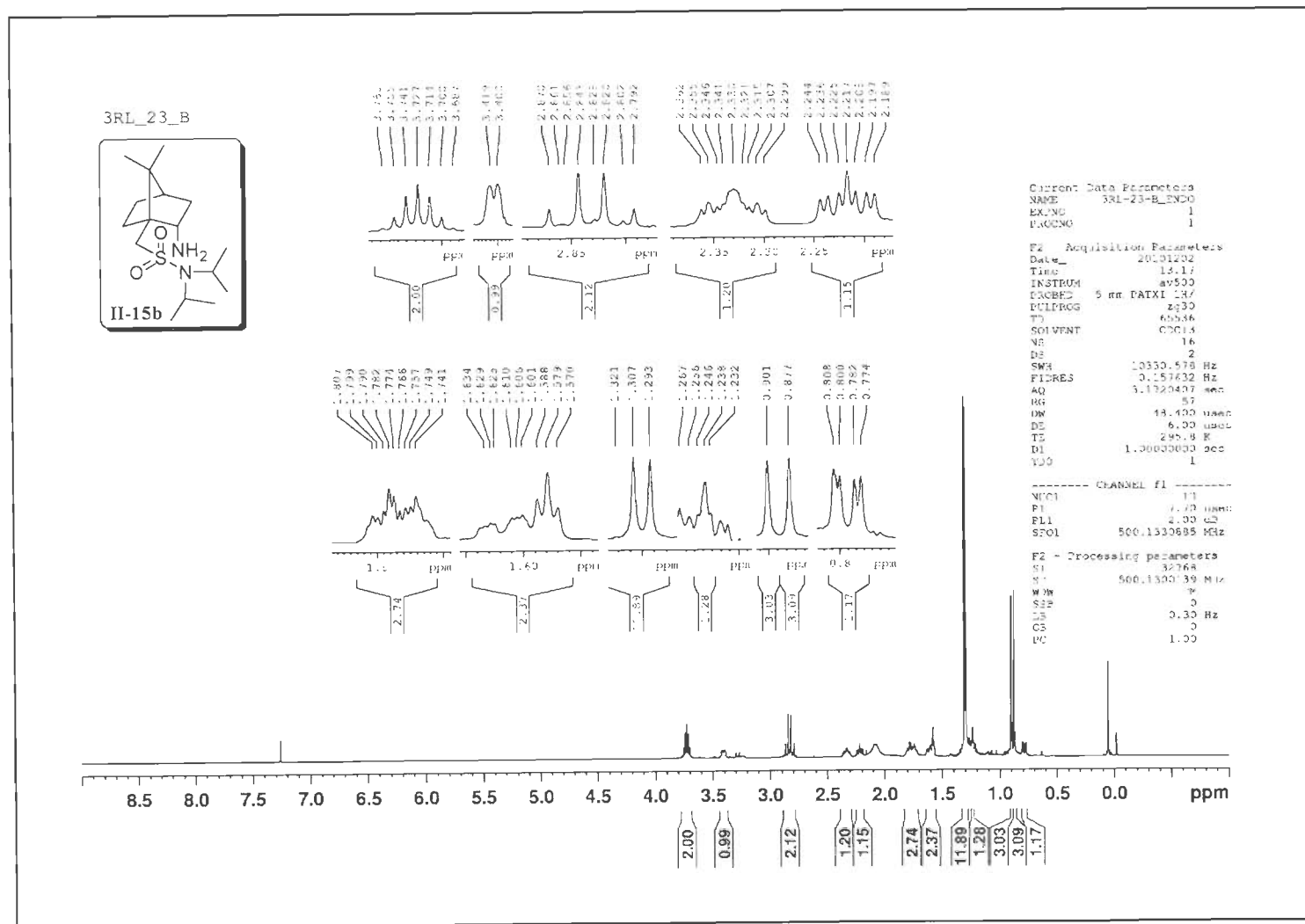


Figure S-29: ¹H-¹H COSY (500 MHz, CDCl₃) Spectrum of II-15a.

Figure S-31: ¹H NMR (500 MHz, CDCl₃) Spectrum of II-15b.

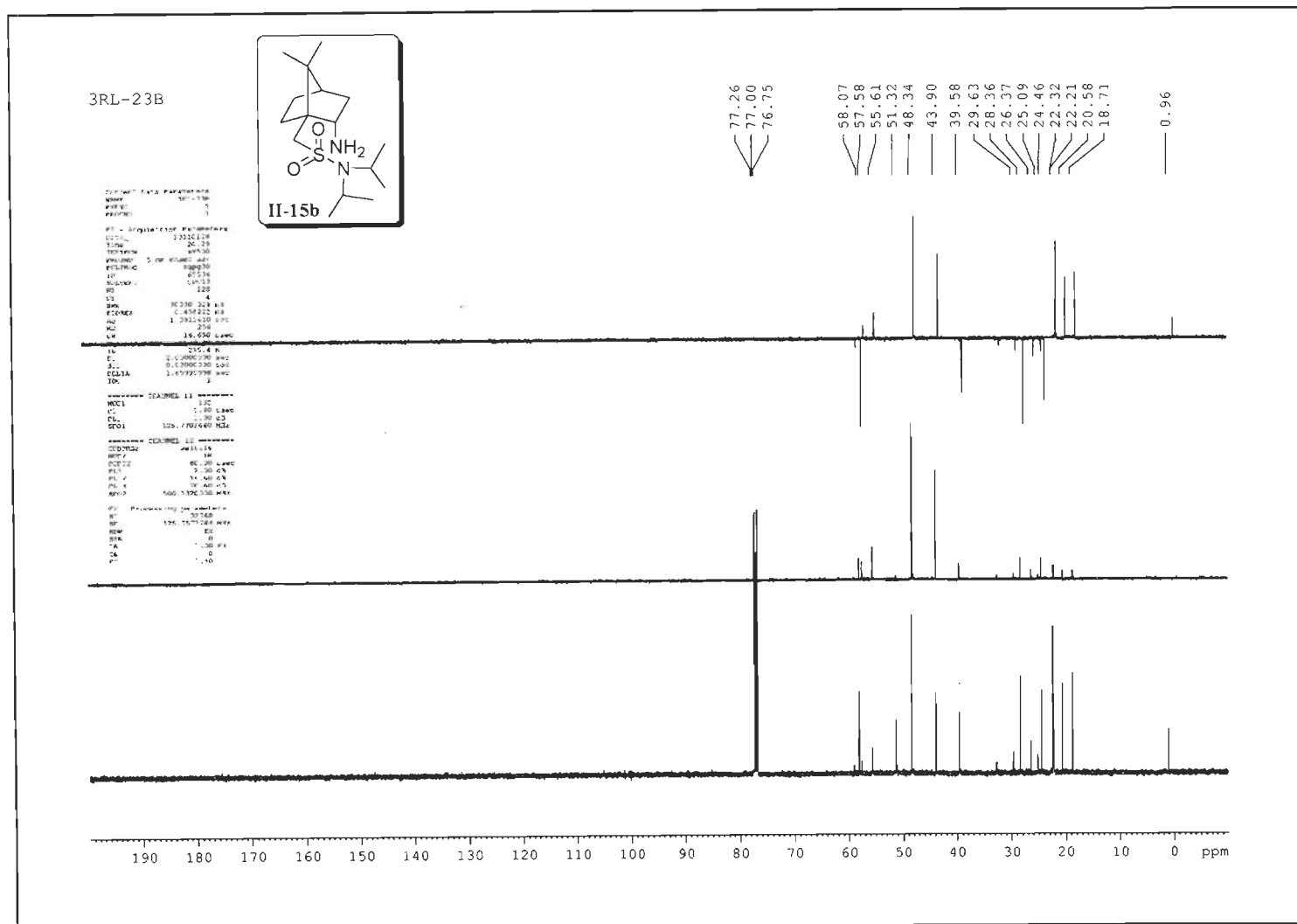


Figure S-32: ^{13}C DEPT (125 MHz, CDCl_3) Spectra of II-15b.

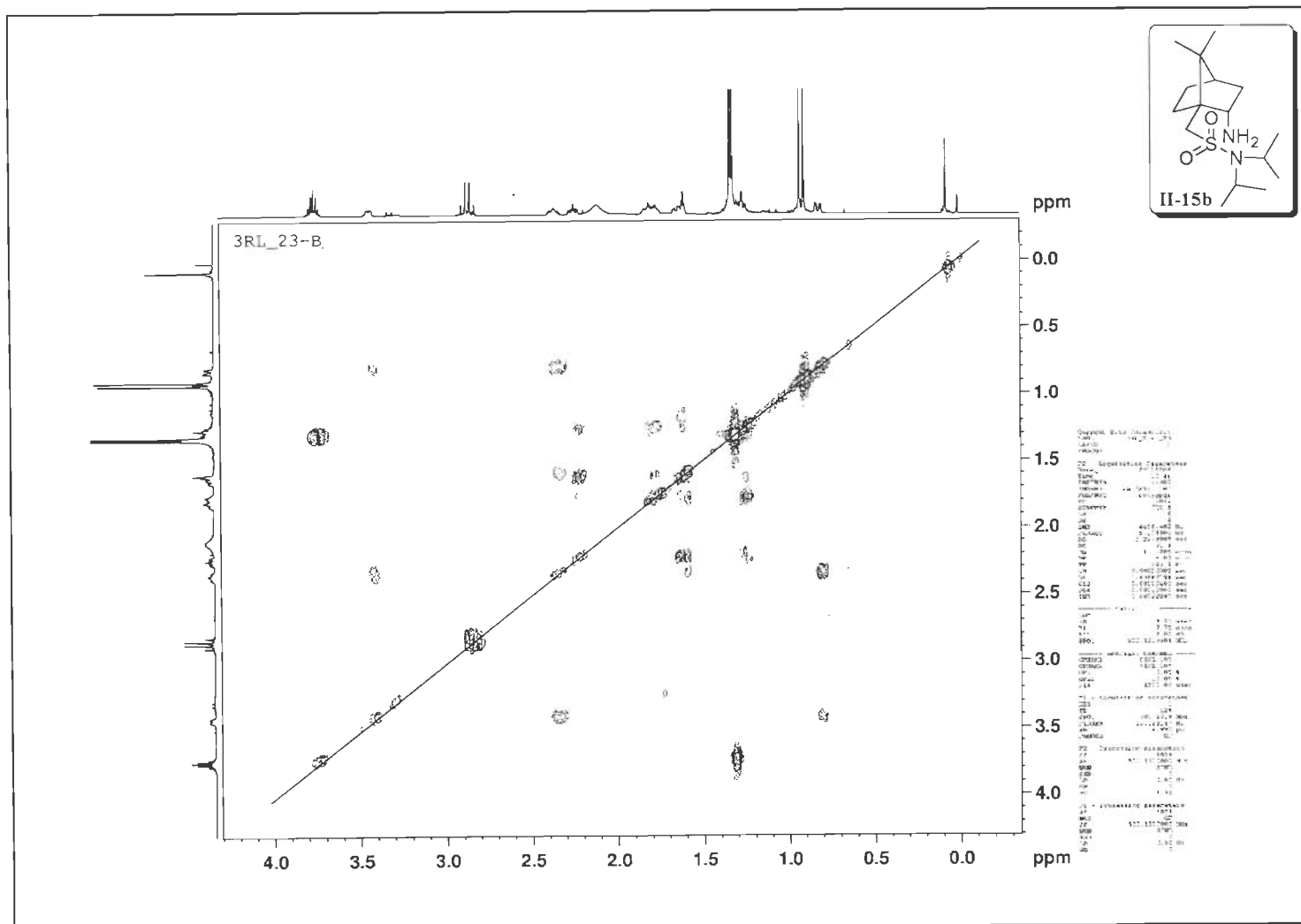


Figure S-33: ^1H - ^1H COSY (500 MHz, CDCl_3) Spectrum of **II-15b**.

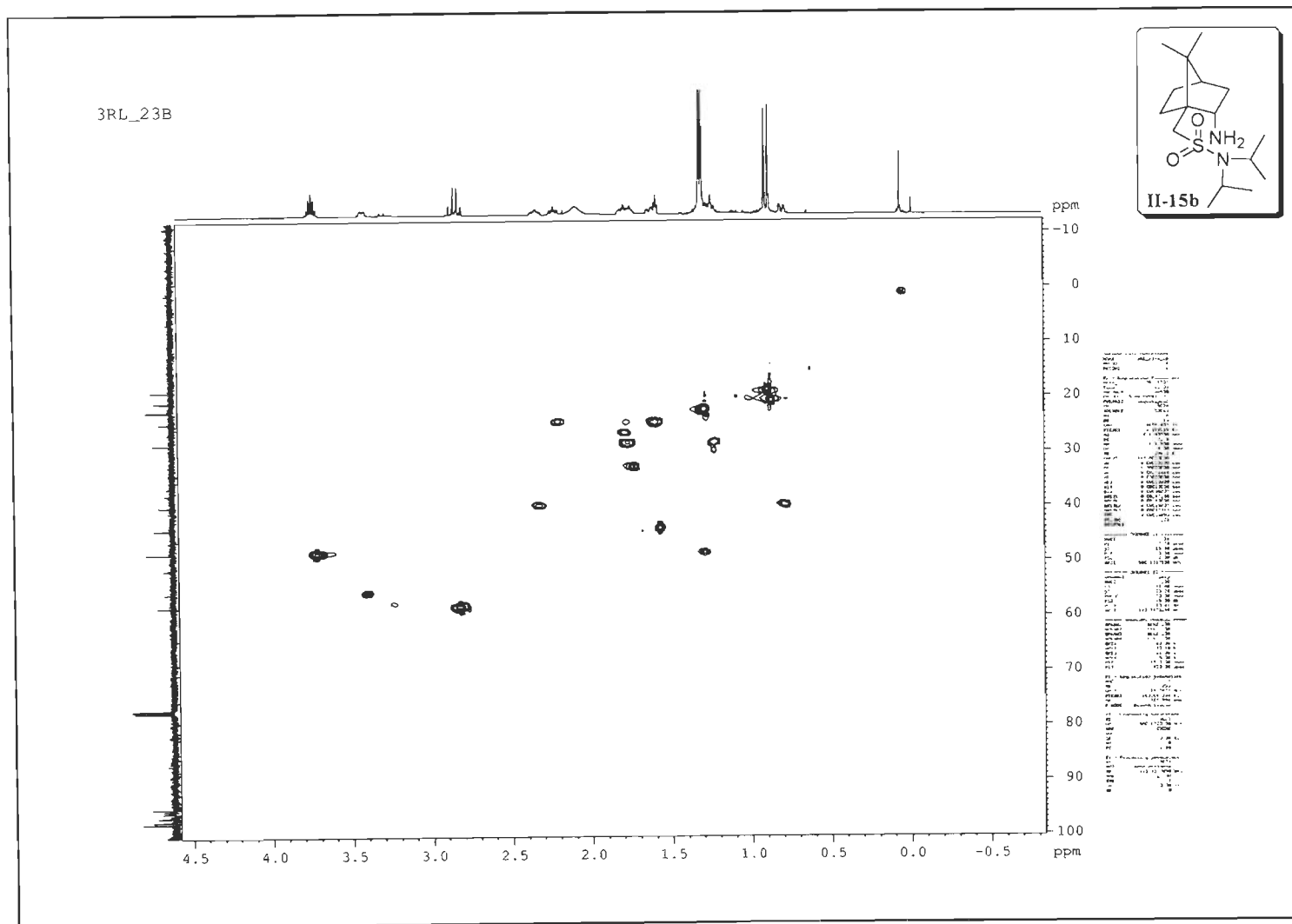
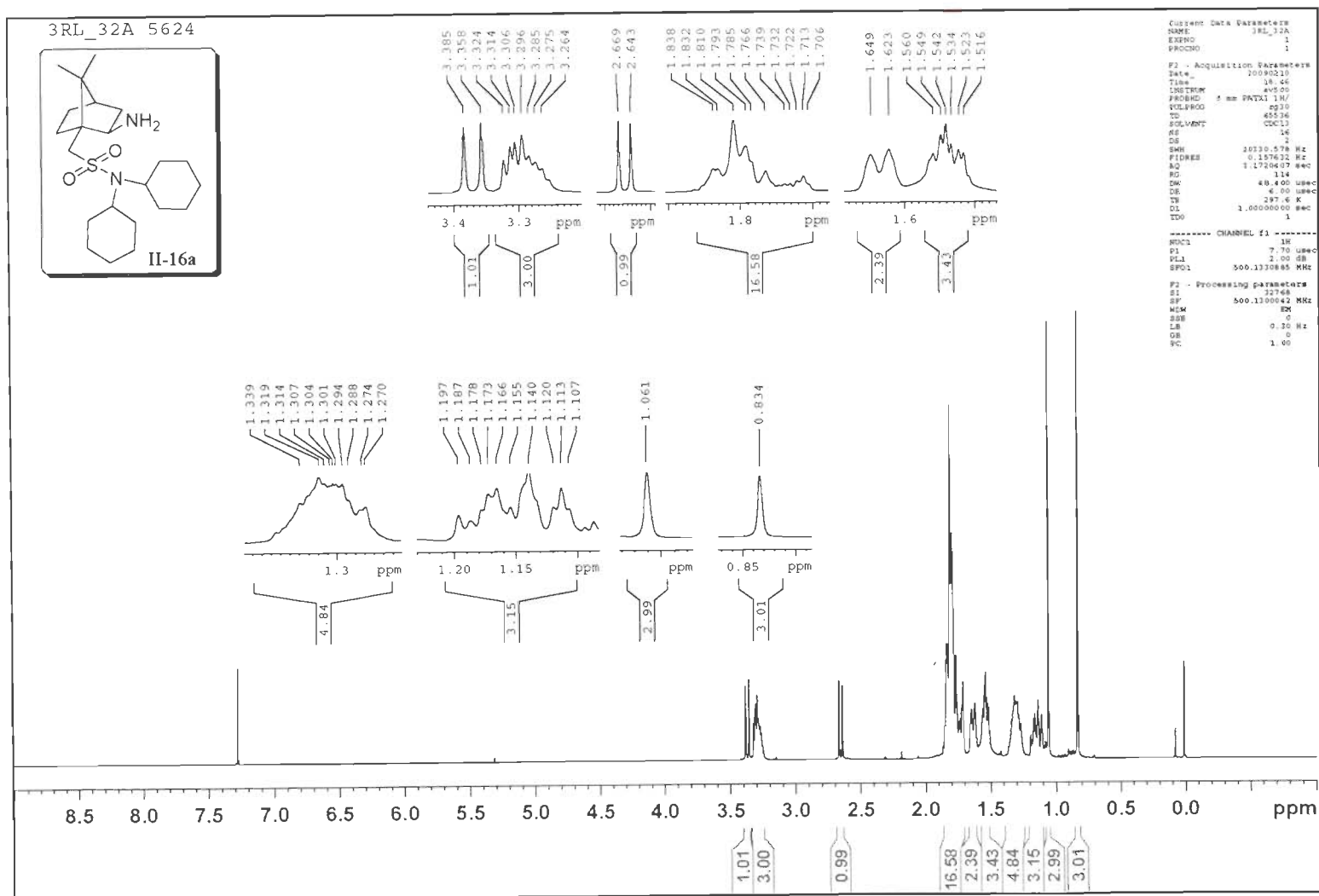


Figure S-34: HSQC (^1H - ^{13}C) (125 MHz, CDCl_3) Spectrum of **II-15b**.

Figure S-35: ^1H NMR (500 MHz, CDCl_3) Spectrum of II-16a.

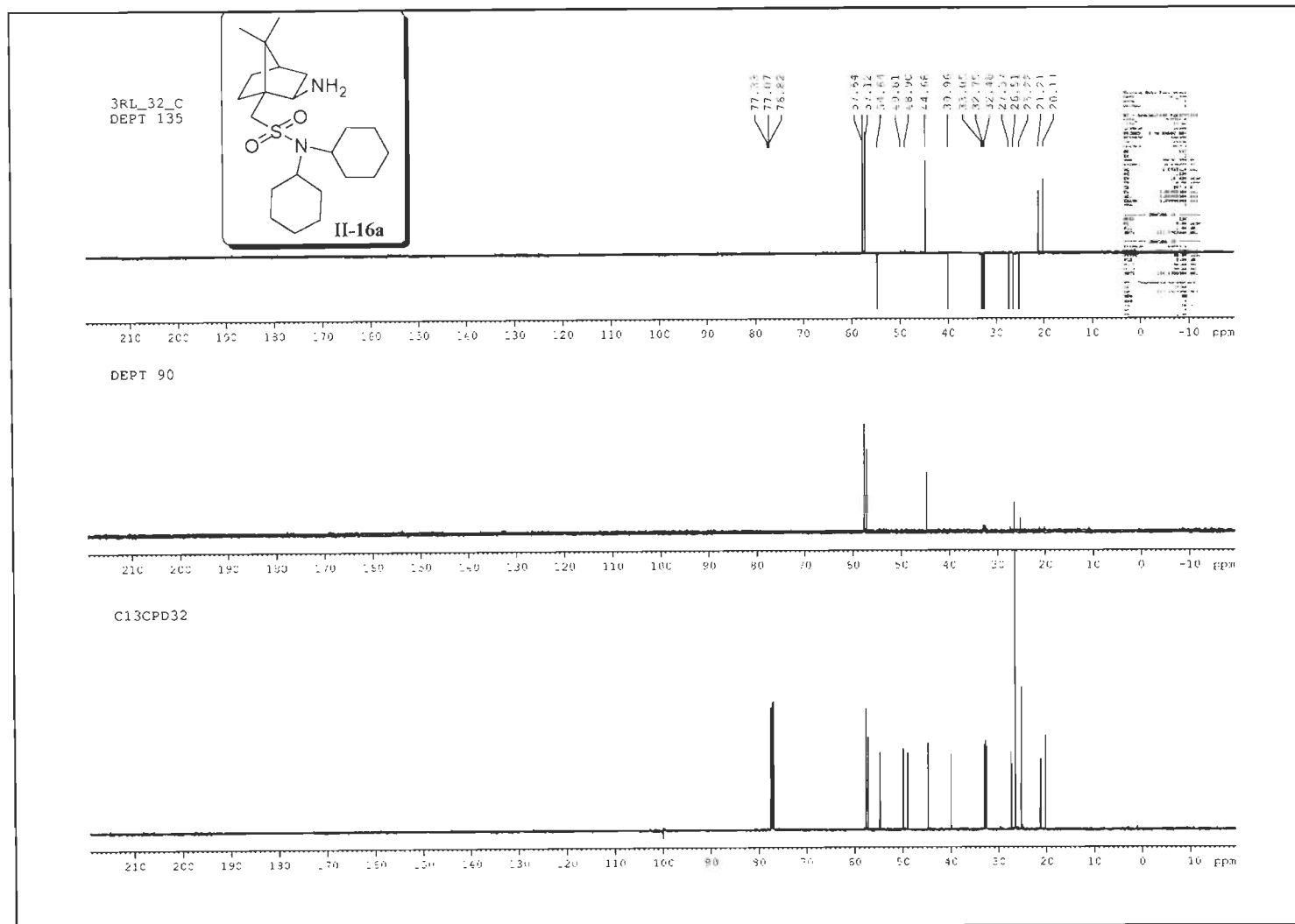


Figure S-36: ^{13}C DEPT (125 MHz, CDCl_3) Spectra of II-16a.

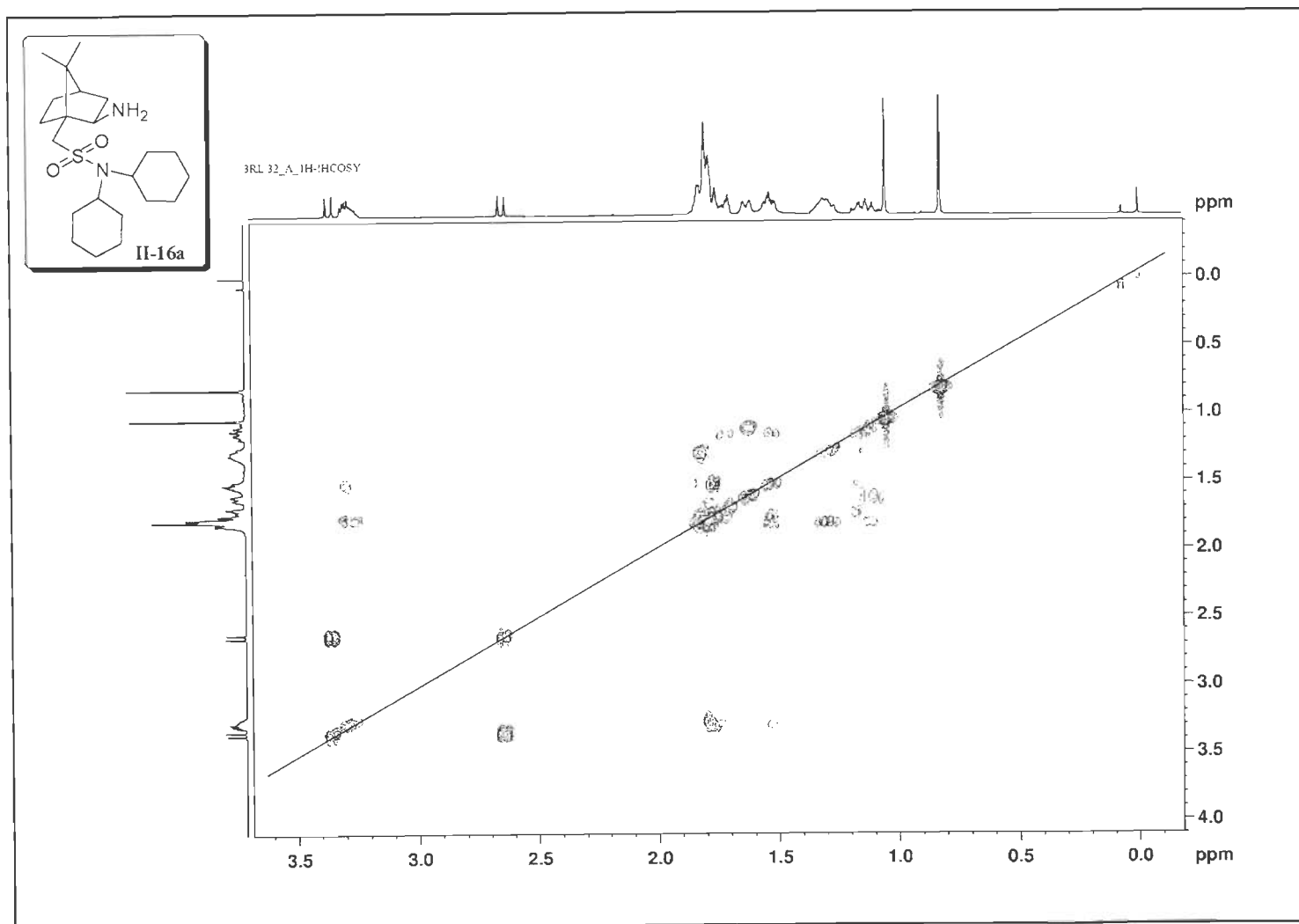


Figure S-37: ^1H - ^1H COSY (500 MHz, CDCl_3) Spectrum of II-16a.

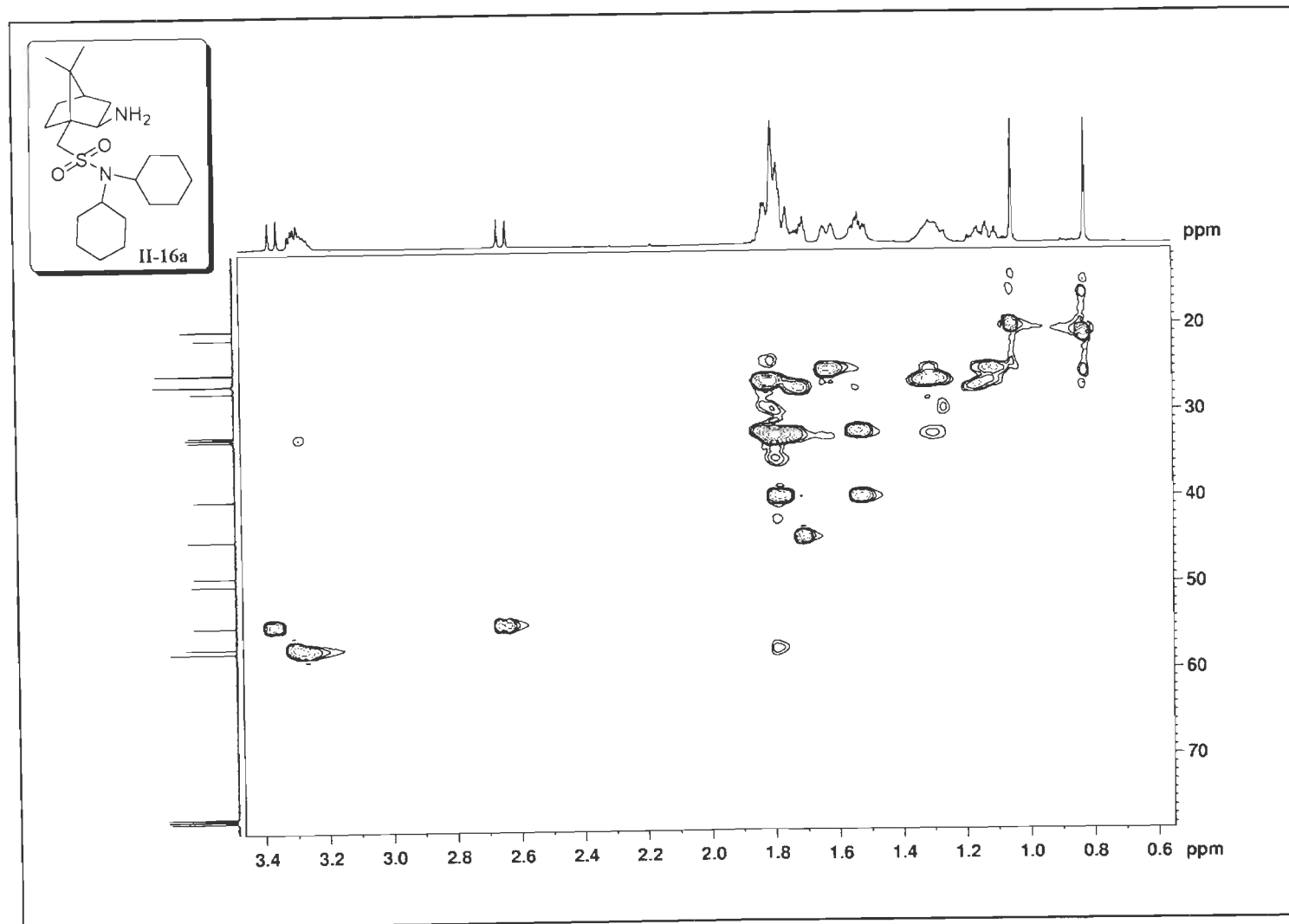


Figure S-38: HSQC (^1H - ^{13}C) (125 MHz, CDCl_3) Spectrum of II-16a.

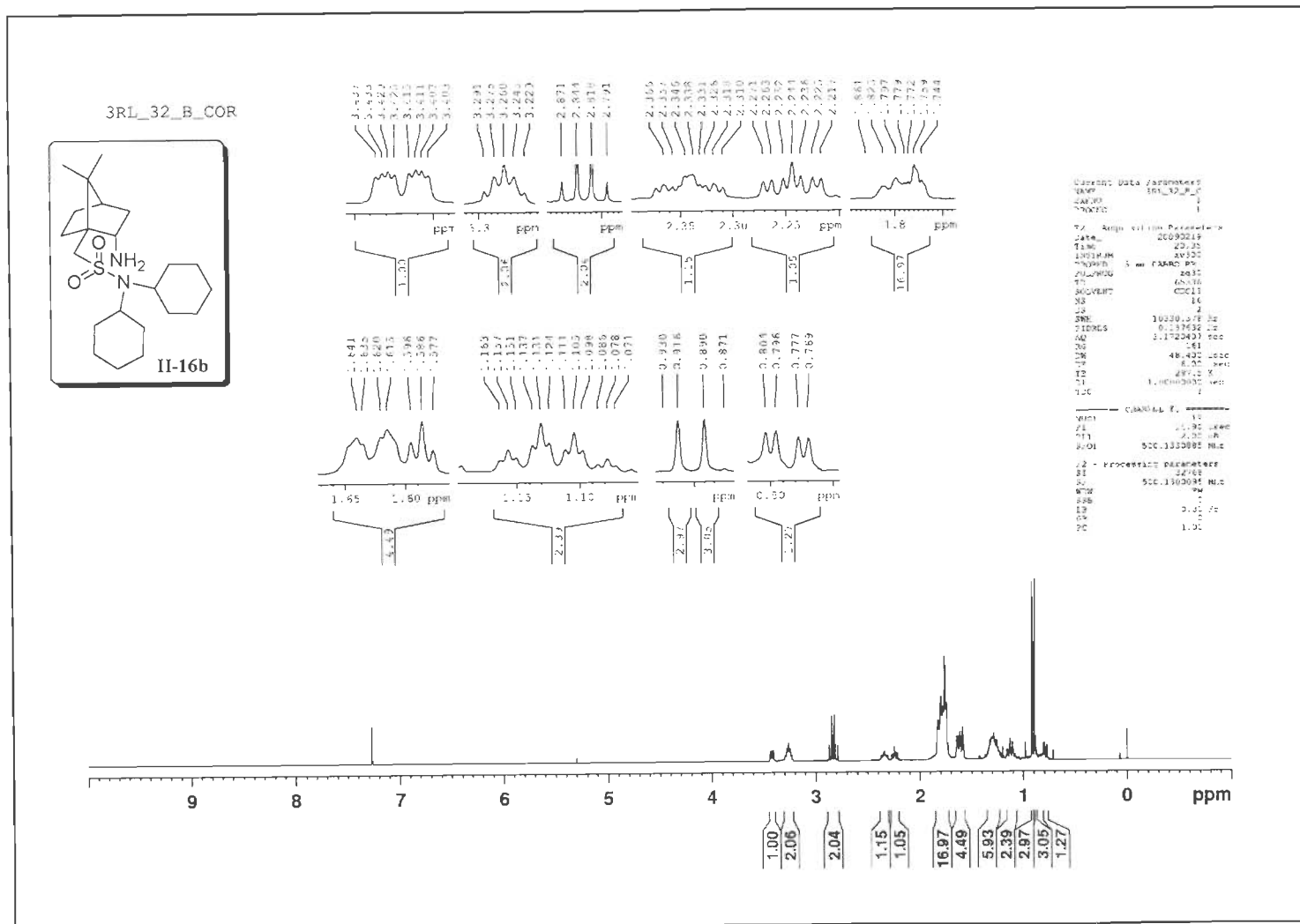


Figure S-39: ^1H NMR (500 MHz, CDCl_3) Spectrum of II-16b.

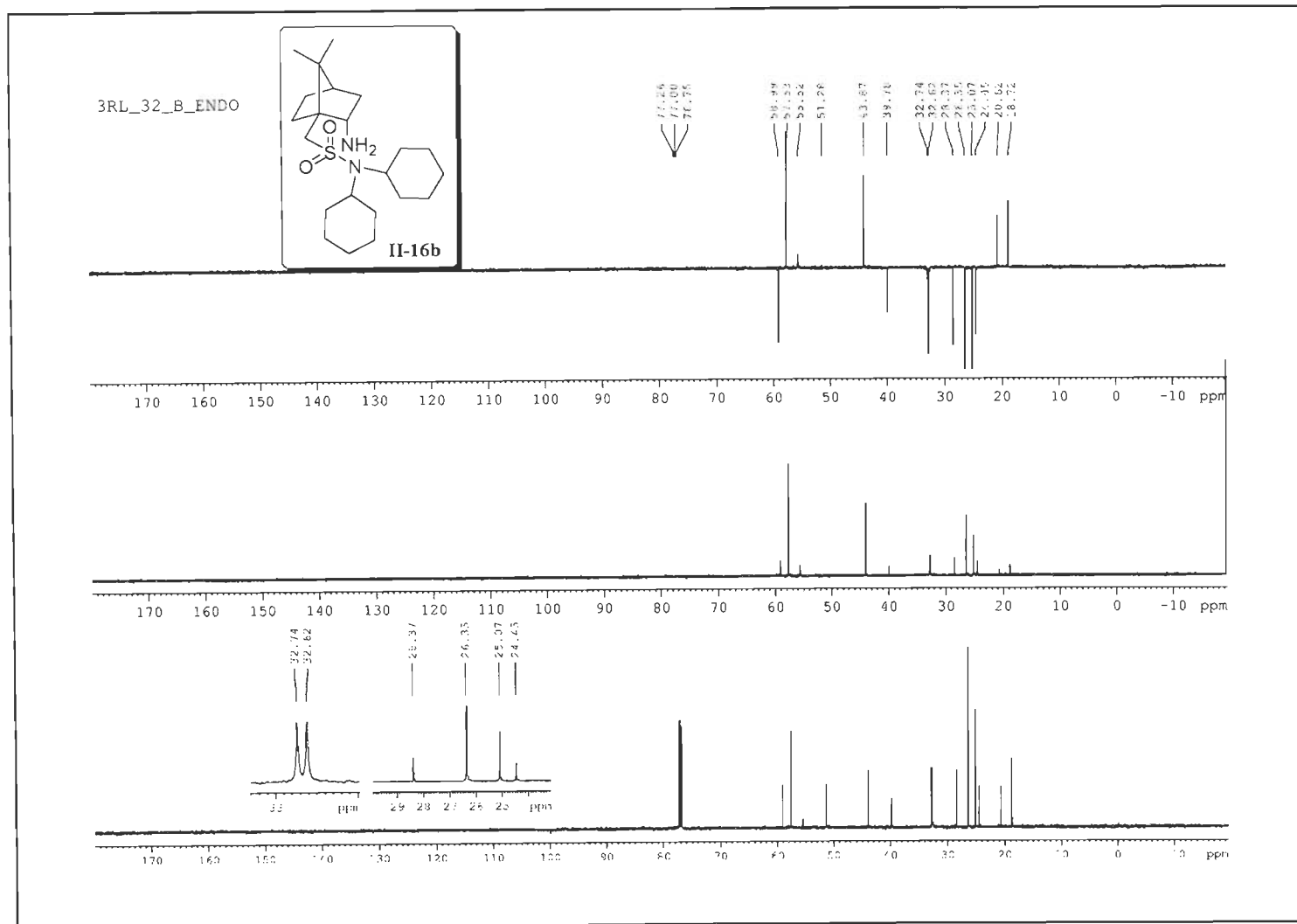


Figure S-40: ^{13}C DEPT (125 MHz, CDCl_3) Spectra of II-16b.

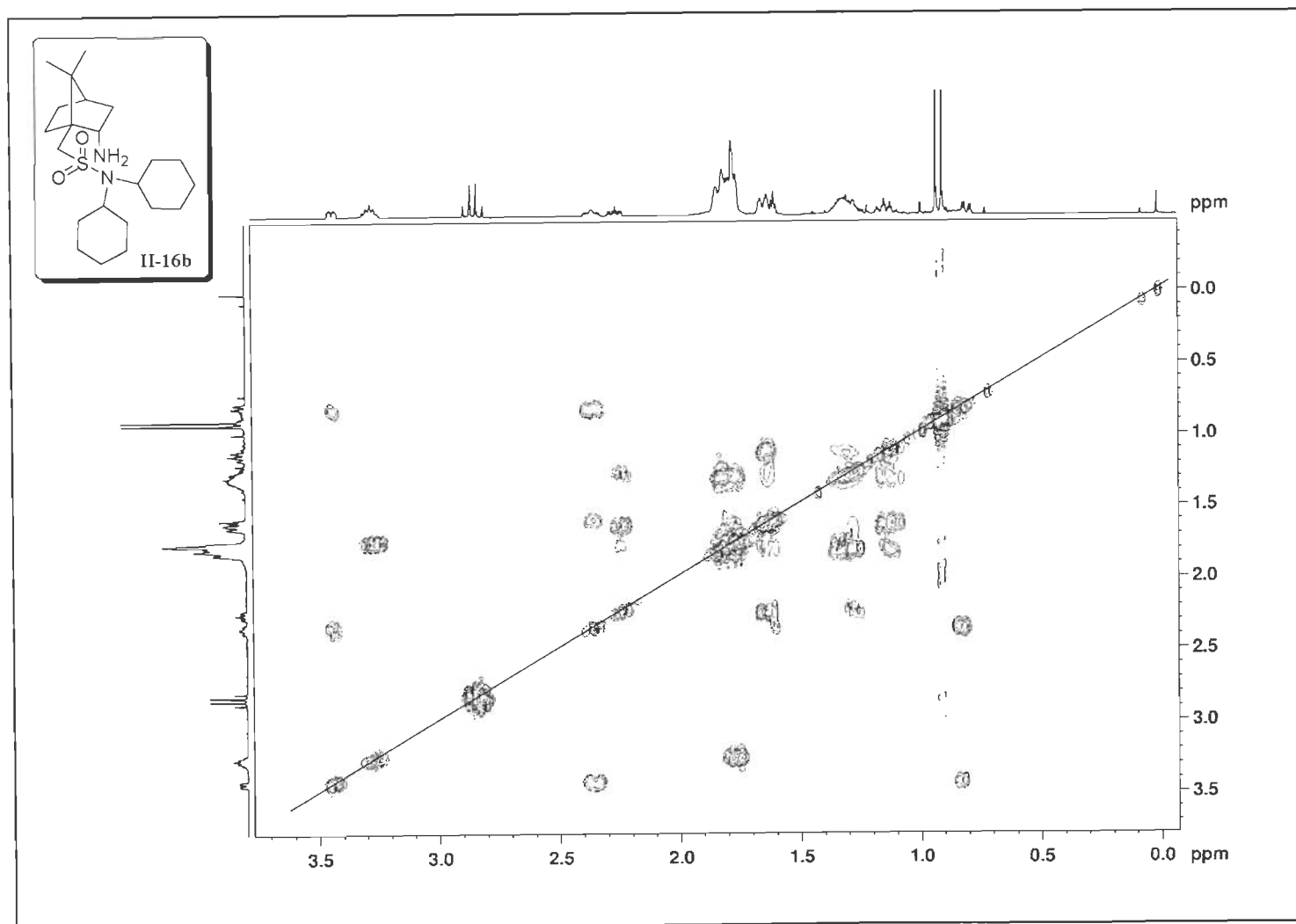


Figure S-41: ^1H - ^1H COSY (500 MHz, CDCl_3) Spectrum of **II-16b**.

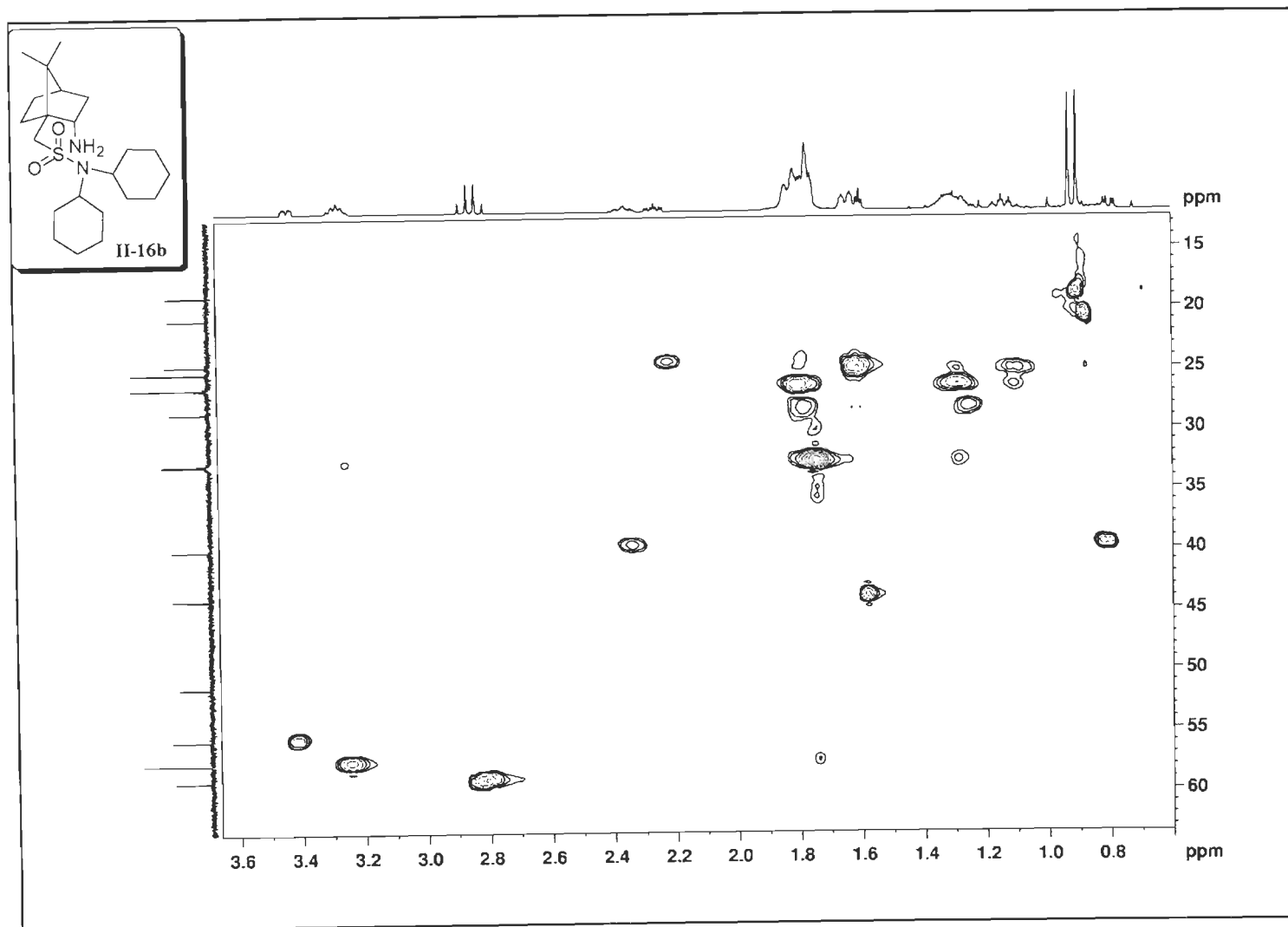


Figure S-42: HSQC (¹H-¹³C) (125 MHz, CDCl₃) Spectrum of **II-16b**.

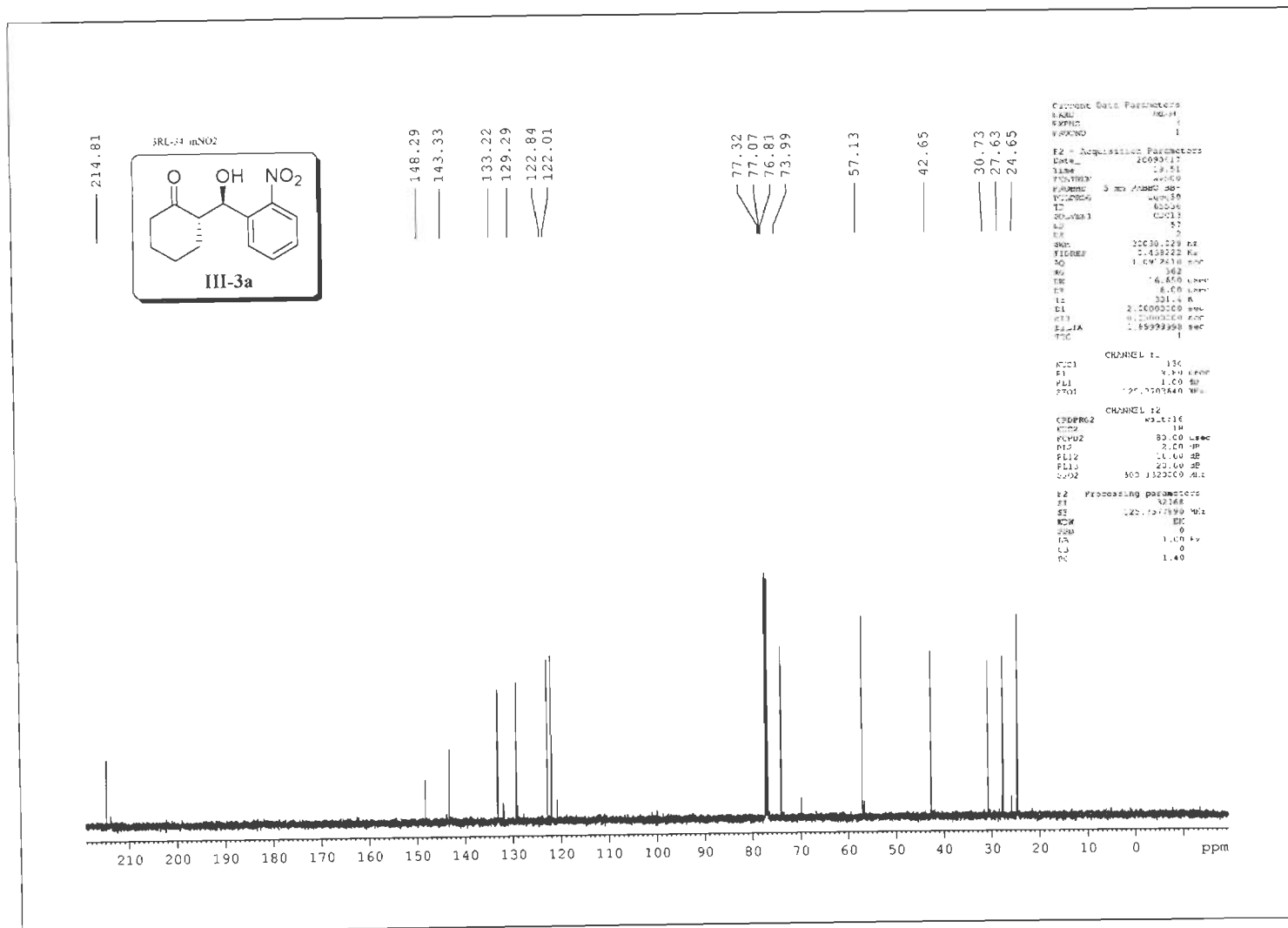


Figure S-44: ¹³C NMR (125 MHz, CDCl₃) Spectrum of III-3b.

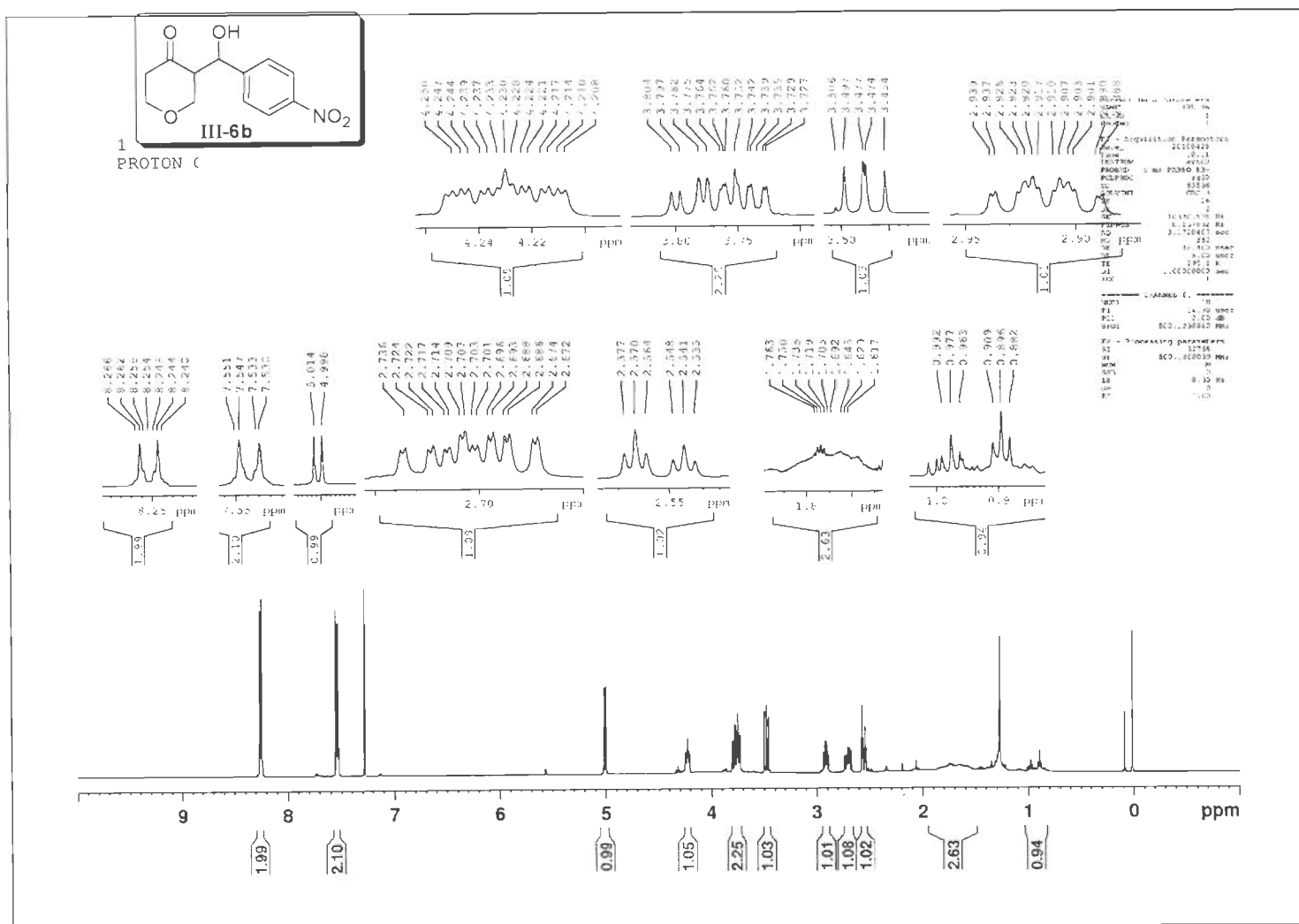


Figure S-45: ^1H NMR (500 MHz, CDCl_3) Spectrum of III-6b.

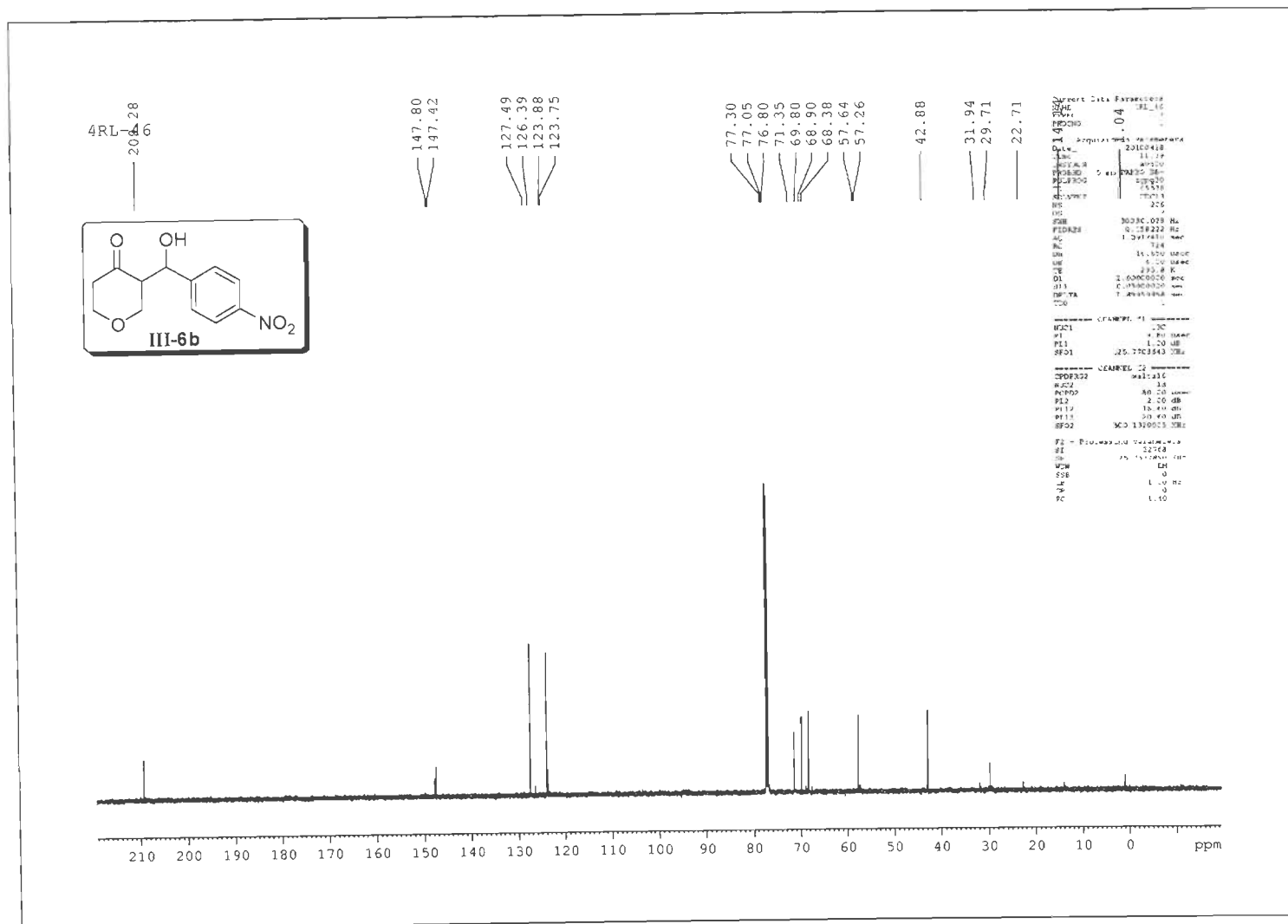


Figure S-46: ¹³C NMR (125 MHz, CDCl₃) Spectrum of III-6b.

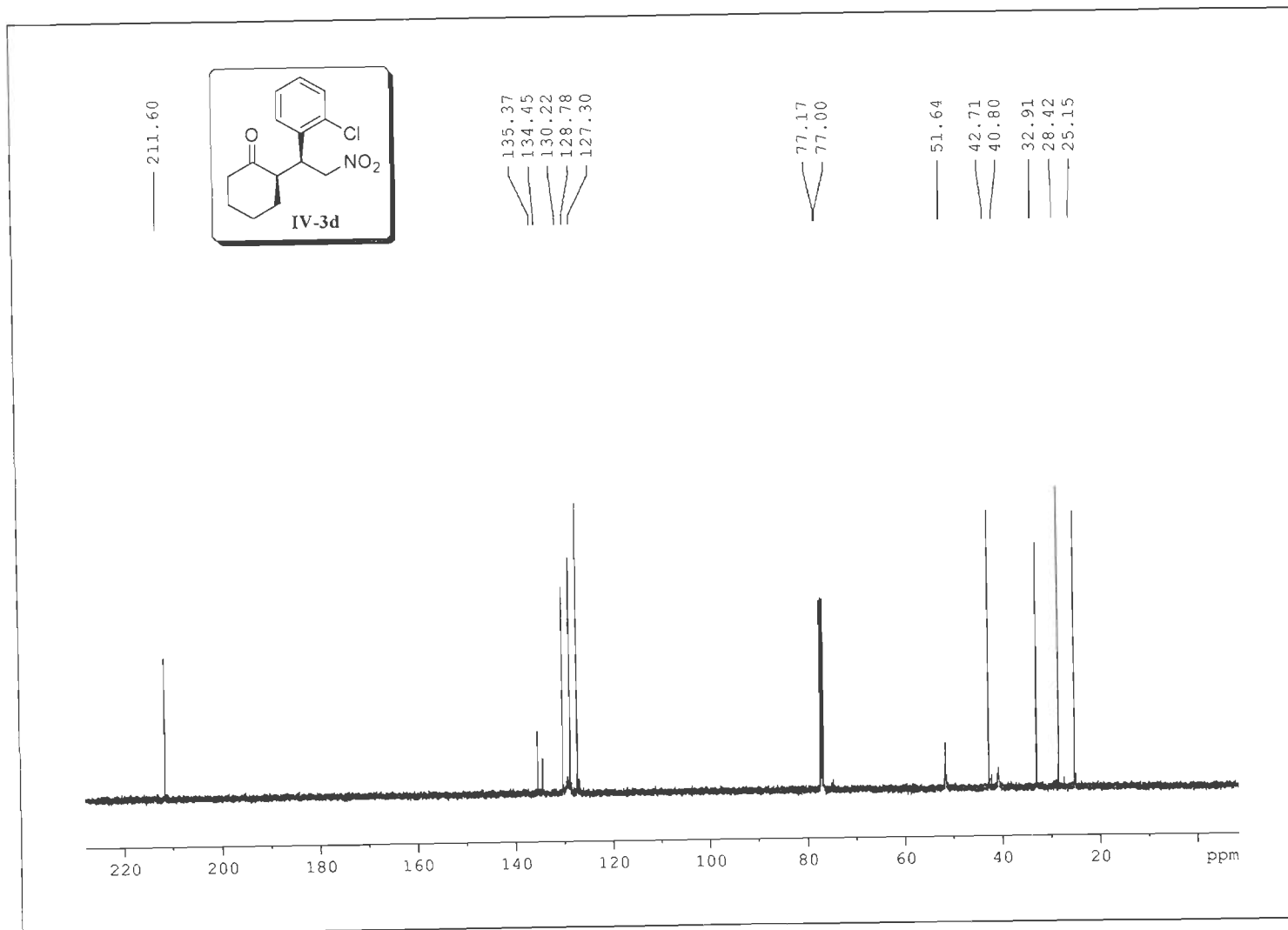
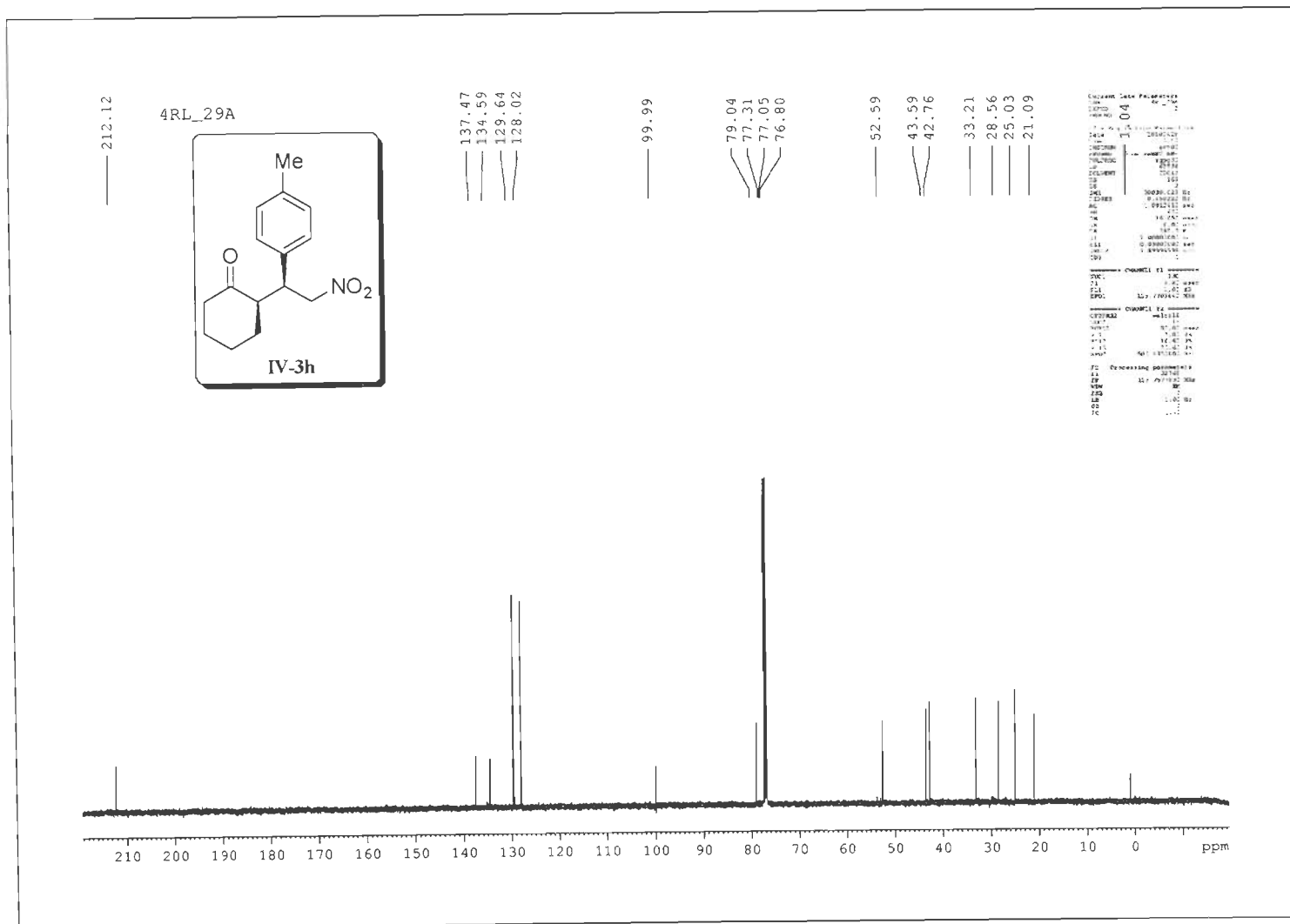


Figure S-48: ¹³C NMR (125 MHz, CDCl₃) Spectrum of IV-3d.

Figure S-50: ^{13}C NMR (125 MHz, CDCl_3) Spectrum of IV-3h.

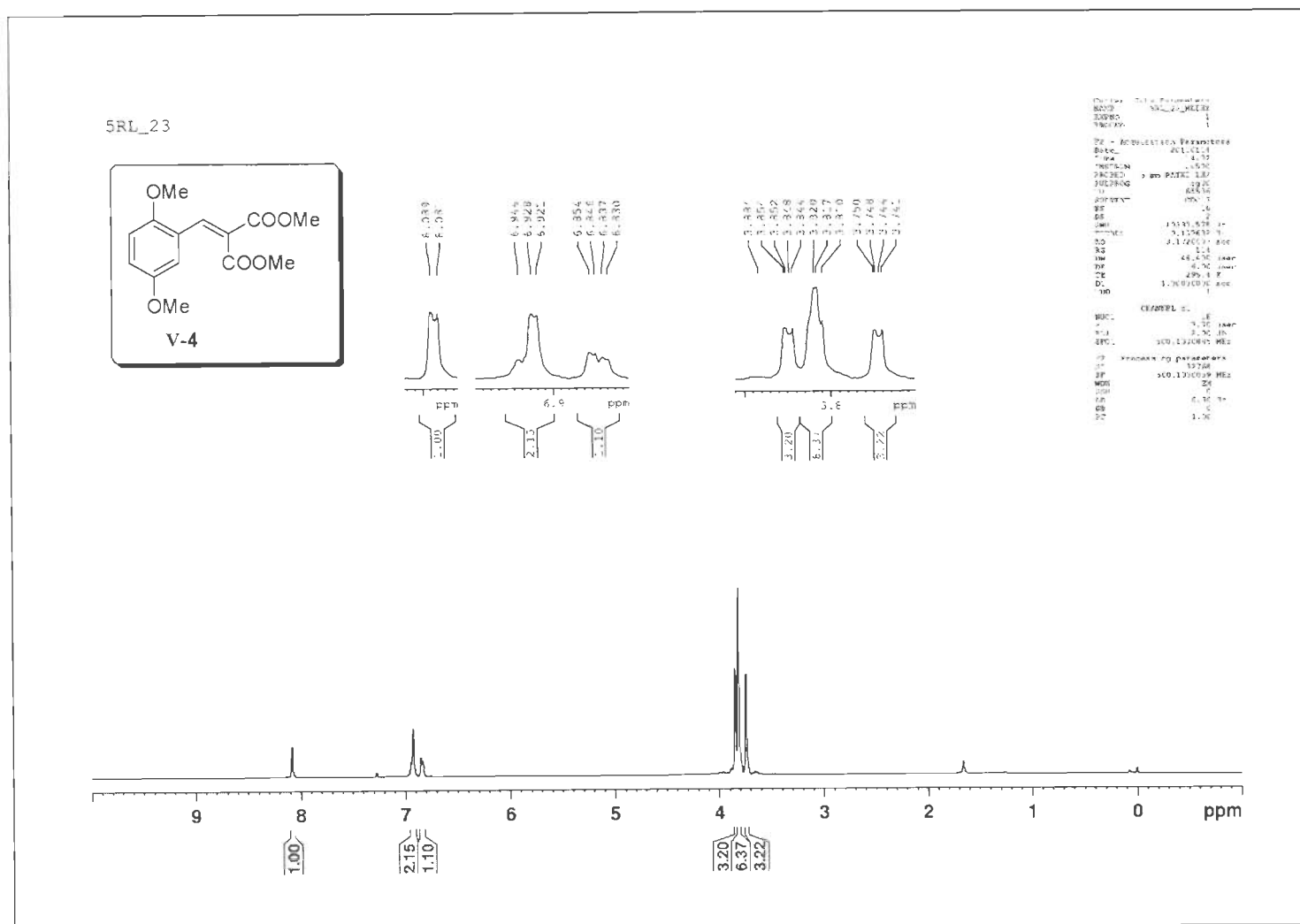


Figure S-51: ^1H NMR (500 MHz, CDCl_3) Spectrum of V-4.

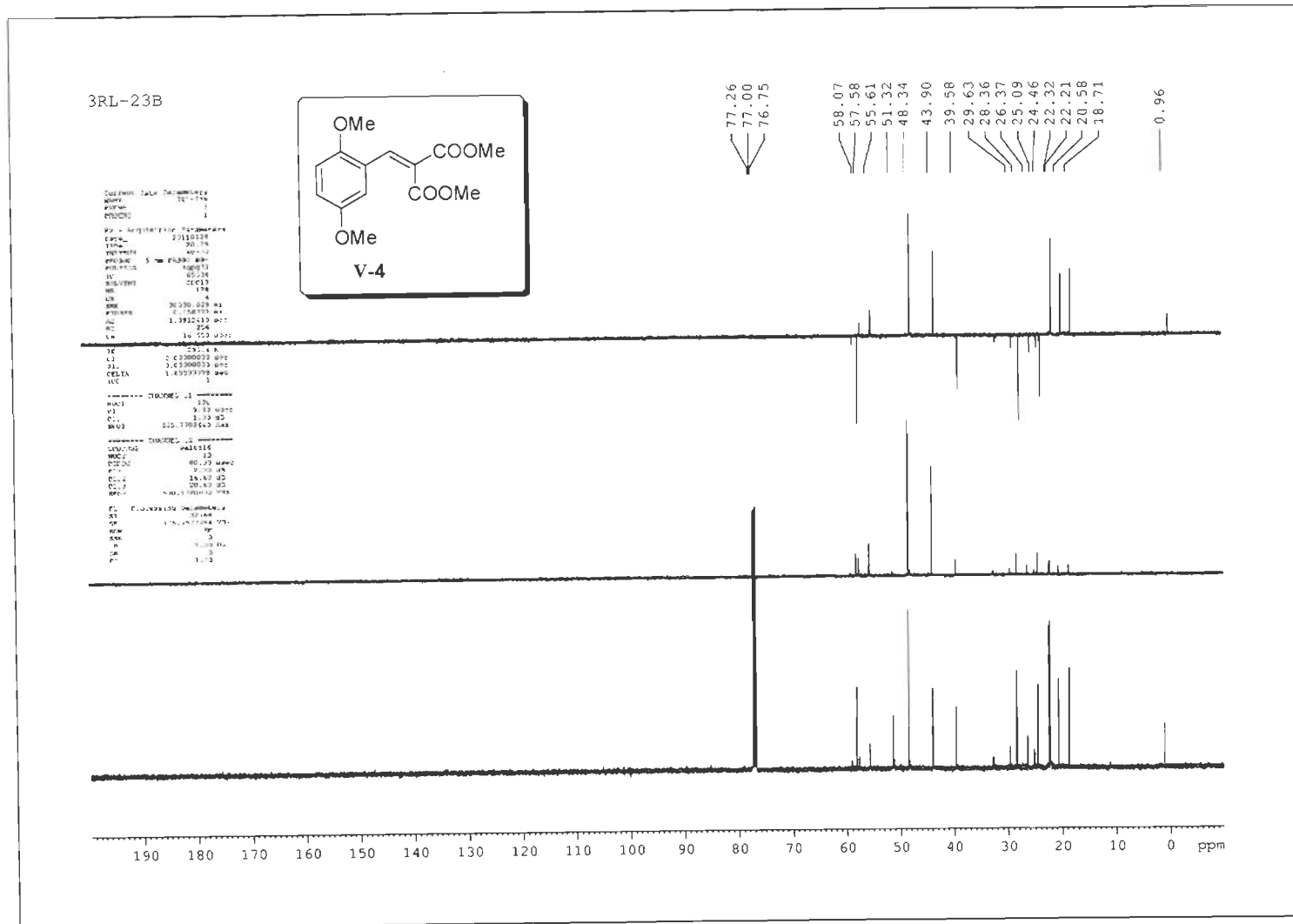


Figure S-52: ¹³C DEPT (125 MHz, CDCl₃) Spectra of V-4.

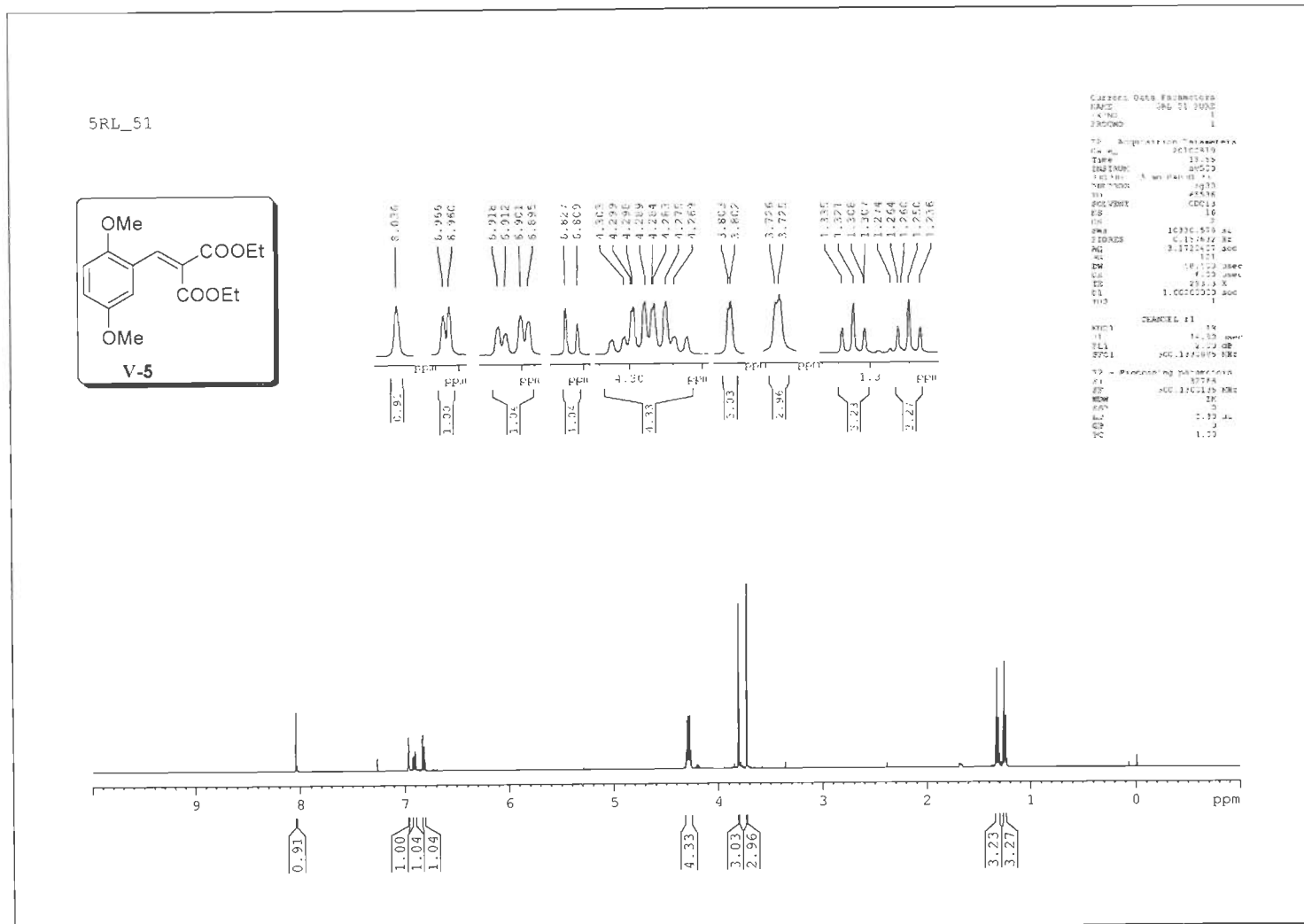


Figure S-53: ¹H NMR (500 MHz, CDCl₃) Spectrum of V-5.

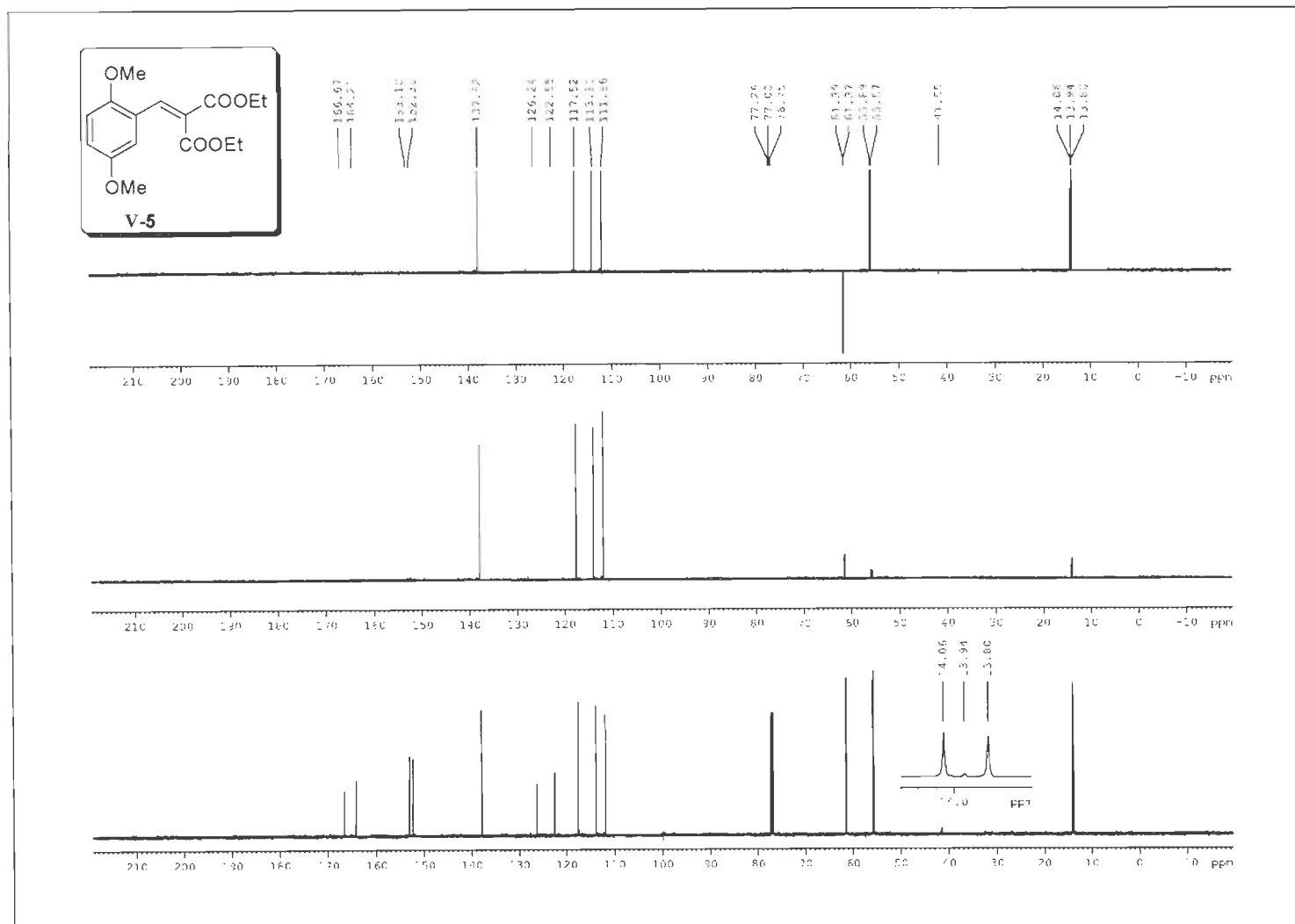


Figure S-54: ^{13}C DEPT (125 MHz, CDCl_3) Spectra of V-5.

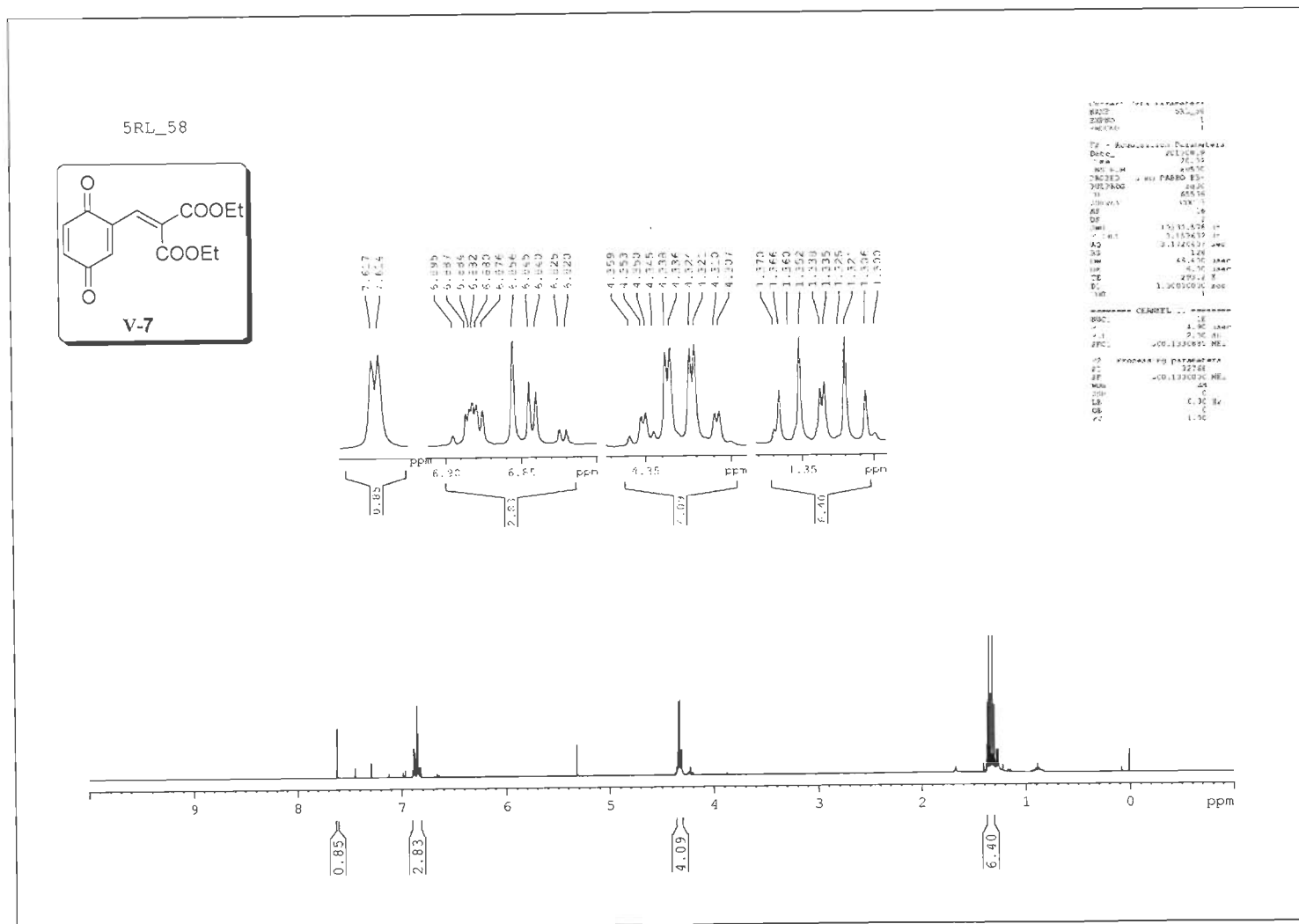


Figure S-55: ^1H NMR (500 MHz, CDCl_3) Spectrum of V-7.

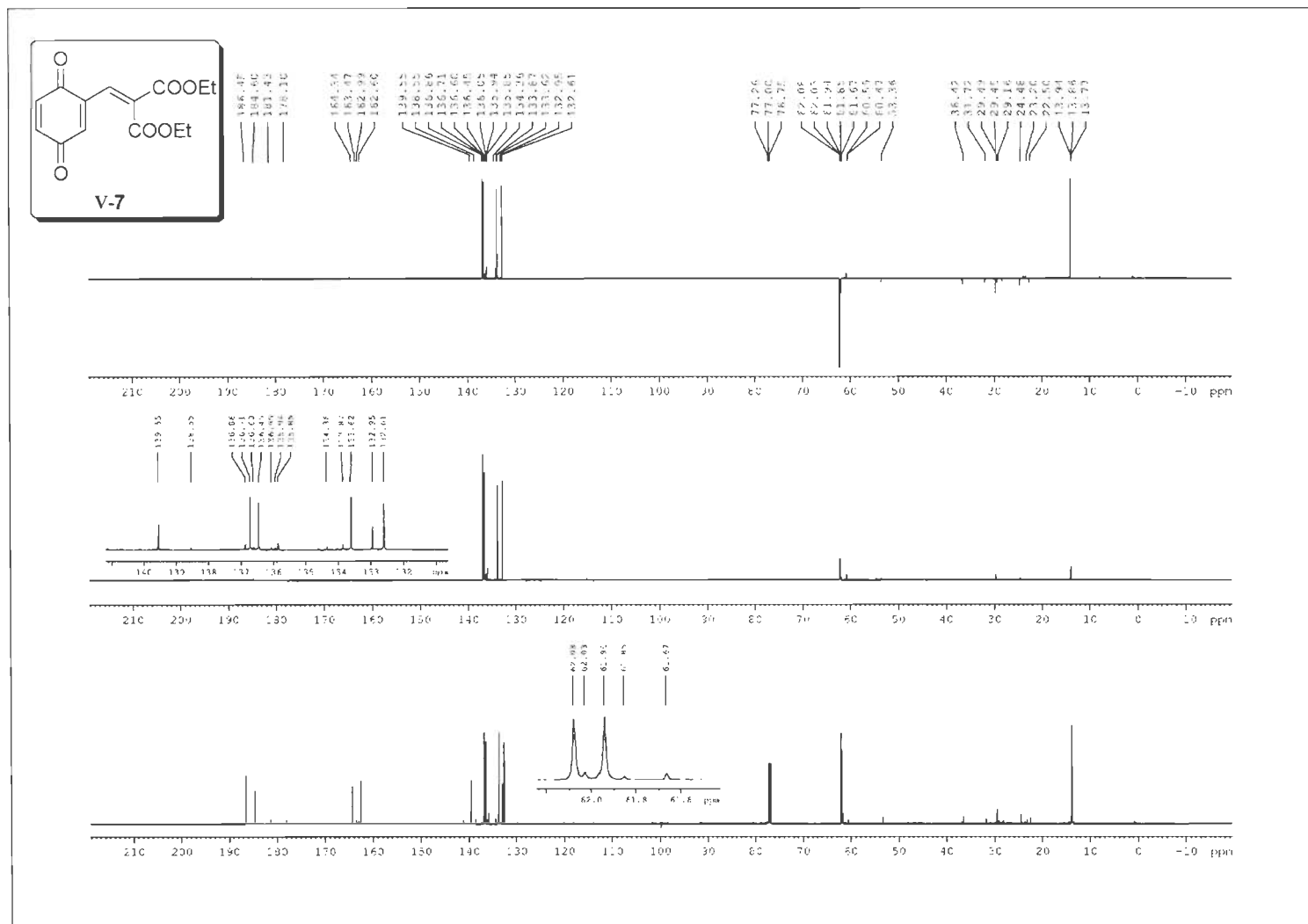


Figure S-56: ^{13}C DEPT (125 MHz, CDCl_3) Spectra of V-7.

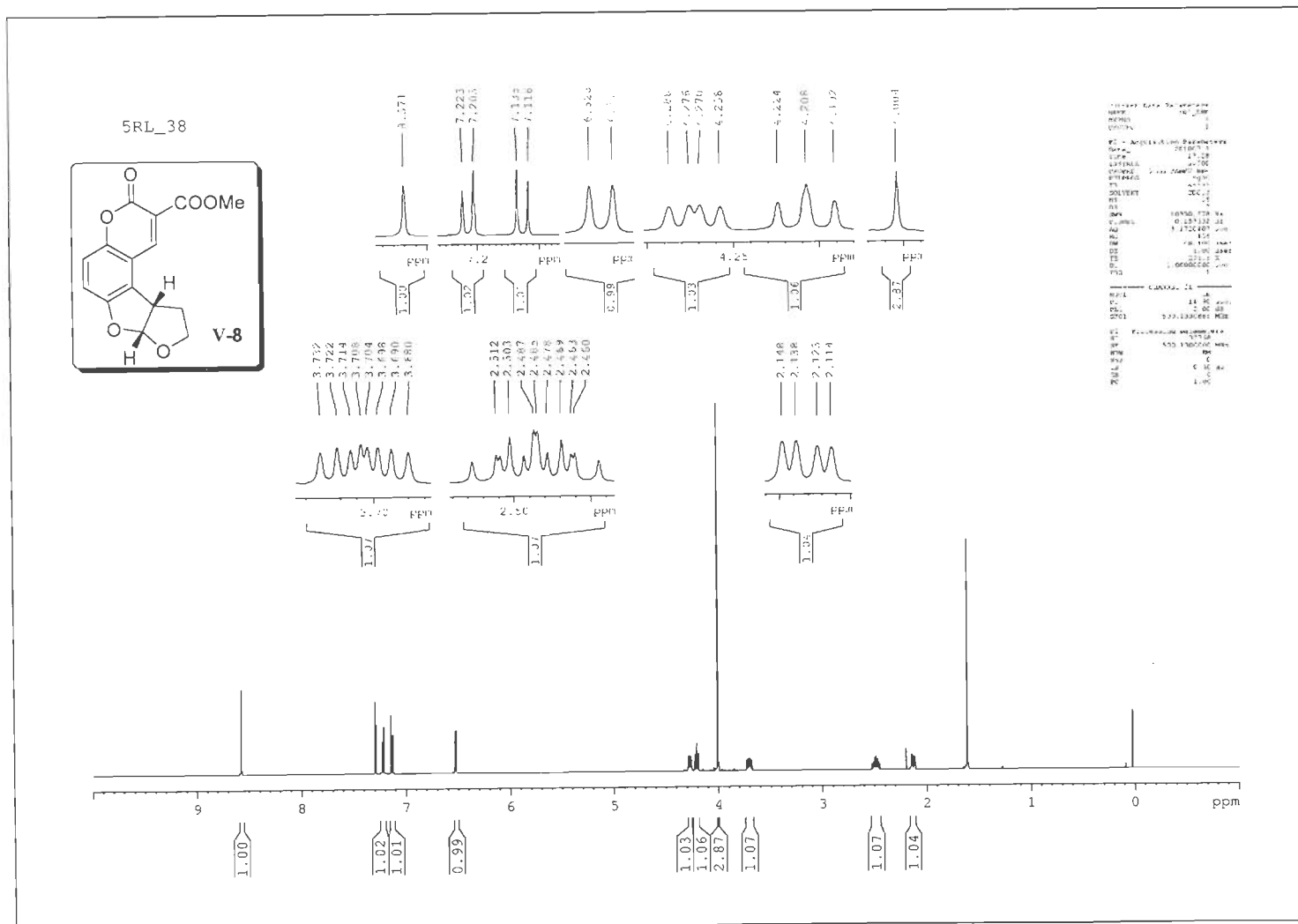


Figure S-57: ^1H NMR (500 MHz, CDCl_3) Spectrum of V-8.

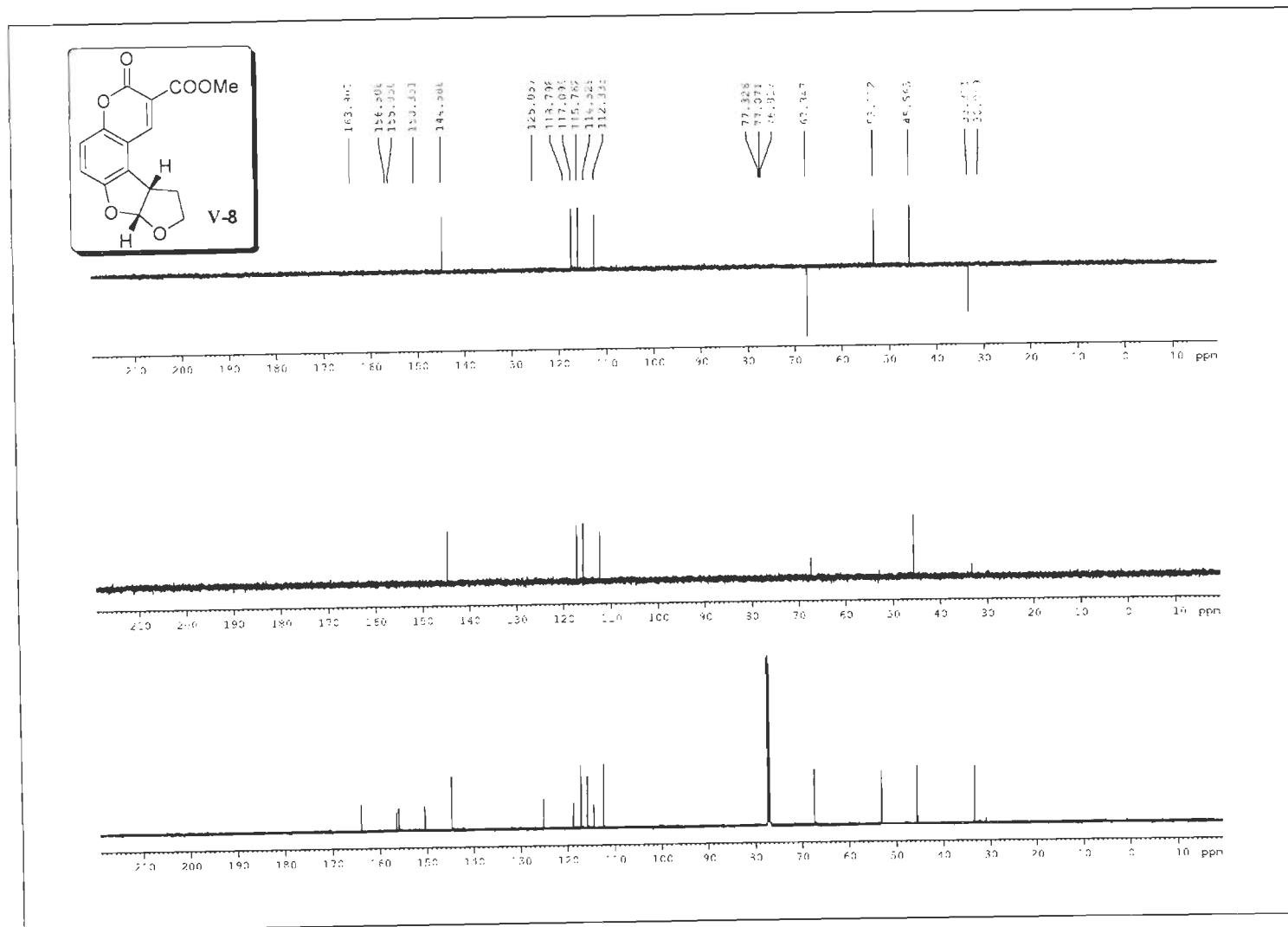


Figure S-58: ^{13}C DEPT (125 MHz, CDCl_3) Spectra of V-8.

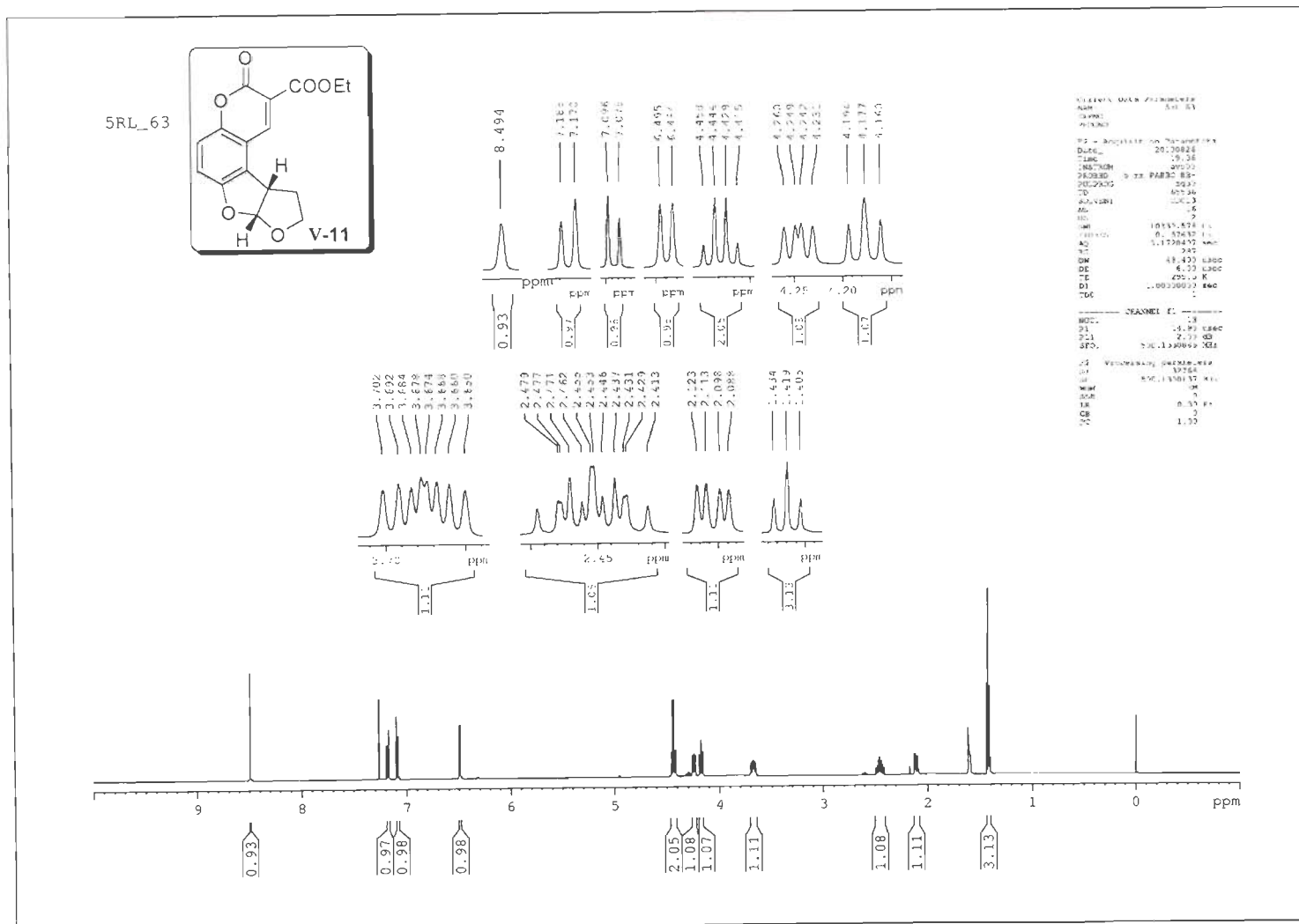


Figure S-59: ^1H NMR (500 MHz, CDCl_3) Spectrum of V-11.

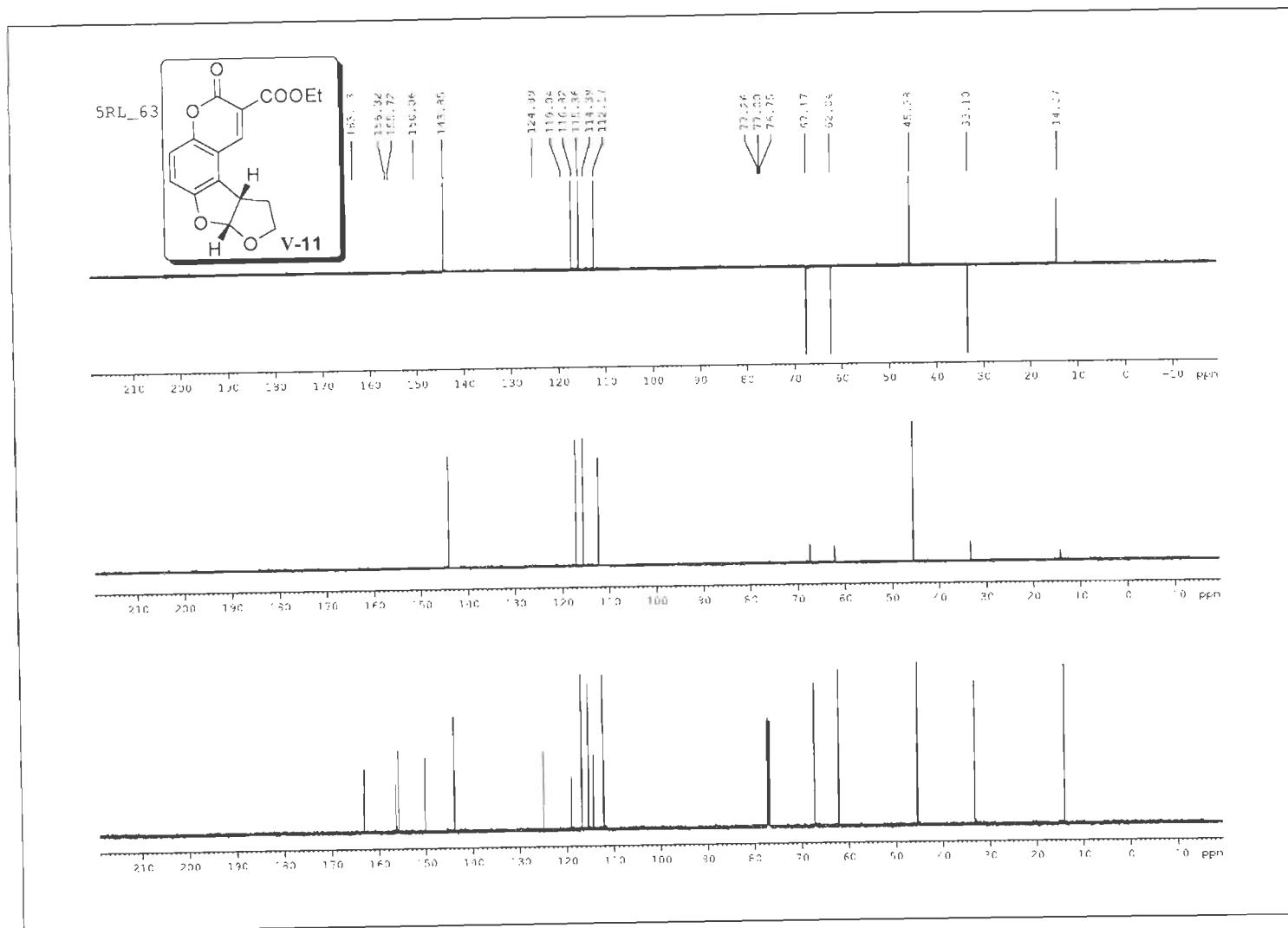


Figure S-60: ^{13}C DEPT (125 MHz, CDCl_3) Spectra of V-11.

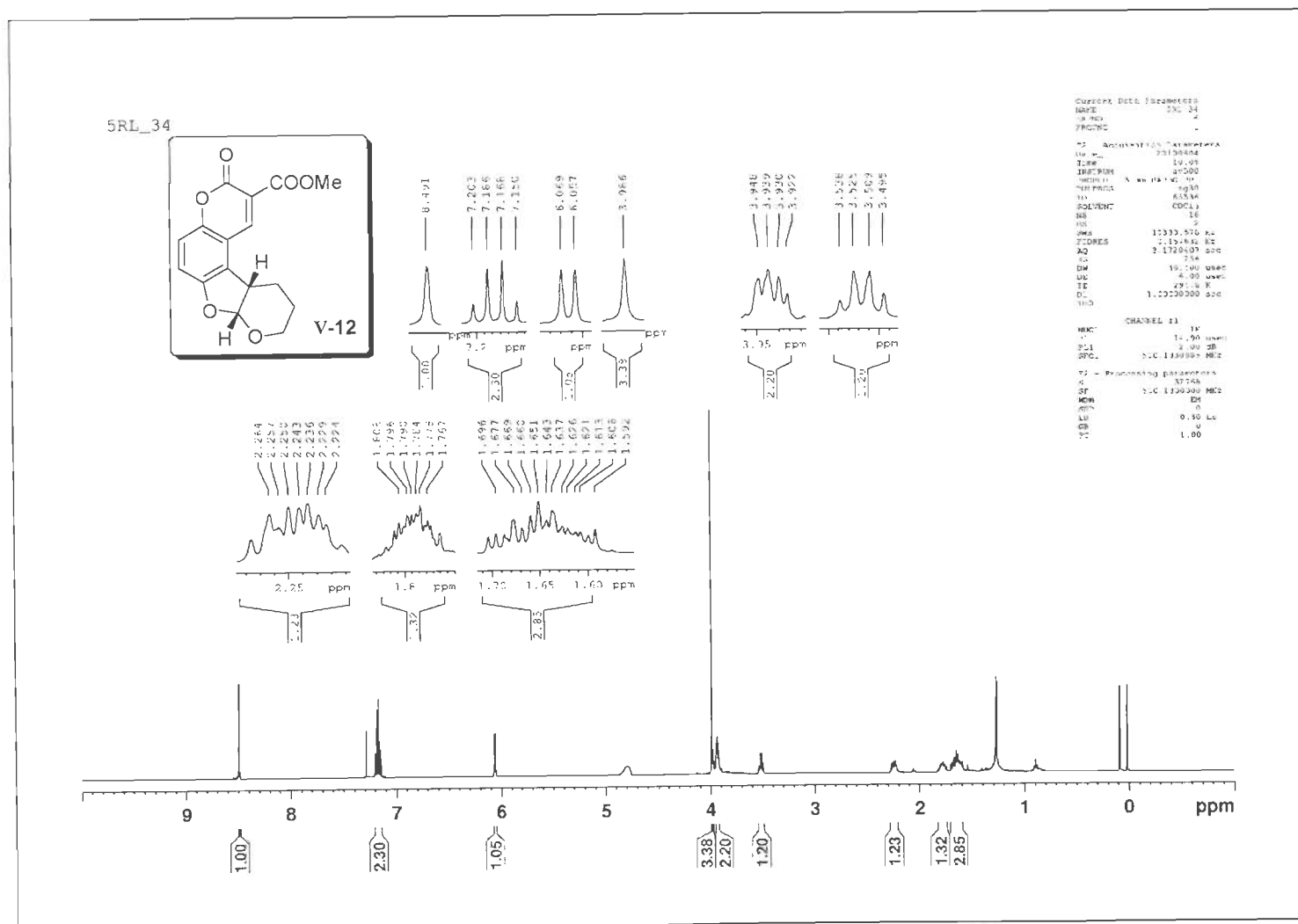


Figure S-61: ^1H NMR (500 MHz, CDCl_3) Spectrum of V-12.

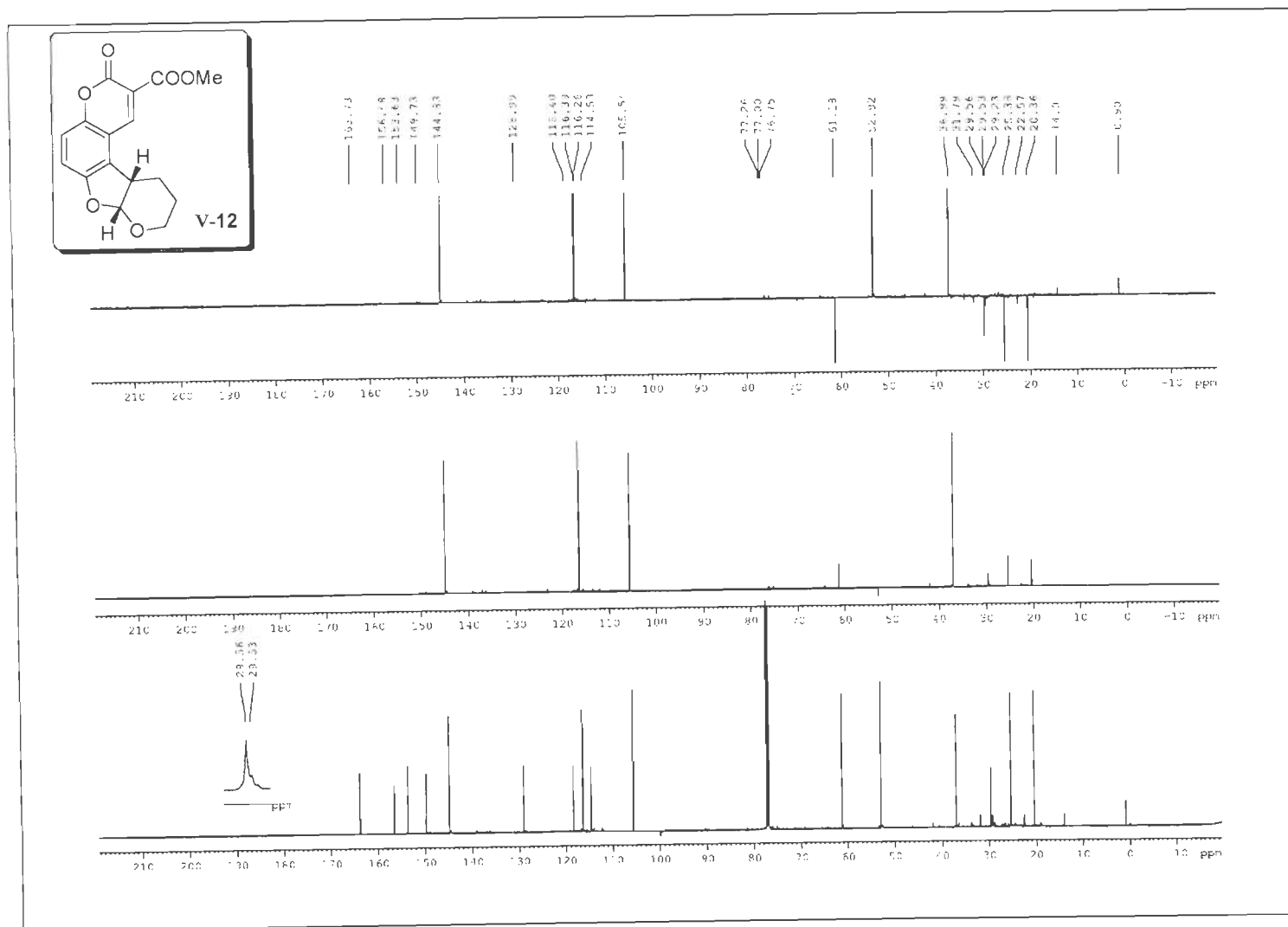


Figure S-62: ^{13}C DEPT (125 MHz, CDCl_3) Spectra of V-12.

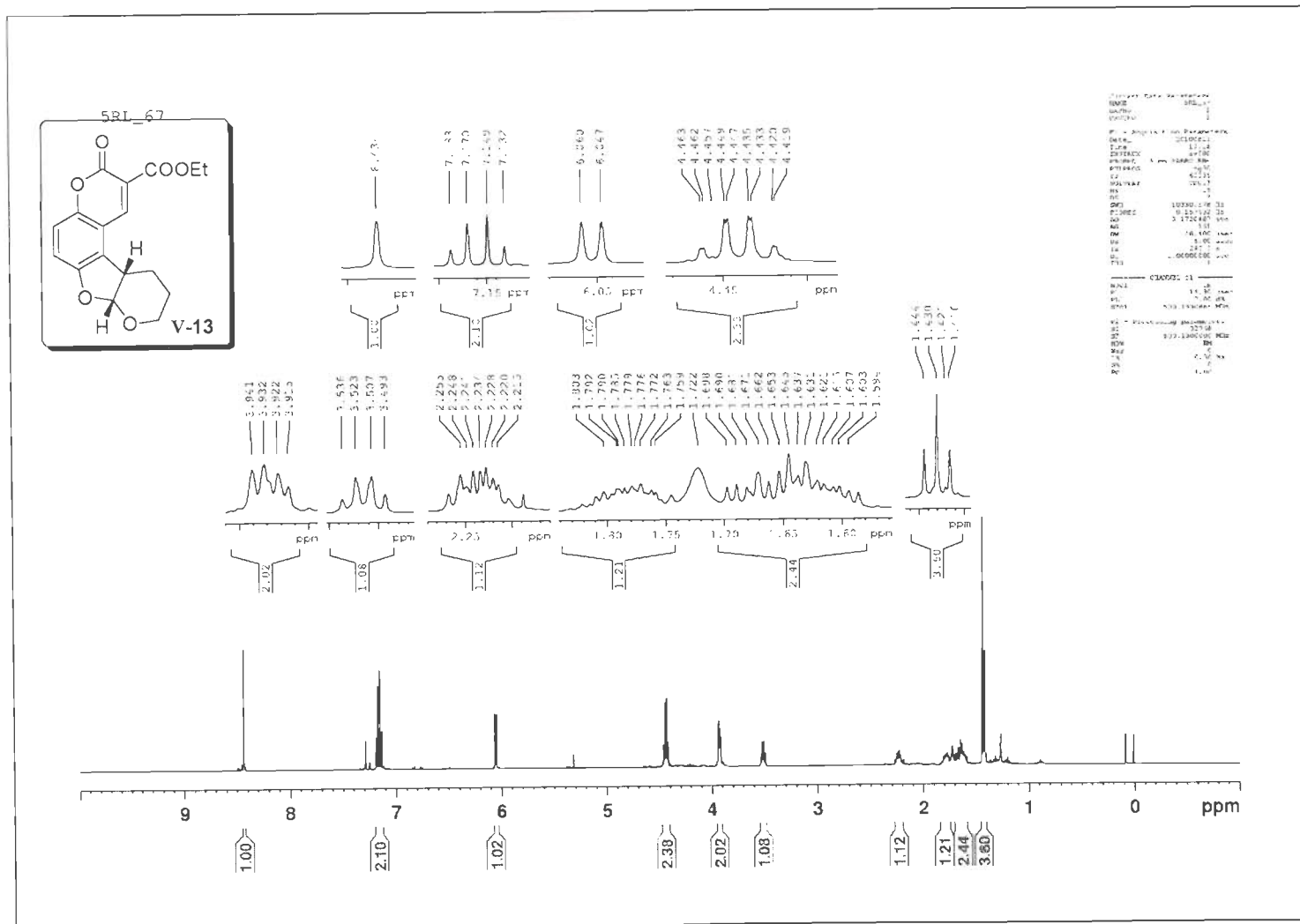


Figure S-63: ¹H NMR (500 MHz, CDCl₃) Spectrum of V-13.

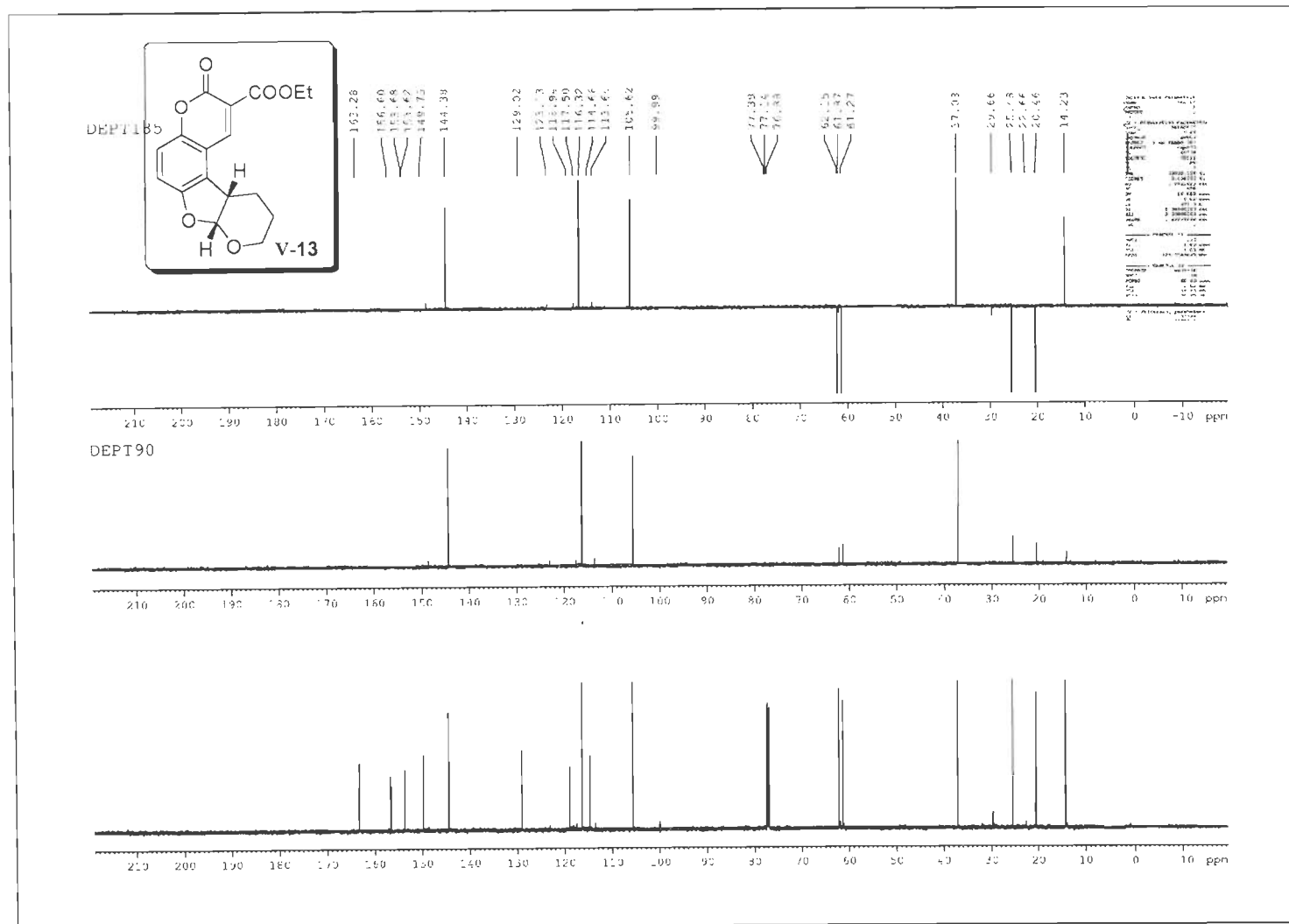


Figure S-64: ^{13}C DEPT (125 MHz, CDCl_3) Spectra of V-13.

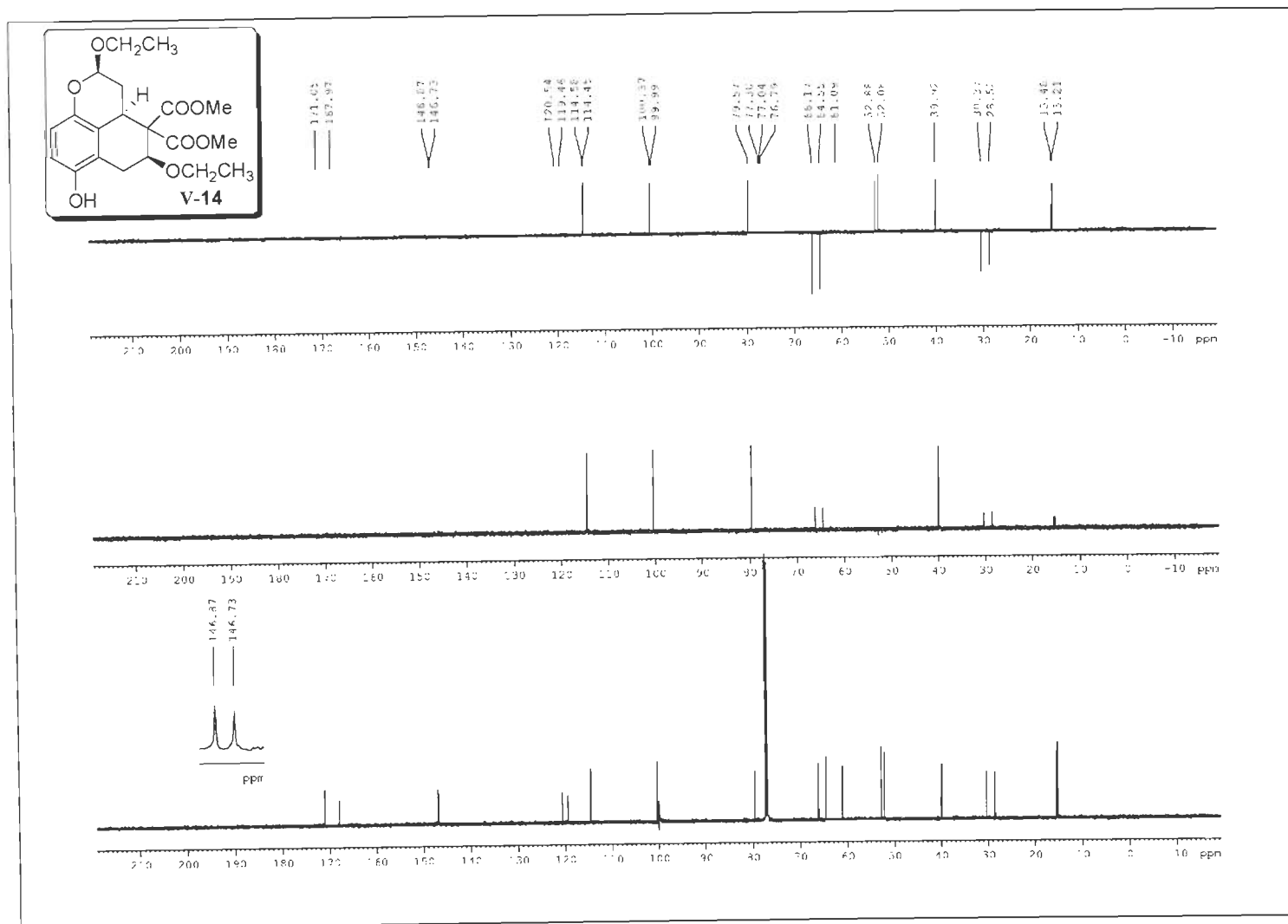
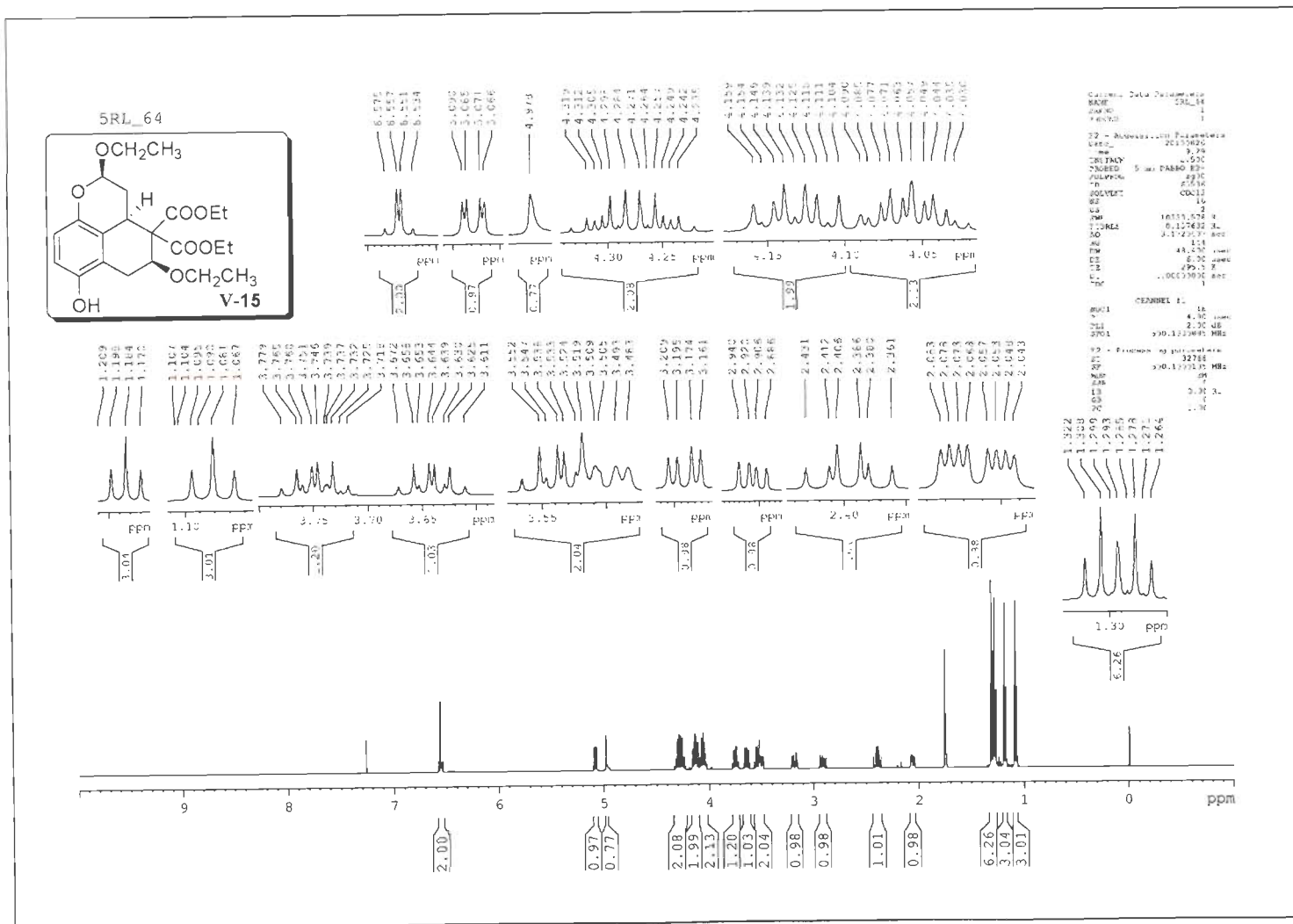


Figure S-66: ^{13}C DEPT (125 MHz, CDCl_3) Spectra of **V-14**.

Figure S-67: ^1H NMR (500 MHz, CDCl_3) Spectrum of V-15.

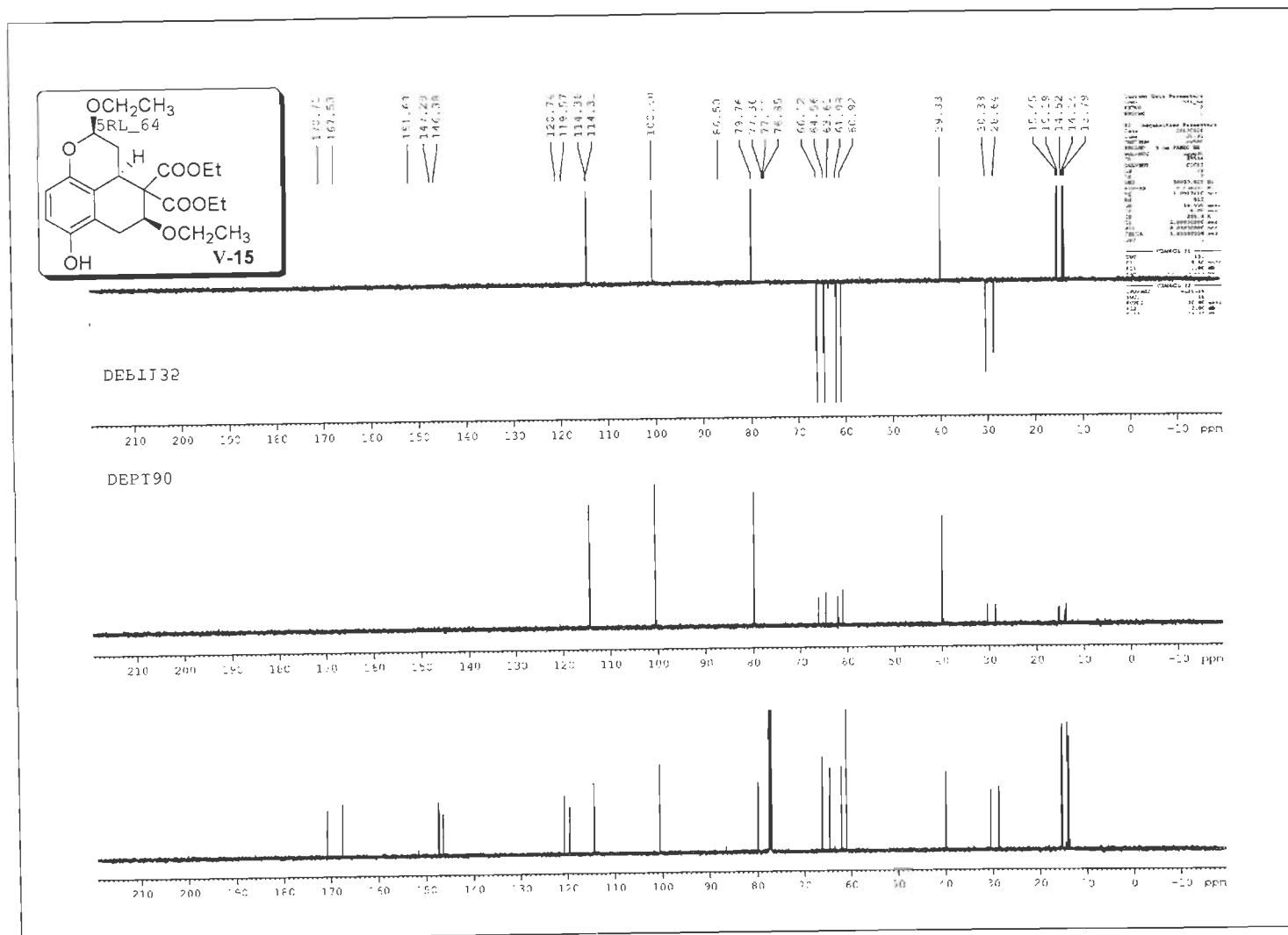


Figure S-68: ^{13}C DEPT (125 MHz, CDCl_3) Spectra of V-15.

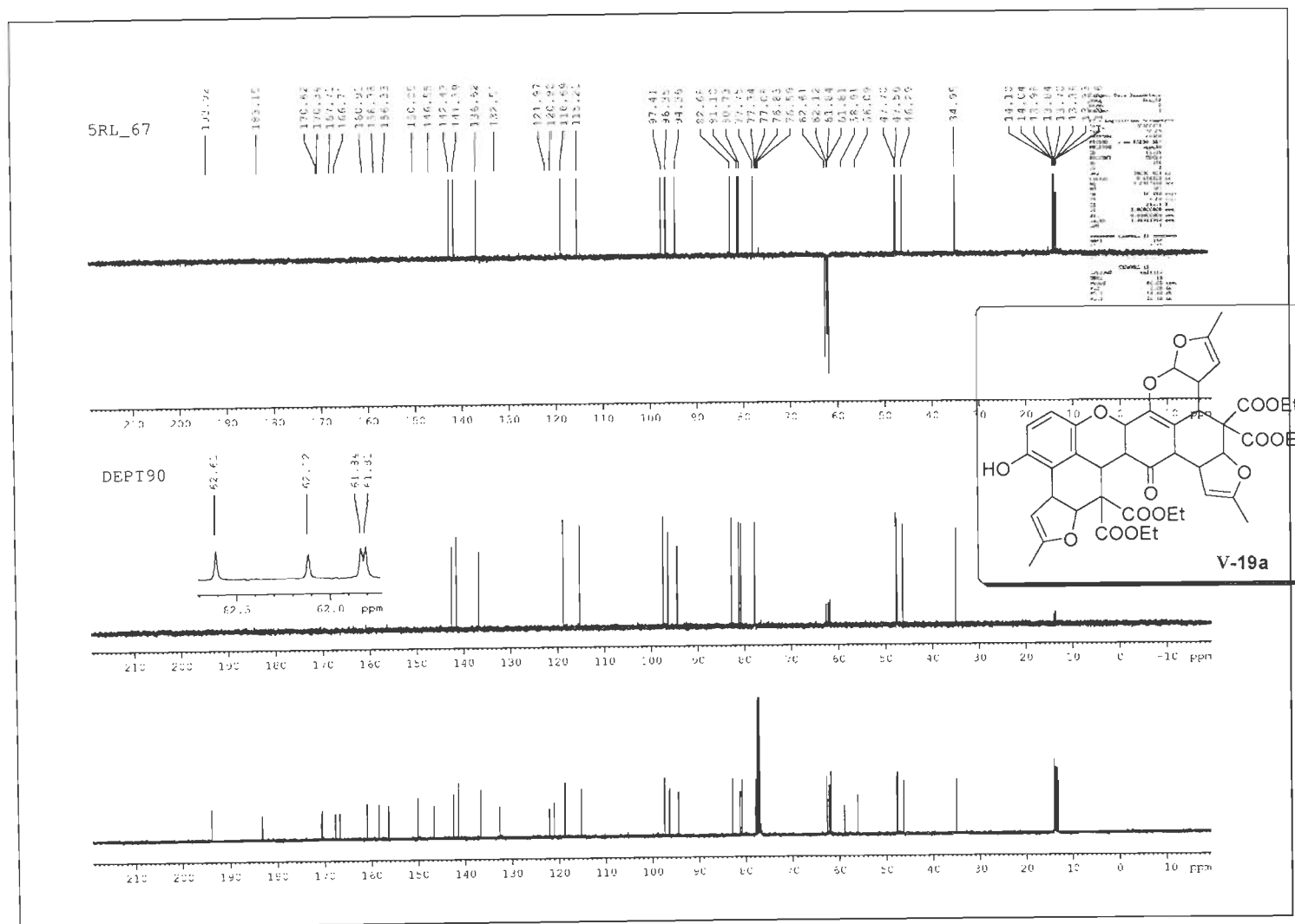


Figure S-70: ^{13}C DEPT (125 MHz, CDCl_3) Spectra of V-19a.

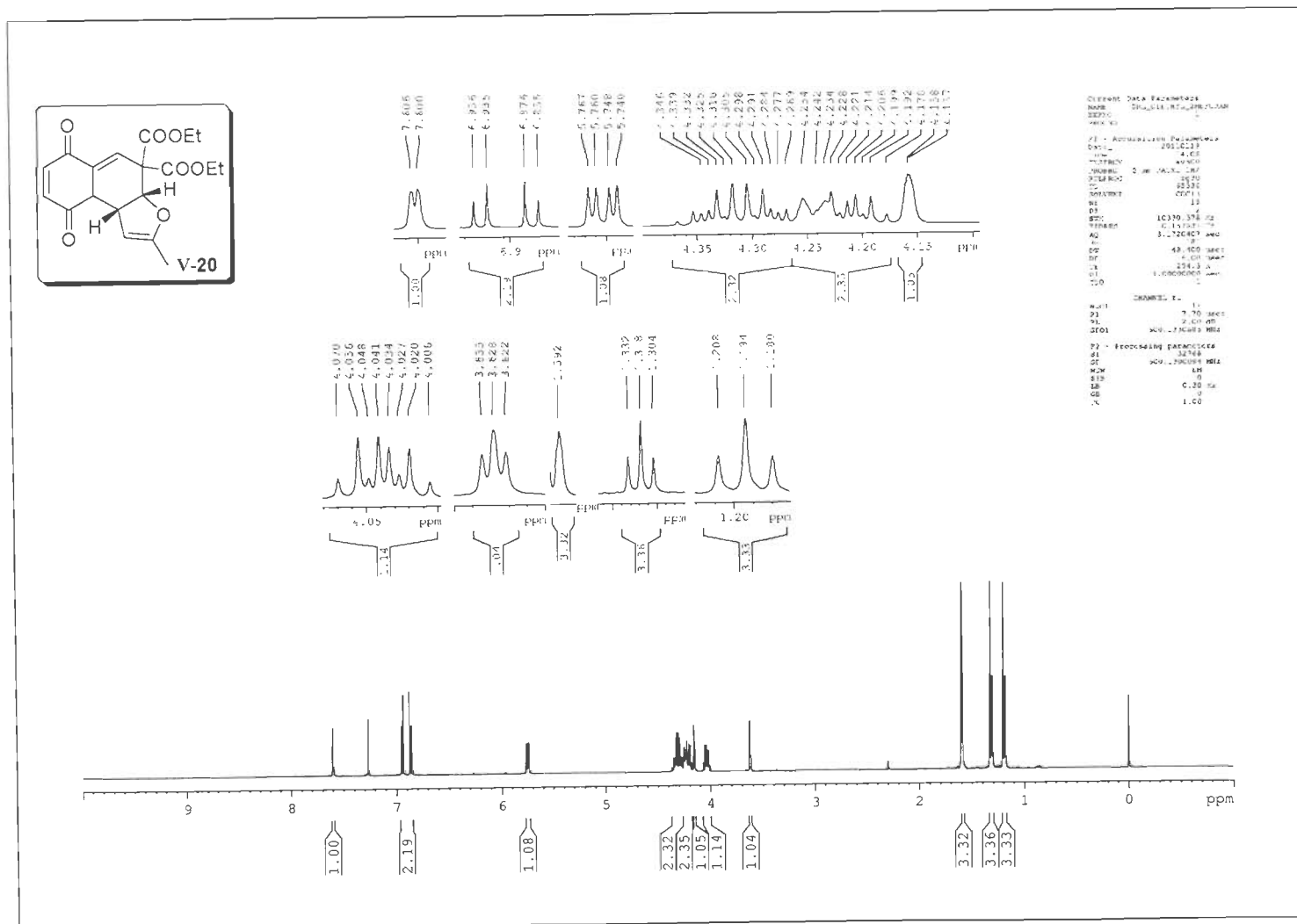


Figure S-71: ^1H NMR (500 MHz, CDCl_3) Spectrum of V-20.

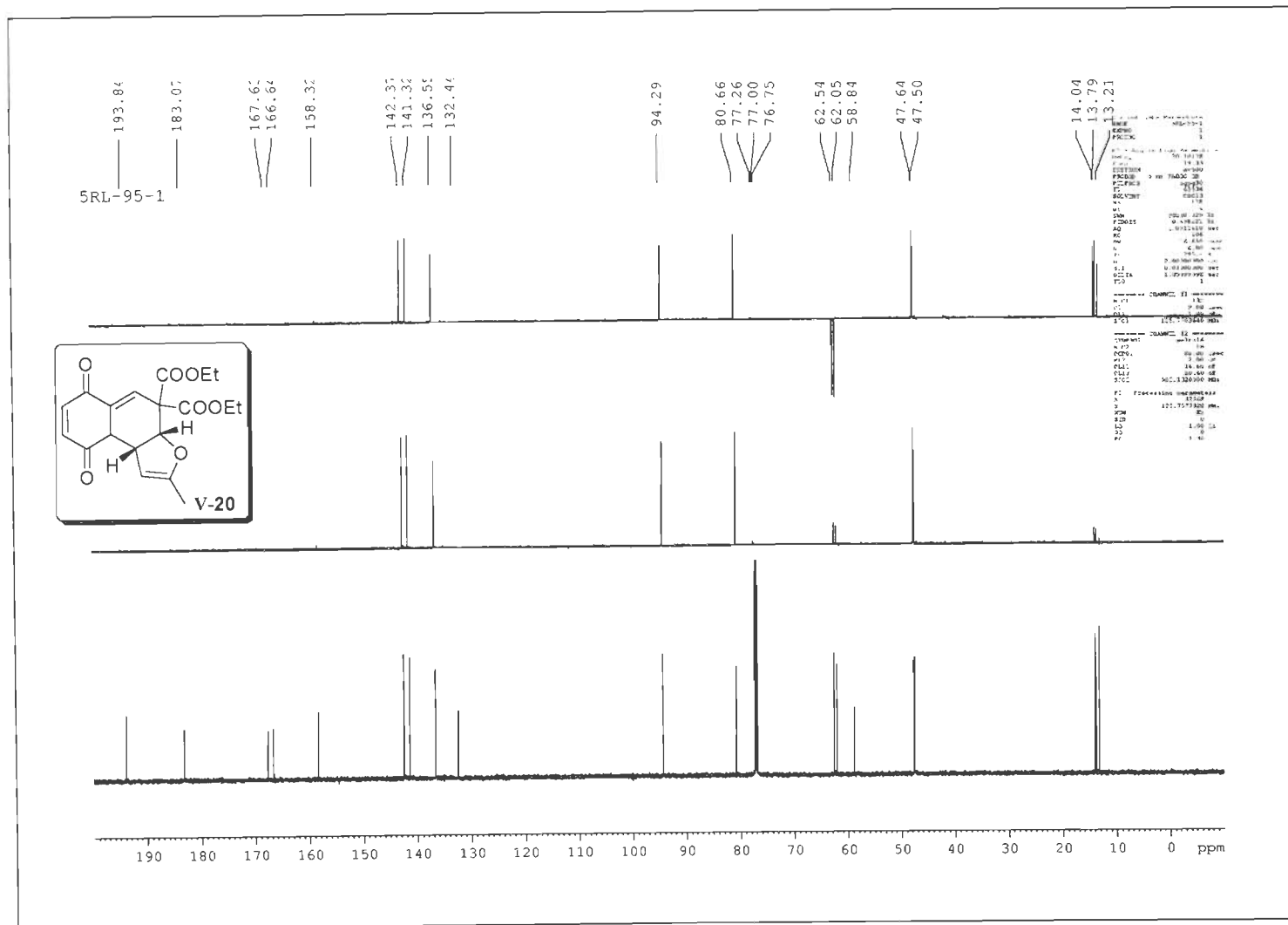


Figure S-72: ^{13}C DEPT (125 MHz, CDCl_3) Spectra of V-20.

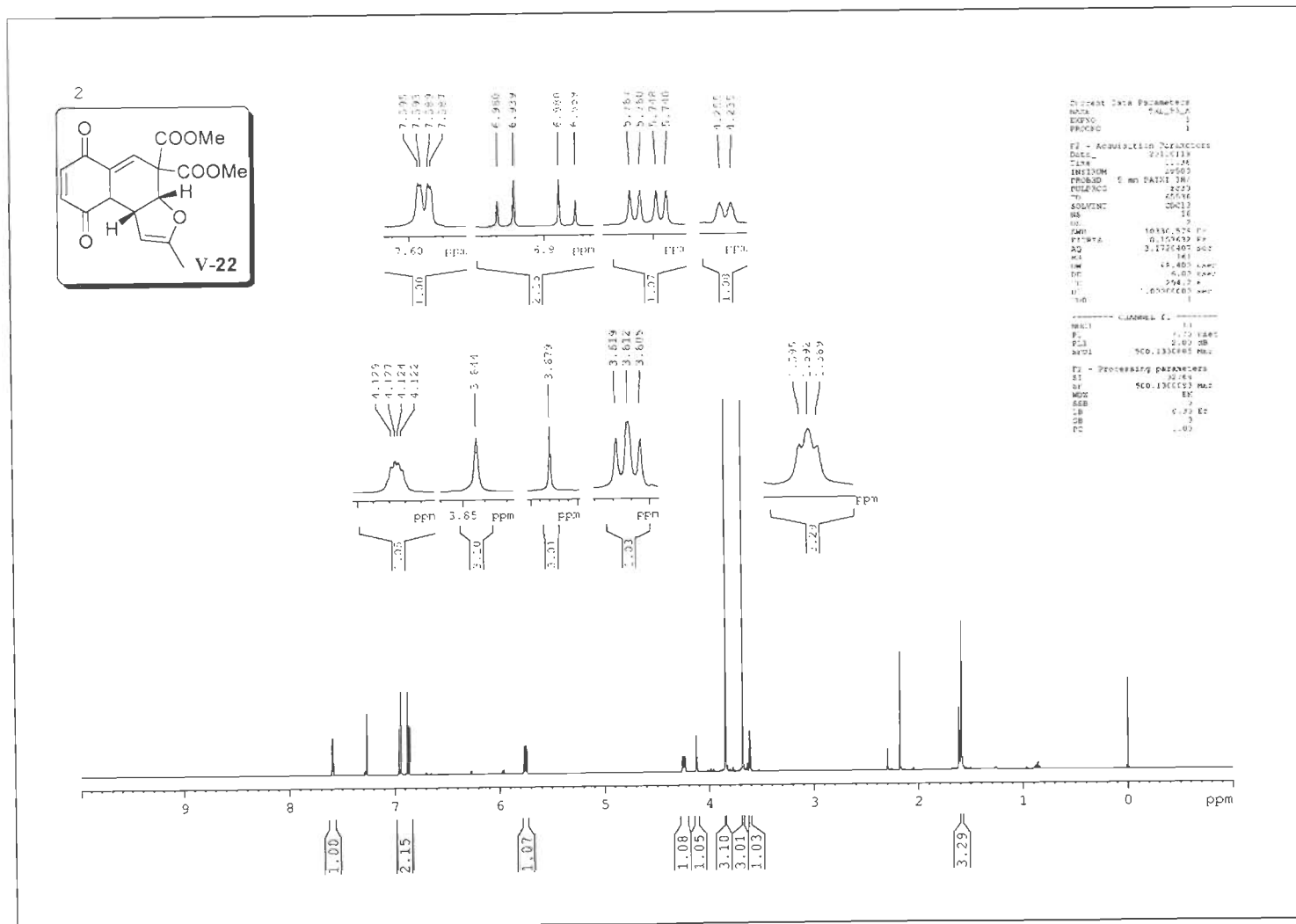


Figure S-73: ^1H NMR (500 MHz, CDCl_3) Spectrum of V-22.

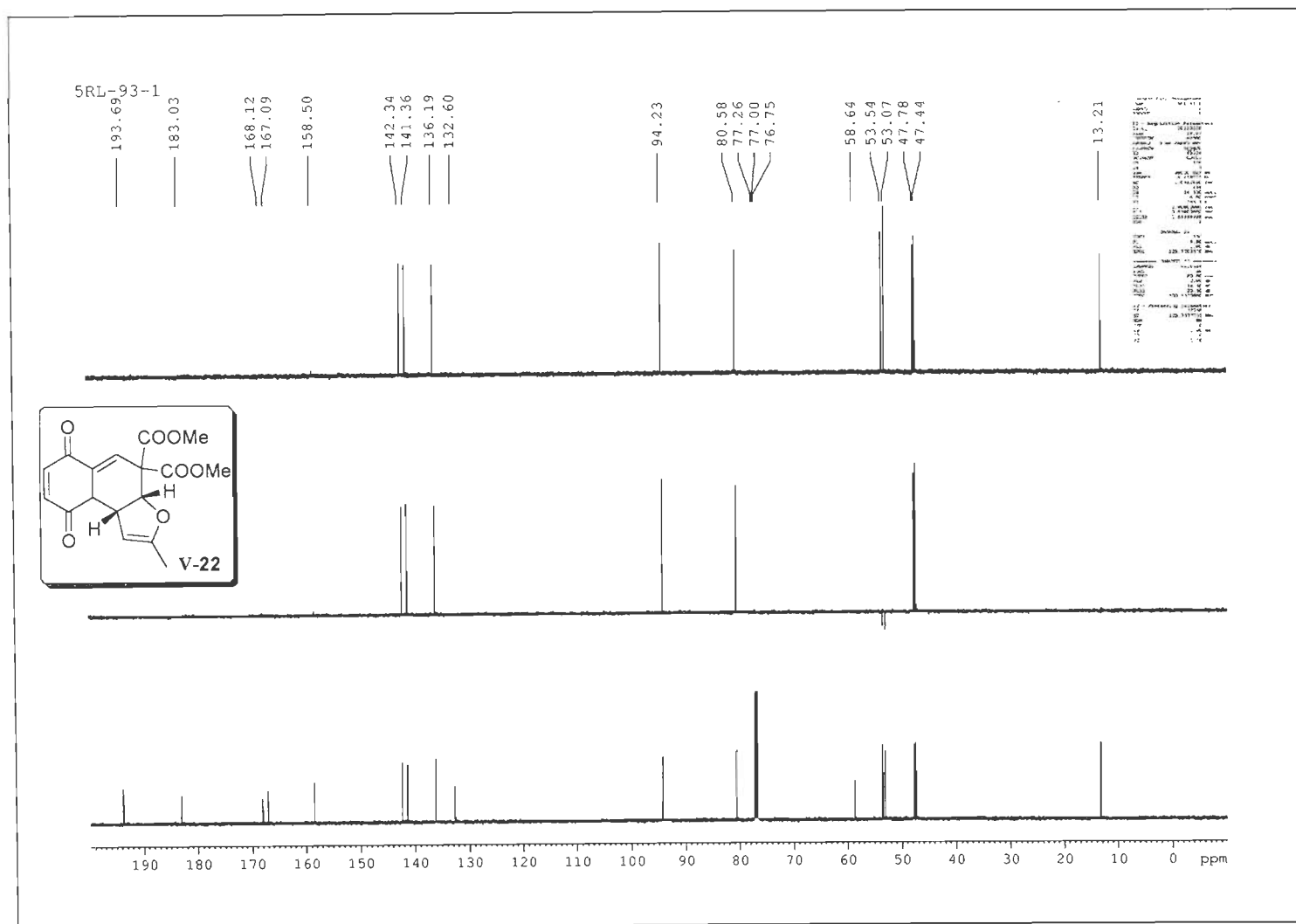


Figure S-74: ^{13}C DEPT (125 MHz, CDCl_3) Spectra of V-22.

LIST OF PUBLICATIONS

1. Aminolysis of Epoxides Using Iridium Trichloride as an Efficient Catalyst.
Jyoti Agarwal, Anju Duley, **Rashmi Rani**, Rama Krishna Peddinti
Synthesis (2009) 2790.
2. Magnesium Chloride-Catalyzed Thiolysis of Epoxides: Synthesis of β -hydroxy Sulfides.
Rashmi Rani, Shankha Pattanayak, Jyoti Agarwal, Rama Krishna Peddinti
Synthetic Communications, 40 (2010) 658.
3. Copper(II) Chloride Catalyzed Friedel-Crafts-type Conjugate Addition of Indoles to α,β -Unsaturated Enones: Synthesis of 3-Substituted Indoles.
Deepika Kanwar, **Rashmi Rani**, Jyoti Agarwal, Rama Krishna Peddinti
Indian Journal of Chemistry, 49B (2010) 1209.
4. Camphor-10-sulfonamide-based Prolinamide Organocatalyst for the Direct Intermolecular Aldol Reaction between Ketones and Aromatic Aldehydes.
Rashmi Rani, Rama Krishna Peddinti
Tetrahedron: Asymmetry 21 (2010) 775.
5. Michael Reaction of Ketones and β -Nitrostyrenes Catalyzed by Camphor-10-sulfonamide-based Prolinamide.
Rashmi Rani, Rama Krishna Peddinti
Tetrahedron: Asymmetry 21 (2010) 2487.
6. Synthesis and Characterization of Camphor-10-sulfonamide Derivatives and Their Application in Direct Intermolecular Aldol and Michael Reactions.
Rashmi Rani, Rama Krishna Peddinti
Submitted for publication.
7. Reactions of Alkenyl-1,4-benzoquinones with Enol Ethers. A Rapid Access to Complex Molecular Architectures.
Rashmi Rani, Rama Krishna Peddinti
Manuscript under preparation.

CONFERENCES

1. A Novel and Efficient Camphor-based Prolinamide Organocatalyst for Intermolecular Direct Aldol Reactions.
Oral Presentation
Uttarakhand State Council For Science and Technology (UCOST), Dehradun (2009)
Awarded Young Scientist Award for Oral Presentation-2009.
2. Asymmetric Reactions Catalyzed by a Novel Camphor-based Organocatalyst.
12th CRSI National Symposium in Chemistry & 4th CRSI-RSC Symposium in Chemistry, Hyderabad-(2010).
Poster Presentation